

August 2016

Molecular Recognition in Water: Design, Synthesis, and Characterization of Rigid Molecular Receptors and Enzymatic Mechanistic Probes

Robert William Hoppe
University of Wisconsin-Milwaukee

Follow this and additional works at: <https://dc.uwm.edu/etd>

 Part of the [Chemistry Commons](#)

Recommended Citation

Hoppe, Robert William, "Molecular Recognition in Water: Design, Synthesis, and Characterization of Rigid Molecular Receptors and Enzymatic Mechanistic Probes" (2016). *Theses and Dissertations*. 1274.
<https://dc.uwm.edu/etd/1274>

This Dissertation is brought to you for free and open access by UWM Digital Commons. It has been accepted for inclusion in Theses and Dissertations by an authorized administrator of UWM Digital Commons. For more information, please contact open-access@uwm.edu.

MOLECULAR RECOGNITION IN WATER:
DESIGN, SYNTHESIS, AND CHARACTERIZATION OF RIGID MOLECULAR RECEPTORS
AND ENZYMATIC MECHANISTIC PROBES

by

Robert William Hoppe

A Dissertation Submitted in
Partial Fulfillment of the
Requirements for the Degree of

Doctor of Philosophy

in Chemistry

at

The University of Wisconsin-Milwaukee

August 2016

ABSTRACT

**MOLECULAR RECOGNITION IN WATER:
DESIGN, SYNTHESIS, AND CHARACTERIZATION OF RIGID MOLECULAR RECEPTORS
AND ENZYMATIC MECHANISTIC PROBES**

by

Robert William Hoppe

The University of Wisconsin-Milwaukee, 2016
Under the Supervision of Alan W. Schwabacher

Molecular recognition can be defined as a selective and reversible binding between two or more molecules through non-covalent interactions. Multiple weakly attractive intermolecular forces work in concert to achieve selectivity in association. Such discrimination is critical to the physiological processes of catalysis, transport, antigen recognition, and storage. To better understand this phenomenon, acyclic synthetic molecular receptors also known as “molecular tweezers” were made to study the inclusion of small molecule guests from water. Three anionic tweezers derivatives with *syn*- cofacial orientation were constructed from a 1,2:4,5-*bis*-Tröger’s Base skeleton that differed in the amount and distribution of negative charge about the receptors. These binding isomers were found to undergo self association to form dimers in solution by inclusion of the naphthalene wall of one tweezers into the cleft of another. Small molecule binding was evaluated at different ionic strengths and under concentration regimes in which either the desired monomeric tweezers or the dimeric complex predominated.

Small molecules were also created in order to probe the mechanisms by which enzymes facilitate their transformations. Cinnamylidene pyruvate and fluorinated pyruvate derivatives were synthesized to better understand why SbADC, an enzyme classified as an acetoacetate decarboxylase, demonstrates aldolase activity.

Enduracidinine is an unsaturated amino acid found in the potent antibiotics mannopeptimycin, teixobactin, and enduracidin. To investigate the biosynthesis of this amino acid, a new preparation of L-vinylglycine was devised. L-vinylglycine is a potential general precursor to the formation β,γ -unsaturated amino acids. Conditions were identified in which such unsaturated amino acids are formed by olefin metathesis of protected L-vinylglycine and alkenes including allylamine derivatives.

© Copyright by Robert William Hoppe, 2016
All Rights Reserved

TABLE OF CONTENTS

List of Figures	x
List of Tables	xvii
List of Abbreviations	xviii
Acknowledgements	xxi
PART ONE: DESIGN, SYNTHESIS, AND CHARACTERIZATION OF RIGID MOLECULAR RECEPTORS	
I. INTRODUCTION	
A. Molecular Recognition	1
B. Precedented Natural and Synthetic Molecular Hosts.	2
1. Cyclic Molecular Receptors.	2
2. Acyclic (non-macrocyclic) Molecular Receptors	6
C. Tröger's Base and <i>bis</i> -Tröger's Base	9
D. Rationale and Design of Target <i>bis</i> -Tröger's Base Molecular Receptor	14
II. RESULTS AND DISCUSSION	
A. Formation of the key intermediate N,N'-di- <i>t</i> -Boc-2,5-diaminoterephthaldehyde.	16
1. Synthesis of Dimethyl 2,5-diaminocyclohexa-1,4-diene-1,4-dicarboxylate	16
2. Synthesis of Dimethyl 2,5-bis((<i>tert</i> -butoxycarbonyl)amino)terephthalate	17
a. Diaryl amine formation	18
b. Exploration on mechanism of diarylamine formation	21
3. Synthesis of Di- <i>tert</i> -butyl (2,5-bis(hydroxymethyl)-1,4-phenylene)dicarbamate	22
4. Synthesis of N,N'-di- <i>t</i> -Boc-2,5-diaminoterephthaldehyde	23
a. Over oxidation from MnO ₂ and alternate Cu(I) catalyzed oxidation	24
B. Synthesis of acyclic <i>bis</i> -Tröger's Base Molecular Receptor	27
1. Preparation of <i>bis</i> -imines	27
2. Synthesis <i>bis</i> - α -aminophosphonates.	30
3. Trögerization Affording Molecular Receptors Isomers.	38
4. Reactions to Generate Water Soluble Molecular Receptors.	45
C. Characterization of Molecular Receptor Isomers.	49
D. Dimerization of Water Soluble Receptor Isomers in Water	52
1. Analysis by ¹ H NMR Spectroscopy	52
2. Analysis by Fluorescent Spectroscopy.	56

3. Analysis by UV-VIS Spectroscopy	64
E. Binding Studies of Molecular Receptor by Small Molecule Titration	66
1. Carbethoxy tetra anion isomers 23 and 24.	68
2. Methyl phosphonate tetra anion isomers 25 and 26.	71
3. Hexa-anionic isomers 27 and 28	79
F. Quinolone Synthesis for Functionalized Walls for <i>bis</i> -Tröger's Base Molecular Receptors .	83
1. Preparation of 7-Amino-4-oxo-1,4-dihydro-quinoline-2-carboxylic acid ethyl ester ..	85
a. From (3-Amino-phenyl)-carbamic acid tert-butyl ester Route.	85
b. From N-(3-aminophenyl)-2,2,2-trifluoroacetamide Route.	87
c. From 3-nitroaniline Route.	88
2. Preparation of 6-Amino-4-oxo-1,4-dihydro-quinoline-2-carboxylic acid ethyl ester ..	92
III. CONCLUSION	92
PART TWO: SMALL MOLECULE SYNTHESIS FOR ENZYMATIC MECHANISTIC PROBES	
IV. SMALL MOLECULE PROBES FOR EVALUATING SbADC ALDOLASE ACTIVITY	97
A. SbADC Background Information.	97
B. Rational for SbADC Molecular Probes.	98
V. RESULTS AND DISCUSSION	101
C. Formation of Cinnamylidenepyruvate and 4-NO ₂ Cinnamylidenepyruvate Salts.	101
D. Difluoropyruvate Synthesis.	104
VI. SMALL MOLECULE PROBES FOR MppR AND MppP	108
A. Enduracididine and Enduracidin Background Information.	108
B. Roles of MppP and MppR	111
C. Attempts to Make Guanidiniumacetaldehyde for MppR Evaluation	116
D. Towards β,γ -dehydroarginine for MppP Evaluation.	118
1. L-Vinylglycine Synthesis	122
a. L-Selenomethionine selenoxide Route.	124
b. L-Methionine sulfoxide Route.	126
i. Gas Phase Pyrolysis	126
ii. <i>in situ</i> Thermolysis.	128

iii. Addition and Distillation Method.	129
2. Olefin Cross Metathesis of L-Vinylglycine Derivatives	139
a. Background on Olefin Metathesis.	139
b. Synthesis and Screening of Allylamine Derivatives for Cross Metathesis	146
c. Cross Metathesis of L-Vinylglycine Derivatives and Selected Allylamine Derivatives.	153
VII. CONCLUSION	156
VIII. EXPERIMENTAL SECTION	159
Dimethyl 2,5-diaminocyclohexa-1,4-diene-1,4-dicarboxylate (1).	160
Dimethyl 2,5- <i>bis</i> ((<i>tert</i> -butoxycarbonyl)amino)terephthalate (2)	161
Dimethyl 2,5-diaminoterephthalate (3).	162
Tetramethyl 5,5'-azanediyl <i>bis</i> (2-((<i>tert</i> -butoxycarbonyl)amino)terephthalate) (4)	163
Dimethyl 2-amino-5-(<i>p</i> -tolylamino)terephthalate (5)	164
Dimethyl 2,5- <i>bis</i> (<i>p</i> -tolylamino)terephthalate (6)	165
Di- <i>tert</i> -butyl (2,5- <i>bis</i> (hydroxymethyl)-1,4-phenylene)dicarbamate (7)	166
N,N'-di- <i>t</i> -Boc-2,5-diaminoterephthaldehyde (8)	167
Ethyl 6-amino-2-naphthoate (12).	169
Diethyl 6,6'-((1 <i>E</i> ,1' <i>E</i>)-((2,5- <i>bis</i> ((<i>tert</i> -butoxycarbonyl)amino)-1,4-phenylene) <i>bis</i> (methanylylidene)) <i>bis</i> (azanylylidene)) <i>bis</i> (2-naphthoate) (13)	170
Diethyl 6,6'-(((1 <i>R</i> ,1' <i>S</i>)-(2,5- <i>bis</i> ((<i>tert</i> -butoxycarbonyl)amino)-1,4-phenylene) <i>bis</i> ((dimethoxyphosphoryl)methylene)) <i>bis</i> (azanediyl)) <i>bis</i> (2-naphthoate) (16)	172
Diethyl 6,6'-(((1 <i>S</i> ,1' <i>S</i>)-(2,5- <i>bis</i> ((<i>tert</i> -butoxycarbonyl)amino)-1,4-phenylene) <i>bis</i> ((dimethoxyphosphoryl)methylene)) <i>bis</i> (azanediyl)) <i>bis</i> (2-naphthoate) (17).	173
C-Me, P-Me <i>rac</i> -tweezers (18)	174
C-Me, P-Me <i>meso</i> -isomer (19)	176
<i>rac</i> - carbethoxy tetra acid tweezers (23)	178

<i>meso</i> - carbethoxy tetra acid isomer (24).	179
<i>rac</i> -methylphosphonate tetra anionic tweezers (25).	180
<i>meso</i> -methylphosphonate tetra anionic isomer (26).	181
<i>rac</i> -hexa anionic tweezers (27)	182
<i>meso</i> -hexa anionic isomer (28)	183
<i>tert</i> -butyl (3-aminophenyl)carbamate (29).	184
2-(3- <i>tert</i> -Butoxycarbonylamino-phenylamino)-but-2-enedioic acid diethyl ester (30).	185
7-Amino-4-oxo-1,4-dihydro-quinoline-2-carboxylic acid ethyl ester (31)	186
Ethyl 5-amino-4-oxo-1,4-dihydroquinoline-2-carboxylate (32).	187
Diethyl 2-((3-(2,2,2-trifluoroacetamido)phenyl)amino)fumarate (34)	187
Ethyl 4-oxo-7-(2,2,2-trifluoroacetamido)-1,4-dihydroquinoline-2-carboxylate (35).	188
Ethyl 4-oxo-5-(2,2,2-trifluoroacetamido)-1,4-dihydroquinoline-2-carboxylate (36).	189
Diethyl 2-((3-nitrophenyl)amino)fumarate (37)	190
Ethyl 7-nitro-4-oxo-1,4-dihydroquinoline-2-carboxylate (38).	191
Ethyl 5-nitro-4-oxo-1,4-dihydroquinoline-2-carboxylate (39).	192
Diethyl 2-((4-nitrophenyl)amino)fumarate (40)	193
Ethyl 6-nitro-4-oxo-1,4-dihydroquinoline-2-carboxylate (41).	193
Ethyl 6-amino-4-oxo-1,4-dihydroquinoline-2-carboxylate (42).	194
Potassium (3E,5E)-2-oxo-6-phenylhexa-3,5-dienoate (45)	195
Potassium (3E,5E)-6-(4-nitrophenyl)-2-oxohexa-3,5-dienoate (46)	197
Sodium trifluoropyruvate (47)	198
5-methyl-2-(2,2,2-trifluoroacetyl)furan (50).	199

5-methyl-2-(2,2-difluoroacetyl)furan (51)	200
Methyl difluoropyruvate methyl hemiacetal (52).	201
Sodium difluoropyruvate hydrate (53)	202
N,N'-Di-Boc-N''-(2,2-dimethoxy-ethyl)-guanidine (54).	203
N-Allyl-N',N''-Di-Boc-guanidine (55).	203
N-allyl guanidinium trifluoroacetate (57)	204
2-Amino-5-hydroxy-4,5-dihydro-3H-imidazolium chloride (58)	205
L-Selenomethionine methyl ester hydrochloride (62).	206
N-Boc-L-Selenomethionine methyl ester (63).	207
N-Boc-L-Selenomethionine oxide methyl ester (64).	208
L-Methionine methyl ester hydrochloride (66).	208
N-Boc-L-Methionine methyl ester (67)	209
N-Boc-L-Methionine sulfoxide methyl ester (68)	210
L-Methionine sulfoxide (70)	211
L-Vinylglycine (71)	212
(S)-2-((R)-2-(((9H-fluoren-9-yl)methoxy)carbonyl)amino)propanamido)but-3-enoic acid (72)	213
(S)-2-(((9H-fluoren-9-yl)methoxy)carbonyl)amino)but-3-enoic acid (73)	214
(S)-2-((<i>tert</i> -butoxycarbonyl)amino)but-3-enoic acid (74)	215
Dicyclohexyl ammonium 2-((<i>tert</i> -butoxycarbonyl)amino)but-3-enoate (75).	216
Allylammonium chloride (76).	217
<i>tert</i> -butyl allylcarbamate (78).	217
(9H-fluoren-9-yl)methyl allylcarbamate (79)	218

N-allyl-2,2,2-trifluoroacetamide (80)	219
3-azidoprop-1-ene (81).	219
(Z)-di- <i>tert</i> .-butyl but-2-ene-1,4-diyl dicarbamate (82)	220
(E)-di- <i>tert</i> .-butyl but-2-ene-1,4-diyl dicarbamate (83)	221
(E)- <i>bis</i> ((9H-fluoren-9-yl)methyl) but-2-ene-1,4-diyl dicarbamate (84)	221
(E/Z)-N,N'-(but-2-ene-1,4-diyl) <i>bis</i> (2,2,2-trifluoroacetamide) (85)	222
(E)-oct-4-enedioic acid (86)	223
(S,E)-2,5- <i>bis</i> ((<i>tert</i> -butoxycarbonyl)amino)hept-3-enoic acid (87).	223
(S,E)-5-((((9H-fluoren-9-yl)methoxy)carbonyl)amino)-2-((<i>tert</i> -butoxycarbonyl)amino)pent-3-enoic acid (88)	224
(S,E)-2-((<i>tert</i> -butoxycarbonyl)amino)hept-3-enoic acid (89).	225
IX. REFERENCES	227
X. APPENDIX	239
A. Characterization Data for Selected Compounds	239
XI. CURRICULUM VITAE	441

LIST OF FIGURES

Figure 1: Equilibrium for association between a molecular receptor (host, H) and an associating molecule (guest, G) in solution to form a complex (C).	2
Figure 2: Example of a cyclodextrins.	3
Figure 3: Cyclic polyether, 18-crown-6, drawn with a potassium ion bound into its cavity.	4
Figure 4: Depiction of an unoriented host adopting a binding conformation before guest inclusion	4
Figure 5: Koga's macrocycle.	5
Figure 6: Whitcock's caffeine based molecular tweezers and a molecular tweezers constructed by Zimmerman	7
Figure 7: <i>bis</i> -Kagan's ether (left) and Harmata's molecular tweezers based on a <i>bis</i> -Kagan's ether architecture	8
Figure 8: Examples of a molecular tweezers (left) and a molecular clip (right) generated by Klärner	9
Figure 9: Formation of the two Tröger's Base isomers from <i>p</i> -toluidine and formaldehyde.	10
Figure 10: A Wilcox molecular tweezers based on Tröger's Base that binds pyrimidin-2-amine	11
Figure 11: Precipitated 1,2:4,3- <i>bis</i> -Tröger's Base isomer and desired 1,2:4,5- <i>bis</i> -Tröger's Base.	12
Figure 12: Retro-synthetic scheme for modular construction of the desired water soluble <i>bis</i> -Tröger's Base molecular tweezers	14
Figure 13: 1,2;4,5- <i>bis</i> -Tröger's Base molecular tweezer with naphthalene walls illustrating their offset nature	15
Figure 14: Overall synthetic sequence to produce key intermediate dialdehyde 8.	16
Figure 15: Synthesis of <i>bis</i> -enamine 1 from dimethyl succinyl succinate	16
Figure 16: Scheme for aromatization and di-Boc protection of <i>bis</i> -enamine 1	17
Figure 17: Deprotection of 2 to afford aromatic diamine 3	20
Figure 18: Compound 4, the diaryl amine side product formed from condensation of 2	20
Figure 19: Mono- and <i>bis</i> - diarylamine formation from <i>bis</i> -enamine	21
Figure 20: Reduction of aromatic diester 2 to desired diol 7.	22

Figure 21: Selective oxidation of diol 7 to desired dialdehyde 8	23
Figure 22: Selective oxidation to dialdehyde with MnO_2	24
Figure 23: Over oxidation of DA to mono-aldehyde mono-carboxylic acid with MnO_2	24
Figure 24: Selective oxidation to DA with Cu(I) catalyst	26
Figure 25: General scheme for <i>bis</i> -imine formation from dialdehyde 8	27
Figure 26: Optimized condition for synthesis of <i>bis</i> -imine 13	28
Figure 27: Formation <i>bis</i> - α -aminophosphonates 14 and 15 from <i>bis</i> -imine 13	30
Figure 28: General "one pot" reaction scheme for <i>bis</i> -aminophosphonate formation.	32
Figure 29: Proposed mechanism for dimethyl methylphosphonate formation with P(OMe)_3	32
Figure 30: Proposed mechanism for reaction of P(OMe)_3 with THF in the presence of Yb(OTf)_3	33
Figure 31: "One pot" <i>bis</i> -aminophosphonate synthesis with HPO(OMe)_2	33
Figure 32: Use of BSA to shift HPO(OMe)_2 equilibrium and to prevent methyl transfer.	36
Figure 33: Trogerization to form desired <i>rac</i> -(18) and control <i>meso</i> - (19) molecular receptors isomers	38
Figure 34: "One pot" molecular tweezers synthetic scheme using HPO(OMe)_2	39
Figure 35: "One pot" molecular tweezers synthetic scheme using diethyl phosphite.	40
Figure 36: "One pot" tweezers synthesis starting from <i>bis</i> -imine	41
Figure 37: Scheme for the synthesis of tetraBoc derivative of 13	43
Figure 38: "One pot" synthesis of molecular tweezers using dimethyl phosphite	44
Figure 39: TMSBr deprotection of tweezers isomers to afford carbethoxy tetra acids derivatives	45
Figure 40: Saponification of tweezers isomers to form the methyl phosphonate tetra anion derivatives	47
Figure 41: Hexa-anionic tweezers isomers formed by saponification of the TMSBr dealkylated derivatives	48

Figure 42: Space filling models for the fully esterified binding <i>rac</i> - isomer (left) and the non-binding <i>meso</i> - isomer (right).	49
Figure 43: ^1H NMR dilution of the fully esterified <i>rac</i> - tweezers 18 in CDCl_3	50
Figure 44: Equation used for the non-linear least squares fit for the dimerization of the fully esterified <i>rac</i> - tweezers utilizing NMR chemical shifts (top) and fit using chemical shift proton A (bottom).	51
Figure 45: Chemical shifts, coupling constants, and NOESY correlations for the full esterified binding <i>rac</i> - isomer 18 in CDCl_3 at $3 \times 10^{-3}\text{M}$ concentration.	51
Figure 46: ^1H NMR spectrum of the fully esterified non-binding <i>meso</i> - tweezers isomer 19.	52
Figure 47: Comparison of the ^1H NMR spectra of <i>rac</i> - carbethoxy tetra anionic tweezers 23 in D_2O and 50% TFA/CDCl_3 versus the non-binding <i>meso</i> - isomer 24 in D_2O	53
Figure 48: Comparison of the ^1H NMR spectra of <i>rac</i> - methyl phosphonate tetra anionic tweezers 25 in D_2O and 50% TFA/CDCl_3 versus the non-binding <i>meso</i> - isomer 26 in D_2O	54
Figure 49: Comparison of the ^1H NMR spectra of <i>rac</i> - hexa anionic tweezers 27 in D_2O and 50% TFA/CDCl_3 versus the non-binding <i>meso</i> - isomer 28 in D_2O	55
Figure 50: Derivation of the equation used to determine K_{dim} for the dimerization of the binding <i>rac</i> - tweezers by fluorescence spectroscopy.	57
Figure 51: Plot of fluorescent emission (445nm) versus concentration for <i>rac</i> - carbethoxy tetra anion 23 tweezers using 300nm excitation.	58
Figure 52: Fluorescence of <i>rac</i> - methyl phosphonate tweezer displaying fine structure at 300nm excitation.	59
Figure 53: Fluorescent emission and plot of fluorescence (430nm) versus concentration for <i>rac</i> - methyl phosphonate tetra anion tweezers 25.	60
Figure 54: Plot of concentration vs. fluorescence for <i>meso</i> - methyl phosphonate isomer 26	61
Figure 55: Fluorescent emission of control <i>meso</i> - methyl phosphonate tetra anion 26 at various excitation wavelengths plotted to include excitation wavelengths.	62

Figure 56: Fluorescent emission and plot of emission (405nm) vs. concentration for <i>rac</i> - hexa anionic tweezers using 345nm excitation	63
Figure 57: Plot of fluorescent emission (405nm) versus concentration for the control <i>meso</i> - hexa anion isomer using 345nm excitation	64
Figure 58: Plot of wavelength vs. epsilon for the binding 25 (left) and the control 26 (right) methyl phosphonate tetra anion isomers.	65
Figure 59: Plot of concentration vs. epsilon for 25 fit by non-linear least squares.	66
Figure 60: Derivation of equation used to determine K_d in small molecule binding titrations where H=host, G=guest, and C=complex	67
Figure 61: Stern-Volmer equation where I_0 = initial fluorescence, I = fluorescence with quencher present, k =quencher rate coefficient, and τ =lifetime of the excited state of the emitting molecule	67
Figure 62: Titration of <i>rac</i> - and <i>meso</i> - carbethoxy tetraanion isomers with L-Tyr Et ester HCl	69
Figure 63: Titration of <i>rac</i> - and <i>meso</i> - carbethoxy tetraanion isomers with methyl viologen	70
Figure 64: Fluorescent emission of tetra anion tweezers 25 with varying excitation wavelength plotted to include excitation wavelengths.	72
Figure 65: Titration of binding <i>rac</i> - and <i>meso</i> - methyl phosphonate isomers with 1-Me nicotinamide chloride in nanopure water	74
Figure 66: 1:1 binding and Stern-Volmer plot for titration of <i>rac</i> - methyl phosphonate tweezers 25 with 1-Me nicotinamide chloride in nanopure water	75
Figure 67: 1:1 binding and Stern-Volmer plot for titration of control <i>meso</i> - methyl phosphonate tetra anion isomer with 1-Me nicotinamide chloride in nanopure water.	76
Figure 68: ^1H NMR comparison of the aromatic region of free <i>meso</i> - methyl phosphonate tetra anion 26, free 1-Me nicotinamide chloride, and a 1:1 mixture of the two at $1.8 \times 10^{-2}\text{M}$ concentration.	77
Figure 69: Comparison of K_d for binding 25 and control 26 isomer to 1-Me nicotinamide chloride in nanopure water and 150mM NaCl, 10mM pH7 phosphate buffer	78
Figure 70: Comparison of fluorescent emissions of the binding <i>rac</i> - hexa anionic tweezers (top) and the non-binding <i>meso</i> - control isomer (bottom). Stern-Volmer plot also included for binding isomer 27.	81
Figure 71: Titration of hexa anionic tweezers 27 with disodium 2-naphthylphosphate	82

Figure 72: 7-Amino-4-oxo-1,4-dihydro-quinoline-2-carboxylic acid ethyl ester and its resulting <i>bis</i> -Tröger's Base tweezer	83
Figure 73: 6-Amino-4-oxo-1,4-dihydro-quinoline-2-carboxylic acid ethyl ester and the possible combinations of <i>bis</i> -Tröger's Base tweezers	84
Figure 74: General scheme for aminoquinolone synthesis.	84
Figure 75: Synthetic route to produce 7-amino-2-carboxy from 1,3-diaminobenzene	85
Figure 76: Synthetic route for quinolone production from mono-trifluoroacetyl protected 1,3-diaminobenzene.	87
Figure 77: Proposed hydrogen bonded intermediate responsible for regioselective cyclization.	88
Figure 78: Quinolone synthetic scheme starting from 3-nitroaniline	88
Figure 79: Synthetic scheme for production of 6-amino-2-carboxy-4-oxoquinolone ethyl ester.	92
Figure 80: 1,2:4,5- <i>bis</i> -Tröger's Base tweezer scheme displaying desired quinolones for future inclusion	96
Figure 81: Proposed use of trifluoropyruvate and difluoropyruvate for mechanistic determination of SbADC aldol pathway.	99
Figure 82: An example synthetic scheme in formation of difluoropyruvate analogues.	100
Figure 83: Formation of cinnamylidene pyruvate sodium salt.	101
Figure 84: Formation of 4-nitrocinnamylidene pyruvate sodium salt.	102
Figure 85: General scheme for isolating sodium pyruvate free cinnamylidene pyruvate analogues	102
Figure 86: ¹ H NMR spectra of 4-nitrocinnamylidene pyruvate over the course of sodium pyruvate removal.	103
Figure 87: Scheme for sodium trifluoropyruvate hydrate	104
Figure 88: Proposed synthetic route for simplified difluoropyruvate formation.	104
Figure 89: Desired E2 elimination of O,O-(<i>bis</i> -trimethylsilyl) ethyl trifluoropyruvate	105
Figure 90: Proposed E2 elimination of O,O-(<i>bis</i> -trimethylsilyl) ethyl trifluoropyruvate that occurred	106
Figure 91: Literature based synthesis for ozonolysis precursor.	106

Figure 92: Ozonolysis scheme for synthesis of methyl difluoropyruvate methyl hemiacetal	106
Figure 93: Enduracididine (left) and allo-enduracididine (right)	110
Figure 94: Enduracidin A (R=H) and Enduracidin B (R=CH ₃). Image provided by Dr. Nicholas Silvaggi.	111
Figure 95: Proposed biosynthesis for enduracididine.	112
Figure 96: Aldol condensation and dehydration product of imidazole carboxaldehyde and sodium pyruvate formed by MppR.	113
Figure 97: Literature route to γ -OH arginine	114
Figure 98: γ -OH arginine synthesis from epichlorohydrin	115
Figure 99: Retro-synthetic analysis for dehydro-L-Arginine by Aldol reactions route	116
Figure 100: Guanidinylation of aminoacetaldehyde dimethyl acetal 54.	116
Figure 101: Formation of 2-aminoimidazole from guanidinylated aminoacetaldehyde dimethyl acetal upon acidic hydrolysis.	117
Figure 102: Desired oxidative cleavage of guanidinylated allylamine.	118
Figure 103: Model reactions to test conditions for oxidative cleavage of an alkene with K ₂ OsO ₄	119
Figure 104: Proposed stabilized complex that prevents dihydroxylation by osmium tetroxide	119
Figure 105: Cyclized hemiaminal generated upon treatment of allylguanidinium trifluoroacetate with osmium tetroxide.	120
Figure 106: Synthethis diBoc protected cyclic hemiaminal from diBoc protected allylguanidine	121
Figure 107: Reaction of di-Boc cyclic hemiaminal 59 with sodium pyruvate	122
Figure 108: α , β -unsaturated ketone formation by arylselenoxide elimination and desired elimination of a methyl selenoxide to form vinylglycine	124
Figure 109: Synthetic scheme of N-Boc-L-vinylglycine methyl ester synthesis from L- selenomethionine.	125
Figure 110: Synthesis of L-vinylglycine methyl ester form L-methionine	126
Figure 111: Illustration of apparatus constructed for gas phase pyrolysis	127

Figure 112: NMR spectra of isolated materials from <i>in situ</i> thermolysis of silylated L-methionine	128
Figure 113: Synthetic scheme for L-vinylglycine formaton by in situ silylation followed by thermolysis with distillation	132
Figure 114: L-Vgy derivatization and HPLC trace demonstrating retention of desired stereocenter	135
Figure 115: Reaction conditions in which L-vinylglycine methyl ester will or will not isomerize	136
Figure 116: Fmoc- and Boc- protection of L-vinylglycine.	138
Figure 117: Examples of intramolecular olefin metathesis with amino acid derivatives.	139
Figure 118: Successful metathesis after saponification of a lactone.	140
Figure 119: Homodimer formation due to isomerization of vinyl sidechain.	140
Figure 120: From left to right Schrock's, Grubb's 1st gen, and Grubb's 2nd gen metathesis catalysts.	141
Figure 121: Afforded yields of cross metathesis product as steric hindrance around olefin increases	141
Figure 122: Effects of increasing steric hindrance on rate of metathesis	142
Figure 123: Hoveyda-Grubbs's 2nd generation metathesis catalyst	144
Figure 124: Ring closing yields using water soluble Hoveyda-Grubbs 2nd gen catalysts.	146
Figure 125: General scheme for homodimer formation via olefin metathesis.	148
Figure 126: Homodimer formation via olefin metathesis of Boc protected allyl amine	152
Figure 127: Example olefin cross metathesis using Hoveyda-Grubbs 2nd generation catalyst.	153
Figure 128: Future direction for dehydroarginine synthesis	158

LIST OF TABLES

Table 1: <i>bis</i> -aminophosphonate diastereomers afforded from deactivated silica gel chromatography.	35
Table 2: Observed dissociation constants from the titration of the proposed <i>rac</i> - carbethoxy tetra anionic tweezers 23 dimer	68
Table 3: Apparent K_d values for small molecules titrated with binding <i>rac</i> - methyl phosphonate tetra anion tweezers	73
Table 4: Apparent K_d values substrate association to binding <i>rac</i> - hexa anionic tweezers at 5.0×10^{-6} M concentrations.	80
Table 5: Quinolone mol ratios with varying substituents and reaction conditions	90
Table 6: Parameters and results in thermolysis of N-Boc-L-selenomethionine oxide methyl ester	125
Table 7: Experimental parameters in screening <i>in situ</i> thermolysis for L-vinylglycine formation.	129
Table 8: Results fom tested conditions <i>in situ</i> thermolysis parameters in L-vinylglycine synthesis	129
Table 9: Experimental parameters from <i>in situ</i> thermolysis with distillation.	130
Table 10: Experimental results from in situ thermolysis with distillation.	131
Table 11: Pseudo- first order kinetic data for the isomerization of L-vinylglycine derivatives. All reactions conducted at 22°C and in $CDCl_3$	137
Table 12: Synthesis of allyl amine derivatives for homodimerization screening	146
Table 13: Alkene reactivities for homodimer formation.	150
Table 14: Summary of results for combinations of metathesis substrates.	156

LIST OF ABBREVIATIONS

1. AcOH	Acetic acid
2. Ar	Aryl
3. b	Broad (NMR)
4. Boc	<i>t</i> -Butyloxycarbonyl
5. BSA	<i>bis</i> -(trimethylsilyl)acetamide
6. CM	Cross metathesis
7. Cy	Cyclohexyl
8. d	Day
9. d	Doublet (NMR)
10. dd	Doublet of doublets (NMR)
11. DEHP	<i>bis</i> -(2-ethylhexyl)phthalate
12. DIPEA	N,N-Diisopropyl ethyl amine
13. DMAP	4-Dimethylaminopridine
14. DME	1,2-dimethoxyethane
15. DMSO	Dimethylsulfoxide
16. DUIS	Dual ionization source (MS)
17. EDTA	Ethylenediaminetetraacetic acid
18. EI	Electron impact (MS)
19. eq.	Equivalents
20. ESI	Electron Spray Ionization
21. EtOAc	Ethyl acetate

22. EtOH	Ethyl alcohol
23. eV	Electron volt (MS)
24. Fmoc	9-Fluorenylmethoxycarbonyl
25. H.G. II	Hoveyda-Grubbs 2 nd generation metathesis catalyst
26. HMDS	Hexamethyldisiloxane
27. h	Hour
28. Hz	Hertz (NMR)
29. IpOH	Isopropyl alcohol
30. IR	Infra-red
31. J	Coupling constant (NMR)
32. m	Multiplet (NMR)
33. MeOH	Methyl alcohol
34. Mes	Mesityl
35. min	Minute
36. mp	Melting point
37. MS	Mass spectrometry
38. "n-methylnicotinamide"	1-Methylnicotinamide chloride
39. Nap	Naphthyl
40. NMR	Nuclear magnetic resonance
41. NOESY	Nuclear Overhauser effect spectroscopy
42. NP Water	Nanopure (18MΩ water)
43. OM	Olefin metathesis

44. Pd-C	Palladium on carbon
45. Ph	Phenyl
46. PhMe	Toluene
47. ppm	Parts per million (NMR)
48. q	Quartet (NMR)
49. R _f	Retention factor
50. RT	room temperature
51. s	Second
52. s	Singlet (NMR)
53. t	time
54. t	Triplet (NMR)
55. TFA	Trifluoroacetic acid
56. THF	Tetrahydrofuran
57. TLC	Thin layer chromatography
58. TMSBr	Bromotrimethylsilane
59. TMSCl	Chlorotrimethylsilane
60. TOF	Time of flight
61. UV	Ultra-violet
62. Vgy	Vinylglycine

ACKNOWLEDGEMENTS

I would like to thank first and foremost the University of Wisconsin-Milwaukee for providing an institution with faculty and facilities that provided me the opportunity to develop my intellect and skills. I will forever be grateful for its existence and the service it provides to members of the local community like myself for the ability to pursue an education so that we may better ourselves and others. I would like to acknowledge the guidance and patience of my advisor, Dr. Alan W. Schwabacher, in providing me the tutelage and in my training as a scientist that challenged my intellect and allowed my knowledge in chemistry to flourish. Thanks to Dr. Nicholas Silvaggi for providing another source of opportunity in collaboration to hone my skills by being able to interact frequently another groups of researchers. I would like to acknowledge Samuel Melton as my closest research collaborator. The dedication, skills, and feedback he has provided in the evaluation of dimerization and binding of the molecular receptors as well as the synthesis of L-vinylglycine were invaluable and will forever be in his debt. I wish him the best of luck in his future education. I would also like to thank John Lukesh III, Chris Meyer, and Curtis Jones who were undergraduate collaborators with me when they attended this university. Having gone onto their own scientific careers I am grateful for the sense of accomplishment they give me in the ability to develop their skills at the earliest stages of their training. To my friends Nina Yuan, Lisa Mueller, Karl Koebeke, it feels unfortunate that I was not able to know you all earlier but will be forever grateful that I did. You all have provided me with the fellowship and support I needed. To John Kestell, Sarah Oehm, Tyler Fenske, Paul Henning, and all of the other fine people in the Chemistry and Biochemistry department I have learned from and met over the years, interacting with all of you has been a pleasure and will never forget the

ways in which you have helped me large and small. I would like to thank my brothers, Christopher and Phillip Hoppe, as they have made things possible for me that were not. Lastly, I would like to thank my mother Sue Hoppe and father Ken Hoppe for their continued support and dedication to me as their son in my pursuit of this goal. Without them, this along with everything else could not have been possible. I will always be thankful for the sacrifices you have made for me. I only hope to one day to be able to give you the support you have given me.

PART ONE: DESIGN, SYNTHESIS, AND CHARACTERIZATION OF RIGID MOLECULAR RECEPTORS

I. INTRODUCTION

A. Molecular Recognition

Molecular recognition can be defined as a selective and reversible binding between two or more molecules through non-covalent interactions. Multiple weakly attractive intermolecular forces work in concert to achieve selectivity and thus makes it substantially more difficult to predict than the formation of covalent chemical bonds. Intercalation of a smaller molecule into the cavity of a larger molecule often describes the mode of action in which two molecules bind together. While net forces like van der Waals attractions or the hydrophobic effect¹, which is a property of the solvent, are primer movers in this phenomenon other electrostatic interactions like dipole-dipole, aromatic stacking², the cation- π effect³, ion pairing⁴, and hydrogen bonding⁵ in arrays⁶, and ditopic coordination⁷ provide the means for exceptionally strong affinities and substrate discrimination in binding.

Molecular recognition also known as Host-Guest chemistry⁸ is critical to the physiological processes of catalysis, transport, antigen recognition, and storage. In studying what can lead to selective and strong binding these powerful capabilities demonstrated by nature could be replicated. For these reasons the concepts of molecular recognition have been applied to molecular actuators⁹, drug discovery¹⁰, and the self assembly of molecular capsules.¹¹

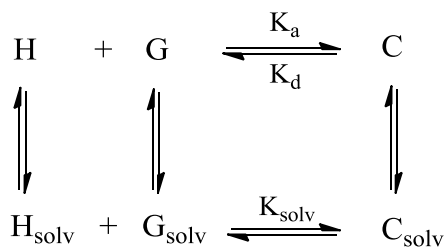


Figure 1: Equilibrium for association between a molecular receptor (host, H) and an associating molecule (guest, G) in solution to form a complex (C)

The strength of the binding interactions is described in terms of an equilibrium constants as either the forward direction of the association of components in complex formation (K_a in units L/mol) or the backwards direction of the dissociation of the complex to the individual compounds (K_d in units mol/L). However as these associations occur in a solvent there exists another equilibrium for the solvation of the host and guest molecules individually to come together to form a solvated complex. The strength of the association to form this solvated complex depends upon solvation energies, temperature, and ionic strength among many other factors lending to a small change in the energies between the two states. For these reasons, predicting what molecules will bind together strongly and selectively is difficult and thus requires the use of experimentation to elucidate fundamental principles to understand this interaction.

B. Precedented Natural and Synthetic Molecular Hosts

1. Cyclic Molecular Receptors

Cyclodextrin, a macrocyclic polysaccharide comprised of glucose units, was the first molecule reported to bind another molecule by way of inclusion of elemental iodine into its

cavity.¹² In the decades following many prominent researchers took up investigating this bucket shaped structure and its propensity to intercalate small molecules

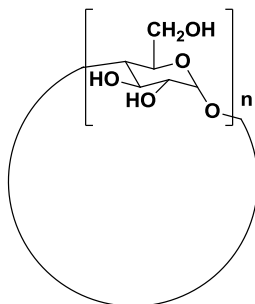


Figure 2: Example of a cyclodextrin: n=6 α -cyclodextrin, n=7 β -cyclodextrin, n=8 γ -cyclodextrin

Cramer and Hettler¹³ were among the first to profile complex formation with cyclodextrins while researchers like Saenger¹⁴ and Breslow¹⁵ studied the inclusion complexes of derivatized cyclodextrins. Cyclodextrins have also been exploited for pharmaceutical purposes to deliver drugs¹⁶ or release over time to create a continuous dosage.

While naturally occurring substances like cyclodextrins and enzymes hold enormous potential for understand what entails the formation of a complex the creation of synthetic molecular receptors could hold even greater potential. Synthetic receptors would allow for the modification of the binding cavity identify of the specific non-covalent interactions responsible for binding. The first artificial host molecule were macrocyclic polyethers synthesized by Pedersen in 1967.¹⁷ This class of compounds dubbed crown ethers were called so for their ability to “crown” metal cations and thioureas¹⁸ by inclusion into their cavity by ion-dipole interactions.

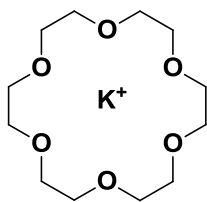


Figure 3: Cyclic polyether, 18-crown-6, drawn with a potassium ion bound into its cavity

These crown ethers, especially 18-crown-6¹⁹, bind cationic substrates with high affinities as all of the oxygens are orientated towards the interior of the macrocycle whereas the alkyl linkers are positioned on the exterior. This demonstrates the concept of “preorganization”. Preorganization⁸ is the concept that the host and guest molecules bind with the strongest affinities if the functional groups responsible for complexation are orientated in a cooperative fashion prior to the components coming into proximity. An example of this would be in the theoretical comparison of 18-crown-6 to its acyclic analogue with the assumption that the acyclic version has the capability to bind potassium ion.

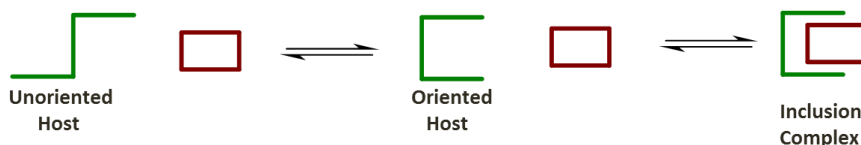


Figure 4: Depiction of an unoriented host adopting a binding conformation before guest inclusion

The acyclic version would not bind the alkali ion as strongly as 18-crown-6 as it contains many more rotational degrees of freedom and thus contains many conformations unsuitable for complex formation. This would result in a lower ΔG term in the Gibbs Free Energy equation compared to the crown ether as the acyclic version ΔS term would be more positive upon complex formation. This loss of entropy results from the acyclic version having to orient

itself to allow for all six oxygen atoms to coordinate to the cation like the crown ether and overall weaker affinity.

From these concepts, Koga reported the first unambiguous example of a water soluble, macrocyclic synthetic molecular receptor.²⁰ Comprised of two diamino diphenylmethanes with two n-butyl alkyl chains linking connecting the amino groups the macrocycle was found to dissolve in aqueous media below pH2.

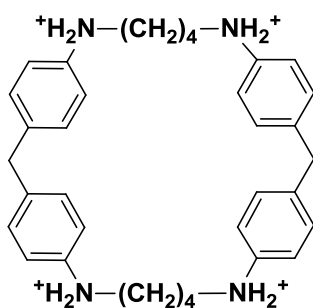


Figure 5: Koga's macrocycle

This host molecule was able to fully include hydrocarbons like durene, naphthalene, and *p*-xylene. A dissociation constant for 8-anilino-1-naphthalene sulfonic acid ($K_d = 1.6 \times 10^{-4}$ M) was determined by fluorescent emission and the orientation of 2,7-dihydroxynaphthalene bound into the cavity was determined using 1H NMR. In using these spectroscopic techniques, Koga was able to demonstrate the utility of these techniques and were widely adopted afterwards. This work went on to inspire others in the study of small molecule binding with significant contributions made by Diedertich and Dougherty. Diederich focused on making macrocyclic receptors that were soluble in water at pH7²¹ that were capable of binding hydrophobic moieties like pyrene and facilitating their transport through aqueous media.²² He was also able to correlate the binding affinities in electron donor-acceptor interactions with electron poor naphthalene derivatives binding stronger to the electron rich macrocycle.²³ Dougherty too

focused on synthetic macrocycles soluble in neutral water. He reported²⁴ that his receptor was able to form inclusion complexes with quaternary ammonium ions. He later went on to show that binding can not only be driven by the hydrophobic effect but by the attraction of the cation to the π electrons in the aromatic walls of the macrocycle.²⁵ This interaction, coined the cation- π effect, was found to be so favorable that it orientated the quaternary ammonium to the interior of the cavity while the hydrophobic part of the ammonium salt was left exposed to the aqueous environment.²⁶

2. Acyclic (non-macrocyclic) Molecular Receptors

Acyclic, synthetic molecular receptors were dubbed “molecular tweezers” by Whitlock in the first known publication of this architecture in 1978.²⁷ Molecular tweezers are usually characterized by two aromatic walls that are approximately parallel to one another in a syn-cofacial configuration and held apart by a rigid linker. This initial design was intended to act as a *bis*-intercalator for DNA that was restricted to a single strand of DNA. Whitlock constructed his tweezers by alkylating caffeine molecules with a rigid diyne linker and prove that it was able to associate to 2,6-dihydroxybenzoate by binding between the aromatic walls to form a sandwich complex by π - π stacking. From this elegant design the next iteration of molecular recognition studies was birthed. Early designs utilized diphenyl glycourils²⁸ or a derivatized Kemp’s triacid²⁹ the work provided by Zimmerman provided foundational examples in constructing molecular tweezers. His motif displays a high degree of preorganization with an aromatic linker and a syn-cofacial arrangement of acridine walls connected in the 9- position.³⁰

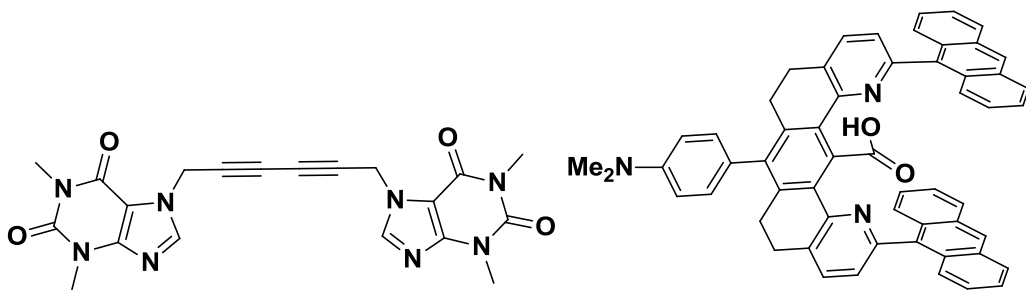


Figure 6: Whittock's caffeine based molecular tweezers and a molecular tweezers constructed by Zimmerman

With the anthracenes twisted out of conjugation due to steric hinderance they can rotate until to walls achieve a conformation until the walls are parallel and approximately 7Å apart so that they can bind a flat, aromatic guest. The import of the rigid spacer was demonstrated in a later publication where Zimmer substituted the rigid linker for a butyl linker to connect the anathcene sized walls and found that the binding affinity towards 2,4,7-trinitrofluorene decreased by a factor at least 40. He also demonstrated that binding affinities can be greatly enhanced through the use of cooperative non-covalent interactions.³¹ When a carboxylic acid group was incorporated into the spacer the combination of π - π interactions and hydrogen bonding the tweezer was able to bind 9-propyladenine with high affinity ($K_d = 4.0 \times 10^{-5}$ M) in $CDCl_3$. When the carboxylic acid was converted to a methyl ester the binding affinity diminished precipitously with no detectable binding was observed by 1H NMR when 9-propyladenine was added to the tweezers in up top four fold stoichiometric excess.

The next contribution in the development of molecular tweezers come from Harmata. His methodology progressed from the synthesis of asymmetric Kagan's ethers³² to symmetrical *bis*-Kagan's ethers.³³ Kagan's ether³⁴ is a diaryl, [6.6.1] bicyclic ether with the oxygen atom bridging the two rings while a *bis*-Kagan's ether is two of these structures connected by a common benzene ring. This structure is more preorganized than Zimmerman's tweezers as the

aromatic walls are enforced into being parallel and are precluded from rotating by being incorporated into the cyclic ether.

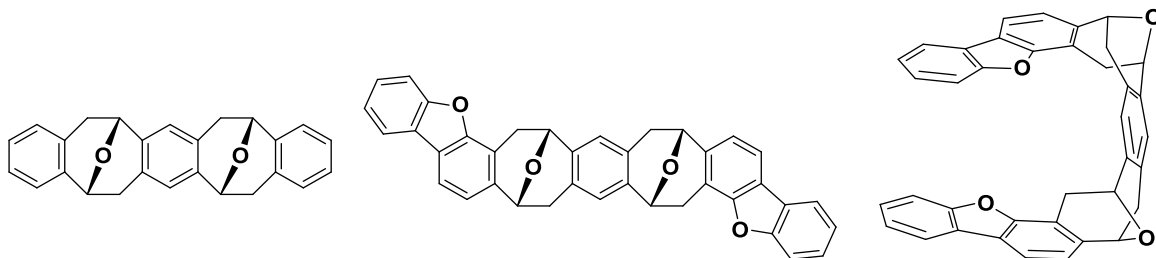


Figure 7: *bis*-Kagan's ether (left) and Harmata's molecular tweezers based on a *bis*-Kagan's ether architecture

However, this structure was not able to bind electron poor, aromatic molecules due to the small aromatic surface area in the cavity. When the benzene walls were replaced with dibenzofurans an X-ray crystal structure was obtained with 1,3,5-trinitrobenzene bound into the 7 Å cavity forming the classic sandwich complex to corroborating the function of the desired shape.³⁵ The use of bicyclic polyethers³⁶ and dibenzofuran sized derivatives as walls³⁷ have seen continued use since Harmata's publication to bind quaternary ammonium ions and aromatic guests respectively.

The molecular tweezers developed by Klärner³⁸ utilized a scheme which employed Diels-Alder reactions to attach a dimethylhydroquinone norbornene derivative to an aromatic norbornadiene. If one Diels-Alder reaction occurs then a U-shaped molecular tweezers is afforded, if done twice then a C-shaped molecular clip is produced. In each of these cases it was found that these structures were able to intercalate electron poor, aromatic small molecules into their cavities.³⁹

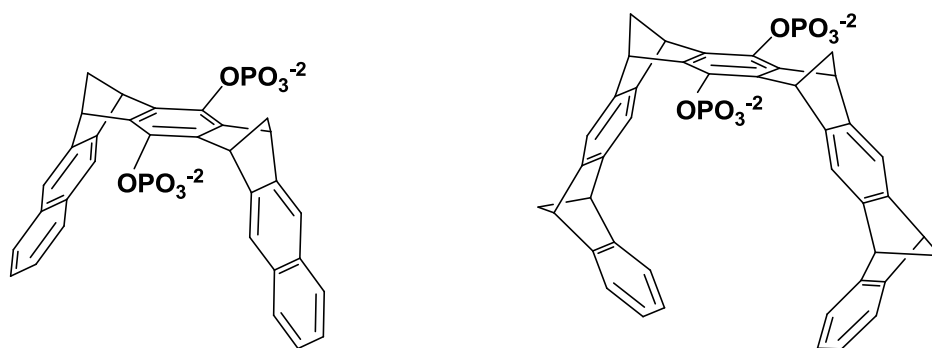


Figure 8: Examples of a molecular tweezers (left) and a molecular clip (right) generated by Klärner

While initially confined to organic solvents, these structures were given water solubility by converting the dimethylhydroquinone ethers to *bis*-phosphates and *bis*-methyl phosphonates which allowed for the binding of thiazolium salts in aqueous media.⁴⁰ These receptors were studied further and found to inhibit enzyme activity in a novel fashion: alcohol dehydrogenase by binding its cofactor NAD^+ ⁴¹ and G6PD by binding to NADP^+ .⁴² In binding to flavium salts⁴³ Klärner observed a spectroscopic response in the UV-Vis region which demonstrates the potential for molecular tweezes to be useful as molecular sensors. To date, this class of water soluble molecular tweezers has shown the most robust utility in small molecule complex formation.⁴⁴

C. Tröger's Base and *bis*-Tröger's Base

While the previously detailed works into molecular tweezers were being published, a parallel strategy was being developed using an easier to synthesize moiety that also generated a well defined cleft for molecular binding. Tröger's Base, composed of two aromatic amines and three formaldehyde equivalents, was chosen by Wilcox to suit these criteria. First synthesized by Julius Tröger in 1887⁴⁵ Tröger's Base is a chiral compound formed from *p*-toluidine and formalin in the presence of concentrated hydrochloric acid. The chirality in this

structure comes not from chiral carbons but from the stereogenic nitrogens in the bicyclic ring system which cannot undergo inversion. If inversion were to occur the bridging methylene unit would have to pass through to the other face of the ring system, ring would place the atoms in the same plane in the process, but the energetic barrier provided by steric hindrance and bond angle strain prevent this.

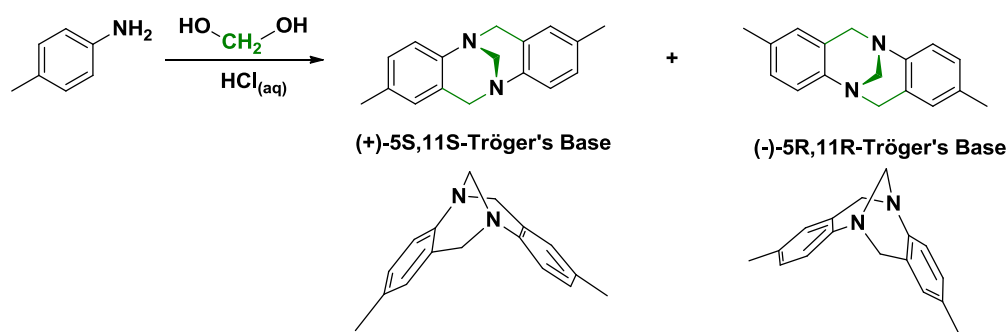


Figure 9: Formation of the two Tröger's Base isomers from *p*-toluidine and formaldehyde

Since its discovery, Tröger's Base was subject of intensive investigation into its structure, mechanism of formation, and origin of its chiral nature. Wganer probed the mechanism of formation by generating Tröger's Base from intermediates isolated along the synthetic pathway⁴⁶ whereas, Spielman was able to confirm the structure of Tröger's Base through its degradation products.⁴⁷ Prelog and Wieland were the first to report the separation of the isomers⁴⁸ the assignment of the absolute configuration of these chiral partners was not conducted until 1967 where circular dichroism was used to analyze the (+)- and (-)- isomers.⁴⁹ From these experiments it was concluded that the (+)- isomer was of the 1R, 3R configuration while the (-)- isomer was 1S, 3S. Later studies however contradicted these assignments with the acquisition of an X-ray crystal structure⁵⁰ and isomeric resolution utilizing a chiral Brønsted acid.⁵¹ It wasn't until 2000 that the initial assignment were unambiguously refuted and the true

configuration of the chiral Tröger's Base isomers were determined as the (+)- being 1S, 3S and the (-)- isomer being 1R, 3R.⁵²

Among the first to take advantage of the shape of Tröger's Base to generate molecular tweezers was Wilcox.⁵³ In taking advantage of the fact the the aromatic faces in Tröger's Base are in the range of 92 to 104° apart, 9,10-dihydro-9,10-ethenoanthracen-2-amine was condensed with formaldehyde to generate a molecular receptor which was found to have two ethanol molecules in its cavity via X-Ray crystallographic analysis.⁵⁴

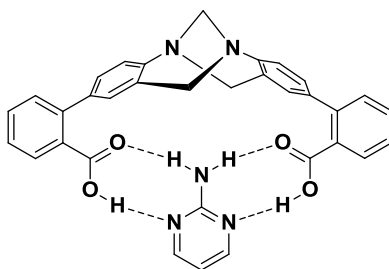


Figure 10: A Wilcox molecular tweezers based on Tröger's Base that binds pyrimidin-2-amine

He later developed a molecular tweezers utilizing a *bis*-carboxylic acid motif to bind to 2-aminopyrimidine through hydrogen bonding⁵⁵ which later elucidated the influence of water included in the active site on binding affinities.⁵⁶ His work demonstrated that the rigid, well defined structure of Tröger's Base was of utility in constructing rigid molecular frameworks that could be incorporated in architectures ranging from metallo-macrocycles⁵⁷ to colorimetric sensors for anion recognition.⁵⁸

Analogous to Harmata's *bis*-Kagan's ether tweezers and the recognition of the perpendicular nature of the aromatic elements in Tröger's Base, 2001 saw the introduction of a *bis*-Tröger's Base into the catalogue of molecular tweezers.⁵⁹ Starting with a Tröger's Base

derived from *p*-toluidine and 4-nitroaniline Pardo *et. al.* was able to synthesize a diastereomeric mixture of *bis*-Tröger's Bases via Friedel-Crafts alkylation. This process was only able to proceed under the fairly harsh conditions of anhydrous ethanol and concentrated hydrochloric acid at 90°C for 24h and resulted in regio-selective cyclization with a 29% overall yield affording the 1,2; 4,5 isomer in a 4:1 ratio of the *syn*-cofacial isomer to the *anti*- isomer.

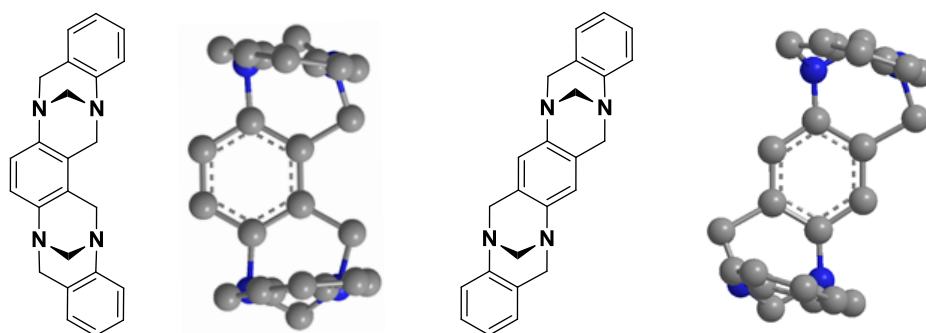


Figure 11: Undesired 1,2:3,4-*bis*-Tröger's Base isomer and desired 1,2:4,5- *bis*-Tröger's Base

This nomenclature is derived from the substitution pattern around the central benzene spacer. The 1 and 4 numbers denote the position of the amino groups in the benzene while the 2 and 3 number describe the positions in that benzene ring where Friedel-Crafts alkylation occurred. The observed ratios invites intriguing questions. What was the reason for the favorability of the *syn*- isomer, the one with the aromatic walls on the same side of the spacer unit, over the *anti*- isomer, the one with the walls on the opposite sides of the linker? What was the origin of the regio-selectivity in cyclization to form the *bis*-Tröger's Base? To address the first question, the Pardo group subjected the *anti*- isomer to the previously described cyclization conditions and recovered the same 4:1 ratio of *syn*- : *anti*- isomers. They attributed this ratio to the *syn*- isomer being more thermodynamically favorable due to the π -stacking interactions of the parallel aromatic walls. While this may be true, I propose it to be a

more complicated mechanism. Under the acidic conditions and isomerization concentrations, this *bis*-Tröger's Base is able to isomerize freely between the two isomers with the *syn*-isomer able to associate with itself, albeit weakly, to form a dimer by π - π stacking interactions. This would remove the self associating *syn*- isomer from the equilibrium and by the Le Châtelier's Principle would drive its continued formation.

With regards to the regioselectivity of Friedel-Crafts alkylation, the Pardo group expected a statistical formation of the 1,2:4,5 isomer alongside the 1,2:4,3 isomer but as stated before observed the latter exclusively. They postulated that even though the 1,2:4,3 isomer is more sterically hindered it was formed preferentially due to the π -stacking of the aromatic walls. This however seems unlikely as the cavity, like the *bis*-Kagan's ether, is approximately 7 Å apart in either configuration.

In a later synthesis of *bis*-Tröger's Base starting from *p*-phenylenediamine, the 1,2:4,3 isomer was also afforded exclusively.⁶⁰ To overcome this regioselectivity, the cyclization to the 1,2:4,5 isomer was enforced by using 1,4-diamino-2,5-dimethylbenzene as the spacer unit.⁶¹ The isolated yield of the cavity shaped *syn*- isomer was 7% en route to generating linear oligo-Tröger's Bases. Dolensky would later go on to incorporate naphthalene sized walls into a *bis*-Tröger's Base tweezers synthesis of the 1,2:4,3 isomer⁶² in order to provide enough aromatic surface area to potentially bind small molecules. The synthetic procedure was improved to utilize a one-pot procedure but only afforded *bis*-Tröger's Bases in low yield (8-13%). To date, there are no known examples of a 1,2:4,5 *bis*-Tröger's Base tweezers without substitution on the core benzene linker to compel the Friedel-Crafts alkylation into this pattern.

D. Rationale and Design of Target *bis*-Tröger's Base Molecular Receptor

Inspired by the design of Harmata's tweezers, the desired 1,2:4,5 *bis*-Tröger's base molecular receptor has the same connectivity to afford parallel naphthalene sized walls held approximately 7 Å apart by a rigid spacer. In reviewing the previous syntheses of *bis*-Tröger's Bases a common feature held in common was the occurrence of the Friedel-Crafts on the central benzene spacer generating the 1,2:4,3- isomer preferentially. The designed spacer unit for desired *bis*-Tröger, the tweezers core, depicted below will circumvent. By already possessing the bonding required for the 1,2:4,5 isomer on the spacer units Trögerization should occur unambiguously to said isomer. This tweezers core not only allows for modular synthesis by condensation with a wide range of aromatic amines but could also facilitate others in their studies of *bis*-Tröger's Base molecular receptors as convenient starting compounds are not readily available.⁶³

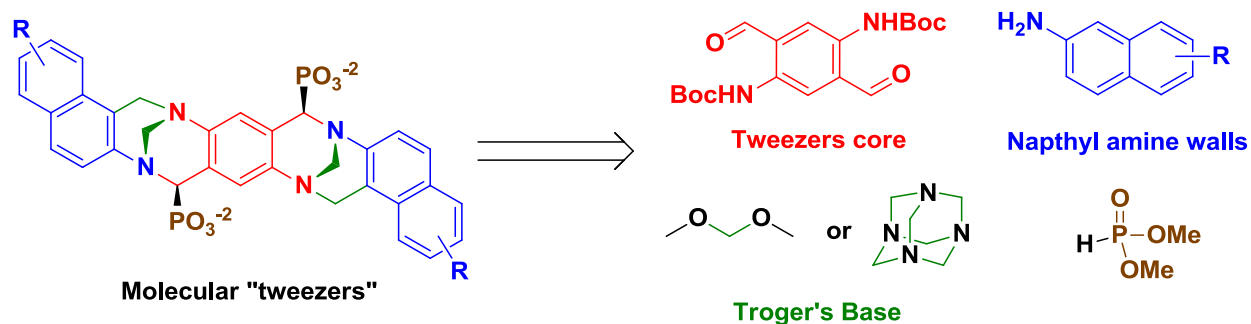


Figure 12: Retro-synthetic scheme for modular construction of the desired water soluble *bis*-Tröger's Base molecular tweezers

Water solubility is installed into the molecular tweezers by the transformation of the imine into an α -amino phosphonate which will then be dealkylated subsequently. Although this functionality provides significant water solubilization it also introduces a not insignificant amount of steric bulk. The consequence of this is that upon cyclization to form the *bis*-Tröger's

Base, the stereochemistry of the bridging methylene is determined by the stereochemistry of the α -aminophosphate to generate the *syn*- cofacial or *anti*- isomers in an expected 1:1 ratio. These orientations cannot be interconverted under acidic conditions as seen in previous *bis*-Tröger's bases as its formation is sensitive to steric interactions.⁶⁴ The alternative to generating a statistical mixture of *syn*-cofacial and *anti*- isomers and isolate more of the desired binding *syn*- isomer would be to either build in water solubilizing functional groups into the walls of the molecule or employ a stereoselective method of forming the α -amino phosphonate.

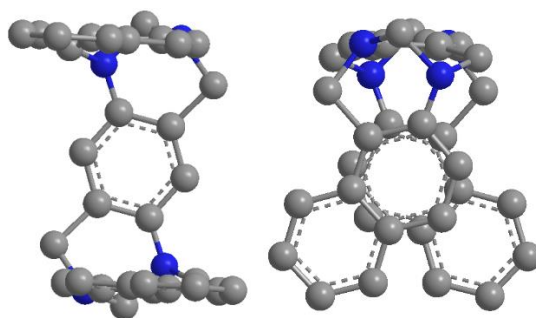


Figure 13: 1,2;4,5-*bis*-Tröger's Base molecular tweezer with naphthalene walls illustrating their offset nature

In contrast to the 1,2;4,3- isomer, inclusion of naphthalene sized hydrocarbons for the walls in the 1,2;4,5- leads to them existing in an offset orientation mimicking the pattern observed in the crystal structure of benzene.⁶⁵ This feature should facilitate easier inclusion of aromatic guest molecules in the cavity compared to the 1,2;4,3- isomer which has its walls directly over one another.

II. RESULTS AND DISCUSSION

A. Formation of the key intermediate N,N'-di-*t*-Boc-2,5-diaminoterephthalaldehyde

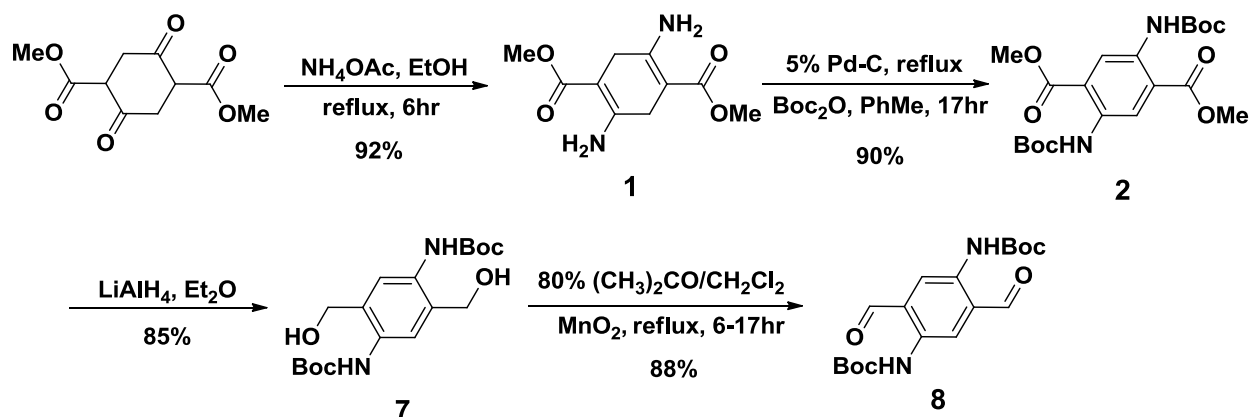


Figure 14: Overall synthetic sequence to produce key intermediate dialdehyde **8**

1. Synthesis of Dimethyl 2,5-diaminocyclohexa-1,4-diene-1,4-dicarboxylate

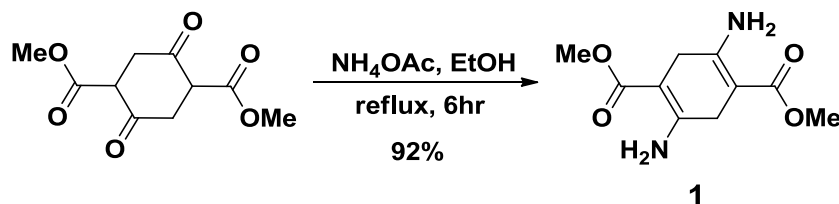


Figure 15: Synthesis of *bisenamine* **1** from dimethyl succinyl succinate

Succinyl succinate diester derivatives have been condensed with amines for over 100 years utilizing molten NH_4OAc ⁶⁶ and NH_3 in ethanol⁶⁷. However, neat alkyl amines⁶⁸ and NH_4OAc in solution⁶⁹ provide for more facile methods to the desired *bis*-enamines. In a method initially developed by Kanchan Tiwari⁷⁰, she chose to go the route of NH_4OAc in ethanol as we needed the primary enamine. Baeyer describes uses ten equivalents of NH_4OAc , but she found that reducing it to five equivalents was sufficient with 95% yield on a one gram scale of

dimethyl succinyl succinate (DMSS). Use of ethanol as the solvent allowed **1** to crystallize from the reaction medium eliminating the need for subsequent purification. In scaling the reaction up to 55g scale, the equivalents of NH_4OAc were reduced to three and four equivalents with each producing yields of 87% and 88% respectively and identical melting points of 212-214°C. On this scale addition of DMSS needs to be added in portions to the refluxing ethanol to ensure it dissolves.

2. Synthesis of Dimethyl 2,5-*bis*((tert-butoxycarbonyl)amino)terephthalate

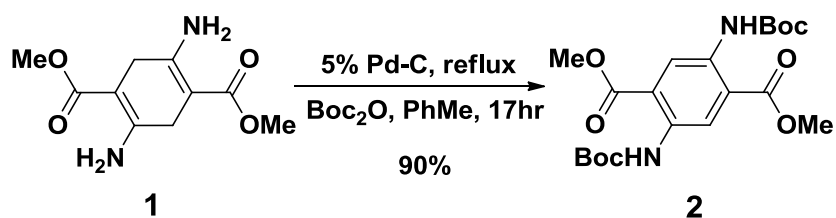


Figure 16: Scheme for aromatization and di-Boc protection of *bis*-enamine **1**

Use of Pd-C has been demonstrated to be able to oxidize heterocycles⁷¹ and cyclic enamines⁷² to the corresponding anilines, but required the use of a sacrificial oxidant to prevent disproportionation of the enamine. Fortunately, refluxing in toluene for 13hr with 30% by weight 10% Pd-C afforded the aromatized **1** in 98% yield with no reduced **1** observed. Boc protection of both amines was accomplished in 66% yield by Kanchan Tiwari in boiling toluene with 5% Pd-C with 4eq Boc_2O followed by 2eq Boc_2O after 4hr. Boc_2O was added in several portions because it is unstable under the reactions conditions and **1** does not acylate until it has been aromatized. This was taken into consideration when increasing the scale of **1** production.

Under my direction, John Lukesh III increased the initial concentration of **1** by a factor of two on a 1g scale. This was considered feasible as **2** is more soluble in boiling toluene than is **1**.

A greater concentrations of Boc_2O (7eq, added in two portions) was utilized with complete conversion to **2** was observed after 22hr. He was able to acquire a 92% yield of the desired product in four crops from recrystallization from CH_2Cl_2 /hexanes. In further testing conditions for scale up, the concentration of **1** was increased further in efforts to decrease the amount of the most expensive reagent, Boc_2O , required for conversion to **2**. Coupled with the aromatization of **1** before the addition of Boc_2O , this alteration to the synthetic methodology was considered to be beneficial. However, this was not the case with side product formation observed. This complication is described subsequently.

a. Diarylamine formation

In the effort to make **8** on a large scale so attempted was **2** but with isolated yields of only ~50%. In the small scale preparations of **2**, Pd-C and Boc_2O were added concurrently to **1** but as Boc_2O thermally decomposes it was thought prudent to aromatize **1** to **3** beforehand. On testing these changes desirable for large scale reaction, it was observed that TLC did not indicate complete reaction over the same time scale. Aromatization initially occurred in distilling toluene to azeotropically remove residual water or ethanol from **1** to prevent it from later reacting with Boc_2O . This resulted in a yellow-green distillate and a pungent smelling vapor being produced that was basic to pH paper. Due to the composition of the mixture and the odor of the gas, it was concluded that ammonia was being produced and was taken as the first evidence that another transformation was occurring.

A potential source of ammonia was residual NH_4OAc in the **1**. This was ruled out by washing with H_2O and EtOH, and use of pure **1** with a melting point of 212-214°C. With

exogenous ammonia ruled out, hydrolysis of the *bis*-enamine was considered the next most likely mechanism. After isolating **2** from the mixture by crystallization, its mother liquor was analyzed by ^1H NMR and observed to be a mixture of DE, Boc_2O , and an unidentified side product that was not mono Boc protected **2**. The excess Boc_2O present suggested that the amine functionality was lost and replaced with something that would not reaction with the Boc_2O , possibly a hydroxyl group. To test the phenol hypothesis, 6g of the concentrated mother liquor was dissolved in CH_2Cl_2 and extracted with sat. Na_2CO_3 . The aqueous phase was removed, acidified to pH6, and extracted with CH_2Cl_2 . After drying the organic phase and concentrating to dryness 1.8mg of material was afforded that identified as not the side product by ^1H NMR. This did not fully rule out the phenol as the side product as the phenoxide may not have been able to be partitioned into water.

To rule out hydrolysis, a portion of **1** was split into two portions for a side by side reaction. The first portion was not azeotropically dried by distillation of toluene and heated at reflux without 5% Pd-C for 3hr with no change in pH paper observed above the condenser. 5% Pd-C was then added and after 12min pH Hydrion paper indicated pH11 vapor above the condenser. After heating at reflux for 18hr, no pH change was observed above the condenser as testing with pH paper. The second portion of **1** was dried azeotropically by distillation of toluene and heated at reflux for 3hr with no observed change in pH paper before the addition of Pd-C. After 5min the pH paper changed to pH9-10. The products from each of the portions were isolated and analyzed by ^1H NMR to afford identical spectra containing **3**.

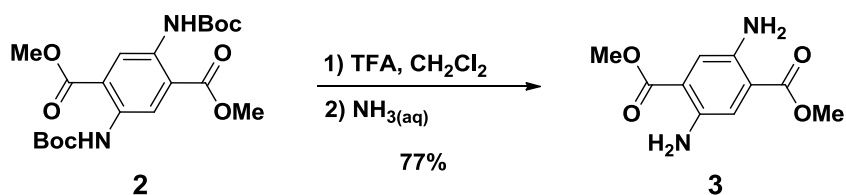


Figure 17: Deprotection of **2** to afford aromatic diamine **3**

To corroborate the signals, a very pure sample of authentic aromatic diamine **3** is was synthesized in 77% overall yield from the TFA deprotection **2** and subsequent deprotonation in 75% conc. $\text{NH}_3(\text{aq})$. No side product was produced with this method. The ^1H NMR spectrum matched that of the aromatic **3** described above. **3** was also exposed to 5% Pd-C in refluxing toluene with no change in composition as observed by TLC. This also ruled out the possibility of **3** reacting with itself to evolve ammonia. It was shown that if the previous protocol of concurrent addition of Pd-C and Boc_2O was used **2** was generated in 88% yield after recrystallization from toluene. **2** was also made from **3** with a 92% yield with no observation of **4** in the isolated product.

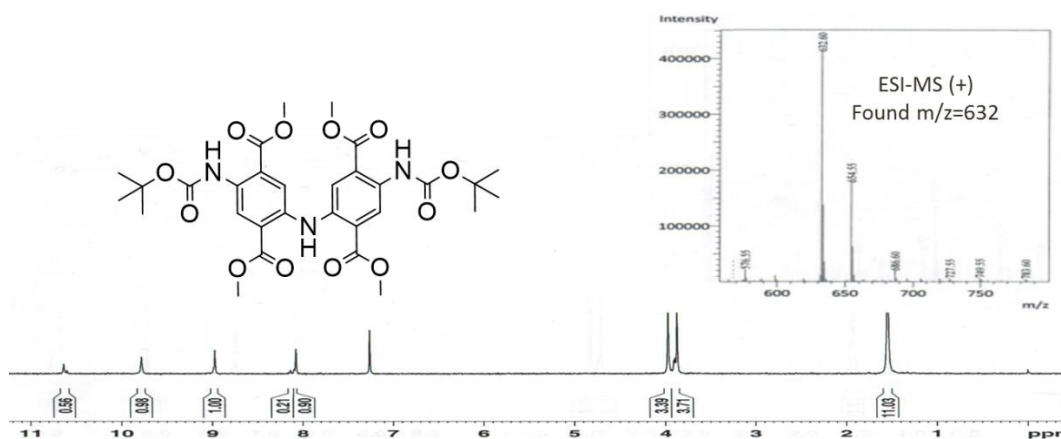


Figure 18: Compound **4**, the diaryl amine side product formed from condensation of **2**

Mass spectrometric analysis of the mother liquor from a synthesis of **2** in which side product formed proved that the side product was not a phenol. The signals produced had a m/z of 442 ($2+Na^+$) and 632 which is consistent with **4**. This data ruled out hydrolysis as a mechanism of side product formation. This mixture was purified by flash chromatography in which diarylamine **4** was isolated and characterized by 1H NMR and ESI-MS confirmed to be the side product generated by Pd-C oxidation. With this diarylamine in hand, it was hypothesized that en route to being aromatized by Pd-C, condenses with itself to form the diaryl amine in the absence of Boc_2O which resulted in the evolution of NH_3 . This surprising results raised the question of when the coupling occurred. The most plausible pathway for condensation would be the transamination of the aromatic amine **3** with the imine form of **2**. As this process is expected to be acid catalyzed it was checked to see if this process could be inhibited by the use of base washed catalyst and glassware. What was determined was that it had no effect in decreasing diarylamine formation.

b. Exploration on mechanism of diaryl amine formation

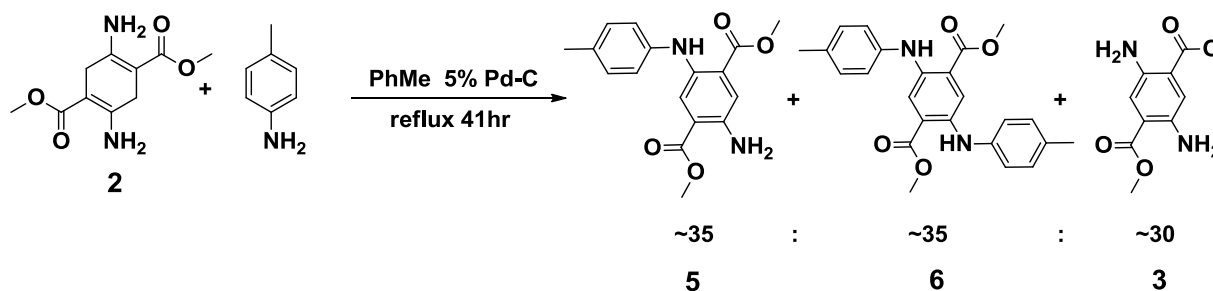


Figure 19: Mono- and bis- diarylamine formation from bis-enamine

To further elucidate this process, **1** and *p*-toluidine were heated in refluxing toluene together without Pd-C. No change was observed by TLC over 17h. Upon addition of 5% Pd-C however, two new spots were observed and after 16-41hr of reflux **5** and **6** were isolated by

flash chromatography in a 1:1 molar ratio with 71% conversion of **1** into the mono- and bis-variants. To ensure exchange of the amine was not due to acid catalysis, the 5% Pd-C was washed with 15% NaOH and rinsed with nanopure water until the filtrate was neutral. Following above procedure, **5** and **6** were observed to be in a 2.3:1 molar ratio respectively with 63% mol conversion of **1** into the desired products. In obtaining compounds **5** and **6**, the hypothesis of having an aniline condense with **1** en route to aromatization was confirmed.

3. Synthesis of Di-tert-butyl (2,5-bis(hydroxymethyl)-1,4-phenylene)dicarbamate

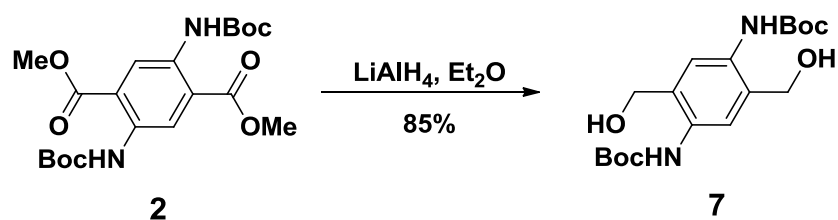


Figure 20: Reduction of aromatic diester **2** to desired diol **7**

LiBH₄ in CH₃OH or IpOH was utilized initially by Kanchan Tiwari reduced diester **2** to afford only trace amounts of diol **3**. When the solvent was switched to THF, a 63% yield by NMR with complete reaction after 4h even though **2** was still only moderately soluble. She observed that if pH7 buffer was not used in the workup of the LiBH₄ the crude product was contaminated with a *bis*-cyclic urethane from the addition of the benzyl alcohol in the the carbonyl of the Boc group. The solubility issues of **2** in the reduction medium were ultimately overcome by a two solvent method employing LiAlH₄.

LiAlH₄ has been used to reduce a vast array of organic compounds⁷³ but we were leery of its use with its ability to reduce the Boc group. This concern did not come to fruition however as deprotonation of the Boc protected NH preserved the protecting group. As LiAlH₄ is soluble in Et₂O but not in CH₂Cl₂ and **2** is readily soluble in CH₂Cl₂ but not in Et₂O a solution was made of

each in the appropriate solvent. **2** in solution was then added to refluxing LiAlH_4 to produce the desired diol in ~2hr over the scale of 0.5g to 27g scale with 71-88% yield. (22g scale, 79% yield, mp 162-166; 27g scale, 82% yield mp 154-157. Most pure product 6g scale, 86% yield, mp 177-180 extracted quenched rxn mix/celite cake with CH_2Cl_2 only)

4. Synthesis of N,N'-di-*t*-Boc-2,5-diaminoterephthalaldehyde

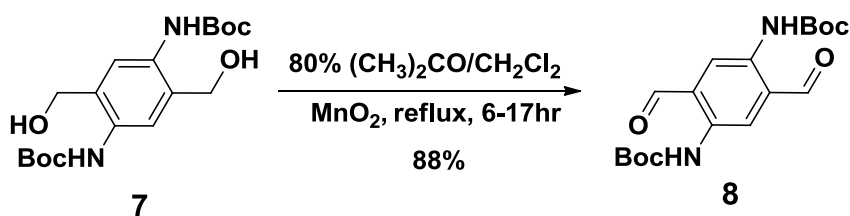


Figure 21: Selective oxidation of diol **7** to desired dialdehyde **8**

MnO_2 has been shown to be a mild oxidant⁷⁴ for selective oxidation of benzylic or vinylic alcohols after systematic testing⁷⁵ and although documented to have difficulty⁷⁶ in oxidizing ortho- amino benzyl alcohols, it was not the case for our particular substrate. Although its chemoselectivity is desired, MnO_2 has many complicating factors in its use. First is that it must be freshly synthesized, usually by the Attenburrow⁷⁷ method, and generates a fine solid that requires a large investment in time to collect by filtration and washed. Its activity also varies based upon its method of production⁷⁸ and to what extent it is dried. If applicable, Goldman⁷⁹ has found that wet MnO_2 can be stored for extended periods of time without precipitous loss in activity which greatly reduces the time in preparing the oxidant. Another issue in MnO_2 oxidation is that it requires a large stoichiometric excess which translates to a large volume of solid and can make efficient stirring tricky although recent work⁸⁰ has found that

substoichiometric “active” MnO_2 from Sigma-Aldrich has been used under an atmosphere of O_2 to circumvent some of these concerns.

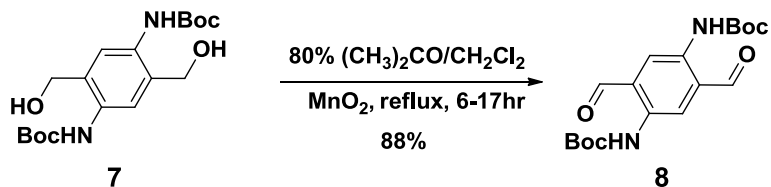


Figure 22: Selective oxidation to dialdehyde with MnO_2

Oxidation of diol **7** to dialdehyde **8** was reliable when carried out using MnO_2 prepared by the Attenburrow procedure and dried in an oven at 110°C with periodic mixing until a free flowing powder resulted. When the oxidation was conducted in refluxing CH_2Cl_2 yields averaged 40%, which was attributed to the inability of the diol and mono-aldehyde to desorb from the MnO_2 surface. Yields improved to 85-95% when the oxidation was carried out in 20% CH_2Cl_2 in acetone. However care needs to be taken in the order of addition of the solvent. If **7** and MnO_2 were mixed together as solid, the addition of a flammable solvent first resulted in ignition of the materials. Combination of the mixed solids with CH_2Cl_2 , followed by acetone avoided combustion.

a. Over oxidation from MnO_2 and alternate Cu(I) catalyzed oxidation

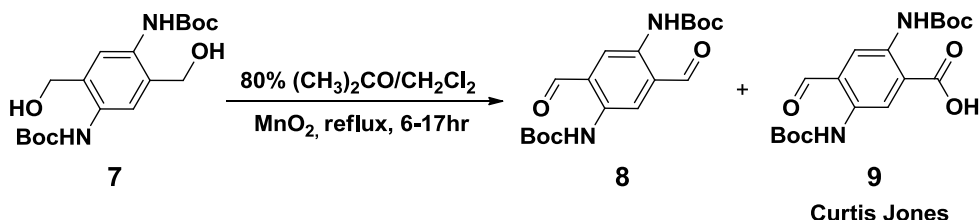


Figure 23: Over oxidation of DA to mono-aldehyde mono-carboxylic acid with MnO_2

Scale up of the oxidation commenced with MnO₂ synthesized via the Attenburrow procedure using newly purchased reagents. Yields of the dialdehyde unexpectedly dipped to a 38% and 53%. Extraction of the MnO₂ from the reaction with 50% CH₃OH/CH₂Cl₂ produced a new solid. Analysis by ¹H NMR in DMSO-d₆ and ESI in negative ion mode confirmed that the reaction with MnO₂ somehow produced the mono carboxylic acid, mono aldehyde **9** by generating m/z= 370 (M-H⁺, 100%) and singlet integrating to 2H at 13ppm. Even though the MnO₂ is described in the literature needing to be alkaline for the reaction to proceed, it was postulated that excess hydroxide or other water soluble contaminants like KMnO₄ were present.

A new batch of MnO₂ was made and washed with water until the filtrate was colorless and neutral to pH Hydrion paper. Reaction with 25eq MnO₂ at 17hr reflux and 35eq MnO₂ at reflux for 24hr produced 58% **8** with 21% mono acid mono aldehyde and 43% **8** with 34% mono acid mono aldehyde **9** respectively. To rule out potential oxidation by Fe⁺³ or other dissolved metal ions from the metal instruments used in the synthesis of MnO₂ ceramic tools with analogous results as described above. Yield improved to 74-87% when the MnO₂ synthesized was washed with hot 0.6M pH7 phosphate buffer. CH₃OH was added to the system to decrease adsorption of **7** to MnO₂ in hopes of limiting the chance of over oxidation. However with a combination of 10% CH₃OH/ 20% CH₂Cl₂/70% acetone the reaction was incomplete over 2d at reflux and 75eq. MnO₂. The carboxylic acid side product began to form after 3d and incomplete transformation of **7** observed.

An alternative method to MnO₂ attracted our attention which would be to make an “active” MnO₂ layer deposited on the surface of activated carbon⁸¹. The solid was easily

filtered. Its washing with water until the filtrate was neutral took a fraction of the time compared to the Attenburrow method. Use of a 12 MnO₂-C : 1 **7** mass ratio was used in 80% THF/CH₂Cl₂ resulted in trace dialdehyde formation after 24h at refluxing temperature. This method was no longer explored proving impractical for our purposes and should not be taken as an indictment of this clever technique. As Carpino noted in his work that the activated carbon employed came from the J.T. Baker company and other sources of activated carbon produced minimally active or non-reactive MnO₂ on C.

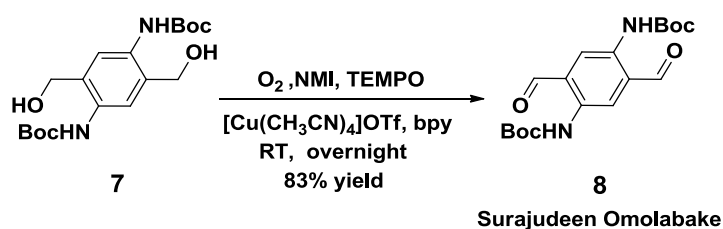


Figure 24: Selective oxidation to DA with Cu(I) catalyst

As the MnO₂ made did not have consistent chemical reactivity over its many preparations coupled with the days required for 100+g scale preparation it was determined to not be worth the effort or the sacrifice of diol. Although the Swern oxidation is known to selectively oxidize an alcohol to an aldehyde and has been optimized⁸², it was not attempted due to concerns of solubility of the diol at the low temperature required. In collaboration with Surajudeen Omolabake we found an aerobic oxidation utilizing Cu(I)⁸³ the ideal for **7**. Complete conversion occurred overnight when exposed to the atmosphere at room temperature with rapid stirring. It was accidentally discovered that the oxidation was able to occur in the absence of 2,2'-bipyridyl with 50% mol ratio NMI as opposed to the 20% prescribed by the literature. Yields in the 80% range were average with crystallization of the product from the reaction medium occurring if CH₃CN was used as the solvent.

B. Synthesis of acyclic *bis*-Tröger's Base Molecular Receptor

1. Preparation of *bis*-imines

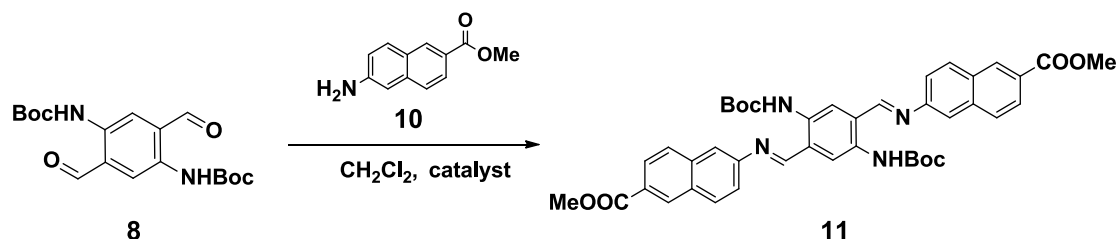


Figure 25: General scheme for *bis*-imine formation from dialdehyde **8**

With the key intermediate dialdehyde in hand, construction of the molecular tweezers began by condensation of a naphthyl amine with it to form a *bis*-imine was first conducted in collaboration with Nzagi Nyakirangani⁸⁴. The naphthyl amine initially chosen was methyl 6-amino-2-naphthoate which was prepared in 94% yield (mp 154-157°C) by refluxing 6-amino-2-naphthoic acid in dry CH_3OH for 2h using 18M H_2SO_4 as the acid catalyst. The dialdehyde was combined with excess **10** in boiling toluene using a Dean-Stark trap to drive the reaction to completion by azeotropic removal of water. Over the course of 17h the dialdehyde was no longer detectable by TLC and an orange solid formed. This orange solid was also observed by Nzagi Nyakirangani who had also had difficulties in identifying this material. This solid was insoluble in ethanol, DMSO, and sparingly soluble in CDCl_3 in which a ^1H NMR spectrum was acquired. From the spectrum the material was speculated to be composed of **10**, the mono imine, and the *bis*-imine but was sufficiently complicated to prohibit confident assignment. The synthesis was conducted again with an acid catalyst, the hydrochloride salt of **10** as well as a chemical dehydrating agent, *bis*-(trimethylsilyl)acetamide (BSA), were employed in an effort to completely form the desired *bis*-imine. After mixing at room temperature overnight a greater

amount of the orange solid was produced, which was sufficiently insoluble to prevent NMR analysis. In order to rule out the possibility that the orange solid was some kind of polymer derived from **8**, a similar reaction was carried out in the absence of naphthylamine **10**. No orange solid was formed, as no new spots were observed by TLC.

The insoluble orange solid was treated in glacial acetic acid with trimethyl phosphite for if the orange solid was indeed the desired *bis*-imine these reagents would be able to convert it into the corresponding *bis*- α -aminophosphonates. After 10d of vigorous stirring at room temperature, the desired aminophosphonates were formed, confirming that the orange solid was indeed the *bis*-imine. The crystallinity of the *bis*-imine was exploited subsequently to drive its formation and eliminate the need for removal of water. Use of CH_2Cl_2 as a solvent and glacial acetic used the acid catalyst gave **11** in 88% yield.

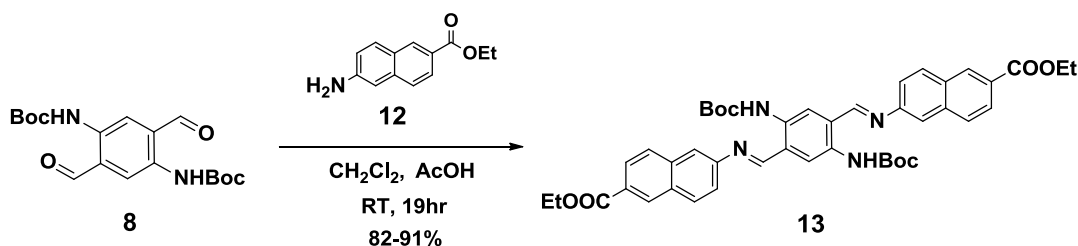


Figure 26: Optimized condition for synthesis of *bis*-imine **13**

Ethyl 6-amino-2-naphthoate **12** was made by Fischer esterification in anhydrous ethanol using concentrated sulfuric acid as the catalyst. After complete esterification and partitioning between CH_2Cl_2 and saturated aqueous NaHCO_3 , yields ranged from 62-97. The purity of the material typically afforded after isolation is usually good enough to carry on without purification. **13** was first made by the condensation of **8** with a slight excess of the two equivalents of **12** needed in CH_2Cl_2 in the presence of $\text{Yb}(\text{OTf})_3$. The lanthanide catalyst was

used to develop conditions later used in a one pot synthesis of the *bis*-aminophosphonates. After 4hr at room temperature **8** was no longer seen by TLC, and a large amount of orange solid was seen in the reaction volume. After collecting by vacuum using ethyl acetate or methanol to transfer, **13** was afforded in 63% and 82% yield respectively. Synthesis was optimized using CH₂Cl₂ and glacial acetic acid on a 1.6g scale of the **8** to give the *bis*-imine in 91% yield in two crops with a melting point of 282-286°C of the first crop when allowed to stir at room temperature overnight and washed with EtOAc. After many preparations it was correlated that a purer crude product was produced after prolonged time stirring at room temperature. Due to its highly crystalline nature and the small amount of the *bis*-imine that can go into solution it is able to selectively complex with itself and enriching the solid in the desired material. *Bis*-imine **13**, with ethyl esters instead of methyl esters, was soluble enough in CDCl₃ to be characterized by ¹H, a ¹³C NMR and MS. In the ¹H NMR spectrum, a singlet is observed at δ11.8 ppm which was attributed to the N-H of the Boc protected amine which is intramolecularly hydrogen bonded to the imine nitrogen. The consequence of this would be to lock all atoms participating in this six membered ring into a planar conformation that enhances crystallinity.

Solvents screened to determine not only a good solvent for recrystallization but a good solvent to put **13** into solution for reaction. The best solvents for dissolving **13** were as follows: THF ≈ CH₂Cl₂ >> EtOAc, toluene, Et₂O >> CH₃CN, DMSO, hexane.

2. Synthesis *bis*- α -aminophosphonates

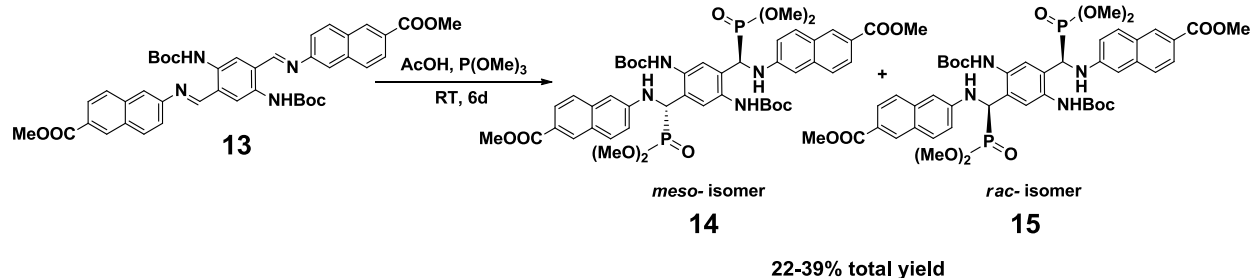


Figure 27: Formation *bis*- α -aminophosphonates **14** and **15** from *bis*-imine **13**

The first attempt to improve *bis*- α -aminophosphonate, elevated temperature to shorten reaction times and to increase the solubility of *bis*-imine **13** were investigated. However, at temperatures above 80°C, the Boc protecting groups were removed. With degradation at higher temperatures and room temperature consigning reaction times to prohibitively long periods, investigation into altering the phosphite and catalyst species was conducted. It has been demonstrated in the literature that metal catalysts based on indium⁸⁵, scandium⁸⁶, and ytterbium⁸⁷ facilitate α -aminophosphonate formation from imines with dialkylphosphites. Of these, ytterbium was chosen by Nzagi Nyakirangani and used by myself due to its ability to catalyze condensation of amines and ketones or aldehydes in β -enamino synthesis⁸⁸, its use in one pot preparations as it poorly catalyzes the dialkyl phosphite addition to the aldehyde⁸⁹, and its future potential for asymmetric aminophosphonation using chiral ligands^{90,91,92}. To confirm that a dialkyl phosphite would not add to **8** in the presence of an ytterbium catalyst a mixture of **8**, Yb(OTf)₃, and dimethyl phosphite in CDCl₃. This was monitored by NMR spectroscopy over the course of a day with no changes observed in the ¹H or ³¹P resonances for the components.

Introduction of P(OMe)_3 however readily added to aldehyde at room temperature, so should only be used if the *bis*-imine is preformed.

When **8**, **10**, Yb(OTf)_3 , and HPO(OMe)_2 were combined in either CH_2Cl_2 or CH_3CN , only trace amounts of the *bis*-aminophosphonates were formed after 4d at room temperature. This lack of activity was attributed to the poor solubility of **11** in either solvent which reduces concentrations below those that rapidly react. When done in neat HPO(OMe)_2 at 50°C for 18h 47% of the *meso*- diastereomer **14** and 31% of the *rac*- diastereomer **15** were isolated after silica gel flash chromatography with Nzagi Nyakirangani initially isolating only the *meso*- isomer. The diastereomers were readily separated on silica as they have marked different R_f values. We tentatively assigned the *meso*- isomer **14** as the faster moving isomer with higher R_f . Presumably, phosphonate group association with silica will dominate chromatographic retention, being most strongly retained when both phosphonates contact the surface While free rotation about the single bond allows placement of phosphonate on either face of the central benzene ring, there must be a lowest energy conformation. In the *rac*- diastereomer **15**, with the same chirality at each of the aminophosphonate centers, both phosphonates will be on the same face in the lowest energy conformation. If formation of **14** and **15** was conducted in neat HPO(OMe)_2 at 90°C the desired materials were not produced. The isolated material resembled neither the starting material nor the products but with apparent loss of the Boc protecting groups. This preliminary data reinforced the idea that the insolubility of the *bis*-imine is the major impediment to reactivity that needs to be overcome.

Bisaminophosphonate synthesis from dialdehyde

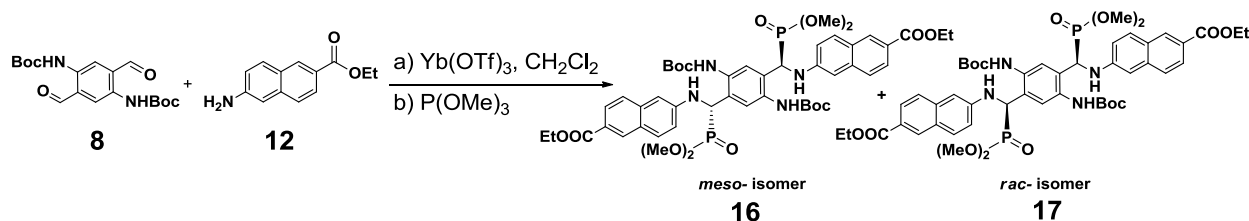


Figure 28: General "one pot" reaction scheme for *bis*-aminophosphonate formation

Investigation into forming **16** and **17** efficiently starting by formation of *bis*-imine **13** *in situ* first using CH_2Cl_2 and glacial AcOH , followed by the addition of $\text{P}(\text{OMe})_3$. The rationale behind this was to determine if the lanthanide catalyst could be omitted and then later used in developing asymmetric phosphonation. What was found though was that even with circa 10x stoichiometric excess of $\text{P}(\text{OMe})_3$ in the presence of acid and at room temperature did not facilitate quantitative transformation. When $\text{Yb}(\text{OTf})_3$ was introduced and the mixture heated to 60°C for 3h the reaction was complete. Analysis by ^1H NMR showed that the Boc groups remained intact but ^{31}P NMR showed signatures for the remaining trimethylphosphite, the *bis*-aminophosphonate diastereomers, and a new signal at $\delta 34$ ppm which is attributed to dimethyl methylphosphonate, believed to be formed by the following mechanism:

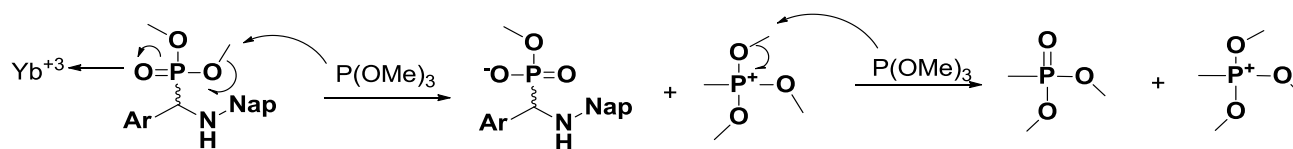


Figure 29: Proposed mechanism for dimethyl methylphosphonate formation with $\text{P}(\text{OMe})_3$

When the solvent was changed to THF using 60°C temperature, the reaction time decreased to 14h but unfortunately $\text{P}(\text{OMe})_3$ was still too reactive and not only formed dimethyl methylphosphonate but reacted with this solvent in the presence of ytterbium (III)

triflate. A side product was tentatively assigned as dimethyl (4-hydroxybutyl)phosphite which was formed, presumably by ring opening of lanthanide coordinated to THF.

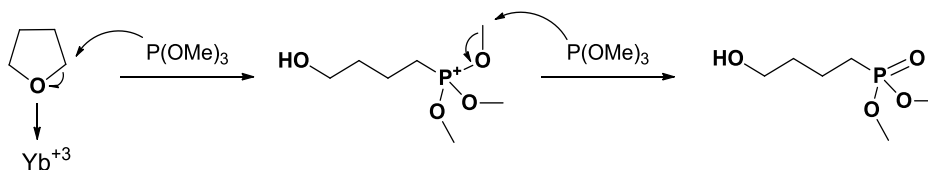


Figure 30: Proposed mechanism for reaction of $P(OMe)_3$ with THF in the presence of $Yb(OTf)_3$

After silica gel flash chromatography the *bis*-aminophosphonates were afforded in an estimated 50% total yield that were not separated from the methyl dimethylphosphate or the dimethyl (4-hydroxybutyl)phosphite. From these results continued use of trialkyl phosphites were put aside due to its demonstrated propensity to form side products at the expense of the desired compounds and focus shifted to conditions in which dialkyl phosphites could be employed.

Bisaminophosphonate Formation using $HPO(OMe)_2$

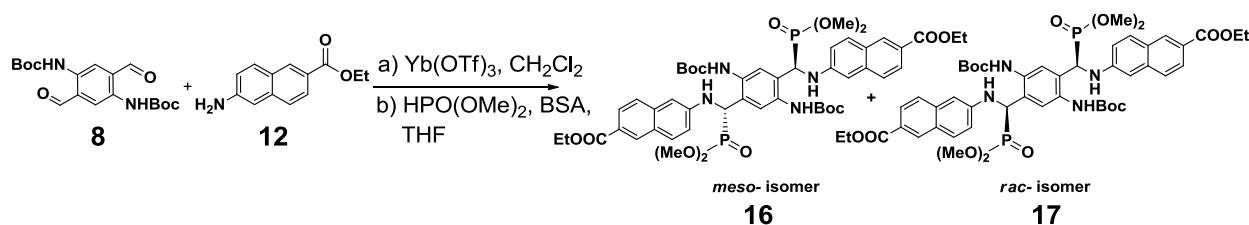


Figure 31: "One pot" *bis*-aminophosphonate synthesis with $HPO(OMe)_2$

It has been shown in the literature that transformation of an imine to an aminophosphonate with a dialkylphosphite and a catalyst as a homogeneous mixture occurs over the range of 0.5 to 4 h⁹³ with a wide range of compatible aldehydes and amines. Building off of the previous work done by Nzagi Nyakirangani, prospecting began using the "one pot"

method for *bis*-aminophosphonate formation. *Bis*-imine **13** was formed first in the presence of Yb(OTf)₃ with 4.5eq dimethyl phosphite in CH₂Cl₂ for 4d to give 34% yield (28% *meso*- **16**, 6% *rac*- **17**) after silica gel chromatography. This contrasted greatly from the 1:1 diastereomeric ratio observed in the NMR of the crude product before purification. Resolution suffered as the remaining dimethyl phosphite interfered with chromatography. Analysis of the diastereomers by ¹H and ³¹P NMR showed clean isolation of products from the dimethyl phosphite, but the *rac*- portion contained more than one signal in the ³¹P spectrum and lower integration ratio of the phosphoesters in ¹H spectrum. From this it was surmised that degradation of the aminophosphonates was occurring on silica gel by the lack of mass balance after this purification technique and the retention of color on the silica. As the ratio of aminophosphonate diastereomers formed should be 1:1 as the conditions for aminophosphonation are unselective, the *rac*- isomer was being degraded to a greater degree as it was isolated in a significantly lower amount. Put forward here is a mechanism by which degradation occurs which seems feasible as it is similar to the removal of a methyl phosphonate ester by excess trimethyl phosphite and provides an explanation as to why the *rac*- isomer is affected disproportionately. The longer contact time with the slower migrating racemic isomer **17** may explain the greater degree of degradation.

If the silica gel acidity was the problem, neutralization may avoid it. The first protocol employed was to expose silica gel to gaseous ammonia. To do this a sample of silica gel was exposed to the vapor over a container holding concentrated aqueous ammonia for one week with periodic mixing over that time. When this silica gel was used for chromatographic separation it indeed significantly decreased the polarity of the eluent needed but caused the

diastereomers to collute. However, if the silica gel that was treated in this manner was left exposed to the atmosphere for a day with periodic mixing the separation was accomplished with the *meso*- isomer being eluted with 40% CH₃CN/CH₂Cl₂ instead of 80% CH₃CN/CH₂Cl₂ and the *rac*- isomer was eluted with 80-100% CH₃CN/CH₂Cl₂ instead of 10% CH₃OH/CH₂Cl₂. Use of the silica gel also produced a lesser degree of degradation upon separation of the diastereomers. Although encouraging we chose not to follow up on this due to questions of reproducibility. With quantitation in mind though, deactivated silica gel was prepared by exposure of silica gel to well defined amounts of Et₃N in CH₂Cl₂ as a slurry. Mixtures of 2.5% and 5% allowed for sufficient deactivation while still affording separation. The 2.5% mixture behaved analogously to the gaseous ammonia exposed silica while the 5% mixture produced the largest disparity in eluents needed to elute the products with the *meso*- isomer being collected with 10% CH₃CN/CH₂Cl₂ and the *rac*- isomer being collected with 100% CH₃CN. Deactivation of the silica indeed afforded a greater amount of the *rac*- isomer but still failed to completely prevent degradation.

% by mass NEt ₃ /silica	Yield 16	Yield 17	Total Yield
0%	28%	6%	34%
2.5%	39%	19%	58%
5%	32%	21%	53%

Table 1: *bis*-aminophosphonate diastereomers afforded from deactivated silica gel chromatography

With the anemic activity of the dimethyl phosphite and the use of trimethyl phosphite producing side products a species of intermediate activity was desired. Dimethyl phosphite is in

equilibrium with its trivalent tautomer but the equilibrium heavily favors that of the pentavalent form. This can be shifted though by the introduction of a silylating agent. BSA was chosen not only for its two equivalents of silylating group per molecule but also acts as a base to facilitate proton transfer in isomerization.

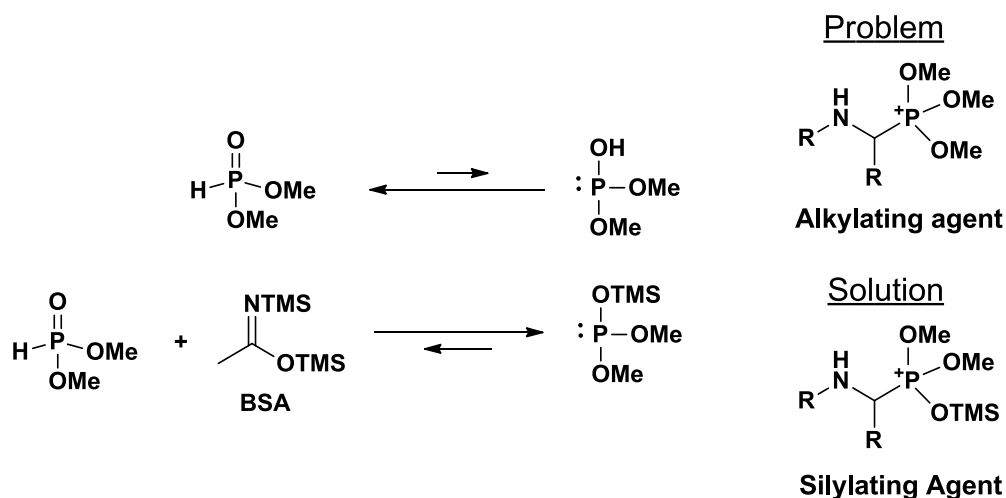


Figure 32: Use of BSA to shift $\text{HPO}(\text{OMe})_2$ equilibrium and prevent to methyl transfer

Dimethylphosphite was combined with BSA and monitored by ^{31}P NMR over the course of a day over which time the signal at $\delta 15$ ppm from $\text{HPO}(\text{OMe})_2$ decreased and a new signal grew in at $\delta 129$ ppm. As this new resonance was similar in chemical shift to $\text{P}(\text{OMe})_3$ ($\delta 141$ ppm) this was taken as evidence of the desired conversion to dimethyl trimethylsilylphosphite⁹⁴. Along with this change another modification to the synthetic procedure was introduced in order to still utilize the large excesses of dimethyl phosphite required but allow it to be removed as this cannot be easily done by simple evaporation. It well known that use of I_2 in pyridine and water can oxidize dimethyl phosphite to a phosphinic acid⁹⁵ which could then be removed by washing with aqueous base. When the dialkyl phosphite was injected with an equimolar amount of BSA reaction times averaged 18-30h at room

temperatures with yield increasing to a consistent 50% of the diastereomeric mixture after silica gel chromatography. It was discovered that quenching of the silylating agent was paramount by addition alcohol prior to being exposed to the I_2 / aqueous pyridine mixture for if this was not done then only trace amounts of the desired products were isolated. This could possibly be attributed to I^- demethylating the methyl phosphonates too quickly under aprotic conditions.

It wasn't until much later that the oxidative workup was suspected to be participating in the dealkylation of the phosphonates in **16** and **17** even after quenching the BSA. This was tested by taking a crude mixture of the diastereomers, splitting it into two portions, and treating one of the halves. Analysis of the untreated half when viewed with ^{31}P NMR showed signals for the excess dimethyl phosphite and the two desired *bis*-aminophosphonates whereas the treated half had the resonances of the products along with an array of signals upfield confirming the removal of the phosphomethyl esters. The mechanism of dealkylation is suspected to be by S_N2 reaction with I^- . This avenue of excess phosphite removal was abandoned as subsequently developed methodologies do not utilize chromatographic separation.

With the susceptibility of the dimethyl phosphonates to degradation on silica gel established the phosphonating agent was switched to diethyl phosphite in order to slow the rate of ethyl phosphonate ester S_N2 cleavage. This approach was validated by isolation of 73% total yield of the *bis*-aminophosphonates after chromatographic separation. From this result it was deemed worthy to carry forward with diethyl phosphite as the phosphonating agent as

well as pursuing tweezers synthesis without isolation of the *bis*-aminophosphonates which will be discussed in a later section.

3. Trögerization Affording Molecular Receptors Isomers

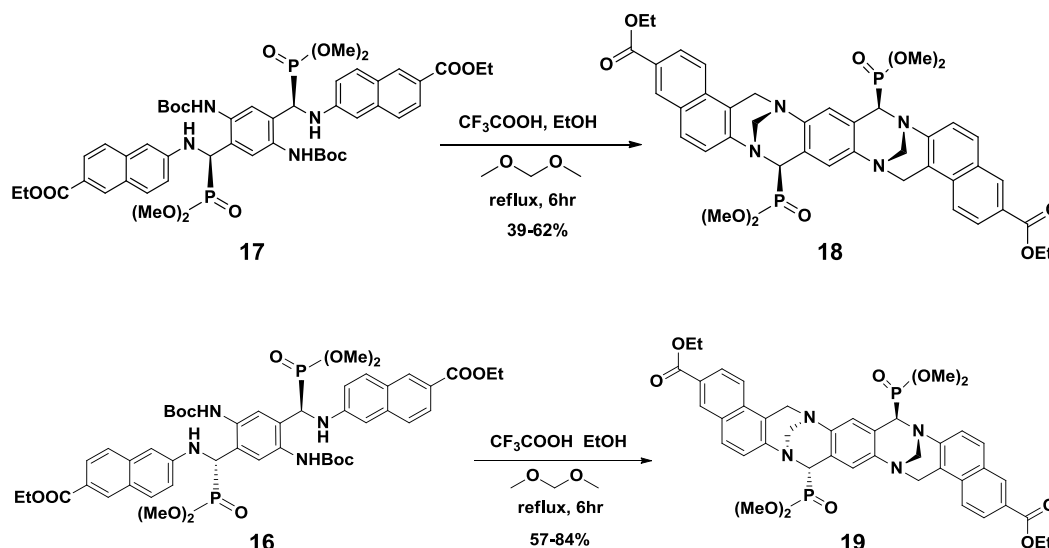


Figure 33: Trögerization to form desired *rac*-(**18**) and control *meso*- (**19**) molecular receptors isomers

With isolated **17** and **16** on hand cyclization to form the *bis*-Tröger's base tweezers commenced. The acid chosen, trifluoroacetic acid (TFA), and the formaldehyde equivalent, dimethoxymethane (DMM), were chosen for Trögerization as both of these required reagents are volatile so that when used in excess remaining amounts of them can be removed under reduced pressure. In using these two as reactive solvents two things were observed: that a reflux temperature at 60°C or above was required to drive Tröger's base formation to completion and that polyformaldehyde was generated as a side product. The polyformaldehyde was not separated from the desired product through silica gel flash chromatography but was able to be removed only after extensive washing with a saturated $\text{NaHCO}_3(\text{aq})$ solution. Fortunately it was found that the addition of either methanol or ethanol as a cosolvent

prevented polyformaldehyde formation by condensing with the formaldehyde equivalent as well as elevating the reflux temperature of the mixture. Additionally crude **17** was cyclized in the presence of dimethyl phosphite, dimethyl methylphosphonate, and dimethyl (4-hydroxybutyl)phosphonate with no observable interference in Tröger's base formation. **18** and **19** molecular tweezers isomers displayed similar behavior on silica gel as its *bis*-aminophosphonate counterparts with regards to degradation occurring over the course of flash chromatography, albeit to a lesser degree. Although these tweezers isomers were not still not separated from the phosphite derivatives they were still able to be identified by ^1H NMR and provided samples for monitoring their formation by TLC.

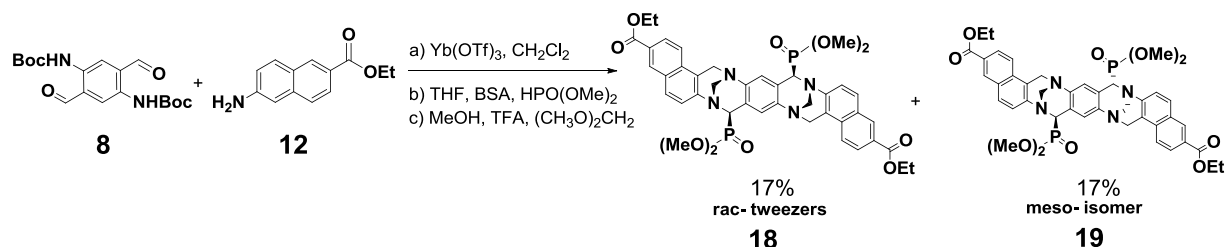


Figure 34: "One pot" molecular tweezers synthetic scheme using $\text{HPO}(\text{OMe})_2$

Synthesis to form the desired molecular tweezers built upon the previous procedure in which the bisimine **13** was formed *in situ* followed by the introduction of the aminophosphinating reagents followed by exposure to condition to form the *bis*-Tröger's base skeleton. Synthesis proceeded in one flask starting with **8** and **12**. The formation of the intermediates **13**, **16**, and **17** were followed by TLC until the desired products were completely formed. When the desired compound was formed the mixture was concentrated by rotary evaporation and exposed to the next set of reaction conditions without removal of $\text{Yb}(\text{OTf})_3$. This proved to be detrimental as the more stable *meso*- isomer **19** was afforded in only 17% yield but a 17% yield the *rac*- isomer **18** was also obtained. Even though this sequence did not

produce an overall increase in yield of the **18** after chromatographic isolation, it did provide an amount of material on par with the protocol utilizing chromatographic isolation in each synthetic step. When the lanthanide was removed prior to cyclization conditions with an EDTA/NaHCO₃ solution, yields did not substantially increase.

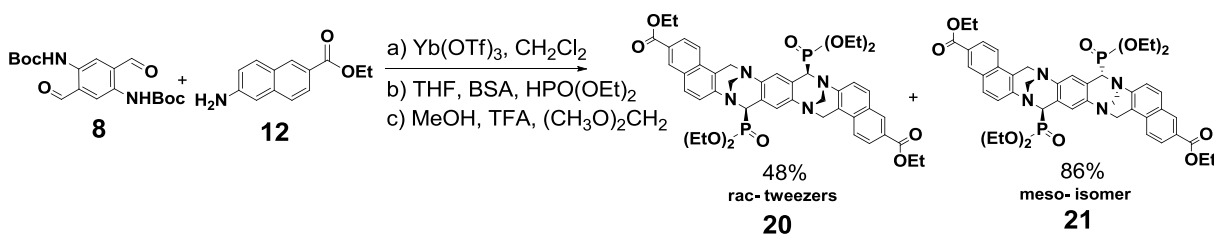


Figure 35: "One pot" molecular tweezers synthetic scheme using diethyl phosphite

With the increased stability of the ethyl phosphonate esters previously demonstrated exploration of the "one pot" synthetic method was conducted using diethyl phosphite with removal of the lanthanide before Trögerization. The resulting tweezers isomers were separated by flash chromatography to afford a substantial increase in yield compared to the dimethyl phosphonate analogues with an average yield of 76% for the *meso*- isomer **21** and 58% average yield for the desired *rac*- isomer **20**. The *meso*- and *rac*- isomers exhibited dramatically different physical properties. For example, the *meso*- isomer was isolated as a crystalline white solid with a fairly high melting point range of 299-303°C while the binding *rac*- isomer is a semi-solid with a low melting point range of 50-60°C.

From these observations and with an appreciable amount of the two isomers now in hand we set about a separation by crystallization. The solubilities of the two were then screened against a panel of solvents. While the *rac*- isomer, **20**, was found to be soluble in all the solvents tested save for hexanes, **21** on the other hand proved to be insoluble or sparingly soluble in

CH₃CN, toluene, ethanol, and EtOAc and could be recrystallized from any of these solvents.

When a mixture of **20** and **21** was triturated with EtOAc, toluene, or CH₃CN the *meso*- isomer remained solid and was isolated by vacuum filtration while the desired *rac*- isomer remained in the supernatants. Most attempts to recrystallize the *rac*- isomer failed: addition of hexanes to a solution of **20** in any of the solubilizing solvents caused oiling out. What was found to be an effective method to solidify **20** was to take a solution in toluene (56mL/g) and add it dropwise to ten volumes of stirring hexanes.

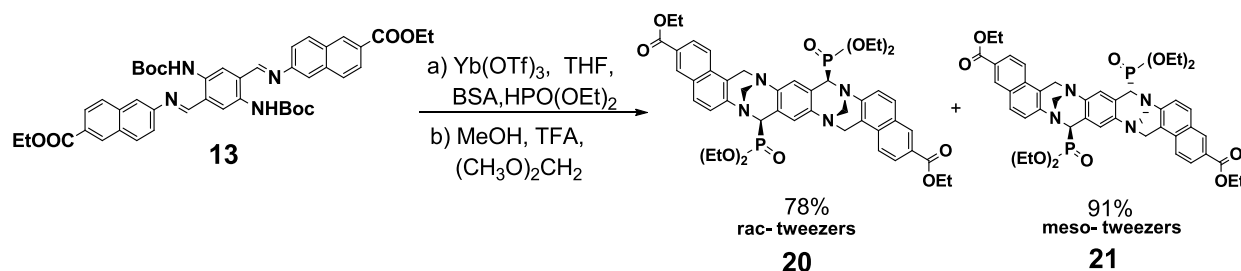


Figure 36: "One pot" tweezers synthesis starting from *bis*-imine

Scale up of the molecular tweezers synthesis was now conducted with an optimized "one pot" procedure and a method of non-chromatographic separation. The synthetic protocol began with the easily isolated and recrystallized *bis*-imine **13** as opposed to forming it *in situ*. This avoids formation of Tröger's base derivative formed from **12**, which required silica gel chromatography for removal. After aminophosphonation, extractive removal of the lanthanide catalyst, and cyclization to form the *bis*-Tröger's bases, the volatiles were removed by rotary evaporation before neutralization. The resulting crude solid was then triturated with hexanes to remove any remaining diethyl phosphite before being triturated with EtOAc to leave behind **21** as a white solid. The EtOAc supernatants were concentrated to dryness, dissolved in toluene, and added dropwise to stirring hexanes to generate the solidified **20**. In the end, an 84% yield

of non-binding *meso*- isomer **21** and a 72% yield of the desired binding *rac*- isomer **20** were afforded. This process was repeated several times to give yields of **21** averaging 86% and **20** averaging 75%.

When this synthesis was done on a 1g scale or above of the *bis*-imine **13** using the developed methodology the transformation to the corresponding *bis*-aminophosphonates was not complete after the usual 18hr time period. Instead, it required three days and additional portions of Yb(OTf)₃, diethyl phosphite, and BSA reaching these final concentrations and ratios: Yb(OTf)₃= 0.39eq, 7x10⁻³M; HPO(OEt)₂ = 99eq, 1.8M; BSA = 49eq, 0.9M. This change in behavior was attributed to the increased purity and thus the increased crystallinity of the **13** used as well as a diminishing in the activity of the lanthanide catalyst over time. As mentioned previously, the chemical literature thoroughly demonstrates rapid aminophosphonation on time scales up to hours in length. This implies that the catalyst is active in this time frame. Undergraduate Angel Corona added various ligands and attempted to study varying catalyst compositions and stoichiometries to maximize reaction rate. He found a dependence on order of ligand addition and irreproducible rates. Sometimes *bis*-imine **13** was solubilized in minutes, with apparent completion of reaction by TLC in that time. Unfortunately, identical conditions required days for completion if the starting imine did not quickly dissolve. We interpret these results to say that a transient lanthanide complex acts as a much more active catalyst before diminishing over time.

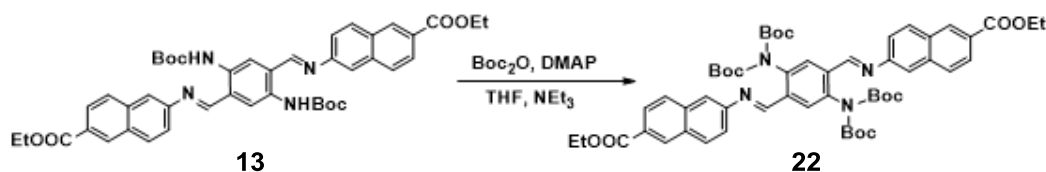


Figure 37: Scheme for the synthesis of tetraBoc derivative of **13**

In an attempt to circumvent the insolubility of the *bis*-imine **13** formation of the tetraBoc derivative was prepared. The reason for this is that the *bis*-imine is a flat, aromatic molecule with a large amount of surface area that allows for a multitude of π - π interactions. If this could be inhibited by reducing its planarity, it would make a poor crystal and more easily dissolve. Addition of another Boc group on the Boc protected nitrogen would eliminate the intramolecular hydrogen bond that enforces the shape. Use of DMAP and Boc₂O in CH₃CN has been shown to accomplish this.⁹⁶ The described conditions did not facilitate additional Boc protection which was attributed again to the poor solubility of **13** in CH₃CN. When the solvent was switched to THF, and triethylamine was added, the desired tetraBoc compound was completely formed after 17hr and isolated in 89% yield of **22** by silica gel chromatography. This material was then exposed to the aminophosphonation conditions as a homogeneous solution with the derivative *bis*-imine being consumed after 4hr. Analysis of the mixture by ³¹P NMR however did not show just the two signals anticipated for the aminophosphonate diastereomers but instead contained ten major peaks in the chemical shift range of the desired materials (δ 25-30ppm). This multitude of signals could have arisen from the transfer of a Boc groups from the phenylamine to the naphthylamine. If this were the case it should not prohibit cyclization as the trifluoroacetic acid in the next reaction step would remove the Boc groups. This technique seems promising for efficient conversion of the **13** on a large scale and should be investigated by future researchers. However, due to the number of the signals and ambiguity in interpretation this avenue was not followed up.

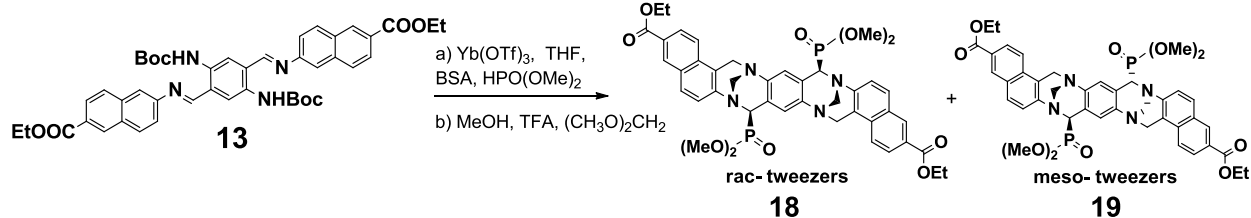


Figure 38: "One pot" synthesis of molecular tweezers using dimethyl phosphite

With a developed "one pot" protocol and the ability to separate the isomers non-chromatographically it was decided to go back to the dimethylphosphonate version of the molecular tweezers. The reason for this would be a simpler ^1H NMR spectrum which would allow for unambiguous interpretation when evaluating conditions for phosphonate ester removal. The ^1H NMR spectrum for the dimethyl phosphonates exist as two doublets as each of the diastereotopic methyl groups is coupled to the phosphorus nucleus. On the other hand the splitting pattern of the diethyl phosphonates is substantially more complex. Each of the two diastereotopic ethyls has a pair of diastereotopic hydrogens that couple each other, are doubled by the ^{31}P , and coupled into a quartet by the neighboring methyl, yielding 4 sets of ddq for 64 peaks in a 0.2ppm spectral range. The carbethoxy group also has a nearby quartet.

Transformation of **13** on a 1.6g scale to **16** and **17** required the same prolonged reaction time; 11d and four additions of $\text{Yb}(\text{OTf})_3$. The tweezers isomers were separated non-chromatographically using toluene to afford an average yield of 86% **19** and 83% **18**. The desired *rac*- isomer was purified by dissolving in minimal 1,4-dioxane and precipitating by addition of eight volumes hexanes. It was observed that the *rac*- isomer **18** needs to be kept in cold storage as the material appears to degrade if kept at room temperature. This was concluded when old samples of **18**, which were kept at room temperature from four months to

one year were combined with toluene which produced a heterogeneous mixture. The degraded material was able to be separated from intact **18** by vacuum filtration as the degraded material was not soluble in toluene. Investigation into the composition of this degraded material was not pursued as proper storage and separation techniques were indentified, but S_N2 attack at the phosphonate methyl is plausible.

4. Reactions to Generate Water Soluble Molecular Receptors

To turn the molecular tweezers into a water soluble form, the esters need to be removed. Detailed below are the formations of three different water soluble derivatives that vary in the amount and distribution of negative charge on the molecular tweezers. Known synthetic methods were employed to take advantage of the selectivity in ester cleavage based on the atom the ester is connected to. These techniques were also used to make water soluble version of the *meso*- tweezers isomers to serve as a negative control in small molecule titration to evaluate complex formation with the desired *rac*- binding isomer.

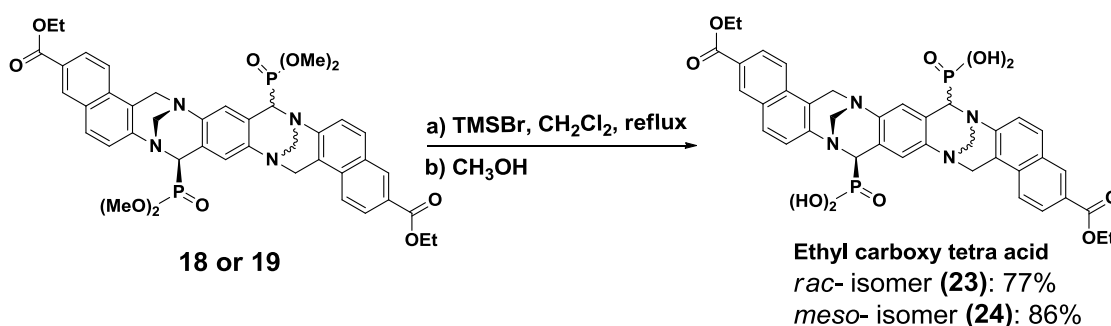


Figure 39: TMSBr deprotection of tweezers isomers to afford carboxy tetra acids derivatives

Bromotrimethylsilane (TMSBr) was first described in 1977⁹⁷ to selectively cleave alkyl phosphonate esters in the presence of carboxylate esters swiftly at room temperature in high yield. For this reason this method has been used subsequently⁹⁸ with demonstrated tolerance

for a multitude of functional groups.⁹⁹ The conversion of **18** to the desired carbethoxy tetraacid compound was done with large excesses (10x stoichiometric) of TMSBr in CH₂Cl₂ at reflux for 1.5 to 16h or at room temperature over 22hr without apparent degradation or side reactions. However, this is dependent upon the purity of the TMSBr. If the TMSBr is colorless or a *faint* yellow color removal of the phosphoesters occurred without complication. If the TMSBr was orange in color or darker, which is indicative of Br₂ from HBr formed, the afforded material could not be identified and was concluded to have been degraded. Complete removal of the P-Me esters was determined by NMR spectroscopy when doublets in ¹H at δ4.04 and 3.98ppm disappeared and signals in ³¹P converged to δ17ppm. After this the volatiles were removed by vacuum in an anhydrous environment to prevent HBr formation until a solid remained after which it was exposed to methanol to remove trimethylsilyl esters. Dealkylation of the *meso*-isomer **19** required refluxing temperature to go to completion in a reasonable amount of time but could also be accomplished in 7d at room temperature if time is not a factor. Both of the isomers were purified by dissolving in boiling EtOH, cooling to room temperature, and precipitation with hexanes to yield 77% **23** and 86% **24** respectively.

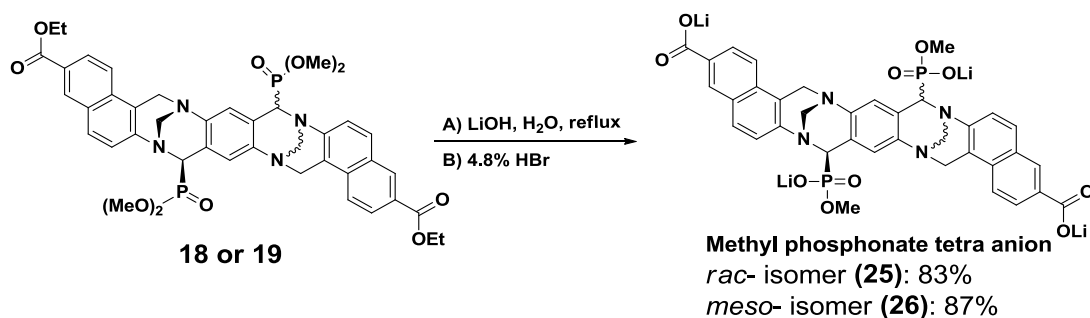


Figure 40: Saponification of tweezers isomers to form the methyl phosphonate tetra anion derivatives

Another water soluble derivative was made when the tweezers isomers were exposed to aqueous hydroxide to saponify the carboxylic esters and selectively remove a single phosphonate methyl ester on each of the phosphonates. Rabinowitz demonstrated this selectivity¹⁰⁰ in dealkylation utilizing aqueous hydroxide at refluxing temperatures over the course of 16h resulting in high yield. The origin of this selectivity is attributed to coulombic repulsion of subsequent hydroxide after the first equivalent breaks the first P-O bond through an addition elimination mechanism.

The saponification procedure was developed using **19** as it was in abundance. Lithium hydroxide was chosen as even though it is the weakest of the alkali hydroxides it can be used in excess as it is readily removed after neutralization with HBr: LiBr is soluble in THF. **19** was mixed with a four fold excess of LiOH in a combination of 1,4-dioxane and D₂O so progress could be monitored by ¹H NMR spectroscopy. TLC analysis would not be able to distinguish the degree of ester removal over time. After 15h all of the desired esters were removed and the absence of the benzyl hydrogen in the aminophosphonate was noted. When submitted to mass spectrometry analysis a m/z of 743 in the negative ion mode and a m/z of 745 were observed suggesting a molar mass of the resulting compound as 744 g/mol. This molar mass is two mass units higher than that of the tetracid form of the saponified *meso*- tweezers which is what seen in MS analysis due to the use of formic acid as the modifier. From this mass increase and lack of signal in the NMR it was determined that H/D exchange occurred on that benzyl position under the aqueous basic conditions before cleavage of the phosphonate ester. This was proved when saponification was performed in H₂O and no loss of benzyl signal was seen and no increase in mass in spectrometric analysis.

The desired saponified tweezers isomers are formed and stable in the refluxing hydroxide solution after 15h after which it is concentrated to dryness to remove the dioxane as to not react with the hydrobromic acid. After redissolving in water, neutralizing to pH7 with 4.8% HBr, and trituration with THF **25** was afforded in 83% yield and **26** was afforded in 87% yield.

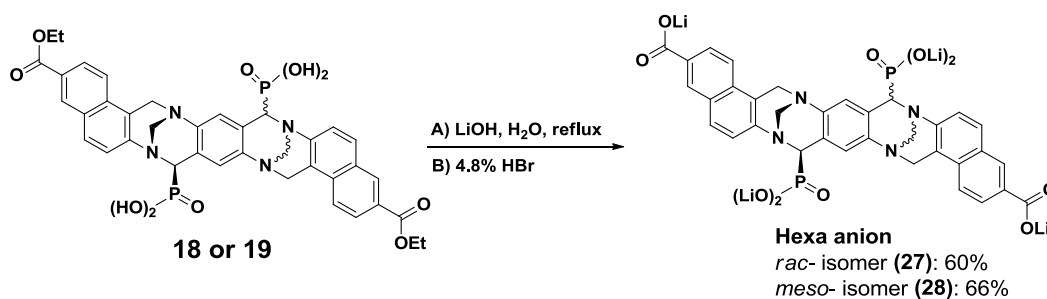


Figure 41: Hexa-anionic tweezers isomers formed by saponification of the TMSBr dealkylated derivatives

The fully deprotected hexa-anionic tweezers were produced by saponification of the bromotrimethylsilane dealkylated water soluble tweezers **18** and **19**. The LiOH saponification protocol described previously was used with saponification complete after 6hr at reflux in the aqueous hydroxide. Neutralization with HBr and trituration with THF afforded **27** in 61% yield and **28** in 66% yield.

C. Characterization of Molecular Receptor Isomers

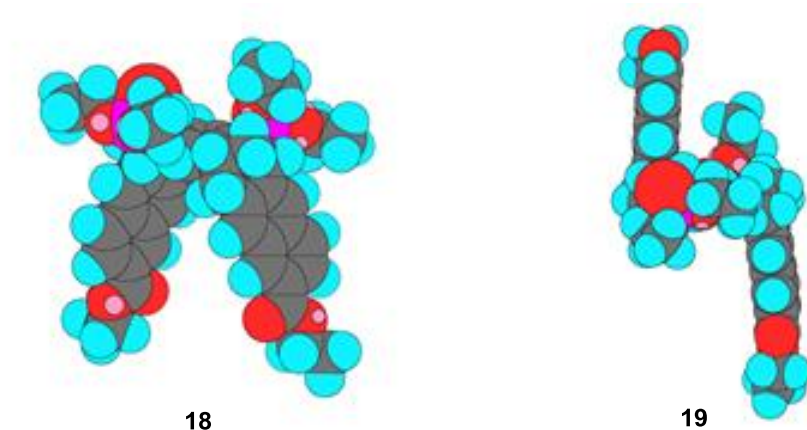


Figure 42: Space filling models for the fully esterified binding *rac*- isomer (left) and the non-binding *meso*- isomer (right)

Isomers **18** and **19** displayed markedly different behaviors when analyzed by ^1H NMR spectroscopy. The fully esterified *rac*- isomer **18** was initially difficult to identify as the resonances seen were very broad but at least were in chemical shifts regions consistent for the chemical bonds for the hydrogen atoms in the desired material. In contrast, the *meso*- isomer **19** gave sharp signals in the same region. To test whether the broadening is due to binding, dimerization only of **18**, we acquired ^1H NMR spectra at various concentrations from 10^{-2}M down to $1.4 \times 10^{-4}\text{M}$, roughly the detection limit for the 300MHz Bruker NMR for 30min acquisition time. Over the course of the dilution, the aromatic hydrogens in the naphthalene walls shifted downfield while the aromatic signals in the benzene core shifted upfield with no more apparent movement at concentrations of $3.4 \times 10^{-4}\text{M}$ and below. This behavior is consistent with the binding, *rac*- form of the molecular receptors self association by the formation of a dimer the inclusion of the naphthalene wall of one molecule of the tweezers into the cavity of another molecule of the tweezers. In dimer formation by this mechanism the

delocalized electrons in the aromatic naphthalene walls from the tweezers would shield the hydrogens on the other copy of the tweezers while the benzene hydrogens would be deshielded by the edge on interaction with the naphthalene quadrupole.

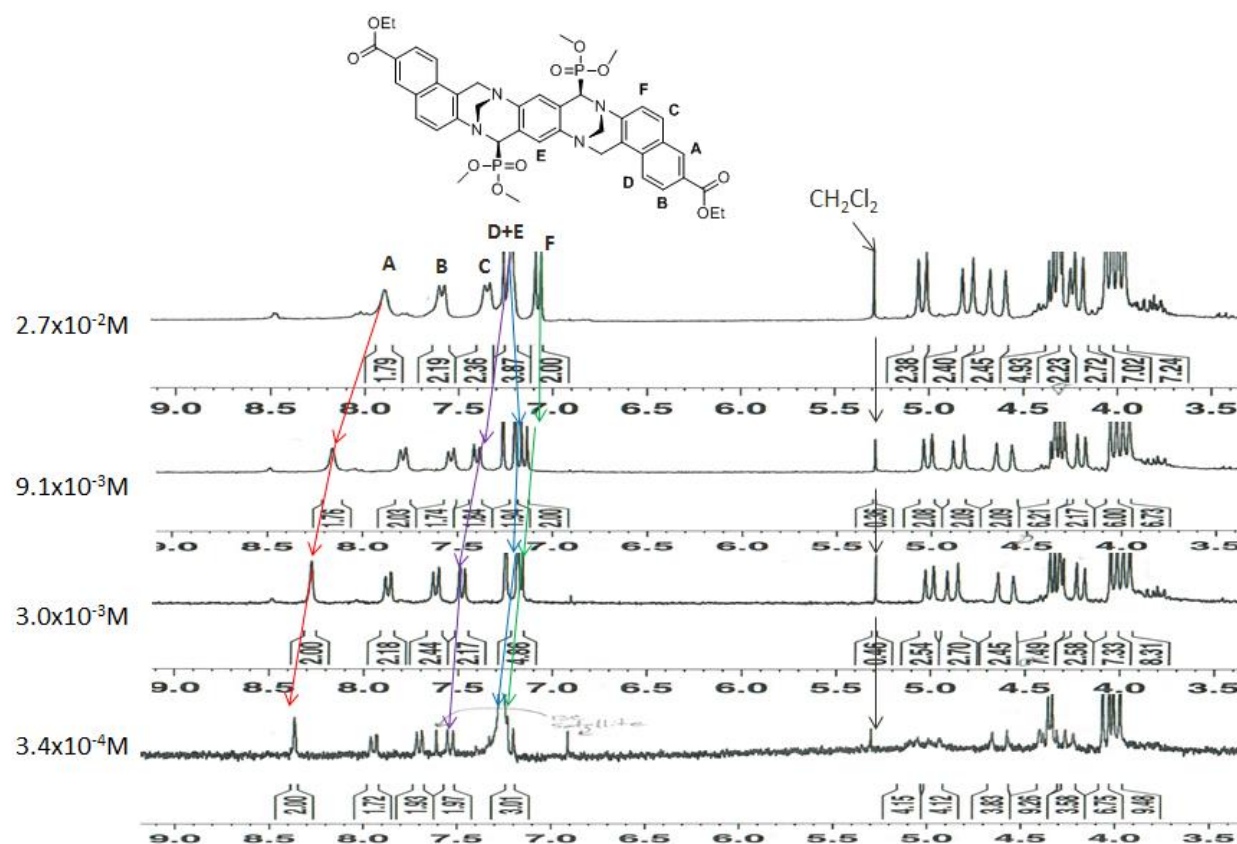


Figure 43: ^1H NMR dilution of the fully esterified *rac*- tweezers **18** in CDCl_3

From the NMR dilution study the chemical shifts of the naphthalene hydrogens versus concentration were plotted and analyzed via non-linear least squares fit via the derived equation below to see whether the changes are consistent with dimerization and to determine the dimerization constant of **18** in CDCl_3 . The value calculated from this data was $1.5 \times 10^{-1} \text{M}$ but it should be stressed that this value is just an estimate based on the number of data points (4) used in the analysis and at least ten data points are required to garner an accurate estimate.

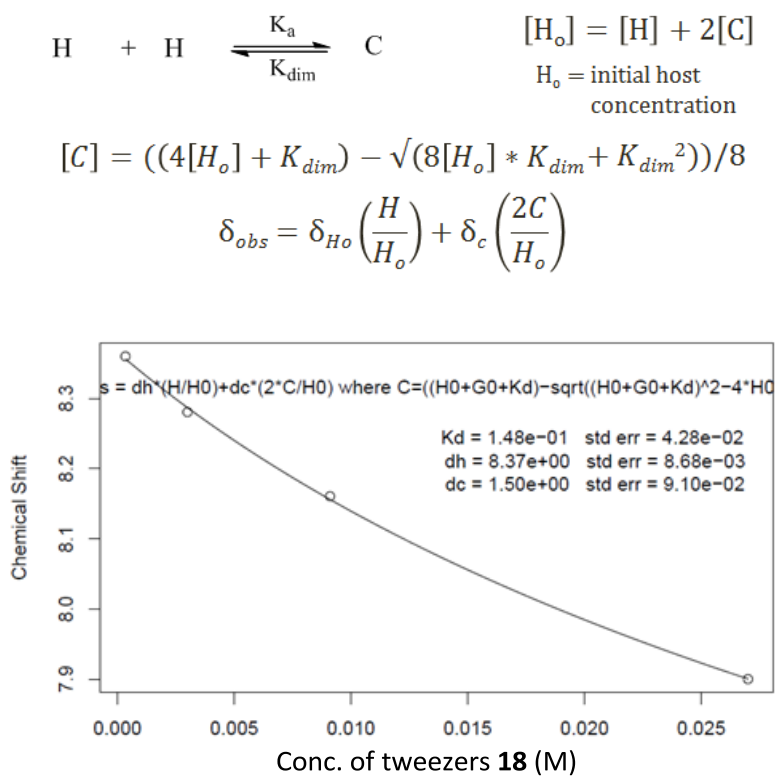


Figure 44: Equation used for the non-linear least squares fit for the dimerization of the fully esterified *rac*-tweezers utilizing NMR chemical shifts (top) and fit using chemical shift proton A (bottom)

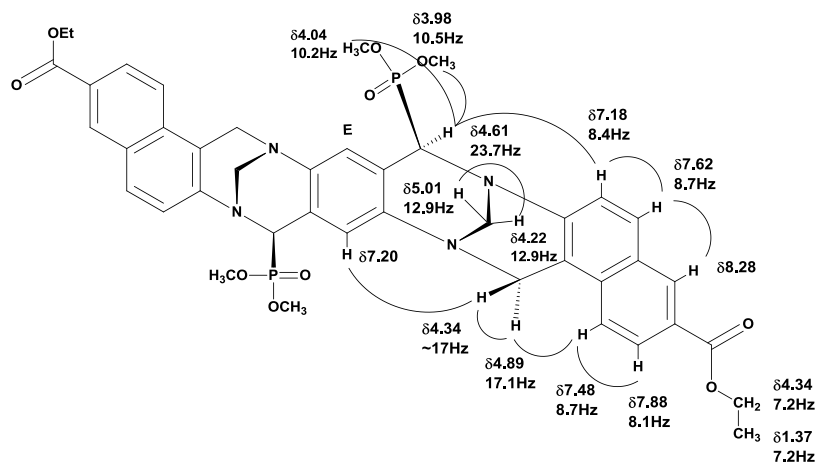


Figure 45: Chemical shifts, coupling constants, and NOESY correlations for the full esterified binding *rac*- isomer **18** in CDCl_3 at $3 \times 10^{-3} \text{ M}$ concentration

When at a concentrations that were monomeric the hydrogen signals of *rac*- isomer **18** in the *bis*-Tröger's base skeleton were able to be distinguished by their distinct coupling

constants. The hydrogens on the methylene bridging the two nitrogens had a coupling constant of 13Hz, the hydrogens on the methylene connecting the naphthalene wall exhibited a coupling constant of 17Hz, and the benzyl hydrogen in the aminophosphonate displayed a signal with 23Hz due to its coupling with the phosphorous.

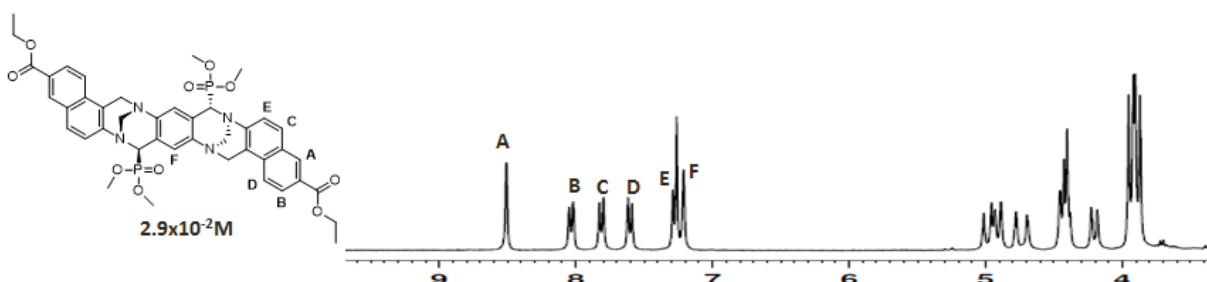


Figure 46: ^1H NMR spectrum of the fully esterified non-binding *meso*- tweezers isomer **19**

When the ^1H NMR spectrum was acquired for the control *meso*- isomer **19** no broadening of the hydrogen signals were observed at concentrations where that phenomenon was seen in the *rac*- isomer. From this it was concluded that *meso*- isomer was not associating with itself while in solution, consistent with our design.

D. Dimerization of Water Soluble Receptor Isomers in Water

1. Analysis by ^1H NMR Spectroscopy

All of the water soluble derivatives of the binding *rac*- isomer also showed the propensity for self assembly in aqueous environments. This made initial characterization of all of these compounds difficult as in the case of carbethoxy tetra anion **23**, which produced a ^1H NMR spectrum containing ill defined signals over broad chemical shift ranges.

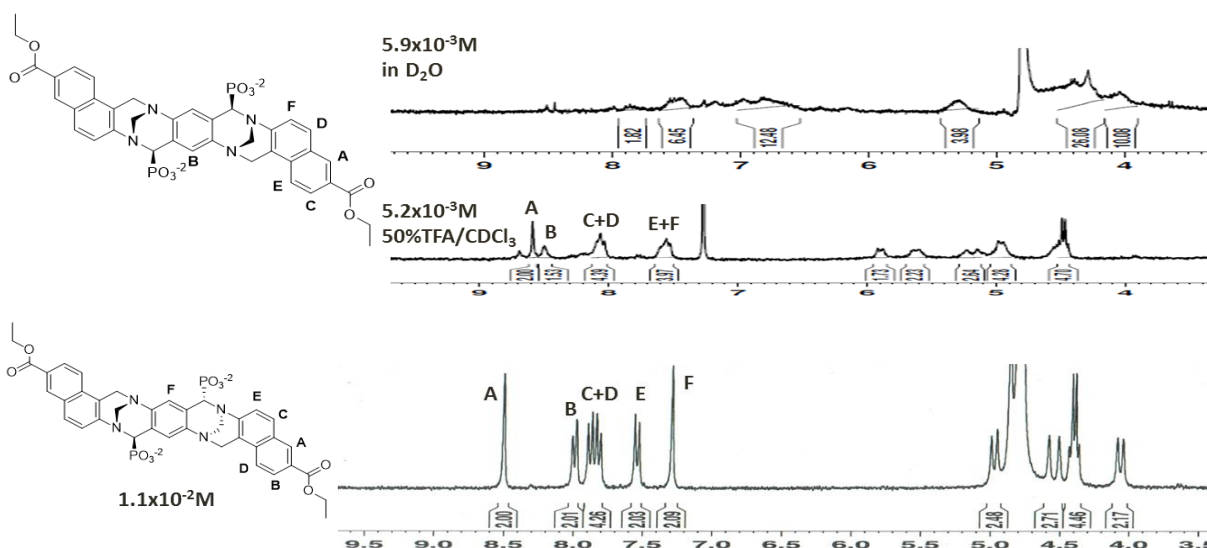


Figure 47: Comparison of the ^1H NMR spectra of *rac*- carbethoxy tetra anionic tweezers **23 in D_2O and 50% TFA/ CDCl_3 versus the non-binding *meso*- isomer **24** in D_2O**

The sample in D_2O was exposed to temperatures ranging from 274K to 313K in hopes of increasing the resolution of the peaks by either increasing or decreasing the rate of exchange of the tweezer molecules in dimer formation but this was not observed. This suggests that rapid exchange on an NMR scale is not accessible at a reasonable temperature. Pyridine- d_5 was used as a solvent in effort to produce monomeric species by insertion into the cavity and did seem to work when the concentration of the *rac*- tweezers **23** was around $5 \times 10^{-4} \text{M}$ but the signals from the residual solvent and their ^{13}C satellite peaks obscured the majority of the aromatic region. DMSO- d_6 was successful in producing a spectrum with resolved aromatic signals but a broad singlet was seen in the spectrum in the 3 to 4ppm range which is in the area needed to evaluate if the P-Me esters are absent. What did produce the best results for characterization was dissolving the initially isolated tetra acid **23** in a mixture of 50% TFA in CDCl_3 . Although not as well resolved as the *meso*- isomer **24**, it produced data sufficient for accurate integration and assignment of the hydrogens. The lack of doublets at $\delta 4\text{ppm}$ with $J=10\text{Hz}$ confirms the absence of methyl phosphonates and the efficiency of the TMSBr dealkylation method. The control

meso- carbethoxy tetra anion isomer **24**, like the full esterified form, gave sharp peaks which was interpreted as no self association in D₂O at concentrations ranges equal to or greater than those where the binding *rac*- isomer **23** appears to do so.

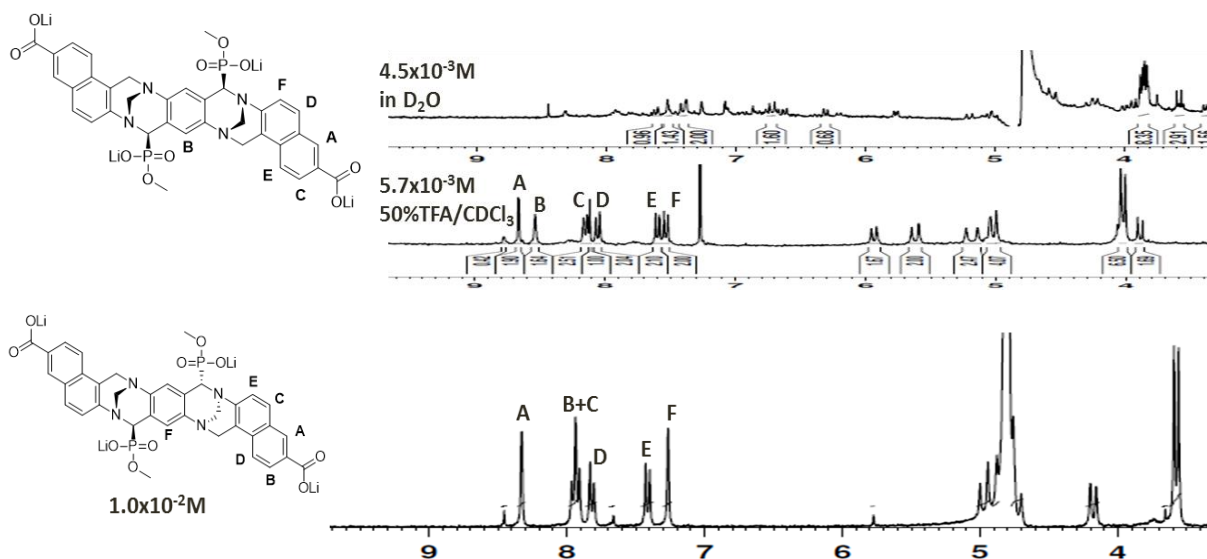


Figure 48: Comparison of the ¹H NMR spectra of *rac*- methyl phosphonate tetra anionic isomer **25** in D₂O and 50% TFA/CDCl₃ versus the non-binding *meso*- isomer **26** in D₂O

As opposed to **23**, the *rac*- methyl phosphonate tetra anionic tweezers **25** when in D₂O did not produce broad signals but an array of signals presumed to be a mixture of species that are exchanging with each other in solution. This presumably is able to occur as this saponified form of the molecular tweezers has an energetic barrier to dimerization from the negatively charged carboxylates on the edges of the naphthalene. The ¹H NMR is consistent with the desired cleavage by hydroxide having taken place. The ¹H NMR simplified slightly upon dilution in D₂O but not to the point of producing a single set of signals. Use of 50% TFA/CDCl₃ in NMR analysis was able to produce a well resolved set of signals that allowed for characterization of **25**. It appears that the molecule is not stable to strongly acidic conditions: an impurity forms

showing a doublet at $\delta 3.9\text{ppm}$ with $J=11\text{Hz}$ in proximity to the methyl phosphonate signal. This may be due to partial transformation of the Tröger's Base skeleton.

This phenomenon also occurs for the *meso*- isomer **26** in 50% TFA/ CDCl_3 but it is not required as like the other control isomers affords well resolved NMR spectra at mM concentrations. The residual solvent signal in D_2O however does reside in the same chemical shift range of the Tröger's base signals and 50% TFA/ CDCl_3 is needed to see these resonances as the residual solvent signals in this mixture do not mask them. After replicating the saponification procedure for both isomers multiple times the integrity of the Tröger's base skeleton remained intact under the alkaline conditions with the TFA/ CDCl_3 needed only to absolutely confirm the structure.

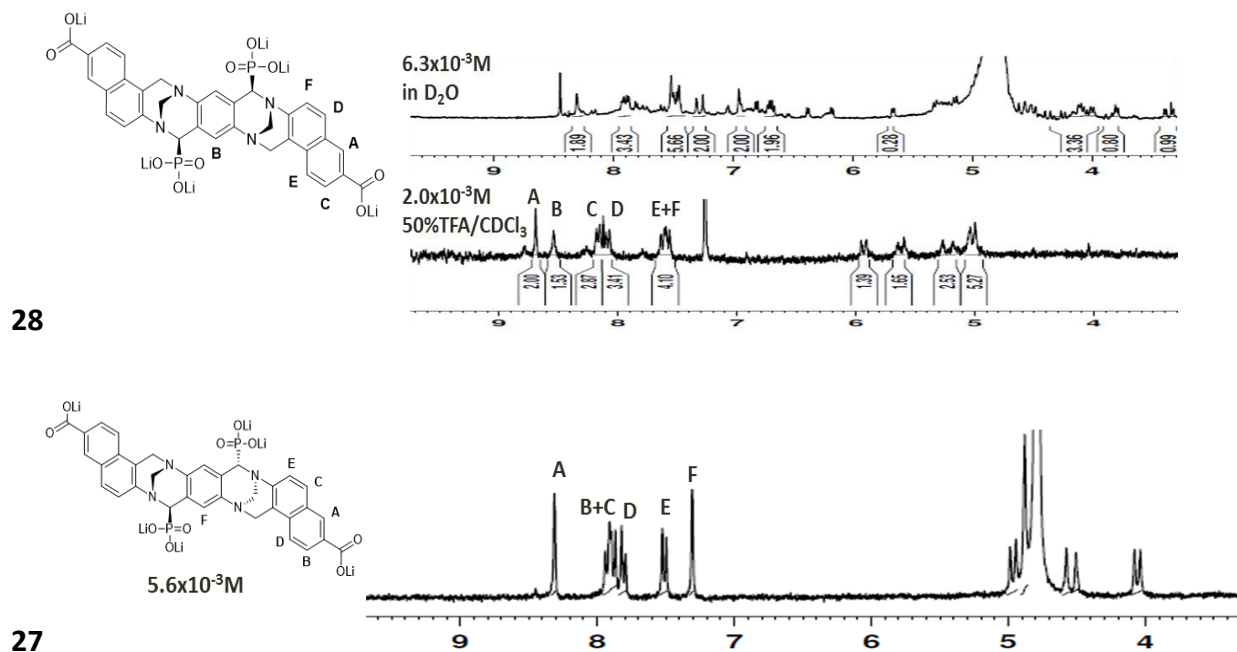


Figure 49: Comparison of the ^1H NMR spectra of *rac*- hexa anionic tweezers **27** in D_2O and 50% TFA/ CDCl_3 versus the non-binding *meso*- isomer **28** in D_2O

The binding *rac*- (**27**) and control *meso*- (**28**) isomers for the fully deprotected hexa anionic derivative exhibited the same behavior in D₂O and 50% TFA/CDCl₃ as their other water soluble counterparts. The set of signals in D₂O were less broad than that of the methyl phosphonate tetra anion and did seem to coalesce to a single set between 6.3x10⁻⁴ and 6.3x10⁻⁵ M but a sufficient signal to noise ratio required to assign the peaks could not be achieved.

2. Analysis by Fluorescent Spectroscopy

BACKGROUND AND GENERAL PROCEDURES

As ¹H NMR spectroscopy could not be used at sufficiently low concentrations to determine a dimerization constant for the water soluble tweezers varieties, fluorescent spectroscopy was used. This technique would allow for the dilution of the tweezers to concentrations below the level of detection of NMR by monitoring its fluorescent emission. It is expected that the dimerized complex and the free monomeric species would emit differently to allow for a way to identify the concentration in which dimerization occurs. A deviation from linearity in fluorescent emission upon dilution of the tweezers would provide evidence of association. If a single species exists in solution its fluorescence will decrease proportionally with concentration with a constant excitation wavelength as described by the Beer-Lambert Law.

$$\begin{aligned}
\text{H} + \text{H} &\xrightleftharpoons[K_{\text{dim}}]{K_a} \text{C} & [\text{H}_o] &= [\text{H}] + 2[\text{C}] & [\text{C}] &= \frac{1}{2}([\text{H}_o] - [\text{H}]) \\
&& \text{H}_o &= \text{initial host} & & \\
&& \text{concentration} & & & \\
&& & & [\text{H}] &= [\text{H}_o] - 2[\text{C}] \\
K_{\text{dim}} &= \frac{[\text{H}][\text{H}]}{[\text{C}]} = \frac{([\text{H}_o] - [\text{C}])([\text{H}_o] - [\text{C}])}{[\text{C}]} = \frac{[\text{H}_o]^2 - 4[\text{H}_o][\text{C}] + 4[\text{C}]^2}{[\text{C}]} \\
&= 4[\text{C}]^2 - [\text{C}](4[\text{H}_o] + K_{\text{dim}}) + [\text{H}_o]^2 = 0 \\
[\text{C}] &= ((4[\text{H}_o] + K_{\text{dim}}) - \sqrt{(8[\text{H}_o] * K_{\text{dim}} + K_{\text{dim}}^2)})/8 \\
I &= I_h([\text{H}_o] - 2[\text{C}]) + I_c[\text{C}]
\end{aligned}$$

Figure 50: Derivation of the equation used to determine K_{dim} for the dimerization of the binding *rac*- tweezers by fluorescence spectroscopy

Correction of fluorescence for screening of exciting light was used. In cases where the absorbance of the tweezers isomers were above a value of 0.1 the intensity of the fluorescent emission was corrected using the equation of $I = I_0 * 10^{-(A/2)}$. The term of $A/2$ was used to compensate for the diminution of emission produced at a point halfway through the sample where fluorescence is monitored. This correction factor was used only for absorbance values between 0.1 and 0.2 as values corrections exceeding 0.2 will be inconsequential.

Carbethoxy tetra acid tweezers 23

The Ocean Optics SD2000 was initially used in trying to determine monomeric concentrations of the *rac*- carbethoxy tetra anion tweezers **23** which was irradiated with broadband light centered at 365nm. A 7.2×10^{-2} M solution in 10mM pH7 phosphate buffer was serially diluted by a factor of 2 until a final concentration of 7.0×10^{-5} M was reached. Linear decrease in fluorescent emission was observed from 2.25×10^{-3} M and lower by monitoring the emission maximum (495nm) of the tweezers. Fluorescence was non-linear in range of 7.2×10^{-2} to 2.25×10^{-3} M with fluorescence increasing upon dilution. This linearized using our screening

correction of the exciting light and not from dimer to monomer transition. The Fluorolog-3 fluorimeter was used subsequently to test concentration ranges below the level of detection of the Ocean Optics, with more control of excitation wavelength.

23 was dissolved in an aqueous solution containing 150mM NaCl and 10mM pH7 phosphate buffer and serially diluted by factors of 1/3 from an initial concentration of 2.50×10^{-5} to a final concentration of 2.89×10^{-7} M. Spectra were acquired using an excitation wavelength of 300nm. A broad emission centered at 445nm was seen down to 10^{-7} M. A plot of tweezers concentration versus fluorescent emission at 445nm showed a linear correlation in the decrease in emission.

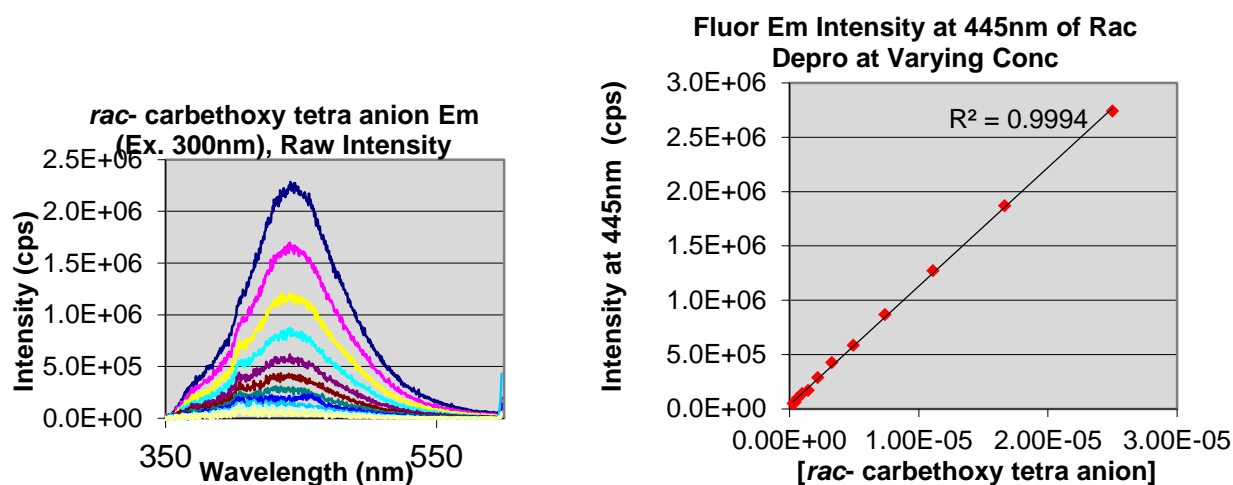


Figure 51: Plot of fluorescent emission (445nm) versus concentration for *rac*- carbethoxy tetra anion **23** tweezers using 300nm excitation

This is consistent with a single species present over this concentration range, either monomer or a dimeric. **23** is expected to dimerize most strongly and if it is dimeric, the $K_{dim} < 3 \times 10^{-7}$ M the limit of detection for this compound with the Fluorolog fluorimeter.

Methyl phosphonate tetra anion isomers 25 and 26

It is expected that the methyl phosphonate tweezers, bearing carboxylate anions on their walls, should not dimerize as readily. To keep ionic strength roughly constant an aqueous solution of 150mM NaCl and 10mM pH7 phosphate buffer was used in the dilution studies. Dimerization behavior was again evaluated using deviation from linearity in fluorescent emission with dilution. Using 300nm excitation the emission spectrum of the binding isomer displayed a fine structure with emission maxima at 405 and 430nm. The *rac*- methyl phosphonate tetra anion isomer **25** was diluted from $2.5 \times 10^{-5} \text{M}$ to $4.3 \times 10^{-7} \text{M}$. A plot of fluorescence at 405nm versus tweezers concentration made and analyzed using the non-linear least squares fit to determine K_{dim} . Although it converged it produced error of equal value to the dimerization constant ($K_{\text{dim}} = 1.9 \times 10^{-4} \text{M} \pm 2.1 \times 10^{-4} \text{M}$) which makes sense as the plot of fluorescence vs. concentration appeared to have only a slight curvature to it, and dimer would be mostly dissociated even at the highest concentration.

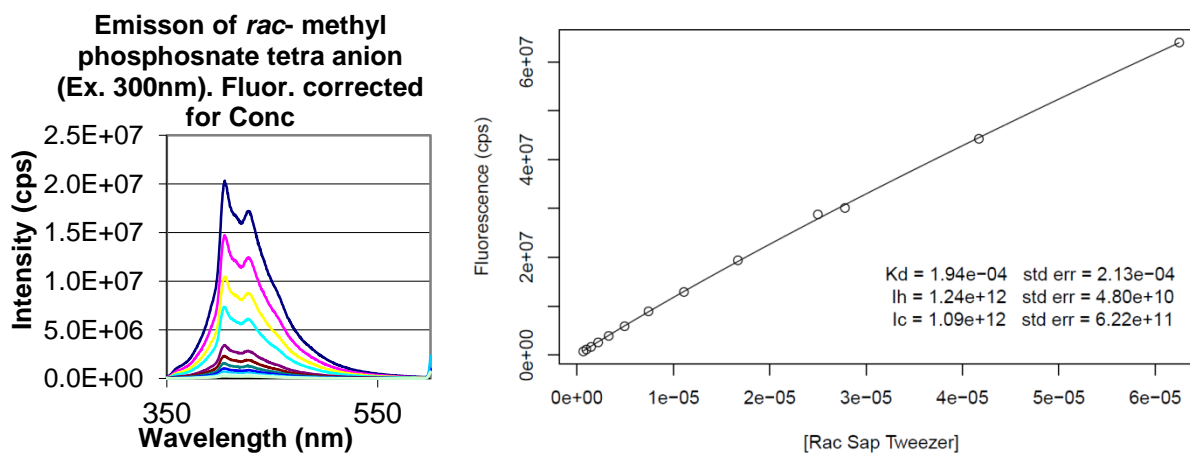


Figure 52: Fluorescence of *rac*- methyl phosphonate tweezer displaying fine structure at 300nm excitation

This result from the concentration range tested again is suggestive of a single species in solution while being diluted. Using 300nm excitation, concentrations above $2.5 \times 10^{-5} \text{M}$ could not be studied because of screening of light. Dilution was repeated using the ionic solution over the range of 2.5×10^{-4} to $1.5 \times 10^{-5} \text{M}$ which was anticipated to be a regime in which dilution would facilitate the change from dimer to monomer. The plot of fluorescent emission at 430nm versus *rac*- isomer concentration produced a line with slightly more curvature resulting in a K_{dim} of $4.5 \times 10^{-4} \text{M} \pm 9.8 \times 10^{-5} \text{M}$ with the standard error being satisfactory for the value for K_{dim} . This suggests a significant association of the tweezers to form a dimer, overcoming a substantial amount of coulombic repulsion in the process.

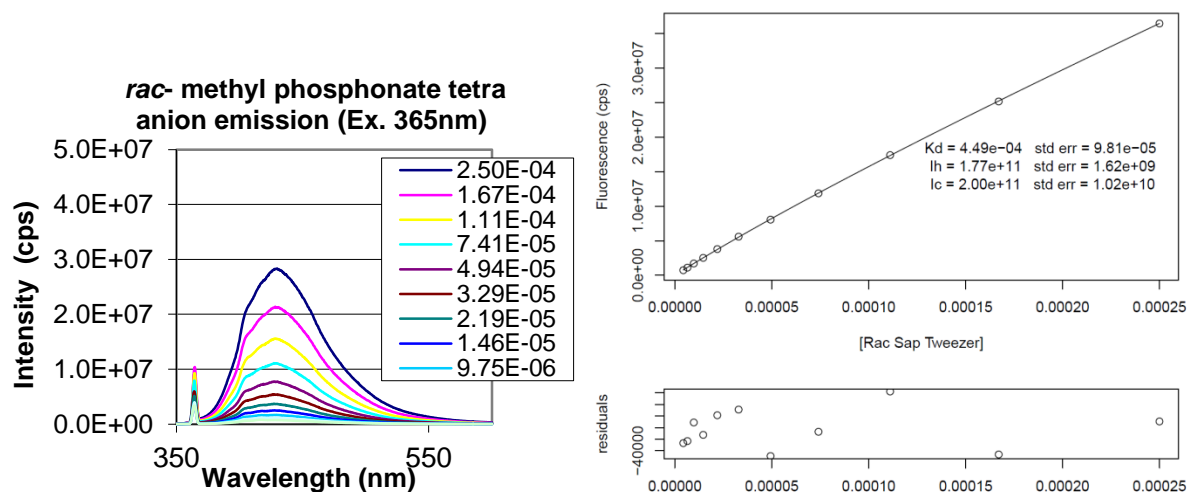


Figure 53: Fluorescent emission and plot of fluorescence (430nm) versus concentration for *rac*- methyl phosphonate tetra anion tweezers 25

From these data it appears that fluorescence spectroscopy is limited in its ability to determine a dimerization constant with low standard error using 300 and 365nm light. 345nm excitation light however may be just right if this dilution is to be repeated as it might allow for solutions of high enough concentration to contain predominantly dimer but not have the rapidly diminishing emission upon dilution so that concentrations lower than $1.5 \times 10^{-5} \text{M}$ can be

investigated. The ideal concentration range to study dimerization would span from 80% dimer to 80% monomer, but this method is limited to 50% dimer. Dimerization was subsequently investigated by UV-Vis spectroscopy and will be discussed in a later section

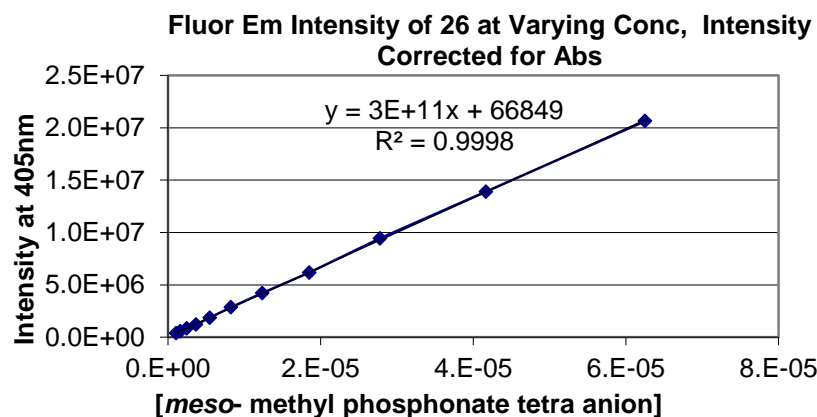


Figure 54: Plot of concentration vs. fluorescence for *meso*- methyl phosphonate isomer **26**

The control isomer, *meso*- methyl phosphonate tetra anion **26**, was diluted from 2.5×10^{-4} M to 4.3×10^{-6} M but only data from 6.25×10^{-5} M and below were used in the plot of emission at 405nm vs. concentration as absorbance values for concentrations above that were above 0.2 using 300nm excitation. As anticipated the resulting plot was linear and was able to converge when fit to a non-linear least squares model producing a K_{dim} of $1.9 \times 10^{-7} \text{ M} \pm 6.8 \times 10^{-6} \text{ M}$. The enormous error range indicates that this behavior is not appropriately modeled by dimerization. The standard amount of error was an order of magnitude larger than the derived value and linear decrease of fluorescence are consistent with the behavior.

To confirm that the *meso*- isomer was not self associating, the fluorescent emission with variable excitation of a 1.8×10^{-4} M solution of the control *meso*- isomer was monitored. As seen previously with the *rac*- isomer **25**, different excitation wavelengths produced different shapes in the fluorescent emission spectrum due to the differences in the absorbance of either the

dimer or monomer. If only a single species is present then a change in fluorescent intensity would be expected with no change in the shape of the emission spectrum.

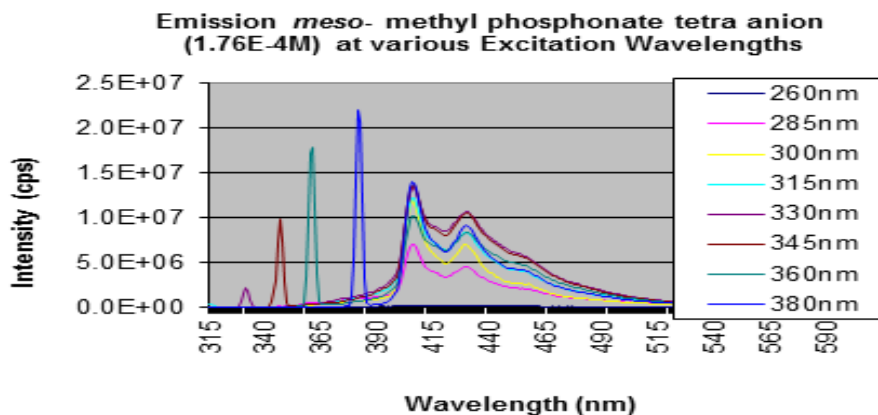


Figure 55: Fluorescent emission of control *meso*- methyl phosphonate tetra anion 26 at various excitation wavelengths plotted to include excitation wavelengths

This is exactly what was observed. Fluorescence increase from 260 to 315nm as screening of the light went away and fluorescent intensity diminished with the longer wavelengths supporting what was observed with NMR that the control *meso*- isomer is not dimerizing when in solution.

Hexa-anions 27 and 28

The final water soluble derivative, the fully de-esterified hexa-anion **27** is expected to dimerize the weakest. It was diluted in the same manner to determine the dimerization equilibrium constant. Using the solution of 150mM NaCl and 10mM pH7 phosphate buffer to dilute to mitigate the change in ionic strength the *rac*- hexa anion was diluted from $2.5 \times 10^{-4} \text{M}$ to $1.7 \times 10^{-7} \text{M}$ using 345nm excitation. The emission at 405nm versus tweezers concentration produced the greatest deviation from linearity in the plot and when fit to the dimerization equation it produced a $K_{\text{dim}} = 1.2 \times 10^{-4} \text{M} \pm 9.0 \times 10^{-6} \text{M}$.

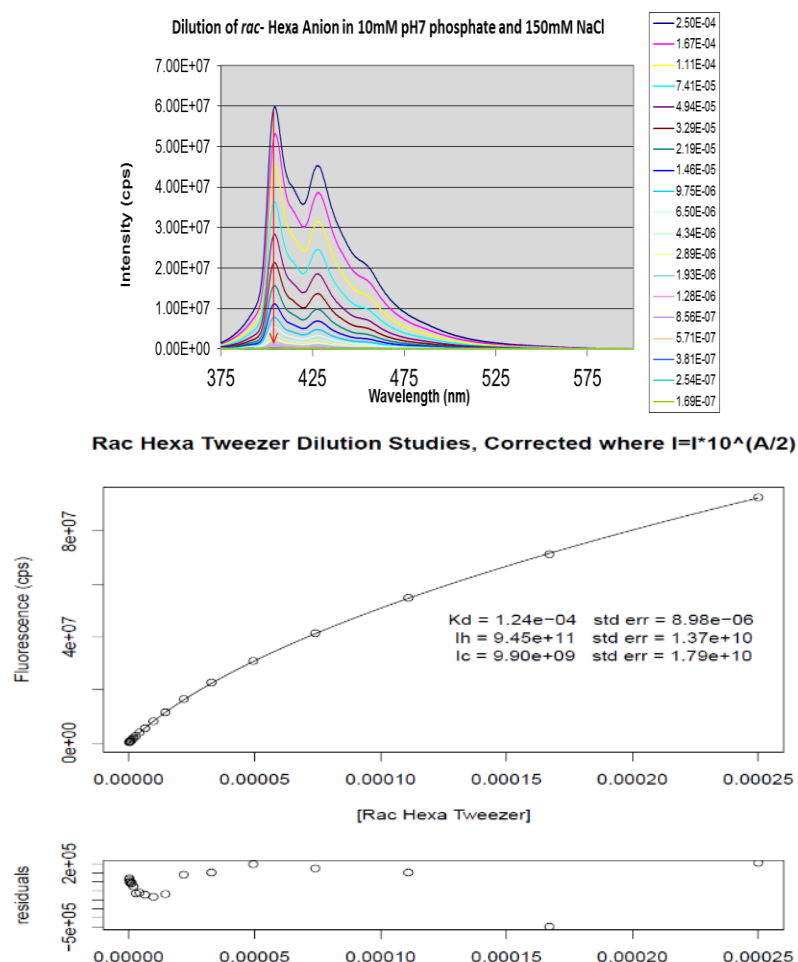


Figure 56: Fluorescent emission and plot of emission (405nm) vs. concentration for *rac*- hexa anionic tweezers using 345nm excitation

From the small error in the K_{dim} value it shows that the model is appropriate in describing the observed phenomenon. The binding *rac*- hexa anion **27** also has the weakest K_{dim} of the three due to the not only the carboxylates on the edge of the tweezers providing the coulombic barrier but also from having the greatest amount of negative charge per tweezers molecule. The average amount of negative charge per hexa- anion in solution at pH7 is presumably that of a penta-anion when comparing it to other *bis*-aminophosphonic acids.¹⁰¹ Overcoming coulombic repulsion to dimerize a penta-anion at 10^{-4} M implies a significant association.

The control *meso*- isomer **28** was evaluated using the same protocol for dilution monitored by fluorescent emission as the *rac*- isomer. When the plot of emission at 405nm versus *meso*- isomer concentration was fit it was able to converge but produced a value or error greater in magnitude for the calculated K_{dim} . This again demonstrated that dimerization is a poor model for characterizing the decrease in fluorescence and that the control *meso*- isomer does not complex with itself in aqueous media.

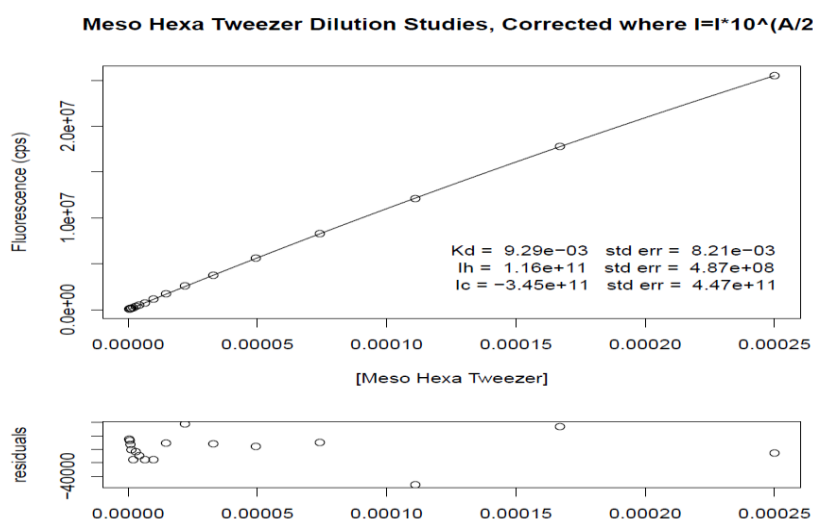


Figure 57: Plot of fluorescent emission (405nm) versus concentration for the control *meso*- hexa anionic isomer using 345nm excitation

3. Analysis by UV-VIS Spectroscopy

Methyl phosphonate tetra anion **25** and **26**

In the effort to find a more convenient alternative to fluorescence for determining dimerization UV-Vis absorbance was investigated. Absorbance spectra for the binding *rac*- (**25**) and control *meso*- (**26**) isomers were monitored over a concentration range of $4.4 \times 10^{-4} \text{ M}$ to $3.4 \times 10^{-6} \text{ M}$ using water containing 150mM NaCl and 10mM pH7 phosphate buffer as the diluent.

Extinction coefficients were calculated for each wavelength by dividing the absorbance spectrum by the concentration of the sample. Plots of wavelength versus these epsilon values at each concentration were constructed. What was seen from this was that at 297nm there were deviation in epsilon for the *rac*- isomer whereas no deviation was seen in the *meso*- isomer at the same wavelength providing another spectroscopic example a difference in behavior for the binding *rac*- isomer **25** and control *meso*- isomer **26**.

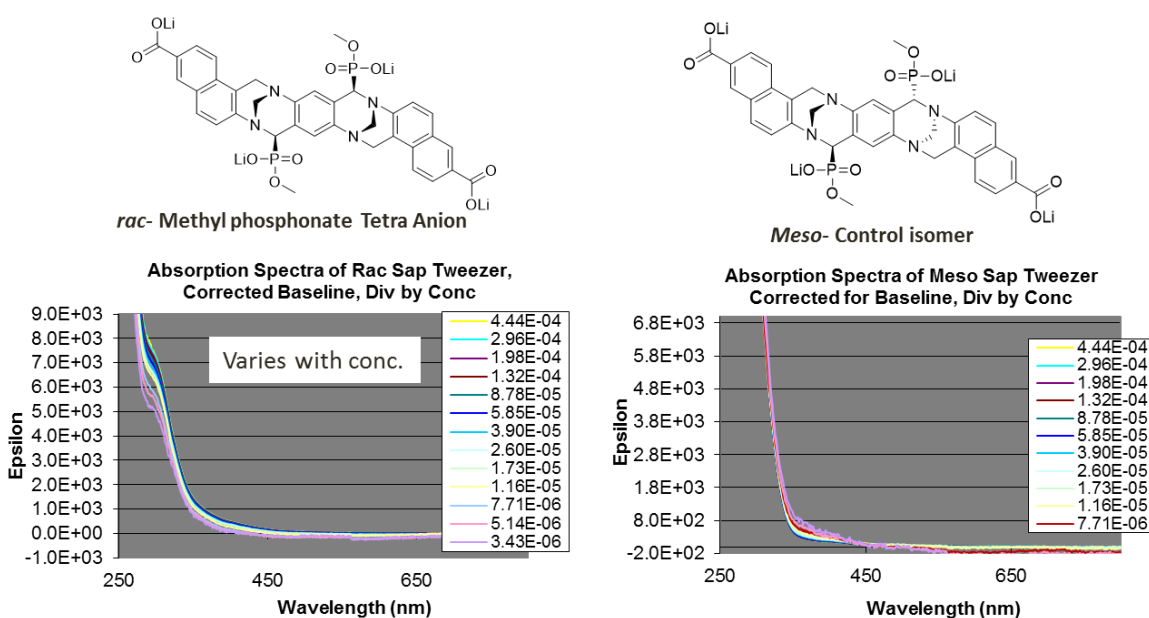


Figure 58: Plot of wavelength vs. epsilon for the binding **25** (left) and the control **26** (right) methyl phosphonate tetra anion isomers

The concentration **25** versus calculated epsilon was plotted and fit using non-linear least squares. The equation used was the same as that for determining K_{dim} using NMR except epsilon values were used instead of chemical shifts. Unfortunately, when fit it produced errors larger than the K_{dim} value but this is not due to dimerization being a poor model. When analyzing the fit, it showed that the majority of the data did not fall on the actual curvature which is required for an accurate calculation. If this dilution study were to be repeated,

absorbance data at concentrations below $7 \times 10^{-6} \text{ M}$ need to be acquired to collect more data points and to get closer to the predicted K_{dim} value.

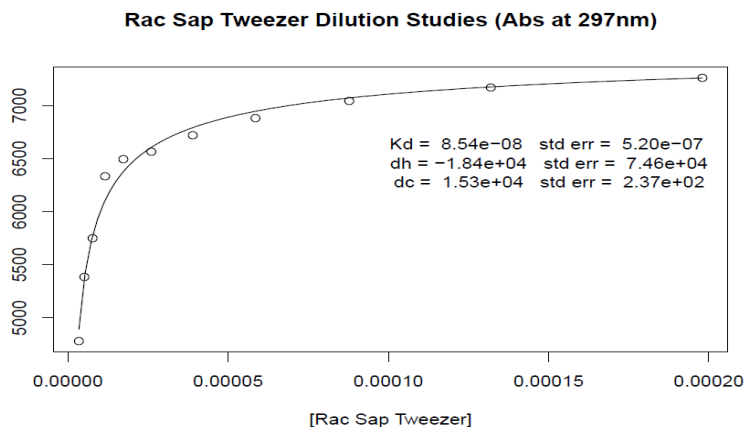


Figure 59: Plot of concentration vs. epsilon for 25 fit by non-linear least squares

E. Binding Studies of Molecular Receptor by Small Molecule Titration

Titration of the water soluble *rac*- binding molecular tweezers and the *meso*-nonbinding control isomer were carried out by fluorescence spectroscopy, monitoring the decrease in fluorescent emission of the tweezers isomer upon titration of the small molecule guest. Guest solutions contained the tweezers isomer at the same concentration as the solution of tweezers isomer being evaluated as not to dilute the tweezers isomer upon addition of the titrant. Fluorescent emission of the host was monitored at a particular wavelength with increasing guest concentration and fit to the equation below which models a 1:1 binding interaction and fit using non-linear least squares to determine the dissociation constant (K_d) of the complex. Adherence to this model would be consistent with decrease in fluorescence by static (intramolecular) quenching. This could be confirmed with fluorescence lifetime

measurements of the host as the fluorescence lifetime of the complex will not change with increasing concentration of the small molecule.

$$\begin{array}{l}
 \text{H} + \text{G} \xrightleftharpoons[\text{K}_d]{\text{K}_a} \text{C} \\
 \\
 \text{K}_d = \frac{[\text{H}][\text{G}]}{[\text{C}]} \qquad \text{K}_d = \frac{[\text{H}_o - \text{C}][\text{G}_o - \text{C}]}{[\text{C}]} \rightarrow [\text{H}_o][\text{G}_o] - ([\text{H}_o] + [\text{G}_o])[\text{C}] + [\text{C}]^2 = \text{K}_d[\text{C}] \\
 \text{H}_o = [\text{H}] + [\text{C}] \\
 \text{G}_o = [\text{G}] + [\text{C}] \\
 \text{I} = \text{I}_o[\text{H}] + \text{I}_c[\text{C}] \\
 \\
 \text{I} = \text{I}_c([\text{H}_o] - [\text{C}]) + \text{I}_c[\text{C}] = \text{I}_o[\text{H}_o] - \text{I}_o[\text{C}] + \text{I}_c[\text{C}] = \text{I}_o[\text{H}_o] + (\text{I}_c - \text{I}_o)[\text{C}] \\
 \rightarrow \text{I}_o[\text{H}_o] + \frac{\text{I}_c - \text{I}_o}{2} ([\text{H}_o] + [\text{G}_o] + \text{K}_d) - \sqrt{([\text{H}_o] + [\text{G}_o] + \text{K}_d)^2 - 4[\text{H}_o][\text{G}_o]}
 \end{array}$$

Figure 60: Derivation of equation used to determine K_d in small molecule binding titrations where H=host, G=guest, and C=complex

The fluorescent data were also fit to the Stern-Volmer equation which models dynamic (intermolecular) quenching of fluorescence with adherence to this model is taken as evidence of intermolecular quenching. Use of fluorescent lifetime measurements could be used if required to confirm dynamic quenching as the fluorescent lifetime of the host molecule will decrease with increasing concentration of the small molecule.

$$\text{Stern-Volmer Equation} \quad \frac{I_o}{I} = 1 + kt[Q]$$

Figure 61: Stern-Volmer equation where I_o = initial fluorescence, I = fluorescence with quencher present, k =quencher rate coefficient, and t =lifetime of the excited state of the emitting molecule

1. Carbethoxy tetra anion isomers **23** and **24**

The titrations of **23** with the small molecules described below were conducted using an Ocean Optics SD2000 fiber optic spectrometer. The titrations of the water soluble tweezers were conducted at concentrations (5×10^{-5} and 1×10^{-5} M) where the self associated dimer predominates. As a consequence, the titrants are presumably in competition with the binding pocket of the dimer.


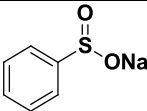
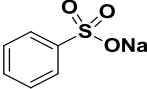
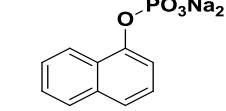
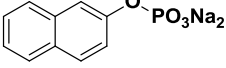
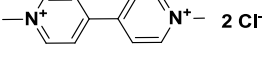
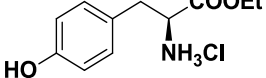
Substrate	Apparent K_d (M) (Titration Medium)
	$2.3 \times 10^{-2} \pm 1.6 \times 10^{-3}$ (10mM pH7 phosphate buffer)
	$3.7 \times 10^{-2} \pm 1.6 \times 10^{-2}$ (10mM pH7 phosphate buffer)
	$>5.5 \times 10^{-2}$ (10mM pH7 phosphate buffer) $3.2 \times 10^{-2} \pm 1.2 \times 10^{-1}$ (10mM pH7 phosphate buffer)
	$1.2 \times 10^{-3} \pm 3.5 \times 10^{-4}$ (10mM pH7 phosphate buffer) $1.4 \times 10^{-3} \pm 4.8 \times 10^{-4}$ (10mM pH7 phosphate buffer)
	$8.3 \times 10^{-4} \pm 3.3 \times 10^{-4}$ (10mM pH7 phosphate buffer) $2.6 \times 10^{-3} \pm 7.0 \times 10^{-4}$ (10mM pH7 phosphate buffer)
	$3.6 \times 10^{-3} \pm 3.0 \times 10^{-4}$ (10mM pH7 phosphate buffer) $2.4 \times 10^{-3} \pm 2.7 \times 10^{-4}$ (10mM pH7 phosphate buffer)
	$3.0 \times 10^{-3} \pm 7.0 \times 10^{-4}$ (100mM pH7 phosphate buffer)

Table 2: Observed dissociation constants from the titration of the proposed *rac*- carbethoxy tetra anionic tweezers **23 dimer**

Hydroquinone and sodium benzenesulfonate were determined to not bind with the dimer. It was concluded that hydroquinone was not able to bind strongly enough into the molecular tweezers to compete with the dimer as evidenced by its adherence to Stern-Volmer behavior. The sodium benzenesulfonate was speculated to not bind because it has too much

steric bulk in proximity to the benzene group. Results from sodium benzenesulfinate titration are suggestive as being able to intercalate into the binding cavity as it did not display a Stern-Volmer relationship but the calculated dissociation constant had fifty percent error. The naphthylphosphates and methyl viologen both appear to bind as they both fit to the binding equation and both deviate from Stern-Volmer behavior. Interestingly enough, both of these substrates have dissociation constant on par with one another yet they are oppositely charged supporting the hypothesis that the carbethoxy tetra anion binding isomer is dimeric.

The preliminary study was continued by selecting the cationic guests, methyl viologen and L-tyrosine ethyl ester hydrochloride, and performing titrations with the *meso*- nonbinding control isomer **24** to determine if the differences in fluorescent quenching would demonstrate binding behavior in the *rac*- binding isomer.

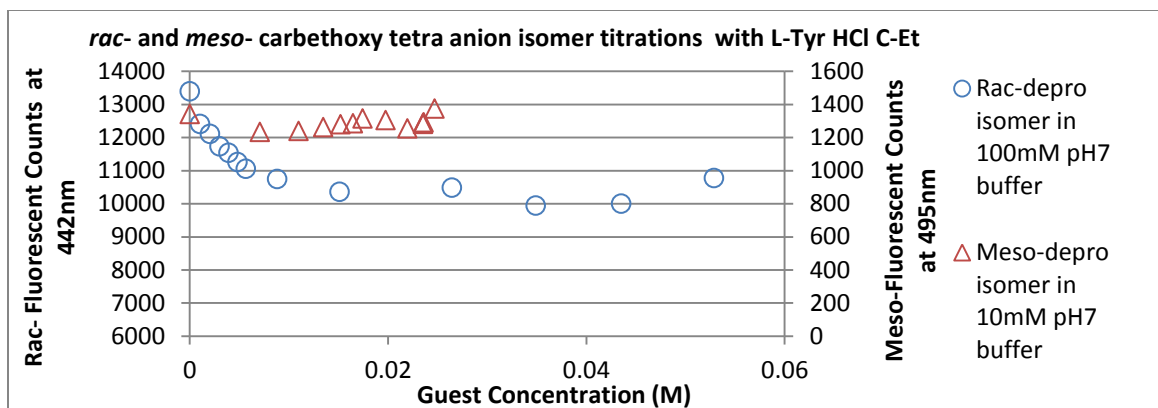


Figure 62: Titration of *rac*- and *meso*- carbethoxy tetraanion isomers with L-Tyr Et ester HCl

When the concentration of L-Tyr ethyl ester hydrochloride versus fluorescent intensity of the tweezers isomers were plotted on the same graph **23** seemed to exhibit binding behavior by the curvature in decrease in fluorescence and its deviation from linearity in the Stern-Volmer plot. From the results of later titrations with cationic guests and the methyl

phosphonate form of the molecular tweezers it was concluded that the guest molecule was likely to be associated with the dimer coulombically not being inserted into the binding isomer's cavity. The fluorescence of **24** stayed fairly constant but increased with increasing concentration of the titrant. It also did not exhibit Stern-Volmer behavior as the value of I_0/I decreased, not increased, with increasing guest concentration. This behavior is counterintuitive as this data suggests that addition of L-Tyr ethyl ester HCl is able increase the fluorescence of the *meso*- isomer by some mechanism as the guest does not emit at the excitation wavelength used to irradiate the non-binding isomer. It is speculated that the *meso*- isomer **24** is not complexing with the guest molecule but the results unfortunately do not provide the evidence for it.

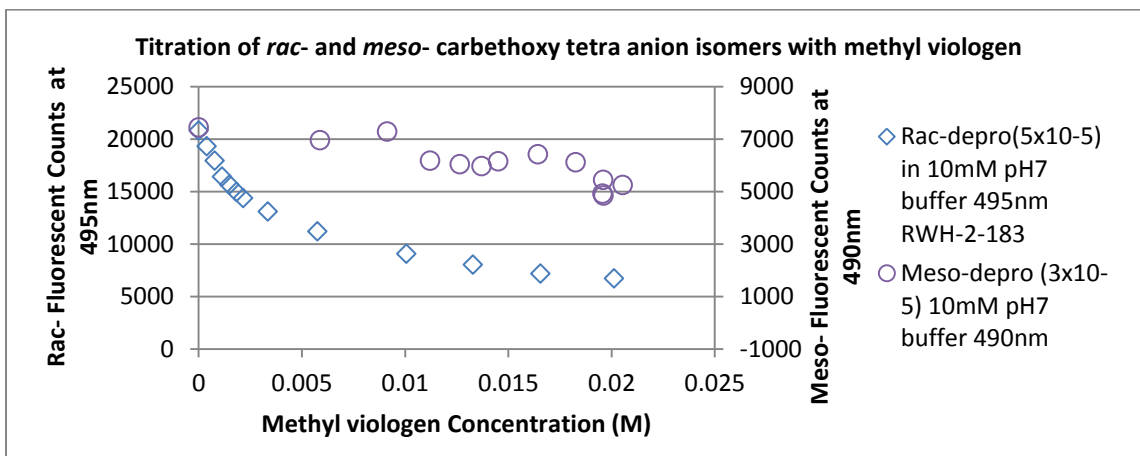


Figure 63: Titration of *rac*- and *meso*- carbethoxy tetraanion isomers with methyl viologen

Titration of the *rac*- and *meso*- carbethoxy tetra-anionic isomers displayed similar fluorescent behavior when titrated with methyl viologen. *Rac*- tweezers **23** appears to be binding methyl viologen by fitting to the 1:1 binding equation and not following Stern-Volmer behavior. However, the quenching of fluorescence for the binding isomer appears to be extrapolating to zero with increasing guest concentration. This is rationalized by having not only

the intramolecular form of quenching occurring but also the quenching of the fluorescence of the complex by intermolecular collision and can be seen in the later half of the titration by an apparent linear decrease in emission. What was expected to be seen on binding however would be a shift in fluorescent emission by formation of a charge transfer complex between the two but this phenomenon was not observed. This suggests that the methyl viologen is associating tightly to the exterior of the tweezers dimer in the low ionic strength of the titration medium to form a complex that is an ion pair. The control isomer **24**'s behavior was consistent with its structure by an overall linear decrease in fluorescence, non-convergence to the binding isotherm, and adherence to the Stern-Volmer relationship. Interestingly when compared to the *meso*- control of the methyl phosphonate tetra-anion, whose decrease in fluorescent emission when titrated with cationic guests mimicked binding, the *meso*- carbethoxy analogue did not. There is no explanation for the difference in the behavior at this time.

As the binding affinities afforded from the titrations were of the same approximate value, it was concluded that the guests were not binding into the cavity of the tweezers.

2. Methyl phosphonate tetra anionic isomers 25 and 26

Fluorescent titrations were conducted on a Fluorolog-3 Model FL3-22 by Horiba Jobin-Yvon using nanopure water as the titration medium. Concentrations used for titration for the *rac*- binding and *meso*-control isomers were either 5.0×10^{-6} or 5.0×10^{-7} M which were assumed to be predominated by monomeric species. This assumption was supported by observing the fluorescent emission of **25** at various excitation wavelengths. If a single species is present,

change in excitation wavelength should change the intensity of the emission but not change the shape of the emission profile which is what was observed.

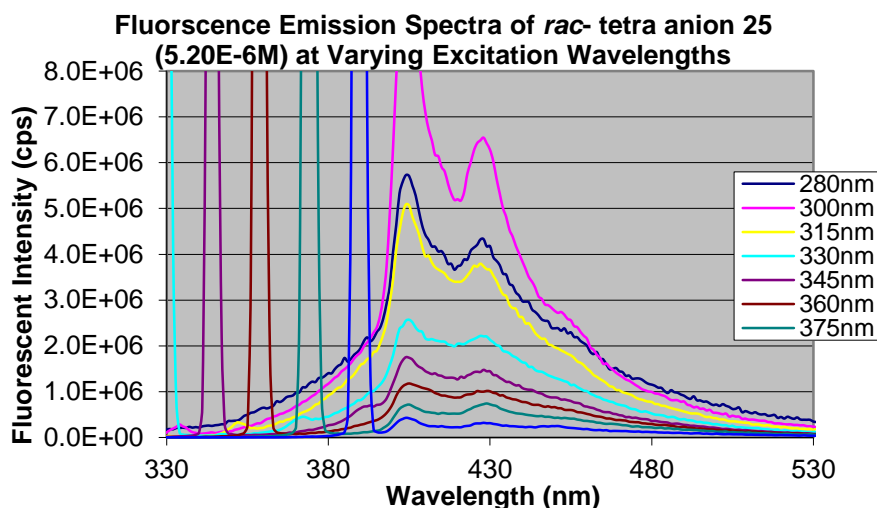


Figure 64: Fluorescent emission of tetra anion tweezers 25 with varying excitation wavelength plotted to include excitation wavelengths

All of the small molecules screened were fit by non-linear least squares to a 1:1 binding equation and did not adhere to intermolecular quenching as described by the Stern-Volmer equation. Titration of neutral and anionic small molecule appeared to bind weakly with K_d 's on the order of 10^{-2} M which was attributed to the small amount of aromatic surface in the benzene sized substrates. For this reason it was expected that 1-naphthylacetic acid would bind stronger than sodium phenylacetate but appeared to bind with the same affinity. This was attributed to the sparing solubility of the 1-naphthylacetic acid in nanopure water which prohibited a solution of sufficient concentration to follow probe the guest. If this material were to be titrated in the future it is suggested to form a salt of the 1-naphthylacetic acid to circumvent the limitation in solubility. The cationic guests afforded dissociation constants on average of an order of magnitude stronger when compared to the other titrants for 1-Me nicotinaminium choride and 100x stronger for methyl viologen.

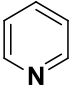
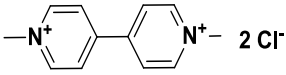
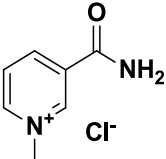
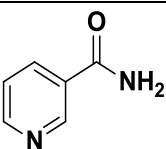
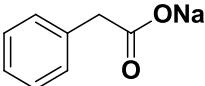
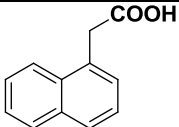
Substrate	Apparent K_d (M)(Titration Medium)
	$5.9 \times 10^{-2} \pm 3.8 \times 10^{-3}$ (NP Water)
	$2.1 \times 10^{-4} \pm 1.6 \times 10^{-5}$ (NP Water)
	$3.6 \times 10^{-3} \pm 1.2 \times 10^{-4}$ (NP Water) $2.5 \times 10^{-3} \pm 1.4 \times 10^{-4}$ (NP Water) $6.0 \times 10^{-3} \pm 5.0 \times 10^{-4}$ (150mM NaCl, 10mM pH7)
	$3.8 \times 10^{-2} \pm 2.2 \times 10^{-2}$ (NP Water)
	$1.8 \times 10^{-2} \pm 3.1 \times 10^{-3}$ (NP Water)
	$4.3 \times 10^{-2} \pm 4.5 \times 10^{-2}$ (NP Water)

Table 3: Apparent K_d values for small molecules titrated with binding *rac*- methyl phosphonate tetra anion tweezers **25**

These results were less encouraging when the small molecules were evaluated against the control isomer **26**. For the non-cationic guests, the shape of the plot of decreasing fluorescence versus titrant concentration and the total decrease in fluorescence were eerily similar save for the last few data points where they began to diverge at the highest concentrations. The plots of **26** had the same slight curvature as the plots for the binding isomer **25** did and for this reason were able to fit to the 1:1 binding equation. These control isomer plots were analyzed for a Stern-Volmer relationship and showed inconsistent behavior. Sodium phenylacetate and nicotinamide showed Stern-Volmer correlation where pyridine did not. With conflicting data for the behavior of **26** in acting as a negative control and noisy data from the minimal response in quenching of fluorescence in the concentration ranges tested for

the small molecules the behaviors between the two isomers could not be distinguished from one another with any confidence. This could possibly be accomplished by future researches with increasing the concentrations of titrant solutions as well as increasing the ionic strength of the titration medium.

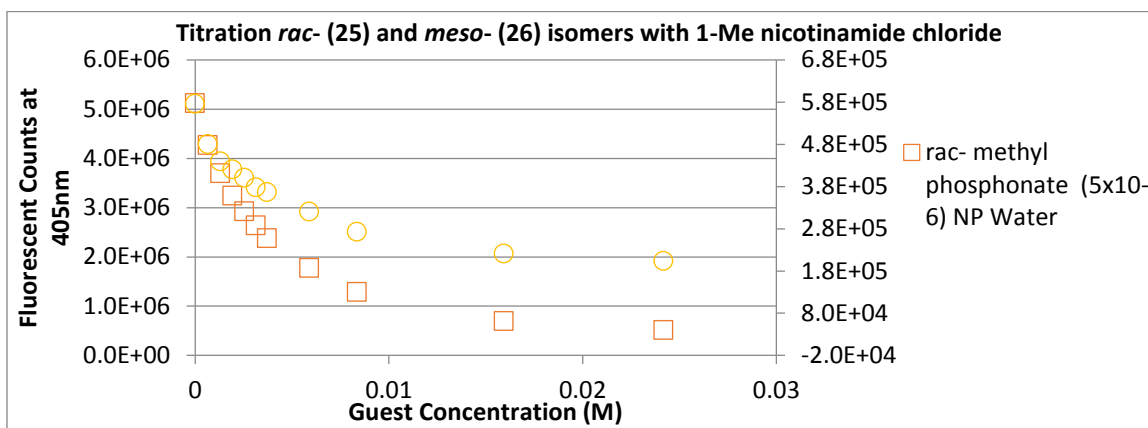


Figure 65: Titration of binding *rac*- and *meso*- methyl phosphonate isomers with 1-Me nicotinamide chloride in nanopure water

In titrations using the cationic guests methyl viologen and 1-Me nicotinamide chloride the binding *rac*- isomer **25** and the control *meso*- isomer **26** looked to be behaving in the same manner as if binding was occurring in both cases. For titrations with methyl viologen both isomers deviated from linearity when modeled by the Stern-Volmer and both converged to the binding equation with $2.1 \times 10^{-4} \text{M} \pm 1.6 \times 10^{-5} \text{M}$ and $6.2 \times 10^{-4} \text{M} \pm 8.7 \times 10^{-5} \text{M}$ for the binding *rac*- isomer and the control *meso*- isomer respectively. Shown below is the data from the titration of the binding *rac*- methyl phosphonate tetra anion tweezers with 1-Me nicotinamide chloride in nanopure water.

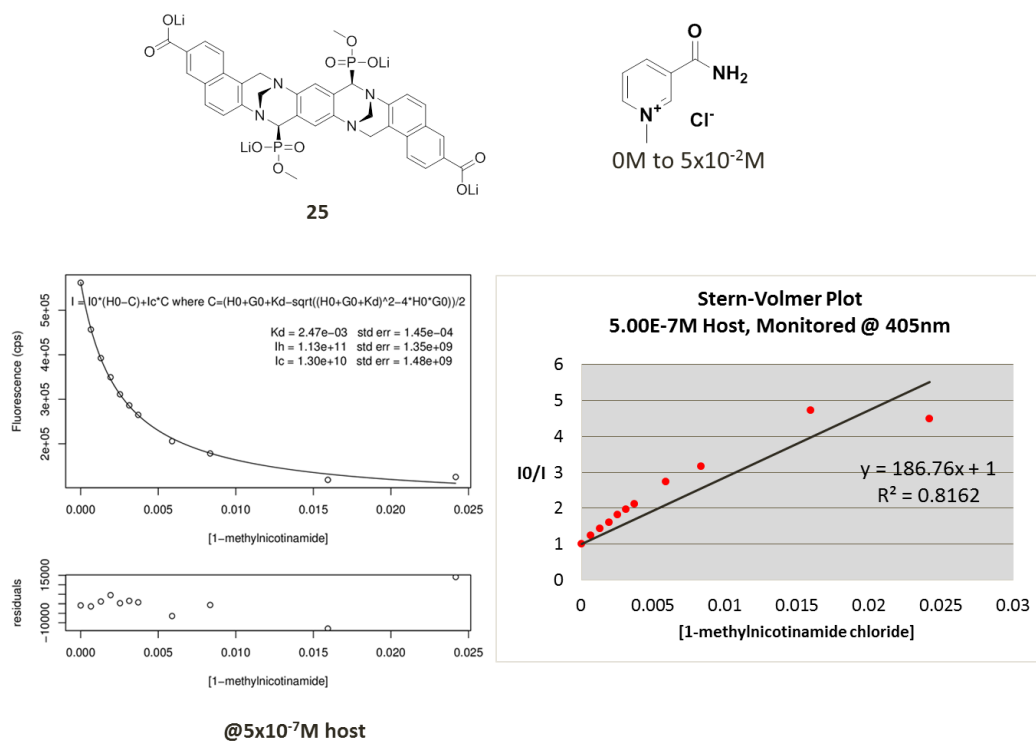


Figure 66: 1:1 binding and Stern-Volmer plot for titration of *rac*-methyl phosphonate tweezers **25 with 1-Me nicotinamide chloride in nanopure water**

The small amount of error and the even distribution of errors as plotted by the residuals in the 1:1 binding fit show that this is a good description for binding interaction of the guest molecule. The curvature of the I_0/I values with increasing guest concentration when compared to the linear regression for the Stern-Volmer plot demonstrate that the decrease in fluorescence observed is not described well by an intermolecular quenching model.

When the negative control *meso*- isomer **26** was titrated with the same protocol it quenched fluorescence in an apparent non-linear fashion but produced errors equal to the calculated K_d when fit to the binding isotherm demonstrating that intramolecular quenching is not a good model as expected for the isomer that lacks the cavity to allow intercalation of a small molecule. However, when the data was evaluated by the Stern-Volmer relationship it demonstrated the same behavior was the binding isomer. It was from the culmination of these

results in titrating cationic guest that the ionic strength of the titration medium was thought to be of import when trying to demonstrate the differences in the isomers of the molecular receptors. In the very low ionic strength condition of nanopure water it was postulated that the cationic guest would be able to mimic the spectroscopic profile of static (intramolecular) quenching by forming a tight ionic pair with the tetra anionic host which would be interesting as the coulombic attraction between the charged species would be more stable than the solvated ion in water.

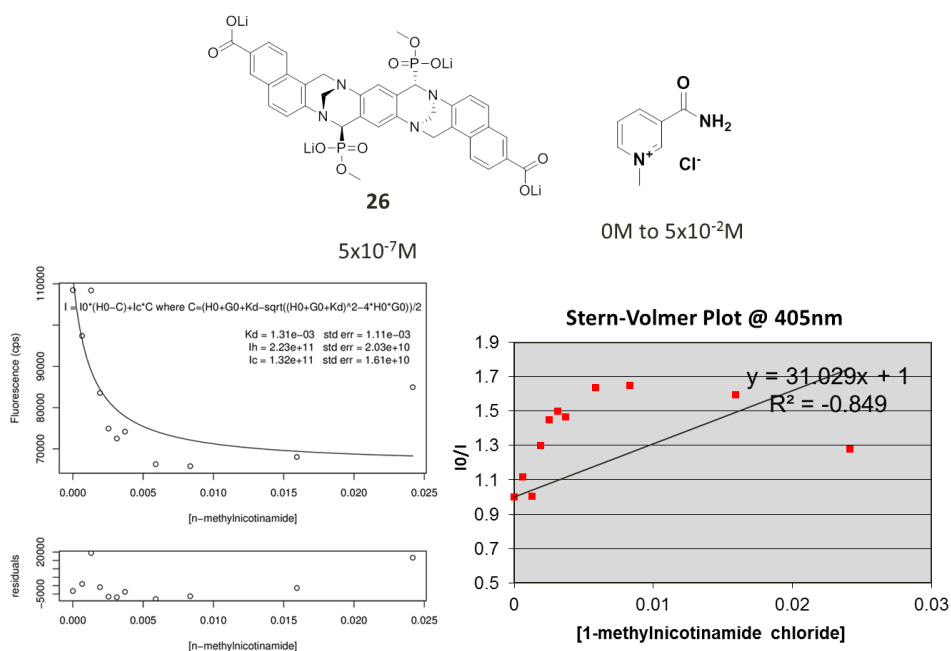


Figure 67: 1:1 binding and Stern-Volmer plot for titration of control *meso*- methyl phosphonate tetra anion isomer with 1-Me nicotinamide chloride in nanopure water

This association was explored using ^1H NMR spectroscopy to compare the chemical shifts of free **26**, free 1-Me nicotinamide chloride, and a 1:1 mixture of the two at a concentration similar to the end points of the titration condition in pure D_2O and D_2O of increased ionic strength. The ionic strength of the D_2O was modified by addition NaCl to

160mM concentration which was approximation of the 150mM NaCl, 10mM pH7 phosphate buffer used in subsequent titration.

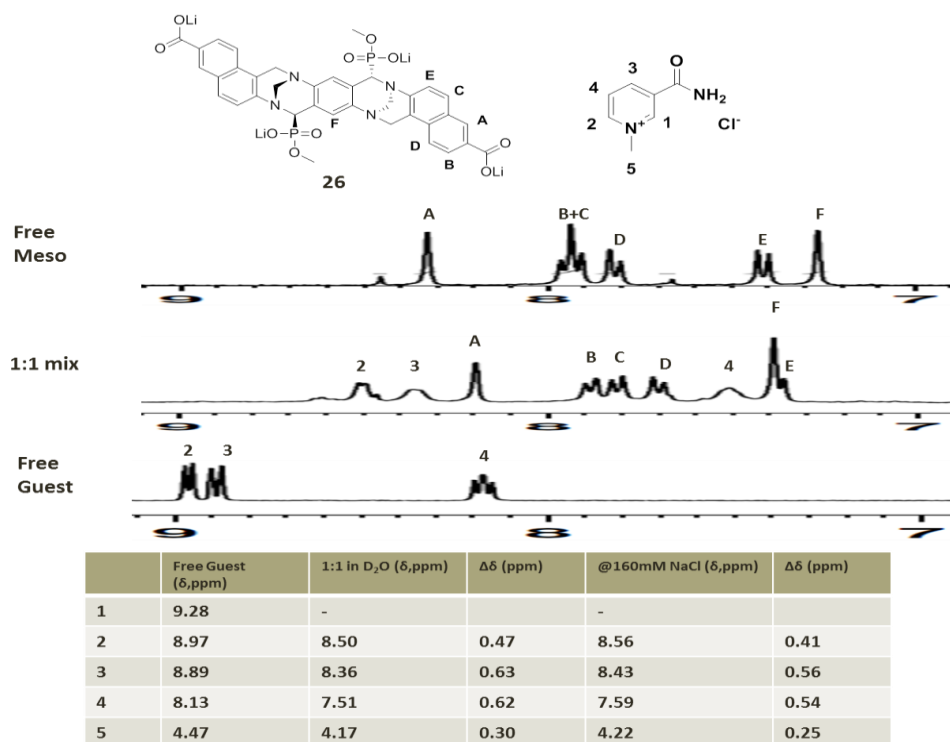


Figure 68: ¹H NMR comparison of the aromatic region of free *meso*- methyl phopshonate tetra anion 26, free 1-Me nicotinamide chloride, and a 1:1 mixture of the two at 1.8×10^{-2} M concentration

When the components were comined in a 1:1 ratio in pure D₂O large upfield shifts were observed in the 1-Me nicotinamide Cl and all but one of the signals in the aromatic region of the *meso*- control. Upon mixing it was also observed that while the *meso*- isomer's signals remained sharp while those of the nicotinamide became broadened, consistent with its associating. From the upfield shifts of the hydrogens in the naphthyl wall of the *meso*- compound along with the concurrent down field shift of hydrogen F that resides on the central benzene ring it is proposed that the nicotinamide salt is associated on the face of the

naphthylene on the opposite side of the phosphonate moiety and perpendicular to the benzene ring. The 1-Me nicotinamide Cl would need to be on the opposite face was when the complex was made using molecular models the 1-Me nicotinamide Cl would not be in proximity to the hydrogens on the benzene core. The ionic strength of the mixture was then adjusted to 160mM strength by the addition of NaCl with only minor downfield shifts for the 1- Me nicotinamide chloride in the ^1H spectrum which shows that even with increased ionic strength the cationic guest and the tetra anionic isomer are still closely associated.

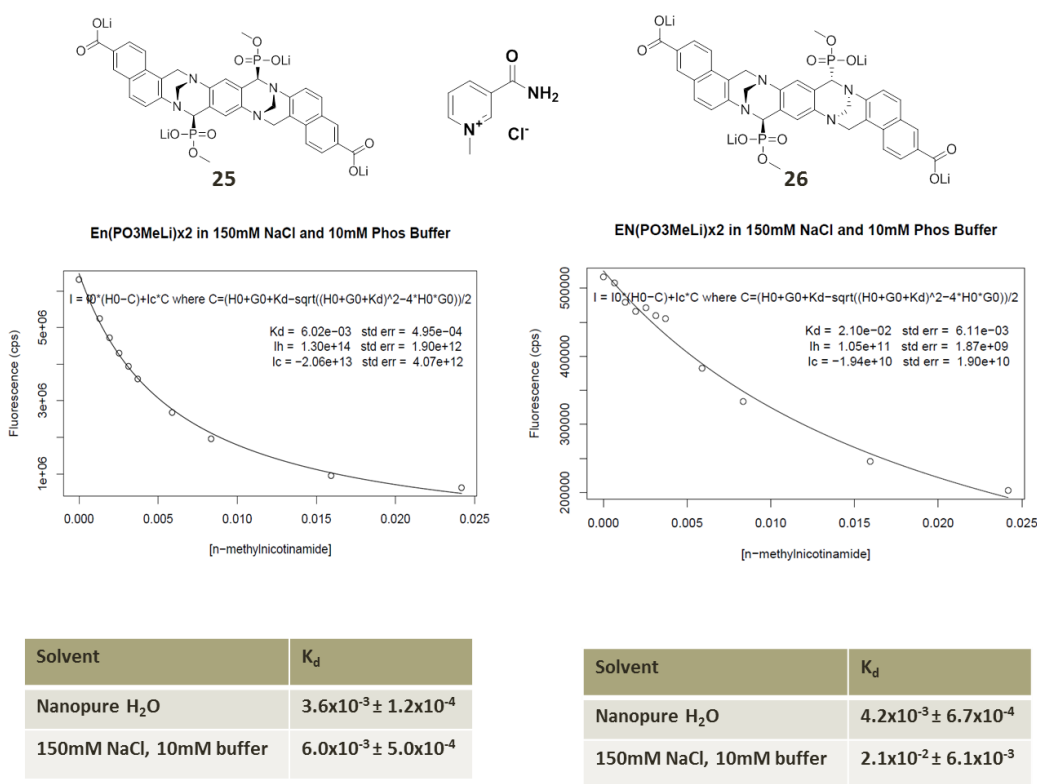


Figure 69: Comparison of K_d for binding 25 and control 26 isomer to 1-Me nicotinamide chloride in nanopure water and 150mM NaCl, 10mM pH7 phosphate buffer

The titration of the methyl phosphonate tetra anion isomer with 1-Me nicotinamide chloride was conducted again but now in aqueous 150mM NaCl, 10mM pH7 phosphate buffer so that the ionic strength of the medium would not appreciable change over the course of the

experiment. What was found was in this solution the dissociation constant for the binding *rac*-isomer decreased by a factor of 1.7 and for the control *meso*- isomer decreased by a factor of 5 which is evidence for the binding isomer forming an inclusion complex with the guest. If the association of the binding isomer was strictly coulombic it would be expected to have its apparent K_d value diminished by the same amount as the control *meso*- isomer. When the K_d values of the binding and control isomer were compared to one another under the new ionic conditions the binding isomer was able to associate with the 1-Me nicotinamide Cl 3.5x stronger whereas in nanopure water the two isomers associated with the guest molecule with the same affinity. This too was taken as evidence as a demonstration of the difference in behavior of the binding isomer **25** and the control isomer **26**.

3. Hexa-anionic isomers **27** and **28**

The best chance of binding a small molecule into the cavity of the *bis*-Tröger's Base tweezers would be with the hexa-anionic derivative. As this form has a dimer that is held together the weakest, it can be titrated at concentrations where one is confident that the tweezers exists as a monomer. In pH9 borate buffer, 1-Me nicotinamide chloride appeared to associate with approximately the same affinity to the hexa anion **27** ($K_d = 8.2 \times 10^{-3}$ M) as it did to the *rac*- methyl phosphonate tetra anion tweezers under the same ionic strength regime. Borate buffer was used to ensure that the hexa-anionic tweezers were fully deprotonated so there was no ambiguity to the charge on the host molecule.

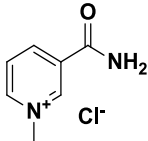
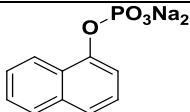
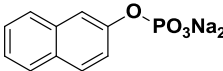
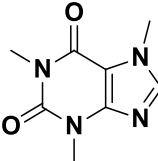
Substrate	Apparent K_d (M) (Titration Medium)
	$8.2 \times 10^{-3} \pm 1.0 \times 10^{-3}$ (150mM NaCl, 10mM pH9 borate buffer)
	$7.2 \times 10^{-3} \pm 4.4 \times 10^{-3}$ (150mM NaCl, 10mM pH7 phosphate buffer)*
	ambiguous
	$4.2 \times 10^{-4} \pm 4.2 \times 10^{-5}$ (150mM NaCl, 10mM pH9 borate buffer)

Table 4: Apparent K_d values substrate association to binding *rac*- hexa anionic tweezers at 5.0×10^{-6} M concentrations. * K_d generated by fitting the curvature in the data to the 1:1 binding equation

Titrations of the *rac*- tweezers **27** and the *meso*- non-binding control **28** with caffeine provided the best evidence for the discrimination between the two. Upon addition, the fluorescence of the binding isomer decreased sharply initially and appeared to reach and asymptotic value. This data did not exhibit Stern-Volmer behavior and when fit this data was fit to the non-linear least squares fit it converged to generate a K_d of 4.2×10^{-4} M which is similar to binding affinity reported by other synthetic acyclic receptors.⁴⁴ In contrast, when the *meso*- hexa anionic **28** was exposed to increasing concentrations of caffeine its fluorescent emission vacillated around a constant value before decreasing, increased at the end of the addition, and did converge when fit to the 1:1 binding equation. This increase in fluorescence is not understood at the present time as the absorbance of caffeine at 365nm is 0.002 and thus should not lead to emission from the guest. However, as their behaviors are so different one can be confident that **27** is actually binding to caffeine presumably via intercalation between its naphthalene walls.

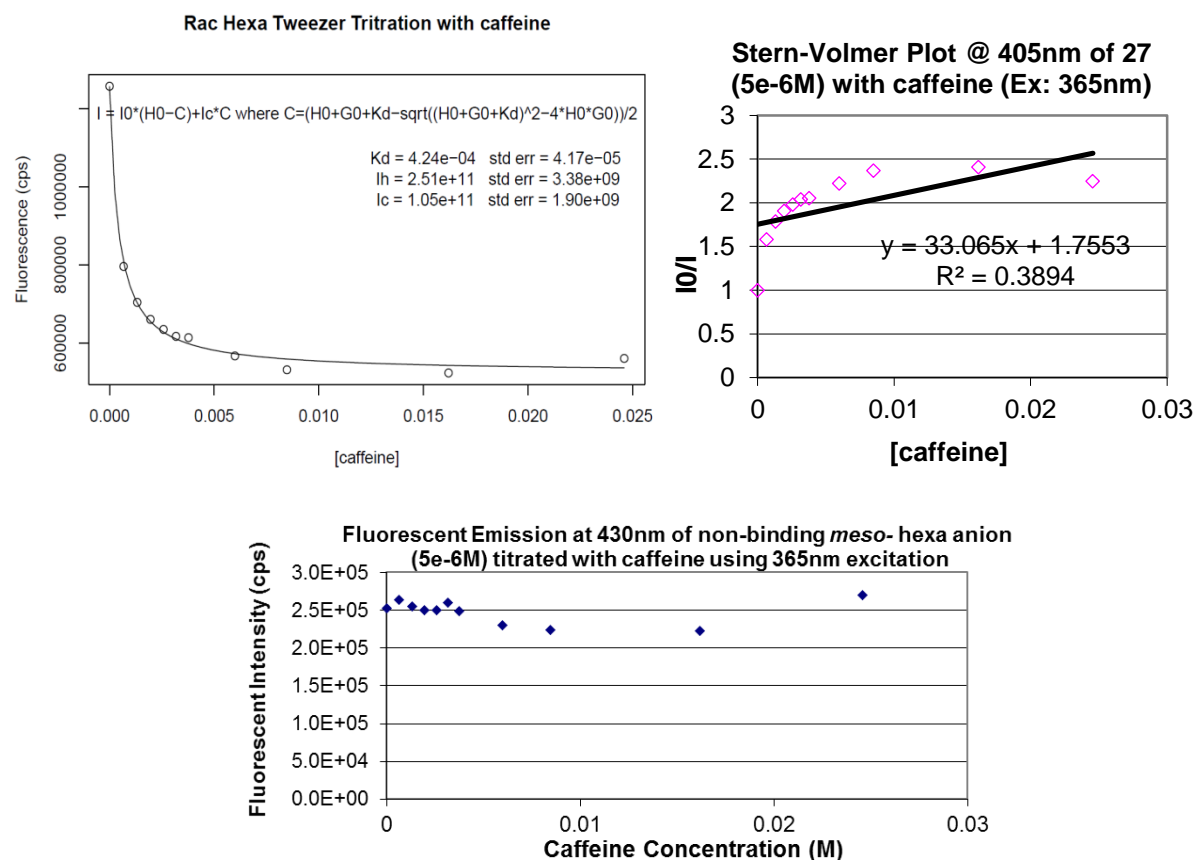


Figure 70: Comparison of fluorescent emissions of the binding *rac*- hexa anionic tweezers (top) and the non-binding *meso*- control isomer (bottom). Stern-Volmer plot also included for binding isomer 27

When titrations of **27** were carried out in water containing 10mM pH7 phosphate buffer, 150mM NaCl with 1- or 2-naphthylphosphate disodium salt the data acquired by fluorescent titrations were ambiguous to say the least. When the 1-naphthylphosphate analogue was titrated with the binding isomer its fluorescent emission increased upon the first addition of guest then fluctuated up and down until 0.06M concentration of the guest was reached. Upon increasing the concentration, the fluorescence of the tweezers decreased to 66% of its initial value before increasing in value after 0.016M of the guest. Then the data points corresponding to the curvature was analyzed with the 1:1 binding model a K_d of 7.2×10^{-3} M was produced after convergence. With regards to the 2-naphthylphosphate, it too

increased in fluorescent emission with the first addition of guest before leveling off until 0.004M of the guest was achieved. After that, fluorescence decreased in a curve before reaching an apparent minimum before increasing with the last addition. When the data in the curvature were analyzed with the 1:1 binding model it did not converge presumably due to the lack data points. These fluorescent data from the naphthylphosphate guest molecules suggests the the mechanism of binding may be either more complexed than initially estimated or that the phenomenon responsible for the increase in emission signature cannot be fully understood at the present time. Due these observations, titrations of the control isomer **28** were not conducted with the phosphate salts.

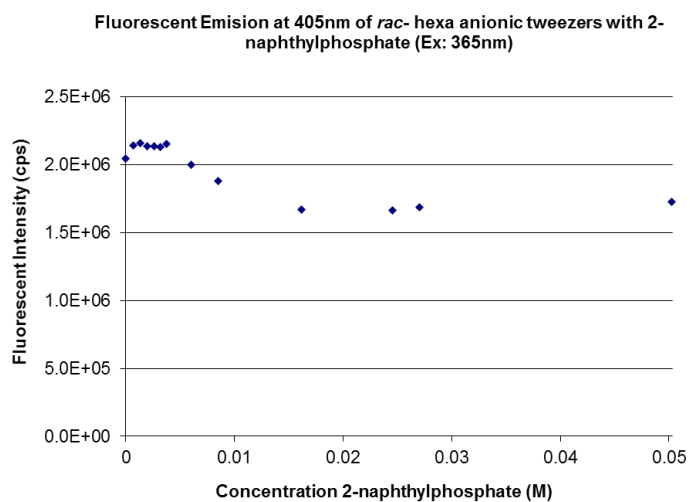


Figure 71: Titration of hexa anionic tweezers **27** with disodium 2-naphthylphosphate

F. Quinolone Synthesis for Functionalized Walls for *bis*-Tröger's Base Molecular Receptors

Quinolones have been reported as therapeutic agents ranging in use from the treatment of Herpes Simplex Type I¹⁰² (HSV-1), as an antitumor agent¹⁰³ for Burkitt's lymphoma, as iron coordinating compounds to inhibit Factor Inhibiting Hypoxia-inducible factor¹⁰⁴, an antilarial chemotherapy agent¹⁰⁵, and an inhibitor to the binding of Nerve Growth Factor p75 to diminish neural apoptosis¹⁰⁶. Although these properties may prove beneficial for specific recognition in the future, the rational in synthesizing the quinolones described below would be to exploit the differences in reactivity of its functional groups to allow for selective instillation of a wide range function groups. The consequence is this would be multiple non-covalent interactions leading to selectivity in substrate binding and could potentially produced catalytic acitivity. However, the dipole moments of the cavity induced by the quinolones in the *bis*-Tröger's base tweezers and its inherent fluorescent properties to monitor binding by fluorescence or absorbance are of immediate interest.

7-Amino-4-oxo-1,4-dihydro-quinoline-2-carboxylic acid ethyl ester when exposed to cyclization conditions should cyclize in the 8 position of the quinolone exclusively yielding a single orientation of tweezers.

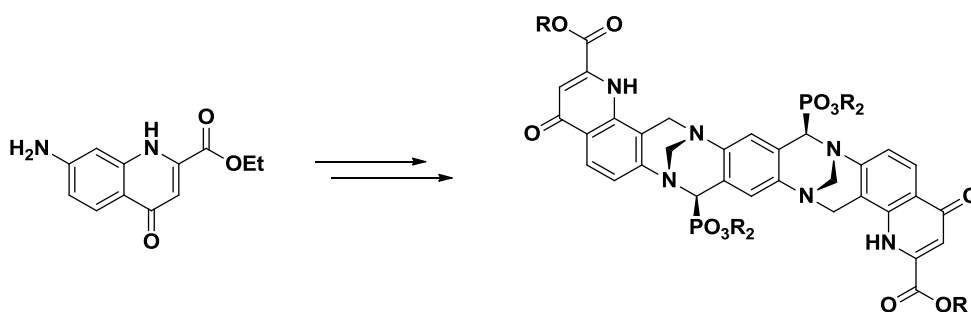


Figure 72: 7-Amino-4-oxo-1,4-dihydro-quinoline-2-carboxylic acid ethyl ester and its resulting *bis*-Tröger's Base tweezer

However when incorporating 6-amino- derivative into the tweezer's architecture there is a question of regioselectivity and could undergo Friedel-Crafts alkylation on the 5 or 7 position of the quinolone to produce a mixture of differently bonded molecular receptors in which some will not have the correct shape to intercalate substrates.

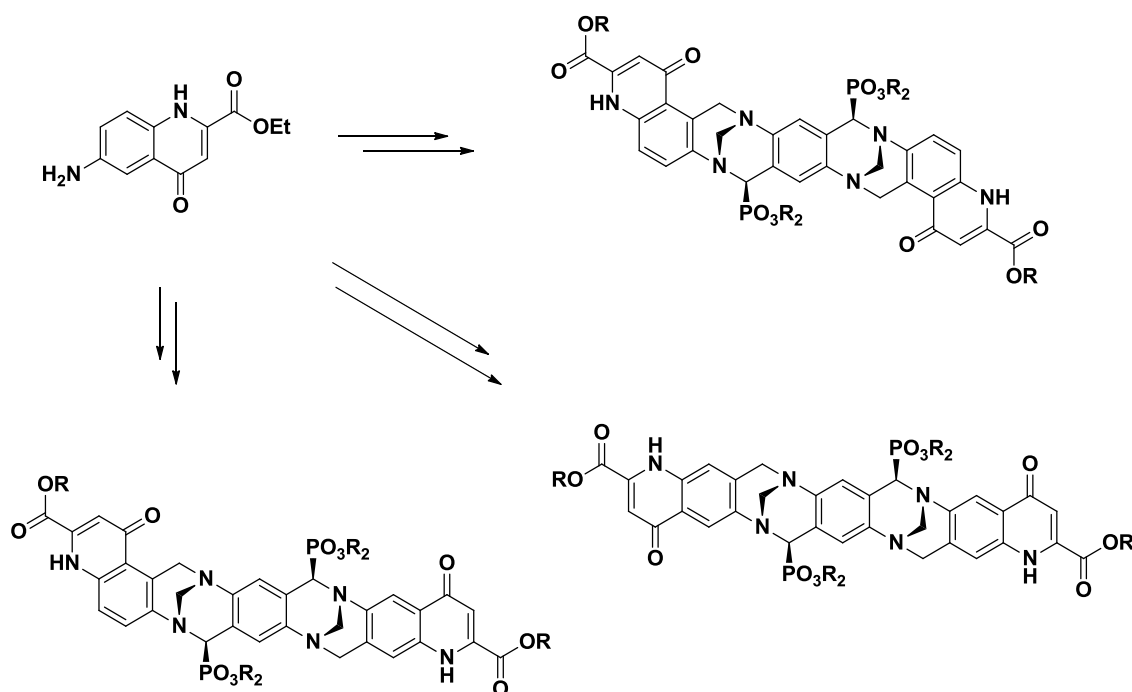


Figure 73: 6-Amino-4-oxo-1,4-dihydroquinoline-2-carboxylic acid ethyl ester and the possible combinations of bis-Tröger's Base tweezers

Below is a general scheme envisioned for the transformations needed to produce the quinolones:

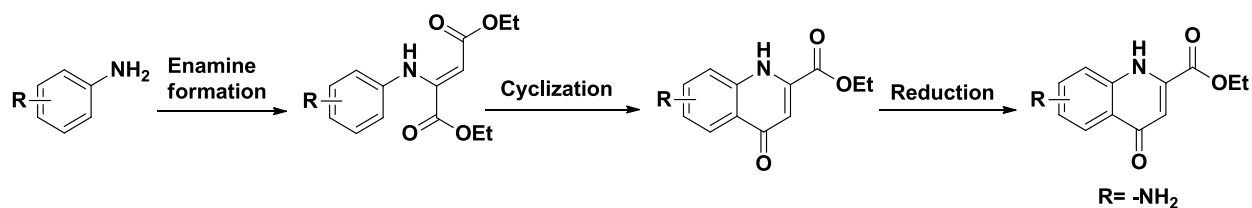


Figure 74: General scheme for aminoquinolone synthesis

Diethyl oxaloacetate was first used¹⁰⁷ and is commonly used to generate the 2-carboxy-4-oxo-quinolone variety along with diethyl acetylenedicarboxylate which can form enamines even with less reactive or sterically hindered anilines¹⁰⁸. Although the reactivity of diethyl acetylenedicarboxylate is greater than that of diethyl oxaloacetate, so is its price leading to the use of diethyl oxaloacetate. Quinolone synthesis has been reported in the literature as early as 1887¹⁰⁹ by Conrad and Limpach reporting the formation of 4-oxoquinolone formation under high temperature conditions which have been modified overtime to induced thermal cyclization^{110,111}. Before 1946 it was contended that cyclizing an enamine made from an aniline and diethyl oxaloacetate generated either a 2-oxo quinolone isomer or the 7- substituted 4-oxo isomer cleanly before Surrey and Hammer demonstrated that the resulting material generated upon thermolysis was that of a mixture of 7- and 5- substituted 4-oxo-quinolones¹¹² and occurs even in the gas phase¹¹³

1. Preparation of 7-Amino-4-oxo-1,4-dihydro-quinoline-2-carboxylic acid ethyl ester

a. From (3-Amino-phenyl)-carbamic acid tert-butyl ester Route

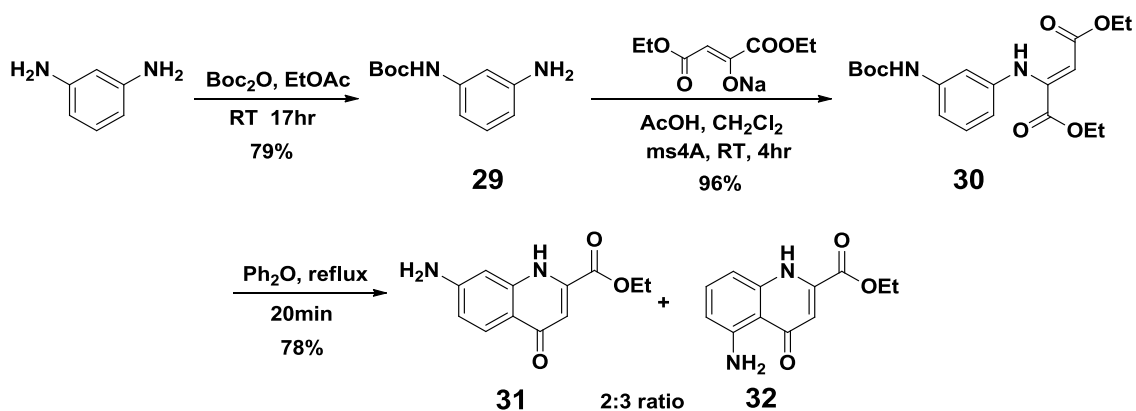


Figure 75: Synthetic route to produce 7-amino-2-carboxy from 1,3-diaminobenzene

Mono-Boc protection of 1,3-diaminobenzene to generate **29** was afforded in 79% yield by using a 100% excess of the diamine over Boc₂O. Utilizing the ability to partition the diamine into water to remove its excess and recrystallization from hexane to remove the diBoc protected side product gave a pure product. Formation of the enamine **30** from the sodium salt of diethyl oxaloacetate in glacial acetic acid cleanly generated the enamine in 4h if 4Å molecular sieves were used to drive the equilibrium by physical removal of water. The excess diethyl oxaloacetate was removed by partitioning the reaction mixture between hexane and sat. Na₂CO₃ to produce the enamine in 96% yield as an orange oil. Diphenyl ether (258°C) was used due to its chemical stability at high temperatures. Refluxing the enamine oil in diphenyl ether for 20min facilitated quinolone formation as well as Boc protecting group removal. Analysis of the quinolone mixture by ¹H NMR spectroscopy revealed a 2:3 ratio of **31** to **32**. This was determined by the ratio of integrations of the doublet of doublets signal at δ6.69ppm for the 7-NH₂ isomer and the triplet at δ7.24ppm indicative of the 5-NH₂ compound. From this data it was hypothesized that when the Boc group was removed and the resulting amino group was able to direct the Friedel-Crafts acylation ortho- to it. The installation of a thermally stable protecting was deemed necessary and thus cyclization with a trifluoroacetyl protecting group was investigated.

b. From N-(3-aminophenyl)-2,2,2-trifluoroacetamide Route

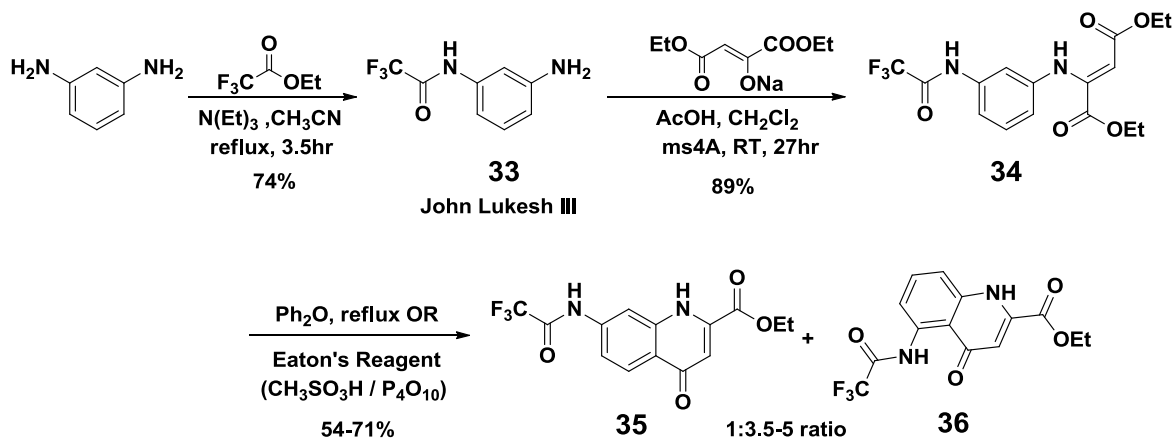


Figure 76: Synthetic route for quinolone production from mono-trifluoroacetyl protected 1,3-diaminobenzene

The mono-trifluoroacetyl 1,3-diaminobenzene (**33**) used was synthesized, isolated, and purified by John Lukesh III which was then condensed using the glacial acetic acid, 4Å molecular sieves and workup method to generate the enamine **34** cleanly in 89% yield as a lime green oil. After exposing the enamine to refluxing diphenyl ether, analysis of the crude product with 1H NMR spectroscopy revealed a mol ratio of 1:5 for the 7-trifluoroacetyl quinolone **35** to 5-trifluoroacetyl quinolone **36** and a 1:3.5 mol ratio of **35**:**36** when the experiment was replicated. As an alternative to thermal cyclization, strongly acidic conditions were also known to facilitate cyclization. Published by Eaton in 1973¹¹⁴ demonstrated that Eaton's reagent (1:10 solution by weight of P_4O_{10} : CH_3SO_3H) not only induced ring closure but sidestepped the difficulties with the physical properties of polyposphoric acid and thus has been used since then as an alternative.¹¹⁵ Unfortunately when Eaton's reagent was used the ratio increased even more in favor of the **36** to a 6.7:1 mol ratio compared to the desired **35**. Ring formation using $POCl_3$ was also used but appeared to produce **36** as the major product. Quinolone formation was attempted with the enamine adsorbed to either silica gel or basic alumina which was placed

into a thermal well in refluxing diphenyl ether which afforded incomplete conversion of the starting material and low mass recovery off of the solid support. From these results it was postulated that this seeming regioselectivity could be due to the formation on an intramolecular hydrogen bond upon the formation of the ketene intermediate.

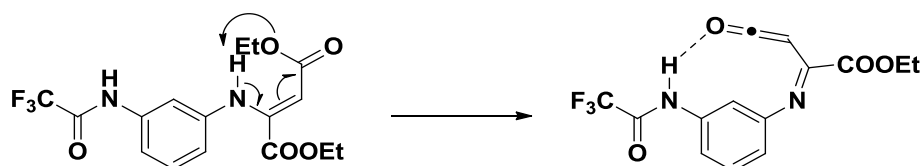


Figure 77: Proposed hydrogen bonded intermediate responsible for regioselective cyclization

If this mechanism were true, then eliminating the ability to hydrogen bond should prevent ortho- direction. This informed the change to a nitro group which would be subsequently reduced to the amine functionality to generate the 7-Amino-4-oxo-1,4-dihydro-quinoline-2-carboxylic acid ethyl ester.

c. From 3-nitroaniline Route

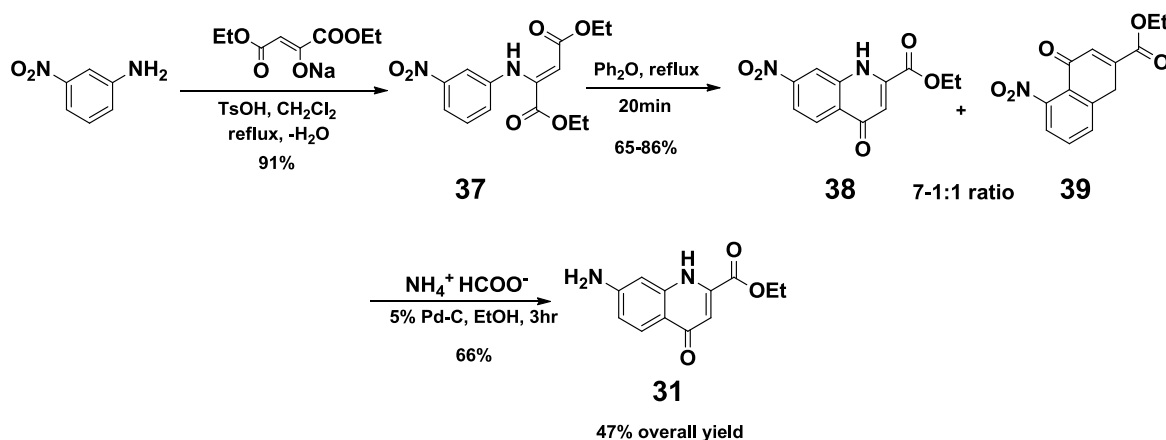


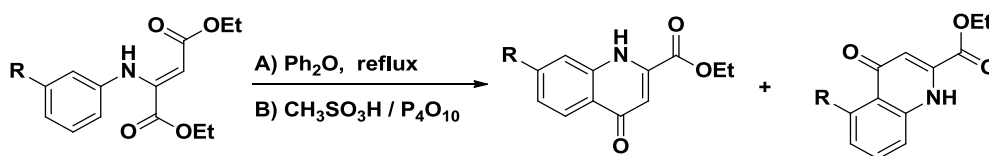
Figure 78: Quinolone synthetic scheme starting from 3-nitroaniline

Enamine formation was first attempt with the glacial acetic acid, 4Å molecular sieves method but only afforded the desired enamine **37** in 54% yield. This was presumably due to the

inductive effect of the nitro reducing the nucleophilicity of the amine and thus requiring harsher conditions to increase yield. Condensation of the 3-nitroaniline and sodium diethyl oxaloacetate was driven then by elevated temperature and physical removal of water via azeotrope with a distilling solvent returned via Dean-Stark trap. It was discovered that choice of solvent was not trivial as use of toluene (b.p. 110°C) or 1,2-dichloroethane (b.p. 84°C) lead to substantial formation of a crystalline, orange side product. This material was not fully characterized but evidence ^1H NMR gave speculation that it was likely produced by condensation of two 3-nitroanilines by reaction of the amine functionality with a protonated nitro group. Dichloromethane (b.p. 40°C) was employed next due to its lower boiling point and ability to azeotropically remove water albeit poor. It was due to this poor azeotrope (99 $\text{CH}_2\text{Cl}_2:1\text{H}_2\text{O}$) that reaction times were extended considerably to ranges of overnight to several days. It was later discovered that on the synthetic scale that this transformation was attempted that the water removed by the dichloromethane was not able to quantitatively separate and allowed for return of water back into the reaction mixture. If however the heavier than water Dean Stark trap was packed with 4Å molecular sieves atop a loosely fit plug of cotton the reaction could be reliably completed overnight. On larger scales though replacing of the sieves may be required to thoroughly remove all of the water generated from the reaction.

37 was then subjected to the thermolytic cyclization protocol of 20min exposure in refluxing diphenyl ether and unfortunately still produced the mixture of 7- NO_2 isomer **38** and 5- NO_2 isomer **39**. In replicating this transformation many times it was observed that although the mol ratio of the quinolone mixture improved with regards to 7- NO_2 to 5- NO_2 isomers it was inconsistent, ranging from 7:1 to 1:1, with no correlation able to be determined for this

observed behavior. Jackie Koch developed a procedure that exploited the greater crystallinity of the quinolone **38** to isolate it exclusively via recrystallization using a mixture of ethanol and toluene and is described in detail in the experimental section. She also found that if only ethanol was used, **38** could still be separated but the amount of material recovered decreased significantly. Interestingly enough when the enamine **37** was cyclized using Eaton's reagent at 110°C the mol ratio of the resulting quinolone mixture was observed to be 2.3:1 in preference of the 5-NO₂ isomer. From these results it appears that although neither the **39** or **38** isomer can be made exclusively there is at least some ability in directing ring closure by either substituent effects or cyclization conditions.



R	Conditions	Mol Ratio	
BocHN-	A	2	3
CF ₃ (CO)HN-	A	1	3.5-5
CF ₃ (CO)HN-	B	1	6.7
O ₂ N-	A	7-1	1
O ₂ N-	B	1	2.3

Table 5: Quinolone mol ratios with varying substituents and reaction conditions

Reduction of the nitro group was first attempted on a mixture of the **38** and **39** using ammonium formate (NH₄O₂CH), 5% Pd-C, and methanol as a solvent. Ammonium formate is attractive as the reducing agent because in the presence of Pd-C it decomposes to produce a concentration of hydrogen gas *in situ* which corresponds to a high pressure of H₂ over the reaction volume. This eliminates the necessity for a specialized high pressure apparatus and the

safety concerns that come with it. Transformation to the amino group occurred as expected but under these conditions trans-esterification with the alcohol solvent occurred resulting in the methyl ester of the corresponding aminoquinolones. Although unexpected in retrospect should not have been wholly unanticipated due to the weakly acidic nature of the ammonium formate. When repeated with ethanol as the solvent the desired aminoquinolone **31** was afforded in 66% yield after isolation by flash chromatography and an average 47% overall yield from the starting 3-nitroaniline.

Attempts to isolate **31** non-chromatographically proved to be problematic. When the starting quinolone **38** was observed to be absent by TLC analysis the mixture was filtered to which CH_2Cl_2 was added to the filtrate to decrease the solvent polarity to cause an unreacted ammonium formate to precipitate. Although precipitation of the salt did occur the removal of the ammonium formate was not quantitative. Reducing the volume of the filtrate or concentrating to dryness resulted in the formation of solid aminoquinolone which was not separated from the excess salt. It was observed that if left to stir for excessive time in the presence of Pd-C the ammonium formate is able to be converted to into insoluble ammonium carbonate however with no way to conveniently monitor this conversion it was not considered as a method of separation. It was later found that use of $\text{H}_{2(\text{g})}$ is not detrimental to the rate of reaction and will be discussed subsequently.

2. Preparation of 6-Amino-4-oxo-1,4-dihydro-quinoline-2-carboxylic acid ethyl ester

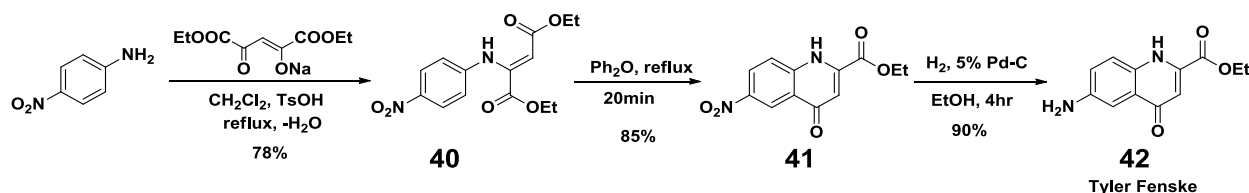


Figure 79: Synthetic scheme for production of 6-amino-2-carboxy-4-oxoquinoline ethyl ester

With a developed methodology in hand, formation of **42** proceeded smoothly especially without question of regioselectivity in ring closure. A major contribution in the reduction step was provided by Tyler Fenske who observed that use of $\text{H}_{2(g)}$ reduced the nitro group at the same rate as that of the ammonium formate and in 90% yield with effortless removal of the excess, gaseous reducing agent.

III. CONCLUSION

The dialdehyde **8** was afforded in a 50% overall yield starting from the dimethyl ester of succinyl succinate without chromatography and the most of the intermediates being able to crystallize from the reaction mixture, eliminating the need for subsequent purification steps. The diarylamino side products were demonstrated to be formed from the bisenamine **2** in the absence of Boc_2O with bis-aryl amino derivatives able to be produced from the corresponding anilines with the mono-substituted version predominating. This opens up a different route by which acridones can be synthesized as well as the possibility for asymmetric quinacridones.

The desired hexa-methyl ester of 1,2:4,5-*bis*-Tröger's Base stereoisomer was afforded as a diastereomeric mixture of the *syn*-cofacially oriented *rac*- isomer and the control *meso*- isomer in 69% overall yield from the key intermediate dialdehyde **8**. This proceeded through

the *bis*-imine formation from the core dialdehyde, transformation into α -aminophosphonates, then cyclization to the final *bis*-Tröger's Base. Each of these isomers was then converted into water soluble analogues via selective dealkylation protocols employing combinations of bromotrimethylsilane and aqueous lithium hydroxide. Two tetra anionic molecular tweezers derivatives were afforded each with a different distribution of charge across its surface along with a fully deprotected hexa anionic receptor.

Each of the organic and water soluble forms of the *rac*- and *meso*- 1,2;4,5-*bis*-Tröger's Bases were characterized using spectroscopic techniques and spectrometric techniques to confirm their identity. It was shown that the desired binding *rac*- isomers underwent self-association to presumably form a dimeric complex in solution whereas the non-binding control *meso*- isomers did not. ^1H NMR analysis of the fully esterified *rac*- isomer in CDCl_3 produced broad resonances that sharpened and shifted downfield upon dilution, which is behavior consistent with the interpretation dimer formation. The water soluble derivatives were not able to produce unambiguous spectra upon dilution in D_2O but were able to generate well resolved spectra in a mixture of 50% TFA/ CDCl_3 to allow for their identification. In contrast, the non-binding *meso*- isomers produced well resolved spectra in all cases even at sample concentrations greater than those where dimerization was observed with the *rac*- isomers. This demonstrated the desired lack of self association for the non-binding *meso*- isomers so that it may serve as a negative control for dimerization and titration studies.

Equilibrium constants for dimer formation were determined for the *rac*- isomers using a combination of ^1H NMR and fluorescence spectroscopy and analyzed using a dimerization equation fit using a non-linear least squares method. K_{dim} for the fully esterified tweezers was

calculated to be 1.5×10^{-1} M in CDCl_3 but this is just an estimate based upon the low number of data points acquired in the NMR dilution experiment. Deviation from Beer's Law in fluorescent emission upon dilution was used to determine the strength of self association for the water soluble molecular tweezers. The *rac*- hexa anionic tweezers formed the weakest dimer with a K_{dim} value of $1.2 \times 10^{-4} \text{ M} \pm 9.0 \times 10^{-6} \text{ M}$. The tetra anions formed progressively stronger dimers with the *rac*- methyl phosphonate analogue producing $K_{\text{dim}} = 4.5 \times 10^{-4} \text{ M} \pm 9.8 \times 10^{-5} \text{ M}$ and the TMSBr deallylated *rac*- carbethoxy $K_{\text{dim}} < 4.4 \times 10^{-7} \text{ M}$. In the case of the *rac*- carbethoxy tweezers a linear decrease in fluorescence was observed upon dilution down the $4.4 \times 10^{-7} \text{ M}$, which was the limit of detection for this compound and prevented fitting to the dimerization model.

Each of the water soluble binding *rac*- and control *meso*- *bis*-Trögers Base derivatives were titrated with small molecules monitoring the decrease in fluorescent emission to acquire the data to be fit to the 1:1 binding model which describes intra-molecular (static) quenching. Data was also fit the Stern-Volmer equation, which models inter-molecular (dynamic) quenching, as a way to discriminate between the binding and non-binding isomers. The *rac*- carbethoxy tetra anion similar dissociation constants (K_d) across a range of guest molecules reinforcing the notion that it exists as a dimer at 10^{-5} M concentration regime the titrations were conducted at. The ionic strength of the aqueous media was also observed to be of import with regards to distinguishing between the binding and non-binding isomers during small molecule titrations. In a low ionic strength environment, like nanopure water, it appeared that both the *rac*- methyl phosphonate and control *meso*- methyl phosphonate tetra anions exhibited binding behavior in the presence of cationic guest molecules like 1-Me nicotinamide chloride. When ionic strength was increased so that the water contained 150mM NaCl and

10mM pH7 phosphate buffer, both isomers were still able to converge to the 1:1 binding model when titrated with 1-Me nicotinamide chloride. However, the calculated K_d diminished by a factor of 5 for the control *meso*- isomer between the low and high ionic strength conditions whereas the K_d for binding *rac*- isomer diminished only by a factor of 1.7.

From this it was concluded that the cationic guest molecule was associating to the control isomer through coulombic attraction which in retrospect is not surprising. To confirm that the nicotinamide salt was indeed forming a pair, ^1H NMR was used to analyze a mixture of the 1-Me nicotinamide chloride with the control *meso*- isomer. What was observed was a significant upfield shift and broadening of the guest's resonances along with minor upfield shift in the naphthyl signature of the *meso*- isomer. When the ionic strength was increased to 160mM NaCl the peaks for the 1-Me nicotinamide chloride shifted only slightly back downfield and still appeared to be significantly associated to the control *meso*- isomer. Titration with charge neutral guest like pyridine or nicotinamide, or anionic guests like sodium phenylacetate did not sufficiently quench either isomer upon addition. This prohibited confidently distinguishing between the modes of intra- or inter-molecular quenching between the two isomers.

The *rac*- hexa anionic tweezers provided the best data with regards to small molecule titrations using cationic or neutral guest. Ionic strength of the aqueous media was accounted for by containing 150mM NaCl and 10mM pH9 borate buffer which ensures that the hexa anionic tweezers fully deprotonated. Titration of the binding *rac*- isomer with 1-Me nicotinamide chloride resulted convergence of the 1:1 binding model, negative Stern-Volmer correlation, and a K_d value of $8.2 \times 10^{-3} \text{M} \pm 1.0 \times 10^{-3} \text{M}$. This value is similar to the dissociation

constant afforded by the *rac*- methyl phosphonate tetra anion tweezers. Titration with caffeine resulted in the same spectroscopic behavior and yielded a K_d value of $4.2 \times 10^{-4} \text{ M} \pm 4.2 \times 10^{-5} \text{ M}$.

The future direction of this work should continue small molecule titration with the binding *rac*- hexa anionic tweezers to determine the scope and trends in its ability to intercalate guest molecules. As it appears that quenching of fluorescence is not adequate in order to determine dissociation constants in some cases it is recommended that the walls of the molecular tweezers be modified to a potentially more responsive moiety.

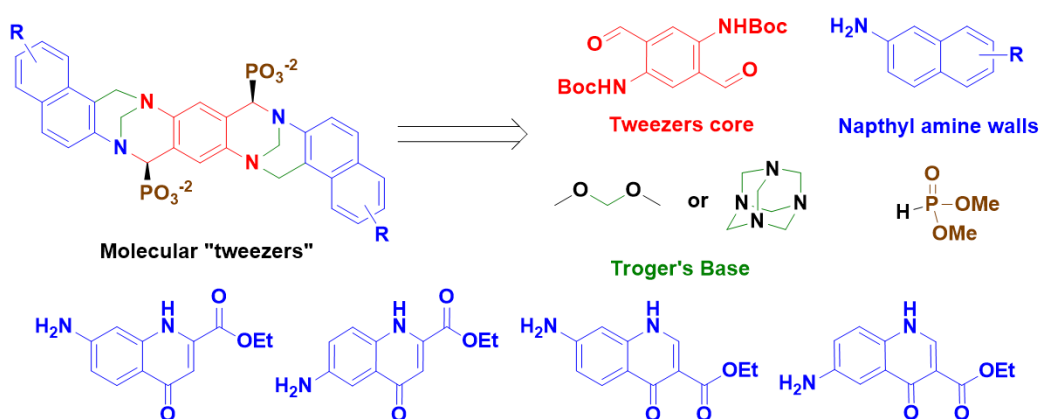


Figure 80: 1,2:4,5-bis-Troger's Base tweezer scheme displaying desired quinolones for future inclusion

This can be accomplished by incorporating the synthesized amino-quinolone derivatives, 7-Amino-4-oxo-1,4-dihydro-quinoline-2-carboxylic acid ethyl ester (47% overall yield) and 6-Amino-4-oxo-1,4-dihydro-quinoline-2-carboxylic acid ethyl ester (60% overall yield), into the modular tweezers synthetic scheme. These structures would provide a different fluorescent signature to monitor binding as well as potentially expand the range of small molecules the tweezers may bind by the presence of dipole-dipole interactions in the cavity.

IV. SMALL MOLECULE PROBES FOR EVALUATING SbADC ALDOLASE ACTIVITY

A. SbADC Background Information

S. Bingchenggensis Acetoacetate Decarboxylase (SbADC) is a tetrameric enzyme first isolated from *Streptomyces Bingchenggensis* from Harbin, China and having sequence homology to that of Group V acetoacetate decarboxylases. However, SbADC does not display the same properties of its brethren and instead was discovered to catalyze Aldol Condensation and Aldol Dehydration as well as the retro variants of these reactions with α -keto acids. It was discovered in the Silvaggi lab that it reacted preferentially with pyruvate and various aldehydes. The purpose of the enzyme for its native species is as of yet unknown but characterization of its aldolase functionality was conducted.

The mode of active site catalysis for SbADC was studied by stop flow, steady state, and inhibition kinetics as well as X-ray crystallography conducted by Lisa Mueller to achieve kinetic parameters in intermolecular interactions in the active site to determine which residues are involved in the transformations. When allowed to react with benzaldehyde; pyruvate and acetoacetate were the only nucleophiles to react with catalytic SbADC action with rates of $2.112\mu\text{M s}^{-1}$ and $0.012\mu\text{M s}^{-1}$ rate where as glyoxylate had non-enzymatic reaction and 2-oxobutyrate did not react leading to the conclusion that pyruvate was the preferred α -keto substrate. Aldehyde substrates were then screened with *trans*-cinnamaldehyde observed to the bind the strongest ($42\text{-}48\mu\text{M}$) with $k_{\text{cat}}/K_{\text{m}} = 3.9 \times 10^5 \text{ M}^{-1}\text{s}^{-1}$. Soaking with hexanal produced no reaction and imidazole-2-carboxaldehyde reacted but did not turn over. Inbetween these

results with increasing reactivity: benzaldehyde < *trans*-2-hexenal, *trans*-2,4-heptadienal < *trans*-2-octenal leading to the conclusion that an α,β -unsaturated aldehyde with required and if steric bulk is in an aldehyde (like a benzyl group) it has to be at least two carbons away from the aldehyde. *Trans*-cinnamaldehyde analogues were screened. Ortho substitution proved detrimental to binding (o-methoxy $K_d=185\mu\text{M}$) while hydrogen bonding substituents in the para position enhanced binding (o-methoxy $K_d=21.5\mu\text{M}$, o-nitro $K_d=7.6\mu\text{M}$)

When SbADC was soaked with sodium pyruvate and the X-ray crystal structure was acquired it appeared as a hemiaminal in three of the four active sites and a Schiff base in the last. However when SbADC had the active site mutation of Y252F and soaked with cinnamylidene pyruvate it was observed to be the Schiff base in all four active sites leading to the speculation that Y252 is needed for the retro Aldol activity as it hydrogen bonds to a water molecule and orients to close to the α -keto moiety. α -Keto acid enones and dieneones have been synthesized from pyruvate for almost one hundred years¹¹⁶ utilizing silyl enol ethers and Lewis acids¹¹⁷, two carbon ethylene homologation¹¹⁸, and base catalyzed Aldol Condensation and Dehydration^{119,120}. For evaluating the X-ray crystal structures of benzylidene pyruvate, cinnamylidene pyruvate, 4-nitrocinnamylidene pyruvate with SbADC the dieneones used were mixtures with pyruvate. For the kinetic studies these substrates were purified to be 98-99% pyruvate free to obtain accurate enzymatic parameters.

B. Rational for SbADC Molecular Probes

In the attempt to elucidate the reason why SbADC does not facilitate the decarboxylation of pyruvate to acetaldehyde, SbADC was to be soaked with various

combinations of substrates to study X-ray crystal structures. This series of X-ray crystal structures when viewed in sequence would produce a “molecular” movie which would show the position of the enzyme’s active site residues, their proximity to substrate functionalities, and thus their role in the catalyzing Aldol reactions. Shown below is the schematic for the desired “molecular movie” showing the steps in the reaction that would be of interest.

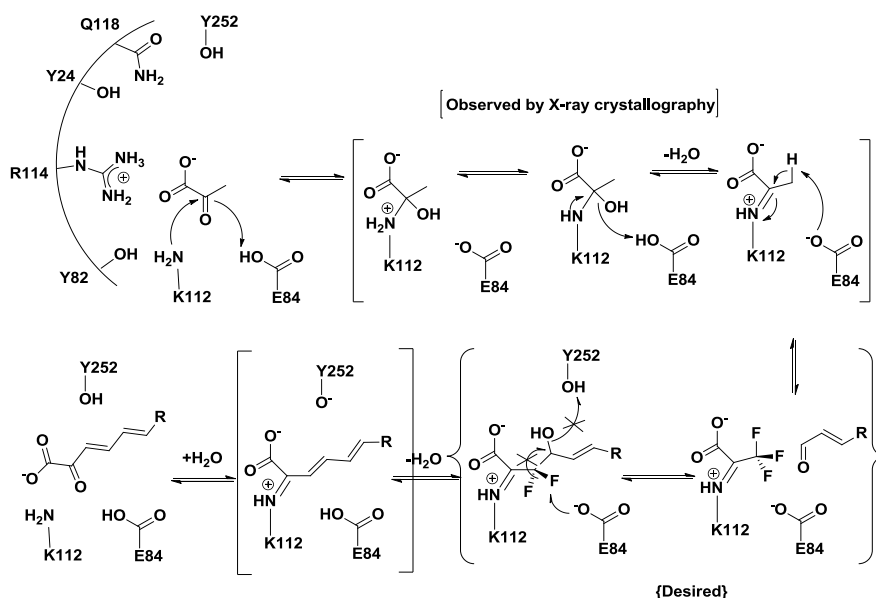


Figure 81: Proposed use of trifluoropyruvate and difluoropyruvate for mechanistic determination of SbADC aldol pathway

The structures in square brackets are the combinations that are already observed by X-ray crystallography while the ones in curly brackets are the ones desired to be produced. For these trifluoropyruvate and difluoropyruvate were synthesized. The purpose of the trifluoropyruvate would be to soak the enzyme with a substrate that cannot undergo Aldol condensation. Trifluoropyruvate would be concurrently soaked with cinnamaldehyde to see the proximity of the substrates to one another and the positions of the active site residues that would be getting into bonding distance of the substrates. Difluoropyruvate would be employed as it is able to undergo aldol condensation but not aldol dehydration. This attenuated reactivity

would also allow for the identification of which side chains participate in Aldol dehydration reaction by their proximity to the Aldol product.

Ethyl trifluoropyruvate is commercially available so the sodium salt of the hydrate of trifluoropyruvate can be made by acidic hydrolysis and neutralization. This method minimizes the presence of excess hydroxide which would denature the enzyme being studied. Ethyl difluoropyruvate is not commercially available so it or an analogue is needed to be made so its salt can be used.

Of the literature examples for synthesizing difluorocompounds, only a few seemed attractive for difluoropyruvate. One of these was as follows:

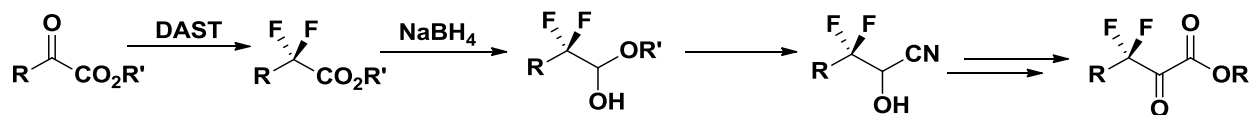


Figure 82: An example synthetic scheme in formation of difluoropyruvate analogues

This method¹²¹ used (diethylamino)sulfur trifluoride (DAST) to make β,β -difluoro compounds by reaction with the α -keto carbonyl and subsequently regenerating it by reduction of the ester to to the aldehyde level followed by substitution with cyanide, oxidation, then acid hydrolysis. This method worked well for cases when R was either alkyl or aryl substituents. No examples of R=H were reported, leading one to believe that it may be unsuccessful with the method. The other route was the Mg^0 promoted mono-defluorination¹²² of trifluoromethyl ketones. This simple preparation was attempted with ethyl trifluoropyruvate even though there was no precedent for an α -keto trifluoromethyl moiety to get to difluoropyruvate directly. The most reliable route and the one ultimately used was trifluoroacetylation of 2-methylfuran by

Friedel-Crafts acylation then Mg^0 promoted monodefluorination¹²³ followed by ozonolysis of the resulting 5-difluoroacetyl-2-methylfuran¹²⁴.

V. RESULTS AND DISCUSSION

C. Formation of Cinnamylidenepyruvate and 4-NO₂ Cinnamylidenepyruvate

The sodium benzylidene pyruvate, sodium and potassium cinnamylidene pyruvate salts, and sodium and potassium 4-nitrocinnamylidene pyruvate salts were synthesized from their corresponding aldehydes using the base catalyzed aldol chemistry. Preliminary studies began with the synthesis of sodium benzylidene pyruvate to determine an appropriate method for cinnamylidene preparation. Benzylidene pyruvate was prepared from benzaldehyde and sodium pyruvate with sodium hydroxide as described⁵ and isolated in 34% purified yield. The initial precipitate from the reaction mixture was isolated and determined to be a mixture of the condensation and dehydration product in ~1:2 molar ratio and free of pyruvate. The mixture was purified from aqueous media and acidified to pH1 with the desired dieneone precipitating from solution. Acidification shifts the α -hydrogen from $\delta 6.9\text{ppm}$ to $\delta 7.6\text{ppm}$.

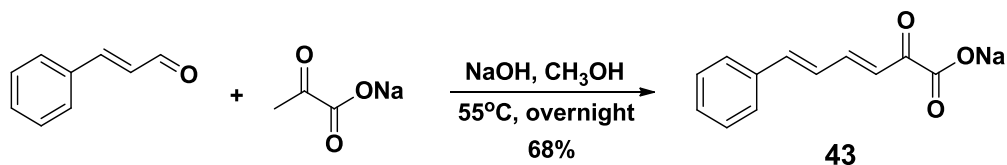


Figure 83: Formation of cinnamylidene pyruvate sodium salt

43 was synthesized using the same method, but at 55°C with a yellow solid precipitating from the reaction mixture in 68% crude yield as mixture of the desired dieneone and pyruvate (27% by mass of the mixture). The mixture was made pyruvate free by the same precipitation

method from acidic aqueous media with a 42% yield and exhibited the same large change in chemical shift of the hydrogen α to the ketone in either the salt or acid form. However the dieneone was reactive to aqueous acid. Extraction of the supernatant of EtOAc afforded a yellow oil in 36% crude mass that was a mix of the desired acid (74% by mass), ethyl acetate, and what was hypothesized to be the Aldol condensation product form by hydration of the dienone. Total estimated yield from the precipitate and extract is ~60%.

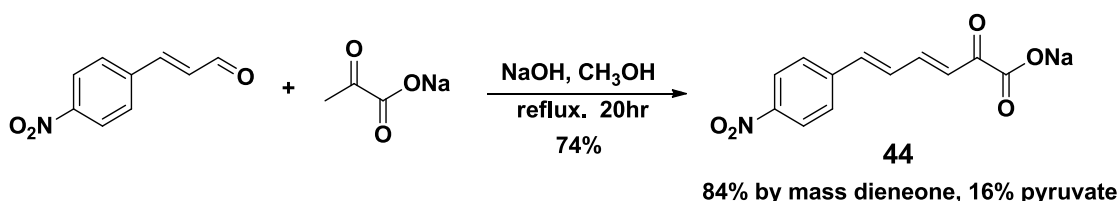


Figure 84: Formation of 4-nitrocinnamylidene pyruvate sodium salt

The 4-NO₂ analogue **44** was synthesized with the previous methods and placed through the same workup protocol but to pH2. This dienone however proved to be very sensitive to aqueous acid and afforded none of the desired material. Synthesis without acidic workup but with precipitation of the salts with isopropyl alcohol afforded a 74% yield of the product as a mixture that was 84% by mass **44** and 14% by mass sodium pyruvate.

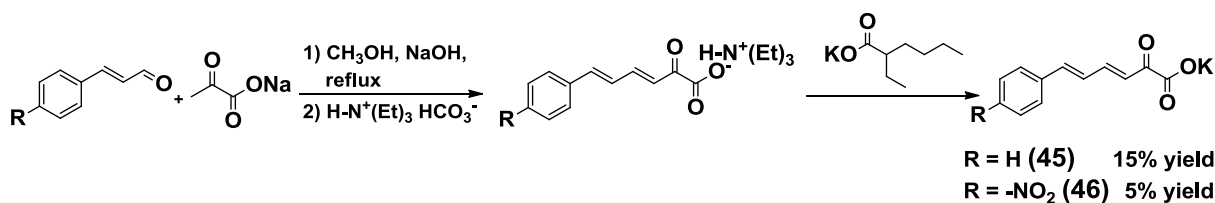


Figure 85: General scheme for isolating sodium pyruvate free cinnamylidene pyruvate analogues

The acid sensitivity of **45** and **46** prevented straightforward extraction to remove contaminating pyruvate. However compounds **45** and **46** could be extracted from their aqueous solutions in triethylammonium bicarbonate into CH₂Cl₂. Evaporation yielded the oily

triethylammonium salts. The crystallize potassium salts were obtained by dissolution in ethyl acetate and precipitated upon addition of a solution of potassium 2-ethylhexanoate¹²⁵ generating 15% yield **46** and 5% yield **46** with 1-2% by mass pyruvate as determined by ¹H NMR spectroscopy. The desired products were able to be isolated pure as when the triethyl ammonium salt acquired from extraction when exposed to ethyl acetate the large majority of it did not dissolve. The resulting supernatant was decanted from the undissolved oil and mixed with a solution of potassium 2-ethylhexanoate in ethyl acetate precipitating the dieneone salt. When the insoluble oil, which was dissolved in CH₂Cl₂, was mixed with potassium 2-ethylhexanoate no precipitate was formed even when the salt was just in large excess. Analysis of the EtOAc insoluble oil by ¹H NMR showed that the doublet characteristic of the hydrogen α to the ketone of the dieneone were reduced to 75% signal intensity relative to the dieneone and instead had a new set of signals from δ3.5 to δ3.2 that appeared to be a triplet and a doublet.

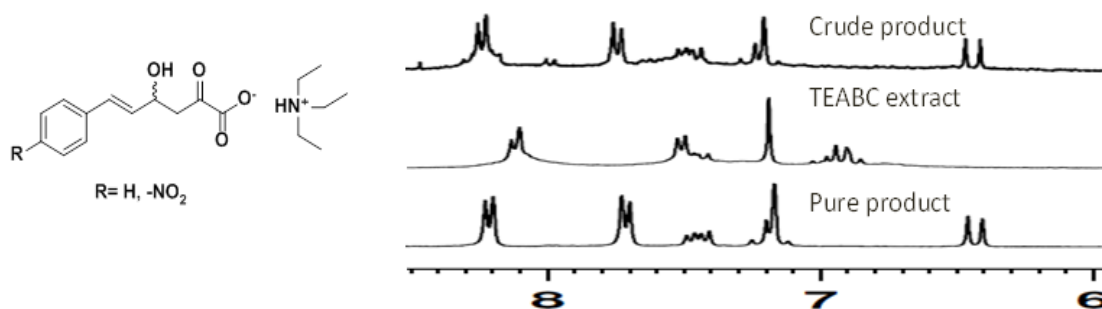


Figure 86: ¹H NMR spectra of 4-nitrocinnamylidene pyruvate over the course of sodium pyruvate removal

A ¹H NMR spectrum was acquired of the triethyl ammonium bicarbonate extract and looked the same as the EtOAc insoluble oil. From this data it was concluded that the dieneones still undergo hydration to form the Aldol product even under these mild conditions. Attempts

to minimize hydration by raising the pH of the reaction mixture to 12 from 8 by bubbling in of CO₂ before exposure to triethylammonium bicarbonate did not mitigate the amount of product degradation. The cinnamylidene pyruvate derivatives containing 1-2% pyruvate were then used by Lisa Mueller to obtain kinetic parameters for SbADC by monitoring the retro Aldol reactions in stop flow experiments.

D. Difluoropyruvate Synthesis

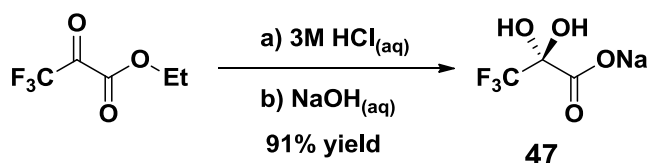


Figure 87: Scheme for sodium trifluoropyruvate hydrate

Ethyl trifluoropyruvate hydrolysis was monitored by ¹H NMR to ensure complete hydrolysis by watching the ester quartet turn to that of the quartet of ethanol. ¹H NMR was deemed necessary for evaluating the reaction mixture as ethyl trifluoropyruvate readily hydrates, analogous to that of hexafluoroacetone, and was unclear if it could migrate upon silica gel for TLC analysis. After overnight reflux with a pyruvate concentration of 0.37M gave a 93% yield of **47** after neutralization with NaOH.

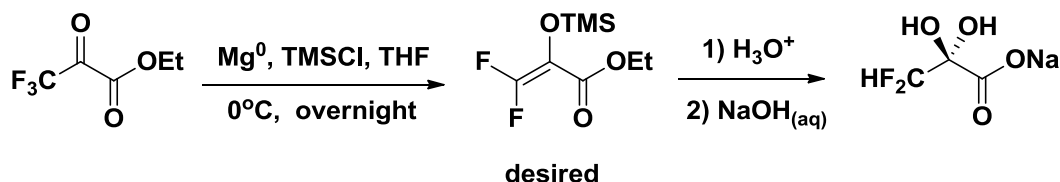


Figure 88: Proposed synthetic route for simplified difluoropyruvate formation

If Mg⁰ reduction and mono defluorination proceeds as for CF₃COAr¹²³, this has the potential to provide a succinct route to difluoropyruvates. When ethyl trifluoropyruvate was

exposed to the mono-defluorination conditions reduction occurred but afforded a mixture of the E and Z isomers of *bis*-silyl enol ether **48** without elimination of fluoride. This material exposed to a range of conditions in efforts to produce ethyl difluoropyruvate (**49**) by the most succinct route known. The first was exposure to aqueous hydrochloric acid. The purpose of this admittedly was not to yield difluoropyruvate but confirm the identity of the product afforded from the monodefluorination reaction. Upon addition of acid the quartet indicative of the ethyl ester of trifluoropyruvate was observed as well as the quartet seen of the alpha hydrogen in ethyl trifluorolactate. The second condition was addition of (Bu)₄NF in portions over time. The goal in using this organic soluble fluoride was to react in an E₂ fashion kicking out fluoride by making trimethylsilyl fluoride in the following fashion:

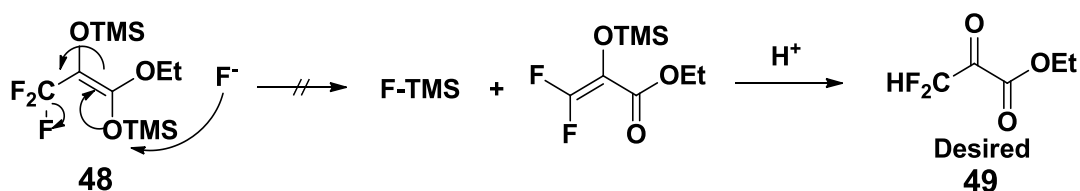


Figure 89: Desired E₂ elimination of O,O-(bis-trimethylsilyl) ethyl trifluoropyruvate

After 20hr with 6eq of (Bu)₄NF added over that time, trifluoroacetic acid was added was to remove the trimethylsilyl groups and to see if a triplet at 6ppm would be produced. This singal is indicative of the desired difluorocompound but no change in the ¹H NMR spectrum observed. If the removal of the silyl groups by fluoride did not occur, then the combination of ethyl trifluoropyruvate and ethyl trifluorolactate would be observed after protonation. The resonances for the compounds were also not seen in the NMR. From this data, it was postulated that the E₂ elimination occurred but the resulting difluoroalkene also acted as a

Michael acceptor which condensed with the *bis*-silylenol ether precursor. The proposed mechanism is diagramed below:

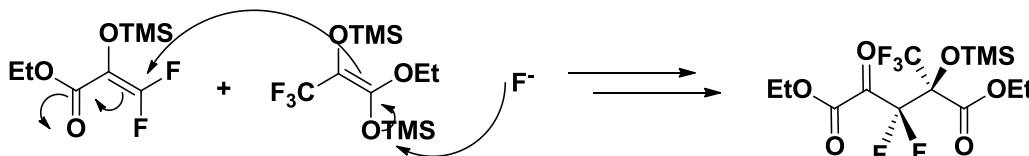


Figure 90: Proposed E2 elimination of O,O-(*bis*-trimethylsilyl) ethyl trifluoropyruvate that occurred

With the limited success using ethyl trifluoropyruvate the ozonolysis scheme was pursued by way of an ozone generator on loan with many thanks to Dr. Tysoe.

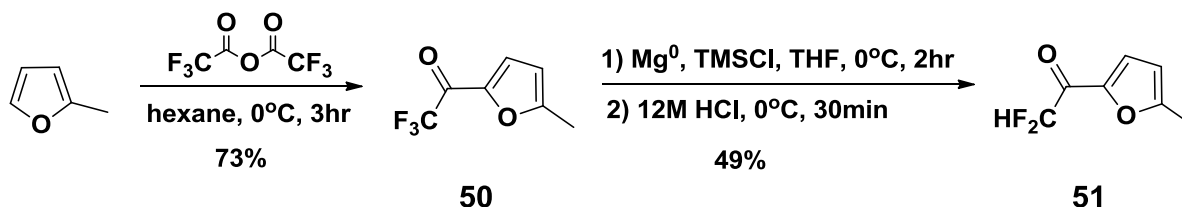


Figure 91: Literature based synthesis for ozonolysis precursor

Trifluoroacetylation of 2-methylfuran with trifluoroacetic anhydride was conducted by the literature procedure to afford **50** in 73% yield followed by the magnesium facilitated mono-defluorination in 44% purified yield after vacuum distillation of **51**.

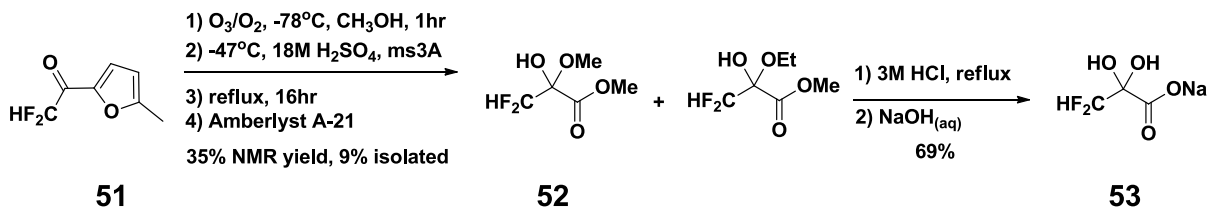


Figure 92: Ozonolysis scheme for synthesis of methyl difluoropyruvate methyl hemiacetal

In the end, ozonolysis of the difluorofuran does produce the methyl ester **52**. Katagiri, Ozaki, and Tanaka¹²⁴ describe ozonolysis “until a green color is formed” which proved to be

problematic in reproducing what they accomplished. We found bubbling of gas into the reaction mixture until a yellow-green color was apparent to produce a mixture of methyl difluoropyruvate hydrate, **52**, and unreacted difluoroacetylmethyl furan. We found if ozone was bubbled into the reaction mixture when the greenish color formed, and then disappeared, the conversion of **51** to **52** was complete.

Separation of **52** from contaminating $\text{CF}_2\text{HCO}_2\text{H}$ was described by passage through silica gel.¹²⁴ Repeated attempts at chromatographic separation on silica failed, using various $\text{CH}_3\text{OH}/\text{CH}_2\text{Cl}_2$ or $\text{CH}_3\text{CN}/\text{CH}_2\text{Cl}_2$ eluents. Acidic byproducts were successfully removed by passage through a column of Amberlyst A-21, a polystyrene supported tertiary amine ion exchange resin. This treatment successfully removed the acidic components but elution with ethanol caused exchange with the methyl hemiacetal of the desired product to produce a mixture of the ethyl and methyl hemiacetals of methyl difluoropyruvate. Using the same methodology for the formation of **47**, compound **53** was afforded in 69% yield after acidic hydrolysis and neutralization.

Soaking SbADC crystals with 50mM **53** did not produce sufficient electron density in the active site to conclude that it was complexed in the cavity. This is more than likely due to the propensity of the difluoropyruvate to hydrate and not have enough of the keto form present to form an imine with the active site lysine. As 50 to 150mM pyruvate was used to generate 1.5Å resolution images, a concentration of 150mM or greater would probably be needed to the **53** to form a Schiff Base with the enzyme. When **47** and cinnamaldehyde were soaked with SbADC concurrently no electron density was observed in the active site. This result was not expected for if the pair would not occupy the active site at least the Schiff base of **47** was expected to be

seen. The reason for this remains unknown but conducting the soaks at various concentrations of the two components might generate the desired crystallographic structure.

VI. SMALL MOLECULE PROBES FOR MppR AND MppP

A. Enduracididine and Enduracidin Background Information

Second to vaccines, antibiotics seem to be the most effective means to treat disease and illness. Unfortunately, this boon is being combated by the organisms we eliminate by their evolution of antibiotic resistance. Infectious agents now exist that are either resistant or immune to our most potent substances like vancomycin or methicillin. The mode of action of these last resort antibiotics, like vancomycin, impede the growth of these bacteria by inhibiting the expansion of their cell walls upon growth causing the cells to lyse in the process due to internal osmotic pressure. Antibiotics such as ramoplanin, enduracidin, and mannopeptimycin¹²⁶ prohibit growth in much the same way but seem to exhibit a peculiar ability to not be adapted against.

All three of these structures are similar in their construction and antibiotic potency. In 2002, Cudic *et. al.* investigated the mechanism of ramoplanin¹²⁷ to inhibit the late stage glycosyltransferase reactions necessary for bacterial growth. Different from the recognition of the N-acyl-D-Ala-D-Ala moiety like vancomycin, Somner and Reynold postulated that it was inhibition of Lipid I to Lipid II conversion that stopped the glycosyltransference.^{128,129} Testing of this hypothesis was problematic for some time as acquisition of pure murG, the enzyme that facilitates transglycosylation, and assay soluble version of Lipid I and II were not available until 1998 when the Walker labs synthesized a biomimetic analogue that was water soluble to test

the activity of the murG enzyme.¹³⁰ It was also stated in this paper that murG has no human equivalent and that the muramyl-pentapeptide moiety is unique to bacterial organisms. Their work continued¹³¹ by following the accumulation of radiolabelled Lipid II in increasing amounts of ramoplanin present to suggest a new mechanism of action for the antibiotic: binding to Lipid II by ramoplanin to prevent its polymerization and thus prevent cell wall biosynthesis. These two modes were tested later in 2006 to confirm which one of these pathways was taken.¹³² Using inhibition kinetics and binding assays it was demonstrated that Lipid II binds approximately ten times stronger to enduracidin and ramoplanin than Lipid I but was only favored in competition experiments by a factor of five. Although capture of Lipid II is slightly favorable both of these pathways appear to happen equally. It is this that makes these antibiotics so resistant to adaptive mutation in that they target and disrupt a process so fundamental to the bacteria's survival that in order to evolve against it would require an alternate method to construct its cellular membranes.

Enduracidin was first observed from *Streptomyces fungicidicus* from the soil of Nishinomia, Japan and found to have potent antibiotic activity against gram-positive bacteria and moderate activity against acid-fast and phytopathogenic organisms while having no activity against gram-negative bacteria, fungi, or yeasts tested.¹³³ Later in the year enduracidin was isolated and characterized¹³⁴ demonstrating its most potent activity against antibiotic resistant strains of *S. aureus* with minimum inhibition concentrations (MIC) ranging from 0.1-0.2µg/mL.

The antibiotic's efficacy was demonstrated¹³⁵ *in vitro* and *in vivo* when administered intravenously, intraperitoneally, and subcutaneously but not orally against *S. aureus*, *S. pyogenes*, and *D. pneumonia*. Digestion of enduracidin in 6M HCl yielded nine types of known

amino acids along with two as of then unidentified residues. In a follow up publication¹³⁶ the structures of the known amino acids were determined and called enduracididine and allo-enduracididine, the enantiomer of enduracididine.



Figure 93: Enduracididine (left) and allo-enduracididine (right)

The origin of enduracididine was investigated by feed experiments of *S. fungicidicus* with radiolabelled amino acids.¹³⁷ For these it was concluded that aspartic acid, threonine, serine, glycine, alanine, ornithine, and citrulline were directly incorporated into the cyclic polypeptide whereas the 4-hydroxyphenyl and 3,5-dichloro-4-hydroxyphenyl glycine residues were derived from tyrosine. For enduracididine it was presumed that either arginine or histidine was the precursor to enduracididine but with this study it shows that the radiolabelled arginine was the amino acid used to make enduracididine providing solid evidence that arginine was the precursor.

B. Roles of MppP and MppR

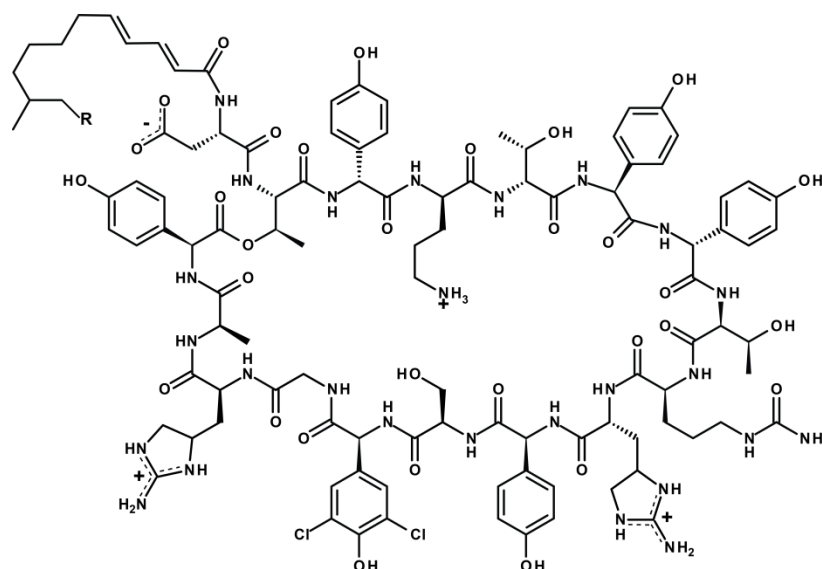


Figure 94: Enduracidin A (R=H) and Enduracidin B (R=CH₃). Image provided by Dr. Nicholas Silvaggi

Using *Streptomyces eurocidius* Eguchi¹³⁸ uncovered more detail as to the specific transformations arginine undergoes along the metabolic pathway to enduracidine when looking at the role of arginine in the biosynthesis of 2-nitroimidazole. When the bacteria was heated at 50°C the production of 2-aminoimidazole, the precursor to 2-nitroimidazole, ended. When arginine was administered to the bacteria followed by 50°C heat treatment a guanidine positive material was seen to accumulate. Exposure of the guanidine positive fraction to H₂O₂ to decarboxylate the amino acids present afforded 3-hydroxy-4-guanidino-butyric acid implying that γ-OH-arginine was the material that was building up. Pyridoxal phosphate (PLP) and oxygen were also confirmed as necessary to the reaction for if the cofactor was omitted and the reaction was conducted under an inert atmosphere 2-aminoimidazole production was not seen.

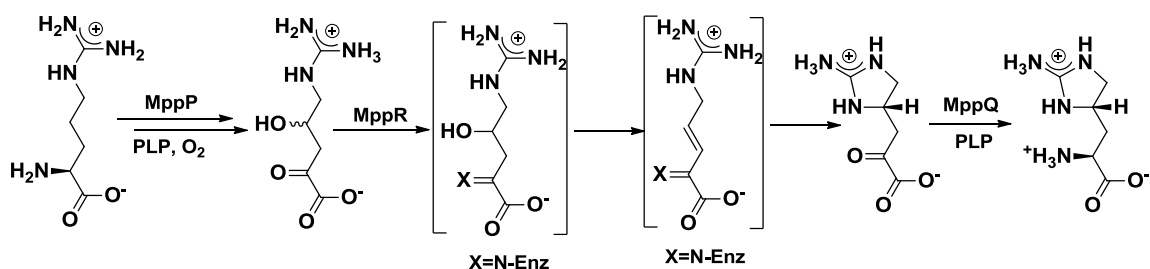


Figure 95: Proposed biosynthesis for enduracididine

The proposed biosynthetic pathway was the oxidation of arginine followed by loss of pyruvate from the oxidized arginine's α -keto analogue to produce 2-aminoimidazole for conversion to the 2-nitroimidazole antibiotic. When given arginine and its cofactors, pyridoxal phosphate and molecular oxygen, 2-aminoimidazole production proceeded. However if deprived of these or if the enzyme was heated to 50°C 2-aminoimidazole was not formed but instead a guanidine positive material accumulated. When this accumulated fraction was treated with H_2O_2 to induce decarboxylation 3-hydroxy-4-guanidinobutyric acid was found as the product implying that the guanidine positive substance was γ -hydroxy-arginine which underwent transamination to the α -keto acid then decarboxylated. Interestingly enough, when γ -OH-arginine was given to the enzyme in the absence of pyridoxal phosphate and/or molecular oxygen 2-aminoimidazole was formed along with an equal amount of pyruvate. Although not identified, it was postulated that an aldolase type enzyme would be required to affect the transformation described above.

Genetic sequencing and experimentation with cloned variants lead to the identification of the 17 amino acid gene cluster for the production of enduracididine.¹³⁹ It was found that both *S. enduracidicus* and *S. hygroscopicus* contained the three gene operon for antibiotic EndP, EndQ, EndR and MppP, MppQ, MppR for the biosynthesis of enduracidin and mannopeptimycin respectively. They also held in common a non-heme based oxygenase that utilized 2-oxo-

glutarate that does not hydroxylate arginine but instead hydroxylates enduracididine in the β position.¹⁴⁰ MppP and MppQ were both shown to be pyridoxal based aminotransferases with the role of MppR still undetermined.

The structural and functional capability of it was later reported¹⁴¹ demonstrating its activity as an aldolase and confirming the previous hypothesis that an aldolase is needed to be present as was postulated by the feed experiments of *S. eurocidius*. Bioinformatic analysis shows that MppR has a low but significant sequence homology to that of a previously uncharacterized group of acetoacetate decarboxylase family with the similarity notably occurring in the active site. X-ray crystallography of MppR crystallized from HEPES buffer showed a HEPES molecule bound in the active site with the sulfonyl group hydrogen bonded to the active site lysine L156. Treatment of MppR with sodium pyruvate either as a soak or being present during crystallization covalently bonded to L156 as a Schiff base with no coordinated water proximal to the former α -keto functionality probably due to the hydrophobic nature of the active site itself.

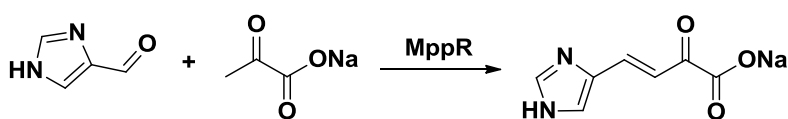


Figure 96: Aldol condensation and dehydration product of imidazole carboxaldehyde and sodium pyruvate formed by MppR

Encouraged by this observation, imidazole-2-carboxaldehyde was soaked with MppR and sodium pyruvate with the resulting crystal structure showing the Aldol product between the two, however, with no enzymatic turnover. HPLC analysis with UV/VIS detection showed none of the enone in the supernatant. To test the role of MppR in the biosynthesis of enduracididine it was treated with 2-oxo- γ -OH-arginine which resulted from the exposure of 4(R/S)-hydroxy-

2(S)-arginine with an L-amino acid oxidase (LAAO) from *C. atrox*. Over time this produced the 2-oxo derivative of enduracididine with the same stereochemistry at C4 as seen in mannopeptimycins and making the same intermolecular interactions with the active site residues as pyruvate did.

(2S,4R)-2-amino-5-guanidino-4-hydroxypentanoic acid, colloquially known as γ -OH-arginine, was first isolated from the sea cucumber *Polycheira rufescens*.¹⁴² Identification of the amino acid was derived from material isolated after reaction of treated extract with an L-argininase and comparing the compounds to synthetically produced γ -OH ornithine and γ -OH-arginine.

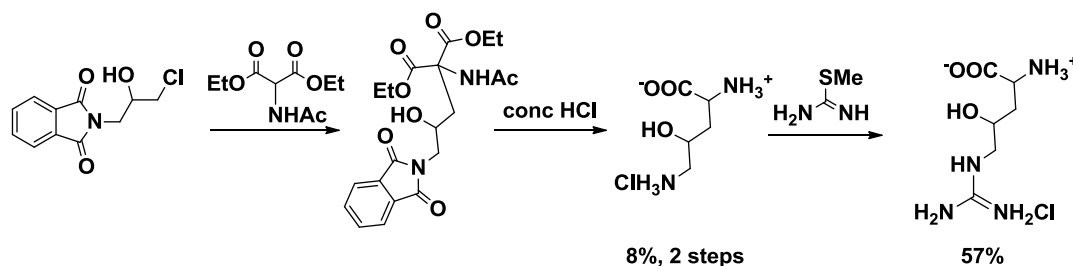


Figure 97: Literature route to γ -OH arginine

γ -OH-arginine was made in 4.6% overall yield by first making γ -OH ornithine which was then treated with S-methylthioisourea to install the guanidino group. The stereochemistry of the γ -OH-arginine isolated from *P. rufescens* was published by Fujita year later¹⁴³ as the S chirality on the hydroxyl containing carbon and R as the chirality of the amino bearing carbon. A later report¹⁴⁴ altered the route used by Fujita by first reacting epichlorohydrin with sodium diethyl malonate instead of phthalamide.

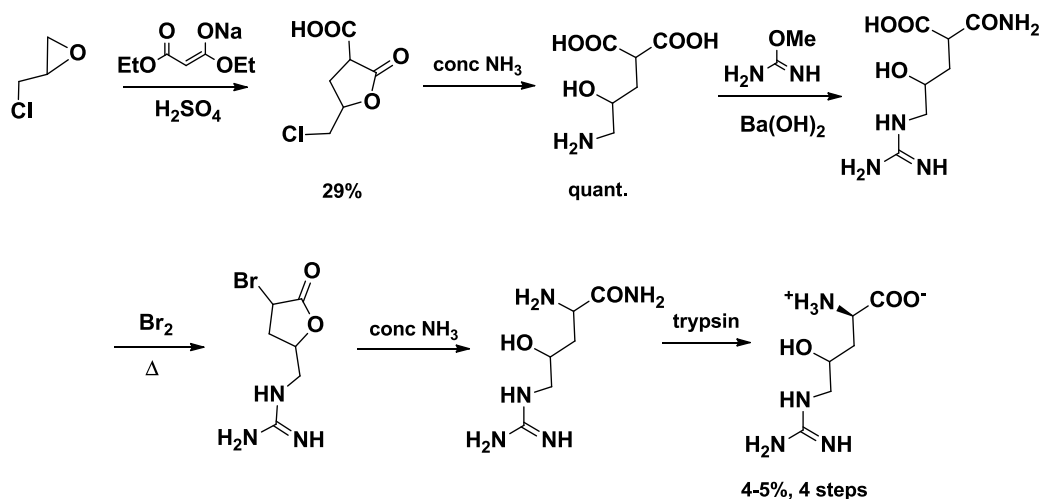


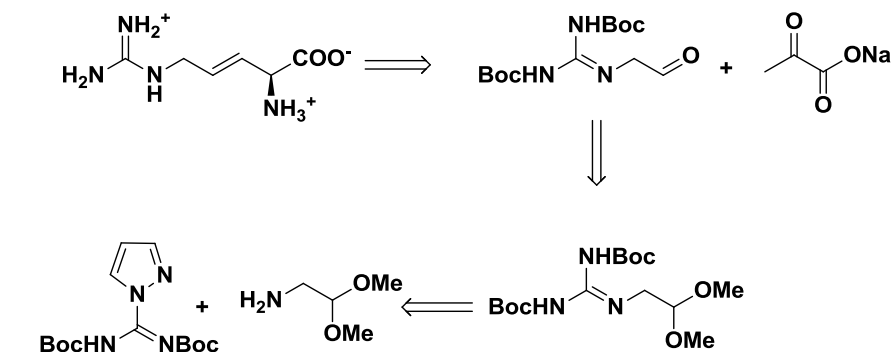
Figure 98: γ -OH arginine synthesis from epichlorohydrin

After treatment with ammonia the guanidine was formed from OMe isourea. Reaction with bromine, then ammonia, then trypsin give the desired product in 1.3% yield as a mixture of the R and S hydroxyl diastereomers with no isolation of the intermediates after formation of the epichlorohydrin malonate adduct. The low yield was attributed to the multitude of side reactions undoubtedly produced by reaction with bromine as well as trypsin hydrolyzing only two of the four total diastereomers present. They also replicated Fujita's method using OMe isourea but did not report a yield however it was stated that use of an acidic eluent for ion exchange chromatography drove the γ -OH-arginine to lactone formation.

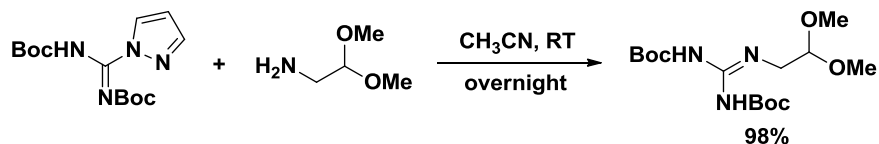
More recent methodologies focus on stereoselectivity to increase yield of the (2S,4R) isomer to study the biosynthesis of enduracidin,¹⁴⁵ synthesis of a fully protected, organic soluble enduracididine in 3-8% overall yield¹⁴⁶ using a single enantiomer of a key aziridine intermediate,¹⁴⁷ and synthesis of β -OH enduracididine derivatives to generate modified mannopeptimycins via peptide coupling.¹⁴⁸ Synthesis of γ -OH-arginine and its dehydro analogue were undertaken to more thoroughly explore MppR as well as to open a pathway to make

modified enduracididines which would hopefully be incorporated into the biosynthesis resulting in modified enduracidins to fight antibiotic resistant bacteria in the future.

C. Attempts to Make Guanidiniumacetaldehyde for MppR Evaluation



The above retrosynthetic analysis shows that the most expedient route to γ -hydroxy-arginine or dehydro-arginine would be through Aldol Condensation of sodium pyruvate with guanidinoacetaldehyde. Good reagents have been developed for installing guanidino functionality on imines¹⁴⁹ but Drake, Petel, and Lebl have made an extremely convenient and efficient guanidinylation agent¹⁵⁰ (used exclusively from here on in) and if reacted with the dimethyl acetal of aminoacetaldehyde acidic hydrolysis would provide the desired material.



When the dimethyl acetal was exposed to the pyrazolyl diBoc-carboxamide the resulting guanidine was afforded in an average of 98% yield with two degree melting point range due to the easy removal of pyrazole side product due to its volatility.

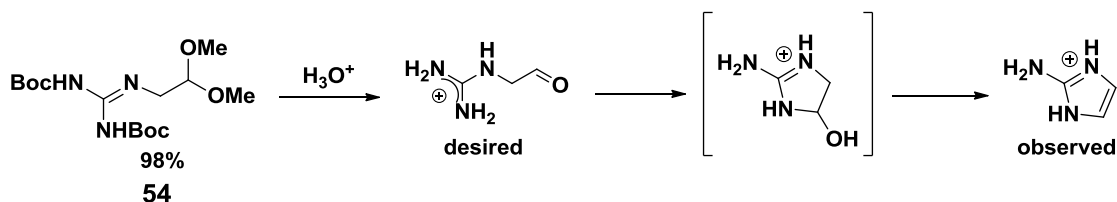


Figure 101: Formation of 2-aminoimidazole from guanidynlated aminoacetaldehyde dimethyl acetal upon acidic hydrolysis

Hydrolysis of dimethyl acetal **54** in 11M trifluoroacetic acid in deuterium oxide was monitored by ^1H NMR with complete removal of the Boc groups after 20min when data was first acquired. When the spectrum of the sample was obtained a second time 18hr later, only singlets corresponding to methanol and 2-aminoimidazole were present. As acid hydrolysis resulted in cyclization and aromatization, removal of the Boc groups to generate the guanidinium salt was conducted in hopes to prevent cyclization. When the acetal was combined with two equivalents of methanesulfonic acid at -78°C and warmed to 0°C no removal of the Boc groups was observed. It was only after warming to room temperature that removal of only one Boc group occurred as determined by ^1H NMR. Even after 46hr at room temperature no change was observed from the now monoBoc guanidine. Hydrolysis was undertaken again but with 12M HCl at 0°C and followed by no D NMR. Complete conversion of the substrate to 2-aminoimidazole occurred in $\leq 48\text{min}$. Under these conditions it was deemed an unsuitable method for formation of the guanidinoacetaldehyde as cyclization and aromatization could not be prevented. In all of these cases the characteristic resonance of an aldehyde in ^1H NMR was not observed, even transiently.

D. Towards β,γ -dehydroarginine for MppP Evaluation

With acidic hydrolysis of the dimethyl acetal demonstrated to not be a viable route to make guanidinoacetaldehyde an alternative method was adopted. Oxidative cleavage of the appropriate alkene precursor to produce the aldehyde first while keeping the Boc groups intact to prevent cyclization was the rationale for the new approach. Guanidinylation of allyl amine to afford **55** averaged yields of 97% with two degree melting point range. Its been shown that generation of OsO_4 *in situ* with NaIO_4 can be used to convert an alkene to a diol which then is cleaved by NaIO_4 to the corresponding carbonyl compounds can be performed conveniently and in decent yield.¹⁵¹ When di-Boc allylguanidine was exposed to these conditions only unreacted starting material was recovered in 83%, even after 35hr time and was not observed anymore on TLC analysis. The reaction was performed again with none of the desired aldehyde **56** observed even after 3days. However, after three days a new signal was observed by ^1H NMR at δ 6.7ppm and interpreted to be the diBoc derivative of 2-aminoimidazole and present in only as minor amount.

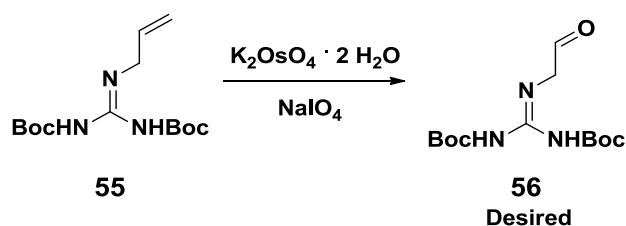


Figure 102: Desired oxidative cleavage of guanidinylated allylamine

Perplexed by this lack of activity on what appeared to be a suitable substrate the quality of the reagents were tested by way of reaction with a different allyl compound.

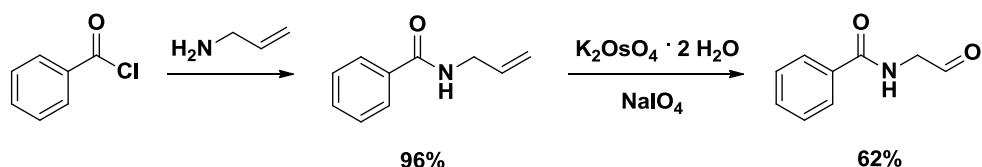


Figure 103: Model reactions to test conditions for oxidative cleavage of an alkene with K_2OsO_4

N-Benzoyl allylamine was synthesized in 96% yield and exposed to the oxidation regime to produce the corresponding aldehyde in 62% yield. In comparing the structure of the di-Boc allylguanidine and the benzoyl allylamine it was hypothesized that the benzoyl analogue was able to react was that the lone pair of electrons on the nitrogen were involved in resonance were as the lone pair on the allyl moiety were sitting as a free lone pair which can coordinate to the osmium when the osmate ester is formed preventing diol formation by either occupying a required coordination site by chelation preventing the ligand transfer needed for the oxidative regeneration of the osmium. The hypothesis was tested by deprotection of **55** in refluxing 50% $\text{CF}_3\text{COOH}/\text{CH}_2\text{Cl}_2$ for 1hr. Elevated temperature was needed as exposure to the acid at room temperature only removed one of the Boc groups which is agreement with previous observations as a di-cation would need to be made to remove the second Boc group.

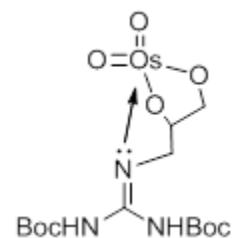


Figure 104:
Proposed stabilized complex that prevents dihydroxylation by osmium tetroxide

The resulting trifluoroacetate salt **57** was treated with the oxidation reagents in a mixture of D_2O and CD_3OD and monitored by ^1H NMR.

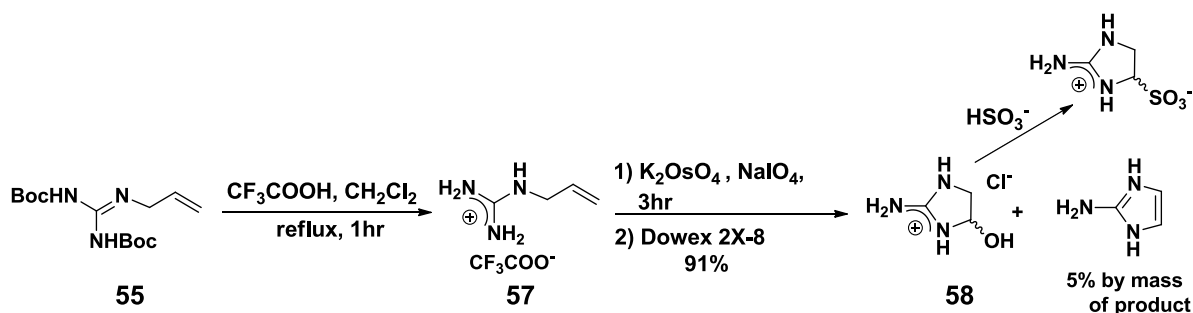


Figure 105: Cyclized hemiaminal generated upon treatment of allylguanidinium trifluoroacetate with osmium tetroxide

After 3.5hr the alkene resonances were no longer observed but neither was that of the desired aldehyde. Instead signals of δ 5.6, δ 3.9, δ 3.5 were seen, each as a doublet of doublets. From this it was concluded that the aldehyde did form but cyclized to hemiaminal **58** even with the protonated guanidine at neutral pH due to the germinal coupling constants. Also observed in the reaction mixture was formalin, corroborating that the oxidative cleavage took place. 2-aminoimidazole was also produced but in trace amounts which implies that **58** is the kinetic product, and aromatization to the imidazole occurs over time.

The reaction mixture was split into two portions to which was added hydroxylamine to one and sodium bisulfite added to the other. Each was added to react with the aldehyde in a manner that could be reversed and to keep it acyclic so it could not aromatize. Exposure to hydroxylamine hydrochloride did not produce the desired oxime but instead catalyzed the transformation to 2-aminoimidazole completely. Addition of 20eq of sodium bisulfite on the other hand did not aromatize the hemiaminal and made the sulfonate of the hemiaminal proving that elimination to the aromatic species is avoidable. After accounting for these two compounds another doublet of doublets was seen but wasn't enough to confirm the presence of the acyclic bisulfite adduct. The splitting pattern, chemical shift, and coupling constants of the cyclic sulfonate shifted upfield to δ 5.3 for methyne hydrogen and downfield shifts of δ 5.0

and δ 4.9 for the methylene hydrogens. Since the identity of the corresponding anion from the reaction may oxidize MppR when exposed to it the reaction was repeated and the hemiaminal was purified to the chloride salt via ion exchange chromatography with Dowex 2X-8 resin.

As hemiaminal **58** had to be produced by cyclization of the guanidine group into an aldehyde, there presumably some mechanism by which the equilibrium can be perturbed so that the aldehyde can be present. Even if it could not open back up, it could lose a hydroxyl group to form an iminium ion which could go on to react with pyruvate in an aldol manner. Based on these possibilities, the Silvaggi group combined **58**, sodium pyruvate, and MppR. Unfortunately, they found that no reaction between the components was observed.

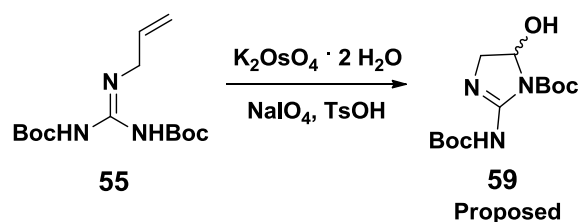


Figure 106: Synthesis of di-Boc protected cyclic hemiaminal from di-Boc protected allylguanidine

With the lone pair hypothesis validated, the di-Boc allylguanidine was treated with K_2OsO_4 and NaIO_4 again but this time in the presence of 1 eq *p*-toluenesulfonic acid to determine if protonation would be a viable way to oxidize the allyl group while keeping the guanidine Boc groups intact. By ^1H NMR it was unable to be determined if the cyclized hemiaminal was a salt or became deprotonated to become neutral but the alkene signals went away and resonances similar to that of **58** were seen. As the mixture was taken in CDCl_3 it was presumed to be the neutral species. The mixture was partitioned against water to remove the inorganic salts and concentrated before being allowed to react with sodium pyruvate as per the cinnamylidene method to produce **59**.

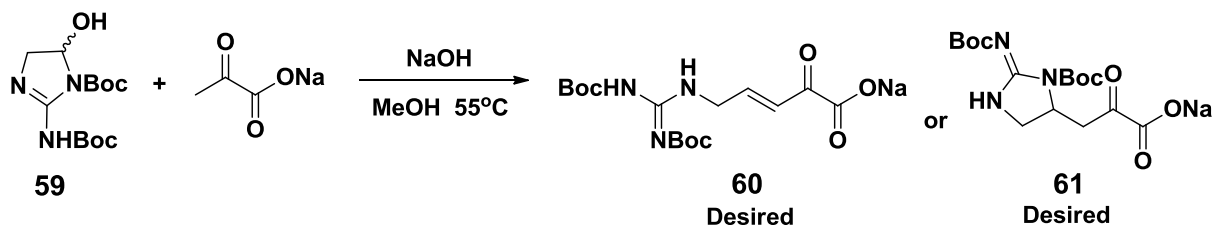


Figure 107: Reaction of di-Boc cyclic hemiaminal **59** with sodium pyruvate

After 17hr at 55°C **59** was longer seen by TLC. Analysis by ^1H NMR in D_2O showed no Boc signals present nor any other the alkene signals anticipated for the Aldol product. The crude product was extracted from triethylammonium bicarbonate with CH_2Cl_2 to isolate the desired product if present. What was observed by ^1H NMR did not have signals correlating to the alkene **60** and the starting material **59** was not isolated. One thought would be that the Boc protected nitrogen in the guanidine could Michael add into the enone product to cyclize to **61**. This was considered a possibility as demonstrated by the guanidine's propensity for cyclization but based on the ambiguity of the ^1H NMR spectrum, and the low amount of material recovered, it was deemed an unattractive method to make the dehydroarginine. However, more investigation should be undertaken to conclude if the material generated was indeed α -keto enduracididine as the methodology used would provide a succinct path for its synthesis.

1. L-Vinylglycine Synthesis

Vinylglycine¹⁵² is a simple chiral substance allowing transformation of each of the three groups bonded to the chiral center.¹⁵³ It has become even more valuable since the development of efficient olefin metathesis catalysts that can convert it to other unsaturated amino acids. The unsaturation diverts pyridoxal-mediated transformations, leading to suicide substrate behavior of substituted vinylglycines with several pyridoxal based enzymes.^{154,155,156} A

GABA transaminase irreversible inhibitor has also been prepared by a similar means.¹⁵⁷ Even in the absence of pyridoxal, the α -proton of vinylglycine ester is considerably more acidic than that of saturated amino acid esters: in mild base β - γ unsaturation of vinylglycine esters is rapidly converted to α - β unsaturation. Even in neutral D₂O, vinylglycine esters α -deuterate and gradually isomerize.¹⁵⁸ This obviously limits the conditions and procedures appropriate for preparation and transformation of such unsaturated amino acids.

Vinylglycine has been prepared by a variety of methods^{159,160} including sulfoxide or selenoxide elimination from methionine derivatives,^{161,162,163,164,165,166} oxidative decarboxylation of glutamic acid,¹⁶⁷ asymmetric allylic substitution and subsequent transformation,¹⁶⁸ vinyl Grignard reaction with an α -bromoglycine,¹⁶⁹ and an interesting route involving Neber rearrangement.¹⁷⁰ All these procedures yield vinylglycine in a protected or racemic form, from which L-vinylglycine itself can be isolated by deprotection and/or enzymatic resolution.

Perhaps the most common route is that reported by the Rapoport group in 1980 involving vapor-phase thermolysis of the Cbz protected methyl ester of methionine sulfoxide.^{92,171} Contamination with isomerization products and variable yields encouraged modifications of conditions over the years, leading ultimately to a 79% yield of 95% pure protected vinylglycine.⁹⁶ Deprotection of chromatographically-isolated Cbz vinylglycine ester in refluxing hydrochloric acid allows subsequent transformation.¹⁶¹ However, the gas phase reaction limits reaction scale, and requires careful control of conditions inconvenient with standard laboratory glassware. Attempts to increase throughput by solution phase approaches met with difficulties.⁹³ Despite this procedure, and the significant number of papers and patents describing vinylglycine and its use,^{172,173} vinylglycine is not readily available commercially.

We report here a modification to the Rappoport approach to unprotected vinylglycine that allows convenient reaction at larger scale using standard apparatus and short reaction times. We have replaced two protection steps, thermolysis, chromatographic purification of protected vinylglycine, and deprotection, with a single simpler process using *in situ* protection, more convenient thermolysis, and a simple workup that effects deprotection and isolation of crystalline vinylglycine without chromatography. We have optimized for convenience rather than yield: conversion of methionine into pure crystalline vinylglycine requires two simple operations.

a. L-Selenomethionine selenoxide Route

The mildest procedures leading to vinylglycines appear to involve phenylselenoxide elimination.¹⁷⁴ A succinct method would be the by β,γ -syn elimination of the selenoxide analogue of L-Methionine with the chemical literature demonstrating that the α,β - elimination to form enones occurs rapidly, usually with no ability to isolate the corresponding selenoxide.

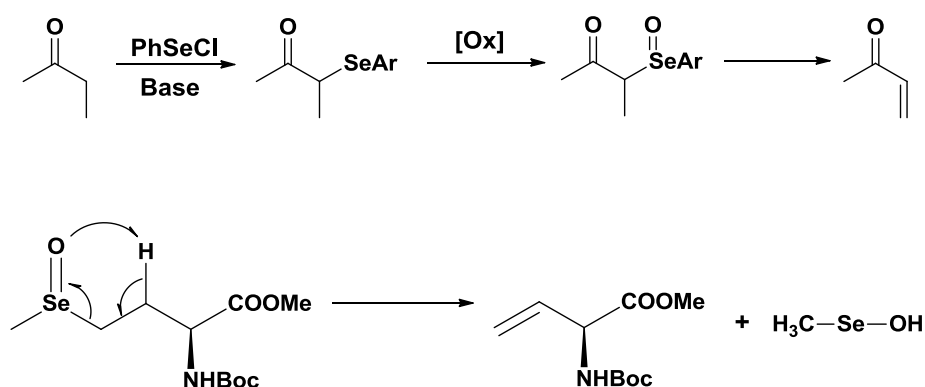


Figure 108: α,β -unsaturated ketone formation by arylselenoxide elimination and desired elimination of a methyl selenoxide to form vinylglycine

While not as facile as the α,β - elimination, the β,γ -elimination was deemed feasible. L-selenomethionine was converted to the methyl ester **62**, N-Boc protected to **63**, and oxidized

the the selenoxide **64** using standard protocols. While the α,β - elimination can occur between -78°C and 0°C, elevated temperature were employed in investigation of the β,γ -elimination to generated the vinylglycine derivative **65**.

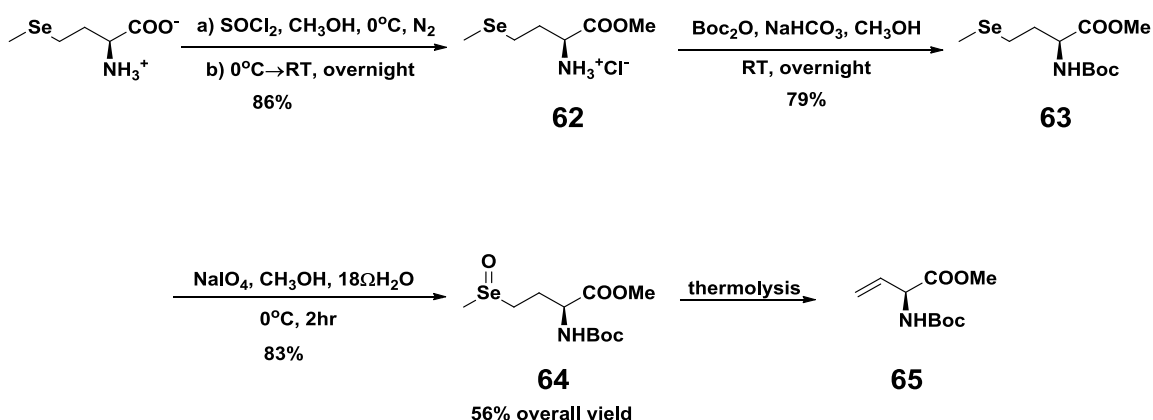


Figure 109: Synthetic scheme of N-Boc-L-vinylglycine methyl ester synthesis from L-selenomethionine

It has been previously reported¹⁰⁶ that a derivative of L-Selenomethionine oxide reduces back to its L-Selenomethionine derivative in acetone over 7d at room temperature in the absence of light. What was surprising was not the extent of this conversion in our experimental observations but the rapidity at which this transformation took place. Tabulated below are the experimental parameters and results from the β,γ -elimination of **64**:

Entry	Conc SeO	Conc P(OMe) ₃	Temp(°C)	Time	Solvent	χ(vinyl:Se)	%yield(NMR)
1	1.0e ⁻² M	-	138	2h	p-xylene	1 : 4	10
2	1.0e ⁻² M	-	81	2h	CH ₃ CN	0 : 1	39 L-MetSe
3	9.0e ⁻³ M	0.09 M	110	20min	Toluene	1 : 2.5	50→0
4	8.0e ⁻³ M	0.10 M	110	20min	Toluene	1 : 1.8	41
5	4.0e ⁻³ M	-	111	25min	P(OMe) ₃	-	0
6	1.0e ⁻² M	3.60 M	reflux	25min	Hexane	1 : 10	15
7	2.0e ⁻² M	0.27 M	110	40min	Toluene	0 : 1	97 L-MetSe
8	1.5e ⁻² M	-	110	20min	Toluene	1 : 2.5	36

Table 6: Parameters and results in thermolysis of NBoc-L-selenomethionine oxide methyl ester

In our hands the methyl selenoxide **64** eliminated less well: only low yields (10-41%) of **65** were obtained on thermolysis. The major product was the preceded reduction to selenide.¹⁷⁵ Poor results were found at various temperatures, even in the presence of excess periodate, though it helped in a related phenylselenoxide case¹⁷⁶.

b. L-Methionine sulfoxide Route

i. Gas Phase Pyrolysis

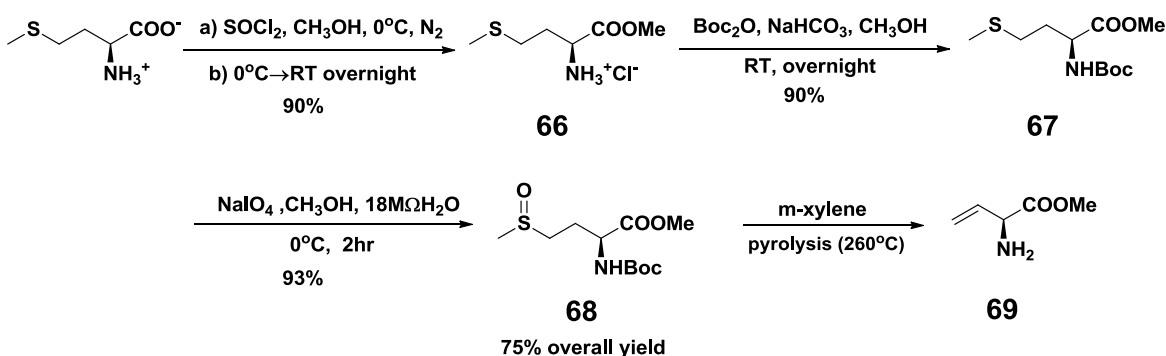


Figure 110: Synthesis of L-vinylglycine methyl ester from L-methionine

With the failure to produce vinyl glycine by β,γ -elimination from **64** in appreciable amounts, we turned to the harsh sulfoxide elimination procedure using the N-Boc methyl ester derivative of methionine sulfoxide, as reported by Rich¹⁶⁴ which provided the most detail for pyrolysis as well as an attractive yield before Rappoport's report and thus this method was chosen.¹⁶¹ L- methionine was converted to **68** using the same protocols in the derivatization of L-selenomethionine to **64**. Vapor or aerosol introduction of **68** in xylene to a hot tube at 266°C led in our hands to variable yields (2-18%) of vinylglycine methyl ester with loss of Boc protection and on average 50% recovery of **68**. Pyrolysis was successful on one account affording a 59% yield of **69** as estimated by NMR a mixture with DEHP. The capricious behavior was attributed

to the low volatility of starting material and to lability of product, as isomerization of desired vinylglycine to α - β unsaturated side product was also observed.

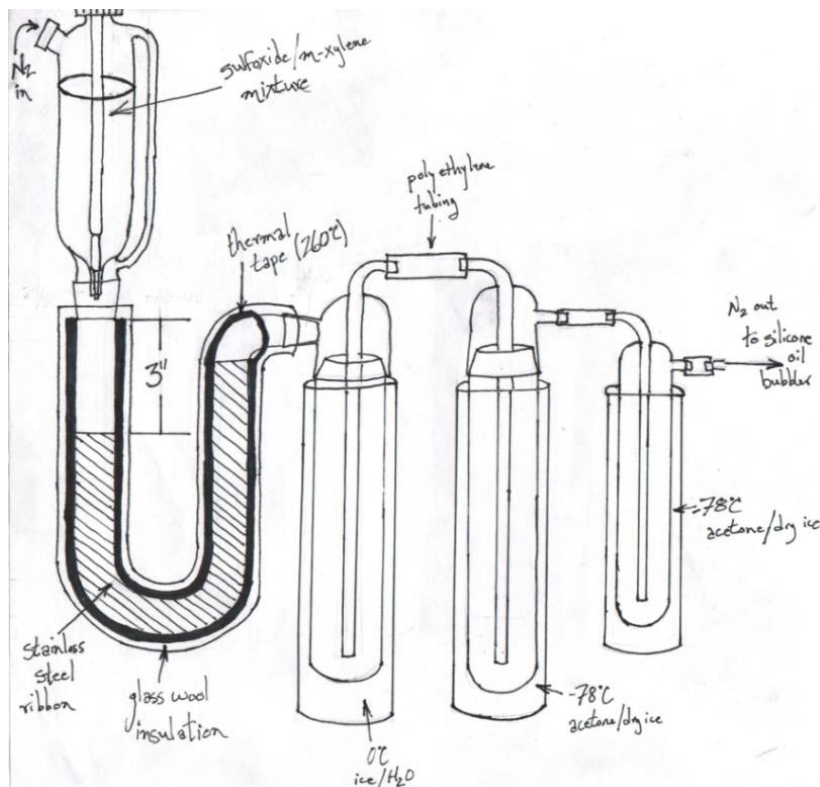


Figure 111: Illustration of apparatus constructed for gas phase pyrolysis

The thermal Boc removal is not entirely unwelcome, as its removal would be the next step in our sequence, but consideration of other protecting groups led to a useful modification. Protection of methionine sulfoxide in an organic soluble and more volatile form is needed, as we found pyrolysis of L-methionine sulfoxide (**70**) itself does not lead to L-vinylglycine (**71**). As stocks of **68** were depleted, pyrolysis of a different protected form of L-Methionine sulfoxide was performed we chose trimethylsilyl groups to protect both the acid and the amine functionality, partly to increase volatility, and partly because both groups could be added before and removed after elimination as one procedure. Vapor phase thermolysis proceeded in a similar efficiency as before, though exposure of product to water caused complete

deprotection to free vinylglycine. Previous solution phase thermolyses led to problems because of decomposition of products on longer high temperature exposure times.¹⁶² Pyrolysis proved successful and reproducible with the silylated methionine sulfoxide. The parameter that determined reproducibility was not only the temperature of pyrolysis, but the position of the stainless steel packing material in the pyrolysis tube.

ii. *in situ* Thermolysis

As the silylated methionine sulfoxide solution was able to be transformed into vinyl glycine by pyrolysis and vinyl glycine was recovered from the packing material at temperatures up to 310°C, it was hypothesized that the reaction could be performed in solution with the high boiling solvent diphenyl ether. The thermolysis was performed with variable amount of time with the solution at reflux. The table below details the distribution of materials was identified by ¹H NMR

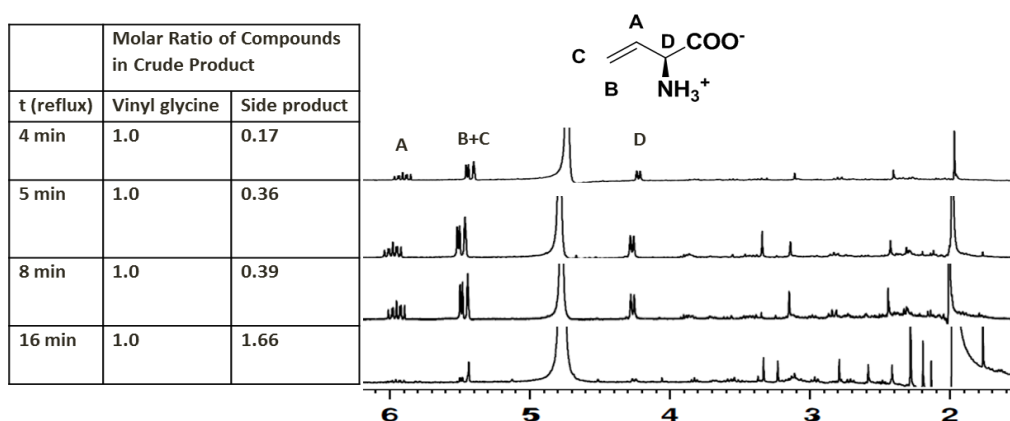


Figure 112: NMR spectra of isolated materials from *in situ* thermolysis of silylated L-methionine

Aqueous workup of the 5min trial afforded a 34% NMR yield of vinyl glycine.

Encouraged, thermolysis of non-silylated **70** was done for 3.5min in refluxing diphenyl ether.

Undetermined degradation products were produced as determined by NMR with signals

observed that did not correspond to L-Methionine sulfoxide, vinyl glycine, or the side product,

concluding that vinyl glycine cannot be produced without the presence of N,O-

(bistrimethylsilyl)acetamide. Thermolysis of the silylated L-Methionine sulfoxide was scaled up

and replicated with experimental parameters and results tabulated below:

Entry	Conc. L-MetSO	Conc. BSA	Mol Ratio L-Met SO:BSA	BSA:Ph ₂ O (v:v)	Time to Reflux	Time at Reflux
1	0.09 M	0.39 M	1 : 4.3	1 : 11	4 min	1 min
2	0.10 M	0.37 M	1 : 3.6	1 : 10	3 min	2 min
3	0.15 M	0.59 M	1 : 4.0	1 : 6	3 min	3 min
4	0.28 M	0.91 M	1 : 3.3	1 : 3.5	2 min	3 min

Table 7: Experimental parameters in screening *in situ* thermolysis for L-vinylglycine formation

Entry	% by mass of the crude product				Estimated NMR yield L-Vgy
	Vinyl Gly	Acetamide	Side Product	L-Met SO	
1	49	37	7	7	68%
2	52	37	11		54%
3	43	39	7	11	68%
4	15	65	20		30%

Table 8: Results from tested conditions *in situ* thermolysis parameters in L-vinylglycine synthesis

iii. Addition and Distillation Method

Because of the expected substantially greater volatility of trimethylsilyl derivatives, we tried solution-phase heating of the silylated methionine sulfoxide. This provides a dramatic operational simplification.

Simply stirring L-methionine sulfoxide¹⁷⁷ in N,O-*bis*(trimethylsilyl)acetamide (BSA) caused gradual dissolution as the zwitterionic starting material was converted to the trimethylsilyl ester and likely the N-trimethylsilyl derivative as well.¹⁷⁸

Surprisingly the material in the still pot after aqueous workup was determined by ¹H NMR to contain trace amounts of vinyl glycine with the majority being the unidentified side product and other degradation products accounting for 15% of the theoretical mass. Analysis of the distillate showed the presence of the silylated vinyl glycine. After aqueous workup the crude product was determined to be 3% by mass side product, 50% by mass acetaminde, and 47% by mass vinyl glycine corresponding to a 48% yield by NMR and the cleanest crude product seen to date. The experiment was replicated with similar success. The tables below are the parameters and results for the subsequent trails:

Entry	Conc SO (M)	Conc. BSA (M)	Ratio BSA:Ph ₂ O(mols)	Time to Reflux	Distill Time
136	0.16	0.56	1:3.5	5.5 min	4 min
138	0.12	0.43	1:3.6	8 min	6 min
130	0.30	0.67	1:2.2	10 min	9 min
140	0.27	1.92	1:7.1	7 min	5 min
142	0.18	0.72	1:4	15 min	4 min

Table 9: Experimental parameters from *in situ* thermolysis with distillation

Entry	Amount Distilled	% by mass of the crude product			% yield
		L-vinylglycine	Acetamide	Side Product	
136	2/3 rxn V	47	50	3	48
138	4/5 rxn V	45	52	3	51
130	To 246°C head temp	16	80	4	22
140	To 246°C head temp	22	73	5	36
142	175-253°C head temp	34	62	4	44

Table 10: Experimental results from in situ thermolysis with distillation

Thermolysis with distillation has consistently lead to the best molar ratios of vinyl glycine to unknown side product (on average 1:0.04 as determined by ratio of vinyl integrals to the triplet at 3.86ppm). Fractions can be collected during the course of distillation to obtain a purer crude product with the head temperature range of 175-246°C containing all of the vinyl product. However, the head temperature range of 175-200°C does contain vinyl glycine it only averages ~1% by mass and ~1% by mass side product with the remainder of the mass being acetamide. Interestingly, a large excess of BSA did not lead to an increased yield of vinyl glycine and corresponded to an increased amount of acetamide. The current hypothesis is that not only does amount of BSA correspond to the best yield but the ratio of volumes of BSA and diphenyl ether. This is presumably due to the time at which the reaction volume reaches the boiling temperature of diphenyl ether.

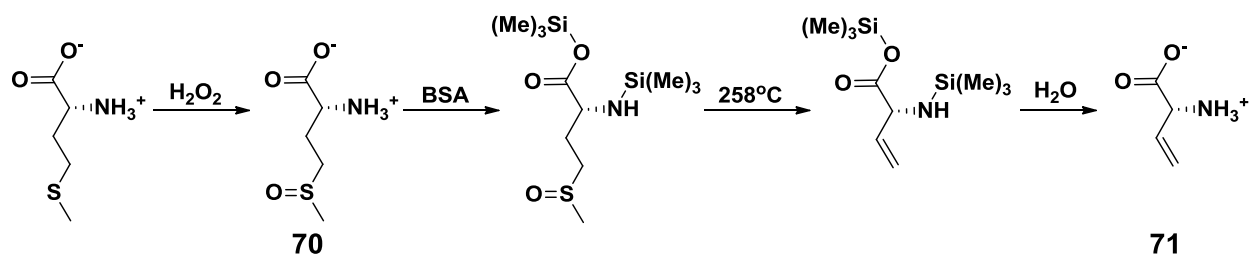


Figure 113: Synthetic scheme for L-vinylglycine formaton by in situ silylation followed by thermolysis with distillation

Though promising the *in situ* silylation and distillation method has the drawback of scale. A volume ratio of diphenyl ether to N,O-(*bis*-trimethylsilyl)acetamide (BSA) of 6:1 was determined to be optimal and therefore the reaction volume increases rapidly with scale. To circumvent this limitation the silylated methionine sulfoxide was added to distilling diphenyl ether. This method proved to be successful in maintaining decent yield along with bringing the silylated mixture to boiling Ph₂O temperature quickly, something not obtainable with lower than 6:1 Ph₂O:BSA . The *In situ* thermolyses where the ratio of Ph₂O to BSA was less than 6:1(v/v) a greater proportion of side product were observed in the isolated material.

Heating caused direct distillation of silylated vinylglycine from the reaction mixture. The addition of the silylated L-methionine sulfoxide mixture via Hirschberg constant addition funnel allowed for the production of vinyl glycine with low amounts of side product (estimated 1%-4% by mass across scale up) while going down to a ratio of Ph₂O:BSA of 2.3:1 (v/v). This protocol was used for reaction scales of 1.4g, 10.6g, 20.1g, 36.0g, and 50.4g with an average yield of vinylglycine of 38%. Of these, the 1.4g scale reaction proved to be anomalous in the fact that no side product was observed in the isolated crude by NMR and would obviously be the ideal method of preparation. The workup procedure was identical across the reactions with regards to hydrolysis and precipitation protocol. In this case, the silylation vessel was flame dried, N₂

flushed, silylated mixture diluted by about half with Ph_2O prior to addition, the pot temperature minimum was 254°C and 40% of the combined volumes used was collected as distillate. This result may be anomalous, as the only factors not carried on throughout the scale were flame dried glassware which was N_2 flushed and only distilling 40% of the combined volumes.

The other concern with scale up, especially with the 50g reaction, is the length of time needed to do the reaction. In this case the addition occurred over 54min at which time almost all Ph_2O was distilled with 92% of the combined volumes being collected as the distillate. Although dilution with Ph_2O does not seem to be needed with smaller scales (1-10g), it is recommended to dilute it with Ph_2O to ensure the distillation pot does not go dry. This also opens up the opportunity to use smaller glassware or work with larger scale as the Ph_2O being distilled is being replaced. Overall, the addition is robust enough with increasing scale while still use standard glassware. The problem of consistently not producing the side product during synthesis remains as well as a way to separate it from the desired product.

The initial isolation of **71** by precipitation of the aqueous phase with CH_3CN was still used, but done twice with scales greater than 20g. At the 20g scale, the crude product was determined to be 28% by mass acetamide which produced a sticky semisolid, whereas if the first precipitate was redissolved in water and precipitated again with acetonitrile, the average mass contribution was 3%. This protocol, although convenient and used for expediency, probably used more water than required to dissolve and thus increased the required amount of acetonitrile to precipitate. If time is not a factor, it is recommended to precipitate once and dry under vacuum overnight followed by trituration of the crude product in boiling ethanol to limit the use of acetonitrile.

Since this method of vinylglycine synthesis appears to be the most succinct when compared to the literature and employs H₂O while still using standard synthetic glassware, exploration of the silylation conditions were carried out to make the overall procedure more amiable to industrial scale up. First, the typical heat treatment was monitored over time with ¹H NMR. The spectra showed from room temperature to 81°C over the course of 100min the α-hydrogen shifted upfield by 0.3ppm and the CH₃ signal transform from a doublet to a singlet. From 125min to 18hr of heating the spectrum did not change from the 100min spectrum and was determined that silylation was complete at 100min. Second, temperatures above 80°C were investigated. Heating at reflux for 2hr and 100°C produced identical spectra which were different from the 80°C and afforded 12% and 6% yield of vinylglycine with an estimated 5:2 and 2:1 molar ratio of vinylglycine to sideproduct. Lastly, cooler temperatures were employed. L-Methionine sulfoxide was silylated at 80°C until the mixture was homogeneous followed by room temperature stirring overnight or stirring at room temperature overnight. These two methods produced NMR spectrum like that of the 80°C overnight silylated product.

However, as slow heating caused starting material decomposition to form side products, and prolonged heating also destroyed the product, we settled upon dropwise addition to distilling diphenyl ether (258°C), which caused rapid heating, elimination, and carryover of product. Hydrolysis, partitioning between water and hexane, and addition of acetonitrile to the aqueous layer caused precipitation of free vinylglycine in 95% purity. This protocol was used for reaction scales of 1-50g, with a 38% average yield of purified vinylglycine with reaction times ranging from 11-54min. No epimerization was apparent as determined by

HPLC separation of the dipeptide diastereomers prepared by reaction of vinylglycine with Fmoc-L-Ala-OSu and Fmoc-D-Ala-OSu.

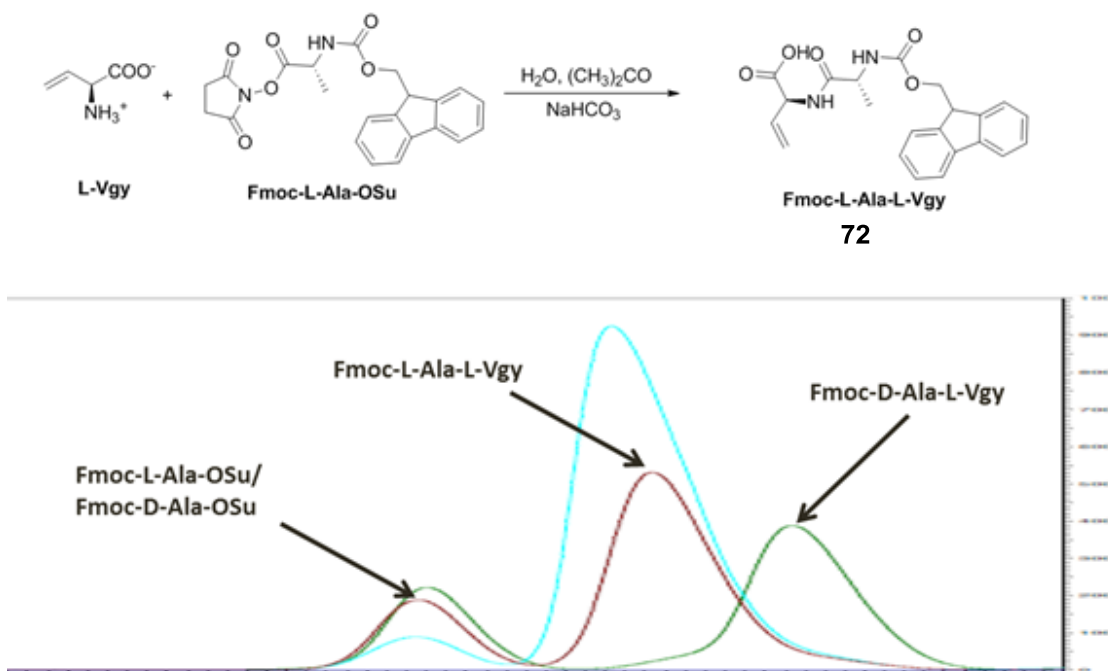


Figure 114: L-Vgy derivatization and HPLC trace demonstrating retention of desired stereocenter

Using these much less careful conditions, we have found effective elimination to vinylglycine without isomerization or epimerization. When N-Cbz vinylglycine methyl ester is used in thermolysis there had been substantial difficulties which are avoided by very short contact times with high temperatures. We wondered which features in our case allowed the simpler reaction conditions. The free acid is, as expected, quite resistant to isomerization compared to the ester: in contrast to the Boc protection of the free acid, bicarbonate in methanol causes complete isomerization during Boc protection of vinylglycine methyl ester in under 4h. In contrast, dissolution of vinylglycine methyl ester in BSA and triethylamine led to no detectable isomerization, even after 50 h. In order to separate effects of ester, and N-substituent on isomerization rates, we carried out the following studies.¹⁷⁹

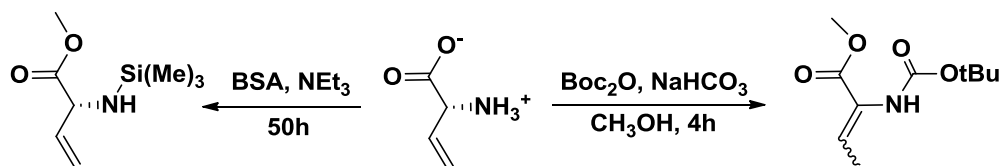


Figure 115: Reaction conditions in which L-vinylglycine methyl ester will or will not isomerize

Comparison of N-Boc with N-TMS groups was made by dissolution of Boc-vinylglycine or free vinylglycine 1 in BSA, followed by addition of Et_3N . Boc vinylglycine TMS ester isomerized with a half time of ca. 1.6h, while the N-TMS derivative had an isomerization half-time of ca. 10^3h , demonstrating that the N protecting group is a substantial part of the difference. We compared TMS with H: vinylglycine methyl ester hydrochloride, on exposure to Et_3N , isomerized with a half time of ca 5.4h while vinylglycine exposed to TMSCl and Et_3N isomerized considerably more slowly, with a half time of ca. $1.7 \times 10^2\text{h}$. While N-Boc facilitates isomerization, it appears the N-TMS group slows it down compared to the N-H material, though the ester also changed. In comparing methyl ester with TMS ester, each in BSA solution, we found that in comparison to the N-TMS TMS carboxy ester half time of ca. 10^3h , the N-TMS methyl ester showed no detectable isomerization in that sample after 50h exposure to Et_3N , corresponding to a half time $>2 \times 10^3\text{h}$. Consequently, the faster isomerization of NH, methyl ester vs NTMS, TMS ester substrate is not due to the ester.

While the low isomerization tendency of silylated vinylglycine may not be critical to the success of the preparation, it is gratifying that this medium is less conducive to isomerization.

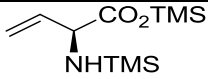
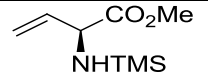
Substrate	Conditions	Solvent	[vinyl] (M)	[S.agent] (M)	[Net ₃] (M)	Time (hr)	Mol Ratio (vinyl:enamine)	t $\frac{1}{2}$ (hr)
	BSA/NEt ₃	CDCl ₃ (77%)	0.092	0.31	1.05	64.5	1 : 0.045	1.0x10 ³
						92.5	1 : 0.06	1.1x10 ³
	TMSCl/NEt ₃	CDCl ₃ (75%)	0.141	0.91	0.99	18	1 : 0.09	1.4x10 ²
						108	1 : 0.73	1.4x10 ²
	BSA/NEt ₃	CDCl ₃ (81%)	0.004	0.25	1.50	50	1 : <0.02	>2.3x10 ³
	TMSCl/NEt ₃	CDCl ₃ (75%)	0.136	0.88	0.96	69	1 : 0.33	1.7x10 ²
	NEt ₃	CDCl ₃ (86%)	0.094	0	0.99	19	1 : 6.7	6.4
						42.5	<1 : 28	<8.7
	BSA/NEt ₃	CDCl ₃ (62%)	0.03	0.95	0.90	1	1 : 2	0.63
						5	<1 : 22	<1.2
	TMSCl/NEt ₃	CDCl ₃ (75%)	0.075	0.91	0.99	1.5	1 : 7	0.3
						18.5	<1 : 33	<3.6

Table 11: Pseudo- first order kinetic data for the isomerization of L-vinylglycine derivatives. All reactions conducted at 22°C and in CDCl₃

Boc group installation attempted on the C-Me L-Vgy HCl with Boc₂O in CH₃OH in the presence of NaHCO₃ to yield a mixture of the enamine isomers exclusively after 4h as observed by TLC and confirmed by ¹H NMR. Properties of derivatives of vinylglycine appropriate to peptide coupling have not been described in the literature, despite the report that incorporation from the Fmoc derivative was superior to incorporation of a phenylselenide followed by elimination: an uncharacterized Fmoc derivative was used.¹⁸⁰ Fmoc vinylglycine (**73**) prepared and characterized. The Boc derivative **74** is an oil at room temperature, so it was converted into its crystalline dicyclohexylammonium salt **75**.

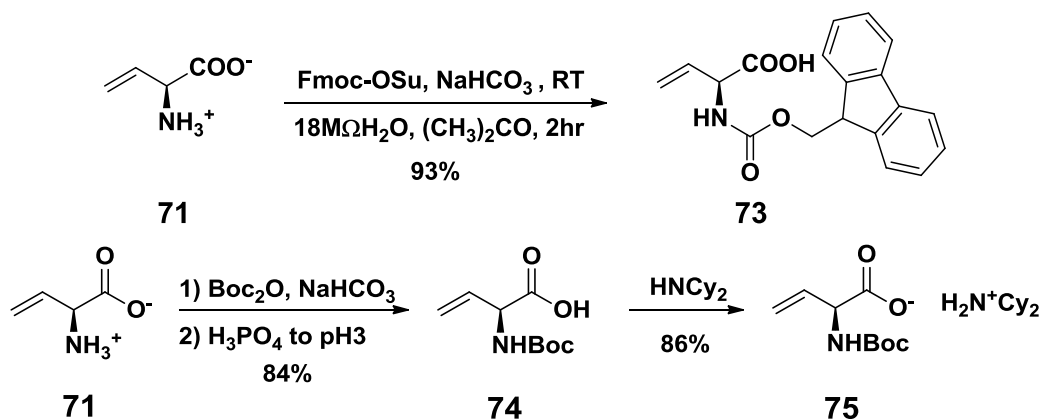


Figure 116: Fmoc- and Boc- protection of L-vinylglycine

Olefin metathesis (OM) can convert vinylglycine into other unsaturated amino acids, though steric hindrance prevents its homodimerization. Olefin metathesis in the presence of a more reactive alkene can lead to crossmetathesis.¹⁸¹ Most examples of efficient vinylglycine and vinyl amine olefin metathesis involves intramolecular reaction.^{182,183} Intermolecular reactions of vinyl glycine derivatives^{100,103,184,185} and related substances¹⁸⁶ are reported, but some attempts have led to other products.¹⁸⁷ As we hoped to prepare unsaturated substances related to arginine for mechanistic studies¹⁸⁸ we screened several allyl derivatives for OM cross coupling to vinylglycine.

While simple terminal alkenes react under olefin metathesis conditions to cross couple with less reactive alkenes such as vinylglycine, the pairing of less reactive alkenes is problematic. Early attempts to cross couple protected allyamine with vinylglycine failed, even in an intramolecular case.¹¹⁸

2. Olefin Cross Metathesis of L-Vinylglycine Derivatives

a. Background on Olefin Metathesis

The net transformation of olefin metathesis is to cleave the strongest (double) bond, and reconnect the fragments. It proceeds by reversible cycloaddition of metallocarbenes to olefins forming a metallocyclobutane. It has become a powerful and versatile tool in the pursuit of sp^2 C-C bond formation. These metal catalysts are either molybdenum or ruthenium based, with each containing a metal carbene bonded to their metal center which serves as the driving force for olefin metathesis.

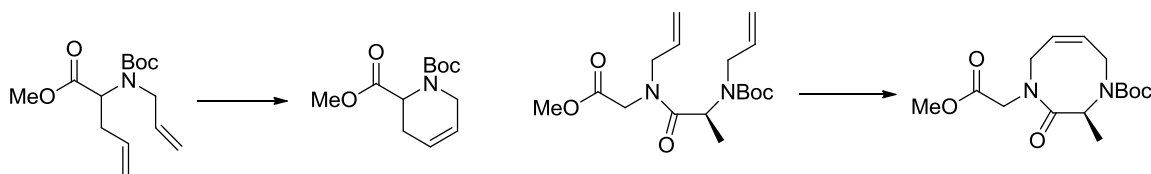


Figure 117: Examples of intramolecular olefin metathesis with amino acid derivatives

Some of the earlier examples of metathesis on amino acid or peptide scaffolds were attempts to perform ring closing metathesis on side chains containing allyl functionalities to make cyclic peptides¹⁸⁹ which remain a topic of interest as cyclic peptides provide a physiologically novel structures.¹⁹⁰ However when one of the allyl groups was for a vinyl group, intramolecular ring closure was prevented.¹⁹¹

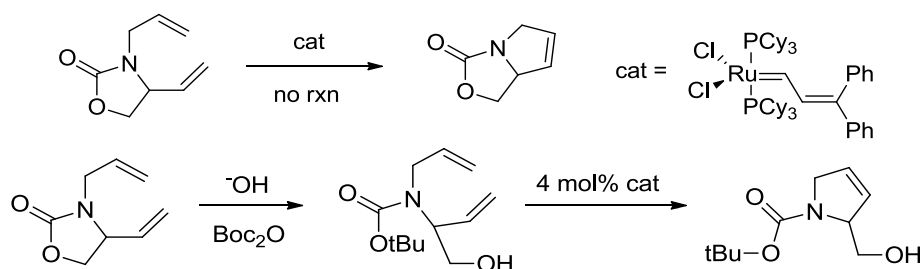


Figure 118: Successful metathesis after saponification of a lactone

Once the lactone was saponified, ring closing metathesis occurred in 95% yield.

Whether this was due to steric hinderence or the pre-Grubbs 1st generation catalyst not being active enough was unknown at the time. Another attempt at ring closing metathesis was an N-allyl derivative of N-Boc-vinylglycine methyl ester.¹⁹² While this did not have the previous constraint of being cyclic, instead of cyclizing with 5mol% catalyst at 25°C, the vinyl side chain isomerized to the α,β -unsaturated side chain and cross metathesized with itself to form a homodimer.

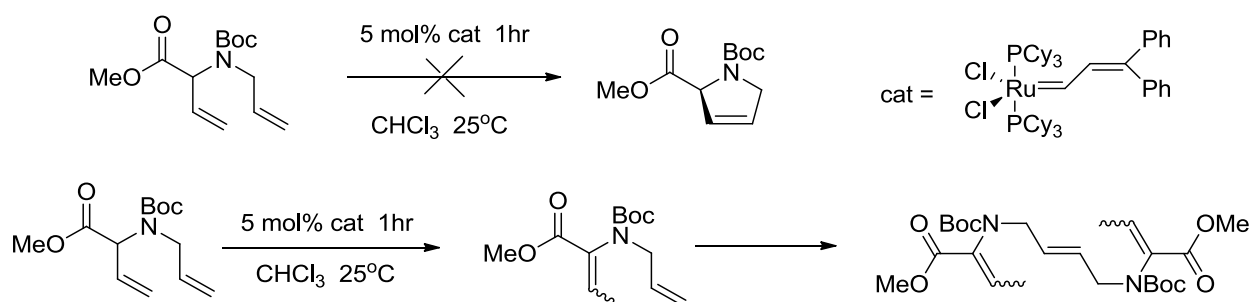


Figure 119: Homodimer formation due to isomerization of vinyl sidechain

The Schrock metathesis catalyst which can have difficulties performing cross metathesis if the substrates are not reactive enough¹⁹³ was employed a year later to perform cross metathesis on N-Cbz-vinylglycine methyl ester without isomerization to the α,β -unsaturated sidechain.¹⁹⁴ The cross metathesis product between the vinyl moiety and allyl trimethylsilane

was accomplished by use of a more reactive alkene, but it is limited in application due to the Schrock catalyst's need anhydrous and anaerobic reaction conditions.

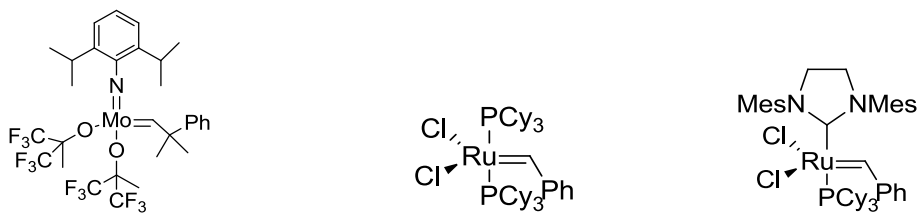


Figure 120: From left to right Schrock's, Grubb's 1st gen, and Grubb's 2nd gen metathesis catalysts

The Grubbs 1st generation catalyst, made by substitution to a styrenyl carbene, was used to perform cross metathesis on unsaturated α -amino acids to systematically test the parameters of C-ester steric hindrance as well as proximity of the olefin to the amino acid backbone with regard to the ability to perform cross metathesis.¹⁹⁵ N-Boc homoallylglycine was used as a model compound to evaluate ester sterics when metathesized with styrene or hexene. The esters were methyl, benzyl, t-butyl, and one instance of the free acid ranged from 52-66% yield showing no appreciable effect from increasing steric bulk at this carbon chain length. The contributing factor that affected the propensity towards cross metathesis was the proximity of the double bond to the amino acid's chiral center: the yield of the desired product decreased as it approached the α -amino carbon. When cross metathesis was conducted using hexene with homoallylglycine, allylglycine, and vinylglycine yields dropped as bulk increased from 66% to 45% to 7% respectively.

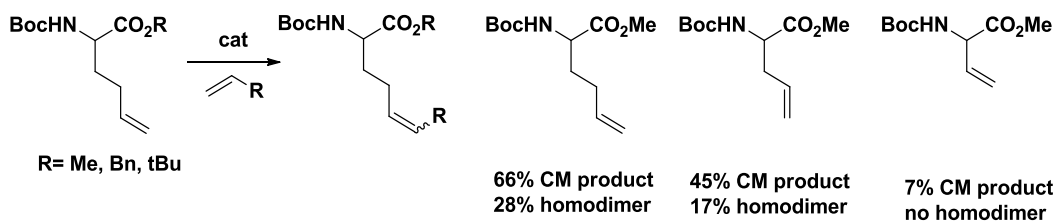


Figure 121: Afforded yields of cross metathesis product as steric hindrance around olefin increases

The sensitivity to sterics for the 1st generation Grubbs catalyst was quantified by the rate of metathesis with increasing encumbrance around the α -carbon to the olefin.¹⁹⁶

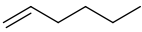
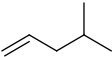
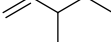
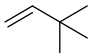
Substrate				
Rate	1.48×10^{-3} L/mol s	1.02×10^{-3} L/mol s	2.5×10^{-4} L/mol s	minor after 4 days

Figure 122: Effects of increasing steric hindrance on rate of metathesis

If hydrogens were substituted for methyl groups β - to the olefins (or presumably even further away) the rate decreased slightly from 1.48 to 1.02×10^{-3} L/mol·s. When this same change in substituents took place α - to the alkene, resulting in a 3° carbon, the rate dropped by an order of magnitude to 2.5×10^{-4} L/mol·s had only trace amounts of metathesis product observed after 4 days if 4° carbon was in proximity. The electronic characteristics were also correlated to a rate which increased by an overall factor of four when changed from *p*-NO₂ styrene to *p*-Me styrene to *p*-OMe styrene, suggesting electron rich species react faster.

Over the course of these studies it was observed that the E isomers were isolated or formed preferentially over the Z isomer. A paper on a new methodology for cross metathesis with Grubbs 1st generation catalyst for greater E selectivity demonstrated homodimerization of terminal olefins before cross metathesis occurred but at the cost of an overall lower yield of the cross metathesis product.¹⁹⁷ The 2nd generation Grubbs catalyst also shares this tendency¹⁹⁸ towards formation of the E isomer. Compatibility with aliphatic alcohol, ester, or ether containing functionalities was no problem affording yields on average of 70% and E:Z ratios ranging from 3-10:1. The only detriment to homodimerization in these cases was reaction temperature. If the temperature were to exceed that of the boiling point of dichloromethane

the yield would decrease, which was attributed to the decomposition of the metathesis catalyst.

The tolerance of alkenes with nitrogen substituents towards metathesis were also studied. Though not as widely explored, the examples of Boc protected allyl amine and amides in peptides did not interfere with cross coupling. What did prevent facile metathesis were amides alpha to the terminal olefin. When metathesis was attempted on N-methoxy-N-methyl-acrylamide, a Weinreb amide, it gave a low yield of 17% and the low E:Z ratio of 1.9:1. This lack of reactivity was speculated to be due to intramolecular coordination of the amide to the ruthenium center when it became attached as a carbene to stabilize it as an intermediate and interrupt the catalytic cycle.

In the year 2000 Hoveyda advanced metathesis technology with his modification to the Grubbs catalyst by replacing the initial styrenyl carbene with an intramolecular coordinating isopropoxystyrene¹⁹⁹ increasing the reactivity of the catalyst, as well as stabilizing it, allowing for a more robust set of experimental conditions in which metathesis may be conducted. This ruthenium carbene complex is known as the Hoveyda-Grubbs 2nd generation catalyst. Substrates previously unresponsive to cross metathesis with previous catalysts were now able to be reevaluated for these purposes. N-Boc-2-vinyl-pyrrolidine was able to do metathesis with methyl 3-butenate²⁰⁰ in 31% yield in a 10:1 E:Z ratio under conditions where the 1st generation Grubbs catalyst could not perform and N-benzyl-N-Boc-ethenamine with methyl 3-butenate in 60% yield. The 1st generation Hoveyda-Grubbs catalyst, in which the tricyclohexylphosphine ligand was replaced with an N,N'-*bis*-mesitylimidazole carbene, is also able to effectuate

vinylglycine metathesis due to the enhanced reactivity of the metal afforded by the additional carbene moiety.

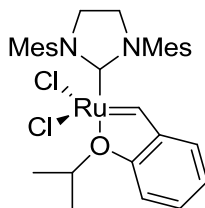


Figure 123: Hoveyda-Grubbs's 2nd generation metathesis catalyst

In the synthesis of D-glycosyl-asparagines, α - or β - allyl glycosides were coupled with vinylglycine derivatives containing different combinations of N-protecting groups and carboxy esters.²⁰¹ What was found from the Orlando group was that metathesis of α - or β - positions displayed slight preference towards the α - position due to the lesser degree of steric interaction. Neither N-Cbz, N-Boc, N-Fmoc nor C-Me, C-Bn- or C-tBu esters altered the yields of the desired glycoside metathesis product substantially. However, when the alkene on the glycoside was change to vinyl from allyl no cross metathesis was observed. Isomerization of the vinyl group in the vinylglycine derivative to the α,β -unsaturated alkene was observed when exposed to refluxing CCl_4 (76°C) and 1,2-dichloroethane (84°C).

Cross metathesis of protected vinylglycines was also used to make other biologically important molecules like diaminopimelic acid,²⁰² a component in peptidoglycan biosynthesis in gram-negative bacteria as well as in the synthetic route to make the natural products Syringolin A and B.²⁰³ Syringolin A and B have been identified as a proteasome inhibitor which act as Michael receptors for conjugate addition to N-terminal threonine residues, acting as virulence factors for plant pathogens as well as a potential therapeutic for human neuroblastoma.

Early in the sequence 4-bromobutene was coupled with a vinylglycine analogue in 69% yield using 10mol% catalyst over two additions and five hours of reaction time.

As these catalysts are non-polar and conducting olefin metathesis in physiological media has become of interest, water soluble varieties of the Hoveyda-Grubbs catalyst have been synthesized and determining their limitations in metathesis has been undertaken. One of the first attempts involved attaching a polyethylene glycol chain to the imidazole ligand in the Hoveyda-Grubbs 2nd generation catalyst which resulted in an average molar mass of 5000g/mol.²⁰⁴ This was able to perform ring closing metathesis on a range of substrates and cross metathesis on allyl alcohol but failed to produce homodimers of acrylic acid or allyl ammonium chloride. Altering the pH of the aqueous media did not perturb the reactivity of the catalyst to either induce metathesis on the unreactive substrates or prohibit the metathesis of the successful species.

The other water solubilizing changes made to the Hoveyda-Grubbs 2nd gen. catalyst were quaternary ammoniums on the isopropoxy styrene ligand²⁰⁵ or use of a solvent mixture consisting of water and an organic cosolvent²⁰⁶ in which the main drawback was the low maximum concentration of the Hoveyda-Grubbs 2nd gen catalyst. Ring closing was able to be performed on secondary ammonium chlorides to form five and six member rings and tertiary amines to close to a five member ring in good yield if the amine was a trifluoroamide or tosylamide. The cases where ring closure did not occur were if quaternary ammoniums were present or if the nitrogen was replaced with a diphenyl silane suggesting that the steric bulk around these moieties hindered metathesis.

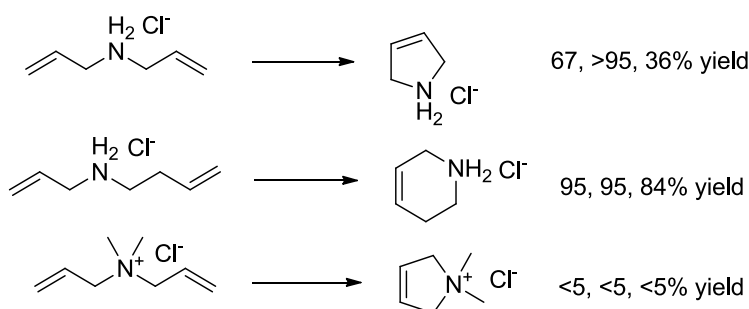


Figure 124: Ring closing yields using water soluble Hoveyda-Grubbs 2nd gen catalysts

b. Synthesis and Screening of Allylamine Derivatives for Cross Metathesis

Our metathesis experimentation began with evaluating the ability of desired alkenes to homodimerize in the presence of Hoveyda-Grubbs 2nd generation catalyst to screen for substrates suitable to perform cross-metathesis on an analogue of vinylglycine. Allyl amine was tried first and when combined with 11mol% of the catalyst in CH₂Cl₂. Upon addition of the amine the color of the solution changed from an emerald green to a brown color and after refluxing for 17hr no metathesis was observed. This was attributed to the coordination of the amine to the ruthenium, inactivating the metal towards metathesis. This observation prompted the creation of a series of derivatives.

$\text{CH}_2=\text{CH}-\text{CH}_2-\text{NH}_2 \xrightarrow[71\%]{12\text{M HCl}} \text{CH}_2=\text{CH}-\text{CH}_2-\text{NH}_3\text{Cl} \quad \mathbf{76}$	$\text{CH}_2=\text{CH}-\text{CH}_2-\text{NH}_2 \xrightarrow[95\%]{\text{Fmoc-OSu, CH}_2\text{Cl}_2} \text{CH}_2=\text{CH}-\text{CH}_2-\text{NH}-\text{Fmoc} \quad \mathbf{79}$
$\text{CH}_2=\text{CH}-\text{CH}_2-\text{NH}_2 \xrightarrow[94\%]{17\text{M AcOH}} \text{CH}_2=\text{CH}-\text{CH}_2-\text{NH}_3\text{OAc} \quad \mathbf{77}$	$\text{CH}_2=\text{CH}-\text{CH}_2-\text{NH}_2 \xrightarrow[76\%]{\text{CF}_3\text{C(O)OEt, EtOH}} \text{CH}_2=\text{CH}-\text{CH}_2-\text{NH}-\text{C(=O)CF}_3 \quad \mathbf{80}$
$\text{CH}_2=\text{CH}-\text{CH}_2-\text{NH}_2 \xrightarrow[75\%]{\text{Boc}_2\text{O, CH}_3\text{OH}} \text{CH}_2=\text{CH}-\text{CH}_2-\text{NH}-\text{Boc} \quad \mathbf{78}$	$\text{CH}_2=\text{CH}-\text{CH}_2-\text{NH}_2 \xrightarrow[68\%]{\text{NaN}_3, \text{NaHCO}_3, \text{H}_2\text{O}} \text{CH}_2=\text{CH}-\text{CH}_2-\text{N}_3 \quad \mathbf{81}$

Table 12: Synthesis of allyl amine derivatives for homodimerization screening

The duo of protonated allyl amines, allyl ammonium chloride and allyl ammonium acetate, were made by combining with 12M HCl and glacial acetic acid respectively. After concentration with rotary evaporation, azeotropic drying by evaporation of toluene, and exposure to vacuum to remove residual solvent, 71% yield of **76** and 94% yield of **77** were obtained. Synthesis of acyl analogues proceeded next. Boc protection of allyl amine occurred quite rapidly using Boc anhydride and excess of allyl amine in methanol at room temperature. Mixing of the two produced a large exotherm and effervescence upon mixing and complete conversion after 20min as seen by TLC (silica, KMnO_4 , 5% $\text{CH}_3\text{OH}/\text{CH}_2\text{Cl}_2$, R_f amine= 0.0, R_f Boc amine= 0.78). The white solid afforded after workup corresponded to 75% yield **78** and had a melting point range of 28-34°C. **78** was also observed to be volatile which was discovered after leaving a previous preparation under vacuum overnight to remove residual solvent to find it had evaporated away. This implies that sublimation should be employed in future preparations to purify this substance.

Fmoc protection used the N-hydroxy succinimide ester of fluorenyl methyloxycarbonyl with an excess of allyl amine in CH_2Cl_2 to produce **79** in 95% yield with 121-122°C melting point in one hour. **80** was created by treating allyl amine with two equivalents ethyl trifluoroacetate, a volatile trifluoroacetylating agent that does not require base to be present. Mixing at room temperature in ethanol produced a large exotherm and complete reaction after 15min (silica gel, 40% EtOAc/hexane, KMnO_4 visualized, R_f product= 0.55). Isolation of the desired product became troublesome as its boiling point was lower than that of either ethanol or ethyl trifluoroacetate meaning that removal of the solvent or excess reagent came at the expense of the yield as the small scale prohibited convenient distillation. From this procedure, the

trifluoroacetate **80** was afforded in 76% yield. Allylamine is the lowest in boiling point of the combination so subsequent syntheses should employ it in excess coupled with its slow addition to ethyl trifluoroacetate in an ice bath using neat conditions.

The final derivative made was **81**. NaHCO_3 , as an extra precaution to prevent the formation of hydrazoic acid, was dissolved in water along with NaN_3 before the addition of allyl bromide as per the literature.²⁰⁷ A biphasic mixture resulted with the organic layer on the bottom. After 30min of stirring at room temperature, the organic phase switched positions with the aqueous phase and is an indication that the reaction is proceeding, but not a sign of complete reaction. After 4hr though TLC showed complete conversion to the allyl azide (silica, 10% EtOAc/hexane, KMnO_4 , R_f amine= 0.57, R_f azide= 0.64). As with **80** and **78**, isolation was problematic due to its volatility. Previous preparations utilized ethyl ether to partition the allyl azide away from the aqueous layer, but use of rotary evaporation or vacuum to remove the solvent also evaporated allyl azide resulting in negligible mass. It was determined then to separate **81** neat and pass it over a column of MgSO_4 in pasteur pipet to give the desired material in 68% yield.

Homodimer Formation

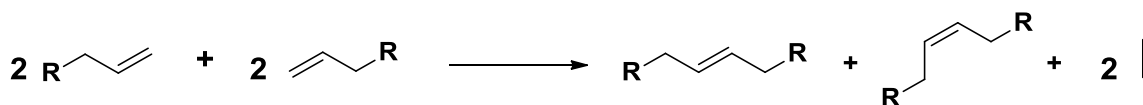


Figure 125: General scheme for homodimer formation via olefin metathesis

Cross metathesis with the vinylglycine moiety is predicated upon the formation of a metathesis homodimer with the allylamine derivatives. This is due to the fact that the allyl

functionalities have a lesser amount of steric hinderence about the olefin compared to the vinyl and thus will undergo metathesis first. As a result, selectivity in cross metathesis can be achieved by having the allyl homodimer then react with the vinyl group. Cross metathesis of L-vinylglycine is desirable as it would provide the most direct route to dehydroarginine.

Allylammonium salts and aqueous cosolvent conditions were used as described by the Raines publication²⁰⁶ to investigate metathesis. A solution of **76** in D₂O as added to a solution of the Hoveyda-Grubbs 2nd generation catalyst (5mol%) in 1,2-dimethoxyethane (DME) which caused some of the catalyst to precipitate. The mixture was stirred at room temperature over the course of five days while being periodically monitored by ¹H NMR with no change observed in the spectra over that time. The same results were seen with **77** in CH₂Cl₂ and H₂O/acetone solvent systems with 10mol% catalyst at reflux and 55°C respectively over the course of 24hr. The mixtures were allowed to sit for an additional 12d at room temperature in the hopes of seeing metathesis proceed, but to no avail. Lack of metathesis was determined to be due to the proximity of the positive charge to the allyl functionality and not the chloride ion.

Alkene	Solvent	Temp (°C)	Cat.(mol%)	Time	Result
	H ₂ O/ acetone	reflux	12	18h	No metathesis
(55)	CDCl ₃	RT	11	72h	No metathesis
(55)	CH ₂ Cl ₂ / AcOH	reflux	13	48h	No metathesis
	CH ₂ Cl ₂	reflux	9	18h	quant. (TLC) 88% isolated
	CH ₂ Cl ₂	reflux	11	19h	No metathesis
(76)	H ₂ O/DME	RT	5	96h	No metathesis
(77)	CH ₂ Cl ₂	reflux	9	21h	No metathesis
(81)	CH ₂ Cl ₂	reflux	8→13	43h	40% yield (NMR)
(78)	CH ₂ Cl ₂	reflux	12	18h	75% isolated
(79)	CH ₂ Cl ₂	reflux	10	4h	quant. (TLC) 47% isolated
(80)	CH ₂ Cl ₂	reflux	12	17h	quant. (TLC) 43% isolated

Table 13: Alkene reactivities for homodimer formation

Allyl guanidinium chloride was investigated next with the thought that maybe a more delocalized cation would not be an impediment. The reaction appeared to proceed with 12mol% catalyst in 20% H₂O/acetone at reflux for 17hr at which time the ¹H spectrum was taken and showed a lack of the starting alkene signals. The mixture was washed with CH₂Cl₂ and the aqueous phase concentrated to give a 68% crude yield. The crude product was analyzed by ESI-MS to give a peak at m/z=307.5 which would correspond to a vapor phase complex between the desired homodimer and allyl guanidinium chloride with a bridging chloride between them and further evidence that metathesis had occurred. However, an M+2 peak at 25% intensity indicative of the ³⁷Cl isotope was absent. Comparison its NMR spectrum to that of the homodimer formed from **78** showed a similar set of signals. The resonances of this homodimer were broad singlets at δ5.62, δ4.57, and δ3.72 and those of the allylguanidinium homodimer were broad singlets at δ5.74, δ5.30, δ4.20, δ4.12 but these signals were only a

fraction of the signals present or their intensities. From these data, metathesis of this substrate appears to occur but is sufficiently ambiguous to prevent a definitive conclusion.

As the cationic allyl amines proved stagnant to homodimerization, **55** was tried next with 11mol% metathesis catalyst in CDCl_3 at room temperature. This mixture was monitored by ^1H NMR over 22.5hr with no appreciable change in the spectral signatures of the catalyst or the starting olefin. Although initially perplexing, recalling the coordination of the imine lone pair to the osmium tetroxide to attempt oxidative cleavage of the alkene and how it prevented reaction could explain this lack of metathesis reactivity. If the lone pair on the guanidine could be occupied by being protonated it could it could facilitate olefin metathesis much like the case of oxidative cleavage to proceed to form **59**. The experiment was replicated with 13mol% catalyst and 10 eq glacial acetic acid and heated at 40°C in CD_2Cl_2 . After heating overnight this mixture only starting materials were observed to be present. The reaction volume was vented with a slow stream of N_2 to the atmosphere and set back to reflux for another 24hr. ^1H NMR analysis showed no ethylene present or starting materials and TLC did show new spots which were isolated with flash chromatography. These spots were then submitted for ESI-MS analysis but did not give any peaks corresponding to the molecular ion of the desired homodimer product. The conclusion from this experiment that as the neutral compound the imine lone pair prevented metathesis by coordination to the ruthenium and trying to circumvent this by protonation also prohibited homodimerization for the same reason as the allyl ammonium compounds, the proximity of the formal positive charge.

Being cationic and sterically bulky has been demonstrated to be detrimental to olefin metathesis allyl azide was exposed to metathesis conditions next. The metathesis catalyst was added at reflux in CDCl_3 with allyl azide in two portions up to a total of 13mol% over the course of two days which resulted in a 1:3 molar ratio of the homodimer to the monomer. The solution changed from a green to a dark brown color upon reaching reflux similar to the attempted metathesis of allyl amine which was assumed to correlate to catalyst decomposition. However when conducted at room temperature with 20mol% catalyst added in two portions over two days a 1:6 molar ratio of homodimer to monomer was produced. Allyl azide also seems to be a poor substrate for olefin metathesis under these conditions.

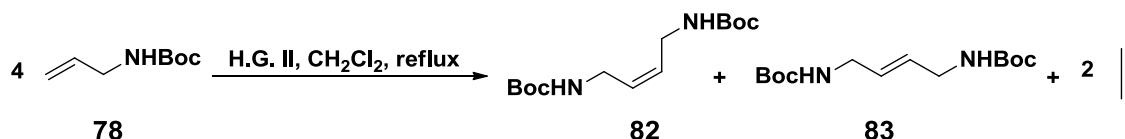


Figure 126: Homodimer formation via olefin metathesis of Boc protected allyl amine

Thankfully not all of the allyl amine derivatives were unreactive. The acyl derivatives were able to homodimerize but with reactivity dependent on solvent observed. In the case of Boc protected **78** use of 30% H_2O /DME resulted in no metathesis while reflux in CH_2Cl_2 afforded complete metathesis in 16hr in a 75% yield in a 1:1.6 ratio of Z:E isomers **82** and **83**. Fmoc derivative **79** underwent complete conversion in refluxing dichloromethane with 10mol% catalyst in 1.5hr. 58% yield of this homodimer **84** was afforded but mass was only acquired from the crystalline material from the reaction mixture, the E isomer. A more quantitative yield can be generated by utilizing flash chromatography on the crude product but was deemed unnecessary, as looking for metathesis activity was the primary goal.

N-allyl-trifluoroacetamide also underwent complete homodimer formation overnight with 12mol% catalyst in refluxing CH₂Cl₂ even though the color of the mixture changed to a dark brown upon reaching reflux temperature. A 43% yield of homodimer **85** was analyzed by ESI-MS (-ion mode) and produced ions corresponding to M-H⁺, M+HCOO⁻, and M+CF₃COO⁻ confirming that metathesis occurred. As expected the less hindered alkene 4-pentenoic acid, underwent olefin metathesis smoothly to form homodimer **86** in 88% isolated yield.

c. Cross Metathesis of L-Vinylglycine Derivatives and Selected Allylamine Derivatives

Even with the lack of precedence of cross metathesis between two ammonium bearing olefins, the metathesis of vinylglycine hydrochloride with allyl guanidinium chloride was attempted to make the dehydroarginine directly. Using conditions described by Raines²⁰⁶, no change was observed in the composition of the mixture by ¹H NMR over the course of 89hr. The next attempt at cross metathesis was done with allyl ammonium acetate (**77**) and N-Boc-L-vinylglycine (**74**) in 28% D₂O/DME with 6mol% catalyst. Even though it seems unlikely as the allyl ammonium acetate did not form a homodimer, it may be possible with a cationic and neutral olefin as opposed to bringing two cationic species together to metathesize into a dicationic species. After heating at 55°C for 24hr the ¹H spectrum remain unchanged. The mixture was brought to room temperature and monitored sporatically over the course of 13d with still no change seen in the resonances.

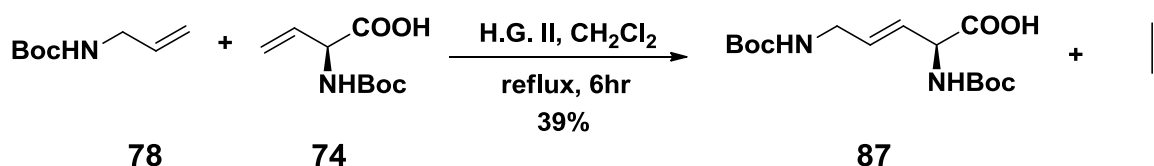


Figure 127: Example olefin cross metathesis using Hoveyda-Grubbs 2nd generation catalyst

Effort was then shifted from the charged olefins to neutral, organic soluble derivatives with the first combination being **78** and **74**. Utilizing 11mol% catalyst and refluxing CH₂Cl₂ only partial reaction was observed over 18hr. The mixture was none the less concentrated, redissolved in EtOAc, and extracted with 29% NH_{3(aq)} to give a crude product that was partially separated by flash chromatography. The fraction containing the largest mol fraction of the cross metathesis product **87** was subjected to ESI-MS (- ion) analysis and produced peaks of m/z= 329 (M-H⁺) and 530 (M⁻+ **74** vapor complex). Accounting for the unreacted **74** a 17% yield based on conversion was isolated. This low yield could be attributed to the low partitioning of the desired product into aqueous ammonia as well as the incomplete reaction. Recommendations in improving the yield of the cross metathesis product can be done by increasing the ratio of 4:1 **78**: **74**, increasing the amount of catalyst to 20mol% in two portions, and chromatography of the reaction mixture should be done in future preparations.

The Fmoc derivatives of vinylglycine coupled to the Boc allyl amine (**78**) is desirable as cross metathesis would generate a product containing orthogonal protecting groups. This will allow for installation of the guanidine functionality unambiguously on the resulting side chain amine. The dicyclohexylammonium salt of Fmoc-L-vinylglycine was prepared and mixed with 6eq Boc allyl amine with 20mol% catalyst in refluxing CH₂Cl₂ for 24hr with no change as seen by TLC. An additional 20mol% catalyst was added and left at reflux for 4d before analysis of the mixture by TLC was done again and still looked like the starting materials. The proton spectrum confirmed that it was still reactants along with the NBoc allyl amine homodimers **82** and **83**. The steric hindrance around the vinylglycine olefin was too bulky to effectuate metathesis.

73 was employed next with Boc allyl amine under similar metathesis conditions but with only 20mol% catalyst. After 4d at reflux no new spots by TLC or a molecular ion from ESI-MS analysis of the reaction mixture was observed.

This continued reticence Fmoc vinylglycine towards metathesis prompted the swapping of the protecting groups on the coupling partners to Fmoc allyl amine and N-Boc-L-vinylglycine (**74**). A minimum of two equivalents Fmoc allyl amine (**79**) and 25mol% metathesis catalyst were left in refluxing CH₂Cl₂ for 4d before TLC analysis which showed the absence of **74**. The reaction, though complete, has yet to have the cross metathesis product **88** isolated. Extraction with ammonia did not partition the product into the aqueous phase, using silica gel flash chromatography with 10% AcOH/CH₂Cl₂, or ion exchange chromatography with Dowex 2X-8 (quaternary ammonium, strong anion exchanger) failed to generate materials that produced the desired molecular ion with ESI-MS. Use of chromatography before any separation should be used subsequently in attempts to isolate the product and should not be abandoned as a possibility.

Metathesis between N-allyl trifluoroacetamide (**80**) and **74** was able to be done with 6eq of **80** and 18mol% catalyst added in two portions in refluxing CH₂Cl₂ over two days. The product was attempted to be isolated by extraction with pH9 water but was not able to partition it into the water and confirmed by lack of molecular ion when analyzed by ESI-MS. This product should be isolated by chromatography.

Success was also found in the coupling of 4-pentenoic acid and **74** with 6eq of the acid and 15mol% metathesis catalyst added in two portions over two days in refluxing CH₂Cl₂ to

generate cross metathesis product. Isolation of the cross metathesis product was accomplished by trifluoroacetic acid removal of the Boc group, dissolving the resulting salt in water, followed by washing with EtOAc to afford **89** in 58% yield.

Entry			Solvent	mol% catalyst	Temp	Time	Result
1			D ₂ O/ (CD ₃) ₂ CO	22	reflux	89h	No cross metathesis
2			28% D ₂ O/DME	6	55°C→RT	1d→1 4d	No cross metathesis
3			CD ₂ Cl ₂	16→40	reflux	6d	No cross metathesis
4			CH ₂ Cl ₂	11	reflux	18h	Cross metathesis
5			CH ₂ Cl ₂	20→42	reflux	5d	No cross metathesis
6			CH ₂ Cl ₂	11	reflux	18h	No cross metathesis
7			CH ₂ Cl ₂	20	reflux	18h	Cross metathesis
8			CH ₂ Cl ₂	12→18	reflux	2d	Cross metathesis
9			CH ₂ Cl ₂	9→15	reflux	2d	Cross metathesis 43% est. yield

Table 14: Summary of results for combinations of metathesis substrates

VII. CONCLUSION

Cinnamylidene pyruvate and (4-nitro)cinnamylidene pyruvate salts were synthesized in a facile manner that allowed subsequent researchers to generate more material and additional pyruvate adducts to further probe the reactivity of SbADC. Triethylammonium bicarbonate extraction of the cinnamylidene pyruvates allowed for the removal of excess sodium pyruvate for kinetic stop flow experiments but at the cost of a large amount of the desired pyruvate

adducts with most of the desired diene reverting back to the Aldol condensation product by hydration of the diene.

The method for sodium difluoropyruvate synthesis was improved on from the described literature methods by detailing ozonolysis conditions that does not generate a mixture of furan starting material and desired difluoropyruvate ester as well as employing an anion exchange resin to simplify the removal of acidic byproducts. Unfortunately the limited amount of material that could be made under the time constraints did not yield solutions of a sufficient concentration to occupy the active site of SbADC to afford unambiguous x-ray crystallography data.

A synthetic route that affords L-vinylglycine in two steps that can be conducted on a 50g scale utilizing conventional laboratory glassware in an average 39% yield was also developed. This method proved to be a dramatic simplification from the literature in the amount of material that could be generated with regard to time invested. Utilizing relatively inexpensive reagents, easily obtainable temperature, and standard laboratory techniques researchers in need of this material are stronger encouraged to use this methodology.

The L-vinylglycine made was derivatized with Boc and Fmoc protecting and made into a crystalline dicyclohexylammonium salt so that it could be used in subsequent screening for olefin metathesis reaction conditions en route to forming β,γ -dehydroarginine. It was found that Boc-L-vinylglycine was able to undergo cross metathesis with Boc protected allyl amine, Fmoc protected allyl amine, trifluoroacetyl allylamine, and 4-pentenoic acid opening up the potential to for other non-canonical dehydro amino acids.

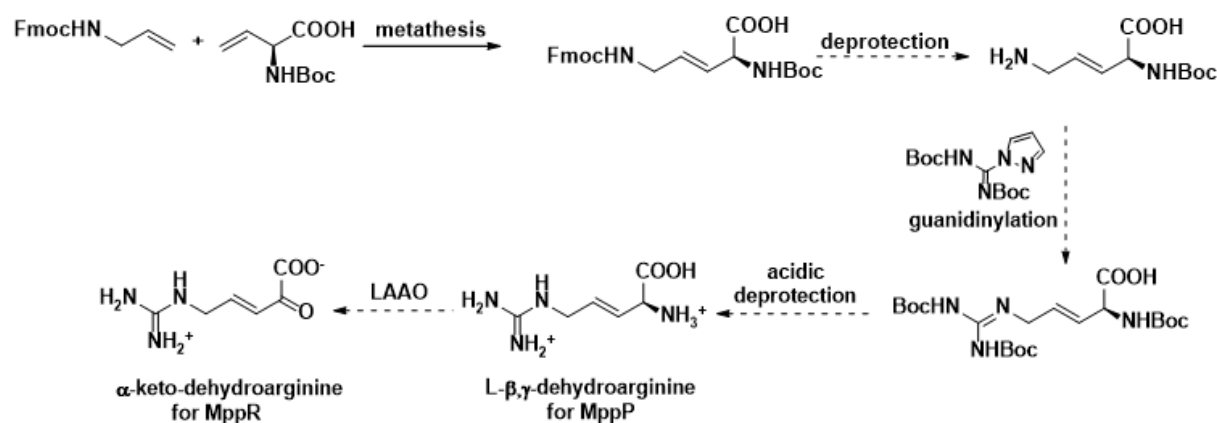


Figure 128: Future direction for dehydroarginine synthesis

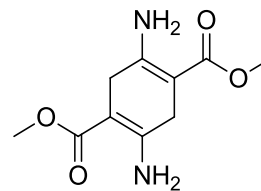
Future researchers who pick up this almost completed project are suggested to follow the route shown above as it is known that cross metathesis between Fmoc allyl amine and Boc-L-vinylglycine is able to go to completion with the presence of the desired product confirmed by ESI-MS. This cross metathesis product is the most desirable as its protecting groups are orthogonal allowing for the Fmoc group to be removed while retaining the Boc group allowing for unambiguous guanidinylation. However, the desired material is yet to be isolated from the reaction mixture with silica gel and reverse phase flash chromatography proving to be ineffective in this task. It is suggested to use preparative HPLC for initial isolation of the desired cross metathesis product followed by development of a method to separate it from the Fmoc allylamine homodimer. The remaining steps in the sequence are well known and described in detail for analogous compounds in the experimental.

VIII. EXPERIMENTAL SECTION

General Procedures:

Reagents and solvents purchased from suppliers were used as received unless otherwise noted in experimental procedures. ^1H NMR spectra were collected on a 300MHz Bruker DPX 300 NMR unless otherwise noted. Chemical shifts (δ) are reported as downfield in parts per million of tetramethylsilane. Coupling constants (J) are reported in Hertz and splitting patterns denoted as singlet (s), doublet (d), doublet of doublets (dd), triplet (t), quartet (q), multiplet (m), and broad (b). ^{13}C NMR spectra were ^1H decoupled and collected on a 300 MHz Bruker DPX 300 NMR with chemical shifts (δ) reported as downfield of tetramethylsilane. The ^{31}P NMR spectra were ^1H decoupled, and collected on a 300MHz Bruker DPX 300 spectrometer with chemical shifts (δ) reported downfield of an 85% H_3PO_4 external standard. Low resolution mass spectrometry data was collected on a Hewlett-Packard 5985 B GC-mass spectrometer and a Shimadzu LCMS-2020 Single Quadrupole. High resolution mass spectrometry data was acquired with a Shimadzu LCMS-IT-TOF. Infrared spectroscopy was performed on a Shimadzu IRAffinity-1S FTIR. Elemental analysis was conducted on a Perkin-Elmer 240C carbon, hydrogen, and nitrogen analyzer. Melting points were determined using a MEL-TEMP II apparatus without correction. HPLC analysis was performed on Agilent Technologies 1220 Infinity LC. UV-Vis absorption data was collected on a Perkin Elmer Lambda 650 using quartz absorbance cells. Fluorescent measurements were collected using right angle scattering on a Fluorolog-3 Model FL3-22 by Horiba Jobin-Yvon using quartz fluorescent cells or an Ocean Optics SD2000 dual channel fiber optic spectrometer. Analytical TLC was conducted on Merck silica gel 60 F₂₅₄

plates and visualized using shortwave ultraviolet light unless noted otherwise. Flash chromatography employed Sorbent Technologies silica gel 60Å, 32-63µm Standard Grade.



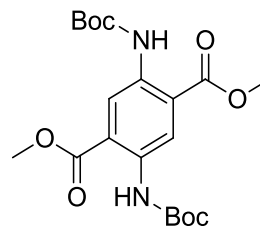
Dimethyl 2,5-diaminocyclohexa-1,4-diene-1,4-dicarboxylate (1)

70.82g (0.9969mol) NH_4OAc was combined with 2.0L anhyd. EtOH, placed under an atmosphere of N_2 , and heated to reflux. 54.93g (0.2407mol) dimethyl 2,5-dioxocyclohexane-1,4-dicarboxylate was added to the boiling solution in three equal portions, waiting for the previous portion to dissolve before the next addition with 400mL anhyd. EtOH added with the last portion. The mixture continued to heat at reflux for 2.5h before TLC showed the reaction to be complete (10% $\text{CH}_3\text{CN}/\text{CH}_2\text{Cl}_2$, silica, $R_{f\text{ SM}} = 0.76$, $R_{f\text{ BE}} = 0.38$) over which time orange crystals formed on the side of the reaction flask. The mixture was allowed to cool to room temperature slowly before being placed into an ice bath for 1h. The resulting orange solid was collected by vacuum filtration and washed with 500mL cold anhyd. EtOH. After drying under vacuum to remove residual solvent overnight 47.72g (88% yield, mp = 212-214°C) of a cream orange colored solid.

^1H NMR (300MHz, CDCl_3): δ 3.71 (s, 6H); 3.13 (s, 4H)

^{13}C NMR (300MHz, CDCl_3): δ 169.3; 155.6; 86.8; 50.8; 30.4

ESI-MS (DUI, + ion): 268 ($\text{M} + \text{CH}_3\text{CNH}^+$, 100%); 227 ($\text{M} + \text{H}^+$, 98%)



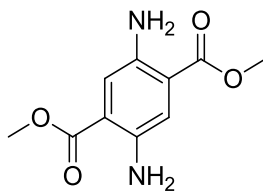
Dimethyl 2,5-bis((tert-butoxycarbonyl)amino)terephthalate (2)

3.708g (16.39mmol) **1** was suspended in 180mL toluene, heated to boiling, and had 80mL toluene removed via distillation. 22.11g (101.3mmol) Boc_2O dissolved in 40mL toluene was added to the reaction mixture followed immediately by 0.409g 5% Pd-C and heated at reflux for 15h before the addition of 3.917g (17.95mmol) Boc_2O dissolved in 8mL toluene. The mixture was allowed to reflux for an additional 8h before the addition of 8.229g (37.71mmol) Boc_2O dissolved in 12mL toluene. With an additional 20h reflux time, TLC showed the reaction to be complete (10% $\text{CH}_3\text{CN}/\text{CH}_2\text{Cl}_2$, silica, R_f product = 0.72). The boiling mixture was filtered over a pad of Celite and rinsed with boiling toluene until the filtrate appeared colorless (90mL). The filtrate was boiled down to 75mL total volume, allowed to cool to room temperature slowly, and placed in an ice bath for 30min. The resulting solid was collected by vacuum filtration, rinsed with three 10mL portions cold toluene, and placed under vacuum overnight to remove residual solvent to yield 6.146g (88% yield, mp = 248.5-250°C) of a lemon yellow solid.

^1H NMR (300MHz, CDCl_3): δ 9.96 (s, 2H); δ 9.03 (s, 2H); δ 3.94 (s, 6H); δ 1.52 (s, 18H)

^{13}C NMR (300MHz, CDCl_3): δ 167.8; 152.8; 135.2; 120.9; 119.2; 80.6; 52.7; 28.2

ESI-MS (DUIS, + ion): 448 (M + CH_3CN + Na^+ , 31%); 442 (M + NH_4^+ , 100%); 310 (56%); 266 (M - 2Boc + CH_3CNH^+ , 30%)



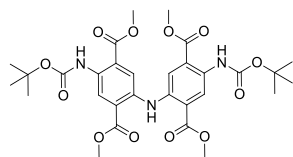
Dimethyl 2,5-diaminoterephthalate (3)

0.4165g (0.9813mmol) **2** was dissolved in 15mL CH₂Cl₂ to which was added 10mL CF₃COOH. The mixture was placed under an atmosphere of nitrogen before it was heated at reflux for 5min at which time TLC showed the deprotection was complete (R_f: 0.62, silica, shortwave UV, 25% CH₃CN/CH₂Cl₂). The reaction mixture was concentrated with rotary evaporation to dryness before being placed under vacuum overnight to remove residual solvent to afford 0.3746g of a yellow solid. The resulting solid was combined with 75% conc. NH_{3(aq)} upon which created a suspension and a color change of yellow to orange in the visible solid. After stirring rapidly for 5min the solid was collected by vacuum filtration, washed with two 10mL portions RT DI H₂O followed by 10mL RT EtOH. (**Note:** Upon EtOH rinse, filtrate turned orange, don't use EtOH to wash away water) The orange solid was placed under vacuum for 1h to remove residual solvent to yield 0.1708g (78% overall yield) of the desired diamine as an orange tinged yellow solid.

¹H NMR (300MHz, CDCl₃): δ7.28 (s, 2H); 4.97 (s, 4H); 3.88 (s, 6H)

ESI-MS (DUI, + ion): 266 (M + CH₃CNH⁺, 100%); 225 (M + H⁺, 93%)

Tetramethyl 5,5'-azanediylbis(2-((tert-butoxycarbonyl)amino)terephthalate) (4)

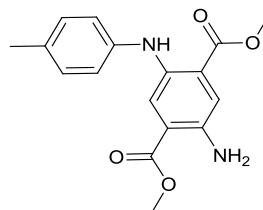


4.541g of the concentrated mother liquor from recrystallization of **2** was combined with 1.085g (14.46mmol) L-Glycine, 4.027g (47.94mmol) NaHCO₃, and 95mL CH₃OH. The mixture was left to stir at room temperature for 17h before the remaining solid was removed by vacuum filtration and rinsed with CH₂Cl₂ until the filtrate ran colorless (150mL). The filtrate was concentrated to dryness with rotary evaporation and placed under vacuum overnight to remove residual solvent to afford 5.199g of a pale orange solid. 5.153g of the resulting solid was boiled in 200mL toluene for 5min before filtering remaining solid with vacuum filtration. The filtrate was washed with three 100mL portion sat. NaHCO₃, dried over MgSO₄, concentrated to dryness with rotary evaporation, and placed under vacuum overnight to remove residual solvent to yield 2.727g of a light orange solid which was determined to be 33% by mass **2** and 67% by mass **4** by ¹H NMR. 0.4081g of the new crude product was purified by flash chromatography (8" silica, 2"/min flow rate, 10mL fraction, eluted with 200mL CH₂Cl₂ then 200mL 5% CH₃CN/CH₂Cl₂) to afford 0.1755g **4**.

¹H NMR (300MHz, CDCl₃): δ10.64 (s, 1H); 9.78 (s, 2H); 8.97 (s, 2H); 8.10 (s, 2H); 3.97 (s, 6H); 3.90 (s, 6H); 1.54 (s, 18H)

ESI-MS (DUIS, + ion): 654 (M + Na⁺, 54%); 632 (M + H⁺, 100%)

HRMS (IT-TOF-ESI, + ion): Calc'd for C₃₀H₃₇N₃O₁₂: 632.2450. Found: 632.2451



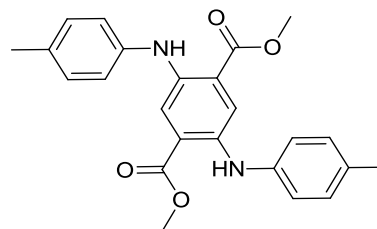
Dimethyl 2-amino-5-(p-tolylamino)terephthalate (5)

0.2764g (1.222mmol) **1** and 1.920g (17.92mmol) *p*-toluidine were combined with 100mL toluene. 30mL toluene was distilled off before the addition of 0.0568g 5% Pd-C. The mixture was then allowed to heat at reflux for 41h (**Note:** pH paper neutral when placed above the condenser periodically over the course of the reaction) after which the boiling reaction mixture was filtered over a pad of Celite and rinsed with boiling toluene until the filtrate was observed to be colorless (75mL). The filtrate was then washed with two 100mL portion pH5 AcOH_(aq) followed by two 100mL pH3 AcOH_(aq). (**Note:** use 4x100mL pH3 portions instead) The organic phase was then removed, dried over MgSO₄, filtered, rinsed with 30mL toluene, concentrated with rotary evaporation, and placed under vacuum overnight to afford 0.335g or a reddish-orange solid (87% crude yield). 0.321g of the crude product from purified via flash chromatography (20mm column, 2in/min flow rate, 10mL fraction, 7.75" silica, 50mL CH₂Cl₂, then 100mL 5% CH₃CN/CH₂Cl₂, 50mL 10% CH₃CN/CH₂Cl₂, then 50mL 100% CH₃CN) Fracs 7-10 5% + Frac 1-3 10% afforded 0.140g **5**.

¹H NMR (300MHz, CDCl₃): δ7.86 (s, 1H); 7.35 (s, 1H); 7.11 (d, J=8.1, 2H); 7.05 (d, J=8.4, 2H); 3.89 (s, 3H); 3.83 (s, 3H); 2.32 (s, 3H)

ESI-MS (DUI, + ion): 356 (M + CH₃CNH⁺, 100%); 315 (M + H⁺, 46%)

HRMS (IT-TOF-ESI, + ion): Calc'd for C₁₇H₁₈N₂O₄: 315.1339. Found: 315.1340



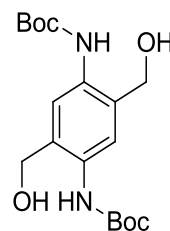
Dimethyl 2,5-bis(p-tolylamino)terephthalate (6)

0.2764g (1.222mmol) **1** and 1.920g (17.92mmol) *p*-toluidine were combined with 100mL toluene. 30mL toluene was distilled off before the addition of 0.0568g 5% Pd-C. The mixture was then allowed to heat at reflux for 41h (**Note:** pH paper neutral when placed above the condenser periodically over the course of the reaction) after which the boiling reaction mixture was filtered over a pad of Celite and rinsed with boiling toluene until the filtrate was observed to be colorless (75mL). The filtrate was then washed with two 100mL portion pH5 AcOH_(aq) followed by two 100mL pH3 AcOH_(aq). (**Note:** use 4x100mL pH3 portions instead) The organic phase was then removed, dried over MgSO₄, filtered, rinsed with 30mL toluene, concentrated with rotary evaporation, and placed under vacuum overnight to afford 0.335g or a reddish-orange solid (87% crude yield). 0.321g of the crude product from purified via flash chromatography (20mm column, 2in/min flow rate, 10mL fraction, 7.75" silica, 50mL CH₂Cl₂, then 100mL 5% CH₃CN/CH₂Cl₂, 50mL 10% CH₃CN/CH₂Cl₂, then 50mL 100% CH₃CN) Fracs 5-8 100% CH₂Cl₂ + f1 5% afforded 0.170g **6**.

¹H NMR (300MHz, CDCl₃): δ8.66 (s, 2H); 7.92 (s, 2H); 7.14 (d, J=8.1Hz, 4H); 7.08 (d, J=8.4Hz, 4H); 3.84 (s, 6H); 2.33 (s, 6H)

ESI-MS (DUIS, + ion): 405 (M + H⁺, 100%); 446 (M + CH₃CNH⁺, 19%)

HRMS (IT-TOF-ESI, + ion): Calc'd for C₂₄H₂₄N₂O₄: 405.1809. Found: 405.1810



N, N'-di-t-Boc-1,4-diamino-2,5-bis-(hydroxymethyl)benzene (7)

13.99g (368.6mmol) LiAlH_4 was combined with 750mL anhydrous Et_2O and heated at reflux for 30min before the addition of 21.95g (51.72mmol) of **2** dissolved in 730mL CH_2Cl_2 . The diester solution was added as quickly as possible while still having the color of the solution disappear upon addition. **Note: Evolution of H_2 gas at this scale can produce increases of pressure that need to be taken into consideration** The reaction was heated at reflux for 1.5h before TLC showed the reaction was complete ($R_f = 0.79$ diester, $R_f = 0.14$ diol 10% $\text{CH}_3\text{CN}/\text{CH}_2\text{Cl}_2$). The mixture was removed from the heat and quenched by sequential, **dropwise**, addition of 14mL DI H_2O , 14mL 15% $\text{NaOH}_{(\text{aq})}$, then 42mL DI H_2O . The mixture was filtered over Celite with the filter pad being removed, boiled in 400mL 50% $\text{Et}_2\text{O}/\text{CH}_2\text{Cl}_2$, for 2min before being filtered over Celite again. The filtrates were combined, dried over MgSO_4 , filtered, concentrated to dryness with rotary evaporation, and placed under vacuum overnight to yield 15.00g (79% yield) of **7** as a white solid (mp = 162-166°C)

^1H NMR (300MHz, CDCl_3): δ 7.78 (s, 2H); 7.59 (s, 2H); 4.67 (s, 4H); 1.92 (s, 2H); 1.51 (s, 18H)

^{13}C NMR (300MHz, CDCl_3): δ 153.7; 133.2; 129.7; 121.7; 80.6; 64.2; 28.5

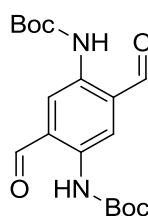
MS (EI, 70eV): 368 (M^+ , 43%); 312 ($\text{M}^+ - \text{C}_4\text{H}_8$, 30%); 256 (312 - C_4H_8 , 100%); 221 ($\text{M}^+ - \text{C}_5\text{H}_{10}\text{O}_2$, 30%); 212 (256 - CO_2 , 48%); 194 (212 - H_2O , 76%); 150 (194 - CO_2 , 88%); 132 (150 - H_2O , 32%)

ESI-MS (DUI, - ion): 367($\text{M} - \text{H}^+$, 90%); 293($\text{M} - 2\text{Boc} + \text{CF}_3\text{COO}^-$, 100%)

HRMS (IT-TOF-ESI, + ion): Calc'd for $C_{18}H_{28}N_2O_6 + NH_4^+$; 386.2291. Found: 368.2288

IR (KBr pellet): IR (KBr pellet): 3384 cm^{-1} (N-H); 3195 cm^{-1} (O-H); 3011 cm^{-1} , 2979 cm^{-1} , 2931 cm^{-1} , 2856 cm^{-1} (C-Hs); 1686 cm^{-1} , 1677 cm^{-1} (C=O); 1537 cm^{-1} (aromatic C-H); 1167 cm^{-1} (C-O)

Elem. Anal.: Calc'd for $C_{18}H_{28}N_2O_6$: C, 58.68; H, 7.66; N, 7.60. Found C, 58.54; H, 7.73; N, 7.52



N,N'-di-*t*-Boc-2,5-diaminoterephthalaldehyde (8)

MnO₂ method

3.018g **7** (8.194mmol) was placed into a 500mL round bottom flask along with 42.47g (488.5mmol) freshly prepared, dried in a 135° C oven until powdery with periodic grinding, MnO₂. 90mL CH₂Cl₂ was added to the reaction vessel before the addition of 210mL acetone. The reflux apparatus was placed under an N₂ atmosphere and heated to reflux while stirring rapidly. After 15h, the reaction was incomplete by TLC (R_f **8** = 0.85, R_f monoaldehyde intermediate = 0.60 10% CH₃CN/CH₂Cl₂) and an additional 4.519g (51.98mmol) 1 day old MnO₂ was added to the reaction and set back to reflux. After an additional 5h TLC showed the reaction was complete. The reaction was filtered hot over a pad of Celite and rinsed with CH₂Cl₂ until the filtrate ran clear (200mL). The MnO₂/Celite pad was placed into a 500mL beaker along with 100mL CH₂Cl₂, 100mL THF, and 100mL MeOH, stirred rapidly, and boiled for ~1-2min before filtering over a pad of Celite. This process was repeated once more. The filtrates were

combined, dried over MgSO_4 , filtered, concentrated with rotary vacuum, and dried over high to remove residual solvent overnight to yield 2.831g **8** (95% yield). 1.015g crude **8** recrystallized from 45mL CH_3CN (44.3mL CH_3CN / g **8**) (58% recovery, mp = 219-221° C) this recovery is not typical though after multiple recrystallizations.

[Cu(MeCN)₄]OTf method

0.3036g (0.8240mmol) **7** was combined with 0.0325g (0.0883mmol) $[\text{Cu}(\text{I})(\text{MeCN})_4]\text{OTf}$, 0.0013g (0.0083mmol) bpy, 13.4 μL (0.168mmol) NMI, 0.0013g (0.0083mmol) TEMPO, and dissolved in 30mL CH_3CN . The mixture was set to stir rapidly open to the air at room temperature for 23h at which time TLC showed incomplete reaction. 0.0130g (0.0832mmol) TEMPO dissolved in 2mL CH_3CN and 20 μL (0.251mmol) NMI were added along with 8mL CH_2Cl_2 to rinse the walls of the vessel. The mixture was set to stir rapidly open to the air for 18h at which time TLC showed complete reaction then filtered over a plug of silica (4.5cm dia., 0.75cm tall) and rinsed with CH_2Cl_2 until the filtrate ran clear (30mL). The filtrate was diluted with 20mL CH_3OH (to prevent bumping), concentrated to dryness with rotary evaporation, and placed under vacuum for 2h to afford 0.286g **8** (95% yield, mp 212-217°C). 0.2641g of crude **8** was recrystallized from 10mL CH_3CN , cooled, and placed in a -20°C freezer overnight to yield 0.2191g (83% recovery, mp = 218-220°C) as orange needles. The mother liquor was concentrated, dissolved in 1.5mL CH_2Cl_2 , and diluted with 12mL hexane. The mixture was boiled down to ½ volume, cooled, and placed in a -20°C freezer overnight to afford 0.0101g DA as yellow plates. **8** afforded in 83% purified yield in two crops from recrystallization.

^1H NMR (300MHz, CDCl_3): δ 10.11 (s, 2H); 10.01 (s, 2H); 8.88 (s, 2H); 1.55 (s, 18H)

^{13}C NMR (300MHz, CDCl_3): δ 195.6; 153.2; 135.3; 126.0; 125.2; 81.5; 28.4

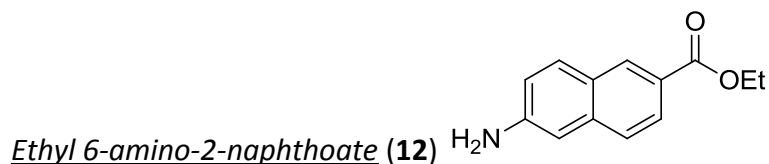
MS (EI, 70eV): 364 (M^+ , 35%); 308 ($\text{M}^+ - \text{C}_4\text{H}_8$, 39); 252 (308 - C_4H_8 , 84%); 208 (252 - CO_2 , 48%); 191 (252 - CH_3NO_2 , 33%); 164 (208 - CO_2 , 100%); 136 (164 - CO , 27%); 108 (136 - CO , 25%)

ESI-MS (DUI, - ion): 458 (54%); 431 ($\text{M}^- + \text{Na}^+ + \text{HCOO}^-$, 78%); 363 ($\text{M} - \text{H}^+$, 100%)

HRMS (IT-TOF-ESI, + ion): Calc'd for $\text{C}_{18}\text{H}_{24}\text{N}_2\text{O}_6 + \text{NH}_4^+$: 382.1978. Found: 382.1973

IR (KBr pellet): 3314cm^{-1} (N-H); 3003cm^{-1} , 2976cm^{-1} , 2933cm^{-1} (methyl C-H); 2886cm^{-1} (aldehyde C-H); 1724cm^{-1} (amide C=O); 1674cm^{-1} (aldehyde C=O); 1550cm^{-1} (aromatic C-H); 1148cm^{-1} (C-O)

Elem. Anal. Calc'd for $\text{C}_{18}\text{H}_{24}\text{N}_2\text{O}_6$: C, 59.33; H, 6.64; N, 7.69. Found: C, 56.68; H, 6.42; N, 7.22



0.9425g (5.035mmol) 6-amino-2-naphthalene-2-carboxylic acid was combined with 24mL anhyd. ethanol to which was added 1.3mL conc. H_2SO_4 , causing a purplish brown solid to precipitate from the mixture. This mixture was placed under an atmosphere of N_2 and heated to reflux, which causing the mixture to become homogeneous. After 2h TLC showed the reaction to be complete. The mixture was then allowed to cool slightly before it was poured into a separatory funnel containing 50mL CH_2Cl_2 and 50mL sat. NaHCO_3 . The organic layer was removed and washed with 50mL sat. NaHCO_3 . Another portion of 50mL CH_2Cl_2 was used to countercurrently extract the two aqueous phases. The organic portions were combined, dried over MgSO_4 , filtered, concentrated with rotary evaporation, and placed under vacuum

overnight to remove residual solvent to afford 1.054g (97%, m.p = 68-71°C) of the desired product as a purple hued brown solid.

^1H NMR (300MHz, CDCl_3): δ 8.45 (s, 1H), 7.94 (dd, J = 8.6 Hz; 1.5Hz, 1H), 7.75 (d, J = 9.3Hz, 1H), 7.58 (d, J = 8.6Hz, 1H), 6.96 (dd, J = overlapped, 1H), 6.95 (d, J = overlapped, 1H), 4.41 (q, J = 7.1Hz, 2H), 3.94 (bs, 2H), 1.42 (t, J = 7.1Hz, 3H)

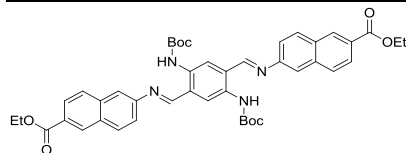
^{13}C NMR (300MHz, CDCl_3): δ 167.2, 146.6, 137.6, 131.1, 131.0, 126.8, 126.1, 125.8, 124.3, 118.8, 108.0, 60.9, 14.9

MS (EI, 70eV) 215 (M^+ , 100%), 187 ($\text{M}^+ - \text{C}_2\text{H}_4$, 38%), 170 ($\text{M}^+ - \text{C}_2\text{H}_5\text{O}$, 79%), 142 ($\text{M}^+ - \text{C}_3\text{H}_5\text{O}_3$), 115 (142 - CHN, 31%)

IR (KBr pellet): Peaks showed the following functional groups: 3431 cm^{-1} , 3349 cm^{-1} (NH_2), 1690 cm^{-1} (C=O); 1294 cm^{-1} (C-O)

Elem. Anal. Calc'd for $\text{C}_{13}\text{H}_{13}\text{NO}_2$: C, 72.54; H, 6.09; N, 6.51. Found C, 71.82; H, 6.13; N, 6.36

Diethyl 6,6'-((1E,1'E)-((2,5-bis((tert-butoxycarbonyl)amino)-1,4-phenylene)bis(methanylylidene))bis(azanylylidene))bis(2-naphthoate) (**13**)



1.003g (2.752mmol) **8** and 1.192g (5.536mmol) **7** were dissolved in 30mL distilled CH_2Cl_2 before the addition of 1.35mL (23.58mmol) glacial acetic acid. The mixture was set to stir at room temperature under an atmosphere of N_2 21h at which time TLC was used to confirm the reaction was complete. Over the course of the reaction it became heterogeneous while orange

solid. The reaction mixture was concentrated to ca. 1/3 volume before diluting with 20mL EtOAc and collecting the orange solid by centrifugation. The supernatant was decanted and the orange solid was combined thoroughly with 20mL EtOAc before centrifuging, decanting and drying the solid under vacuum overnight. 1.792g (86%, mp = 280-282°C) **13** was afforded as a bright orange solid. The supernatants were combined, concentrated with rotary evaporation, diluted with 10mL EtOAc, and centrifuged to collect another portion of orange solid. The supernatant was decanted, washed with 7mL EtOAc, centrifuged, supernatant decanted, and dried under vacuum for 5h to afford 0.1086g (5%) **13** as an orange solid for a total of 1.900g (91% yield)

¹H NMR (300MHz, CDCl₃): δ 11.84 (s, 2H); 8.85 (s, 2H); 8.77 (s, 2H); 8.63 (s, 2H); 8.12 (d, J=8.7Hz, 2H); 8.04 (d, J=9Hz, 2H); 7.92 (d, J=8.7, 2H); 7.72 (s, 2H); 7.56 (d, J=8.7Hz, 2H); 4.47 (q, J=7.2Hz, 4H); 1.59 (s, 18H); 1.47 (t, J=7.2Hz, 6H)

¹³C NMR (300MHz, CDCl₃): δ 166.8; 163.2; 153.8; 149.3; 136.4; 135.0; 131.7; 131.0; 130.9; 128.4; 128.0; 126.3; 124.2; 123.2; 121.7; 118.7; 80.6; 61.3; 28.6; 14.6

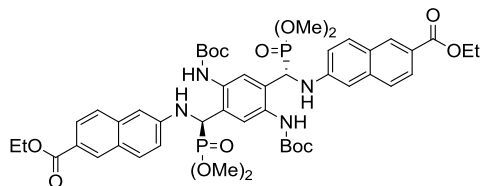
IR (KBr pellet) 3410cm⁻¹; 2975 cm⁻¹; 2359 cm⁻¹; 2341 cm⁻¹; 1713 cm⁻¹; 1273 cm⁻¹, 1241 cm⁻¹

ESI-MS (DUIS, + ion): 759 (M + H⁺, 100%)

HRMS (IT-TOF-ESI): Calc'd for C₄₄H₄₆N₄O₈ + H⁺: 759.3388 Found: 759.3381

Elem. Anal.: Calc'd for C₄₄H₄₆N₄O₈ C: 69.64; H: 6.11; N: 7.38. Found C: 67.45; H: 6.16; N: 6.80

Diethyl 6,6'-(((1*R*,1'*S*)-(2,5-bis((*tert*-butoxycarbonyl)amino)-1,4-phenylene)bis((dimethoxyphosphoryl)methylene))bis(azanediyl))bis(2-naphthoate) (16)



0.1072g (0.4981mmol) **12**, 0.0865g (0.2374mmol) **8**, and 0.0543g (0.0875mmol)

$\text{Yb}(\text{OTf})_3$ were combined and dissolved in 5mL CH_2Cl_2 under an atmosphere of N_2 . After 2.75h TLC showed that NEDA fully formed. The mixture was made homogeneous with the addition of 7mL CH_2Cl_2 before the addition of 0.25mL (4.240mmol) $\text{P}(\text{OMe})_3$. After 21h, the mixture was observed to be homogenous but with the monoamine, mono-aminophosphonate still present so 0.20mL (1.696mmol) $\text{P}(\text{OMe})_3$ was added. After stirring for 21h the reaction appeared complete by TLC. The mixture was poured into a sep. funnel containing 50mL 80% sat. Na_2CO_3 and 25mL CH_2Cl_2 . The organic layer was countercurrently washed with 50mL 80% sat. Na_2CO_3 . A 40mL portion CH_2Cl_2 run through the countercurrent extraction apparatus before the organic layers were combined, dried over MgSO_4 , filtered, concentrated with rotary evaporation, and placed under vacuum to remove residual solvents to afford **16** and **17** (0.2337g, 100%) as a brown solid. Purified by flash chromatography (100mL 10% $\text{CH}_3\text{CN}/\text{CH}_2\text{Cl}_2$, 200mL 40% $\text{CH}_3\text{CN}/\text{CH}_2\text{Cl}_2$, 200mL CH_3CN) to afford **16** (0.0377g, 32%) as an off white solid.

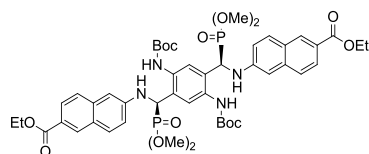
^1H NMR (300MHz, CDCl_3): δ 8.39 (s, 2H); 7.86 (dd, $J=8.6;1.6$, 2H); 7.77 (bs, 2H); 7.72 (d, $J=8.7$, 2H); 7.59 (bs, 2H); 7.38 (d, $J=8.7$, 2H); 6.99 (dd, $J=8.8;2.3$, 2H); 6.54 (nd, $J=1.9$, 2H); 5.13 (dd, $J=22.1$; 5.4, 2H); 4.99 (dd, $J=10.2;5.7$, 2H); 4.39 (q, $J=7.1$, 4H); 3.67 (d, $J=10.5$, 6H); 3.61 (d, $J=10.3$, 6H); 1.51 (s, 18H); 1.41 (t, $J=7.1$, 6H)

^{13}C NMR (300MHz, CDCl_3): δ 167.1, 154.0, 137.4, 134.3, 130.9, 130.8, 128.6, 127.1, 126.1, 126.0, 125.8, 124.6, 118.7, 106.2, 80.5, 60.9, 55.5, 53.8, 53.0, 51.1, 28.6, 14.1

^{31}P NMR (300MHz, CDCl_3): δ 24.94

ESI-MS (DUI, + ion): 997 ($\text{M} + \text{H}^+$, 100%)

Diethyl 6,6'-(((1*S*,1'*S*)-(2,5-bis((*tert*-butoxycarbonyl)amino)-1,4-phenylene)bis((dimethoxyphosphoryl)methylene))bis(azanediyl))bis(2-naphthoate) (17)



0.1072g (0.4981mmol) **12**, 0.0865g (0.2374mmol) **8**, and 0.0543g (0.0875mmol)

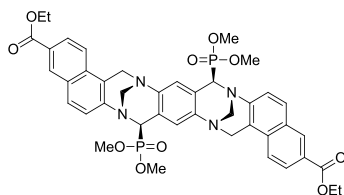
$\text{Yb}(\text{OTf})_3$ were combined and dissolved in 5mL CH_2Cl_2 under an atmosphere of N_2 . After 2.75h **13** fully formed. The mixture was made homogeneous with the addition of 7mL CH_2Cl_2 before the addition of 0.25mL (4.2402mmol) $\text{P}(\text{OMe})_3$. After 21h, the mixture was observed to be homogenous but with the monoamine, mono-aminophosphonate still present so 0.20mL (1.696mmol) $\text{P}(\text{OMe})_3$ was added. After stirring for 21h the reaction appeared complete by TLC. The mixture was poured into a sep. funnel containing 50mL 80% sat. Na_2CO_3 and 25mL CH_2Cl_2 . The organic layer was countercurrently washed with 50mL 80% sat. Na_2CO_3 . A 40mL portion CH_2Cl_2 run through the countercurrent extraction apparatus before the organic layers were combined, dried over MgSO_4 , filtered, concentrated with rotary evaporation, and placed under vacuum to remove residual solvents to afford **16** and **17** (0.2337g, 99.7%) as a brown solid. Purified by flash chromatography (100mL 10% $\text{CH}_3\text{CN}/\text{CH}_2\text{Cl}_2$, 200mL 40% $\text{CH}_3\text{CN}/\text{CH}_2\text{Cl}_2$, 200mL CH_3CN) to afford EDPB (0.0344g, 29%) as a tan solid.

^1H NMR (300MHz, CDCl_3): δ 8.38 (s, 2H), 8.00 (bs, 2H), 7.87 (dd, $J = 8.6; 1.6$, 2H), 7.77 (s, 2H), 7.69 (d, $J = 8.8$, 2H), 7.44 (d, $J = 8.6$, 2H), 6.96 (dd, $J = 8.8; 2.2$, 2H), 6.65 (s, 2H), 5.08 (dd, $J = 2.94; 6.7$), 4.99 (d, $J = 7.0$, 2H), 4.39 (q, $J = 7.1$, 4H), 3.58 (d, $J = 10.5$, 2H), 1.46 (s, 18H), 1.41 (t, $J = 7.1$, 6H)

^{13}C NMR (300MHz, CDCl_3): δ 167.1, 153.8, 145.7, 145.5, 137.3, 134.1, 130.8, 130.8, 127.1, 126.5, 126.1, 124.6, 118.7, 106.5, 80.5, 60.9, 54.7, 54.2, 52.5, 28.5, 14.5

^{31}P NMR (300MHz, CDCl_3): δ 25.65

ESI-MS (DUIS, - ion): 977 ($\text{M} - \text{H}^+$, 100%)



C-Me, P-Me rac- tweezers (**18**)

0.1107g (0.1122mmol) EDPB was combined with 3mL (74.064mmol) MeOH and 1.5mL (16.932mmol) methylal and placed under an atmosphere of N_2 before the addition of 7mL (90.861mmol) CF_3COOH . The mixture was heated at reflux for 22hr before concentration over rotary evaporation. The mixture was poured into a sep. funnel containing 55mL 80% sat. Na_2CO_3 and 30mL CH_2Cl_2 and 15mL sat. NaCl. The organic layer was removed and countercurrently washed with 55mL 80% sat. Na_2CO_3 and 15mL sat. NaCl 20mL CH_2Cl_2 run through the extraction apparatus before the organic portions were combined, dried over MgSO_4 , filtered, concentrated with rotary evaporation, and placed under vacuum to remove residual solvents to afford 0.0835g **18** (90% yield) as a tan solid. Purified by flash chromatography (silica, 75% $\text{CH}_3\text{CN}/\text{CH}_2\text{Cl}_2$, 10% MeOH/ CH_2Cl_2).

Largest Scale:

1.886g (1.927mmol) of the 1:1 mixture of **16** and **17** was combined with 14.0mL anhyd. ethanol, 14.0mL methylal (90mmol), and 34.0mL CF₃COOH. The mixture was placed under an atmosphere of N₂ and heated at reflux for 20hr after which it was cooled to room temperature, diluted with 30mL toluene and concentrated to dryness with rotary evaporation. The concentrate was dissolved in 100mL CH₂Cl₂ and washed with two 50mL portions sat. NaHCO₃. The aqueous washes were combined and back extracted with two 30mL portions CH₂Cl₂. The organic extracts were combined, dried over MgSO₄, filtered, concentrated to dryness with rotary evaporation and placed under vacuum overnight to remove residual solvent to afford 1.6862g of a beige solid. 0.577g of the crude product was combined with 30mL boiling toluene, concentrated to 25mL total volume, cooled to room temperature, and placed on ice for 15min. The resulting mixture was filtered and rinsed with 15mL toluene. The filtrate was concentrate to dryness with rotary evaporation, dissolved in 10mL 1,4-dioxane and precipitate using 100mL hexane. The solid was collected by centrifugation, washed with 40mL hexane, and placed under vacuum overnight to remove residual solvent to afford 0.2253g (81% yield, mp = 308°C (s), 320°C (d)) of the light tan solid **18**.

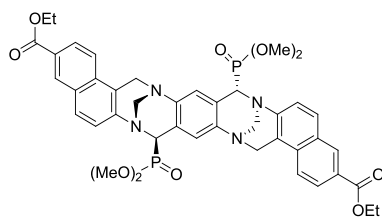
¹H NMR (300MHz, CDCl₃, at 3x10⁻³M): δ8.28 (s, 2H); 7.88 (d, J=7.8Hz, 2H); 7.62 (d, J=8.7Hz, 2H); 7.48 (d, J=8.7, 2H); 7.20 (s, 2H); 7.18 (d, J=8.4Hz, 2H); 5.01 (d, J=12.0Hz, 2H); 4.89 (d, J=17.1Hz, 2H); 4.61 (d, J=23.7Hz, 2H); 4.36 (d, overlapped, 2H); 4.34 (q, J=7.2Hz, 4H); 4.22 (d, J=13.0Hz, 2H); 4.04 (d, J=10.2Hz, 6H); 3.98 (d, J=10.5Hz, 6H); 1.34 (t, J=7.2Hz, 6H)

^{13}C NMR (300MHz, CDCl_3): δ 166.7; 166.5; 147.9; 133.6; 133.2; 131.5; 131.1; 130.2; 129.9; 129.4; 126.8; 126.5; 126.1; 125.6; 124.9; 124.7; 123.3; 122.3; 121.3; 64.4; 63.6; 62.3; 61.25; 61.20; 56.4; 55.3; 53.2; 28.2; 14.5

^{31}P NMR: δ 23.8

ESI-MS (DUI, + ion): 868($\text{M} + \text{CH}_3\text{CNH}^+$, 100%); 827($\text{M} + \text{H}^+$, 42%)

HRMS (IT-TOF-ESI, + ion): Calc'd for $[\text{C}_{42}\text{H}_{44}\text{N}_4\text{O}_{10}\text{P}_2 + \text{H}^+]$ 827.2605 Found: 827.2610



C-Me, P-Me meso-isomer (**19**)

0.1501g (0.1521mmol) **16**, 1.2mL (13.545mmol) methylal, and 2.5mL MeOH (61.720mmol) were combined under an atmosphere of N_2 before 4mL (341.36mmol) CF_3COOH was added. The mixture was heated at reflux for 21hr concentrating the mixture with rotary evaporation. 10mL CH_2Cl_2 was to the concentrate and countercurrently washed with 50mL 80% sat. Na_2CO_3 in the first sep. funnel and 50mL 80% sat. Na_2CO_3 and 30mL sat. NaCl in the second sep.funnel. 60mL CH_2Cl_2 run through the extraction apparatus before the organic portions were combined, dried over MgSO_4 , filtered, concentrated with rotary evaporation, and placed under high vacuum to afford **19** (0.1062g, 84%) as a solid. Crude product is purified by flash chromatography (40% $\text{CH}_3\text{CN}/\text{CH}_2\text{Cl}_2$, 5% $\text{MeOH}/\text{CH}_2\text{Cl}_2$, and 10% $\text{MeOH}/\text{CH}_2\text{Cl}_2$ if not eluted out in the 5% portion).

Largest Scale:

1.886g (1.927mmol) of the 1:1 mixture of **16** and **17** was combined with 14.0mL anhyd. ethanol, 14.0mL methylal (90mmol), and 34.0mL CF₃COOH. The mixture was placed under an atmosphere of N₂ and heated at reflux for 20hr after which it was cooled to room temperature, diluted with 30mL toluene and concentrated to dryness with rotary evaporation. The concentrate was dissolved in 100mL CH₂Cl₂ and washed with two 50mL portions sat. NaHCO₃. The aqueous washes were combined and back extracted with two 30mL portions CH₂Cl₂. The organic extracts were combined, dried over MgSO₄, filtered, concentrated to dryness with rotary evaporation and placed under vacuum overnight to remove residual solvent to afford 1.6862g of a beige solid. 0.577g of the crude product was combined with 30mL boiling toluene, concentrated to 25mL total volume, cooled to room temperature, and placed on ice for 15min. The resulting mixture was filtered with 15mL toluene used to rinse the collected solid which was then placed under vacuum overnight to afford 0.241g (84% yield, mp = 322°C (s), 338°C (d)) of the *meso*-isomer **19**.

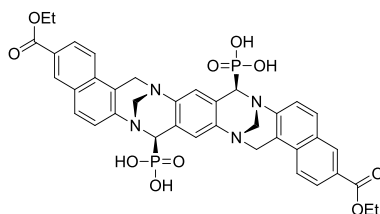
¹H NMR (300MHz, CDCl₃): δ 8.52 (s, 2H); 8.05 (d, J=8.7Hz, 2H); 7.84 (d, J=9.0Hz, 2H); 7.61 (d, J=9.0Hz, 2H); 7.31 (s, 2H); 7.28 (d, overlapped, 2H); 5.07 (d, J=16.8Hz, 2H); 5.00 (d, J=13.8Hz, 2H); 4.75 (d, J=24.3Hz, 2H); 4.45 (d, overlapped, 2H); 4.43 (q, overlapped, 4H); 4.25 (d, J=12.9Hz, 2H); 3.94 (d, J=10.5Hz, 6H); 3.85 (d, J=10.8Hz, 6H); 1.43 (t, J=7.2Hz, 6H)

¹³C NMR (300MHz, CDCl₃): δ 166.8; 133.7; 131.6; 130.3; 129.8; 127.1; 126.5; 125.8; 124.9; 123.5; 122.2; 121.4; 64.4; 63.6; 62.3; 61.2; 57.1; 55.2; 53.3; 14.5

³¹P NMR (300MHz, CDCl₃): δ 23.7

ESI-MS (DUI, + ion): 827 ($M + H^+$, 100%); 424 ($(M + 2H^+)/2$, 40%); 270 (26%)

HRMS (IT-TOF-ESI, + ion): Calc'd for $[C_{42}H_{44}N_4O_{10}P_2 + H^+]$ 827.2605 Found: 827.2600



rac-carbethoxy tetra acid tweezers (23)

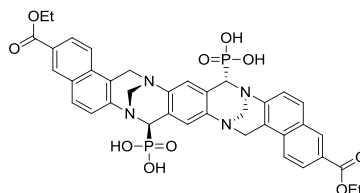
0.121g (0.146mmol) *rac*- naphthyl tweezers was dissolved in 6mL CH_2Cl_2 (distilled from CaH_2) and placed under an atmosphere of N_2 before the addition of 0.80mL (6.0mmol) bromotrimethylsilane. The mixture was stirred at room temperature for 16hr before the mixture was concentrated to dryness with vacuum. The crude product was dissolved in 10mL boiling ethanol and cooled to room temperature before the addition of 40mL hexane causing a solid to precipitate and stored overnight at $-20^\circ C$. The solid was collected by centrifugation, washed with 15mL hexane, and placed under vacuum overnight to remove residual solvent to afford 0.087g (77% yield, mp = $350^\circ C$ (d)) **23**.

1H NMR (1:1 dTFA/ $CDCl_3$): δ 8.58 (s, 2H); 8.49 (s, 2H); 8.07 (d, $J=9.3Hz$, 2H); 8.04 (d, $J=9.6Hz$, 2H); 7.58 (d, $J=9.0Hz$, 2H); 7.53 (d, $J=9.0$, 2H); 5.89 (d, $J=11.4Hz$, 2H); 5.62 (d, $J=15.0Hz$, 2H); 5.19 (d, $J=25.5Hz$, 2H); 4.94 (overlapped, 4H); 4.47 (q, $J=6.9Hz$, 4H); 1.45 (t, $J=7.2Hz$, 6H)

^{31}P NMR (300MHz, DMSO- d_6): δ 17.2

ESI-MS (DUI, - ion): 769 ($M + H^+$, 100%)

HRMS (IT-TOF-ESI, + ion): Calc'd for $C_{38}H_{34}N_4O_{10}P_2 + H^+$: 771.1979 Found: 771.1975



meso-carbethoxy tetra acid isomer (24)

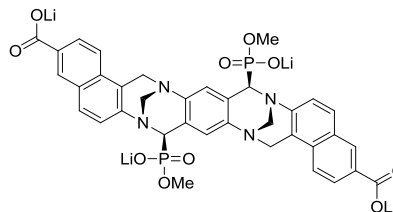
0.212g (0.1256mmol) **19** was suspended in 10mL CH_2Cl_2 (distilled from CaH_2) and placed under an atmosphere of N_2 before the addition of 0.90mL (6.8mmol) bromotrimethylsilane. The mixture was heated at reflux for 18hr after which time none of the starting material was seen by TLC (R_f = 0.35, 10% CH_3OH/CH_2Cl_2 , silica). The reaction mixture was concentrated to dryness under vacuum. The 16mL boiling ethanol was added to the crude product, allowed to cool to room temperature, diluted with 25mL hexane, and stored overnight at $-20^\circ C$. The solid was collected by centrifugation, washed with 15mL hexane, and placed under vacuum overnight to remove residual solvent to yield 0.170g (86% yield, mp = $340^\circ C$ (darkens), $380^\circ C$ (shrinks), $>400^\circ C$) of **24**.

1H NMR (300MHz, D_2O): δ 8.50 (s, 2H); 7.99 (d, J =8.4Hz, 2H); 7.88 (d, J =8.7Hz, 2H); 7.82 (d, J =8.7Hz, 2H); 7.54 (d, J =9.0Hz, 2H); 7.29 (s, 2H); 4.98 (d, J =12.3Hz, 2H); 4.9-4.7 (obscured by HOD, 4H); 4.55 (d, J =21.3Hz, 2H); 4.40 (q, J =6.9Hz, 4H); 4.07 (d, J =11.7Hz, 2H); 1.40 (t, J =7.2Hz, 6H)

^{31}P NMR (300MHz, D_2O): δ 18.2

ESI-MS (DUIS, - ion): 770 ($M - H^+$, 100%); 384 ($M - 2H^+$, 40%)

HRMS (IT-TOF-ESI, + ion): [Calc'd for $C_{38}H_{34}N_4O_{10}P_2 + H^+$] 771.1979 Found: 771.1970



rac-methyl phosphonate tetra anionic tweezers (25)

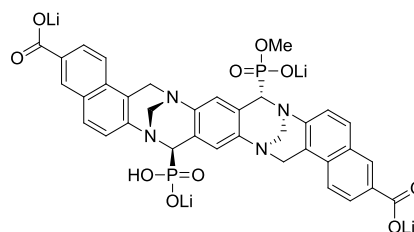
0.076g (0.0092mmol) **18** was dissolved in 2mL 1,4-dioxane to which was added 0.018g (0.752mmol) LiOH in 5.5mL 18 Ω H₂O and heated at reflux for 22hr. The mixture was allowed to cool to room temperature, concentrated to dryness with rotary evaporation, dried azeotropically by the evaporation of 50mL toluene, and placed under vacuum overnight to yield 0.0734g of a mixture that was 87% by mass **25**. 0.0491g of the crude solid was dissolved in 10mL 18 Ω H₂O, titrated to pH7 with 4.8% HBr (0.89M), concentrated to dryness with rotary evaporation, dissolved in 12mL 18 Ω H₂O, and concentrated to dryness again. 10mL THF was added to the solid and swirled periodically over the course of 20min after which the THF was removed. This process was repeated with a 20mL portion THF then followed by a 6mL portion THF before being placed under vacuum for 3d to remove residual solvent to afford 0.0401g of **25** (96% by mass, 90% recovery) as a mixture with THF.

¹H NMR (1:1 TFA:CDCl₃): δ 8.67 (s, 2H); 8.52 (s, 2H); 8.16 (d, J=8.7Hz, 2H); 8.06 (d, J=9.0Hz, 2H); 7.60 (d, J=9.0Hz, 2H); 7.54 (d, J=8.7Hz, 2H); 5.94 (d, J=11.7Hz, 2H); 5.63 (d, J=17.1Hz, 2H); 5.19 (d, J=25.8Hz, 2H); 5.02 (overlapped, 4H); 4.14 (d, J=10.8Hz, 6H)

³¹P NMR (1:1 TFA:CDCl₃): δ 17.2

ESI-MS (- ion mode): 748 (M - 2H⁺ + Li⁺, 50%); 741 (M - H⁺, 100%)

HRMS (IT-TOF-ESI, + ion): Calc'd for C₃₆H₃₂N₄O₁₀P₂ + H⁺: 743.1666 Found: 743.1671



meso-methylphosphonate tetra anionic isomer (26)

0.095g (0.115mmol) **19** was suspended in 15mL 1,4-dioxane to which was added 0.025g (1.03mmol) LiOH in 4.5mL 18Ω H₂O. The mixture was placed under an atmosphere of N₂ and heated at reflux for 29hr. The mixture was concentrated to dryness with rotary evaporation, combined with 4mL 18Ω H₂O, and filtered through a plug of Celite. The filtrate was concentrated to dryness with rotary evaporation, dried azeotropically by the evaporation of 25mL toluene, and placed under vacuum for 3d for yield 0.0889g of **26** in 86% yield as an 85% by mass mixture with LiOH. 0.0125g of the crude product was dissolved in 10 mL 18Ω H₂O and titrated to pH7 with 4.8% HBr (0.89M). The mixture was concentrated to dryness with rotary evaporation and triturated with 10mL THF by period swirling over 20min. The THF was decanted and the process was repeated one more time before the solid was placed under vacuum overnight to remove residual solvent to afford 0.011g **26** (100% recovery)

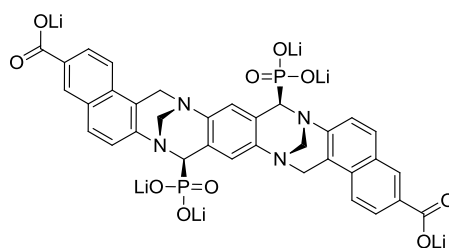
¹H NMR (300MHz, D₂O): δ8.46 (s, 2H); 7.94 (d, overlapped, 2H); 7.94 (d, overlapped, 2H); 7.82 (nd, J=7.2Hz); 7.42 (d, J=8.7Hz, 2H); 7.27 (s, 2H); 4.97 (d, J=16.5Hz, 2H); 4.95-4.55 (obscured by HOD, 6H); 4.18 (d, J=12.0Hz, 2H); 3.56 (d, J=9.0Hz, 6H)

^{13}C NMR (300MHz, D_2O): δ 176.1; 146.8 (d); 143.5; 133.6; 132.8; 130.7; 130.4; 130.1; 127.2; 126.2; 125.6; 125.2; 122.5; 121.9; 65.1; 63.0 (d); 56.8; 53.1

^{31}P NMR (300MHz, D_2O): δ 16.9

ESI-MS (DUI, - ion): 747(M - H^+ - Li^+ , 100%); 741(M - H^+ , 58%)

HRMS (IT-TOF-ESI): Calc'd for $\text{C}_{36}\text{H}_{32}\text{N}_4\text{O}_4\text{P}_2 + \text{H}^+$: 743.1666 Found: 743.1666



rac-hexa anionic tweezers (27)

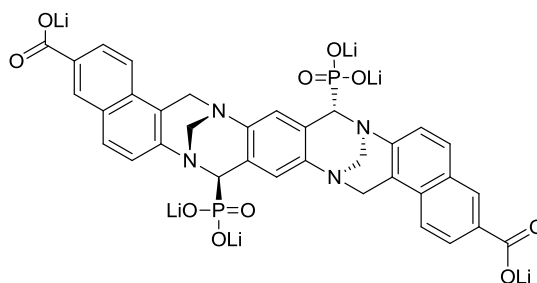
0.041g (0.053mmol) **23** was combined with 0.024g (0.994mmol) LiOH and 8mL 18 Ω H_2O . The mixture was heated at reflux for 24hr after which time the mixture was allowed to cool to room temperature and brought to pH7 by dropwise addition of 4.8% HBr (0.89M). The mixture was concentrated to dryness with rotary evaporation, dissolved in 10mL 18 Ω H_2O , and concentrated to dryness again. The crude product was combined with 11mL THF, mixed thoroughly, centrifuged, and THF decanted. This process was repeated twice more before the solid was placed under vacuum for 2d to remove residual solvent to afford 0.0276g **27** as a 90% by mass mixture (62% yield) with THF.

^1H NMR (300MHz, 50% TFA/ CDCl_3): δ 8.69 (s, 2H); δ 8.54 (s, 2H); δ 8.16 (d, $J=8.1\text{Hz}$, 2H); δ 8.08 (d, $J=7.8\text{Hz}$, 2H); δ 7.62 (d, $J=8.1\text{Hz}$, 2H); δ 7.58 (d, $J=9.3\text{Hz}$, 2H); δ 5.93 (d, $J=12.9\text{Hz}$, 2H); δ 5.62 (d, $J=14.1\text{Hz}$, 2H); δ 5.22 (d, $J=25.2\text{Hz}$, 2H); δ 5.02 (d, overlapped, 4H)

^{31}P NMR (50% TFA/ CDCl_3): δ 17.6

ESI-MS (DUI, - ion): 713 ($\text{M} - \text{H}^+$, 85%); 473 (100%)

HRMS (IT-TOF-ESI, + ion): Calc'd for $\text{C}_{34}\text{H}_{28}\text{N}_4\text{O}_{10}\text{P}_2 + \text{H}^+$: 715.1353 Found: 715.1357



meso-hexa anionic isomer (28)

0.079g (0.103mmol) **24** was combined with 0.050g (0.207mmol) LiOH in 10mL 18 Ω H_2O and heated at reflux for 25hr after it was allowed to cool to room temperature and neutralized to pH7 with 4.8% HBr (0.89M). The mixture was concentrated to dryness with rotary evaporation, redissolved in 10mL 18 Ω H_2O , and concentrated to dryness again. The crude solid was mixed thoroughly with 10mL THF, centrifuged, and THF was decanted. This process was repeated twice more before being placed under vacuum overnight to afford 0.0517g (66% yield) of the meso-hexa anion tweezer as a pale yellow solid.

^1H NMR (50% TFA/ CDCl_3): δ 8.80 (s, 2H); 8.28 (d, obscured, 2H); 8.27 (s, 2H); 8.17 (d, $J=8.7\text{Hz}$, 2H); 7.80 (d, $J=8.4\text{Hz}$, 2H); 7.58 (d, $J=8.7\text{Hz}$, 2H); 5.87 (d, $J=12.6\text{Hz}$, 2H); 5.61 (d, $J=15.9\text{Hz}$, 2H); 5.20 (d, $J=22.5\text{Hz}$, 2H); 5.11 (d, $J=16.2\text{Hz}$, 2H); 4.97 (d, $J=12.3\text{Hz}$, 2H)

^{31}P NMR (50% TFA/ CDCl_3): δ 16.0

ESI-MS (DUIS, - ion): 713 ($\text{M} - \text{H}^+$, 100%); 473 (89%)

HRMS (IT-TOF-ESI, + ion): Calc'd for $\text{C}_{34}\text{H}_{28}\text{N}_4\text{O}_{10}\text{P}_2 + \text{H}^+$: 715.1353 Found: 715.1398



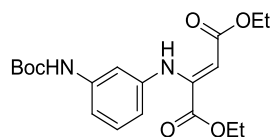
2.064g 1,3-diaminobenzene (19.09mmol) was dissolved in 15mL of EtOAc at room temperature to which was added 2.033g Boc_2O (9.315mmol) dropwise under an atmosphere of N_2 . After 90min, the starting diamine and mono Boc material observed by TLC. At 120min the diacylated product started to show by TLC (50% EtOAc/ CH_2Cl_2 , silica, short UV, R_f diamine = 0.34 R_f mono Boc = 0.72, R_f DiBoc = 0.92). The reaction mixture was diluted with 50mL of CH_2Cl_2 and washed with eight 250mL portion DI H_2O . The organic layer was removed, dried over MgSO_4 , concentrated over rotary vacuum, and dried over vacuum overnight to yield 1.528g **29** (79% yield) as a smokey white solid. Recrystallized from hexanes using hot filtration to afford white crystals (mp = 108-109°C).

^1H NMR (300MHz, CDCl_3): δ 7.32 (t, $J=8.0\text{Hz}$, 1H); 6.92 (1H, s); 6.56 (ddd, $J=7.3$; 1.8; 0.6, 1H); 6.56 (s, 1H); 6.33 (ddd, $J=7.9$; 2.1; 0.7, 1H); 3.23 (bs, 2H); 1.51 (s, 9H)

^{13}C NMR (300MHz, CDCl_3): δ 152.6; 147.2; 139.3; 129.6; 109.8; 108.5; 105.0; 80.2; 28.3

MS (EI, 70eV): 208 (M^+ , 25%); 152 ($\text{M}^+ - \text{C}_4\text{H}_8$, 100%); 108 (152 - CO_2 , 78%); 57 (C_4H_9^+ , 84%)

2-(3-tert-Butoxycarbonylamino-phenylamino)-but-2-enedioic acid diethyl ester (30)

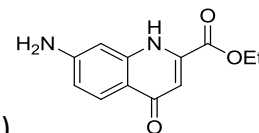


0.9982g (4.794mmol) tert-butyl (3-aminophenyl)carbamate **29** and 2.192g (10.43mmol) sodium diethyl oxaloacetate were added to 11mL CH_2Cl_2 and 8.9mL glacial AcOH. The mixture was stirred until homogeneous before the addition of 4Åms (25% reaction volume). The mixture was swirled periodically over 4h at which time TLC showed the reaction was done (25% EtOAc/ CH_2Cl_2 , silica, short UV, R_f amine=0.5, R_f enamine=0.9). The mixture was poured into 125mL sat. Na_2CO_3 and 100mL hexanes. The organic phase was removed and the aqueous layer was extracted with an addition two 100mL portions hexanes. The organic extracts were combined, washed with four 100mL portions DI H_2O then 60mL pH2 phosphate buffer before drying over MgSO_4 . After drying the mixture was filtered, concentrated with rotary evaporation, and placed under vacuum overnight to yield the 1.558g (96% yield) desired enamine **30** as an orange oil.

^1H NMR (300MHz, CDCl_3): δ 9.61 (s, 1H); 7.15 (unresolved, 2H); 6.95 (dd, J =6.7 Hz; 1.4 Hz, 1H); 6.57 (dd J =6.9 Hz; 2.0 Hz, 1H); 6.42 (s, 1H); 5.37 (s, 1H); 4.20 (q, J =7.1 Hz, 4H); 1.51 (s, 9H); 1.32 (t, J =7.1Hz, 3H); δ 1.15 (t, J =7.1Hz, 3H)

^{13}C NMR (300MHz, CDCl_3): δ 169.8; 164.7; 152.7; 148.6; 141.4; 139.6; 129.7; 115.6; 114.2; 111.2; 94.5; δ 81.0; 62.5; 60.3; 28.6; 14.7; 14.0

MS (EI, 70eV): 378 (M^+ , 18%); 322 ($M^+ - C_4H_8$, 22%); 249 (322 - $C_3H_5O_2$, 39%); 203 (249 - C_2H_6O , 68%); 185 (203 - H_2O , 36%); 159 (203 - CO_2 , 100%); 132 (159 - CO , 32%)



7-Amino-4-oxo-1,4-dihydro-quinoline-2-carboxylic acid ethyl ester (31)

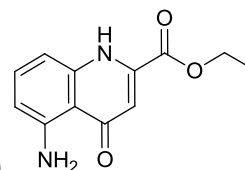
0.0326g (0.1243mmol) **38** and 0.0109g 5% Pd-C were suspended in 10mL anhyd. EtOH to which was added 0.1930g (3.061mmol) ammonium formate. The mixture was stirred rapidly for 3h before TLC showed the absence of starting material (50% EtOAc/ CH_2Cl_2 , silica, short UV R_f nitro= 0.39, R_f amino= 0.08). The mixture was filtered through Celite, rinsed with 40mL anhyd. EtOH, and concentrated to dryness with rotary evaporation. The crude was dissolved in 5.5mL EtOH and diluted with 30mL CH_2Cl_2 causing NH_4O_2CH to precipitate which was removed by filtration. The filtrate was concentrated to dryness with rotary evaporation and purified by flash chromatography (5% IpOH/ CH_3CN) to yield 0.019g (66% yield) of **31**.

1H NMR (300MHz, DMSO- d_6): δ 11.40 (s, 1H); 8.03 (d, $J=8.7$ Hz, 1H); 6.81 (d, $J=1.8$ Hz, 1H); 6.64 (dd, $J=8.8$; 2.1Hz, 1H); 6.42 (d, $J=2.1$ Hz, 1H); 6.03 (s, 2H); 4.41 (q, $J=7.1$ Hz, 2H); 1.42 (t, $J=7.1$ Hz, 3H)

^{13}C NMR (300MHz, DMSO- d_6): δ 162.8; 153.1; 142.8; 137.1; 126.4; 117.7; 114.4; 110.6; 110.0; 98.1; 62.6; 14.3

MS (EI, 70eV): 232 (M^+ , 49%); 158 ($M^+ - C_3H_5O_2$, 10%); 130 (158 - CO); 104 (130 - C_2H_2 , 27%); 57 ($C_3H_5O^+$, 56%)

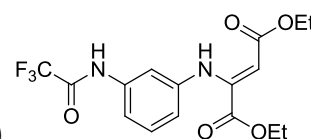
ESI-MS (DUIS, + ion): 465 (2M + H^+ , 28%); 291 (M + 59, 38%); 233 (M + H^+ , 100%)



Ethyl 5-amino-4-oxo-1,4-dihydroquinoline-2-carboxylate (**32**)

^1H NMR (300MHz, DMSO- d_6): δ 11.52 (s, 1H); 7.51 (bs, 2H); 7.23 (t, $J=8.8\text{Hz}$, 1H); 6.86 (dd, $J=7.3$; 0.8Hz, 1H); 6.40 (d, $J=1.9\text{Hz}$, 1H); 6.20 (dd, $J=7.4$; 0.7Hz, 1H); 4.40 (q, $J=7.1\text{Hz}$, 2H); 1.35 (t, $J=7.1\text{Hz}$, 3H)

^{13}C NMR (300MHz, DMSO- d_6): δ 181.9; 162.4; 151.1; 142.7; 137.2; 133.6; 112.7; 110.7; 107.0; 103.7; 62.8; 14.3



Diethyl 2-((3-(2,2,2-trifluoroacetamido)phenyl)amino)fumarate (**34**)

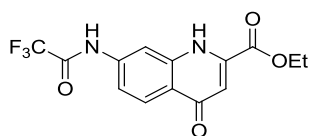
0.154g (0.753mmol) N-(3-aminophenyl)-2,2,2-trifluoroacetamide (**33**) and 0.404g (1.92mmol) sodium diethyl oxaloacetate were dissolved in 5mL CH_2Cl_2 and 0.3mL glacial AcOH. After homogeneous 0.709g 4Åms were added to the mixture and swirled periodically over the course of 27h at which time the reaction was observed to be complete by TLC (1:1:1 EtOAc/ CH_2Cl_2 / NEt_3 , silica, short UV R_f amine=0.54, R_f enamine=0.82). The reaction volume was poured into 20mL sat. Na_2CO_3 and 100mL hexanes. The organic phase was removed and the aqueous layer was extracted with an addition two 50mL portions hexanes. The organic extracts were combined, washed with 20mL sat. Na_2CO_3 , dried over MgSO_4 , filtered, concentrated with rotary evaporation, and placed under vacuum overnight to remove residual solvent to yield 0.252g (89% yield) of **34** as a yellow green oil.

^1H NMR (300MHz, CDCl_3): δ 9.61 (s, 1H); 8.15 (s, 1H); 7.26(obsured, 1H); 7.24 (t, $J=8.0\text{Hz}$, 1H); 7.14 (d, $J=8.2\text{Hz}$, 1H); 6.73 (d, $J=7.8\text{Hz}$, 1H); 5.47 (s, 1H); 4.24 (q, $J=7.2\text{Hz}$, 4H); 1.30 (t, $J=7.1\text{Hz}$, 3H); 1.18 (t, $J=7.1\text{Hz}$, 3H)

^{13}C NMR (300MHz, CDCl_3): δ 169.3; 164.2; 154.8; 147.3; 141.0; 136.2; 129.5; 118.0; 115.7; 115.5; 112.7; 95.4; 62.4; 60.8; 14.1; 13.5

MS (EI, 70eV): 374 (M^+ , 12%); 301 ($\text{M}^+ - \text{C}_3\text{H}_5\text{O}_2$, 13%); 255 (301 - $\text{C}_2\text{H}_6\text{O}$, 100%); 228 (256 - CO, 18%)

Ethyl 4-oxo-7-(2,2,2-trifluoroacetamido)-1,4-dihydroquinoline-2-carboxylate (35)



Thermolysis method

0.0526g (0.1405mmol) diethyl 2-((3-(2,2,2-trifluoroacetamido)phenyl)amino)fumarate (**34**) was combined with 25mL Ph_2O and heated at reflux under an atmosphere of N_2 for 20min after which it was cooled to room temperature below the addition of 170mL hexane. The mixture was stored in a 0°C refrigerator with crystals being collected by vacuum filtration the following day. After rinsing with hexanes and residual solvent removed 0.0249g (54% yield) quinolones afforded in a 1:3.5 mol ratio of the 7- : 5-trifluoroacetyl isomers.

Eaton's Reagent method

0.149g (0.394mol) **34** was dissolved in 10mL Eaton's Reagent and heated at 116°C for 50min after which the reaction volume was poured into 20mL CH_2Cl_2 to which was added sat.

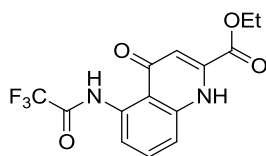
Na₂CO₃ until no more effervescence was observed. The organic layer was removed and the aqueous phase was extracted with two 60mL portions CH₂Cl₂. The organic layers were combined, dried over MgSO₄, filtered, concentrated with rotary evaporation, and placed under vacuum to remove residual solvent yield 0.105g (81% yield) of the quinolones in a 1:7 mol ratio of the 7- : 5-trifluoroacetyl isomers.

¹H NMR (300MHz, DMSO-d₆): δ12.26 (s, 1H); 11.64 (s, 1H); 8.13 (d, J=8.9Hz, 1H); 7.96 (d, J=2.0Hz, 1H); 7.52 (dd, J=9.0; 2.1Hz, 1H); 6.89 (s, 1H); 4.47 (q, J=7.1Hz, 2H); 1.39 (t, J=7.1Hz, 3H)

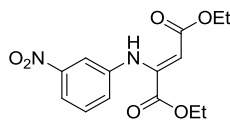
¹³C NMR (300MHz, DMSO-d₆): δ168.7; 165.3; 161.4; 155.1; 140.5; 138.9; 131.9; 127.1; 123.5; 115.8; 114.2; 107.3; 62.3; 14.2

MS (EI, 70eV): 328 (M⁺, 100%); 299 (M⁺ - C₂H₅, 25%); 256 (299 +H - CO₂, 34%); 203 (256 + H - C₃H₂O, 16%); 157 (256 - H - C₂HF₃O, 22%); 132 (157 + H - C₂H₂, 40%); 69 (CF₃⁺, 45%)

Ethyl 4-oxo-5-(2,2,2-trifluoroacetamido)-1,4-dihydroquinoline-2-carboxylate (36)



¹H NMR (300MHz, CDCl₃): δ14.79 (s, 1H); 9.26 (s, 1H); 8.57 (d, J=8.1Hz, 1H); 7.69 (t, J=8.3Hz, 1H); 7.23 (d, J=8.4; 0.9Hz, 1H); 6.96 (s, 1H); 4.52 (q, J=7.1Hz, 2H); 1.45 (t, J=7.1Hz, 3H)



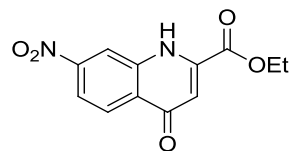
Diethyl 2-((3-nitrophenyl)amino)fumarate (37)

1.024 (7.417mmol) m-nitroaniline, 3.118g (14.84mmol) sodium diethyl oxaloacetate, 2.982g TsOH·H₂O(15.68mmol) were combined in 60mL of CH₂Cl₂, fitted with a heavier than water Dean-Stark Trap and heated to reflux overnight. After the starting aniline had been seen to be consumed (silica,1:1:1 EtOAc: CH₂Cl₂: NEt₃, short UV R_f aniline=0.65, R_f enamine=0.83) the reaction mixture was poured into 50mL of hexane and washed with 200mL of a 0.1M K₃PO₄ solution. The organic phase was then washed with 200mL of DI H₂O, dried over MgSO₄, filter, concentrated over rotary vacuum, and placed on high vacuum to removal residual solvent to yield 2.085g (92% yield) of the desired enamine as a yellow oil.

¹H NMR (300MHz, CDCl₃): δ9.77 (s, 1H); 7.92 (dd, J=8.1; 1.5Hz, 1H); 7.72 (t, J=2.1Hz, 1H); 7.44 (t, J=8.1Hz, 1H); 7.20 (dd, J=8.0; 2.1Hz, 1H); 5.62 (s, 1H); 4.24 (q, J=7.2Hz, 4H); 1.32 (t, J=7.1Hz, 3H); 1.21 (t, J=7.1Hz, 3H)

¹³C NMR (300MHz, CDCl₃): δ169.2; 163.5; 148.7; 146.3; 141.8; 129.8; 126.2; 118.3; 115.0; 97.6; 62.5; 60.5; 14.3; 13.8

MS (EI, 70eV): 308 (M⁺, 18%); 235 (M⁺ - C₃H₅O₂, 28%); 189 (235 - C₂H₆O, 100%); 162 (189 - CO, 23%); 143 (189 - NO₂, 24%); 89 (C₃H₇NO₂⁺, 23%); 76 (C₆H₄⁺, 49%)



Ethyl 7-nitro-4-oxo-1,4-dihydroquinoline-2-carboxylate (38)

Thermolysis

0.282g (0.916mmol) **37** was dissolved in 80°C 40mL Ph₂O. The reaction mixture was degassed and backfilled with N₂ three time, placed under an atmosphere of N₂, and heated at reflux for 21min before the mixture was allowed to cool to room temperature over which time a yellow solid precipitated. 50mL hexanes were added to ensure complete precipitation before the solid was collected by vacuum filtration, washed with an additional 100mL hexane, and dried under vacuum overnight to remove residual solvent to generate 0.194g (81%) of the quinolones in a mol ratio of 4:1 of the 7-NO₂ : 5-NO₂ isomers.

Eaton's Reagent

0.273g (0.886mmol) **37** to which was added 5mL Eaton's Reagent. The mixture was placed under a N₂ atmosphere and heated at 110°C 3h over which time it changed color to a dark red color and was removed from the heat. After 20h at room temperature the mixture was poured into 50mL CH₂Cl₂ and 60mL sat. Na₂CO₃. The organic layer was removed and the aqueous phase was extracted with an addition two 40mL portions CH₂Cl₂. The organic extracts were combined, dried over MgSO₄, filtered, concentrated with rotary evaporation, and placed under vacuum overnight to remove residual solvent to yield 0.254g (109% yield) of the quinolones in a mol ration of 1:2.3 of the 7-NO₂ : 5-NO₂ isomers.

Recrystallization procedure developed by Jackie Koch

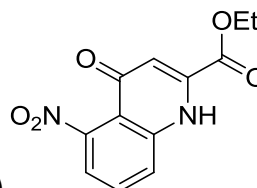
0.1006 g of a 2.6:1 mol ratio 7-NO₂ : 5-NO₂ quinolone isomers mixture was suspended in 8mL boiling EtOH for 3 min to which was added 10mL boiling toluene and continued to heat at boiling for 9 min. The mixture was placed on ice for 15 min with the resulting solid collected by centrifugation. It was then washed with 20mL hexanes and placed under vacuum overnight to afford 0.0639 g of the **38** in 88% recovery (mp = 308-310°C)

¹H NMR (300MHz, DMSO-d₆): δ12.47 (s, 1H); 8.87 (d, J=2.2Hz, 1H); 8.29 (d, J=8.9, 1H); 8.09 (dd, J=8.9; 2.2Hz, 1H); 6.79 (s, 1H); 4.44 (q, J=7.1Hz, 2H); 1.38 (t, J=7.1, 3H)

¹³C NMR (300MHz, DMSO-d₆): saturated solution too dilute to acquire all signals

Signals observed: δ161.8; 149.6; 128.5; 127.0; 117.5; 111.1; 62.8; 13.9

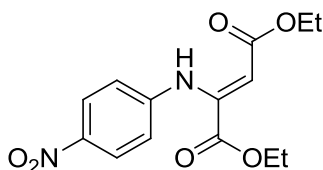
MS (EI, 70eV): 262 (M⁺, 67%); 188 (M⁺ - C₃H₆O₂, 98%); 142 (188⁺ - NO₂); 114 (142⁺ - CO, 75%); 88 (114⁺ - C₂H₂, 61%); 75 (C₃H₇O₂⁺, 100%); 62 (88⁺ - C₂H₂, 58%)



Ethyl 5-nitro-4-oxo-1,4-dihydroquinoline-2-carboxylate (39)

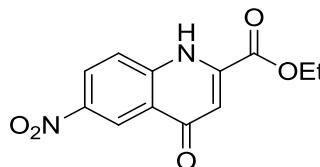
¹H NMR (300MHz, DMSO-d₆): δ14.86 (1H, s); 8.19 (d, J=8.5, 1H); 7.86 (1H, t, J=7.9Hz); 7.62 (1H, d, J=7.4Hz); 6.69 (1H, s); 4.47 (2H, q, J=6.8Hz); 1.40 (3H, t, J=7.4Hz)

Diethyl 2-((4-nitrophenyl)amino)fumarate (**40**)



0.6405g (4.637mmol) p-nitroaniline, 1.951g (9.282mmol) sodium diethyl oxaloacetate, 1.855g (9.752mmol) TsOH·H₂O, and 50mL CH₂Cl₂ were combined in heated at reflux with a heavier than water Dean-Stark trap with 0.596g loosely packed cotton contained within. After 3d the aniline was no longer seen by TLC (1:1:1 EtOAc:CH₂Cl₂:NEt₃, silica, shortUV, R_f aniline=0.37, R_f enamine=0.86) and the mixture was allowed to cool to room temperature before being poured into 120mL hexanes. The mixture was washed with three 200mL portions sat. Na₂CO₃. The aqueous phase was back extracted with 200mL hexane. The organic extracts were combined, dried over MgSO₄, filtered, concentrated with rotary evaporation, and placed under vacuum overnight to yield 1.216g of the desired product as a mixture with the starting aniline. The desired enamine **40** was present in a 92:8 mol ratio to provide an NMR yield of 78% ¹HNMR (300MHz, CDCl₃): δ9.82 (s,1H); 8.15 (d, J=9.0Hz, 2H); 6.90 (d, J=9.0Hz, 2H); 5.69 (1H, s); 4.27 (q, J=7.1Hz, 2H); 4.23 (q, J=7.1Hz, 2H); 1.31 (q, J=7.1Hz, 3H); 1.23 (q, J=7.1Hz, 3H)

Ethyl 6-nitro-4-oxo-1,4-dihydroquinoline-2-carboxylate (**41**)



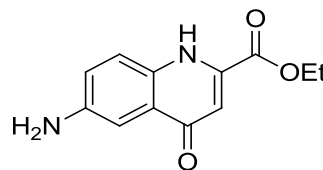
1.112g (3.607mmol) **40** was combined with 25mL Ph₂O, placed under an atmosphere of N₂, and heated at reflux for 20min. The mixture was cooled to room temperature, diluted with 250mL hexanes, and left to sit overnight. The resulting precipitate was collected by vacuum

filtration and placed under vacuum overnight to afford 0.807g (85% yield) of the desired quinolone **41**.

^1H NMR (300MHz, DMSO- d_6): δ 12.54 (s, 1H); 8.80 (d, J =2.6Hz, 1H); 8.48 (dd, J =9.2; 2.6Hz, 1H); 8.11 (d, J =9.2Hz, 1H); 6.76 (s, 1H); 4.44 (q, J =7.1Hz, 2H); 1.38 (q, J =7.1Hz, 3H)

^{13}C NMR: δ 177.1; 161.7; 143.8; 143.1; 139.2; 126.5; 124.7; 121.4; 121.2; 111.3; 62.9; 13.8

MS (EI, 70eV): 262 (M^+ , 96%); 216 (M^+ - $\text{C}_2\text{H}_6\text{O}$, 25%); 188 (216 - CO, 100%); 142 (188 - NO_2 , 40%)



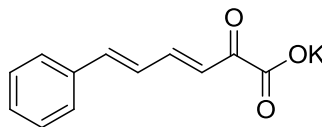
Ethyl 6-amino-4-oxo-1,4-dihydroquinoline-2-carboxylate (42)

0.1075g (0.4100mmol) **41**, 0.6093g (9.577mmol) $\text{NH}_4\text{O}_2\text{CH}$, 0.0282g 5% Pd-C, and 5mL anhyd. EtOH were combined under an atmosphere of N_2 . The mixture was mixed at a rapid pace for 6d at which time the mixture was filtered over Celite and rinsed with 60mL anhyd. EtOH. The filtrate was concentrated to dryness with rotary evaporation and placed under vacuum for 10d to generate 0.096g (100% yield) of the desired product.

^1H NMR (300MHz, CDCl_3): δ 9.01 (s, 1H); 7.55 (d, J =2.6, 1H); 7.29 (d, J =8.8Hz, 1H); 7.09 (dd, J =8.7; 2.6Hz, 1H); 6.91 (s, 1H); 4.47 (q, J =7.1Hz, 2H); 3.91 (s, 2H); 1.43 (t, J =7.1Hz, 3H)

MS (EI, 70eV): 232 (M^+ , 73%); 186 (M^+ - $\text{C}_2\text{H}_6\text{O}$, 9%); 158 (186 - CO, 100%); 130 (158 - CO, 17%); 104 (130 - C_2H_2 , 16%)

Potassium (3E,5E)-2-oxo-6-phenylhexa-3,5-dienoate (45)



3.292g (24.91mmol) cinnamaldehyde, 2.804g (25.48mmol) sodium pyruvate, and 0.1123g (2.808mmol) NaOH were combined with 25mL CH₃OH before being placed under an atmosphere of N₂ and heated to reflux for 17h. The volume was observed to be heterogeneous with yellow solid but TLC showed that the starting aldehyde was still present (25% CH₃CN/CH₂Cl₂ R_f: 0.85) and concentrated to dryness with rotary evaporation. 0.4030g (10.08mmol) NaOH and 46mL CH₃OH were placed into the reaction vessel and heated at reflux for 3h before the starting aldehyde was no longer visible by TLC. The yellow solid was collected by vacuum filtration, rinsed with two 100mL portions CH₃OH, and placed under vacuum overnight to afford 2.083g (37% crude yield). CO₂ was bubbled into the filtrate until it reached pH 8 before being concentrated to dryness with rotary evaporation before being combined with 150mL 18Ω H₂O and 75mL triethylamine (TEA). CO₂ was bubbled into the mixture while on ice until it became homogeneous before being extracted with five 50mL CH₂Cl₂. The organic portions were combined, dried over MgSO₄, filtered, concentrated with rotary evaporation, and placed under vacuum overnight to yield 2.050g of an auburn oil. The oil was combined with 100mL EtOAc, heated to boiling, decanted from the remaining undissolved semisolid, and cooled to room temperature. The supernatant was combined with 1.643g (9.013mmol) potassium 2-ethylhexanoate (K-2EHA) dissolved in 30mL EtOAc which produced a precipitate. The solid was collected by centrifugation, washed with two 30mL portions EtOAc, and placed under vacuum overnight to remove residual solvent to afford 0.433g of crude **45** as a yellow solid. 2.045g of the initially isolated yellow solid was dissolved in 185mL 2.4M

triethylammonium bicarbonate (TEABC) and extracted with four 50mL portions CH_2Cl_2 . The organic extracts were combined, dried over MgSO_4 , filtered, concentrated with rotary evaporation, and placed under vacuum overnight to yield 1.0963g of an auburn oil. The oil was combined with 50mL EtOAc and stirred at room temperature before the supernatant was decanted and mixed with 0.8073g (4.429mmol) K-2EHA producing a solid upon mixing. The solid was collected by centrifugation, washed with three 30mL portions EtOAc, and dried under vacuum to afford 0.7836g of crude **45** as a yellow solid. 1.118g of crude **45** was recrystallized from 55mL CH_3OH and 100mL EtOAc and boiled down to 1/3 of the total volume and stored in a -10°C freezer overnight. The resulting solid was collected by centrifugation and dried under vacuum to yield 0.914g **45** as a yellow solid (15% yield, 99.4% **45**, 0.6% by mass pyruvate, mp = 204°C (darkens to tan), 228°C (shrinks, darkens to brown), 260°C (d)

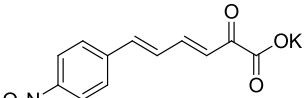
^1H NMR (300MHz, D_2O): δ 7.63 (d, $J=8.1\text{Hz}$, 2H); 7.51 (q_{AB}, $J=15.6\text{Hz}$, 9.6Hz, 1H); 7.48-7.41(m, 3H); 7.20-7.07 (m, $J=15.6\text{Hz}$; 8.7Hz, 2H); 6.40 (d, $J=15.6\text{Hz}$, 1H)

^{13}C NMR (300MHz, D_2O): δ 198.3; 173.0; 151.7; 144.7; 136.4; 130.6; 129.7; 128.4; 127.4; 126.0

ESI-MS (DUIS, + ion): 519 ($2\text{M} + \text{K}^+$, 100%); 279 ($\text{M} + \text{K}^+$, 96%)

ESI-MS (DUIS, - ion): 441 ($2\text{M}^- + \text{K}^+$, 89%); 201 (M^- , 100%)

UV-VIS: $\lambda_{\text{max}}=335\text{nm}$; $\epsilon=38868 \text{ L mol}^{-1} \text{ cm}^{-1}$

Potassium (3E,5E)-6-(4-nitrophenyl)-2-oxohexa-3,5-dienoate (46) 

1.456g (8.222mmol) 4-nitrocinnamaldehyde and 1.351g (12.28mmol) sodium pyruvate were suspended in 25mL. 0.1133g (2.832mmol) NaOH was dissolved in 25mL CH₃OH, added to the reaction mixture, and quantitatively transferred with 10mL CH₃OH. The mixture was placed under an atmosphere of N₂ and heated at reflux for 3.5h before the starting aldehyde was no longer visible by TLC (25% CH₃CN/CH₂Cl₂ R_f: 0.87). The mixture was allowed to cool to room temperature, concentrated with rotary evaporation, and placed under vacuum overnight to afford 2.133g of a brown solid. 2.132g of the crude product was added to 120mL 18Ω H₂O and 100mL TEA. CO₂ was bubbled into the mixture until it became homogeneous, extracted with six 100mL portions CH₂Cl₂. The organic extracts were combined, dried over MgSO₄, filtered, concentrated with rotary evaporation, and placed under vacuum to yield 2.372g of a dark brown solid. 1.539g of the dark brown solid was mixed with 140mL EtOAc and heated to boiling before the supernatant was decanted, cooled to room temperature. 1.357g potassium 2-ethylhexanoate dissolved in 50mL EtOAc was added to the supernatant, producing a precipitate. The solid was collected by centrifugation, washed with two 40mL portions EtOAc, and dried under vacuum to produce 0.2123g of the crude product which was recrystallized from 12mL CH₃OH and 15mL EtOAc. After concentrating to 10mL total volume the mixture brought to room temperature and placed on ice for several minutes before collecting the solid by centrifugation and drying under vacuum to yield 0.1257g (5% yield) **46** (98% pure, 2% pyruvate mp = 198°C (darkens from brown to dark brown), > 400°C

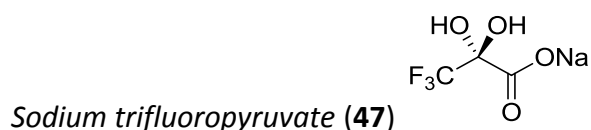
^1H NMR (300MHz, D_2O): δ 8.21 (d, $J=8.4\text{Hz}$, 2H); 7.72 (d, $J=8.7\text{Hz}$, 2H); 7.46 (q_{AB} , $J=15.3\text{Hz}$, 8.4Hz, 1H); 7.20 (m, 2H); 6.46 (d, $J=15.6\text{Hz}$, 2H)

^{13}C NMR (300MHz, D_2O): δ 198.9; 173.6; 150.9; 149.0; 144.1; 142.4; 132.3; 129.9; 129.0; 125.8

MS (DUIS, + ion): 324 ($\text{M} + \text{K}^+$, 89%), 150 ($\text{C}_8\text{H}_7\text{NO}_2 + \text{H}^+$, 100%)

MS (DUIS, - ion): 531 ($2\text{M}^- + \text{K}^+$, 65%); 493 ($2\text{M}^- + \text{H}^+$, 69%); 246 (M^- , 38%); 202 ($\text{M}^- - \text{CO}_2$, 100%);

UV-VIS: $\lambda_{\text{max}}=356\text{nm}$; $\epsilon=16922 \text{ L mol}^{-1} \text{ cm}^{-1}$



3.760g ethyl trifluoropruvate was combined with 50mL 1.2M HCl and heated at reflux for 21h at which time hydrolysis appeared complete by TLC (R_f ester= 0.22, R_f prod=0.0, 10% $\text{CH}_3\text{CN}/\text{CH}_2\text{Cl}_2$, DNP stain). The reaction mixture was concentrated to dryness with rotary evaporation, redissolved in 50mL 18 Ω H_2O , and concentrated to dryness with rotary evaporation again. The crude product was dissolved in 30mL 18 Ω H_2O neutralized to pH7 with $\text{NaOH}_{(\text{aq})}$, concentrated to near dryness with rotary evaporation, and azeotropically dried by evaporation of toluene. The **47** was placed under vacuum overnight to generate 3.542g (91% yield, mp = 206 $^\circ\text{C}(\text{d})$) as a white solid.

^1H NMR (300MHz, D_2O): no signals observed

^{13}C NMR (300MHz, D_2O): δ 171.1; 122.4 (q); 92.2 (q)

ESI-MS (DUI, - ion): 227 ($M + HCO_2^-$, 41%); 159 (M^- (hydrate), 100%); 141 (M^- (keto form), 85%)



8.0mL 2-methylfuran (88.67mol) and 60mL hexane were combined in a 200mL round bottom flask. The reaction mixture was placed under an atmosphere of N_2 and submerged into an ice bath and stirred for 20min to allow for thermo-equilibration. 8.25mL (59.35mmol) trifluoroacetic anhydride was then injected into the reaction mixture dropwise and stirred rapidly at $0^\circ C$ for 2.5h. The reaction mixture was concentrated with rotary evaporation to 1/6 volume before being poured into a separatory funnel containing 150mL $0^\circ C$ sat. $NaHCO_3$ and 30mL Et_2O . The organic layer was removed with the aqueous phase being countercurrently extracted with three 30mL portions of Et_2O . The organic phases were combined, dried over $MgSO_4$, filtered, rinsed with 10mL Et_2O , and concentrated with rotary evaporation to afford 12.439g (118% crude yield) of a free flowing orange liquid. The crude product was purified by vacuum distillation with the following parameters:

Pressure: 20torr Fraction 1 collected with $80^\circ C$ head temp and oil bath temp $119-126^\circ C$

Pressure: 20torr Fraction 2 collected with $80^\circ C$ head temp and oil bath temp $128-139^\circ C$

Fraction 1: 6.7228g Fraction 2: 1.0354g were both **50** to generate a 74% purified yield

1H NMR (300MHz, $CDCl_3$): δ 7.45 (d, bs, 1H); 6.33 (d, $J=3.6Hz$, 1H); 2.48 (s, 3H)

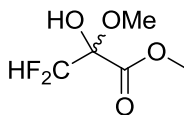


1.354g Mg⁰ (55.71mmol) was crushed with a mortar and pestle, placed into a 250mL round bottom flask, and placed under an atmosphere of N₂. 110mL THF (distilled, Na⁰/benzophenone) and 14mL (110.3mmol) TMSCl were placed into the reaction vessel before being submerged in an ice bath while stirring rapidly. A solution of 5.004g (28.09mmol) **50** in 28mL THF was added dropwise at the rate of 1drop/5sec. After 1h the reaction mixture darkened to a blackish blue. 30min after all of the **50** solution was added the reaction mixture was filtered. The crude yellow liquid was combined with 20mL THF and added to rapidly stirring 4.4mL conc. HCl on an ice bath. The mixture was stirred at 0°C for 30min before being poured into a separatory funnel containing 30mL Et₂O and 35mL sat. NaHCO₃. The organic layer was removed and the aqueous phase was extracted with two 30mL portions of Et₂O. The organic portions were combined, dried over MgSO₄, filtered, concentrated with rotary evaporation, and placed under vacuum to remove residual solvent for 30s to afford 3.838g (85% crude yield) of a yellow liquid. ¹H NMR analysis determined the crude product was 88% by mass for afford a corrected mass to be 3.3889g (75% NMR yield). The reaction mixture was concentrated to 1/8 total volume with rotary evaporation before diluting with 300mL hexane, causing a white solid to precipitate. The white solid was removed via filtration over Celite. The filtrate was concentrated with rotary evaporation and placed under vacuum to remove residual solvent for 30s to afford 5.200g (80% crude yield) of a yellow liquid. Crude **51** purified by vacuum distillation with the following parameters: Pressure: 20torr Fraction 1: 96-105°C head temp,

130-140°C oil temp, Pressure: 20torr Fraction 2: 105-103°C head temp, 140-160°C oil temp.

64% yield of pure **51**

¹H NMR (300MHz, CDCl₃): δ7.39 (bs, 1H); 6.24 (d, J=3.6Hz, 1H); 6.12 (t, J=53.7Hz, 1H); 2.40 (s, 3H)



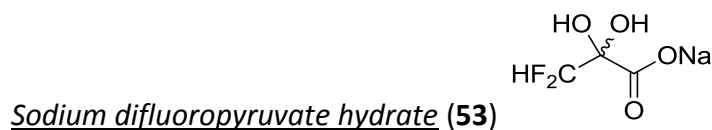
Methyl difluoropyruvate methyl hemiacetal (52)

0.518g (3.237mmol) **51** was combined with 16mL CH₃OH in a 50mL round bottom flask was placed under a nitrogen atmosphere and submerged in a -78°C bath. After stirring for 3min a mixture of O₃/O₂ was bubbled into the reaction mixture with the following parameters: A2Z O₃ generator Model#A2Z5-5GLAB, 0.56Amp on meter(100% production), 13PSI O₂ from the regulator, 0.5L/min bubble flow rate. After 25min of bubbling the reaction mixture was observed to be faint greenish yellow in color and after 35min of bubbling, the reaction mixture became colorless. After 1h, the O₃/O₂ bubbling was ceased and N₂ then bubbled through the reaction mixture for 18min. The reaction vessel was then moved to a -47°C bath (m-xylene/N₂(l)) for 2min before the dropwise addition of 0.07mL conc. H₂SO₄ and 0.2126g 3Å molecular sieves. After warming to room temperature the mixture was heated at reflux for 16h. The reaction mixture was concentrated to ~4mL total volume with rotary evaporation. The H₂SO₄ was removed by passing over a column (49mmx24mm) silica gel and eluted with 10% CH₃OH/CH₂Cl₂ collecting 2.5mL fractions. Desired product collected in fractions 5-16 with ¹H NMR yield of the 35% of the desired product as a mixture with CF₂HCOOH. (Note: Use ionic exchange technique only)

Removal of the acidic side product via ion exchange chromatography by the following method:

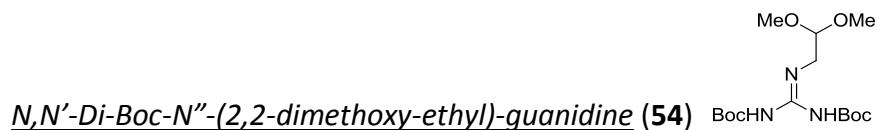
10.2231g Amberlyst A-21 (swollen with 18.1MΩ H₂O) was used to make a 10.25" tall by 10mm wide column. 300mL 5M NH₃ was passed through the column followed by 18.1Ω H₂O until the effluent was neutral to pH Hydron paper then 150mL MeOH. The reaction concentrate was loaded on top of the column and eluted with MeOH. Seventeen 3mL fraction were collected at a rate of ~1drop/s. Eight 5mL fraction were then collected at a rate of ~2drops/s. Fractions 3-19 contained the desired product was visualized by KMnO₄ stain on silica.

¹H NMR (300MHz, CDCl₃): δ5.81 (t, J=54.9Hz, 1H); 3.94 (s, 3H); 3.34 (s, 3H)



0.0652g (0.4178mmol) mixture of **52** and the ethyl hemiacetal derivative were dissolved in 20mL 3M HCl, placed under an atmosphere of N₂, and heated to reflux for 17h being cooled to room temperature. The reaction mixture was filtered (as specks of brown solid formed in the mixture overnight), concentrated with rotary evaporation, and dried azeotropically with CH₃CN and toluene, and placed under vacuum to remove residual solvent for 2h to afford 0.0464g (78% crude yield) of a yellow solid (difluoropyruvic acid). The crude product was dissolved in 15mL 18.1MΩ H₂O and titrated to neutrality with a solution of NaOH. The mixture was concentrated with rotary evaporation, dried azeotropically with CH₃CN and toluene, and placed under vacuum overnight to remove residual solvent to afford 0.0470g (69%crude yield) of a tannish solid.

^1H NMR (300MHz, D_2O): δ 5.94 (t, J =55.2Hz, 1H)

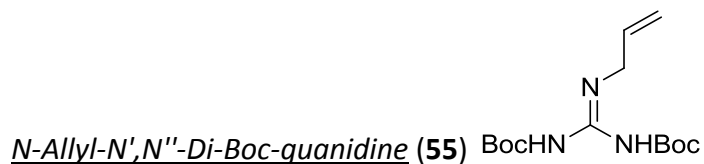


0.253g (0.816mmol) *N,N'*-Di-Boc-1H-pyrazole-1-carboxamidine was placed under an atmosphere of N_2 before being dissolved in 4.1mL CH_3CN . The mixture was set to stir before the addition of 0.27mL (2.48mmol) aminoacetaldehyde dimethyl acetal. The mixture was allowed to stir for 1.5h before TLC showed only the presence of the desired product (0.43 25% EtOAc/ CH_2Cl_2 , silica). The mixture was concentrated with rotary evaporation and placed under vacuum overnight to remove residual solvent to afford 0.218g **54** (99% yield, mp = 101-104°C) as a white solid.

^1H NMR (300MHz, CDCl_3): δ 11.46 (s, 1H); 8.48 (s, 1H); 4.48 (t, J =5.4Hz, 1H); 3.59 (q_{AB}, J =5.4Hz, 2H); 3.40 (s, 6H)

^{13}C NMR (300MHz, CDCl_3): δ 163.6; 156.4; 153.1; 102.0; 83.2; 79.4; 54.1; 42.3; 28.4; 28.2

MS (EI, 70eV): 347 (M^+ , 100%); 290 ($\text{M}^+ - \text{C}_4\text{H}_8$, 30%); 236 (35%)



0.159g (0.512mmol) *N,N'*-Di-Boc-1H-pyrazole-1-carboxamidine was dissolved in 3mL CH_3CN before 0.12mL (1.600mmol) allyl amine was added to the reaction mixture and subsequently

placed under an inert atmosphere. The mixture was allowed to stir at room temperature for 3h before the reaction mixture was concentrated with rotary evaporation and placed under vacuum overnight to remove residual solvent to afford 0.147g (96% yield) of off-white solid **55**.

^1H NMR (300MHz, CDCl_3): δ 11.52 (s, 1H); 8.41 (s, 1H); 5.89 (m, J = 15.9; 10.2; 5.1Hz, 1H); 5.24 (d, J = 17.1; 1.2Hz, 1H); 5.17 (d, J = 10.2Hz, 1H); 4.08 (dd, J = 5.4; 1.2Hz, 2H); 1.50 (s, 18H)

^{13}C NMR (300MHz, CDCl_3): δ 163.7; 156.2; 153.4; 133.4; 116.9; 83.7; 79.5; 43.4; 28.4; 28.2

MS (CI): 299 (M^+ , 10%); 243 ($\text{M} - \text{C}_3\text{H}_7\text{N} + \text{H}^+$, 17%); 188 ($\text{M}^+ - 111$, 100%)



0.106g (0.355mmol) **55** was dissolved in 3.0mL CH_2Cl_2 before the addition of 1.0mL CF_3COOH .

The reaction mixture was set to stir and heated at reflux for 3h. The reaction mixture was allowed to cool to room temperature, concentrated by rotary evaporation, and dried azeotropically via evaporation of toluene. After being placed under vacuum overnight to remove residual solvent afforded 0.0819g (108%) **57**.

^1H NMR (300MHz, D_2O): δ 5.86 (m, 1H); 5.28 (dd, J = 12.3; 0.9Hz, 1H); 5.23 (dd, overlapped, 2H); 3.83 (d, J = 4.8Hz, 2H)

^{13}C NMR (300MHz, CD_3CN): δ 158.8; 133.6; 117.3; 44.2

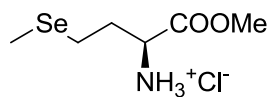
ESI-MS (DUI, + ion): 100 ($\text{M} - \text{CF}_3\text{COO}^-$, 100%)

2-Amino-5-hydroxy-4,5-dihydro-3H-imidazolium chloride (58) 

0.0331g (0.1459mmol) 1-allylguanidinium trifluoroacetate and 0.0856g (0.4002mmol) NaIO₄ were combined in a 25mL pear bottom flask along with 0.08mL CD₃OD. 0.0037g (0.0100mmol) K₂OsO₄·2H₂O was dissolved in 0.50mL D₂O, injected into the reaction mixture, and quantitatively transferred with 0.50mL D₂O. The mixture was allowed to stir at room temperature. Shortly after mixing, a white solid was observed to precipitate from the reaction mixture. The reaction was allowed to mix for 2.5 h before being analyzed by ¹H NMR at which point the reaction was determined to be complete. The reaction mixture was filtered, rinsed with 6mL CH₃OH, and combined with NMR sample. Dowex 2-X8 ion exchange resin was swelled with 3M HCl. A column 28cm tall and 2cm wide was constructed with the resin and rinsed with 300mL 3M HCl. 18.1Ω H₂O was run through the column until the effluent was neutral to pH Hydron paper(180mL) followed by 150mL CH₃OH. The methanolic solution was loaded on the column and eluted with CH₃OH. Twenty 10mL fractions were collected at the rate of 10mL/min. All fractions were negative to starch iodide paper with TLC showing the majority of the material collected in fractions 3-8. All fractions were combined, concentrated with rotary evaporation, dried azeotropically by evaporation of toluene, and placed under vacuum overnight to remove residual solvent to afford 0.0254g (128% crude yield). ¹H NMR analysis in D₂O showed the product to be 92% by mass **58**, 5% by mass 2-aminoimidazole, and 3% by mass toluene.

¹H NMR (300MHz, D₂O): δ5.57 (dd, J= 6.9; 1.5Hz, 1H); 3.89 (dd, J= 11.7; 6.9Hz, 1H); 3.52 (dd, J= 11.7; 1.5Hz, 1H)

L-Selenomethionine methyl ester hydrochloride (62)



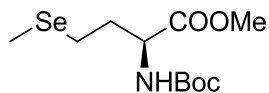
12.0mL anhyd. CH₃OH was placed into a flame dried 25mL round bottom flask placed into an ice/salt bath, allowed to thermoequilibrate before the dropwise addition of 1.0mL (13.71mmol) SOCl₂. 0.5242g (2.673mmol) L-Selenomethionine added to the mixture, placed under an atmosphere of N₂, septum wired on, and allowed to warm to room temperature in the air while stirring for 22h. TLC was take and showed the reaction to be complete (4:1:1 nBuOH:AcOH:H₂O, silica, KMnO₄, R_f a.a: 0.65, R_f ester: 0.38) Note: Mixture should be concentrated with rotary evaporation to dryness and dissolved in CH₃OH before precipitation. The reaction mixture was quantitatively transferred to a beaker with 5.0mL distilled CH₃OH before the addition of 150mL cold, anhyd. Et₂O. The beaker was placed into an ice bath for 5 min before the collection of the white solid that formed by vacuum filtration and dried under vacuum overnight 0.4598g (70% yield, mp = 158-161°C) **62** as a white solid.

¹H NMR (300MHz, D₂O): δ4.29 (t, J=6.3, 1H); 3.86 (s, 3H); 2.67 (t, J=6.9Hz, 2H); 2.23 (m, 2H); 2.02 (s, 3H)

¹³C NMR (300MHz, D₂O): δ176.3; 59.5; 58.4; 24.7; 9.1

ESI-MS (DUIS, + ion): 253 (M⁺ + CH₃CN, 57%); 212 (M⁺, 100%); 210 (M⁺ (⁷⁸Se), 56%)

N-Boc-*L*-Selenomethionine methyl ester (**63**)

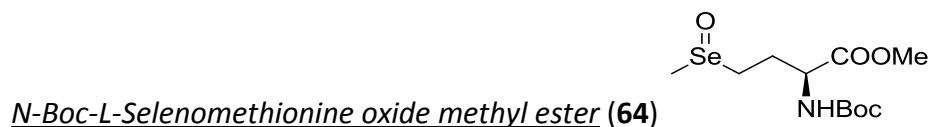


0.4078g (1.6538mmol) **62** and 0.4644g (5.529mmol) NaHCO₃ were combined in 5.0mL distilled CH₃OH. 0.6652g (3.048mmol) Boc₂O was dissolved in 3.0mL distilled CH₃OH, injected into the reaction mixture, and quantitatively transferred using 2.0mL distilled CH₃OH. The mixture was placed under an atmosphere of N₂ and stirred at room temperature for 15h at which time TLC was taken and showed the reaction to be complete (4:1:1 nBuOH:AcOH:H₂O, silica, KMnO₄ visualized R_f SM: 0.44, R_f prod: 0.94). 0.1131g (1.507mmol) glycine was added to the reaction mixture and stirred for 1h before the reaction mixture was filtered and concentrated with rotary evaporation before being diluted with 20mL CH₂Cl₂ and poured into a separatory funnel containing 50mL sat. NaHCO₃ and 20mL CH₂Cl₂. The organic layer was removed and the aqueous phase was extracted with two 25mL portions CH₂Cl₂. The organic portions were combined, dried over MgSO₄, filtered, concentrated with rotary evaporation, and placed under vacuum overnight to remove residual solvent to afford 0.4046g (79% yield) of the desired product **63** as a pale yellow oil.

¹H NMR (300MHz, CDCl₃): δ5.09 (s, 1H); 4.41 (s, 1H); 3.76 (s, 3H); 2.55 (t, J=8.1Hz, 2H); 2.20 (m, 1H); 2.00 (m, 1H); 2.00 (s, 3H); 1.45 (s, 9H)

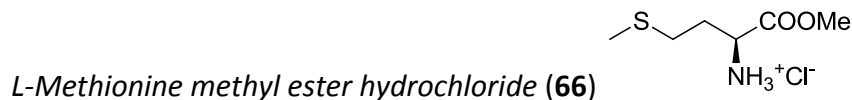
¹³C NMR (300MHz, CDCl₃): δ172.7; 155.2; 79.7; 53.4; 52.2; 33.1; 28.2; 20.3; 4.0

ESI-MS (DUIS, + ion): 312 (M + H⁺, 33%); 253 (M + H⁺ - COOMe, 54%); 212 (M + H⁺-Boc, 100%)



0.3192g (1.029mmol) **63** was dissolved in 13mL distilled CH₃OH, diluted with 7.0mL 18Ω H₂O, and submerged in an ice bath. The mixture was allowed to thermoequilibrate before the addition of 0.2347g (1.097mmol) NaIO₄. The mixture was set to stir rapidly in the ice bath for 2h before it was confirmed to be complete by TLC (4:1:1 nBuOH/AcOH/H₂O, silica, KMnO₄ R_fSe: 0.94, R_fSeO: 0.60). The reaction mixture was filtered, rinsed with 10mL distilled CH₃OH, and concentrated with rotary evaporation to remove the methanolic portion before it was diluted with 13mL 80% sat. NaCl. The aqueous phase was then countercurrently extracted with three 40mL portions EtOAc. The organic portions were combined, dried over MgSO₄, filtered, concentrated with rotary evaporation, and placed under vacuum overnight to afford 0.2335g of a pale yellow oil that was 4.6% by mass EtOAc to yield 0.2247g (67% yield) **64**.

¹H NMR (300MHz, CDCl₃): δ5.57 (d, J=6.6Hz, 1H); 4.41 (m, 1H); 3.78 (s, 3H); 2.95 (m, 1H); 2.79 (m, 1H); 2.54 (s, 3H); 2.27 (m, 1H); 2.13 (m, 1H); 1.45 (s, 9H)



12.0mL CH₃OH (distilled from Mg⁰/I₂) was placed into a 25mL flame dried round bottom flask. The vessel was submerged in an ice/salt bath (-12°C) and allowed to thermoequilibrate before the dropwise addition of 2.5mL (34.27mmol) SOCl₂. 1.003g (6.721mmol) L-Methionine was then added to the methanolic mixture, placed under an atmosphere of N₂, septum wired

on, and allowed to warm to room temperature in air for 17h. TLC was then taken, showing the reaction to be complete. (4:1:1 nBuOH/AcOH/H₂O, silica, KMnO₄, L-Met R_f a.a.: 0.35, R_f ester:0.45) Note: Reaction mixture should be concentrated with rotary evaporation to dryness and dissolved in MeOH before continuing The reaction mixture was cooled to 0°C before the addition of 150mL cold Et₂O, causing a white solid to precipitate. The white solid was collected by vacuum filtration and dried under vacuum overnight (1st crop). White solid was observed to have formed in the filtrate which was collected by vacuum filtration and dried under vacuum overnight (2nd crop). The two crops were combined to afford 1.215g **66** (90% yield) as a white solid.

¹H NMR (300MHz, D₂O); δ4.29 (t, J=6.3Hz, 1H); 3.86 (s, 3H); 2.69 (t, J=7.2Hz, 2H); 2.26 (m, 2H); 2.12 (s, 3H)



0.7251g (3.631mmol) **66** and 0.7234g (8.613mmol) NaHCO₃ were combined with 5.0mL distilled CH₃OH. 1.083g (4.963mmol) Boc₂O was dissolved in 3.0mL distilled CH₃OH, injected into the reaction mixture, and quantitatively transferred using 2.0mL distilled CH₃OH. The mixture was placed under an atmosphere of N₂, and stirred rapidly at room temperature for 18h. TLC was taken, showing only the presence of **67** (4:1:1 nBuOH:AcOH:H₂O, silica, KMnO₄ visualized R_f SM: 0.49, R_f prod: 0.93). 0.1828g (2.435mmol) glycine was added to the reaction mixture and stirred at room temperature for 3h before the mixture was filtered, concentrated with rotary evaporation to near dryness, diluted with 20mL CH₂Cl₂ and poured into a separatory funnel containing 20mL CH₂Cl₂ and 50mL sat. NaHCO₃. The organic layer was removed and the

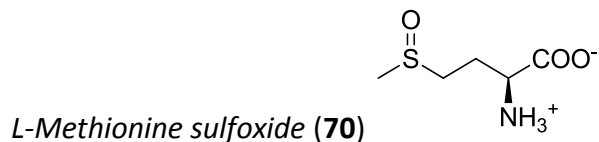
aqueous phase was extracted with two 25mL portions CH₂Cl₂. The organic portions were combined, dried over MgSO₄, filtered, concentrated with rotary evaporation, and placed under vacuum overnight to remove residual solvent to afford 0.8652g (90% yield) of **67** as a pale yellow oil.

¹H NMR (300MHz, CDCl₃): δ5.11 (s, 1H); 4.41 (s, 1H); 3.76 (s, 3H); 2.54 (t, J=7.8Hz, 2H); 2.10 (s, 3H); 2.10 (m, 1H); 1.94 (m, 1H); 1.45 (s, 9H)



0.5496g (2.087mmol) **67** was dissolved in 7.0mL distilled CH₃OH to which was added 4.0mL 18Ω H₂O. The mixture was submerged in an icebath and stirred rapidly for 3min to thermoequilibrate before the addition of 0.4712g (2.203mmol) NaIO₄. The mixture was stirred rapidly for 1.5h during which a white solid formed in the reaction volume. After 1.5h TLC showed the reaction to be complete (4:1:1 nBuOH:AcOH:H₂O, silica, KMnO₄ visualized S R_f: 0.93, SO R_f: 0.58). The reaction mixture was filtered and concentrated with rotary evaporation to near dryness before being diluted with 15mL 80% sat. NaCl. The aqueous phase was countercurrently extracted with four 40mL portions of EtOAc. The organic phases were combined, dried over MgSO₄, filtered, concentrated with rotary evaporation, and placed under vacuum overnight to remove residual solvent to afford 0.6495g of a pale yellow oil which was determine to be 16.9% by mass EtOAc to yield 0.5397g (93% yield) **68**.

^1H NMR (300MHz, CDCl_3): δ 5.27 (s, 1H); 4.43 (m, 1H); 3.78 (s, 3H); 2.79 (t, $J=7.8$, 2H); 2.57 (s, 3H); 2.35 (m, 1H); 2.14 (m, 1H); 1.45 (s, 9H)

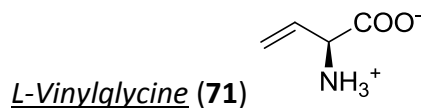


3.005g (20.14mmol) L-Methionine was suspended in 10mL DI H_2O in a 25mL round bottom flask. 2.2mL 30% H_2O_2 was added to the suspension in the following manner: 0.36mL over the course of 2min, dropwise with 5min of stirring until 1.44mL total volume of 30% H_2O_2 was added. At this point the mixture became homogeneous. The mixture was allowed to stir for 1.5h (Note: Does not appear to be necessary). After this time 0.36mL 30% H_2O_2 followed by a 0.40mL 30% H_2O_2 portion added to the reaction in the same manner as described above. After 1.2h of stirring at RT, TLC showed all of the starting material consumed. 150mL 200proof EtOH was then added to the aqueous solution causing a white solid to precipitate. The mixture sat at room temperature for 30min before the white solid was collected by vacuum filtration, rinsed with 20mL 200proof EtOH, and dried under vacuum overnight to remove residual solvent to afford 3.096g **70** (93% yield, mp = 254°C(d)) as a white solid.

^1H NMR (300MHz, D_2O): δ 3.87 (q, $J=6.3\text{Hz}$, 1H); 3.02 (m, 2H); 2.74 (s, 3H); 2.33 (q, $J=7.2\text{Hz}$, 2H)

^{13}C NMR (300MHz, D_2O): δ 173.8; 54.0; 48.9; 37.1; 24.4

ESI-MS (DUI, + ion): 188 ($\text{M} + \text{Na}^+$, 100%); 166 ($\text{M} + \text{H}^+$, 14%)



20.09g (0.1216mol) L-Methionine sulfoxide was combined with 120mL (0.4872mol) *bis*-(trimethylsilyl)acetamide and set to stir in a 25-80°C oil bath for 19h after which it was diluted with 80mL Ph₂O. The mixture was added to 300mL boiling Ph₂O over the course of 33.5min. Distillate was collected with pot temperature not dropping below 250°C and a head temperature range of 238-248°C. The 275mL EtOH and 30mL H₂O was poured into the distillate (417mL). The resulting mixture thickened and required being shaken by hand periodically over 20min. Volatiles were removed by rotary evaporation before the addition of 20mL H₂O and 150mL hexane. The mixture was shaken well and allowed to separate before the removal of the organic phase. The aqueous phase was washed with another 150mL hexane before the addition of 400mL CH₃CN which caused a tan solid to precipitate. The solid was collected by vacuum filtration, rinsed with 40mL CH₃CN, and placed under vacuum overnight to remove residual solvent to afford 7.672g. 7.267g of the crude product was triturated with 155mL boiling anhyd. EtOH for 5min before being collected by vacuum filtration, rinsed with 20mL cold EtOH, and dried under vacuum overnight to yield 4.568g **71** (37% yield, 95% purity as estimated by NMR, mp = 216°C(d)) (35% yield overall).

¹H NMR (300MHz, D₂O): δ5.97 (ddd, J=10.2; 6; 4.5Hz, 1H); 5.48 (d, J= 10.2Hz, 1H); 5.48 (d, J=6.3Hz, 1H); 4.27 (d, J=4.5Hz, 1H)

¹³C NMR (300MHz, D₂O); δ173.5; 130.8; 122.0, 57.7

ESI-MS (DUIS, + ion): 102 (M + H⁺, 22%)

HRMS (IT-TOF-ESI, + ion): Calc'd C₄H₇NO₂ (M + H⁺): 102.0550. Found: 102.0553

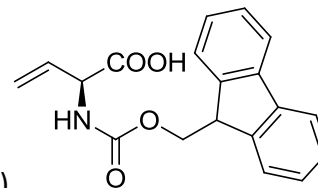
(S)-2-((*R*)-2-(((9*H*-fluoren-9-yl)methoxy)carbonyl)amino)propanamido)but-3-enoic acid (**72**)

0.3371g (0.8090mmol) 98% Fmoc-L-Ala-OSu was dissolved in 10mL acetone to which was added 0.1317g (1.568mmol) NaHCO₃ dissolved in 5mL H₂O (using 2mL H₂O to quant. trans.) which caused the bicarbonate to precipitate. 0.1144g (1.075mmol) **71** dissolved in 5mL H₂O was then added to the mixture, using 2mL H₂O to quantitatively transfer. Upon addition the mixture became homogeneous and was set to stir at room temperature for 3h at which time TLC showed the reaction to be complete ($R_{f\text{ OSu}}=0.54$, silica, 10% CH₃OH/CH₂Cl₂). The mixture was acidified to pH1 with 1mL 12M HCl and extracted with three 35mL CH₂Cl₂. The organic portions were combined, washed with three 35mL portions 3M HCl, dried over MgSO₄, filtered, concentrated with rotary evaporation, and placed under vacuum overnight to remove residual solvent to afford 0.3131g of the desired dipeptide **72** as a white solid (98% yield, mp = 176°C (shrinks), 184-188°C)

¹H NMR (300MHz, CD₃OD): δ7.79 (d, J=7.5Hz, 2H); 7.67 (dd, J=7.2Hz, 2H); 7.39 (t J=7.2Hz, 2H); 7.31 (t, J=7.2Hz, 2H); 6.00 (m, J=16.8, 10.5; 4.8Hz 1H); 5.38 (d, J=16.8Hz, 1H); 5.25 (d, J=10.2Hz, 1H); 4.98 (d, J=5.1Hz, 1H); 4.36 (t, J=6.9Hz, 2H,; 4.22 (d, J=6.6Hz, 1H,; 4.22 (d, J=6.6Hz, 1H); 1.37 (d, J=7.2Hz, 3H)

¹³C NMR (300MHz, CD₃OD): δ175.3; 173.1; 158.3; 145.4; 145.2; 142.6; 133.5; 128.8; 128.2; 126.3; 120.9; 117.9; 68.0; 56.0; 51.8; 18.2

HRMS (IT-TOF-ESI, -ion): Calc'd (C₂₂H₂₂N₂O₅): 393.1456. Found: 393.1458



(S)-2-((((9H-fluoren-9-yl)methoxy)carbonyl)amino)but-3-enoic acid (73)

1.024g (2.974mmol) Fmoc-OSu was dissolved in 13mL acetone to which was added 0.3344g (3.143mmol) **71** dissolved in 11mL H₂O and 0.5330g (6.344mmol) NaHCO₃ dissolved in 9mL H₂O. Upon addition, the vinylglycine precipitated out. The mixture was heated at 65°C for 1h before the mixture was observed to be homogeneous. The mixture was removed from the heat and stirred at room temperature for 26h at room temperature at which time TLC did not show Fmoc-OSu (*R*_f=0.73, silica, 10% CH₃OH/CH₂Cl₂). The mixture was then acidified to pH1 with 1mL 12M HCl and extracted with three 35mL portions CH₂Cl₂. The organic phases were combined, washed with three 35mL portions 4M HCl, dried over MgSO₄, filtered, rinsed with 20mL CH₂Cl₂, concentrated with rotary evaporation, and placed under vacuum overnight to remove residual solvent to afford 0.876g of the desired product as an off-white solid (91% yield, mp = 146-149°C) 0.0484g of the crude product was dissolved in 0.6mL EtOAc and diluted with 14mL hexane producing a cloudy white mixture which was allowed to sit at room temperature for 1h to produce crystals. The solid was collected by centrifugation, washed with 10mL hexane, and dried under vacuum to remove residual solvent to afford 0.0448g **73** (93% recovery, mp = 160-161°C).

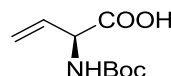
¹H NMR (300MHz, CD₃OD): δ7.80 (d, *J*=7.5Hz, 2H); 7.68 (d, *J*=6.9Hz, 2H); 7.39 (t, *J*=7.5Hz, 2H); 7.31 (t, *J*=7.5Hz, 2H); 6.01 (ddd, *J*=16.8; 10.2, 5.7Hz, 1H); 5.36 (d, *J*=17.4Hz, 1H); 5.26 (d, *J*=10.2Hz, 1H); 4.78 (d, *J*=5.4Hz, 1H); 4.36 (m, 2H); 4.24 (t, *J*=7.2Hz, 1H)

^{13}C NMR (300MHz, CD_3OD): δ 145.3; 145.2; 133.9; 128.8; 128.2; 128.2; 126.5; 120.9; 117.8; 68.1; 57.8; 48.4

MS (DUIS, - ion): 322 ($\text{M} - \text{H}^+$, 100%)

HRMS (IT-TOF-ESI, - ion): Calc'd $\text{C}_{19}\text{H}_{17}\text{NO}_4$ ($\text{M} - \text{H}^+$): 322.1085. Found: 322.1091

(S)-2-((tert-butoxycarbonyl)amino)but-3-enoic acid (74)



0.1624g L-Vinylglycine (1.542mmol) was combined with 0.5228g (2.428mmol) Boc_2O , 0.6813g (8.112mmol) NaHCO_3 , and suspended in 12mL CH_3OH . The mixture was set to stir at room temperature for 24h at which time TLC show complete reaction (10% $\text{AcOH}/\text{CH}_2\text{Cl}_2$ R_f : 0.42). The mixture was filtered and the filtrate was concentrated to dryness with rotary evaporation, and dissolved in 20mL CH_2Cl_2 and 20mL sat. NaHCO_3 . The organic layer was removed and the aqueous phase was washed with two 20mL CH_2Cl_2 before acidifying to pH3 with conc. H_3PO_4 . After extracting with four 20mL portion EtOAc the organic phases were combined, dried over MgSO_4 , filtered, concentrated with rotary evaporation, diluted with 30mL toluene, concentrated to dryness, and placed under vacuum overnight to remove residual solvent to yield 0.2601g (84%) of a pale yellow oil.

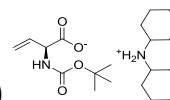
^1H NMR (300MHz, CD_3OD): δ 5.97 (ddd, $J=16.8$; 10.8; 4.5Hz, 1H); 5.34 (d, $J=17.1$ Hz, 1H); 5.23 (d, $J=10.5$ Hz, 1H); 4.69 (d, $J=4.5$ Hz, 1H); 1.45 (s, 9H)

^{13}C NMR (300MHz, CD_3OD): δ 174.0; 157.7; 134.3; 117.4; 80.7; 57.5; 28.7

ESI-MS (DUIS, - ion): 423 ($2\text{M}^- + \text{Na}^+$, 52%); 401 ($2\text{M}^- + \text{H}^+$, 100%); 200 ($\text{M} - \text{H}^+$, 72%)

HRMS (IT-TOF-ESI, + ion) Calc'd $\text{C}_9\text{H}_{15}\text{NO}_4\text{Na}$ ($\text{M}+\text{Na}^+$): 224.0893. Found 224.0890

Dicyclohexyl ammonium 2-((tert-butoxycarbonyl)amino)but-3-enoate (75)



0.1682g (0.8360mmol) **74** was dissolved in 1.5mL CH₂Cl₂ to which was added 0.20mL (1.006mmol) dicyclohexylamine. The mixture was brought to a boil, diluted with 12mL hexanes added at a rate that kept the mixture boiling, and concentrated to one third total volume. The mixture was allowed to cool to room temperature before being placed into a -20°C freezer for 1.5h. The solid was collected by centrifugation, washed with 10mL hexane, and placed under vacuum overnight to remove residual solvent to afford 0.2760g (86% yield, mp = 152°C (d)) of the desired salt **75** as a yellow solid.

¹H NMR (CDCl₃): δ6.00 (m, J=16.2; 11.1; 6.3Hz, 1H); 5.62 (d, J=17.1Hz, 1H); 5.25 (d, J= 4.8Hz, 1H); 5.09 (d, J= 10.2Hz, 1H); 4.48 (s, 1H); 2.95 (m, cyclohexyl, 2H); 1.99-1.67 (cyclohexyl, 10H); 1.43 (s, 9H); 1.40-1.20 (cyclohexyl, 10H)

¹³C NMR (CDCl₃): δ176.6; 157.2; 137.7; 114.2; 80.2; 59.9; 54.4; 30.6; 28.8; 26.2; 25.5

ESI-MS (DUIS, + ion): 223 (H₂NCy₂ + CH₃CN, 76%); 182 (HNCy₂ + H⁺, 100%)

ESI-MS (DUIS, - ion): 401 (2M⁻ + H⁺, 44%); 246 (M + HCOO⁻, 72%); 200 (M - H⁺, 100%)

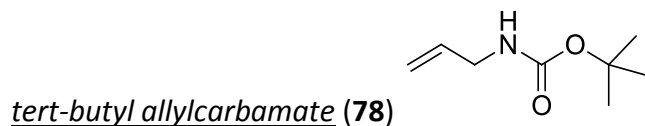
HRMS (IT-TOF-ESI, + ion): calc'd C₁₂H₂₃N (HNCy₂ + H⁺): 182.9000. Found: 182.9003

HRMS (IT-TOF-ESI, - ion): calc'd (C₉H₁₅NO₄ - H⁺): 200.0928. Found: 200.0925

Allylammonium chloride (76)

3mL (40.02mmol) allyl amine was added to 6mL 12M HCl. The mixture was concentrated to dryness with rotary evaporation, dissolved in 15mL DI H₂O, and concentrated again using 5mL CH₃OH and 15mL toluene to dry by azeotropic evaporation. The resulting white solid was placed under vacuum overnight to yield 2.668g **76** (71% yield).

¹H NMR (300MHz, D₂O): δ5.94 (m, 1H); 5.43 (d, J=18.3Hz, 1H); 5.41 (d, J=9.9Hz, 1H); 3.62 (d, J=5.7Hz, 2H)



2.096g (9.125mmol) Boc₂O was dissolved in 10mL CH₃OH. The mixture was set to stir rapidly before the slow addition of 0.85mL (11.330mmol) allyl amine. Upon addition the reaction volume became exothermic and evolved gas. After 30min TLC showed the consumption of Boc₂O (5% CH₃OH/CH₂Cl₂ R_f prod= 0.78, R_f Boc₂O= 0.96). The reaction mixture was concentrated to near dryness with rotary evaporation, diluted with 20mL toluene, concentrated to dryness with rotary evaporation, and placed under vacuum for 1.5h to afford 1.075g (75% yield, mp = 28-34°C) of **78** as a yellow solid.

Note: Product is volatile and will evaporate away if left under vacuum overnight. 1.5h appears to be the amount of time needed at this scale to give the driest product with the best yield.

¹H NMR (300MHz, CDCl₃): δ5.84 (m, J=17.1; 10.2; 1.5Hz, 1H); 5.18 (dd, J=17.1; 1.5Hz, 1H); 5.11 (dd, J=10.2; 1.2Hz, 1H); 4.60 (s, 1H); 3.75 (nt, unresolved, 2H); 1.45 (s, 9H)

¹³C NMR (300MHz, CDCl₃): δ115.9; 135.0; 115.8; 79.4; 43.2; 28.5

ESI-MS (DUIS, + ion): 315 (2M + H⁺, 100%)

(9H-fluoren-9-yl)methyl allylcarbamate (79) 

2.000g (5.810mmol) Fmoc-OSu was dissolved in 20mL CH₂Cl₂ (distilled from CaH₂). 2.0mL (26.12mmol) allyl amine was injected into the mixture was set to stir at room temperature 1h after which time the Fmoc-OSu was not seen by TLC (R_f Fmoc-OSu= 0.16, R_f prod= 0.33). The mixture was filtered with vacuum over a pad of Celite and rinsed with 20mL CH₂Cl₂. The filtrate was washed with four 40mL portions 0.1M HCl_(aq). The organic phase was dried over MgSO₄, filtered, concentrated with rotary evaporation, and placed under vacuum overnight to remove residual solvent to yield 1.5476g **79** (95% yield, mp = 121-122°C.) as a white solid.

¹H NMR (300MHz, CDCl₃): δ 7.77 (d, J=7.2Hz, 2H); 7.60 (d, J=7.5Hz, 2H); 7.40 (t, J=7.2Hz, 2H); 7.31 (t, J=7.5Hz, 2H); 5.84 (m, 1H); 5.18 (d, J=17.4Hz, 1H); 5.14 (d, J=10.2Hz, 1H); 4.82 (t, J=7.5Hz, 2H); 4.43 (d, J=6.9Hz, 2H); 4.23 (t, J=6.9Hz, 1H); 3.83 (t, unresolved, 2H)

¹³C NMR (300MHz, CDCl₃): δ 156.4; 144.1; 141.4; 134.6; 127.8; 125.2; 120.1; 116.2; 66.8; 47.4; 43.6;

ESI-MS (DUIS, + ion): 581 (2M + Na⁺, 95%); 334 (M + Na⁺+CH₃OH, 54%); 302 (M + Na⁺, 100%); 297 (M + NH₄⁺, 94%); 280 (M + H⁺, 65%); 179 (9-methylene-9H-fluorene+H⁺, 26%)

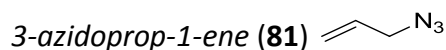


2.0mL (26.66mmol) allyl amine with combined with 2.0mL (54.62mmol) ethyl trifluoroacetamide producing a large exotherm upon addition. (Note: Use no solvent and an excess of allyl amine instead as it is more volatile and add it in portions to stirring ethyl trifluoroacetate stirring in an ice bath) After 15min TLC confirmed that the reaction was complete (silica gel, KMnO₄ visualized, R_f product= 0.55 40% EtOAc/hexane). The mixture was concentrated with rotary evaporation and placed under high vacuum for 25min to yield 3.117g (76% yield) of **80** as a light yellow liquid.

¹H NMR (300MHz, CDCl₃): δ7.52 (s, 1H); 5.77 (m, J=16.2; 10.2; 5.7; 0.9Hz, 1H); 5.18 (dd, J=16.2; 0.9Hz, 1H); 5.15 (dd, J= 10.2; 1.2Hz, 1H); 3.89 (t, J=5.7Hz, 2H)

¹³C NMR (300MHz, CDCl₃): δ157.7 (q, J= 147Hz); 131.9; 117.7; 116.0 (q, J=1143Hz); 42.2

ESI-MS (DUIS, + ion): 329 (2M + Na⁺, 32%); 231 (69%); 211 (100%)



0.0872g (1.038mmol) NaHCO₃ and 3.078g (47.34mmol) NaN₃ were combined and dissolved in 11mL DI H₂O. 2.5mL (28.89mmol) allyl bromide was then added to the mixture resulting in a biphasic solution. The mixture was set to stir rapidly at room temperature for 30min at which time the aqueous phase was observed to be the bottom layer. TLC of the reaction mixture after 4h showed that it was complete (silica, 10% EtOAc/hexane, KMnO₄ visualized, R_f allyl bromide= 0.56, R_f product= 0.61). The aqueous phase was removed and the organic phase was passed over a 2cm tall column of MgSO₄ in a glass Pasteur pipet to afford

1.6258g (68% yield) of **81** as a yellow liquid. (Note: Do not place product under vacuum for a prolonged period of time as it is volatile and cannot be separated from diethyl ether by means of rotary evaporation even)

^1H NMR (300MHz, CDCl_3): δ 5.87 (m, 1H); 5.33 (d, J =17.1Hz, 1H); 5.30 (d, J =11.1Hz, 1H); 3.78 (d, J =6Hz, 2H)



0.0507g (0.3225mmol) **78** was placed into a flame dried, N_2 flushed 25mL round bottom flask to which was added 0.0235g (0.0375mmol) Hoveyda-Grubbs 2nd generation catalyst. The mixture was dissolved in 10mL CH_2Cl_2 (distilled from CaH_2), placed under an atmosphere of N_2 , and heated at reflux for 18.5h at which time TLC showed the reaction to be complete (10% $\text{CH}_3\text{CN}/\text{CH}_2\text{Cl}_2$ $R_{f\text{ SM}} = 0.73$, $R_{f\text{ prod}} = 0.41$). The mixture was concentrated with rotary evaporation to dryness and placed under vacuum to remove residual solvent for 30min to yield 0.0897g (194% yield). The crude solid was purified by flash chromatography (silica gel 60, 9" silica, 10mm column, 2'/min flow rate, 5mL fraction, 100mL 10% $\text{CH}_3\text{CN}/\text{CH}_2\text{Cl}_2$, 50mL 20% $\text{CH}_3\text{CN}/\text{CH}_2\text{Cl}_2$) fraction 7-12 10% were combined, concentrated with rotary evaporation, and placed under vacuum overnight to afford 0.0134g **82** as a brown oil (58% yield of (Z)- TY)

^1H NMR (300MHz, CDCl_3): δ 5.39 (s, 2H); 4.72 (s, 2H); 3.44 (m, 2H); 3.25 (m, 2H); 1.46 (s, 9H); 1.44 (s, 9H)

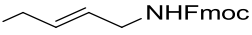
ESI-MS (DUIS, + ion): 309 ($\text{M} + \text{Na}^+$, 54%); 304 ($\text{M} + \text{NH}_4^+$, 100%); 287 ($\text{M} + \text{H}^+$, 42%)

(E)-di-tert.-butyl but-2-ene-1,4-diyl dicarbamate (83) 

0.0507g (0.3225mmol) **78** was placed into a flame dried, N₂ flushed 25mL round bottom flask to which was added 0.0235g (0.0375mmol) Hoveyda-Grubbs 2nd generation catalyst. The mixture was dissolved in 10mL CH₂Cl₂ (distilled from CaH₂), placed under an atmosphere of N₂, and heated at reflux for 18.5h at which time TLC showed the reaction to be complete (silica, ninhydrin, 10% CH₃CN/CH₂Cl₂ R_f SM= 0.73, R_f prod= 0.36). The mixture was concentrated with rotary evaporation to dryness and placed under vacuum to remove residual solvent for 30min to yield 0.0897g (194% yield). The crude solid was purified by flash chromatography (silica gel 60, 9" silica, 10mm column, 2'/min flow rate, 5mL fraction, 100mL 10% CH₃CN/CH₂Cl₂, 50mL 20% CH₃CN/CH₂Cl₂) fraction 13-21 10% were combined, concentrated with rotary evaporation, and placed under vacuum overnight to afford 0.0213g **83** as a tan solid (92% yield of (E)- TY)

¹H NMR (300MHz, CDCl₃): δ 5.62 (s, 2H); 4.57 (s, 2H); 3.72 (s, 4H); 1.45 (s, 18H)

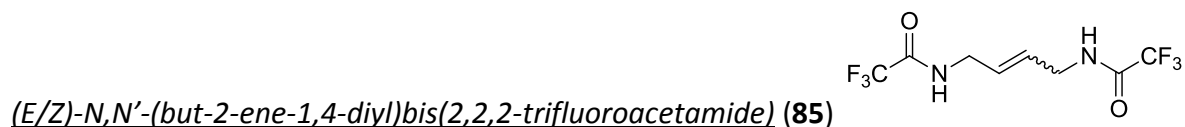
ESI-MS (DUIS, + ion): 309 (M + Na⁺, 100%); 304 (M + NH₄⁺, 50%)

(E)-bis((9H-fluoren-9-yl)methyl) but-2-ene-1,4-diyl dicarbamate (84) 

0.0510g (0.1826mmol) **79** was combined with 0.0115g (0.0184mmol) Hoveyda-Grubbs 2nd generation catalyst and dissolved in 5mL CH₂Cl₂ (distilled from CaH₂). The mixture was placed under an atmosphere of N₂ and reflux for 4h at which time ¹H NMR showed consumption of the allyl amine. The mixture was diluted with 6mL hexanes and cooled to -78°C before the solid present was collected by centrifugation. The supernatant was removed, the white solid was washed with 12mL 50% CH₂Cl₂/hexane, and placed under vacuum overnight to remove residual solvent to afford 0.0229g (47% yield, mp = 191-192°C) **84** as a white solid.

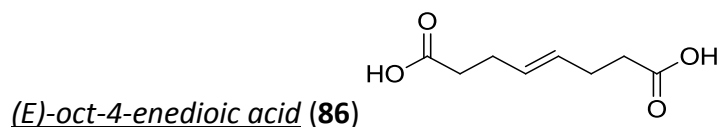
^1H NMR (300MHz, CDCl_3): δ 7.76 (d, $J=7.2\text{Hz}$, 4H); 7.60 (d, $J=7.2\text{Hz}$, 4H); 7.40 (t, $J=7.2\text{Hz}$, 4H); 7.31 (t, $J=7.2\text{Hz}$, 4H); 5.60 (s, 2H); 4.79 (s, 2H); 4.44 (d, $J=6.6\text{Hz}$, 4H); 4.22 (t, $J=6.0\text{Hz}$, 2H); 3.80 (s, 2H)

ESI-MS (DUI, + ion): 553 ($\text{M} + \text{Na}^+$, 100%); 548 ($\text{M} + \text{NH}_4^+$, 39%)



0.0539g (0.3521mmol) **80** was injected into a solution of 0.0266g (0.0424mmol) Hoveyda-Grubbs 2nd generation catalyst dissolved in 2mL CH_2Cl_2 and quantitatively transferred using two 2mL portions CH_2Cl_2 . The mixture was placed under an atmosphere of N_2 and heated at reflux for 18h. 4min after mixing, the color of the mixture darkened to a brownish green color and turned completely brown after 13min when reflux was achieved. After 18h, TLC indicated that the reaction was complete by absence of the starting alkene (silica gel, KMnO_4 , 40% EtOAc/hexane, R_f SM= 0.55, R_f Z and E products= 0.63 and 0.42). The mixture was concentrated to dryness with rotary evaporation and placed under vacuum overnight to remove residual solvent to yield 0.0478g of **85** (43% yield after subtraction of catalyst mass). ESI-MS of crude product acquired.

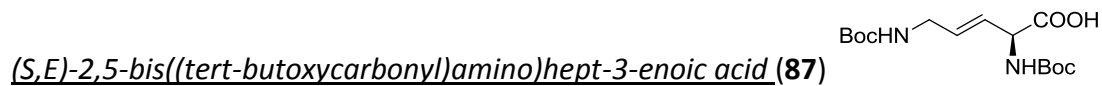
ESI-MS (DUI, - ion): 391 ($\text{M} + \text{CF}_3\text{COO}^-$, 47%); 323 ($\text{M} + \text{HCOO}^-$, 26%); 277 ($\text{M} - \text{H}^+$, 100%)



0.05mL (0.4899mmol) 4-pentenoic acid was combined with 0.0273g (0.0436mmol) Hoveyda-Grubbs 2nd generation catalyst dissolved in 10mL CH₂Cl₂ (distilled from CaH₂). The mixture was placed under an atmosphere of N₂ and heated at reflux for 16.5h after which the solution was observed to still be green in color. Analysis of a concentrated aliquot by ¹H NMR in CD₃CN showed no more of the starting alkene. The reaction mixture and NMR sample were combined, dissolved in a combination of 5mL CH₃CN and 15mL CH₂Cl₂, and extracted with 20mL sat. NaHCO₃. The aqueous layer was removed and the organic phase was extracted with an additional 20mL sat. NaHCO₃. The aqueous phases were combined, washed with two 20mL portions CH₂Cl₂, and acidified to pH1 were 12M HCl. The aqueous phase was extracted with two 35mL EtOAc. The organic extracts were combined, dried over MgSO₄, filtered, concentrated with rotary evaporation to dryness, and placed under vacuum overnight to remove residual solvent to yield 0.0185g (44% yield) **86** as an off white solid.

¹H NMR (300MHz, DMSO-d₆): δ12.05 (s, 2H); 5.43 (m, 2H); 2.27-2.18 (m, 8H)

ESI-MS (DUI, - ion): 387 (35%); 365 (2M⁻ + Na⁺, 100%); 343 (M + M⁻, 86%); 171 (M - H⁺, 72%)



0.0392g (0.2494mmol) **78** dissolved in 2.5mL CH₂Cl₂ was added to 0.0188g (0.0934mmol) **74** and 0.0067g (0.0107mmol) Hoveyda-Grubbs 2nd generation catalyst dissolved in 5mL CH₂Cl₂. The mixture was set to stir heated at reflux under an atmosphere of N₂ for 18h at

which time the mixture was analyzed by ^1H NMR revealing that the vinylglycine was almost gone. The reaction mixture was concentrated to dryness with rotary evaporation, dissolved in 15mL EtOAc, and extracted with four 7mL portion conc. NH_3 . The aqueous extracts were combined, concentrated by rotary evaporation and dried azeotropically by evaporation of 5mL CH_3OH and 15mL toluene. The concentrate was placed under vacuum overnight to yield 0.0333g (102% yield). 0.0144g of the crude product was separation was attempted by flash chromatography (10mm column, 7.5" silica, 2"/min flow rate, 5mL fractions, slurry packed and eluted with 100mL (2.5% AcOH/7.5%IPA/90% CH_2Cl_2) to afford the desired product **87** as a 3:1 mixture with **74** (0.0043g, 32% yield, 39% based on conversion)

^1H NMR (300MHz, CDCl_3): δ 5.81-5.66 (m, 2H); δ 4.65 (d, J =17.7Hz, 1H); 3.65 (d, J =10.2Hz, 2H); 1.44 (s, 9H); 1.43 (s, 9H)

MS (DUI, -ion): 530 ($\text{M}^- + \text{NBoc-L-Vgy}$, 31%); 329 ($\text{M} - \text{H}^+$, 100%)

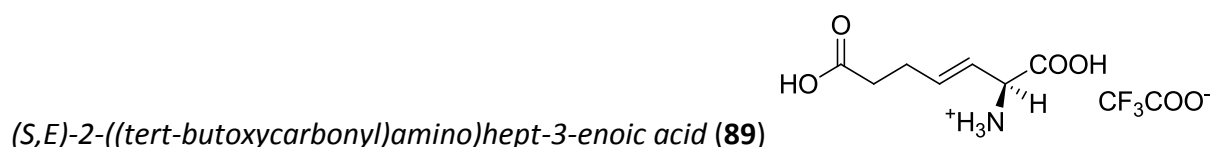
(S,E)-5-((((9H-fluoren-9-yl)methoxy)carbonyl)amino)-2-((tert-butoxycarbonyl)amino)pent-3-



0.0613g (0.9387mmol) **73** and 0.2622g (0.3047mmol) **79** were combined to which was added 0.0315g (0.0503mmol) Hoveyda-Grubbs 2nd generation catalyst dissolved in 3mL CH_2Cl_2 , using two 2mL portions CH_2Cl_2 to quantitatively transfer. The mixture placed under an atmosphere of N_2 and heated at reflux for 21h over which time the initial emerald green color of the solution changed to an orange-green to brown in the first 1h of heating. After 21h TLC showed that the vinylglycine was still present. The mixture was removed from the heat for 24h before the addition of 0.0406g (0.1453mmol) **79**, 0.0150g (0.0239mmol) Hoveyda-Grubbs 2nd

generation catalyst and 3mL CH₂Cl₂ and heated at reflux for another 13h at reflux at which time the NBoc-L-Vgy was no longer seen by TLC (silica, ninhydrin, 10% AcOH/CH₂Cl₂, R_f NBoc-L-Vgy= 0.38, R_f homodimer= 0.56, R_f CM product= 0.20). The mixture was concentrated to dryness with rotary evaporation and placed under vacuum overnight to remove residual solvent to yield 0.4060g crude product (294% yield). 0.1173g of the crude product was dissolved in 20mL CH₂Cl₂ and 10mL toluene and extracted with three 10mL portions sat. NaHCO₃. The aqueous portions were combined and washed with 10mL CH₂Cl₂. The aqueous phase was acidified to pH3 and extracted with three 30mL portions EtOAc. The organic extracts were combined, dried over MgSO₄, filtered, concentrated with rotary evaporation, and placed under vacuum overnight to remove residual solvent to afford 0.1200g which was submitted to MS analysis to afford M+NH₄⁺ of the desired product.

ESI-MS (DUIS, - ion): 475 (M + Na⁺, 98%); 470 (M + NH₄⁺, 100%)



0.1292g (0.6421mmol) **74** was dissolved in 6mL CH₂Cl₂ to which was added 0.20mL (1.956mmol) 4-pentenoic acid followed by 0.0377g (0.0602mmol) Hoveyda-Grubbs 2nd generation catalyst dissolved in 6mL CH₂Cl₂. The mixture was placed under an atmosphere of N₂ and heated to reflux for 24h after which time TLC showed the reaction to be incomplete. 0.20mL 4-pentenoic acid and 0.0259g (0.0413mmol) Hoveyda-Grubbs 2nd generation catalyst were added before resuming reflux for another 21h with a white precipitate forming over the course of the reaction (pentenoic acid homodimer). TLC analysis after this time showed that

starting vinylglycine was no longer present (silica, ninhydrin, 10% AcOH/CH₂Cl₂, R_f NBoc-L-Vgy= 0.35, R_f homodimer= 0.57, R_f product= 0.22). The mixture was filtered to remove the white precipitate, concentrated to dryness with rotary evaporation, and dissolved in 30mL CH₂Cl₂. The solution was extracted with three 10mL portions sat. NaHCO₃. The aqueous portions were combined, washed with two 25mL portions CH₂Cl₂, and acidified to pH2 with 85% H₃PO₄, and extracted with three 25mL portions EtOAc. The organic layers were combined, dried over MgSO₄, filtered, concentrated with rotary evaporation and placed under vacuum overnight to remove residual solvent to afford 0.1725g (98% crude yield). 0.0465g of the crude product was dissolved in 10mL CH₂Cl₂ and 10mL CF₃COOH and heated at reflux for 1.5h before concentrating with rotary evaporation to dryness. The concentrated crude was dissolved in 30mL EtOAc to which was added 15mL DI H₂O. The aqueous phase was removed and the organic phase was extracted with an addition two 10mL portions H₂O. The aqueous portions were combined, washed with three 20mL portions EtOAc, then concentrated with rotary evaporation to near dryness before being dried azeotropically by evaporation CH₃OH and toluene to afford 0.0290g of **89** as a light tan solid (16% yield, 58% based on amount used)

Boc protected CM product

ESI-MS (DUIS, - ion): 567 (2M⁻ + Na⁺, 30%); 545 (M + M⁻, 75%); 272 (M - H⁺, 100%)

Deprotected TFA salt of CM product

¹H NMR (300MHz, CDCl₃): δ6.01 (dt, J=15.6; 6.9Hz, 1H); 5.64 (dd, J= 15.6; 7.5Hz 1H); 4.29 (d, J= 8.1Hz, 1H); 2.52 (t, J= 6.3Hz, 2H); 2.41 (m, J= 14.1Hz; 6.9Hz, 2H)

ESI-MS (DUIS, - ion): 249 (M-2H⁺+NH₄⁺+AcO⁻, 92%); 172 (M-H⁺, 100%)

IX. REFERENCES

1. Southall, N.; Dill, K.; Haymet, A.D. *J. Phys. Chem. B.*, **2002**, *106*(3), 521-533)
2. Newcomb, L.; Gellman, S. *J. Am. Chem. Soc.*, **1994**, *116*, 4993-4994
3. Ma, J.; Dougherty, D. *Chem. Rev.*, **1997**, *97*(5), 1303-1324
4. Smith, P.; Wilcox, C.S. *J. Org. Chem.*, **1990**, *55*, 5675-5678
5. Kollman, P.; Allen, L.; *Chem. Rev.*, **1972**, *72*, 283-303
6. Murray, T.; Zimmerman, S. *J. Am. Chem. Soc.*, **1992**, *114*, 4010-4011
7. Lee, J.; Schwabacher, A. W. *J. Am. Chem. Soc.*, **1994**, *116*, 8382-8383
8. Cram, D. *Angew. Chem. Int. Ed. Engl.*, **1986**, *25*(12), 1039-1134
9. Zhang, Z.; Han, M.; Zhang, H.; Liu, Y. *Org. Lett.*, **2013**, *15*(7), 1698-1701
10. Gschwend, D.; Good, A.; Kuntz, I. *J. Mol. Recogn.*, **1996**, *9*(2), 175-186
11. Kang, J.; Santamaría, J.; Hilmersson, G. Rebek, Jr., J. *J. Am. Chem. Soc.*, **1998**, *120*(29), 7389-7390
12. Freudenberg, K.; Meyer-Delius, M. *Ber. Dtsch. Chem. Ges.*, **1938**, *71*, 1596
13. Cramer, F.; Hettler, H. *Die Naturwissenschaften*, **1967**, *54*, 625
14. Saenger, W. *Angew. Chem. Int. Ed. Engl.*, **1980**, *19*, 344-362
15. Breslow, R. *Acc. Chem. Res.*, **1995**, *28*(3), 146-153
16. Brewster, M.E.; Loftsson, T. *Adv. Drug Deliv. Rev.*, **2007**, *59*(7), 645-666
17. Pedersen, C. J. *J. Am. Chem. Soc.*, **1967**, *89*(26), 7017
18. Pedersen, C. J. *J. Org. Chem.*, **1971**, *36*(12), 1690-1693
19. Gokel, G.; Cram, D. *J. Org. Chem.*, **1974**, *39*(16), 2445-2446
20. Odashima, K.; Itai, A.; Iitaka, Y.; Koga, K. *J. Am. Chem. Soc.*, **1980**, *102*(7), 2504-2505

21. Diederich, F.; Dick, K. *Angew. Chem. int. Ed. Engl.*, **1983**, 22(9), 715-716
22. Diederich, F.; Dick, K. *J. Am. Chem. Soc.*, **1984**, 106, 8024-8036
23. Ferguson, S.; Diederich, F. *Angew. Chem. Int. Ed. Engl.*, **1986**, 25, 1127-1129
24. Sheppodd, T.; Petti, M.; Dougherty, D. *J. Am. Chem. Soc.*, **1986**, 108, 6085-6087
25. Petti, M.; Sheppodd, T.; Barrans, Jr., R.; Dougherty, D. *J. Am. Chem. Soc.*, **198**, 110, 6825-6840
26. Dougherty, D.; Stauffer, D. *Science*, **1990**, 250, 1558-1560
27. Chen, C. W.; Whitlock, Jr., H. W. *J. Am. Chem. Soc.*, **1978**, 100(15), 4921-4922
28. Smeets, J. W.; Sijbesona, R.; Niele, F. G.; Spek, A.; Smeets, W. J. Nolte, R. J. *J. Am. Chem. Soc.*, **1987**, 109, 928-929
29. Williams, K.; Askew, B.; Bullester, P.; Buhr, C.; Jeong, K.; Jones, S.; Rebek, Jr., J. *J. Am. Chem. Soc.*, **1989**, 111, 1090-1094
30. Zimmerman, S.; VanZyl, C. *J. Am. Chem. Soc.*, **1987**, 109, 7894-7896
31. Zimmerman, S.; Wu, W. *J. Am. Chem. Soc.*, **1989**, 111, 8054-8055
32. Harmata, M. ; Murray, T. *J. Org. Chem.*, **1989**, 54(16), 3761-3763
33. Harmata, M.; Barnes, C. *Tet. Lett.*, **1990**, 31(13), 1825-1828
34. Kagan, J.; Chen, S.-Y.; Agdeppa, Jr., D.A. *Tet. Lett.*, **1977**, 18(51), 4469-4470
35. Harmata, M.; Barnes, C. *J. Am. Chem. Soc.*, **1990**, 112, 5655-5657
36. He, Z.; Yang, X.; Jiang, W. *Org. Lett.*, **2015**, 17, 3880-3883
37. Legouin, B.; Uriac, P.; Tomasi, S.; Toupet, L.; Bondon, A, van de Weghe, P. *Org. Lett.*, **2009**, 11(3), 745-748

38. Klärner, F.-G.; Benkhoff, J.; Boese, R.; Burket, U.; Kameith, M.; Naatz, U. *Angew. Chem. Int. Ed. Engl.*, **1996**, *35*(10), 1130-1133
39. Klärner, F.-G.; Kahlert, B. *Acc. Chem. Res.*, **2003**, *36*, 919-932
40. Schrader, T.; Fokkens, M.; Klärner, F.-G.; Polkowska, J.; Bastkowski, F. *J. Org. Chem.*, **2005**, *70*, 10227-10237
41. Talbiersky, P.; Bastkowski, F.; Klärner, F.-G.; Schrader, T. *J. Am. Chem. Soc.*, **2008**, *130*, 9824-9828
42. Kirsch, M.; Talbiersky, P.; Polkowska, J.; Bastkowski, F.; Schaller, T.; de Groot, H.; Klärner, F.-G.; Schrader, T. *Angew. Chem. Int. Ed. Engl.*, **2009**, *48*(16), 2886-2890
43. Gomes, R.; Parola, A. J.; Bastkowski, F.; Polkowska, J.; Klärner, F.-G. *J. Am. Chem. Soc.*, **2009**, *131*(25), 8922-8938
44. Klärner, F.-G.; Schrader, T. *Acc. Chem. Res.*, **2013**, *46*(4), 967-978
45. Tröger, J. *J. prakt. Chem.*, **1887**, *36*(2), 227
46. Wagner, E.C. *J. Am. Chem. Soc.*, **1935**, *57*(7), 1296-1298
47. Spielman, M. A. *J. Am. Chem. Soc.*, **1935**, *57*, 583
48. Prelog, V.; Weiland, P. *Helv. Chim. Acta.*, **1944**, *27*, 1127
49. Mason, S. F.; Vane, G. W.; Schofield, K.; Wells, R. J.; Whitehurst, J. S. *J. Chem. Soc. B.*, **1967**, 553-556
50. Larson, S. B.; Wilcox, C. S. *Acta. Cryst.*, **1986**, *C42*, 224-227
51. Wilen, S.; Qi, J. Z.; Willard, P. *J. Org. Chem.*, **1991**, *56*, 485-487
52. Aamouche, A.; Devlin, F. J.; Stephens, P. J. *J. Am. Chem. Soc.*, **2000**, *122*, 2346-2354
53. Wilcox, C. S. *Tet. Lett.*, **1985**, *26*(47), 5749-5752

54. Wilcox, C. S.; Greer, L. M.; Lynch, V. *J. Am. Chem. Soc.*, **1987**, *109*, 1865-1867
55. Adrian, Jr., J. C.; Wilcox, C. S. *J. Am. Chem. Soc.*, **1991**, *113*, 678-680
56. Adrian, Jr. J. C.; Wilcox, C. S. *J. Am. Chem. Soc.*, **1992**, *114*, 1398-1403
57. Kiehne, U.; Weilandt, T.; Lutzen, A. *Org. Lett.*, **2007**, *9*(7), 1283-1286
58. Boyle, E. M.; Comby, S.; Molloy, J. K.; Gunnlaugsson, T. *Org. Lett.*, **2013**, *78*, 8312-8319
59. Pardo, C.; Sesmilo, E.; Gutiérrez-Puebla, E.; Monge, A.; Elguero, J. Fruchier, A. *J. Org. Chem.*, **2001**, *66*, 1607-1611
60. Mas, T.; Pardo, C.; Salort, F.; Elguero, J.; Rosario Torres, M. *Eur. J. Org. Chem.*, **2004**, 1097-1104
61. Dolenský, B.; Valík, M.; Sýkora, D.; Král, V. *Org. Lett.*, **2005**, *7*(1), 67-70
62. Havlík, M.; Král, V.; Kaplânek, R.; Dolenský, B. *Org. Lett.*, **2008**, *10*(21), 4767-4769
63. Havlík, M.; Král, M.; Dolenský, B. *Org. Lett.*, **2006**, *8*(21), 4867-4870
64. Sucholeik, I.; Lynch, V.; Phan, L.; Wilcox, C. S. *J. Org. Chem.*, **1988**, *53*, 98
65. Cox, E.G. *Rev. Mod. Phys.*, **1958**, *30*, 159
66. Bogert, M.; Dox, A. *J. Am. Chem. Soc.*, **1905**, *27*(10), 1302-1305.
67. Sinnreich, J., *Synthesis*, **1980**, *7*, 578-580.
68. Stenger-Smith, J.; Zarras, P.; Merwin, L. *Macromolecules*, **1998**, *31*, 7566-7569.
69. Baeyer *Ber.*, **1886**, *19*, 430.
70. Tiwari, K. Synthesis of a versatile building block for binding site preparation, M.S. Thesis, The University of Wisconsin-Milwaukee, December 2006
71. Clark, T.; Sperry, J. *Synlett*, **2012**, *23*, 2827-2829.
72. Cossy, J.; Belotti, D. *Org. Lett.*, **2002**, *4*(15), 2557-2559.

73. Nystran, R.; Brown, W. *J. Chem. Soc.*, **1947**, 69(5), 1197-1199.
74. Ball, S.; Goodwin, T.; Morton, R. *Biochem. J.*, **1948**, 42(4), 516-523.
75. Pratt, E.; van de Castle, J. *J. Org. Chem.*, **1961**, 26(8), 2973-2975.
76. Black, D.; Rothnie, N. *Aust. J. Chem.*, **1983**, 36, 1149-1157.
77. Attenburrow et al, *J. Chem. Soc.*, **1952**, 26(8), 1094-1111.
78. Gritter, R.; Dupre, G.; Wallace, T. *Nature*, **1964**, 202(4928), 179-181.
79. Goldman, I. *J. Org. Chem.*, **1969**, 34(6), 1979-1981.
80. Kamimura, A.; Komatsu, H.; Moriyama, T.; Yuichiro, N. *Tetrahedron*, **2013**, 69, 5968-5972.
81. Carpino, L. *J. Org. Chem.*, **1970**, 35(11), 3971-3972.
82. Perrone, D.; Dondoni, A. *Org. Synth.*, **2000**, 77, 64.
83. Hoover, J.; Stahl, S., **2013**, 90, 240-250.
84. Nyakirangani, N. Synthetic Procedures For Molecular Receptors Ph.D. Dissertation, The University of Wisconsin-Milwaukee, December 2009
85. Ranu, B.; Hajra, A.; Jana, U. *Org. Lett.*, **1999**, 1(8), 1141-1143).
86. Manabe, K.; Kobayashi, S. *Chem. Commun.*, **2000**, 669-670.
87. Bhagat, S.; Chakraboti, A. *J. Org. Chem.*, **2007**, 72, 1263-1270.
88. Epifano, F.; Genovese, S.; Cuirih, M. *Tetrahedron Letters*, **2007**, 48, 2717-2720.
89. Qian, C.; Huang, T. *J. Org. Chem.*, **1998**, 63, 4125-4128.
90. Ingle, G.; Liang, Y.; Mormino, M.; Li, G.; Fronczek, F.; Antilla, J. *Org. Lett.*, **2011**, 13(8), 2054-2057.
91. Joly, G.; Jacobsen, E. *J. Am. Chem. Soc.*, **2004**, 126, 4102-4103.

92. Pettersen, D.; Marcolini, M.; Bernardi, L.; Fini, F.; Herrera, R.; Sgarzani, V.; Ricci, A. *J. Org. Chem.*, **2006**, *71*, 6269-6272.
93. Bhagat, S.; Chakraborti, A. *J. Org. Chem.*, **2008**, *73*, 6029-6032.
94. Chernyshev, E. A.; Bugerenko, E.F.; Akat'eva, A.S.; Naumov, A.D. *Zhurnal Obshche Khimii*, **1975**, *45(1)*, 242-243
95. Knerr, L.; Paunecouke, X.; Schmitt, G.; Luu, B. *Tetrahedron Letters*, **1996**, *37(29)*, 5123-5126.
96. Grehn, L.; Gunnarsson, K.; Ragnarsson, U. *Acta Chemica Scandinavica B*, **1986**, *40*, 745-750.
97. McKenna, C.; Higa, M.; Cheung, N.; McKenna, M. *Tetrahedron Letters*, **1977**, *2*, 155-158.
98. Norén, J.; Helgstrand, E.; Johansson, N.; Misiorny, A.; Stening, G. *J. Med. Chem.*, **1983**, *26*, 264-270.
99. McKenna, C.; Schmidhauser, J. *J. Chem. Soc. Chem. Commun.*, **1979**, 739.
100. Rabinowitz, R.; *J. Am. Chem. Soc.*, **1960**, *82*, 4564-4567.
101. Van Wazer, J. *Phosphorous and Its Compounds*, Vol. I New York Interscience Encyclopedias, Inc. 1958.
102. Lucero, B.; Gomes, C.; Frugulhetti, I.; Faro, L.; Alvarenga, L.; Souza, M.; Souza, T.; Ferreira, V. *Bioorganic and Medicinal Chemistry Letters*, **2006**, *16(4)*, 1010-1013.
103. Nakamura, S.; Kozuka, M.; Bastow, K.; Tokuda, H.; Nishino, H.; Suzuki, M.; Tatsuzuki, J.; Natschke, S.; Kuo, S.; Lee, K. *Bioorganic and Medicinal Chemistry Letters*, **2005**, *13*, 4396-4401.
104. Banerji, B.; Conejo-Garcia, A.; McNeill, L.; McDonough, M.; Buck, M.; Hewitson, K.; Oldham, N.; Schofield, C. *Chem. Commun.*, **2005**, 5438-5440.

105. Srivastava, S.; Chauhan, P.; Bhadur, A.; Fatima, N.; Chatterjee, R. *J. Med. Chem.*, **2000**, *43*, 2275-2279.
106. Jean, J.; Laborde, E.; Busch, R.; Caprathe, B.; Sorenson, R.; Fergus, J.; Spiegel, K.; Marks, J.; Dickerson, M.; Davis, R. *J. Med. Chem.*, **1995**, *38*, 4439-4445.
107. Kermack, W.; Webster, W. *J. Chem. Soc.*, **1942**, 213-216.
108. Heindel, N.; Bechara, I.; Lemke, L.; Fish, V. *J. Org. Chem.*, **1967**, *32*(12), 4155-4157.
109. Conrad, M.; Limpach, L. *Ber.*, **1887**, *20*, 944.
110. Limpach, L. *J. Am. Chem. Soc.*, **1931**, *64*, 969.
111. Gould, Jr., G.; Jacobs, W. *J. Am. Chem. Soc.*, **1939**, *61*, 2890-2895.
112. Surrey, A. ; Hammer, H. *J. Am. Chem. Soc.*, **1946**, *68*, 133-116.
113. Al-Awadi, N.; Abdelhamid, A.; Al-Etaibi, A.; Elnagdi, M. *Synlett*, **2007**, *14*, 2205-2208.
114. Eaton, P.; Carlson, G.; Lee, J. *J. Org. Chem.*, **1973**, *38*(23), 4071-4073.
115. Zewge, D.; Chen, C.; Deer, C.; Dormer, P.; Hughes, D. *J. Org. Chem.*, **2007**, *72*, 4276-4279.
116. Reimer, M. *J. Am. Chem. Soc.*, **1931**, *53*(8), 3147-3149.
117. Sugimura, H.; Yoshida, K. *Bull. Chem. Soc. Jpn.*, **1992**, *65*, 3209-3211.
118. Mahata, P.; Barun, O.; Ila, H.; Junjappa, H. *Synlett*, **2000**, *9*, 1345-1347.
119. Thangavel, V.; Chadta, A. *Tetrahedron*, **2007**, *63*, 4126-4133.
120. Zhu, L.; Meng, Q.; Fan, W.; Xie, X.; Zhang, Z. *J. Org. Chem.*, **2010**, *75*, 6027-6030.
121. Parisi, M.; Gattuso, G.; Notti, A.; Raymo, F. *J. Org. Chem.*, **1995**, *60*, 5174-5179.
122. Amii, H.; Kobayashi, T.; Hatamoto, Y.; Uneyama, K. *Chem Commun.*, **1999**, 1323-1324.
123. Takahashi, S.; Jukurogi, T.; Katagari, T.; Uneyama, K. *CrystEngComm*, **2006**, *8*, 320-326.
124. Katagiri, T.; Ozaki, F.; Tanaka, Y. *Journal of Fluorine Chemistry*, **2009**, *130*, 682-683.

125. Raju, R.; Prasad, K. *Tetrahedron*, **2012**, *68*, 1341-1349.
126. He, H.; Willaimson, R.; Shen, B.; Graziani, E.; Yang, H.; Sakya, S.; Petersen, P.; Carter, G. *J. Am. Chem. Soc.*, **2002**, *124*, 9729-9736.
127. Cudic, P.; Kranz, J.; Behenna, D.; Kruger, R.; Tadesse, H.; Wand, A.; Velclich, Y.; Weisel, J.; McCafferty, D. *Proc. Natl. Acad. Sci.*, **2002**, *99*(4), 7384-7389.
128. Reynold, P.; Somner, E. *Drugs. Exp. Clin. Res.*, **1990**, *16*(8), 385-389.
129. Reynold, P.; Somner, E. *Antimicrob Agents Chemother.*, **1990**, *34*(3), 413-419.
130. Men, H.; Park, P.; Ge, M.; Walker, S. *J. Am. Chem. Soc.*, **1998**, *120*(10), 2484-2485.
131. Lo, M.; Men, H.; Branstrom, A.; Helm, J.; Yao, N.; Goldman, R.; Walker, S. *J. Am. Chem. Soc.*, **2000**, *122*(14), 3540-3541.
132. Fang,X.; Tiyanont, K.; Zhang, Y.; Wanner, J.; Boger, D.; Walkers. *Mol. BioSyst.*, **2006**, *2*, 69-76.
133. Higashide, E.; Hatano, K.; Shibata, M.; Nakazawa, K. *J. Antibiotics*, **1968**, *21*(2), 126-137.
134. Asai, M.; Muroi, M.; Sugita, N.; Kawashima, H.; Mizuno, K.; Miyaki, A. *J. Antibitotics*, **1968**, *21*(2), 138-146.
135. Tsuchiya, K.; Kondo, M.; Oishi, T.; Yamazaki, T. *J. Antibiotics*, **1968**, *21*(2), 147-153.
136. Horii, S.; Kameda, Y. *J. Antibiotics*, **1968**, *21*(4), 665-667.
137. Hatano, K.; Nogami, I.; Higashide, E.; Kishi, T. *Agric. Biol. Chem.*, **1984**, *48*(6), 1503-1508.
138. Nakane, A.; Nakamura, T.; Eguchi, Y. *Journal of Biological Chemistry*, **1977**, *252*(12), 5267-5273.
139. Yin, X.; Zabriskie, T.M. *Microbiology*, **2006**, *152*, 2969-2983.

140. Halti, B.; Tan, Y.; Magarvey, N.; Wagenaar, M.; Yin, X.; Grunstein, M.; Hucul, J.; Zabriskie, T.M. *Chem. Biol.*, **2005**, *12*(11), 1163-1168.
141. Burroughs, A.; Hoppe, R.; Goebel, N.; Sayyed, B.; Voegtline, T.; Schwabacher, A.; Zabriskie, T.M.; Sivaggi, N. *Biochemistry*, **2013**, *52*, 4492-4506.
142. Fujita, Y. *Bull. Chem. Soc. Japan*, **1959**, *32*(5), 439-442.
143. Fujita, Y. *Bull. Chem. Soc. Japan*, **1960**, *32*(10), 1379-1381.
144. Rossa, B.A.; Viswanatha, T. *Can. J. Biochem.*, **1968**, *46*, 725-728.
145. Yoon, G.; Zabriskie, T.M. *Journal of Radiolabelled Compounds and Radiopharmaceuticals*, **2008**, *52*(2), 53-55.
146. Sanière, L.; Leman, L.; Bourguignon, J.; Dauban, P.; Dodd, R. *Tetrahedron*, **2004**, *60*, 5889-5897.
147. Leman, L.; Sanière, L.; Dauban, P.; Dodd, R. *ARKIVOC*, **2003**, (vi), 126-134.
148. Schwörer, C.; Oberthür, M. *Eur. J. Org. Chem.*, **2009**, 6129-6139.
149. Frédérick, R.; Charlier, C.; Robert, S.; Wouters, J.; Maserel, B.; Pachet, L. *Bioorganic and Medicinal Chemistry Letters*, **2006**, *16*, 2017-2021.
150. Drake, B.; Patek, M.; Lebl, M. *Synthesis*, **1994**, *6*, 579-582.
151. Behrens, C.; Paquette, L. *Org. Syn. Coll.*, **2004**, *10*, 41.
152. Dardeen, G.; Casimir, J.; Marlier, M.; Larsen, P. *Phytochemistry*, **1974**, *13*(9), 1897-1900.
153. Angst, C. *Pure Appl. Chem.*, **1987**, *59*(3), 373-380.
154. Rando, R.; Relyea, N.; Cheng, L. *J. Biol. Chem.*, **1976**, *251*(11), 3306-3312.
155. Rando, R. *Biochemistry*, **1974**, *13*(19), 3859-3863.
156. Feng, L.; Kirsch, J. *Biochemistry*, **2000**, *39*(10), 2436-2444.

157. Brodie, J.; Figueroa, E.; Dewey, S. *Synapse*, **2003**, 50(3), 261-265.
158. Goto, Y.; iwaski, K.; torikai, K.; Murakami, H.; Suga, H. *Chem. Commun.*, **2009**, 3419-3421.
159. Friis, P.; Helboe, P.; Larsen, P. *Acta Chemica Scandinavica B*, **1974**, 28, 317-321.
160. Berkowiz, D.; Charette, B.; Kurukurichi, K.; McFadden, J. *Tet. Assymetry*, **2006**, 17, 869-882.
161. Afzali-Ardakani, A.; Rapoport, H. *J. Org. Chem.*, **1980**, 45, 4817-4820.
162. Rajenda, G.; Miller, M. *J. Org. Chem.* **1987**, 52(20), 4471-4477.
163. Itaya, T.; Shimizu, S.; Nakagawa, S.; Morisue, M. *Chem. Pharm. Bull*, **1994**, 42(9), 1927-1930.
164. Rich, D.; Tam, J. *J. Org. Chem.*, **1977**, 42(24), 3815-3820.
165. Kuchenthal, C.; Migenda, J.; Polednia, M.; Maison, W. *Amino Acids*, **2010**, 39(2), 443-448.
166. Shirasishi, S., Nomoto, S. *Agric. Biol. Chem.*, **1998**, 52 (6), 1601-1602.
167. Hanessian, S.; Sahoo, S. *Tetrahedron Letters*, **1984**, 24(14), 1425-1428.
168. Berkowitz, D.; Maiti, G. *Org. Lett.*, **2004**, 6(16), 2661-2664.
169. Biagini, S.; Gibson, S.; Keen, S. *J. Chem. Soc. Perkin Trans. 1*, **1998**, 2485-2499.
170. Hallinan, K.; Crout, D.; Errington, W. *J. Chem. Soc. Perkin Trans. 1*, **1994**, 3537-3543.
171. Carrasco, M.; Jones, R.; Kamel, S.; Rapoport, H.; Truong, T., *Organic Syntheses*, **1998**, Coll. Vol. 9, 63-68.
172. Pirrung, M.; Biswas, G; Ibarra-Rivera, T. *Org. Lett.*, **2010**, 12, 2402-2405.
173. Hoffmann, T.; Waibel, R.; Gmeiner, P. *J. Org. Chem.* **2003**, 68, 62-69.
- 174 a. Sharpless, K.; Lauer, R.; Teranishi, A. *J. Am. Chem. Soc.*, **1973**, 95, 6137-6139.
- b. Reich, H.; Renga, J. *J. Org. Chem.*, **1975**, 40(22), 3313-3314.

- c. Reich, H.; Renga, J.; Reich, I. *J. Am. Chem. Soc.*, **1975**, *97*, 5434-5447.
175. Walter, R.; Roy, J. *J. Org. Chem*, **1971**, *36*(17), 2561-2563.
176. Lebar, M.; Lupoli, T.; Tsukamoto, H.; May, J.; Walker, S.; Kahne, D. *J. Am. Chem. Soc.*, **2013**, *135*, 4632-4635.
177. Bodanszky, M.; Bodanszky, A. *The Practice of Peptide Synthesis* 1984 Springer-Verlag Berlin New York Tokyo.
178. NMR indicates changes subsequent to dissolution that correlate with higher yields.
Possibly this corresponds to a greater degree of N-silylation.
179. In each, base was held constant at 1M triethylamine, and isomerization monitored at 25°C by ¹H NMR. As we did not collect full time course data, and analysis times varied, we have chosen to express half times calculated assuming pseudo first order kinetics and using only 1-2 data points.
180. Kastrinsky, D.B.; Kumar, P.; Marriner, G.A.; Barry, C. E. III, *Synthesis* **2012**; *44*, 3043-3048.
181. Chatterjee, A.K.; Choi, T-L.; Sanders, D.P.; Grubbs, R.H. *J. Am. Chem. Soc.*, **2003**, *125*, 11360-11370.
182. Binder, J.; Blank, T.; Raines, R. *Org. Lett.*, **2007**, *9*(23), 4885-4888.
183. Huwe, C.; Blechert, S. *Tet. Lett.*, **1995**, *36*(10), 1621-1624.
184. Brümmer, O.; Rückert, A.; Blechert, S. *Chem. Eur. J.*, **1997**, *3*(3), 441-446.
185. Nolen, E.; Kurish, A.; Wong, K.; Orlando, M. *Tet. Lett.*, **2003**, *44*(12), 2449-2453.
186. Vasbinder, M.; Miller, S. *J. Org. Chem.*, **2002**, *67*, 6240-6242.
187. Miller, S.; Blackwell, H.; Grubbs, R. *J. Am. Chem. Soc.*, **1996**, *118*, 9606-9614.
188. Han L., Schwabacher, A.W., Moran G.R., Silvaggi N.R. *Biochemistry*, **2015**, *54*, 7029–7040.

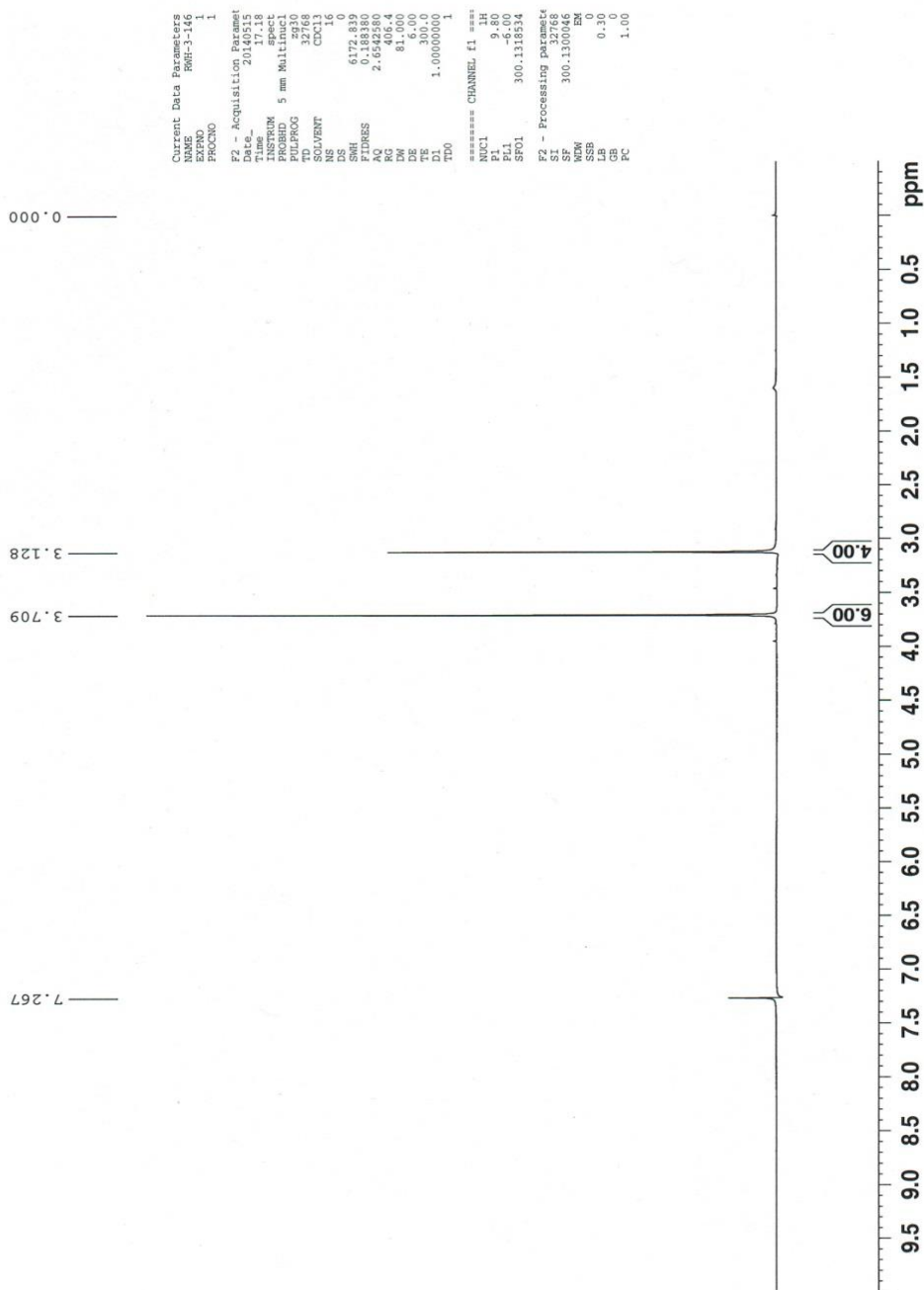
189. Miller, S.; Grubbs, R. *J. Am. Chem. Soc.*, **1995**, *117*(21), 5855-5856.
190. Hoffman, T.; Waibel, R.; Gmeiner, P. *J. Org. Chem.*, **2003**, *68*, 62-69.
191. Huwe, C.; Biechert, S. *Tet. Lett.*, **1995**, *36*(10), 1621-1624.
192. Miller, S.; Blackwell, H.; Grubbs, R. *J. Am. Chem. Soc.*, **1996**, *118*, 9606-9614.
193. Fu, G.; Grubbs, R. *J. Am. Chem. Soc.*, **1992**, *114*, 5426-5427.
194. Brümmer, O.; Rückert, A.; Biechert, S. *Chem. Eur. J.*, **1997**, *3*(3), 441-446.
195. Biagini, S.; Gibson, S.; Keen, S. *J. Chem. Soc., Perkin Trans.1*, **1998**, *16*, 2485-2499.
196. Ulman, M.; Grubbs, R. *Organometallics*, **1998**, *17*(12), 2484-2489.
197. Blackwell, H.; O'Leary, D.; Chatterjee, A.; Washenfelder, R.; Bussman, D.; Grubbs, R. *J. Am. Chem. Soc.*, **2000**, *122*(1), 58-74.
198. Chatterjee, A.; Grubbs, R. *Org. Lett.*, **1999**, *1*(11), 1751-1753.
199. Garber, S.; Kingsbury, J.; Gray, B.; Hoveyda, A. *J. Am. Chem. Soc.*, **2000**, *122*(34), 8168-8179.
200. Vasbinder, M.; Miller, S. *J. Org. Chem.*, **2002**, *67*, 6240-6242.
201. Nolan, E.; Kurish, A.; Wong, K.; Orlando, M. *Tet. Lett.*, **2003**, *44*(12), 2449-2453.
202. Chowdhury, A.; Boons, G. *Tet. Lett.*, **2005**, *46*(10), 1675-1678.
203. Pirrung, M.; Biswas, G.; Ibarra-Rivera, T. *Org. Lett.*, **2010**, *12*(10), 2402-2405.
204. Hong, S.; Grubbs, R. *J. Am. Chem. Soc.*, **2006**, *128*(11), 3508-3509.
205. Jordan, J.; Grubbs, R. *Angew. Chem. Int. Ed.*, **2007**, *46*(27), 5152-5155.
206. Binder, J.; Blank, J.; Raines, R. *Org. Lett.*, **2007**, *9*(23), 4885-4888.
207. Schwabacher, A.; Lane, J.; Schiesher, M.; Leigh, K.; Johnson, C. *J. Org. Chem.*, **1998**, *63*, 1727-1729.

X. APPENDIX

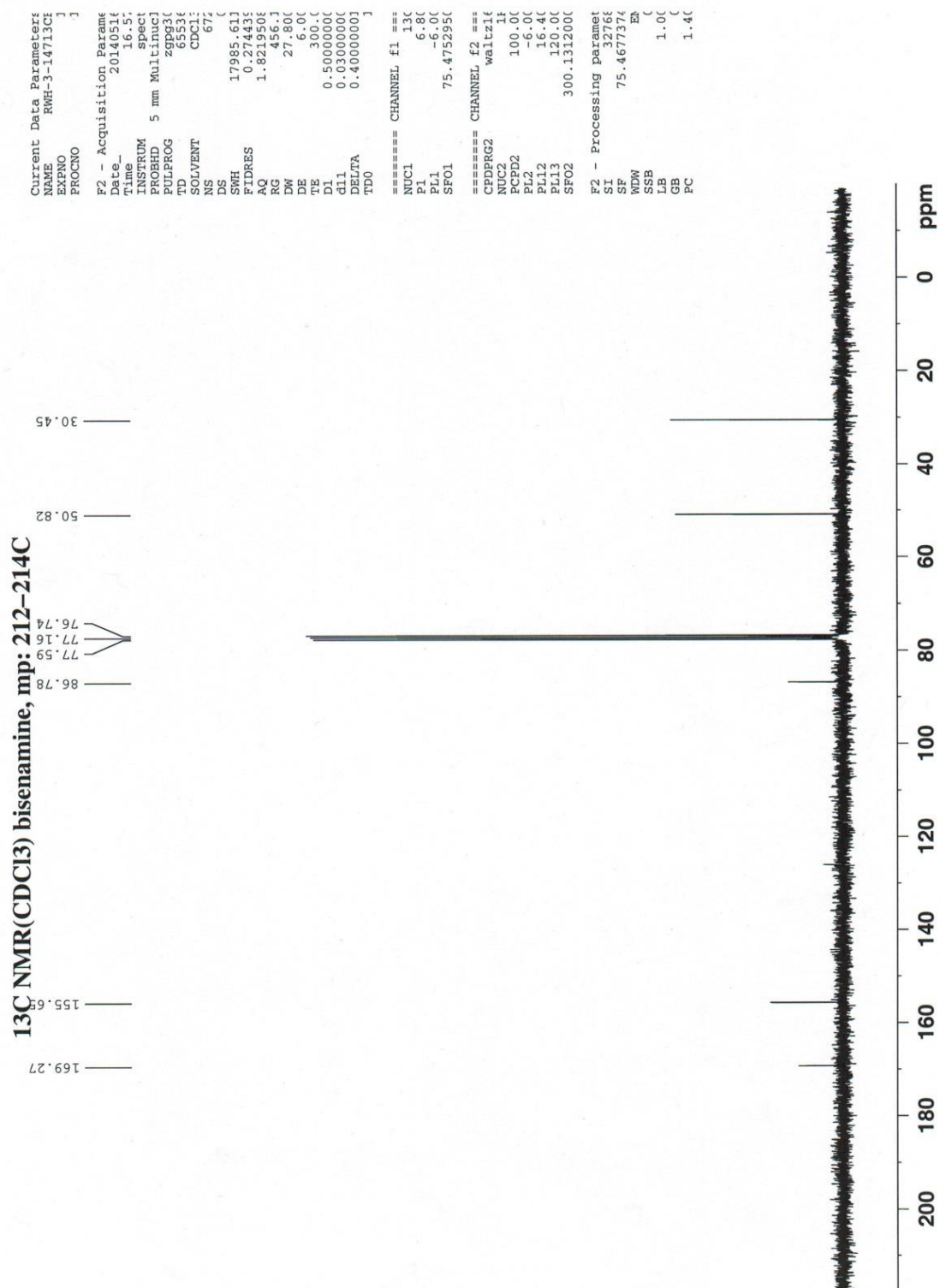
A. Characterization Data for Selected Compounds

^1H NMR Dimethyl 2,5-diaminocyclohexa-1,4-diene-1,4-dicarboxylate (1)

^1H NMR(CDCl_3) sat. bisenamine soln: 20.2mg sample, filtered mp:212–214C



¹³C NMR Dimethyl 2,5-diaminocyclohexa-1,4-diene-1,4-dicarboxylate (1)



MS Dimethyl 2,5-diaminocyclohexa-1,4-diene-1,4-dicarboxylate (1)

11/4/2014 10:18:24 AM Page 1 /

Shimadzu LCMS-2020 Data Report

Mass Spectrum for Sample
RWH-3-147 02.lcd

Operator: Mark Wang

Data Filename: C:\LabSolutions\Data\Schwabacher Alan\RWH-3-147 02.lcd

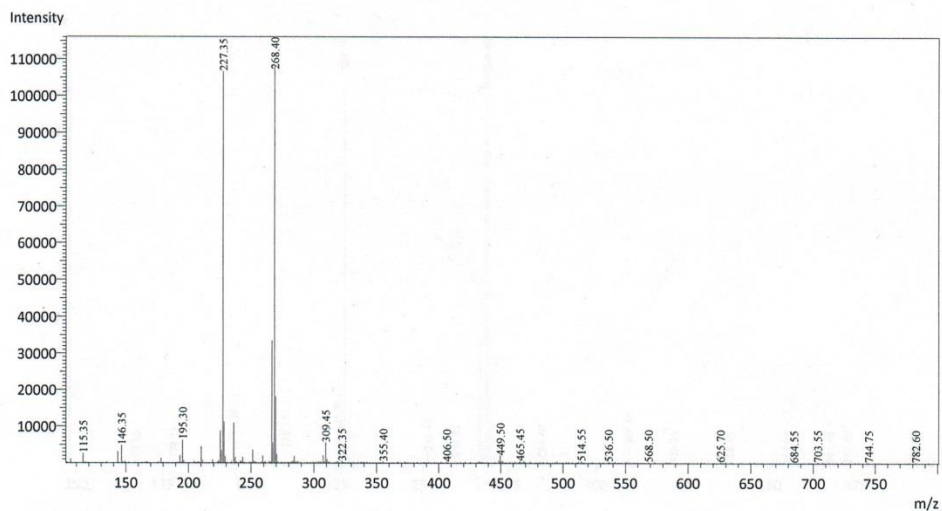
Spectrum Mode: Averaged

Retention Time: ----

Interface Type (ESI, APCI, DUIS): DUIS

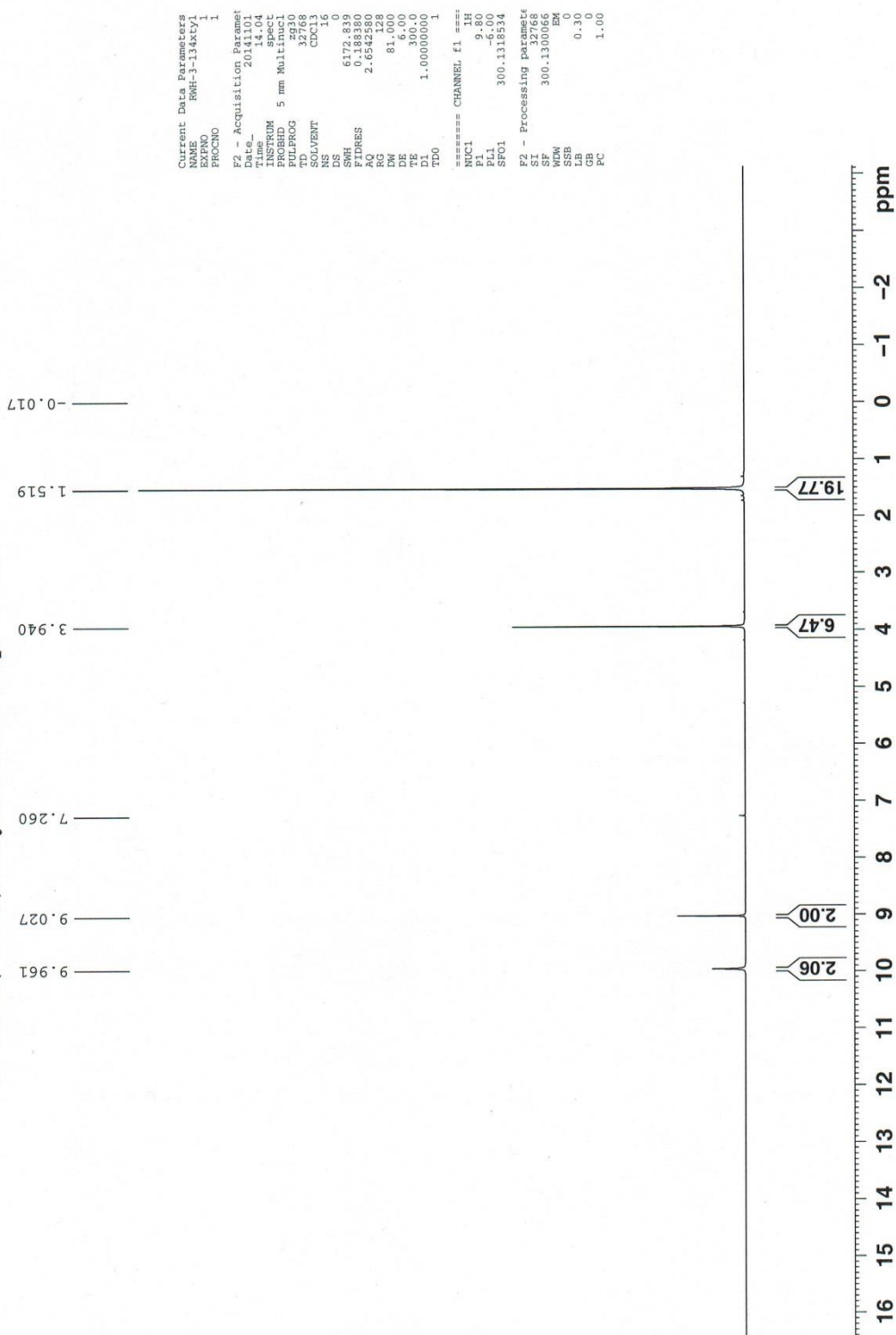
Acquisition Mode (Scan, SIM, Profile): Scan

Polarity: +

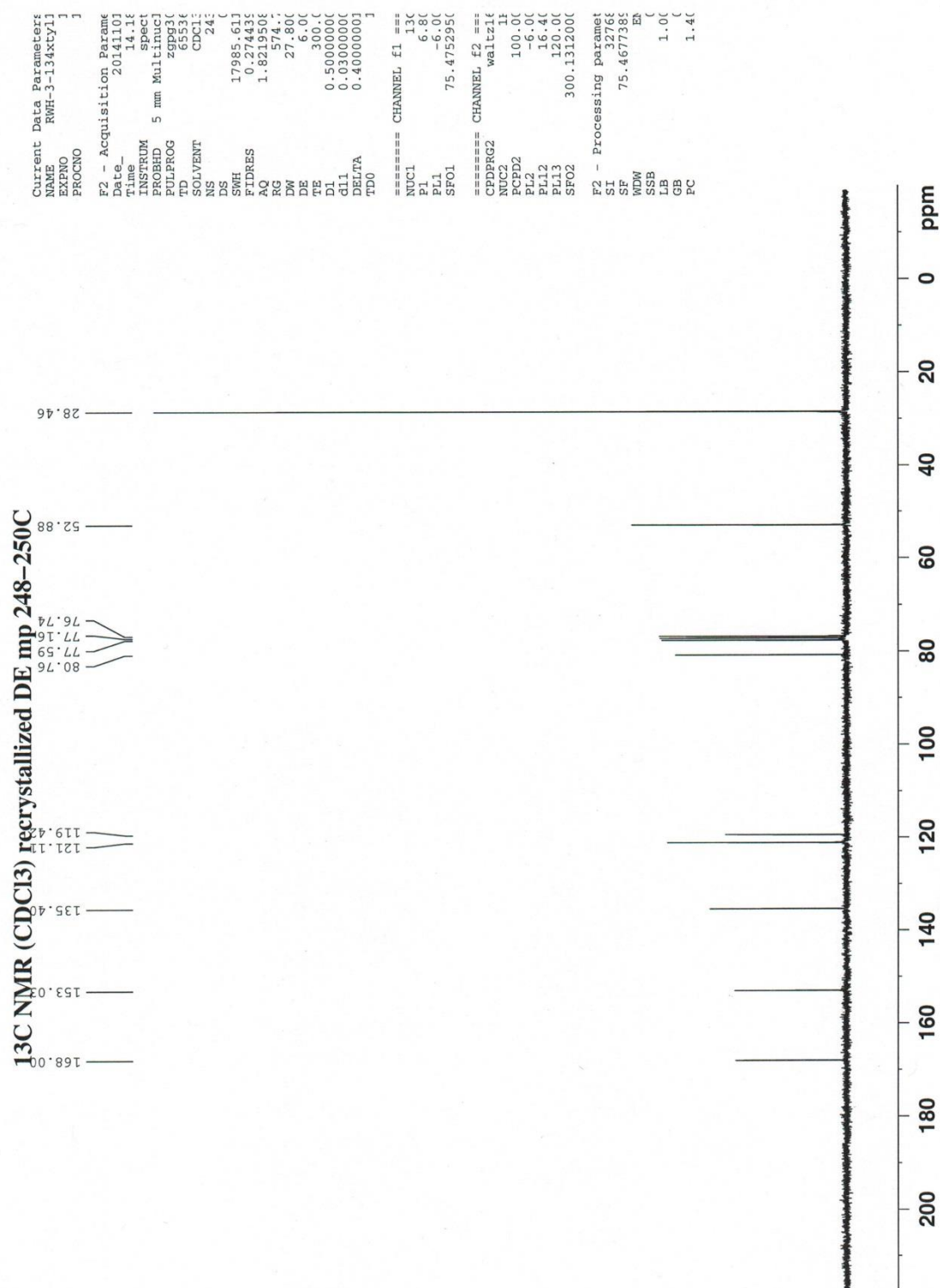


¹H NMR Dimethyl 2,5-bis((tert-butoxycarbonyl)amino)terephthalate (2)

¹H NMR (CDCl₃) recrystallized DE mp 248–250C



¹³C NMR Dimethyl 2,5-bis((tert-butoxycarbonyl)amino)terephthalate (2)



Shimadzu LCMS-2020 Data Report

Mass Spectrum for Sample
RWH-3-134 02.lcd

Operator: Mark Wang

Data Filename: C:\LabSolutions\Data\Schwabacher Alan\RWH-3-134 02.lcd

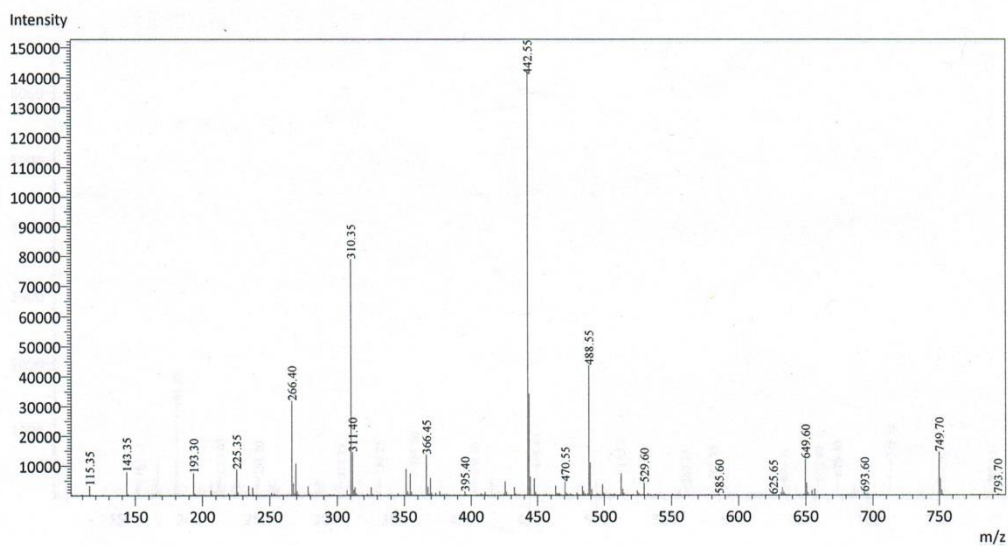
Spectrum Mode: Averaged

Retention Time: ----

Interface Type (ESI, APCI, DUIS): DUIS

Acquisition Mode (Scan, SIM, Profile): Scan

Polarity: +



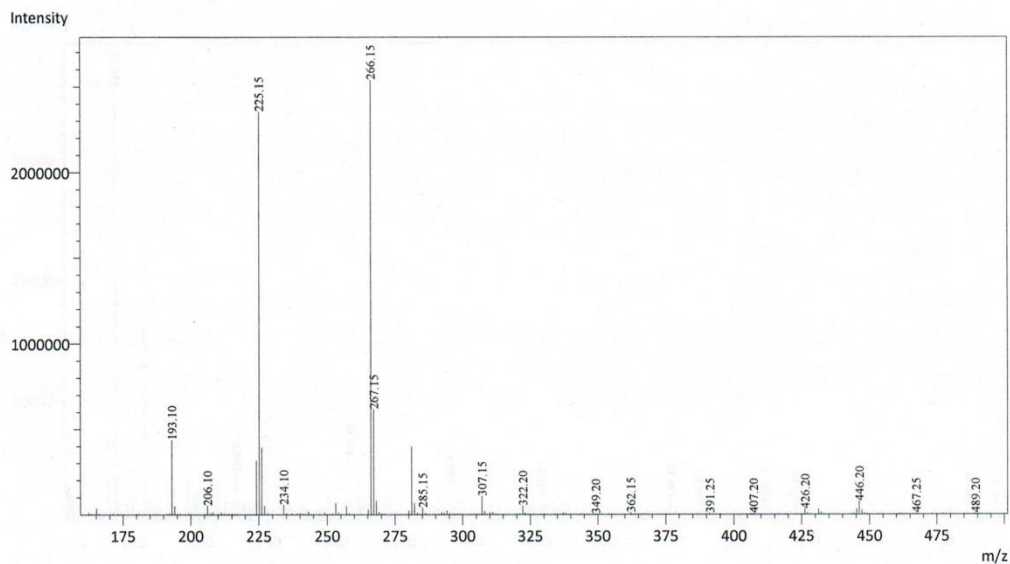
**¹H NMR (CDCl₃) yellow solid from NH₃(aq) workup of TFA deprotected DE
4.8 mg sample**

Current Data Parameters
NAME: RHF-4-918
EXPNO: 1
PROCNO: 1
F2 - Acquisition Parameters
Time: 20.00
Time: 14.53
INSTRUM: spect
PROBHD: 5 mm Multinuc
PULPROG: zgpg30
TD: 32768
SOLVENT: CDCl₃
NS: 16
DS: 4
SWH: 6172.839
FIDRES: 0.188380
AQ: 0.022280
RG: 2.000
DE: 81.000
TE: 300.0
D1: 1.00000000
===== CHANNEL f1 =====
NUC1: ¹H
P1: 9.80
PL1: -6.00
SFO1: 300.1318534
F2 - Processing parameters
SI: 32768
SF: 300.1300064
WDW: EM
SSB: 0
LB: 0.30
GB: 0
PC: 1.00

Shimadzu LCMS-2020 Data Report

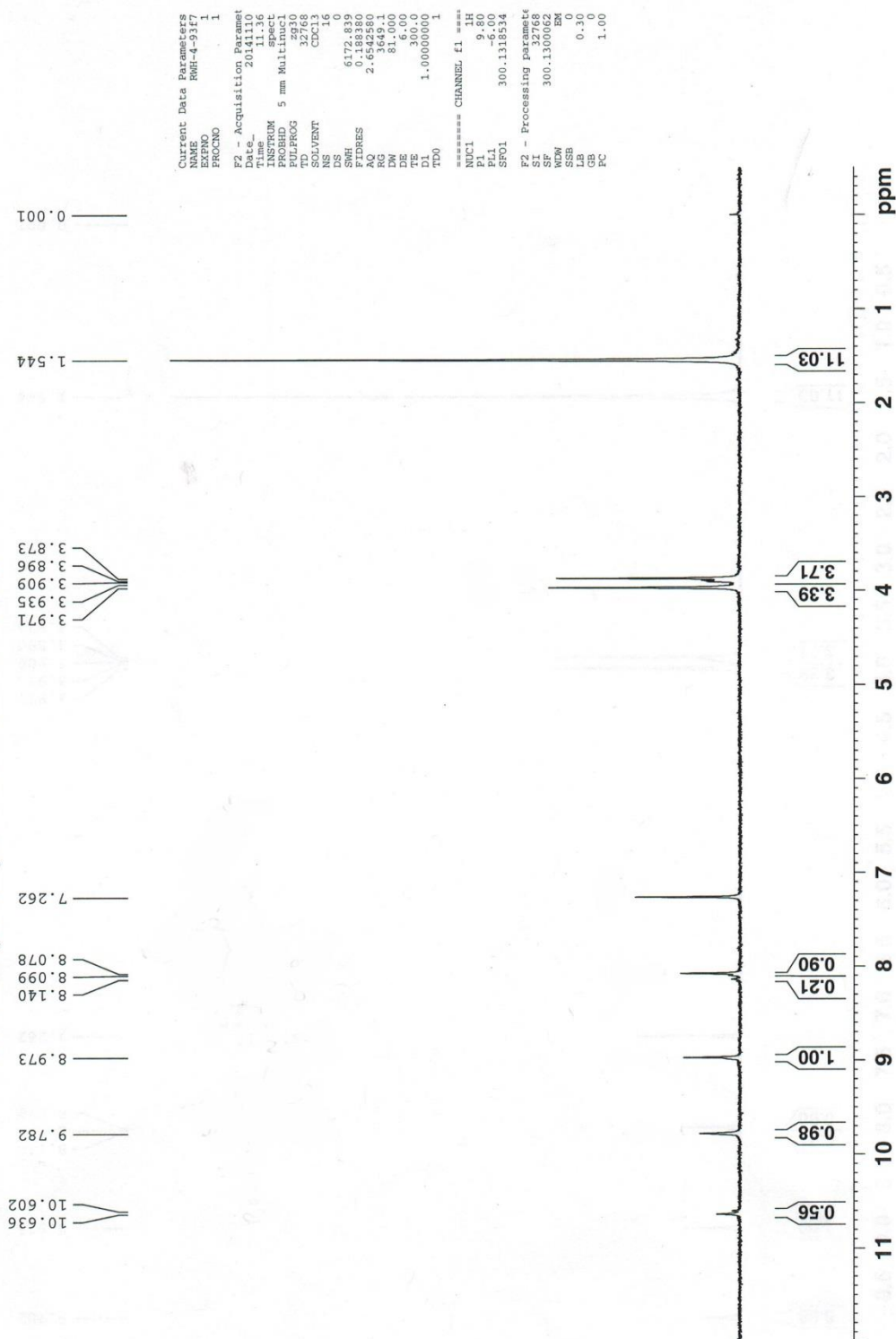
Mass Spectrum for Sample
RWH-4-91 01.lcd

Operator: Mark Wang
Data Filename: C:\LabSolutions\Data\Schwabacher Alan\RWH-4-91 01.lcd
Spectrum Mode: Averaged
Retention Time: ----
Interface Type (ESI, APCI, DUIS): DUIS
Acquisition Mode (Scan, SIM, Profile): Scan
Polarity: +



¹H NMR Tetramethyl 5,5'-azanediylbis(2-((tert-butoxycarbonyl)amino)terephthalate) (**4**)

¹H NMR (CDCl₃) f7-9 5% CH₃CN/CH₂Cl₂



Shimadzu LCMS-2020 Data Report

Mass Spectrum for Sample
RWH-4-93.lcd

Operator: Mark Wang

Data Filename: C:\LabSolutions\Data\Schwabacher Alan\RWH-4-93.lcd

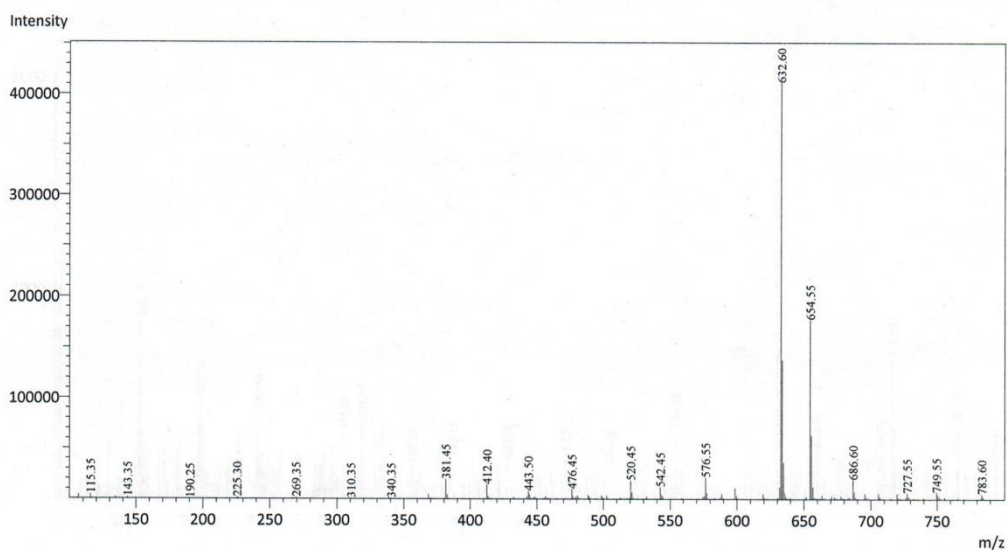
Spectrum Mode: Averaged

Retention Time: ----

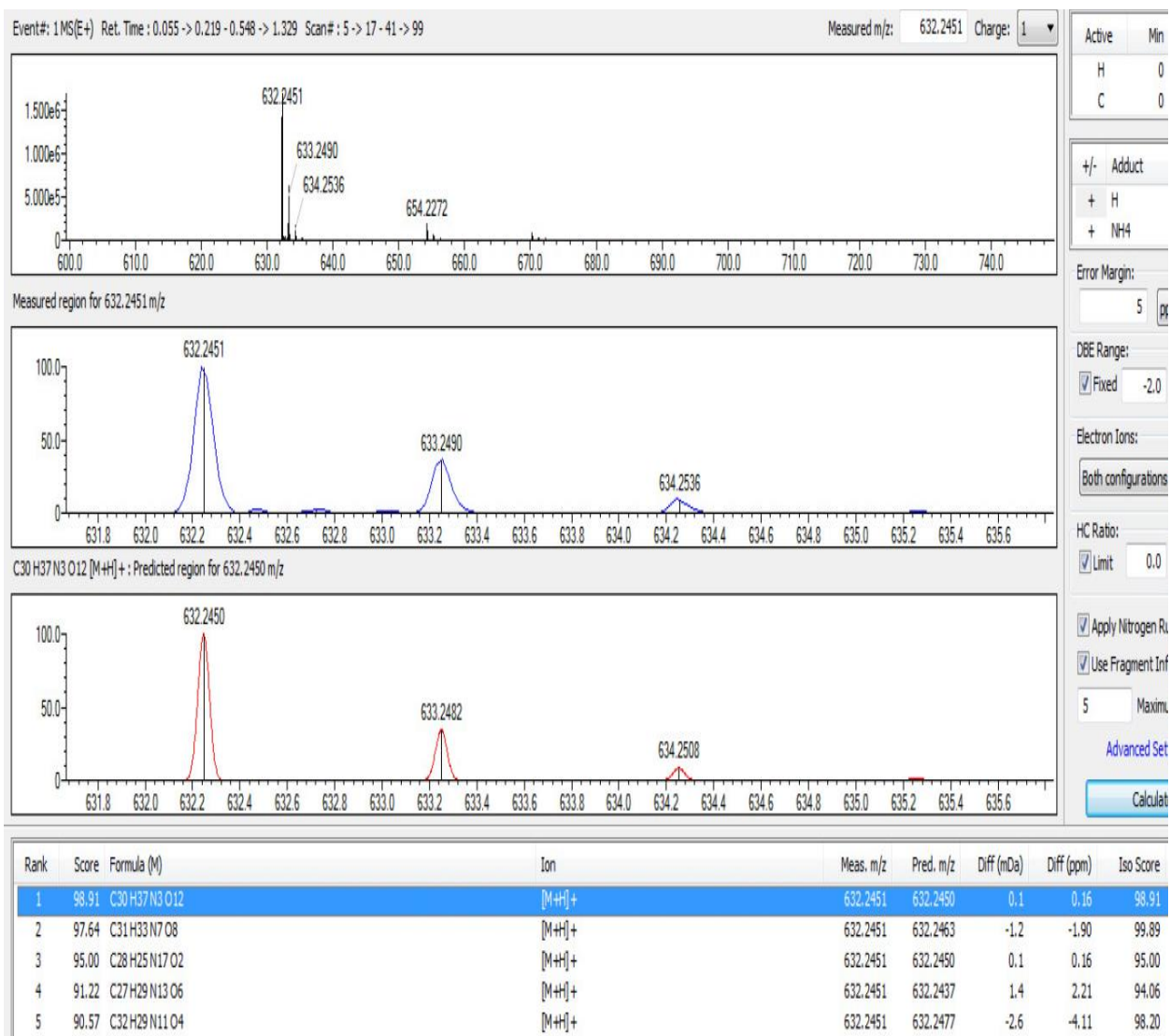
Interface Type (ESI, APCI, DUIS): DUIS

Acquisition Mode (Scan, SIM, Profile): Scan

Polarity: +

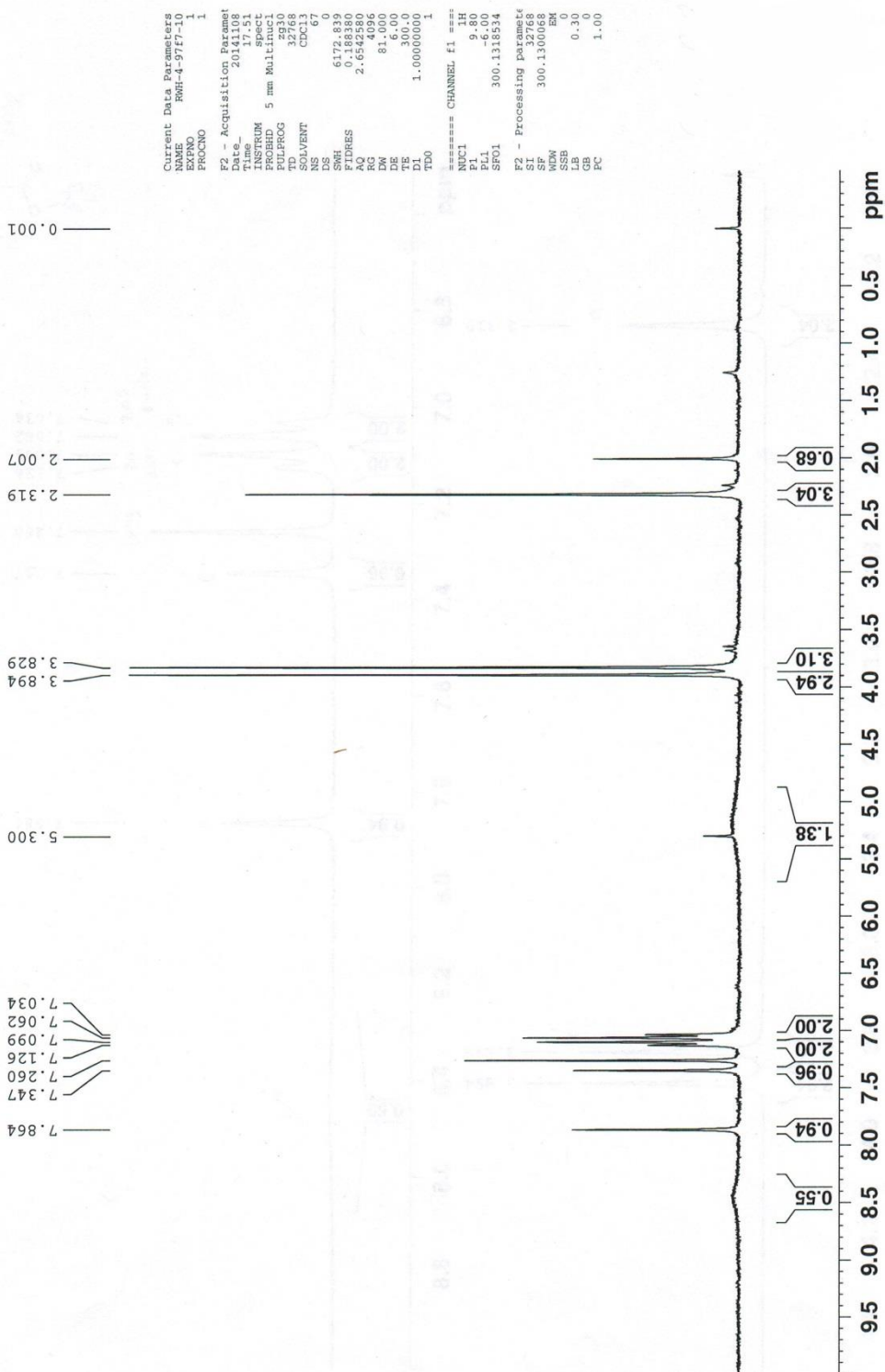


HRMS Tetramethyl 5,5'-azanediylbis(2-((tert-butoxycarbonyl)amino)terephthalate) (4)



¹H NMR Dimethyl 2-amino-5-(p-tolylamino)terephthalate (5)

¹H NMR (CDCl₃) f5-8 5% ACN/DCM + f1-3 10% ACN/DCM



Shimadzu LCMS-2020 Data Report

Mass Spectrum for Sample
RWH-4-97f10 01.lcd

Operator: Mark Wang

Data Filename: C:\LabSolutions\Data\Schwabacher Alan\RWH-4-97f10 01.lcd

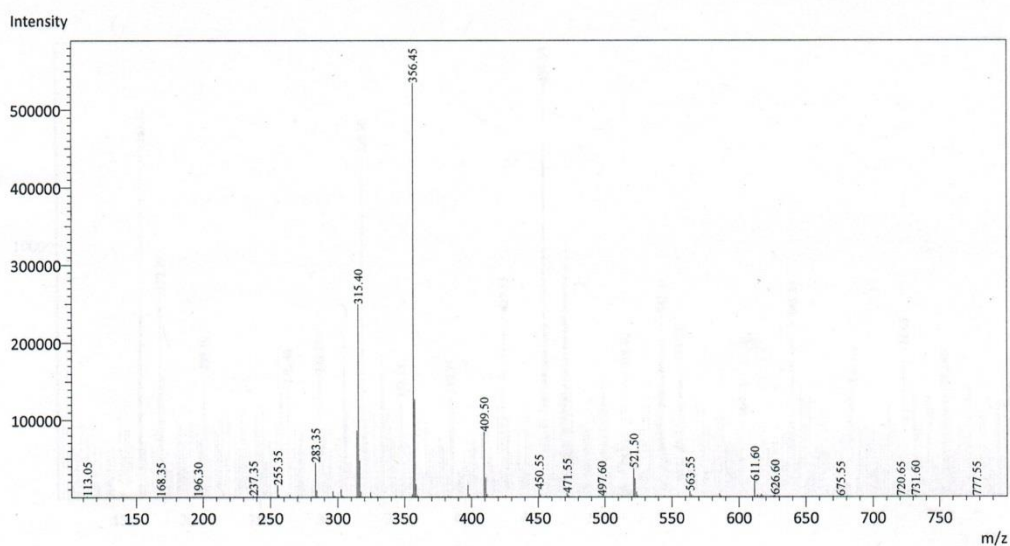
Spectrum Mode: Averaged

Retention Time: ----

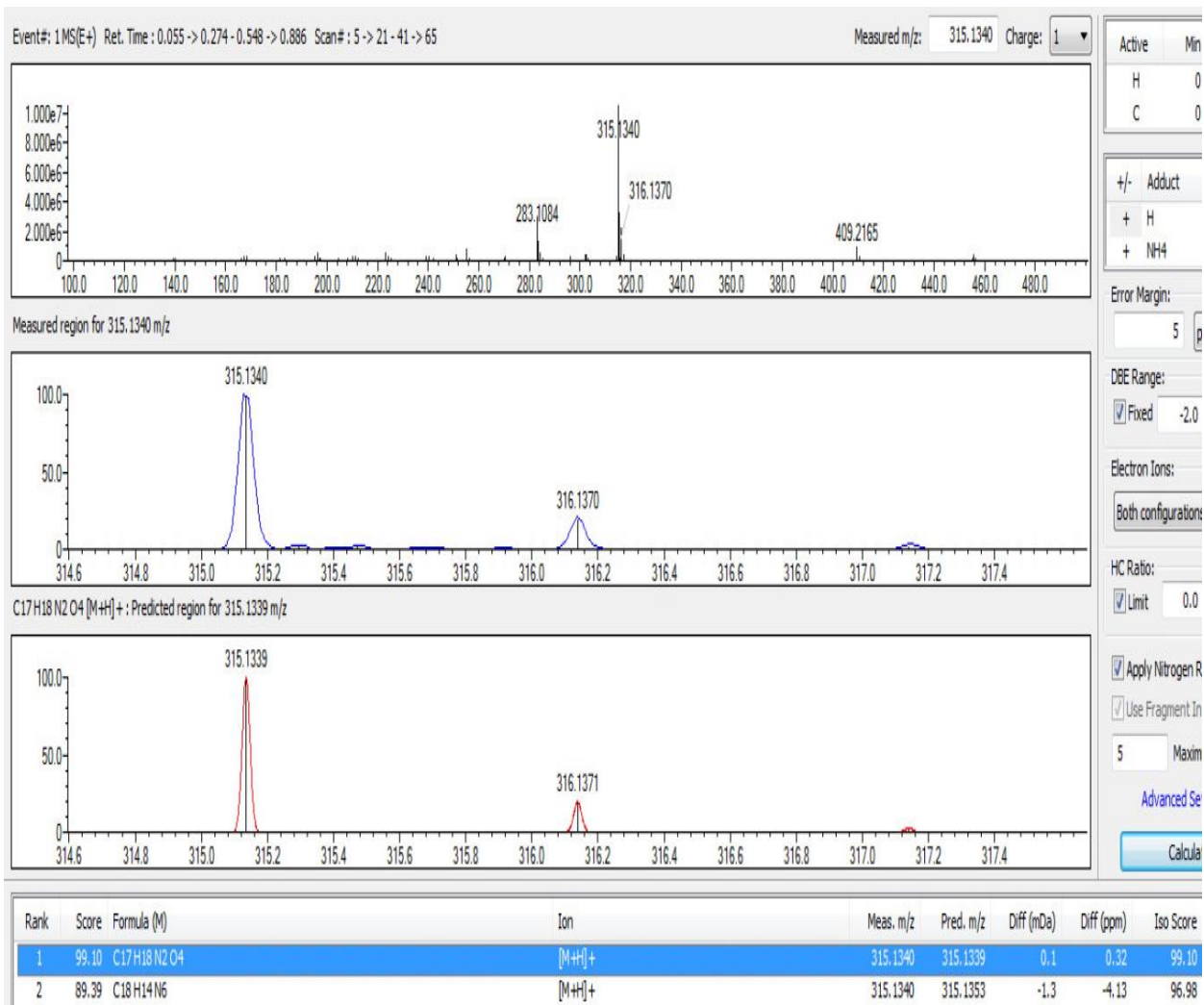
Interface Type (ESI, APCI, DUIS): DUIS

Acquisition Mode (Scan, SIM, Profile): Scan

Polarity: +

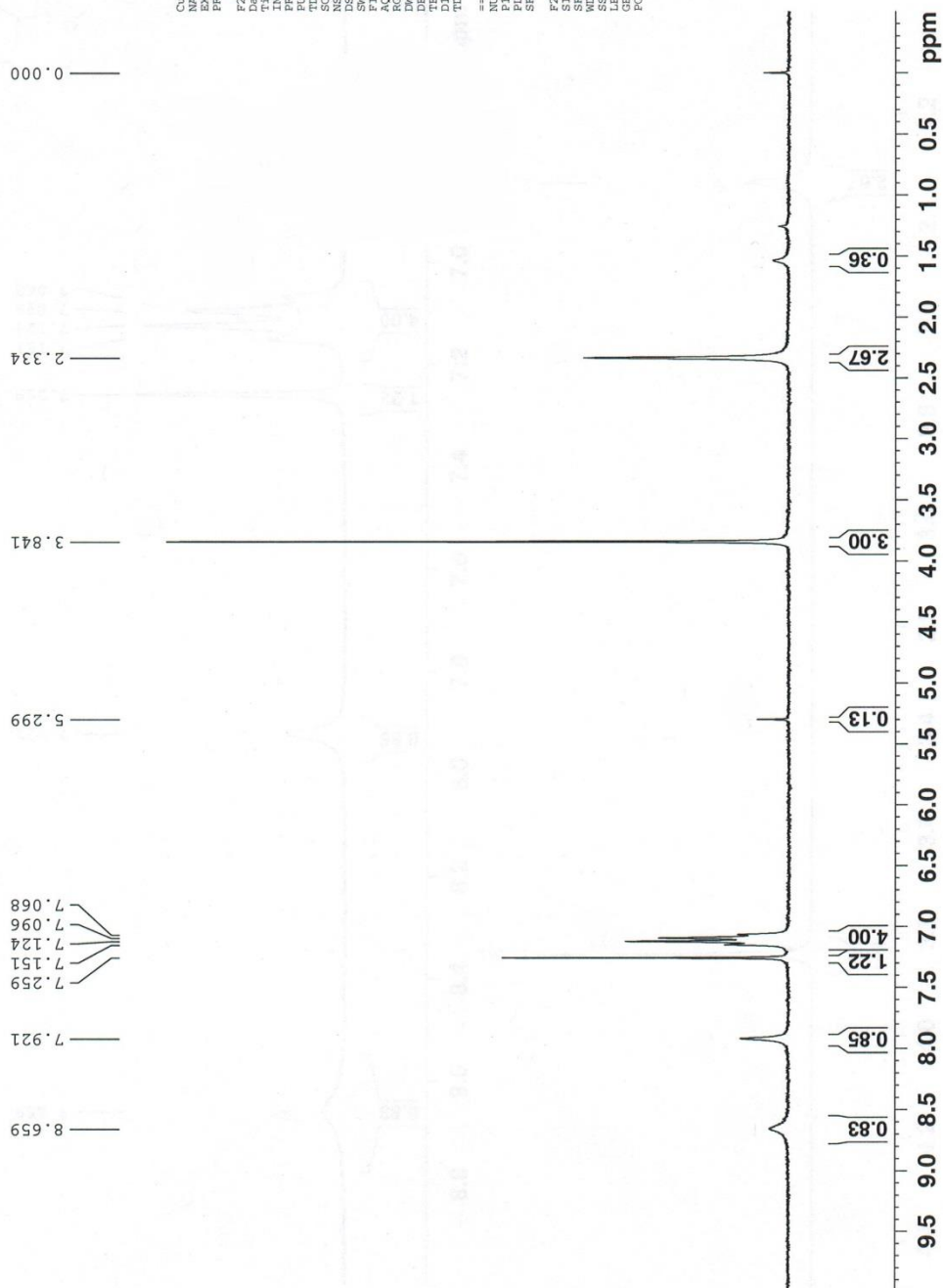


HRMS *Dimethyl 2-amino-5-(p-tolylamino)terephthalate (5)*



¹H NMR Dimethyl 2,5-bis(p-tolylamino)terephthalate (6)

¹H NMR (CDCl₃) f5-8 100% DCM + f1 5% ACN/DCM



Current Data Parameters
 NAME FWH-4-97f5-8
 EXPNO 1
 PROCNO 1
 F2 - Acquisition Parameters
 Date_ 20141108
 Time 14:53
 INSTRUM spect
 PROBRD 5 mm Multinucl
 PULPROG zg30
 FIDRES 0.161
 SOLVENT CDCl₃
 NS 62
 DS 0
 SH 0
 FTRES 0.163380
 AQ 2.6542580
 RG 4597.6
 DW 81.000
 DE 800.0
 TE 300.0
 D1 1.00000000
 TDO 1
 ===== CHANNEL f1 =====
 NUC1 1H
 P1 9.80
 PL1 0.00
 SFO1 300.1318334
 F2 - Processing parameters
 SI 32768
 SF 300.1300721
 WDW EM
 SSB 0
 LB 0.30
 GB 0
 PC 1.00

Shimadzu LCMS-2020 Data Report

Mass Spectrum for Sample
RWH-4-97f5 01.lcd

Operator: Mark Wang

Data Filename: C:\LabSolutions\Data\Schwabacher Alan\RWH-4-97f5 01.lcd

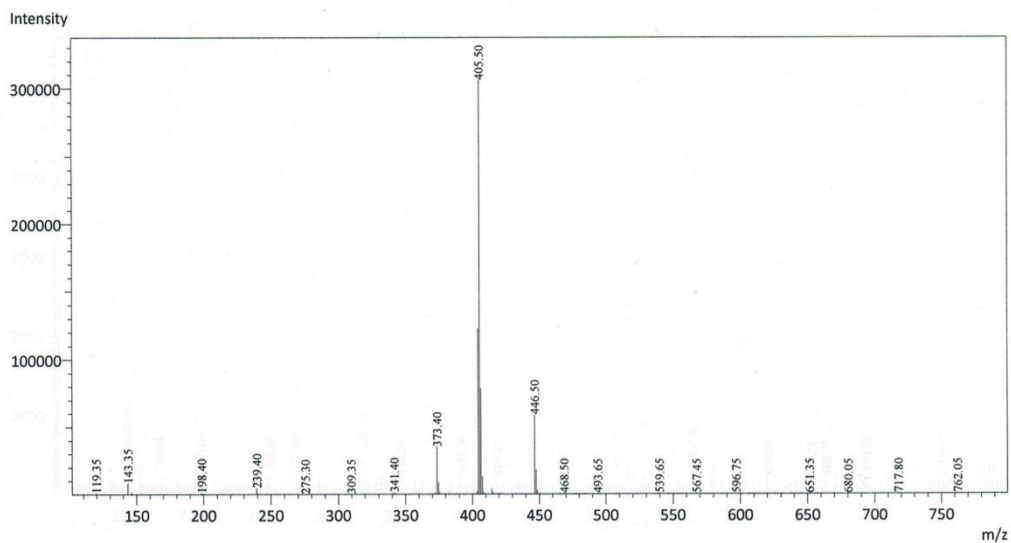
Spectrum Mode: Averaged

Retention Time: ----

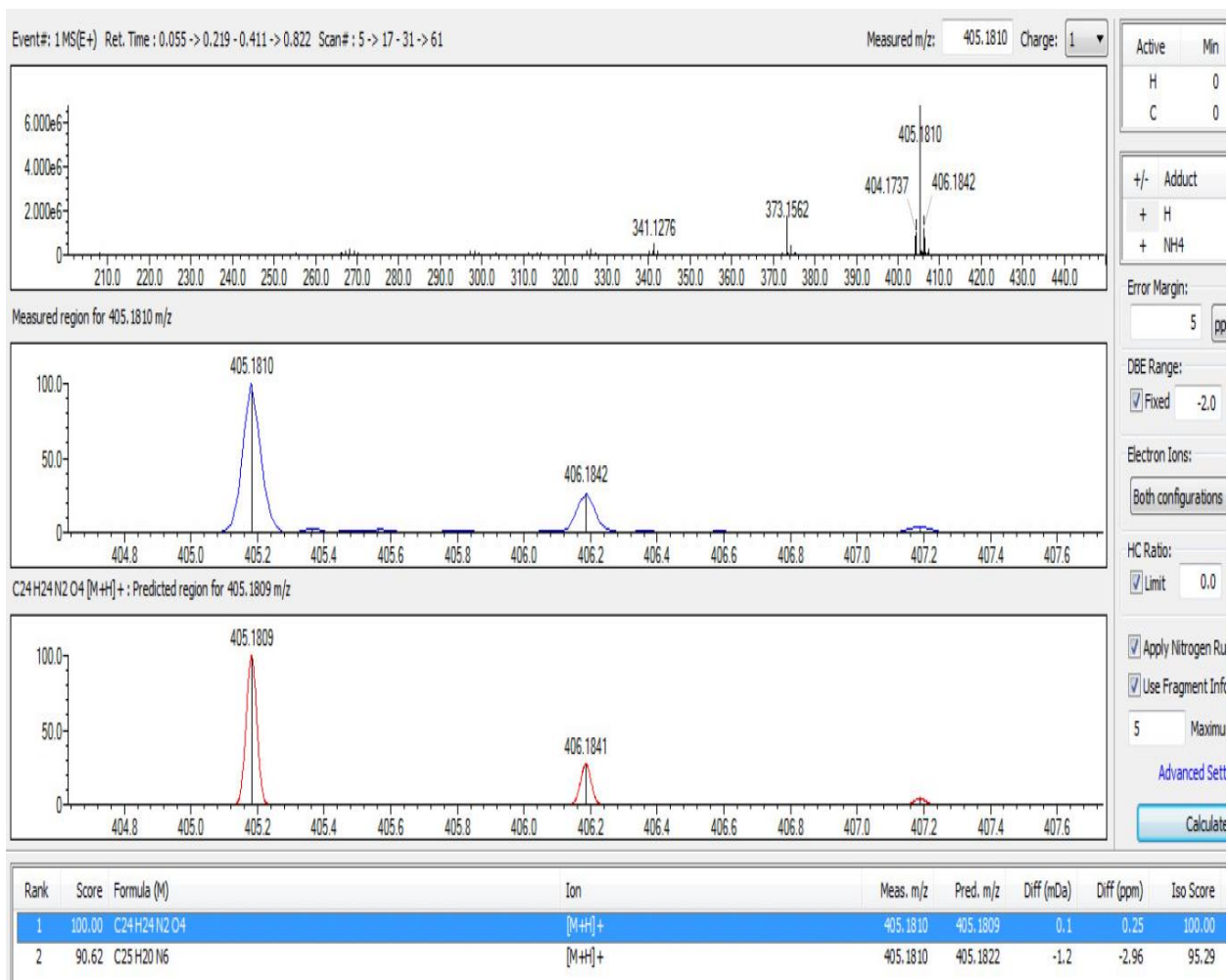
Interface Type (ESI, APCI, DUIS): DUIS

Acquisition Mode (Scan, SIM, Profile): Scan

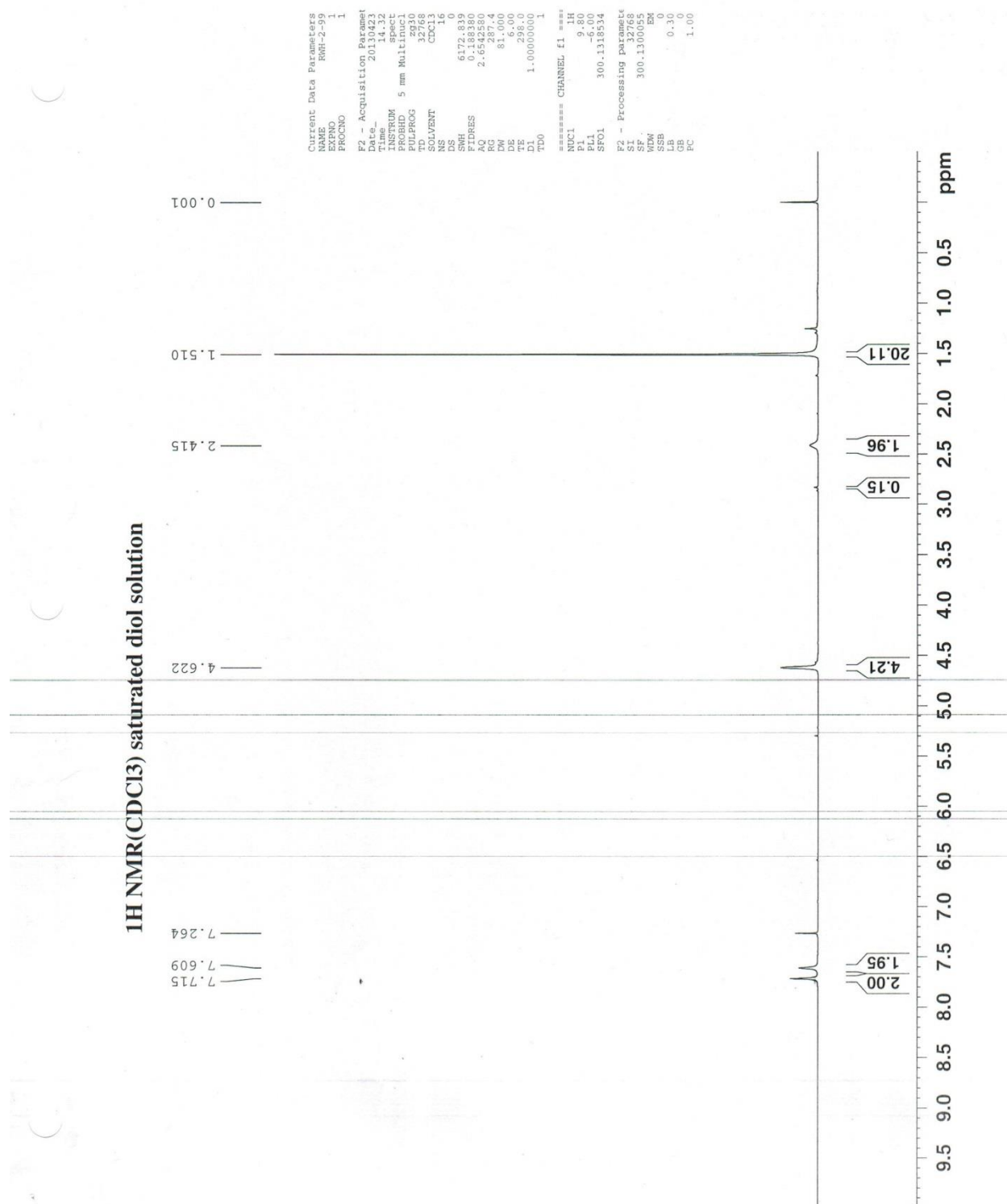
Polarity: +



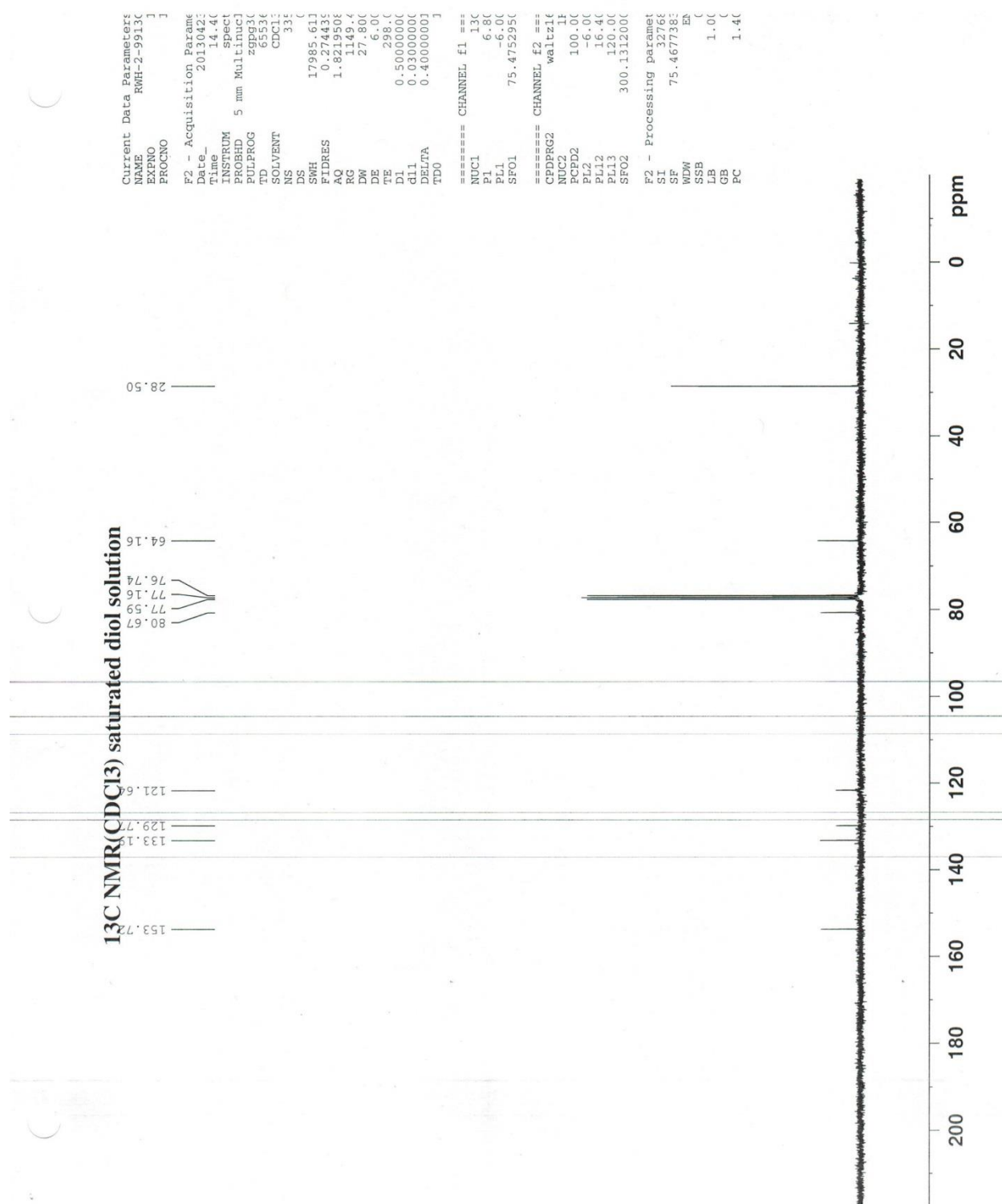
HRMS *Dimethyl 2,5-bis(p-tolylamino)terephthalate (6)*



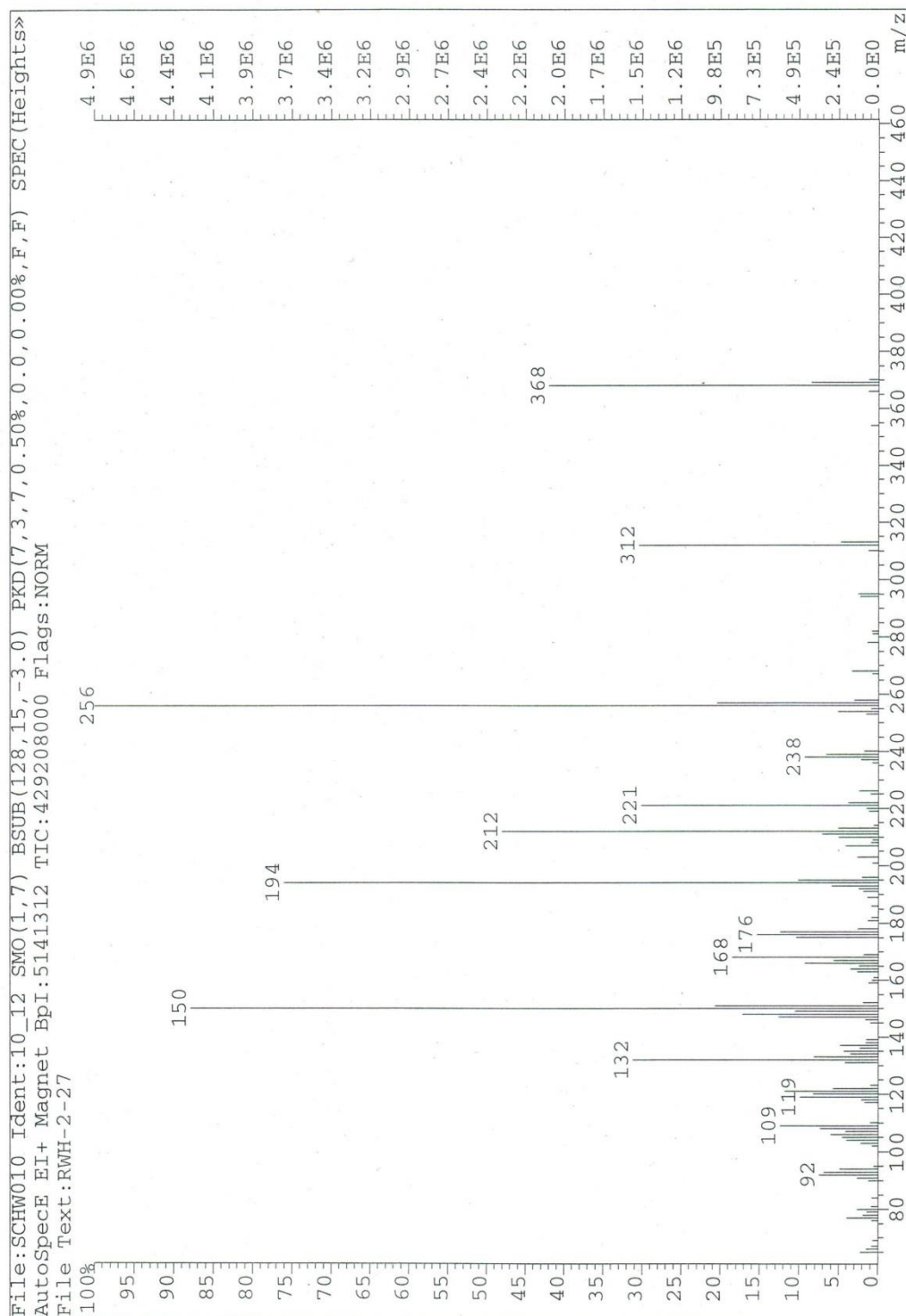
¹H NMR Di-tert-butyl (2,5-bis(hydroxymethyl)-1,4-phenylene)dicarbamate (7)



¹³C NMR Di-tert-butyl (2,5-bis(hydroxymethyl)-1,4-phenylene)dicarbamate (7)



MS (EI, 70eV): Di-tert-butyl (2,5-bis(hydroxymethyl)-1,4-phenylene)dicarbamate (7)

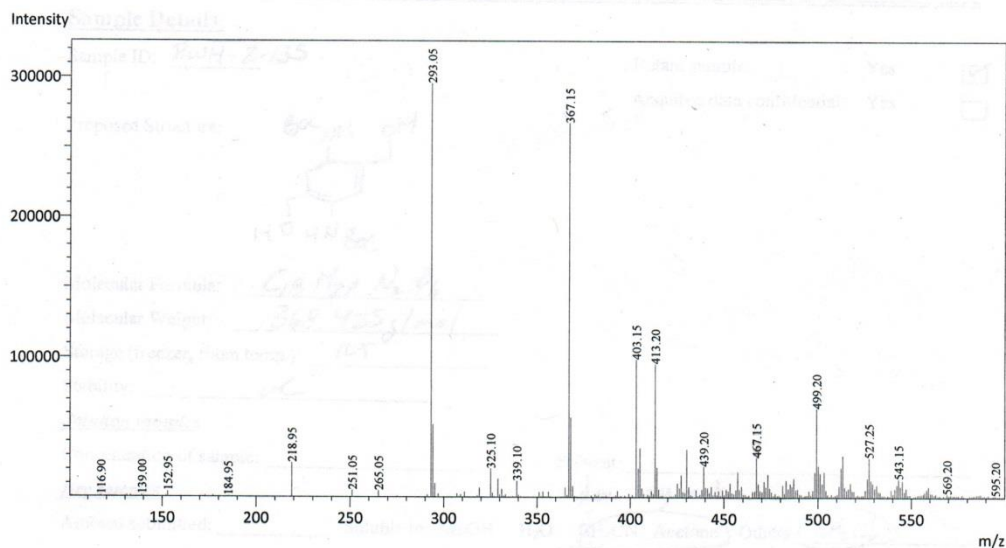


Shimadzu LCMS-2020 Data Report

Mass Spectrum for Sample
RWH-2-135 01.lcd

Operator: Mark Wang

Data Filename: C:\LabSolutions\Data\Schwabacher Alan\RWH-2-135 01.lcd
Spectrum Mode: Averaged
Retention Time: ----
Interface Type (ESI, APCI, DUIS): DUIS
Acquisition Mode (Scan, SIM, Profile): Scan
Polarity: -



HRMS (IT-TOF) Di-tert-butyl (2,5-bis(hydroxymethyl)-1,4-phenylene)dicarbamate (7)

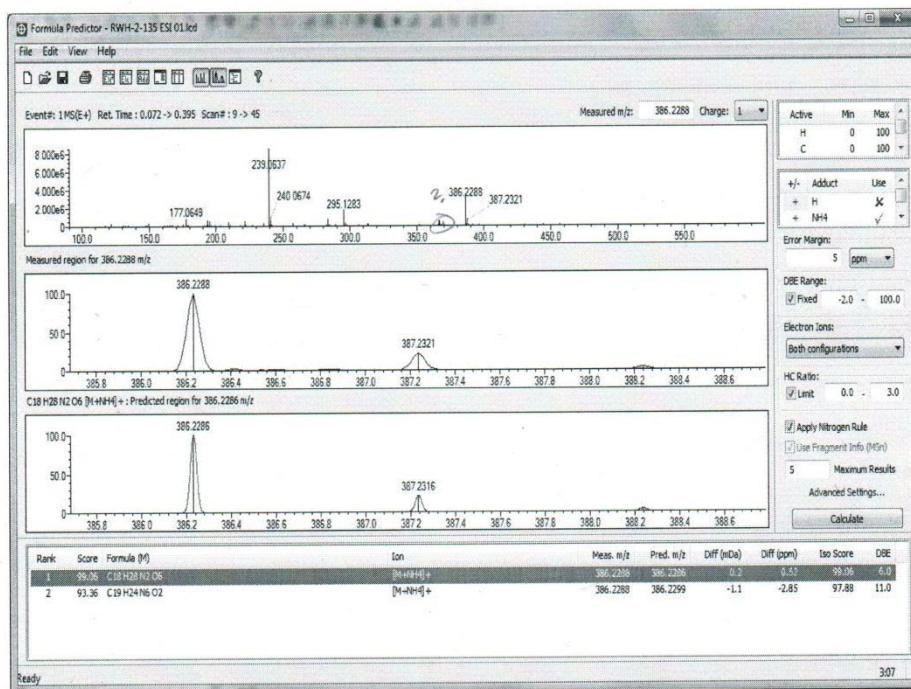
Shimadzu LCMS-IT-TOF Analysis Report

Feb 26, 2015

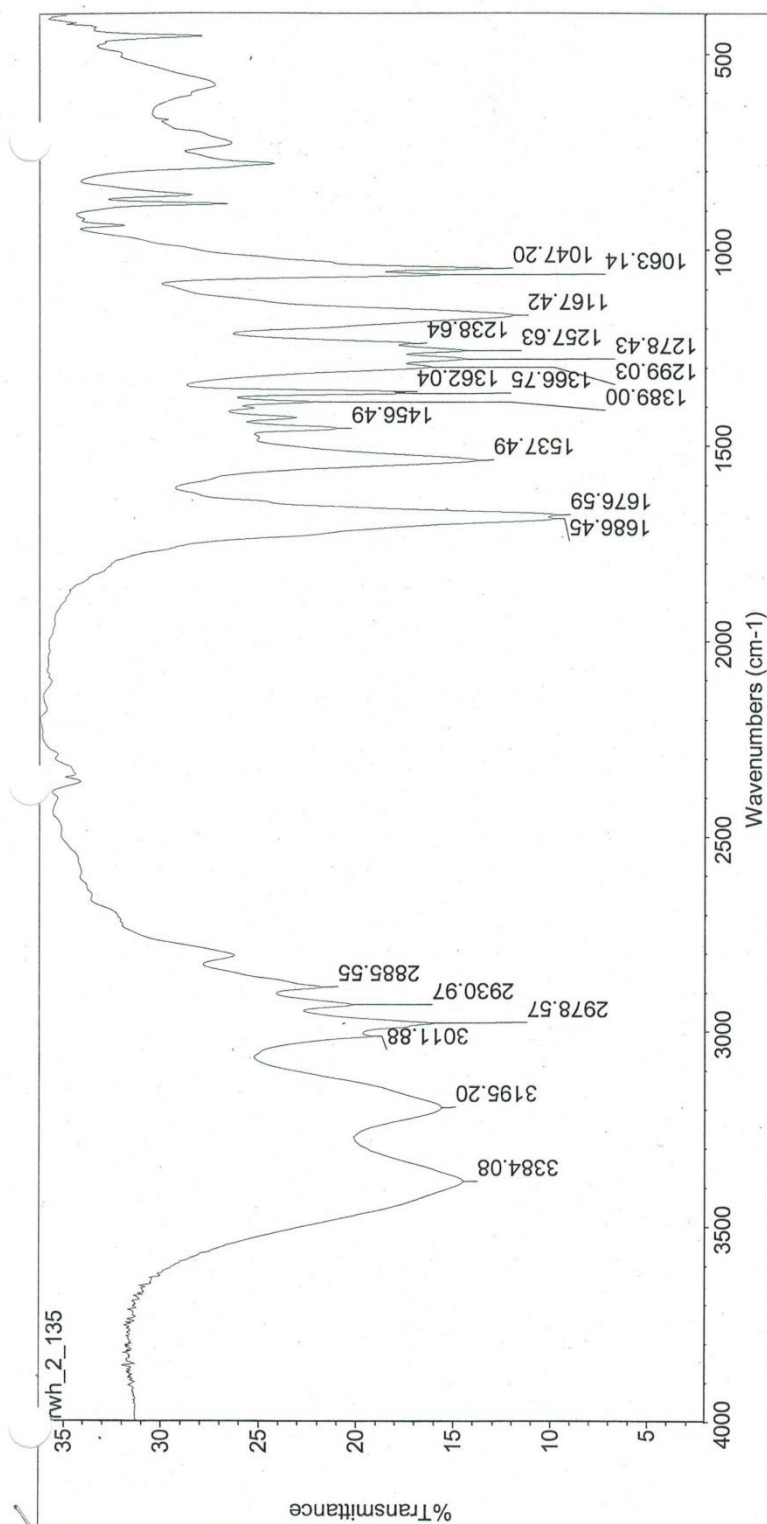
Acquired by : Mark Wang, Department of Chemistry and Biochemistry, UW-Milwaukee

Mass analyzer type: IT-TOF
 Ionization method : ESI (Electrospray Ionization)
 Sample Name: RWH-2-135 ESI
 Sample ID: RWH-2-135 ESI
 Vial #: 21
 Injection Volume: 5 uL
 Data File Name: RWH-2-135 ESI 01.lcd
 Method File Name: MW Manual (MS-MS, +, -).lcm
 Data Acquired: 2/26/2015 2:48:09 PM
 Data Processed: 2/26/2015 2:50:10 PM

Formula Prediction Results



IR Di-tert-butyl (2,5-bis(hydroxymethyl)-1,4-phenylene)dicarbamate (7)



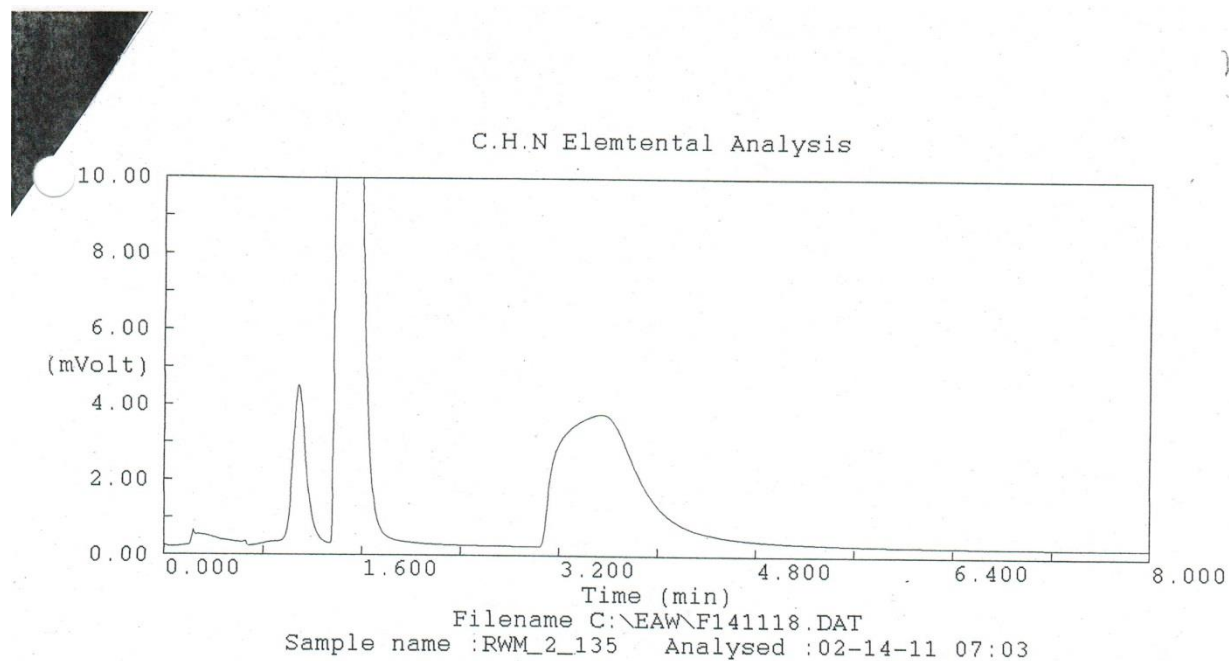
Wed Jan 26 13:41:18 2011 (GMT-06:00)

FIND PEAKS:

Spectrum: nwh_2_135(dil)
 Region: 4000.00 400.00
 Absolute threshold: 22.950
 Sensitivity: 70
 Peak list:

Position:	Intensity:
1047.20	12.746
1063.14	15.445
1167.42	11.920
1238.64	17.138
1257.63	14.282
1278.43	14.368
1299.03	16.144
1362.04	17.610

Elem. Anal. Di-tert-butyl (2,5-bis(hydroxymethyl)-1,4-phenylene)dicarbamate (7)



C.H.N Elemental Analysis

/W version : 1.06
 Operator ID : Mark Wang
 Method Name : Minute8
 Analysed : 02-14-11 07:03

Company Name : UWM Chemistry
 Method File : MINUTE8.MTH
 Printed : 2/15/2011 03:19

Sample ID : RWM_2_135 (# 21)
 Analysis Type : UnkNown (Area)
 Chromatogram : C:\EAW\F141118.DAT

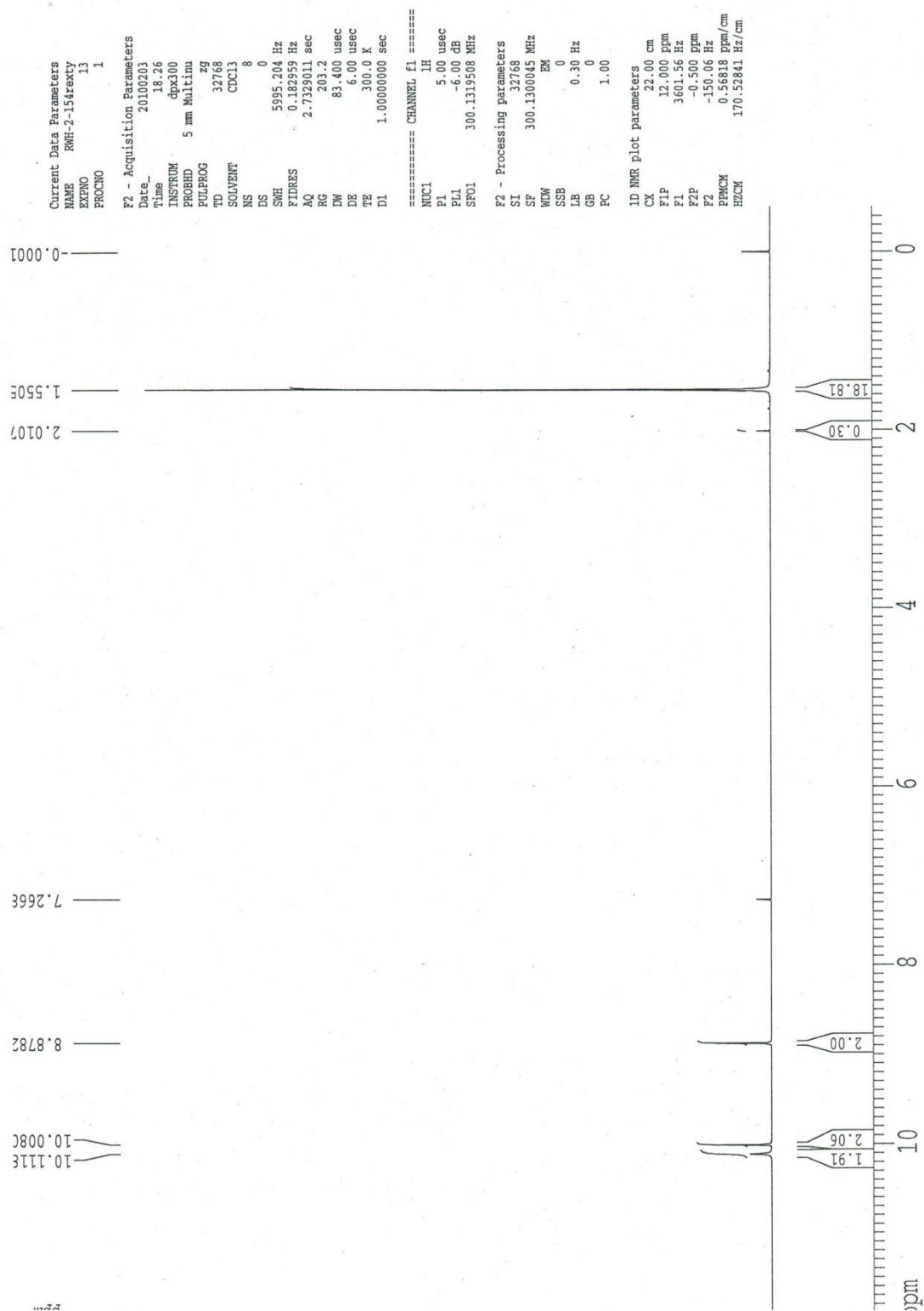
Channel : E.A. Channel A
 Sample weight : 1.493

Calib. method : using 'K Factors'

Element Name	Element %	Ret.Time	Area	BC	Area ratio	K factor
Nitrogen	7.5158	1.08	338641	FU	13.853140	.285272E+07
Carbon	58.5419	1.41	4691234	FU	1.000000	.535241E+07
Oxygen	7.7307	3.53	1704779	RS	2.751813	.147704E+08

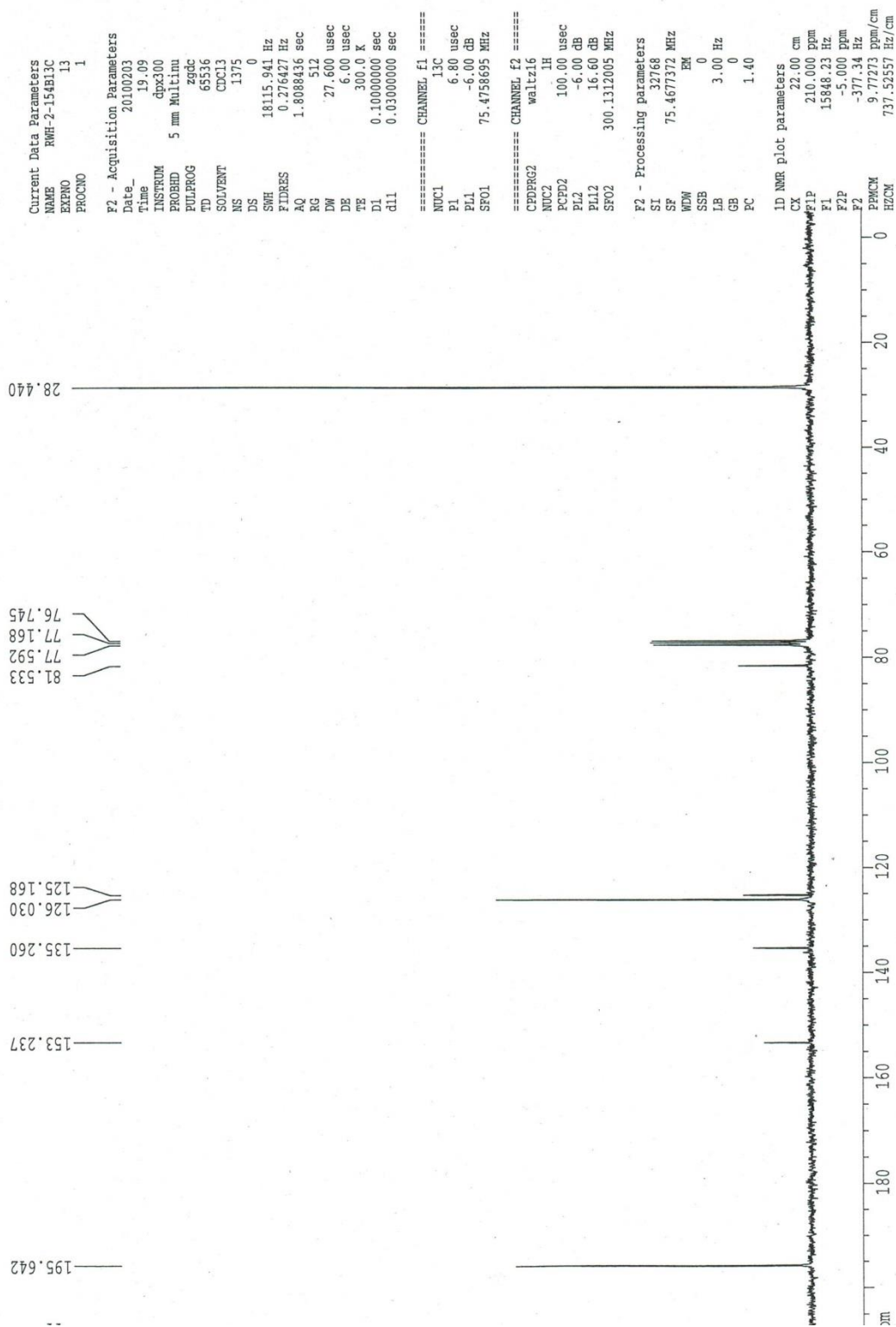
¹H NMR *N,N'*-di-*t*-Boc-2,5-diaminoterephthaldehyde (8)

Proton Spectrum

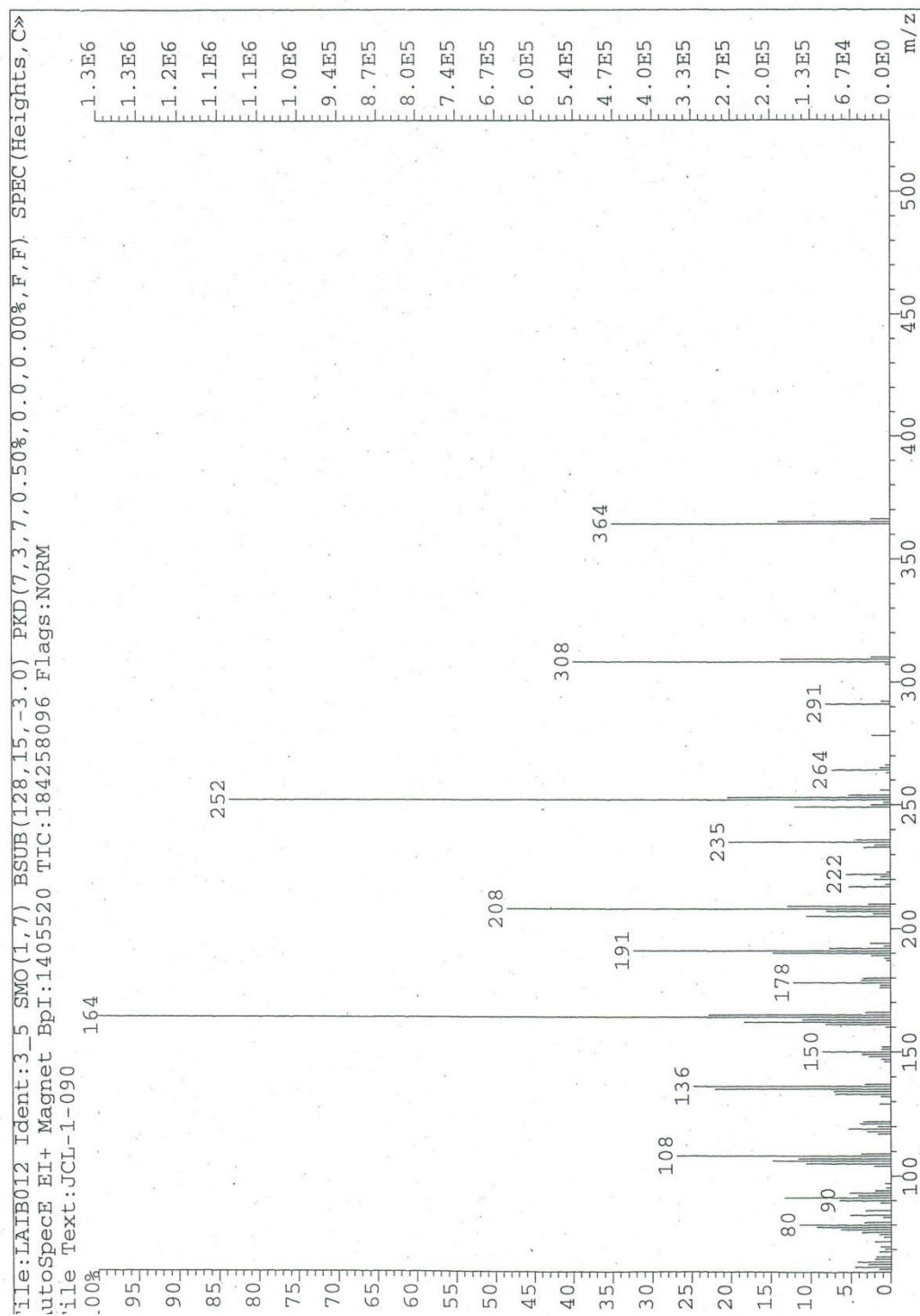


¹³C NMR *N,N'*-di-*t*-Boc-2,5-diaminoterephthaldehyde (8)

Carbon Spectrum



MS (EI, 70eV) *N,N'*-di-*t*-Boc-2,5-diaminoterephthaldehyde (8)



Shimadzu LCMS-2020 Data Report

Mass Spectrum for Sample
RWH-3-174 01.lcd

Operator: Mark Wang

Data Filename: C:\LabSolutions\Data\Schwabacher Alan\RWH-3-174 01.lcd

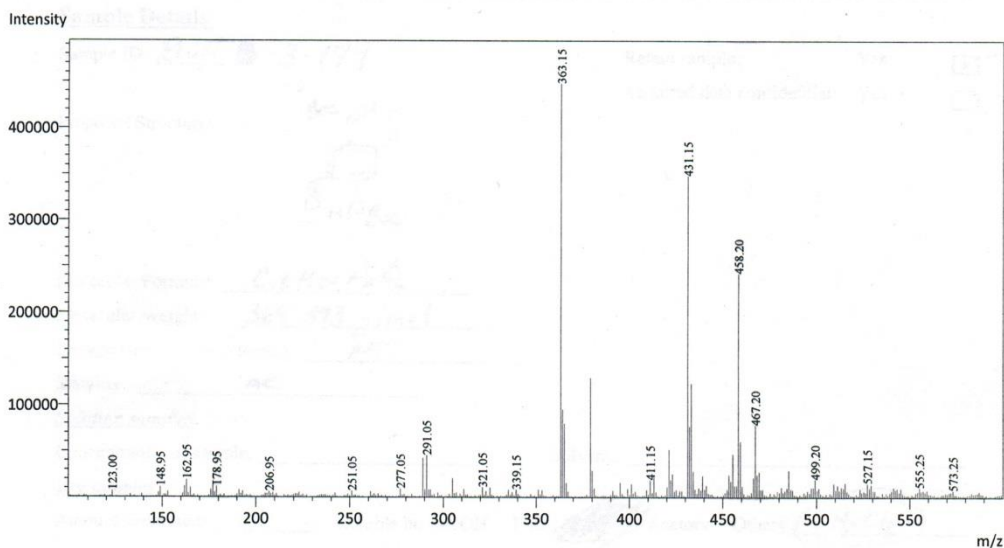
Spectrum Mode: Averaged

Retention Time: ---

Interface Type (ESI, APCI, DUIS): DUIS

Acquisition Mode (Scan, SIM, Profile): Scan

Polarity: -



HRMS (IT-TOF) *N,N'*-di-*t*-Boc-2,5-diaminoterephthaldehyde (8)

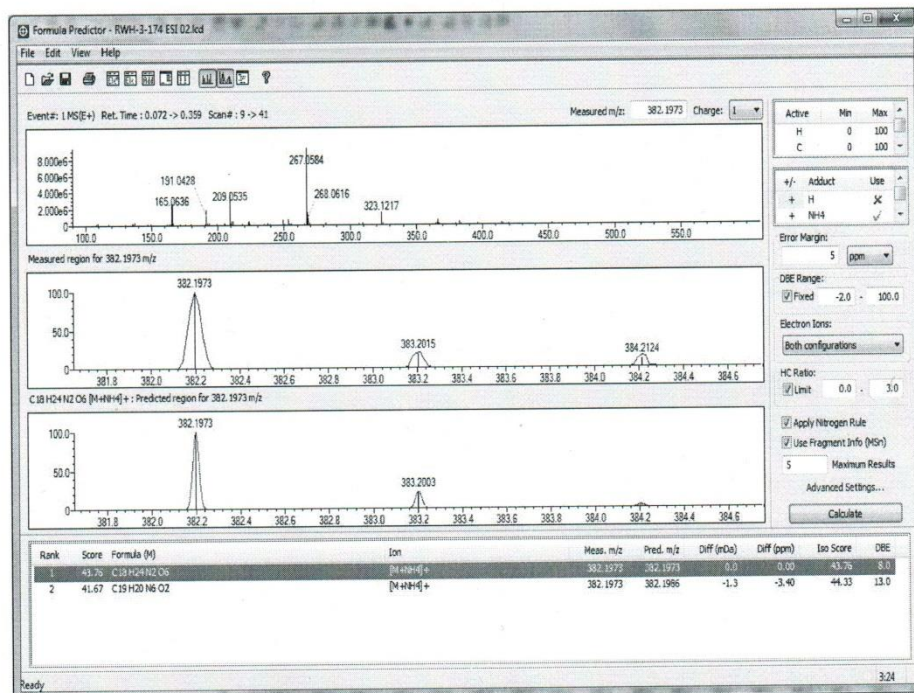
Shimadzu LCMS-IT-TOF Analysis Report

Feb 26, 2015

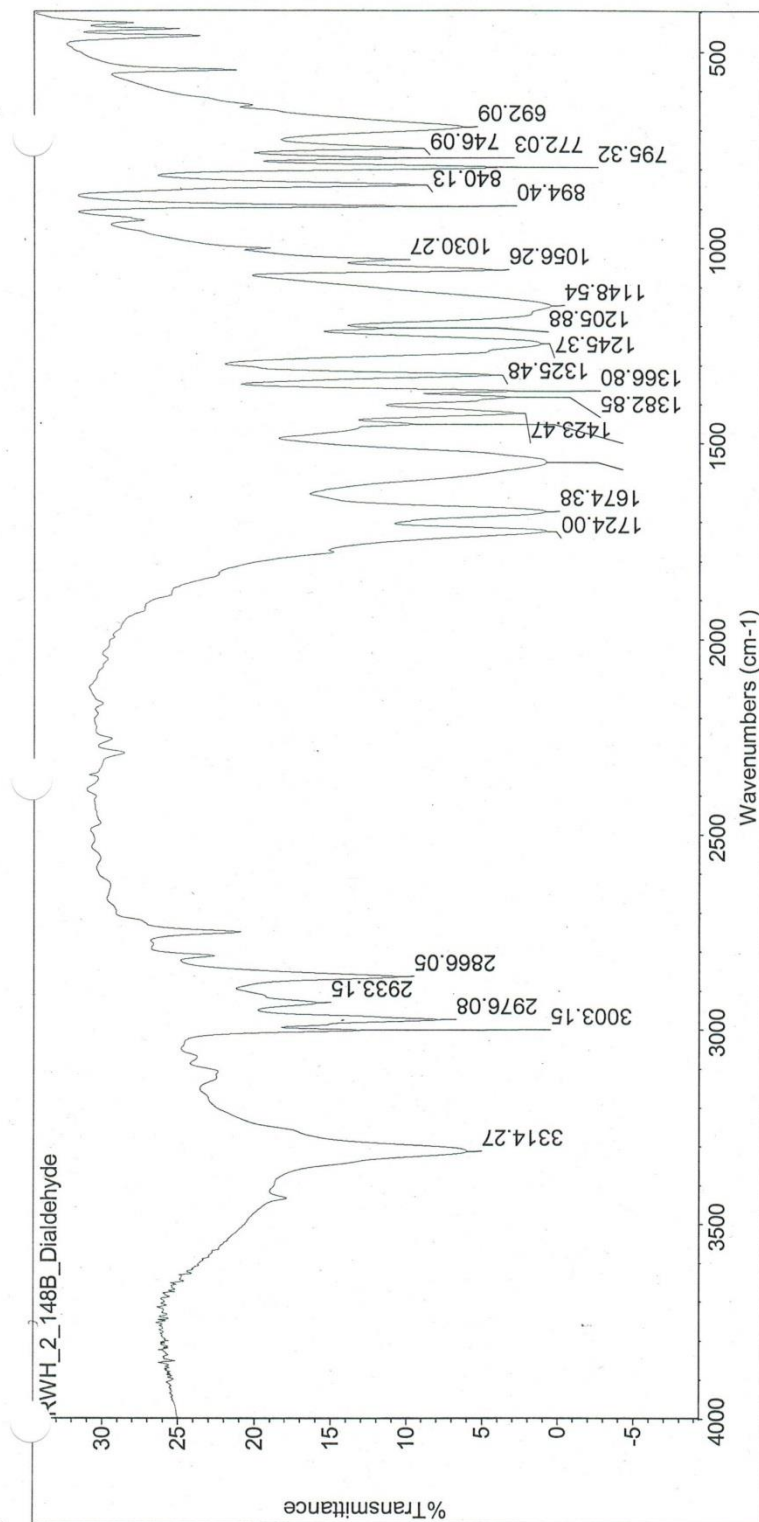
Acquired by : Mark Wang, Department of Chemistry and Biochemistry, UW-Milwaukee

Mass analyzer type: IT-TOF
 Ionization method : ESI (Electrospray Ionization)
 Sample Name: RWH-3-174 ESI
 Sample ID: RWH-3-174 ESI
 Vial #: 1
 Injection Volume: 5 uL
 Data File Name: RWH-3-174 ESI 02.lcd
 Method File Name: MW Manual (MS-MS, +, -).lcm
 Data Acquired: 2/26/2015 3:20:38 PM
 Data Processed: 2/26/2015 3:22:42 PM

Formula Prediction Results



IR (KBr pellet) *N,N'*-di-*t*-Boc-2,5-diaminoterephthaldehyde (**8**)



Wed Jan 26 14:04:06 2011 (GMT-06:00)

FIND PEAKS:

Spectrum: RWH_2_148B_Dialdehyde

Region: 4000.00 400.00

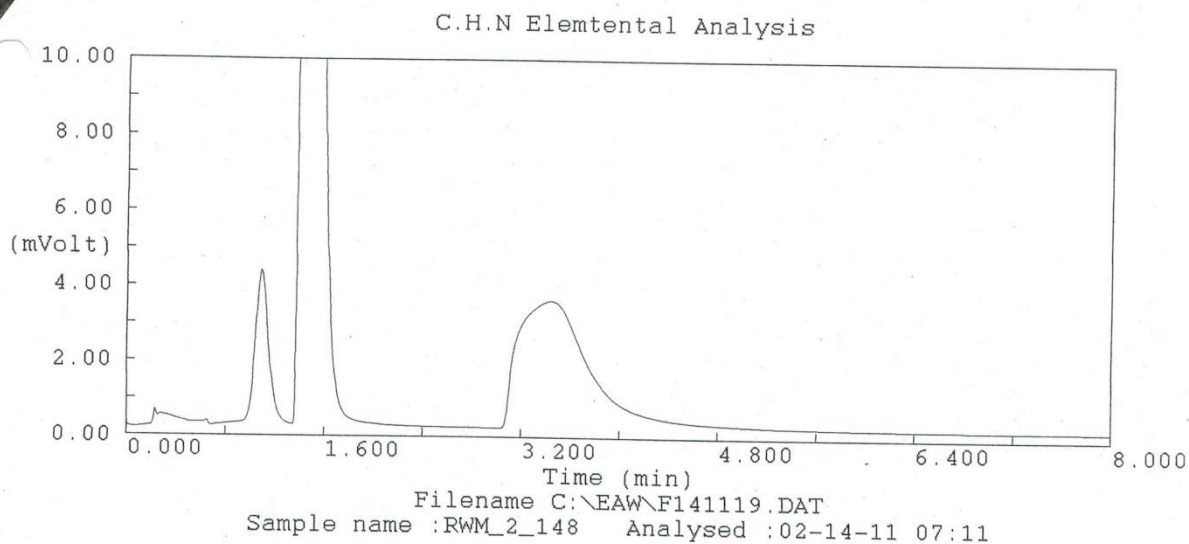
Absolute threshold: 17.458

Sensitivity: 65

Peak list:

Position:	Intensity:
692.09	6.304
746.09	9.364
772.03	10.310
795.32	3.798
840.13	9.137
894.40	9.713
1030.27	10.776
1056.26	4.127

Elem. Anal. *N,N'*-di-*t*-Boc-2,5-diaminoterephthaldehyde (8)



C.H.N Elemental Analysis

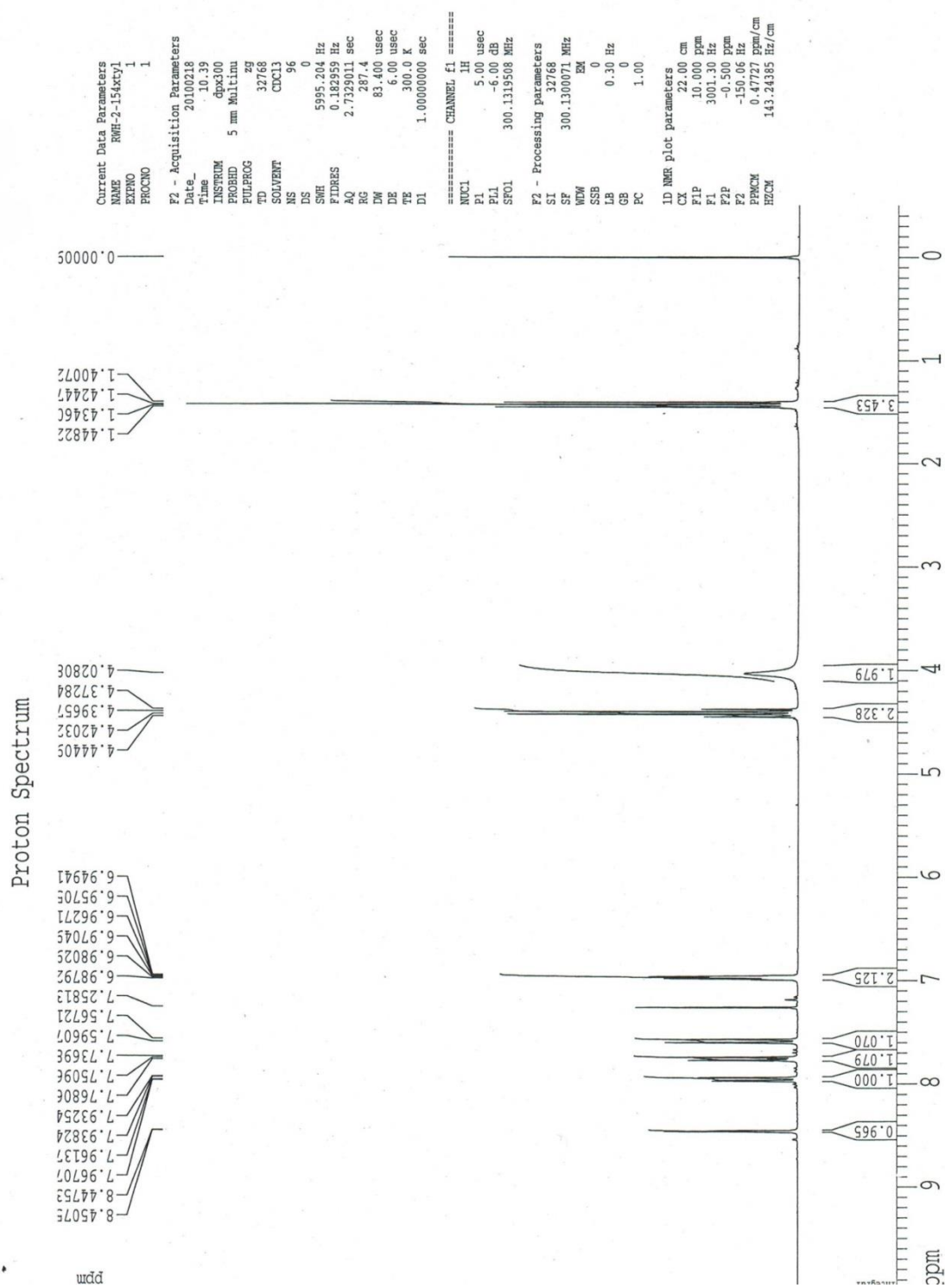
/w version : 1.06
 operator ID : Mark Wang
 Method Name : Minute8
 analysed : 02-14-11 07:11
 Company Name : UWM Chemistry
 Method File : MINUTE8.MTH
 Printed : 2/15/2011 03:21

Sample ID : RWM_2_148 (# 22)
 Analysis Type : UnkNown (Area)
 Chromatogram : C:\EAW\F141119.DAT
 Channel : E.A. Channel A
 Sample weight : 1.485

Calib. method : using 'K Factors'

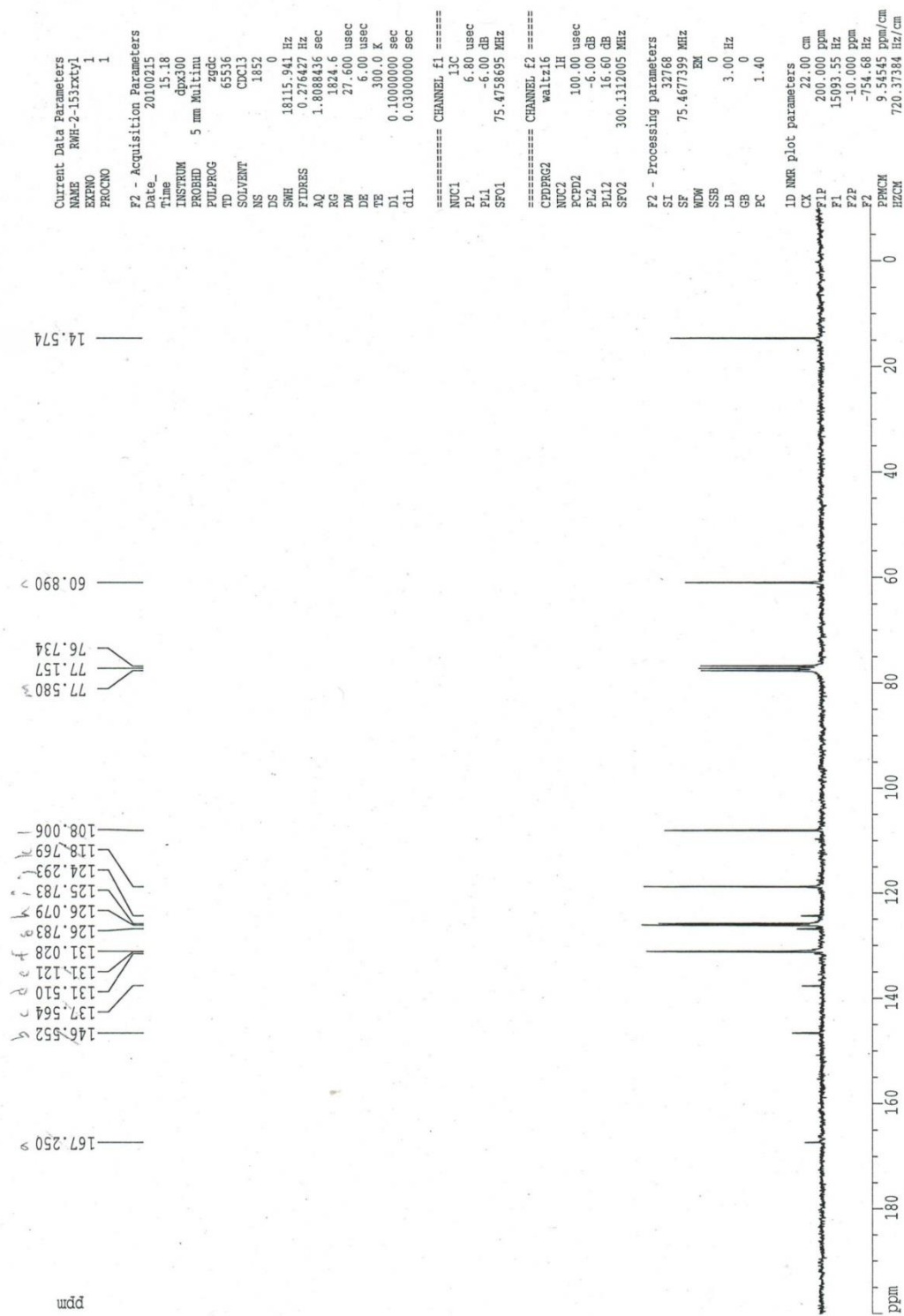
Element Name	Element %	Ret.Time	Area	BC	Area ratio	K factor
Nitrogen	7.2235	1.08	324540	FU	13.923130	.285272E+07
Carbon	56.6855	1.42	4518617	FU	1.000000	.535241E+07
Hydrogen	6.4252	3.44	1409310	RS	3.206262	.147704E+08

¹H NMR Ethyl 6-amino-2-naphthoate (12)

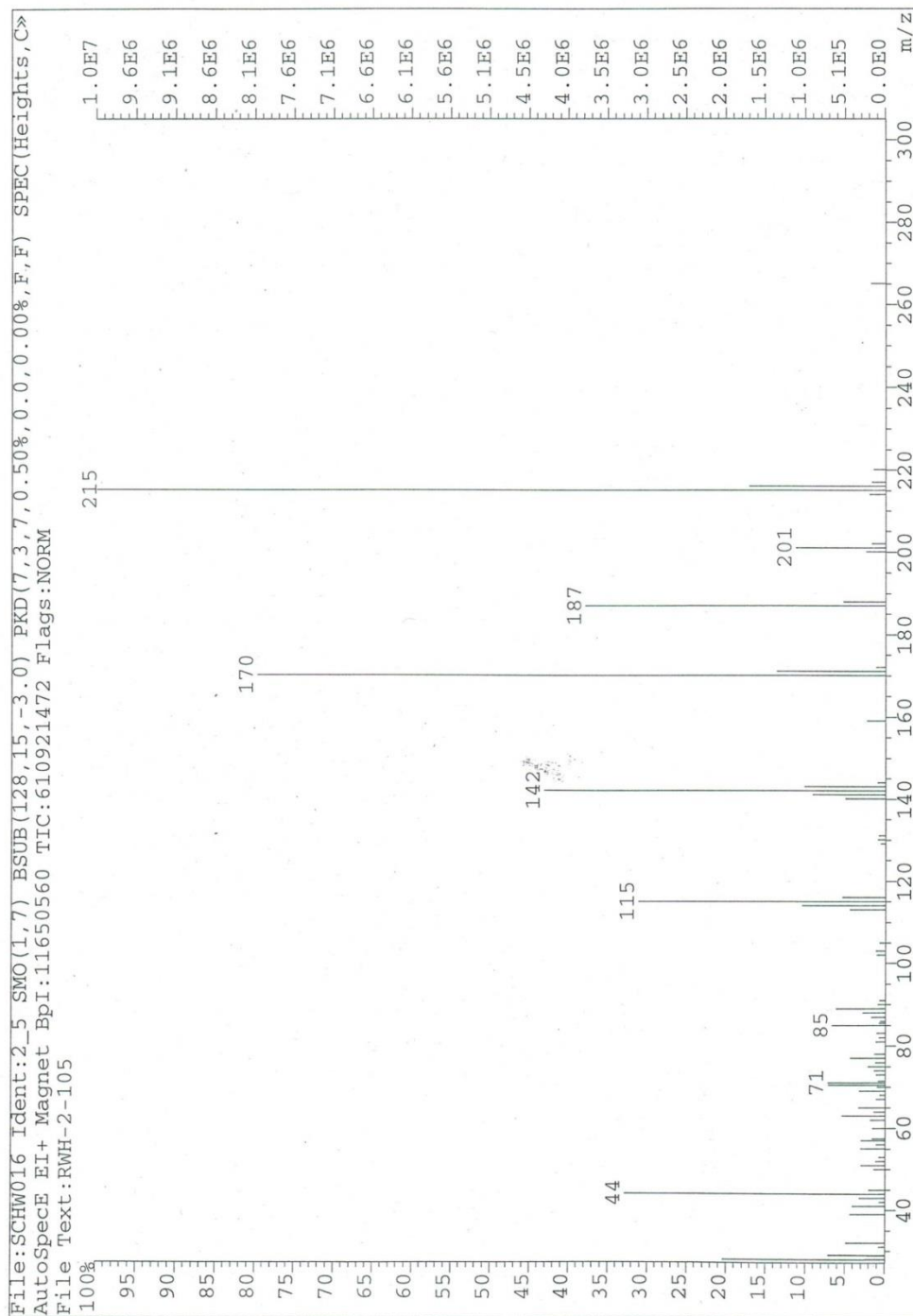


¹³C NMR Ethyl 6-amino-2-naphthoate (12)

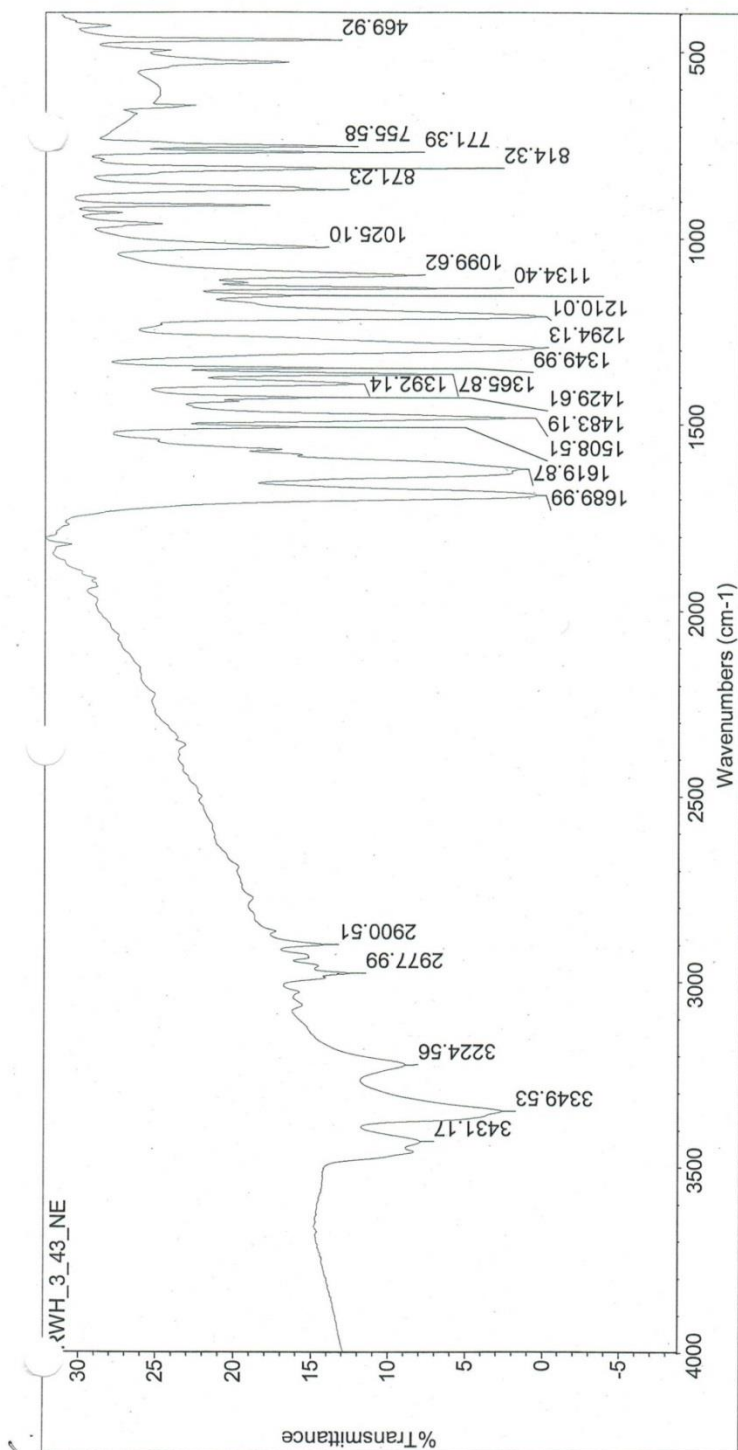
¹³C NMR(CDC13) rextyl NE 76-78C mp range 18.7mg sample



MS Ethyl 6-amino-2-naphthoate (12)



IR Ethyl 6-amino-2-naphthoate (12)



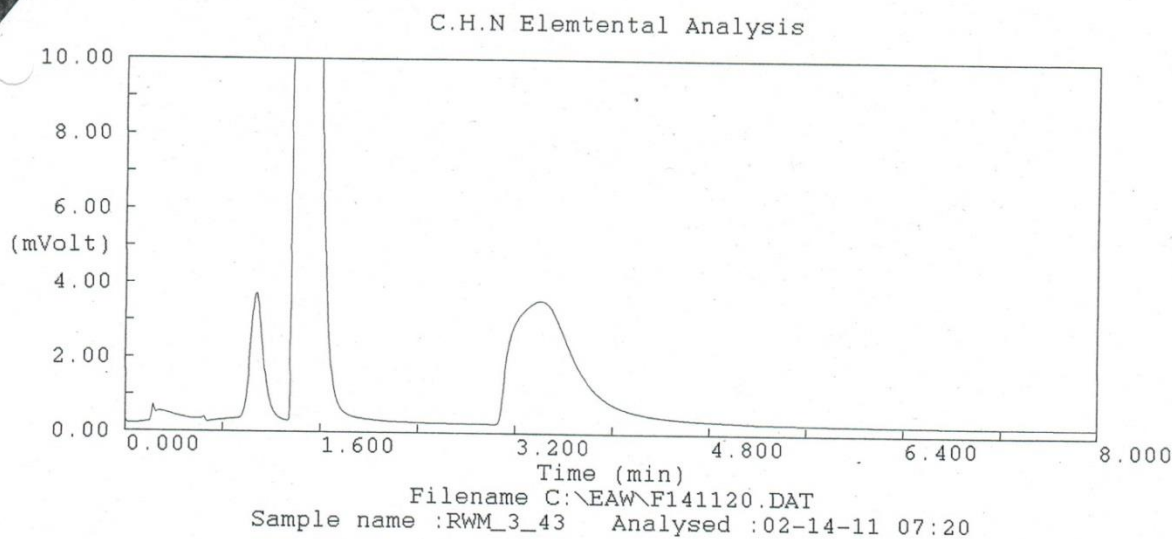
Wed Jan 26 14:27:26 2011 (GMT-06:00)

FIND PEAKS:

Spectrum: RWH_3_43_NE
 Region: 4000.00 - 400.00
 Absolute threshold: 16.295
 Sensitivity: 50
 Peak list:

Position:	Intensity:
469.92	12.992
755.58	12.229
771.39	13.633
814.32	13.489
871.23	13.466
1025.10	14.686
1099.62	8.575
1134.40	5.651

Elem. Anal. Ethyl 6-amino-2-naphthoate (NE)



C.H.N Elemental Analysis

```

Software version : 1.06
Operator ID      : Mark Wang
Method Name     : Minute8
Analysed        : 02-14-11 07:20
Company Name    : UWM Chemistry
Method File     : MINUTE8.MTH
Printed         : 2/15/2011 03:23
  
```

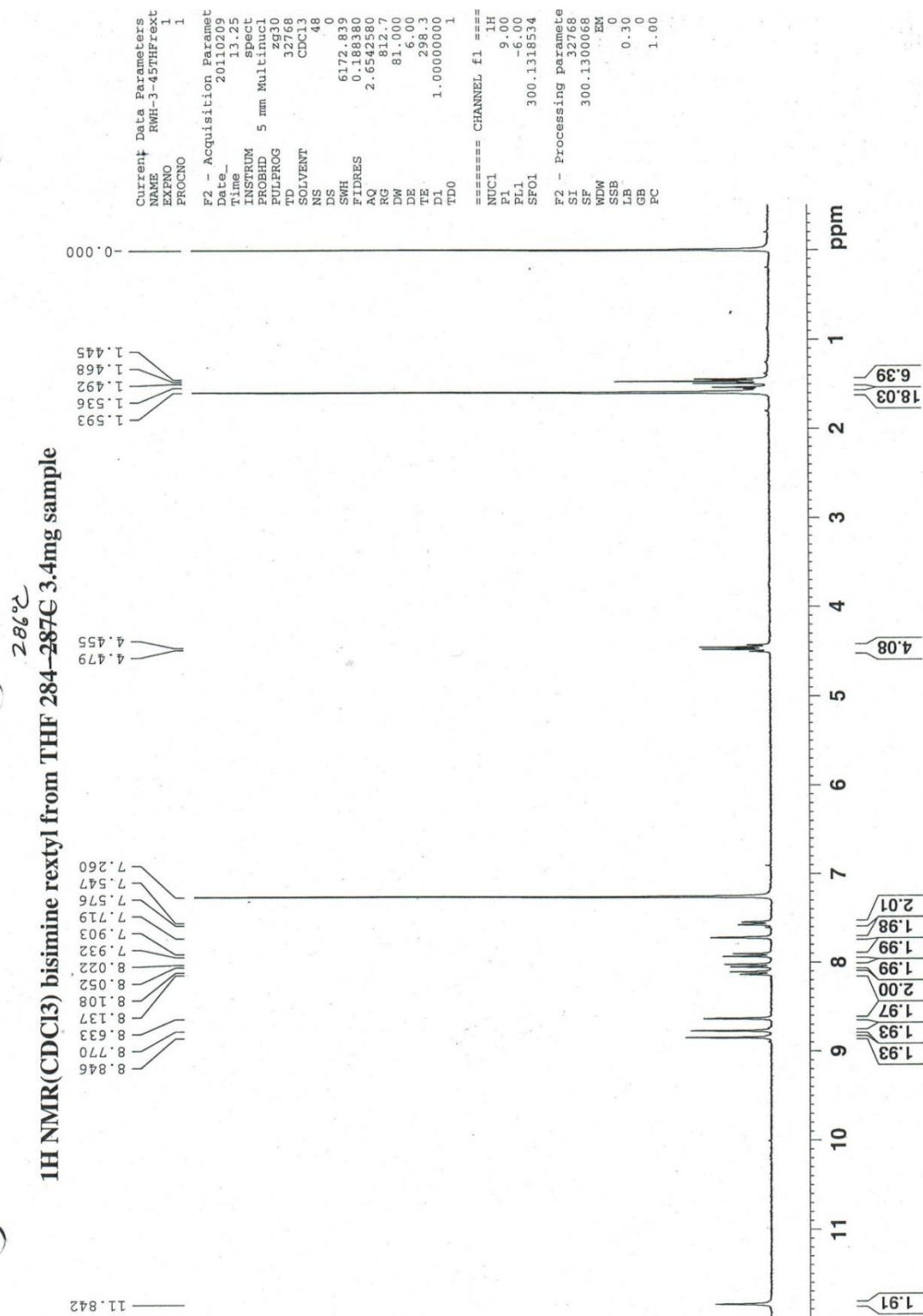
```

Sample ID       : RWM_3_43 (# 23)
Analysis Type   : UnkNown (Area)
Chromatogram    : C:\EAW\F141120.DAT
Channel         : E.A. Channel A
Sample weight   : 1.436
  
```

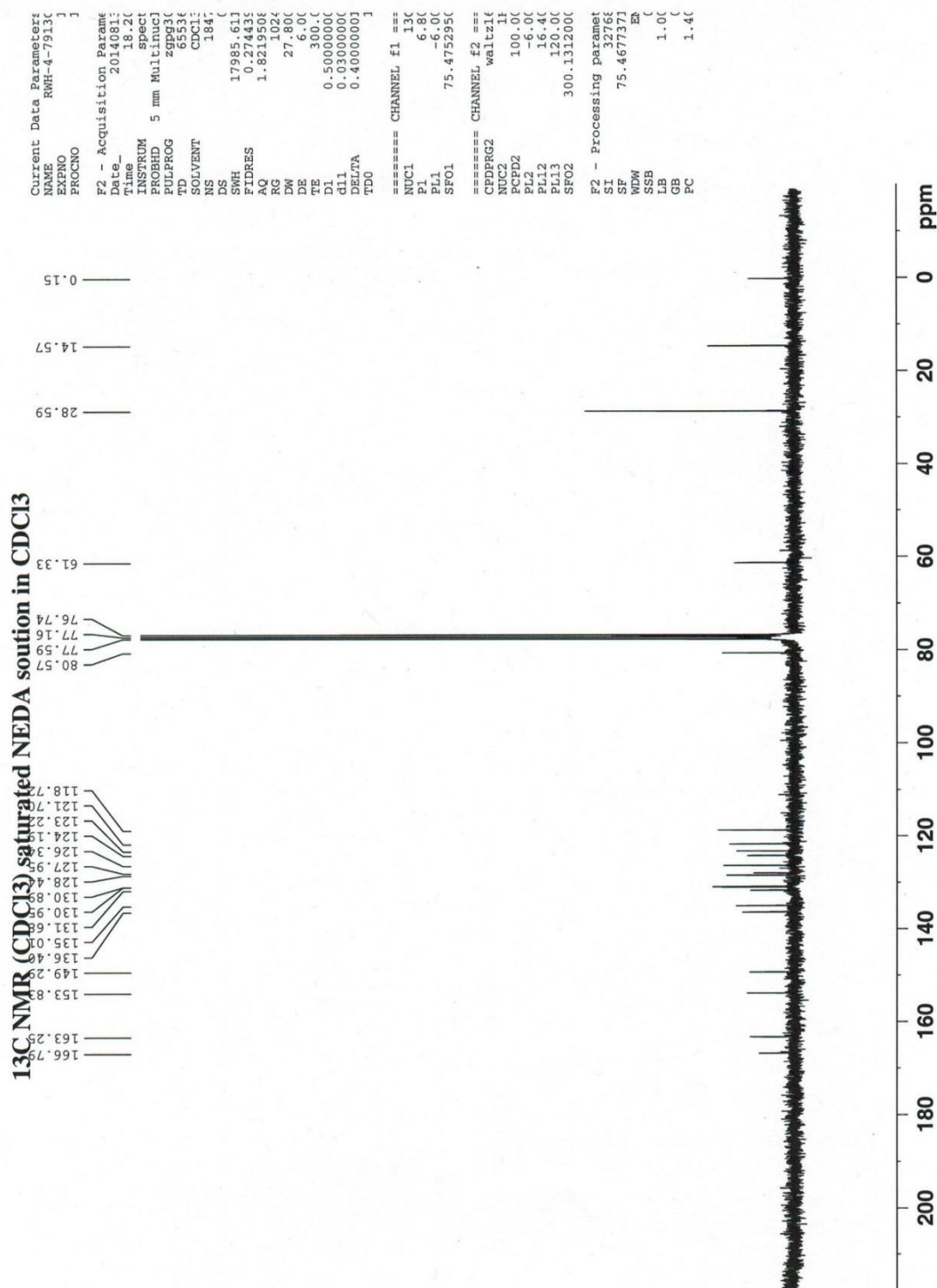
Calib. method : using 'K Factors'

Element Name	Element %	Ret.Time	Area	BC	Area ratio	K factor
Nitrogen	6.3557	1.07	278897	FU	19.840360	.285272E+07
Carbon	71.8228	1.40	5533412	FU	1.000000	.535241E+07
Hydrogen	6.1295	3.41	1300089	RS	4.256179	.147704E+08

¹H NMR Diethyl 6,6'-((1E,1'E)-((2,5-bis((tert-butoxycarbonyl)amino)-1,4-phenylene)bis(methanylylidene))bis(azanylylidene))bis(2-naphthoate) (13)



¹³C NMR Diethyl 6,6'-((1E,1'E)-((2,5-bis((tert-butoxycarbonyl)amino)-1,4-phenylene)bis(methanylylidene))bis(azanylylidene))bis(2-naphthoate) (13)



ESI-MS Diethyl 6,6'-((1E,1'E)-((2,5-bis((tert-butoxycarbonyl)amino)-1,4-phenylene)bis(methanylylidene))bis(azanylylidene))bis(2-naphthoate) (13)

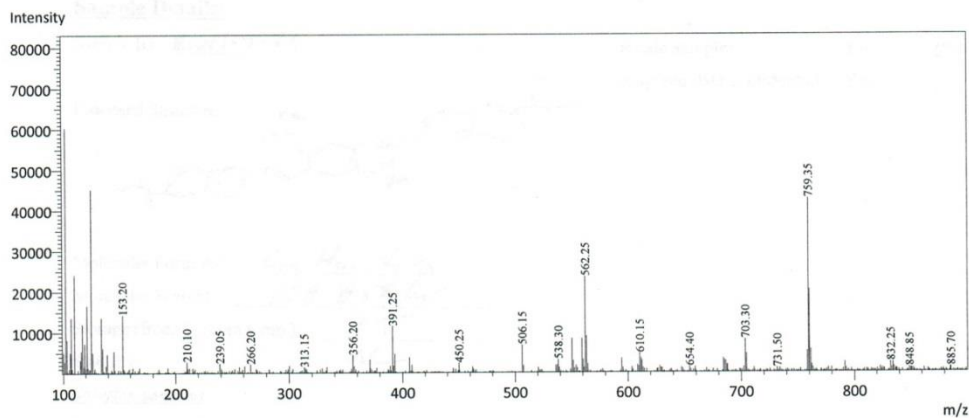
9/23/2015 10:21:59 AM Page 1 / 1

Shimadzu LCMS-2020 Data Report

Mass Spectrum for Sample
RWH-4-80.lcd

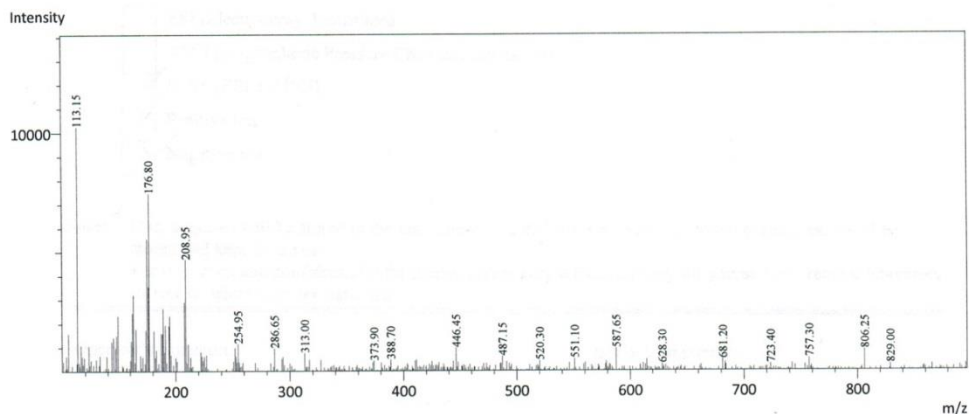
Operator: Tyler Fenske

Data Filename: C:\LabSolutions\Data\Schwabacher Alan\RWH-4-80.lcd
Spectrum Mode: Averaged
Retention Time: ----
Interface Type (ESI, APCI, DUIS): DUIS
Acquisition Mode: (Scan, SIM, Profile): Scan
Polarity: +
H₂O/0.1% HCOOH, CH₃CN/0.1% HCOOH

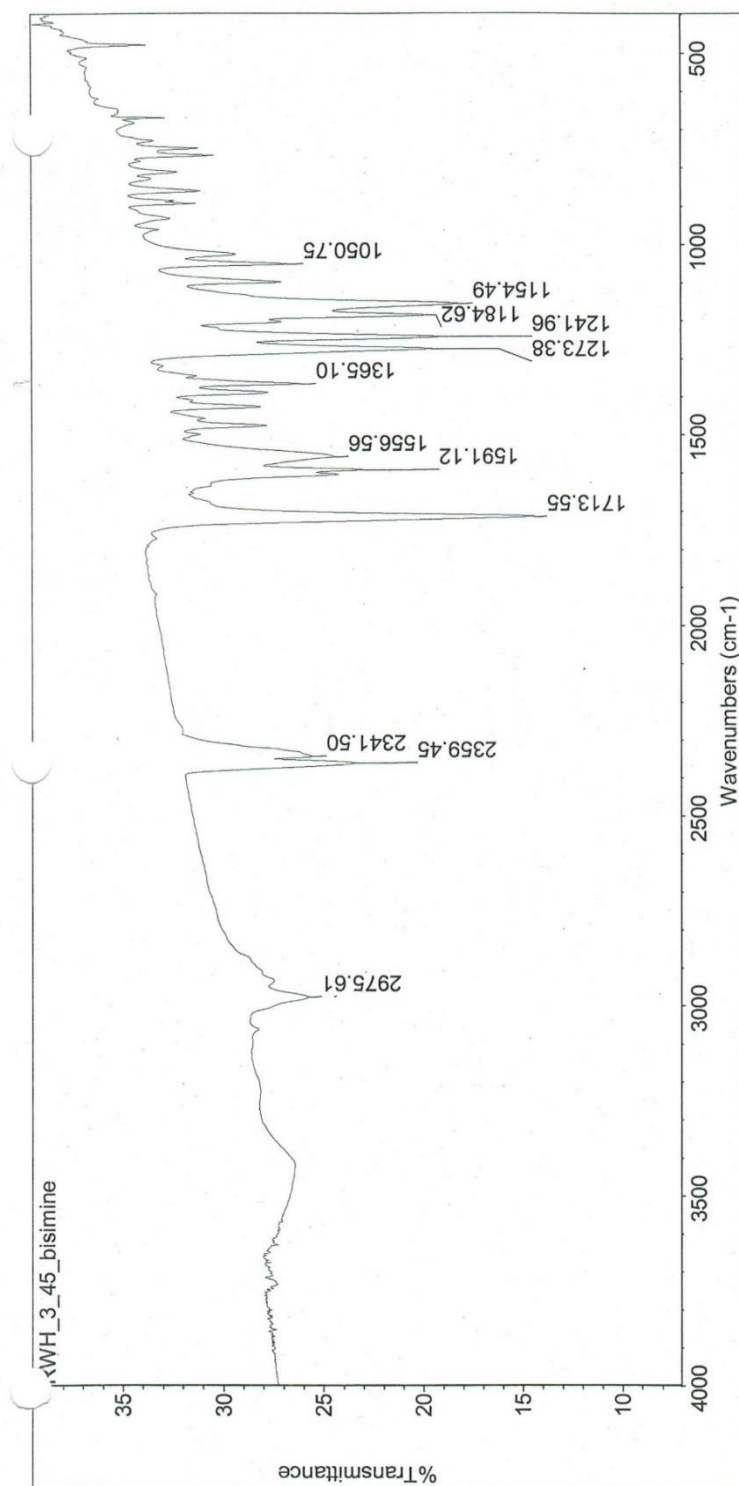


Operator: Tyler Fenske

Data Filename: C:\LabSolutions\Data\Schwabacher Alan\RWH-4-80.lcd
Spectrum Mode: Averaged
Retention Time: ----
Interface Type (ESI, APCI, DUIS): DUIS
Acquisition Mode: (Scan, SIM, Profile): Scan
Polarity: -
H₂O/0.1% HCOOH, CH₃CN/0.1% HCOOH



IR *Diethyl 6,6'-(1E,1'E)-((2,5-bis((tert-butoxycarbonyl)amino)-1,4-phenylene)bis(methanylylidene))bis(azanylylidene))bis(2-naphthoate) (13)*



Wed Feb 09 14:43:38 2011 (GMT-06:00)

FIND PEAKS:

Spectrum: RWH_3_45_bisimine

Region: 4000.00 400.00

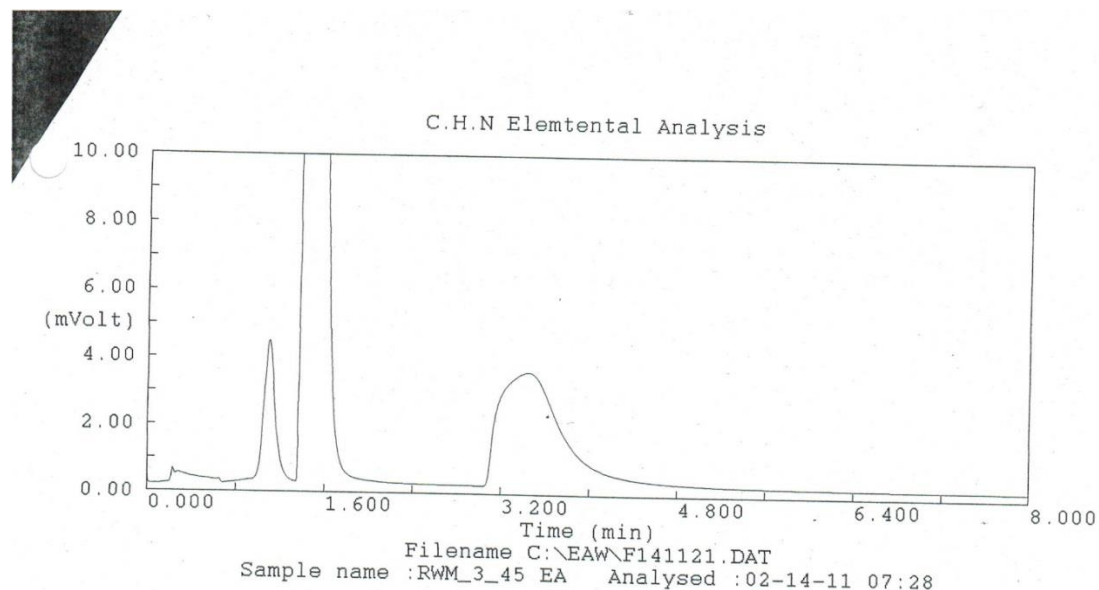
Absolute threshold: 26.926

Sensitivity: 37

Peak list:

Position:	Intensity:
1050.75	26.658
1154.49	18.146
1184.62	19.705
1241.96	19.060
1273.38	19.369
1365.10	26.031
1556.56	24.452
1591.12	22.840

Elem. Anal. Diethyl 6,6'-((1E,1'E)-((2,5-bis((tert-butoxycarbonyl)amino)-1,4-phenylene)bis(methanylylidene))bis(azanylylidene))bis(2-naphthoate) (13)



C.H.N Elemental Analysis

Version : 1.06
Operator ID : Mark Wang
Method Name : Minute8
Analysed : 02-14-11 07:28
Company Name : UWM Chemistry
Method File : MINUTE8.MTH
Printed : 2/15/2011 03:25

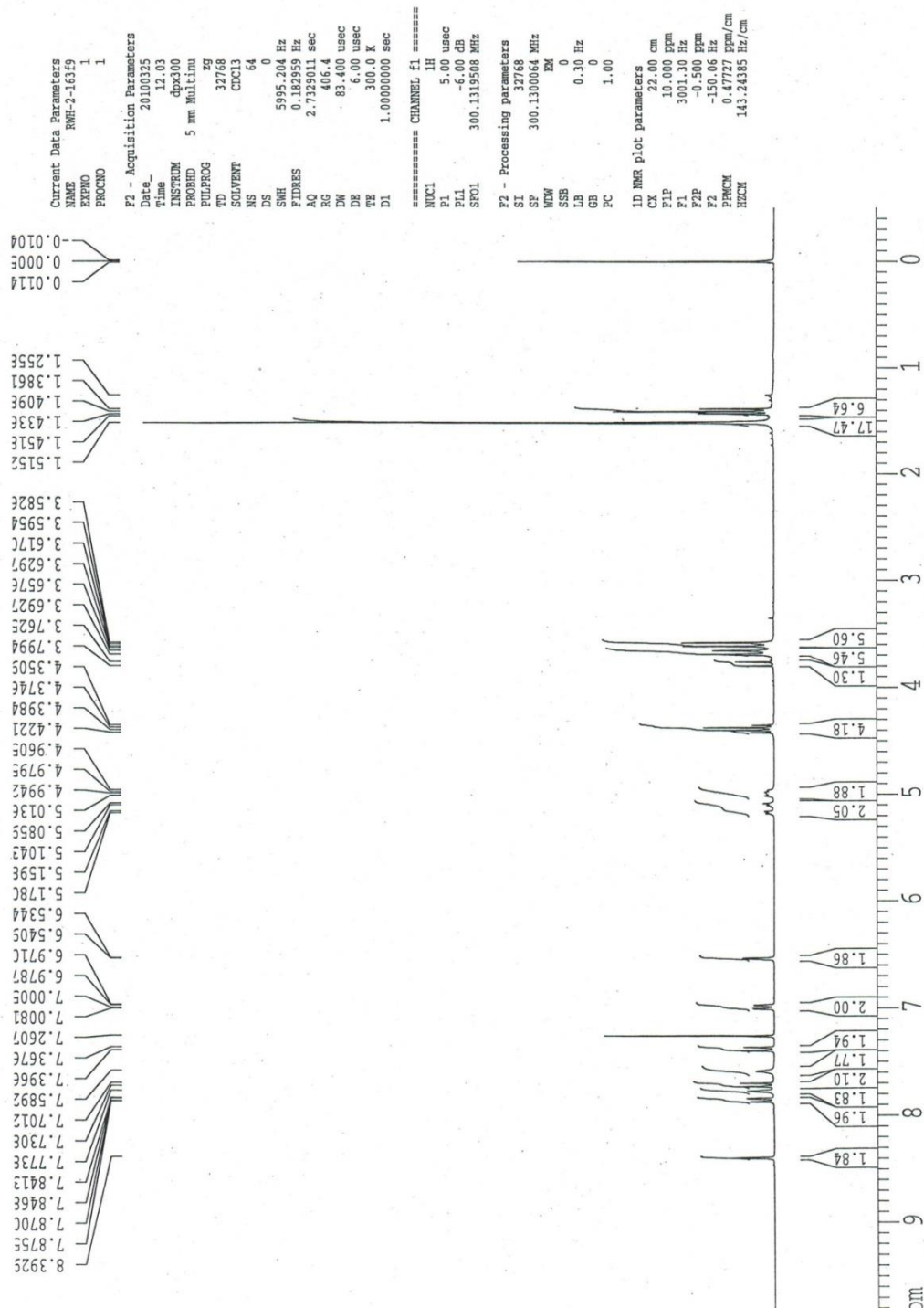
Sample ID : RWM_3_45 EA (# 24)
Analysis Type : UnkNown (Area)
Chromatogram : C:\EAW\F141121.DAT
Channel : E.A. Channel A
Sample weight : 1.547

Calib. method : using 'K Factors'

Element Name	Element %	Ret.Time	Area	BC	Area ratio	K factor
Nitrogen	6.7996	1.09	318612	FU	17.569540	.285272E+07
Carbon	67.4477	1.41	5597861	TL	1.000000	.535241E+07
Hydrogen	6.1159	3.44	1397467	CR	4.005720	.147704E+08

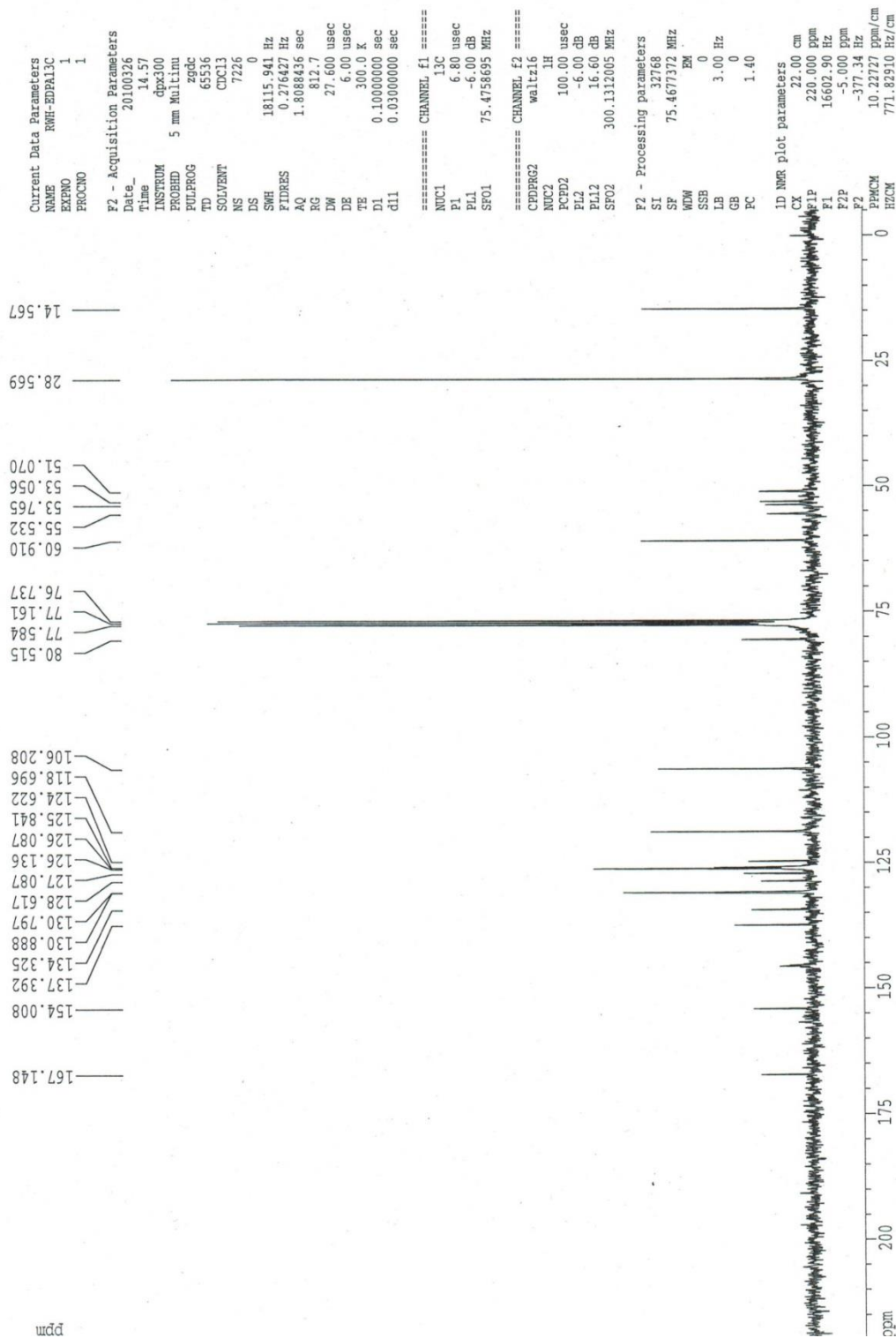
¹H NMR Diethyl 6,6'-(((1R,1'S)-(2,5-bis((tert-butoxycarbonyl)amino)-1,4-phenylene)bis((dimethoxyphosphoryl)methylene))bis(azanediyl)))bis(2-naphthoate) (16)

¹H NMR (CDCl₃) f9-19 40%ACN/DCM EDPA



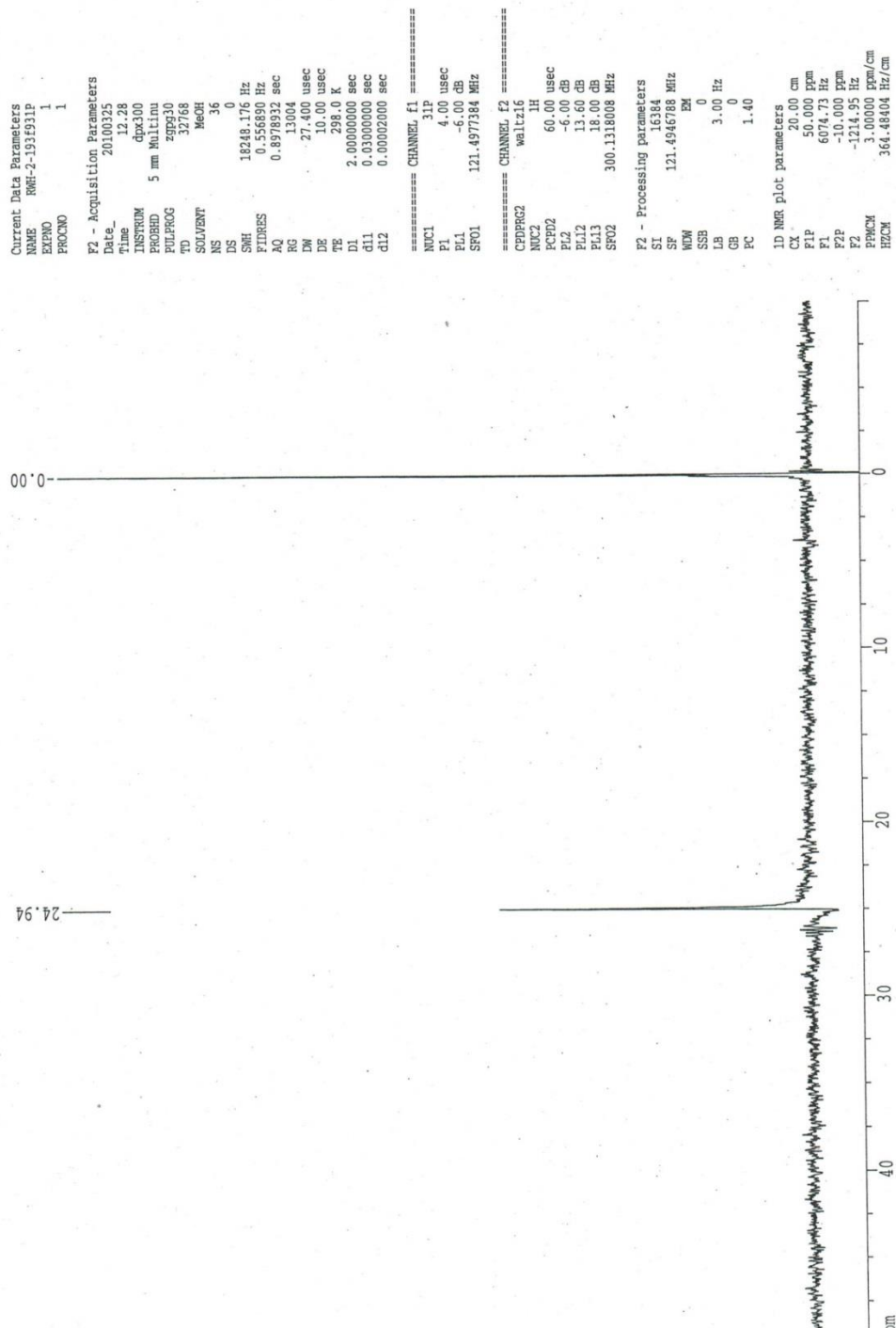
¹³C NMR Diethyl 6,6'-(((1R,1'S)-(2,5-bis((tert-butoxycarbonyl)amino)-1,4-phenylene)bis((dimethoxyphosphoryl)methylene))bis(azanediyl)))bis(2-naphthoate) (16)

¹³C NMR (CDCl₃) RWH-2-163 EDPA



³¹P NMR Diethyl 6,6'-(((1R,1'S)-(2,5-bis((tert-butoxycarbonyl)amino)-1,4-phenylene)bis((dimethoxyphosphoryl)methylene))bis(azanediyl)))bis(2-naphthoate) (16)

31P NMR(CDC13) f9-19 40%ACN/DCM EDPA



ESI-MS Diethyl 6,6'-(((1R,1'S)-(2,5-bis((tert-butoxycarbonyl)amino)-1,4-phenylene)bis((dimethoxyphosphoryl)methylene))bis(azanediyl))bis(2-naphthoate) (16)

9/5/2014 10:57:16 AM Page 1 / 1

Shimadzu LCMS-2020 Data Report

Mass Spectrum for Sample
RWH-4-84 01.lcd

Operator: Mark Wang

Data Filename: C:\LabSolutions\Data\Schwabacher Alan\RWH-4-84 01.lcd

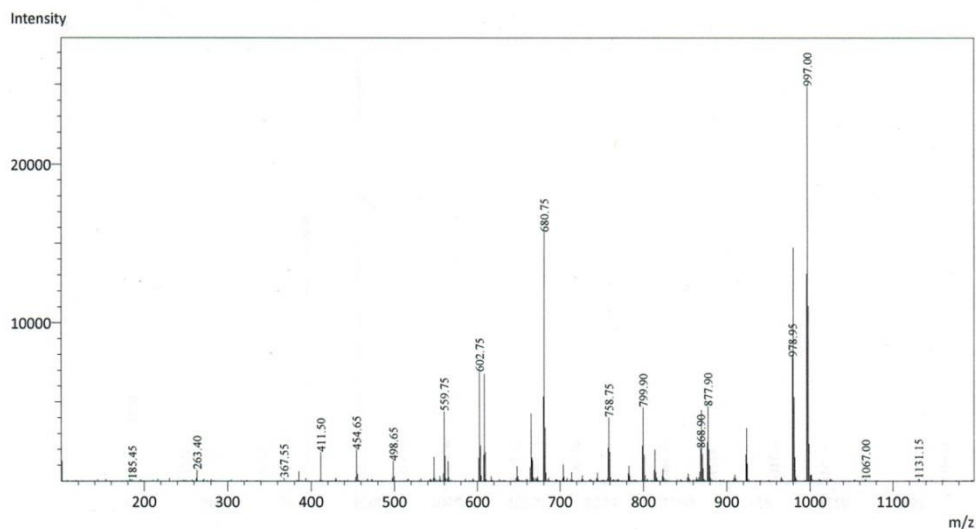
Spectrum Mode: Averaged

Retention Time: ----

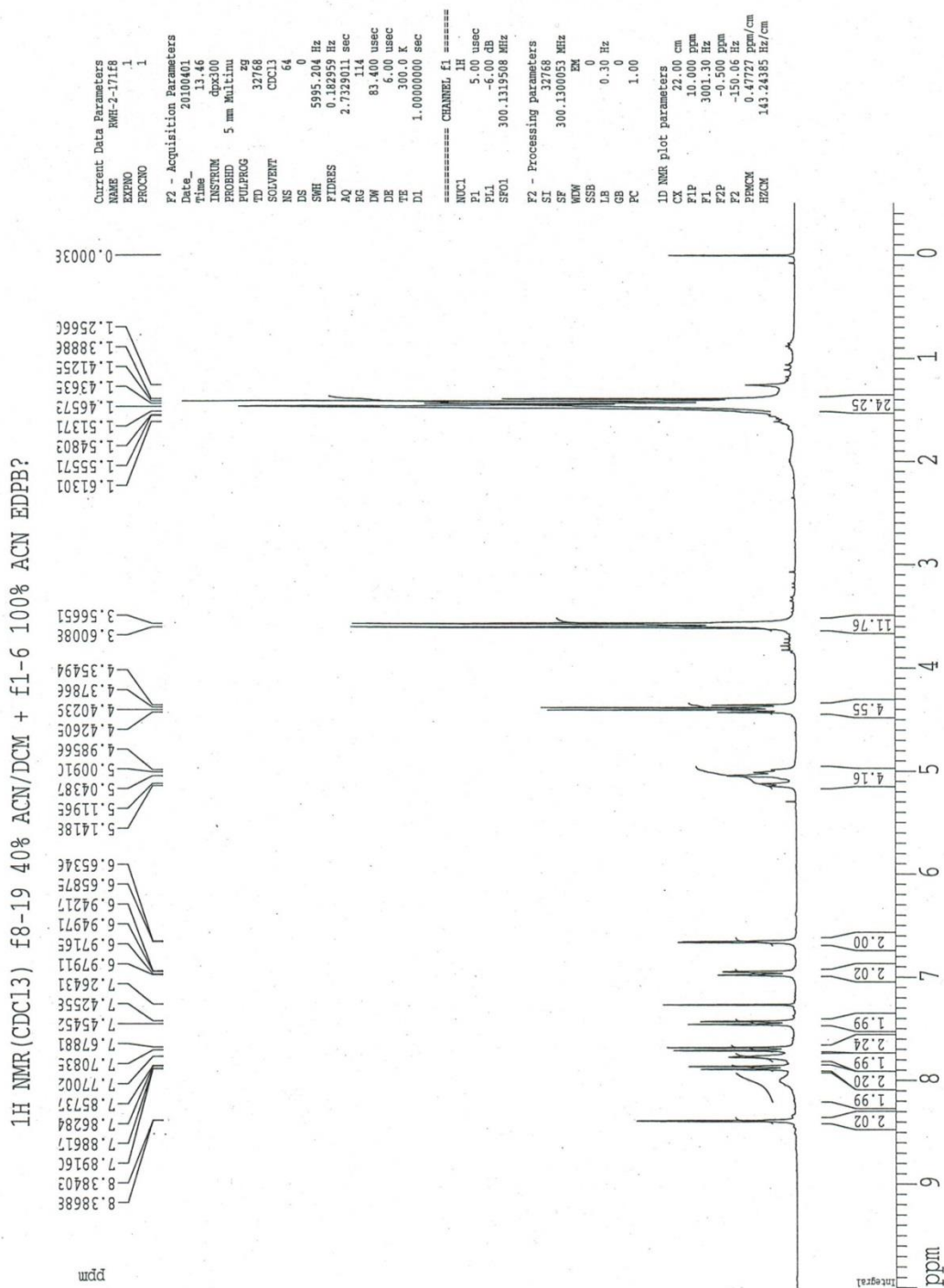
Interface Type (ESI, APCI, DUIS): DUIS

Acquisition Mode (Scan, SIM, Profile): Scan

Polarity: +

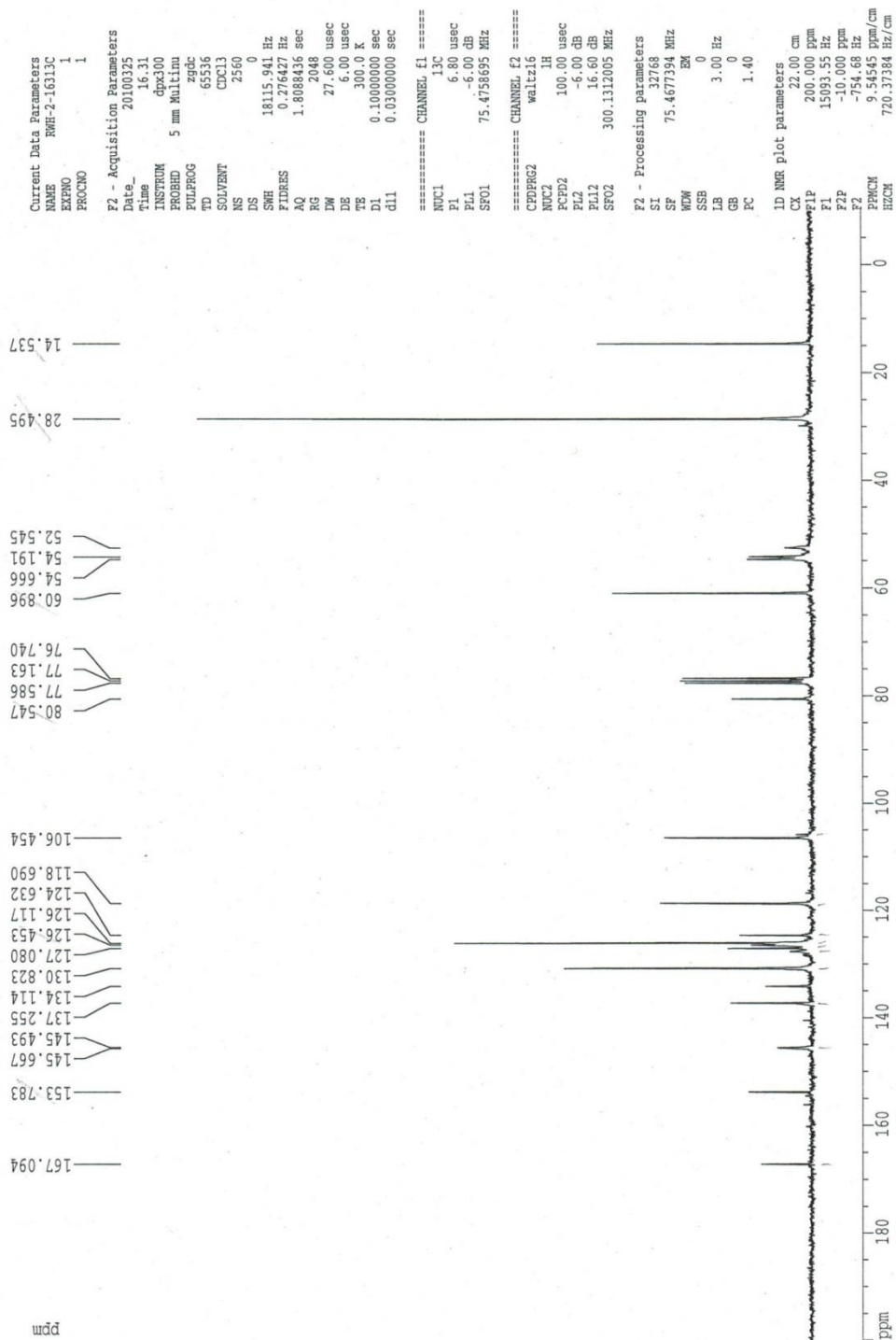


¹H NMR Diethyl 6,6'-(((1S,1'S)-(2,5-bis((tert-butoxycarbonyl)amino)-1,4-phenylene)bis((dimethoxyphosphoryl)methylene))bis(azanediyl)))bis(2-naphthoate) (17)



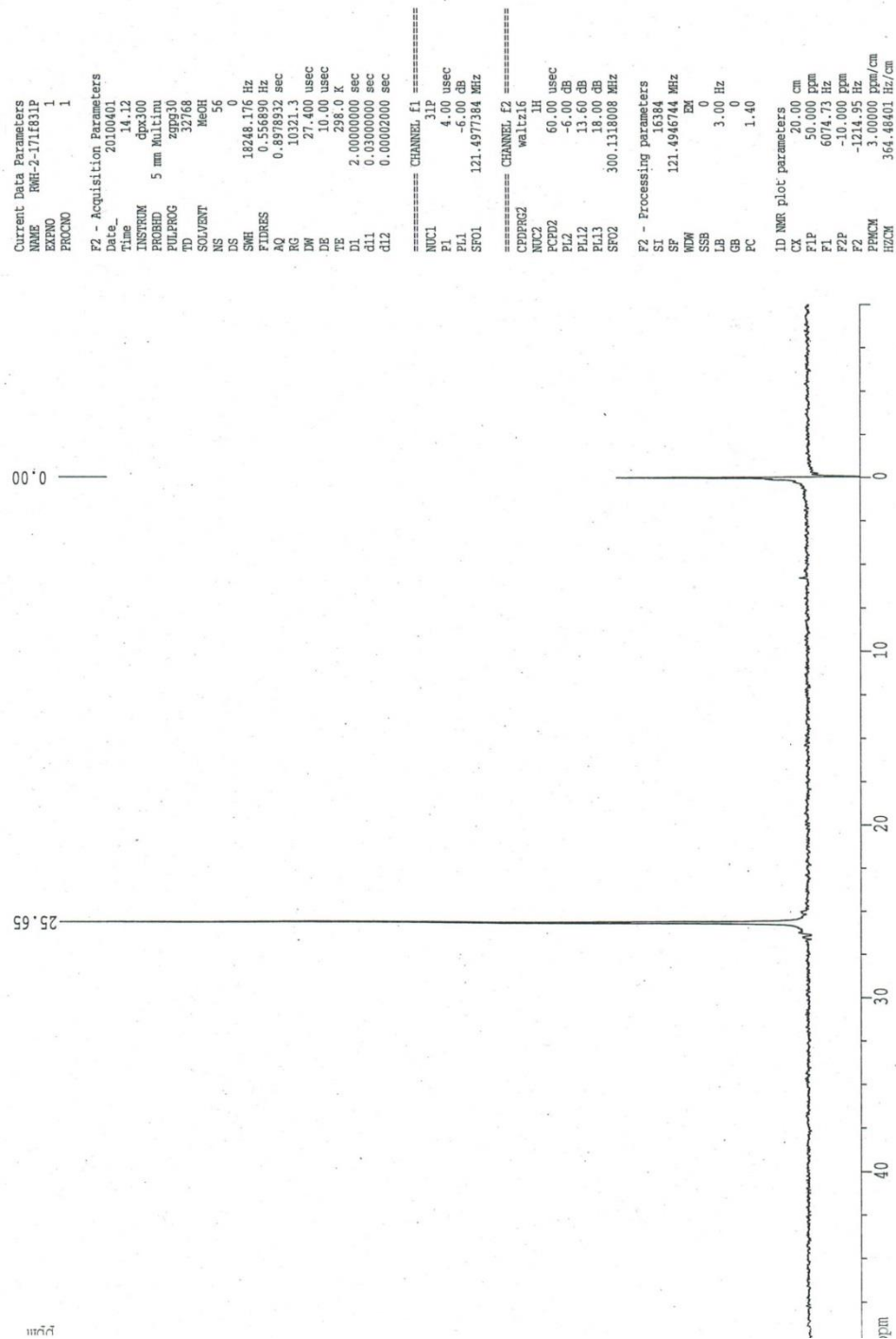
¹³C NMR Diethyl 6,6'-(((1S,1'S)-(2,5-bis((tert-butoxycarbonyl)amino)-1,4-phenylene)bis((dimethoxyphosphoryl)methylene))bis(azanediyl)))bis(2-naphthoate) (17)

¹³C NMR (CDCl₃) RWH-2-163 EDPB



³¹P NMR Diethyl 6,6'-(((1S,1'S)-(2,5-bis((tert-butoxycarbonyl)amino)-1,4-phenylene)bis((dimethoxyphosphoryl)methylene))bis(azanediyl)))bis(2-naphthoate) (17)

31P NMR (CDCl3) f8-19 40% ACN/DCM + f1-6 100% ACN EDPB



ESI-MS Diethyl 6,6'-(((1S,1'S)-(2,5-bis((tert-butoxycarbonyl)amino)-1,4-phenylene)bis((dimethoxyphosphoryl)methylene))bis(azanediyl))bis(2-naphthoate) (17)

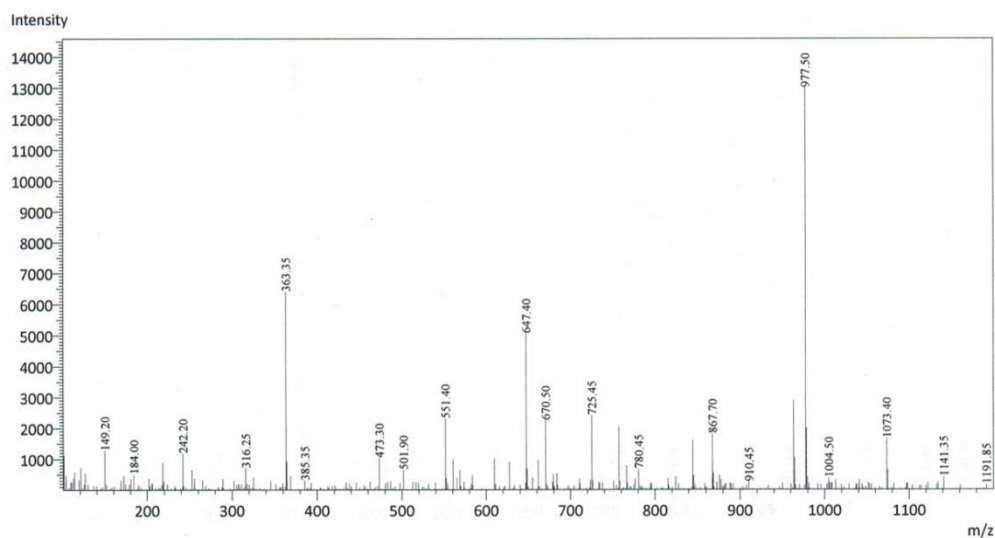
9/5/2014 10:57:29 AM Page 1 / 1

Shimadzu LCMS-2020 Data Report

Mass Spectrum for Sample
RWH-4-84 01.lcd

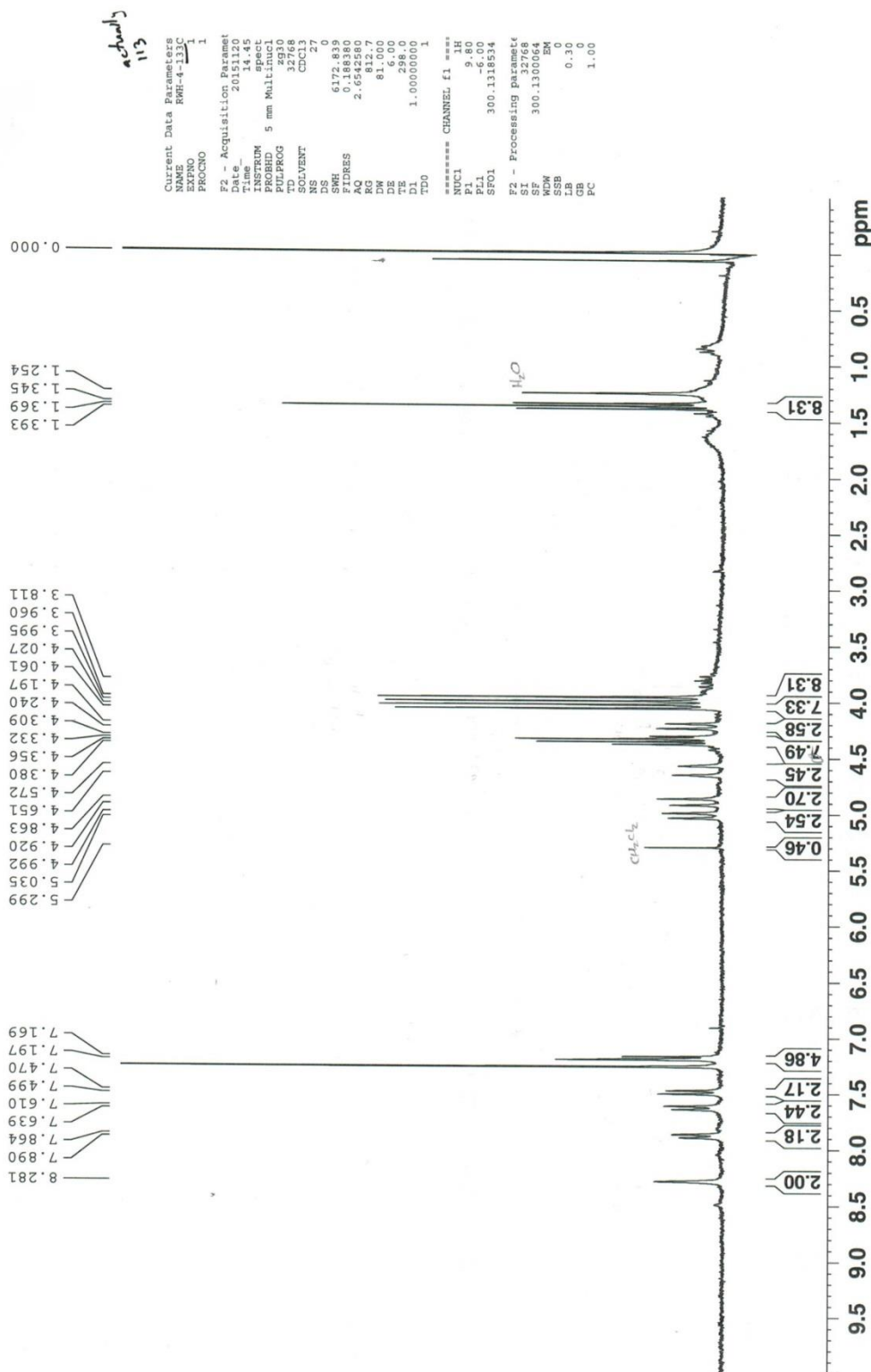
Operator: Mark Wang

Data Filename: C:\LabSolutions\Data\Schwabacher Alan\RWH-4-84 01.lcd
Spectrum Mode: Averaged
Retention Time: ---
Interface Type (ESI, APCI, DUIS): DUIS
Acquisition Mode: (Scan, SIM, Profile): Scan
Polarity: -



¹H NMR C-Me, P-Me rac-tweezers (18)

¹H NMR (CDCl₃) 3.0x10⁻³M P-Me, C-Et rac tweezers



¹³C NMR C-Me, P-Me rac-tweezers (18)

¹³C NMR (CDCl₃) rac- P-Me, C-Et naphthyl tweezers 21.3mg sample

```

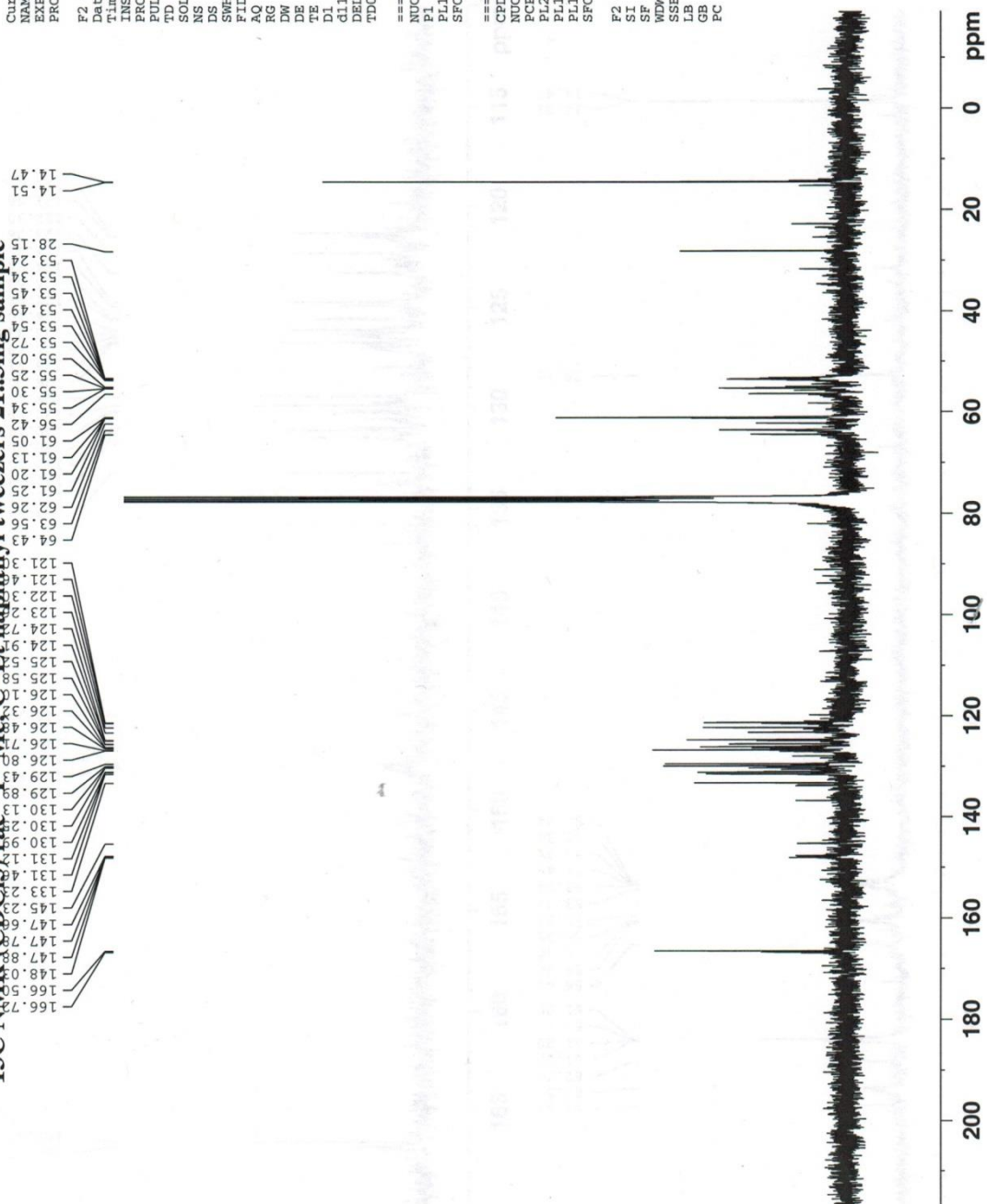
Current Data Parameters:
NAME      RWH-4-61rac13
EXPNO     1
PROCNO    1

F2 - Acquisition Parameters
Date_     20140614
Time      17.4
INSTRUM   spect
PROBHD    5 mm Multinuc
PULPROG   zgpg30
TD        65536
SOLVENT   CDCl3
NS        2400
DS        4
SWH        17985.613
FIDRES     0.274435
AQ         1.8219506
RG         645.1
DE         27.800
TE         300.2
D1         0.50000000
d11        0.03000000
DELTA     0.40000001
TDO        0

===== CHANNEL f1 =====
NUC1       13C
P1         6.80
PL1        -6.00
SFO1       75.4752950

===== CHANNEL f2 =====
CPDPRG2    waltz16
NUC2       1H
PCPD2      100.00
PL2        -6.00
PL12       16.40
PL13       120.00
SFO2       300.1312000

F2 - Processing parameters
SI         32768
SF         75.4677385
WDW         EM
SSB         0
LB         1.00
GB         0
PC         1.40
  
```



³¹P NMR C-Me, P-Me rac-tweezers (18)

³¹P NMR (CDCl₃) conc. toluene mother liquor from rextl of tweezers mix

```

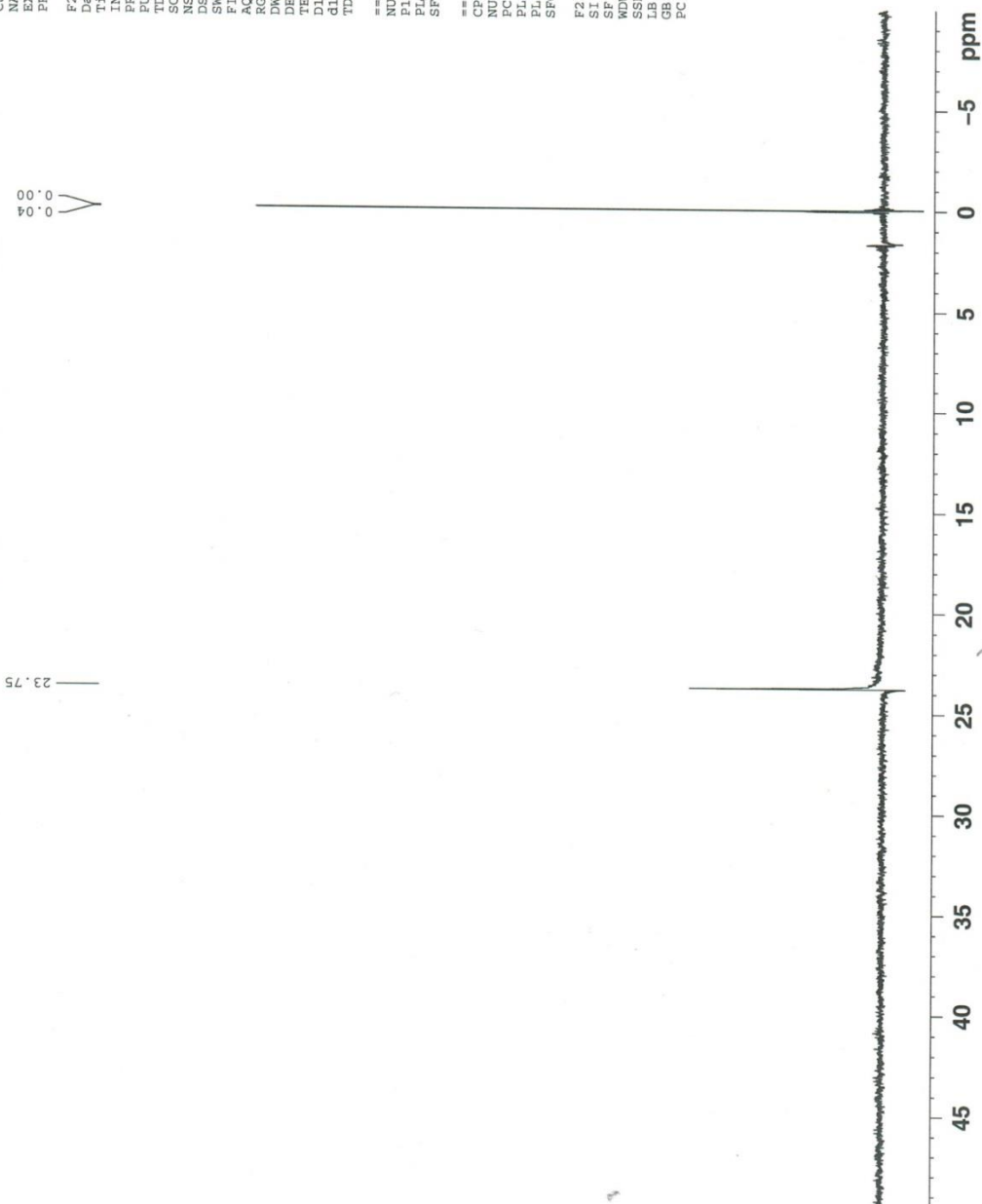
Current Data Parameters:
NAME      RWH-4-108rac31
EXPNO     1
PROCNO    1

F2 - Acquisition Parameters
Date_     20151101
Time      17.01
INSTRUM   spect
PROBHD    5 mm Multinucl
PULPROG   zgpg30
TD        65536
SOLVENT   CDCl3
NS         4
DS         4
SWH        17985.611
FIDRES     0.27443
AQ         1.82190
RG         319.0
DE         27.80
TE         300.2
D1         0.2000000
d11        0.0300000
TD0        1

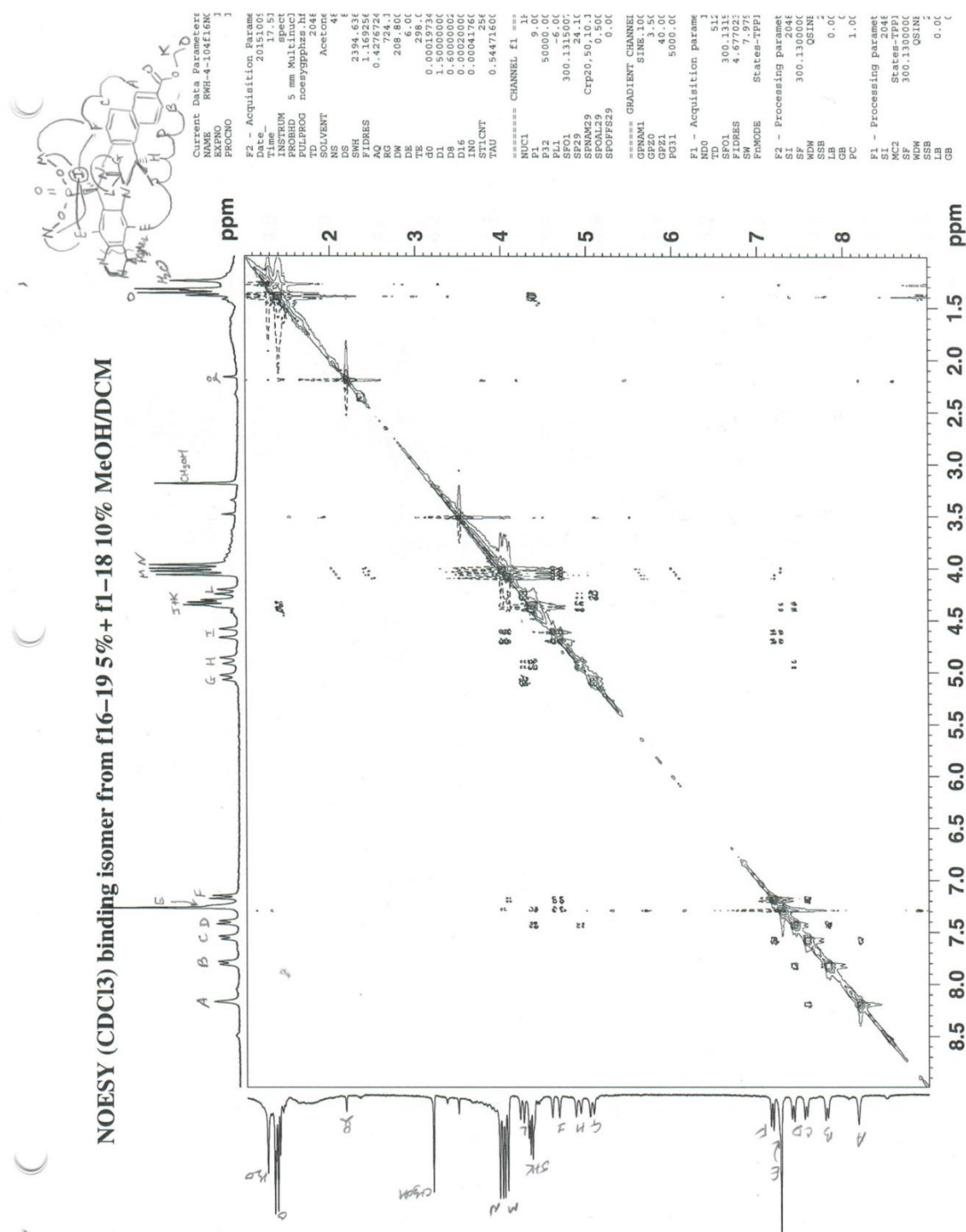
===== CHANNEL f1 =====
NUC1       31P
P1         8.00
PL1        -6.00
SFO1       121.497281

===== CHANNEL f2 =====
CPDPRG2    waitz16
NUC2       1H
PCPD2      100.00
PL2        -6.00
PL12       17.85
SFO2       300.131200

F2 - Processing parameters
SI         32768
SF         121.494682
WDW        EM
SSB        0
LB         1.00
GB         0
PC         1.40
  
```



COSY *C*-Me, *P*-Me *rac*-tweezers (18)



Shimadzu LCMS-2020 Data Report

Mass Spectrum for Sample
RWH-4-108rac.lcd

Operator: Robert Hoppe

Data Filename: C:\LabSolutions\Data\Schwabacher Alan\RWH-4-108rac.lcd

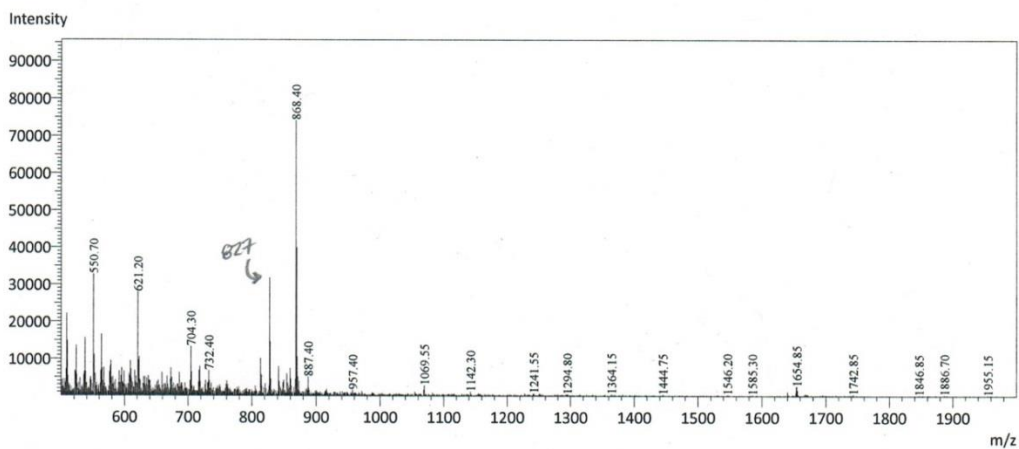
Spectrum Mode: Averaged

Retention Time: ----

Interface Type (ESI, APCI, DUIS): DUIS

Acquisition Mode: (Scan, SIM, Profile): Scan

Polarity: +

H₂O/0.1% HCOOH, CH₃CN/0.1% HCOOH

Operator: Robert Hoppe

Data Filename: C:\LabSolutions\Data\Schwabacher Alan\RWH-4-108rac.lcd

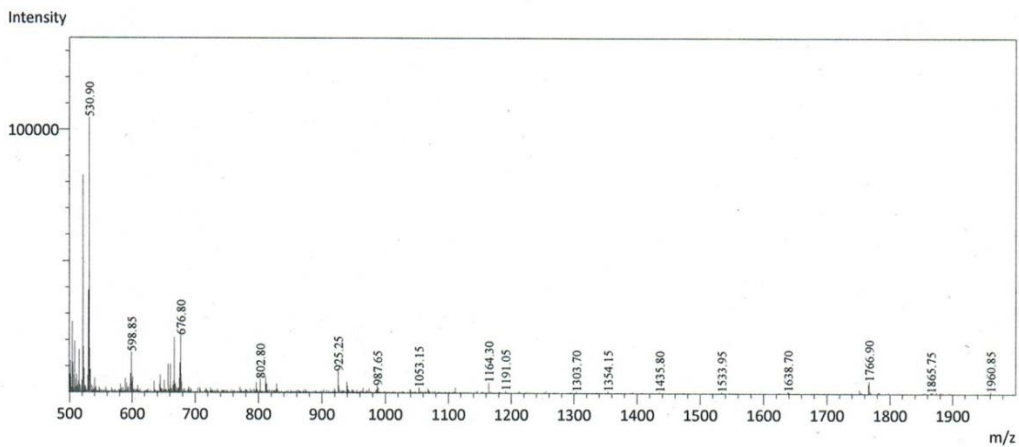
Spectrum Mode: Averaged

Retention Time: ----

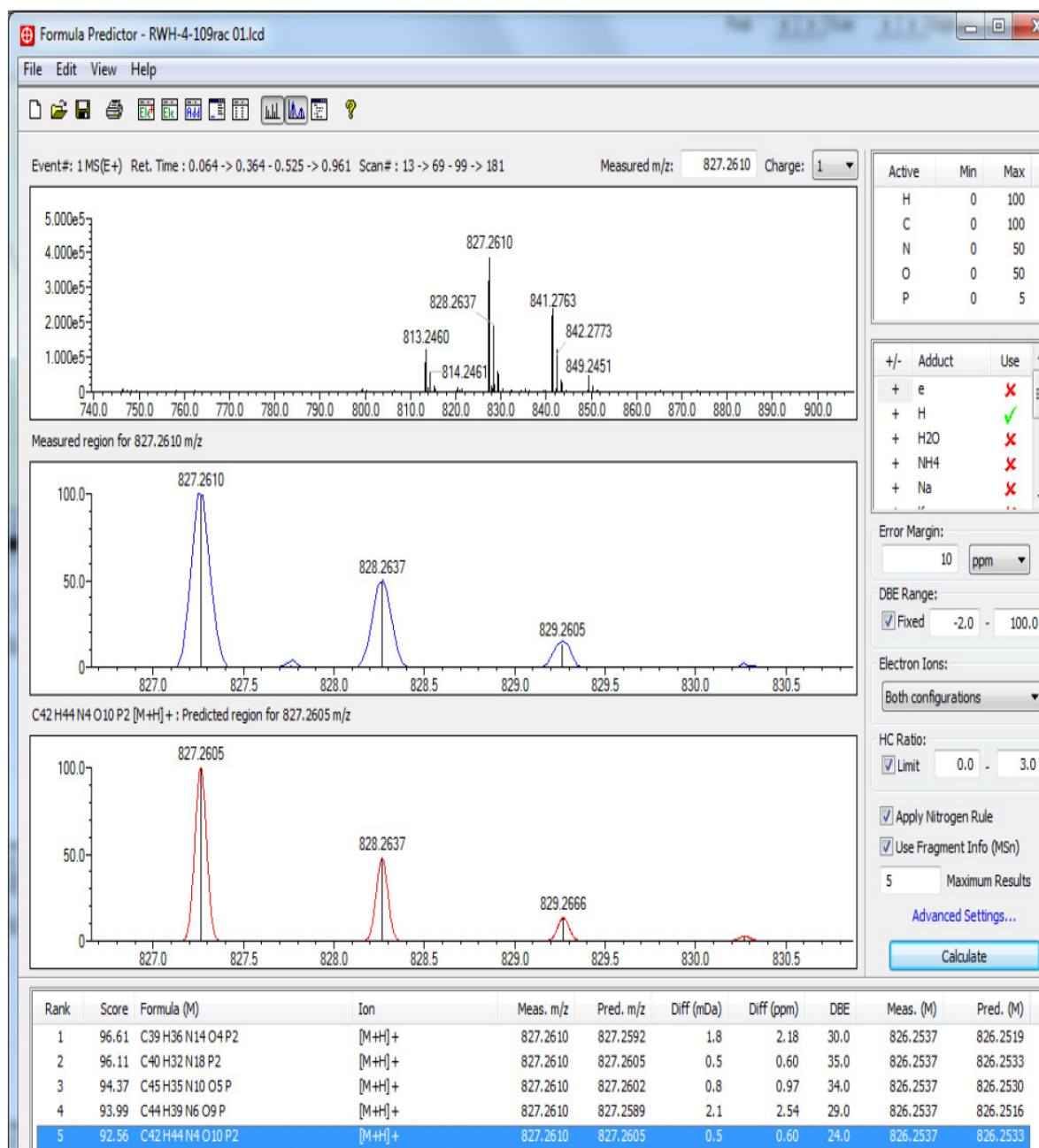
Interface Type (ESI, APCI, DUIS): DUIS

Acquisition Mode: (Scan, SIM, Profile): Scan

Polarity: -

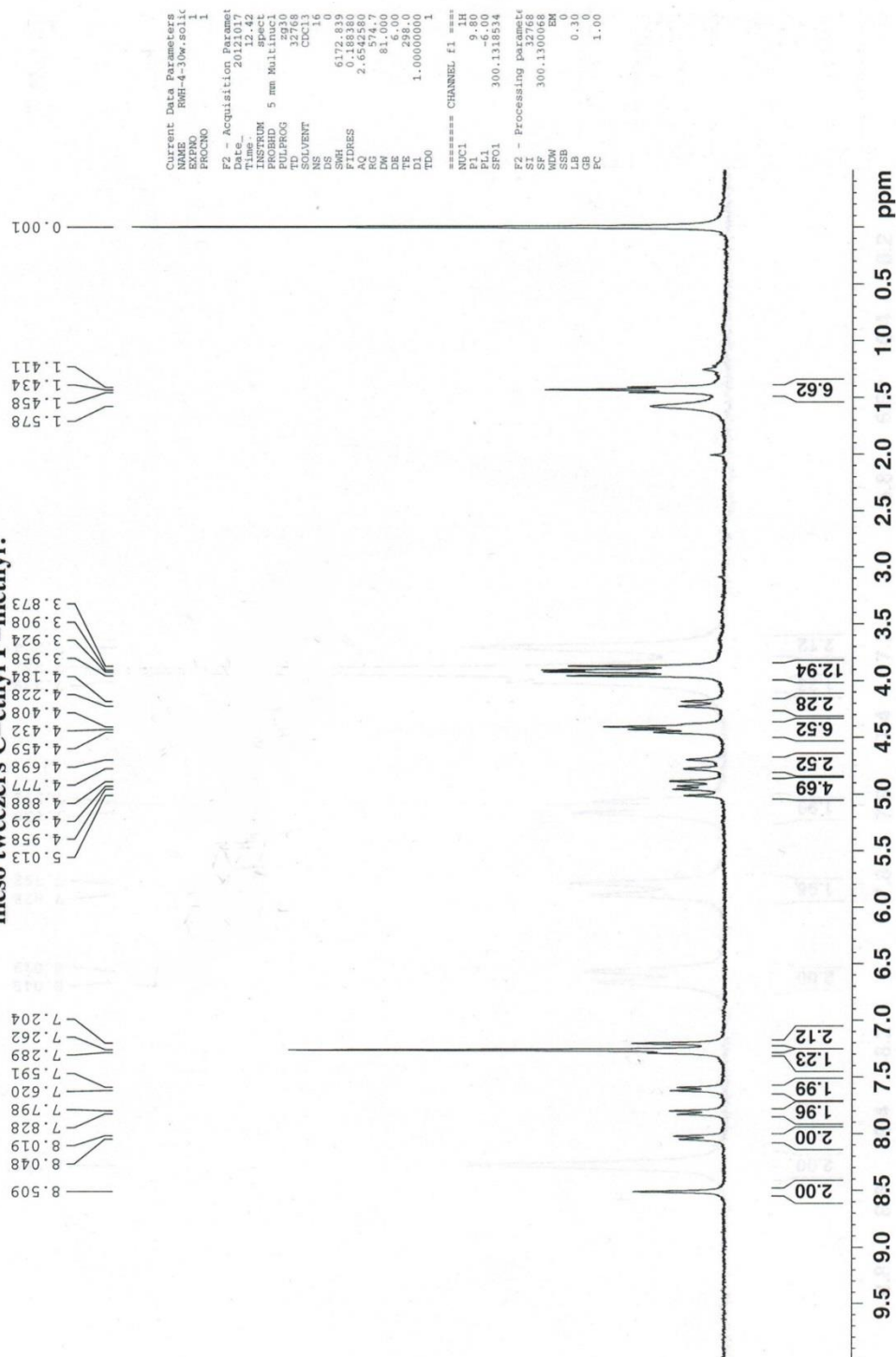
H₂O/0.1% HCOOH, CH₃CN/0.1% HCOOH

HRMS *C-Me, P-Me rac-tweezers* (**18**)

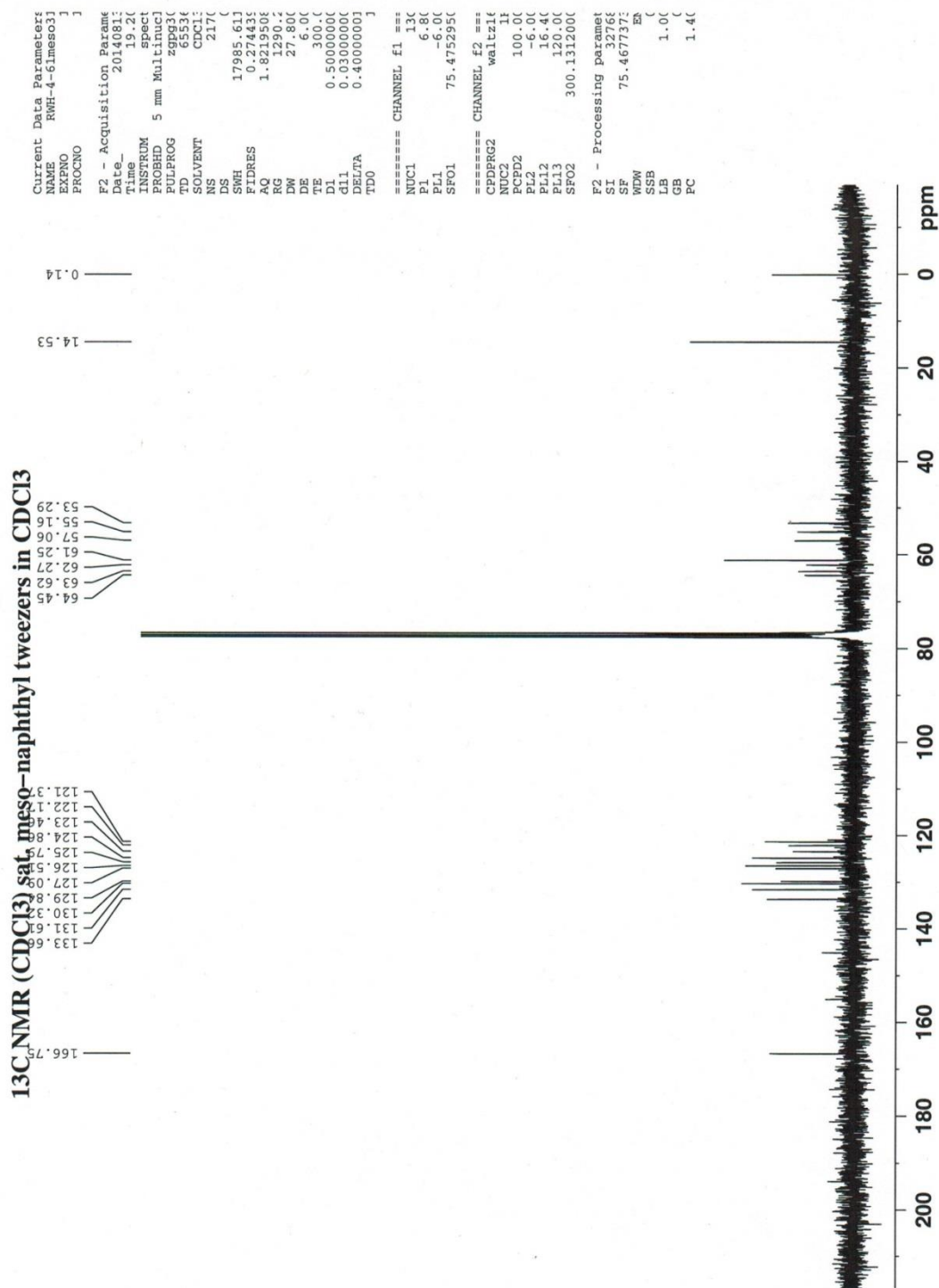


¹H NMR *C*-Me, *P*-Me meso-isomer (19)

¹H NMR(CDC13) white solid from trogerization 4.5mg sample
meso tweezers *C*-ethyl *P*-methyl?



¹³C NMR C-Me, P-Me meso-isomer (19)



³¹P NMR C-Me, P-Me meso-isomer (19)

³¹P NMR (CDCl₃) 1st crop meso from rextyl with crude tweezers mix with toluene

```

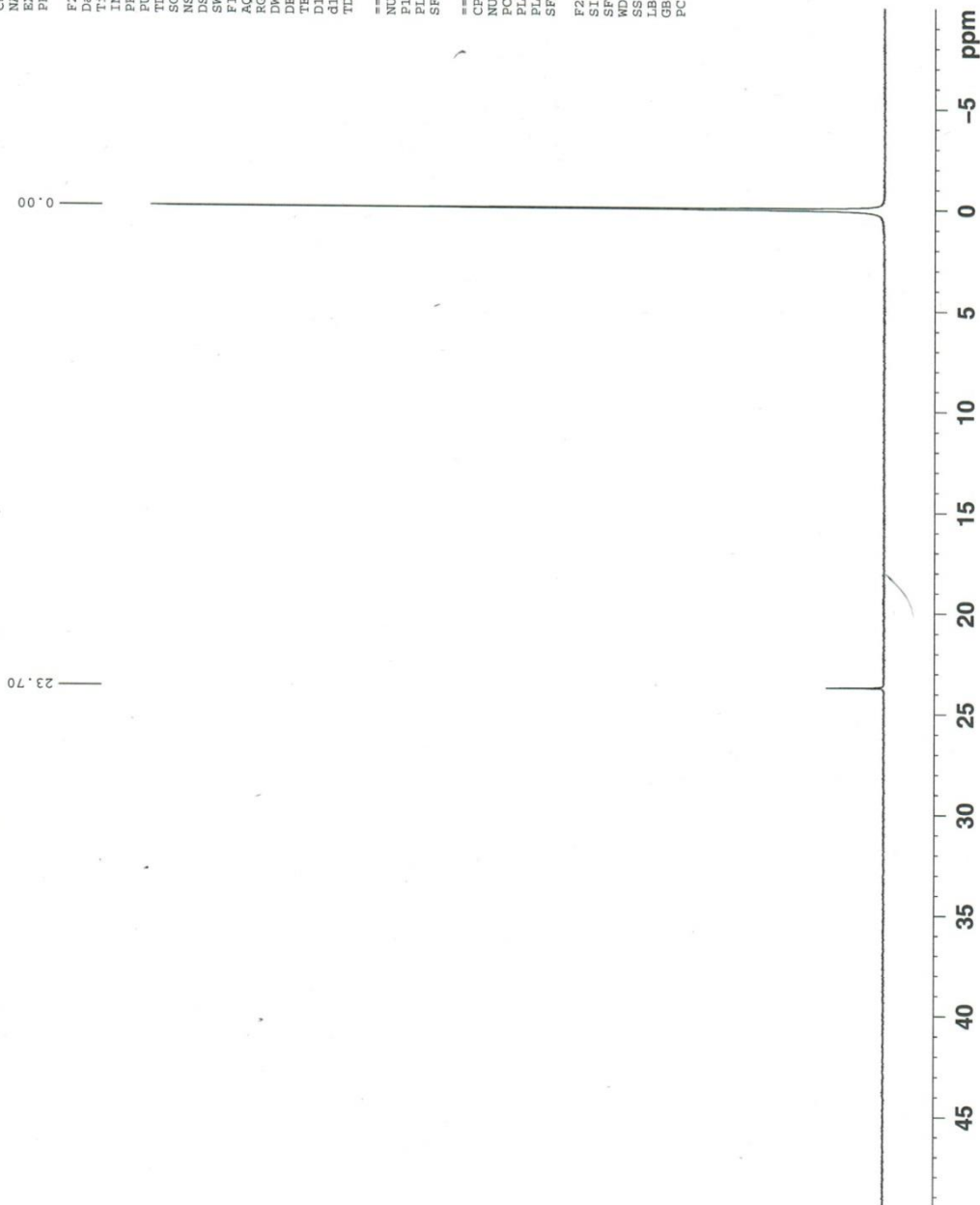
Current Data Parameters:
NAME      RWH-4-10meso
EXPNO     1
PROCNO    1

F2 - Acquisition Parameters
Date_     20151101
Time      16.52
INSTRUM   spect
PROBHD    5 mm Multinucl
PULPROG   zgpg30
TD        65536
SOLVENT   Acetone
NS        3
DS        4
SWH        17985.611
FIDRES     0.27443
AQ         1.8213504
RG         100.00
DE         27.80
TE         298.2
D1         0.20000000
d11        0.03000000
TD0        1

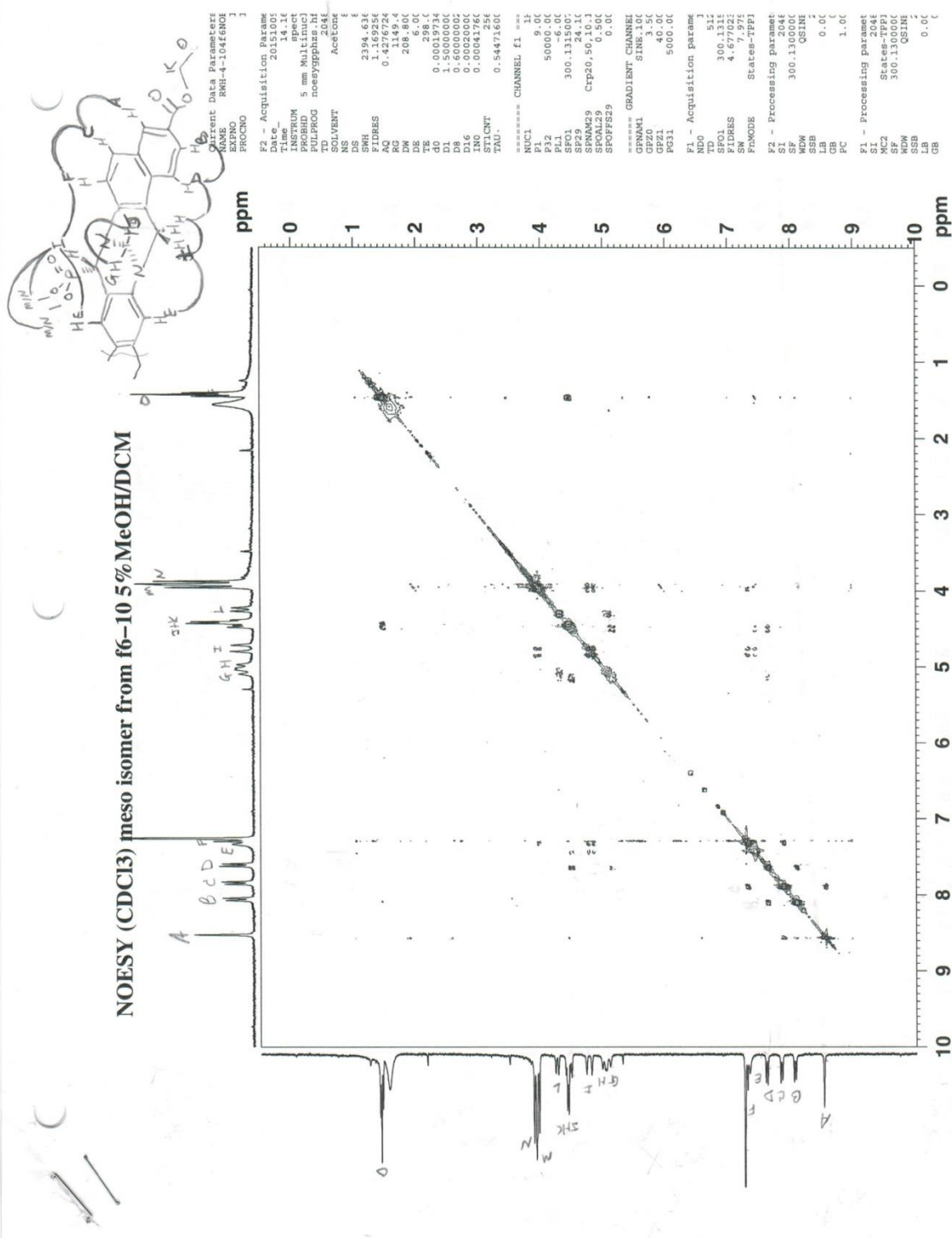
===== CHANNEL f1 =====
NUC1       31P
P1         8.00
PL1        -6.00
SFO1       121.4972810

===== CHANNEL f2 =====
CPDPRG2    waltz16
NUC2       13C
PCPD2      100.00
PL2        -6.00
PL12       17.85
SFO2       300.1312000

F2 - Processing parameters
SI         32768
SF         121.4946835
WDW        EM
SSB        0
LB         1.00
GB         0
PC         1.40
  
```



COSY C-Me, P-Me meso-isomer (19)



Shimadzu LCMS-2020 Data Report

Mass Spectrum for Sample
RWH-4-30 01.lcd

Opeator: Mark Wang

Data Filename: C:\LabSolutions\Data\Schwabacher Alan\RWH-4-30 01.lcd

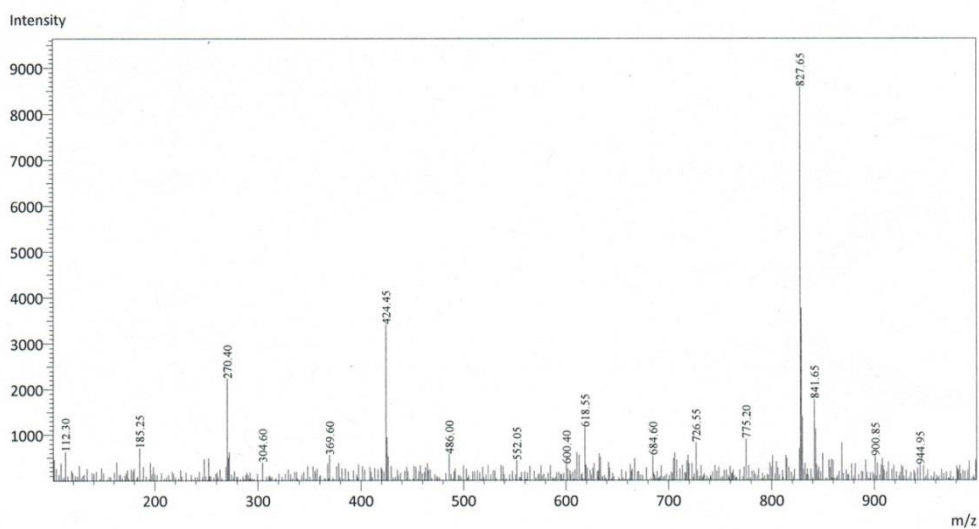
Spetrum Mode: Averaged

Retention Time: ----

Interface Type (ESI, APCI, DUIS): DUIS

Aquisition Mode: (Scan, SIM, Profile): Scan

Polarity: +

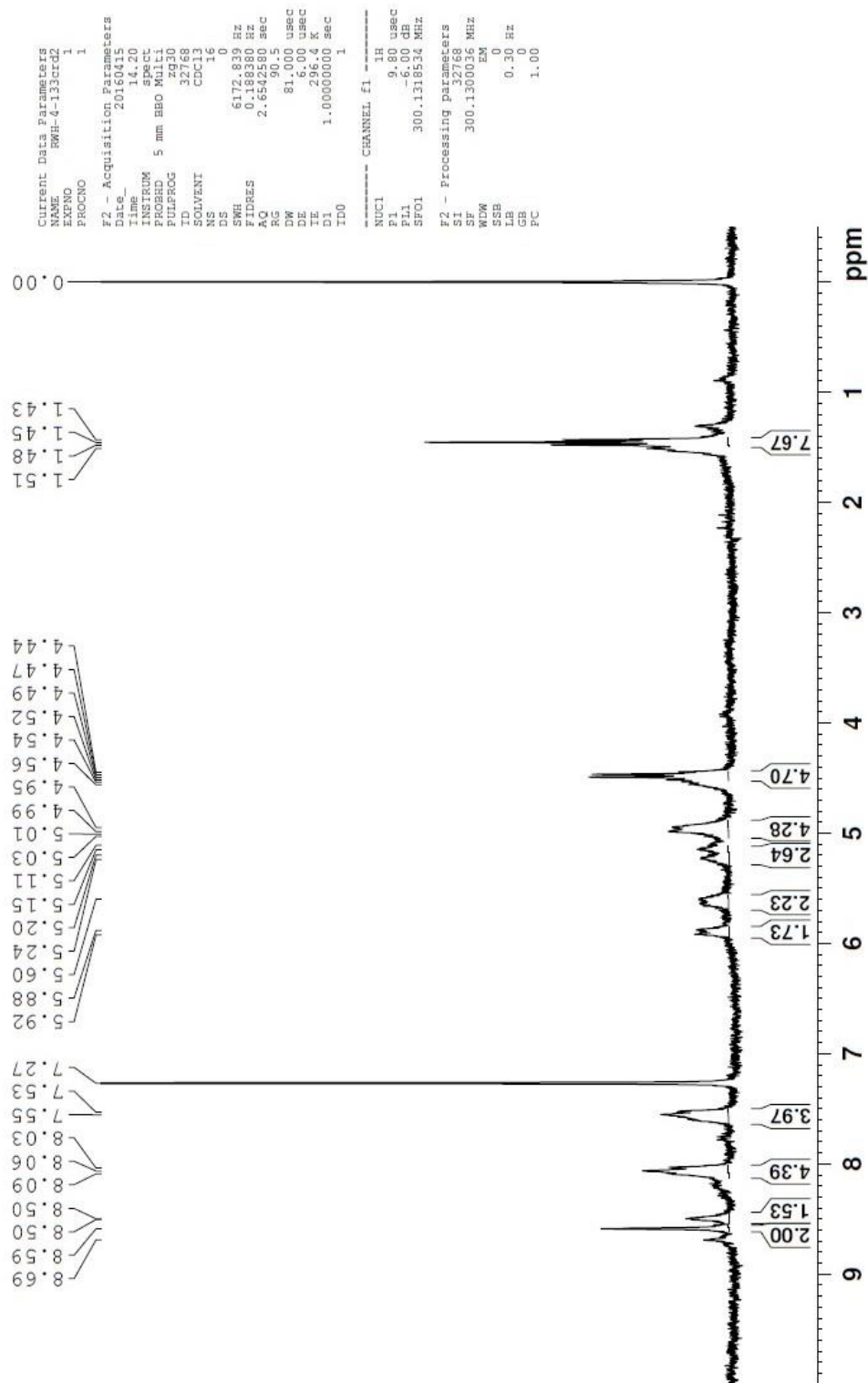


HRMS *C-Me, P-Me meso-isomer* (19)



¹H NMR *rac*- carboxy tetra acid tweezers (23)

¹H NMR (CDCl₃/TFA) prod after ppt from crd prod of TMSBR depro of En, 4.0mg sample



³¹P NMR rac- carboxy tetra acid tweezers (23)

³¹P NMR (DMSO-d₆) TMSBr depro rac naphthyl tweezers crude product 3.3mg

```

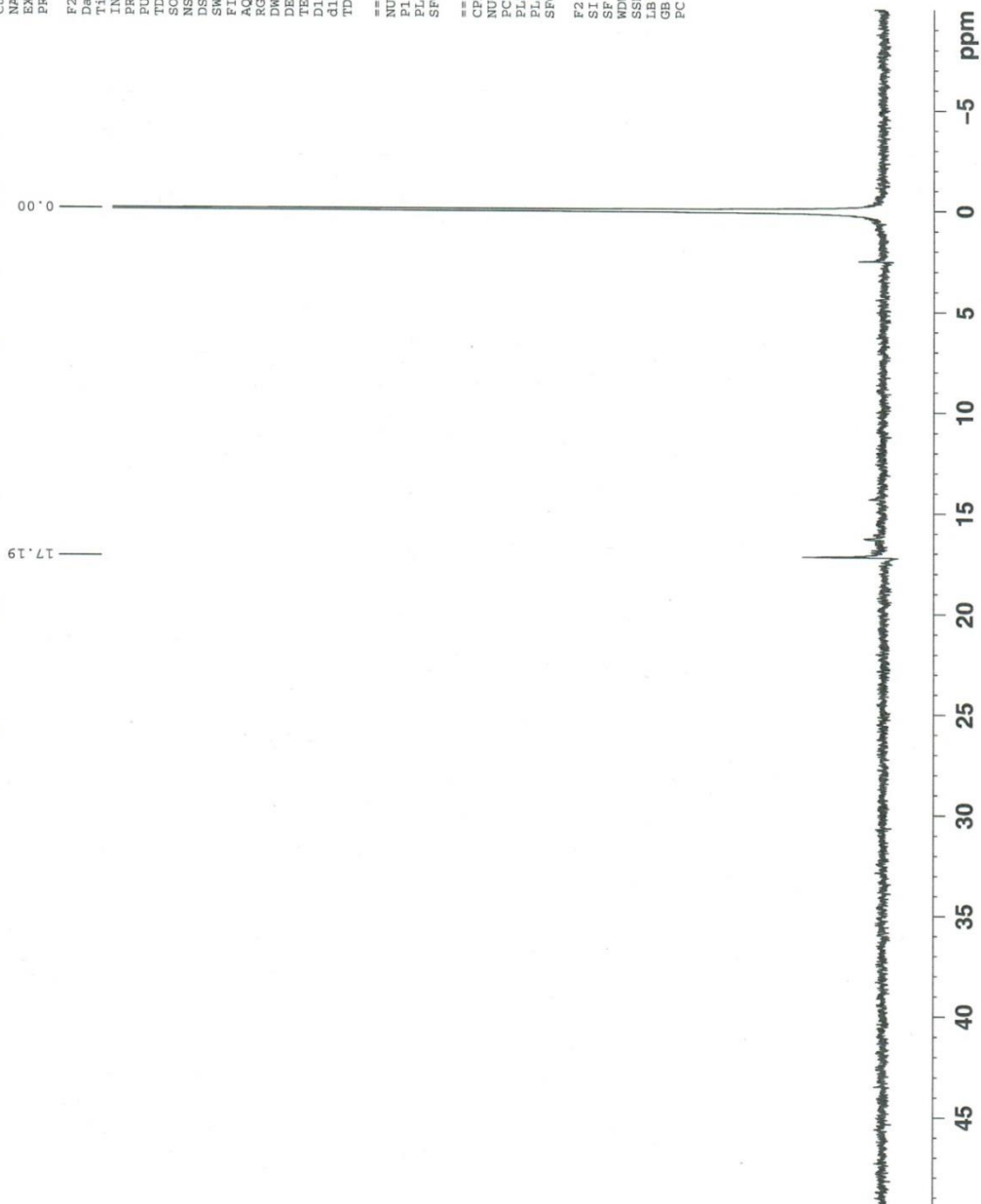
Current Data Parameters
NAME      RMH-4-116C131
EXPNO     1
PROCNO    1

F2 - Acquisition Parameters
Date_     20160121
Time      11.14
INSTRUM   spect
PROBHD    5 mm Multinuc
PULPROG   zgpg30
TD        65536
SOLVENT   Acetone
NS        64
DS        4
SWH        17985.611
FIDRES     0.274433
AQ         1.8219506
RG         228.1
DW         27.800
DE         6.00
TE         298.15
D1         0.20000000
d11        0.03000000
TD0        1

===== CHANNEL f1 =====
NUC1       31P
P1         4.00
PL1        0.00
SFO1       121.4972816

===== CHANNEL f2 =====
CPDPRG2    waltz16
NUC2       1H
PCPD2      100.00
PL2        -6.00
PL12       16.40
SFO2       300.1312000

F2 - Processing parameters
SI         32768
SF          121.4947186
WDW         EM
SSB         0
LB          1.00
GB          0
PC          1.40
  
```



Shimadzu LCMS-2020 Data Report

Mass Spectrum for Sample
RWH-4-72 01.lcd

Operator: Mark Wang

Data Filename: C:\LabSolutions\Data\Schwabacher Alan\RWH-4-72 01.lcd

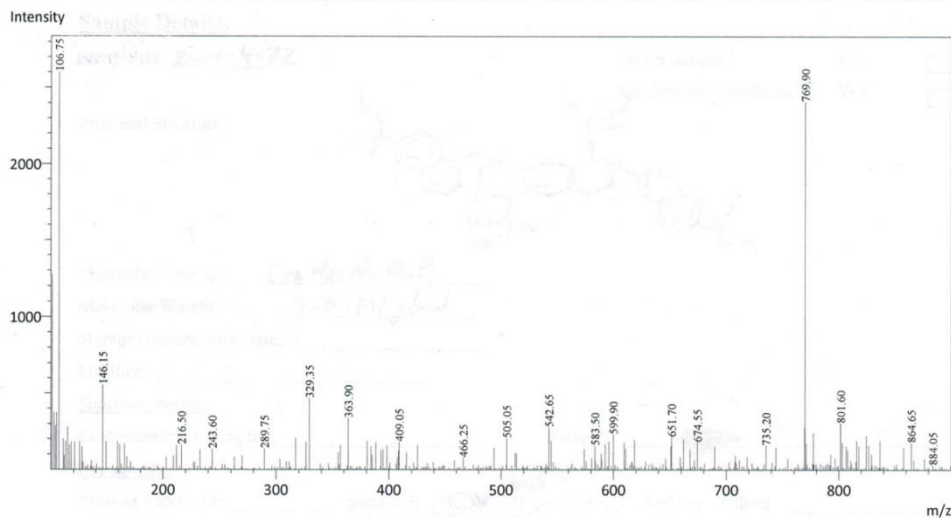
Spectrum Mode: Averaged

Retention Time: ----

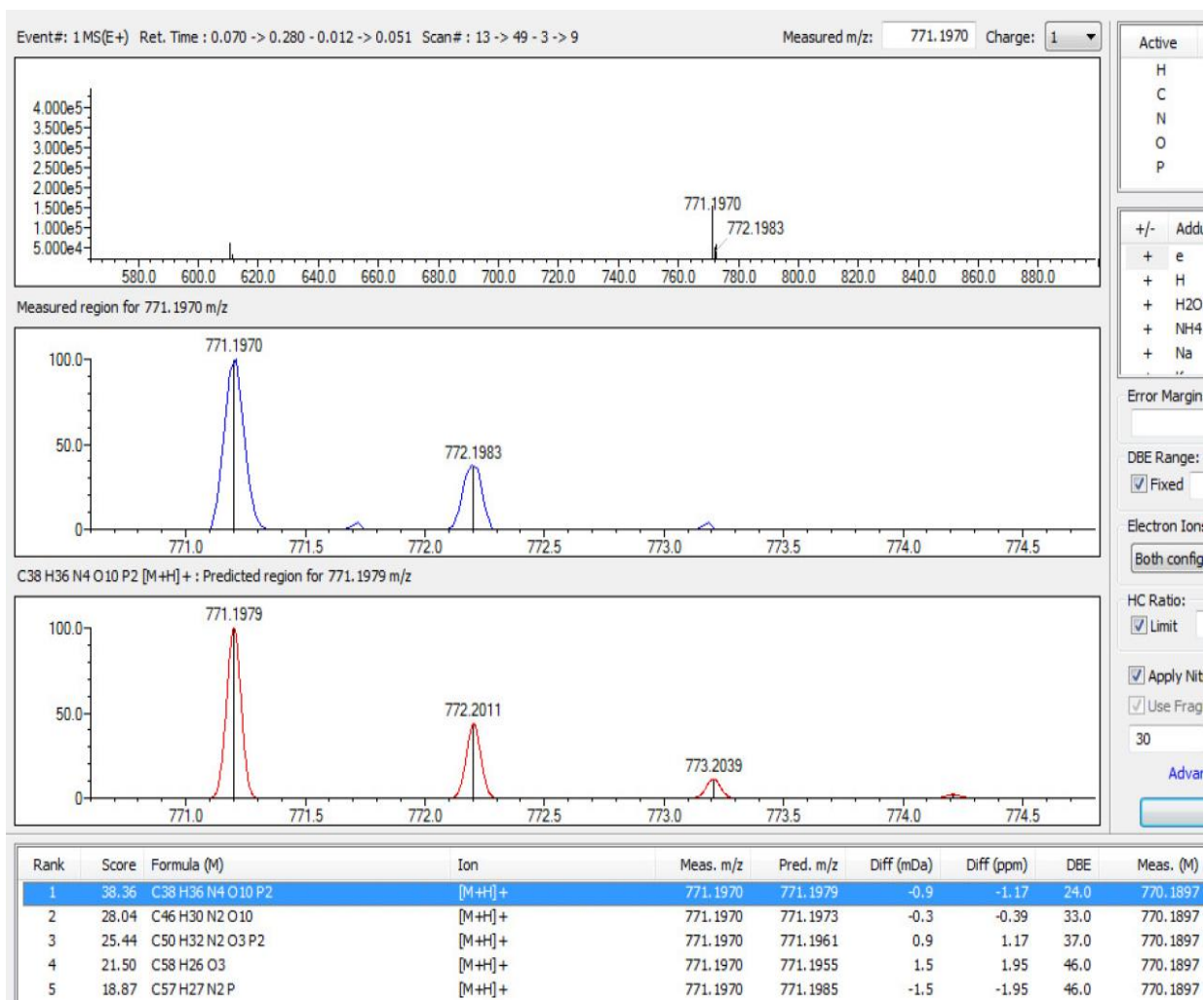
Interface Type (ESI, APCI, DUIS): DUIS

Acquisition Mode (Scan, SIM, Profile): Scan

Polarity: -

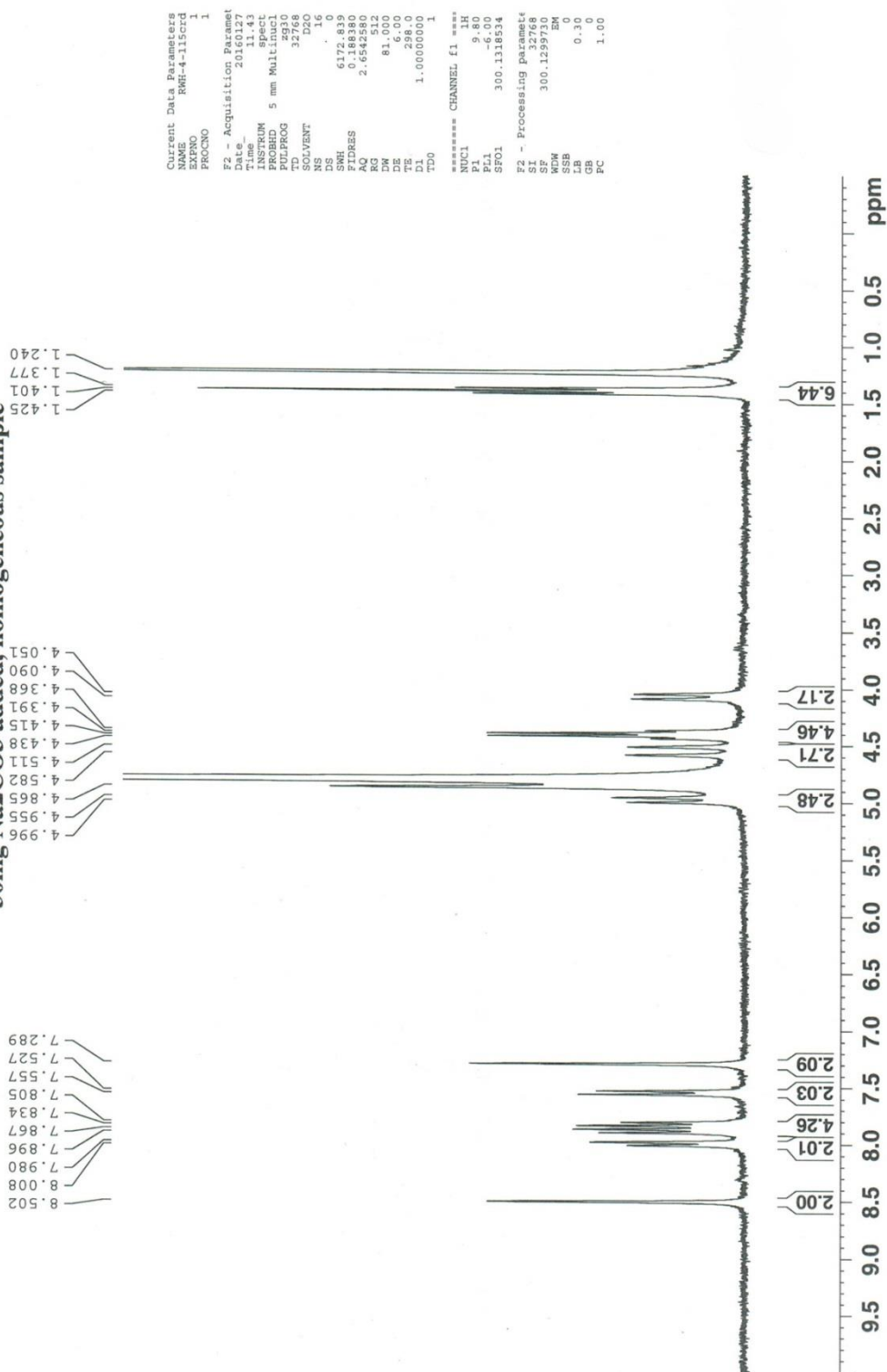


HRMS *rac*- carboxy tetra acid tweezers (23)



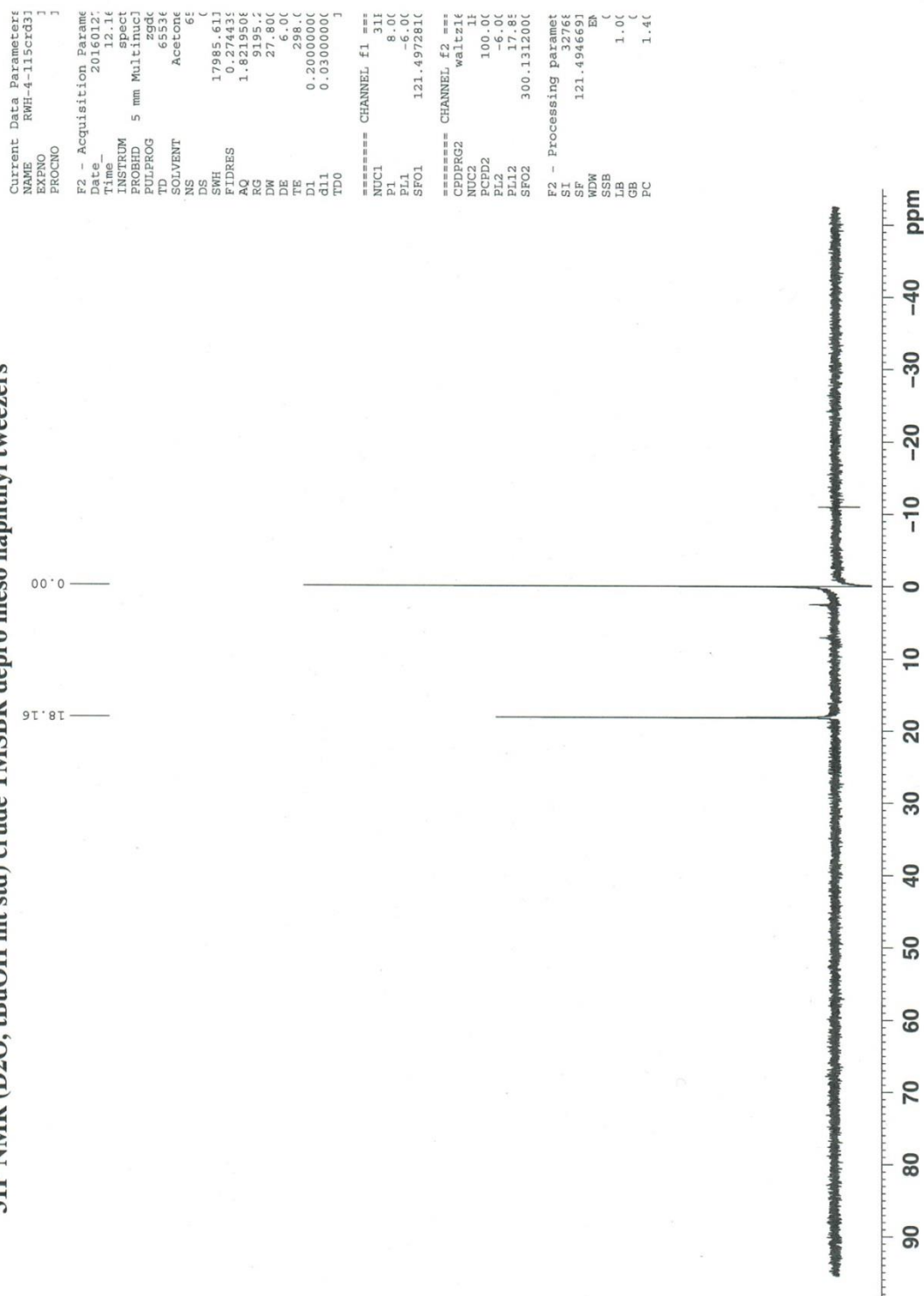
¹H NMR *meso*- carbethoxy tetra acid isomer (24)

¹H NMR (D₂O, tBuOH int std) crude TMSBr depro meso naphthyl tweezer 6.0mg
30mg Na₂CO₃ added, homogeneous sample



³¹P NMR meso- carbethoxy tetra acid isomer (24)

31P NMR (D2O, tBuOH int std) crude TMSBR depro meso naphthyl tweezers



Shimadzu LCMS-2020 Data Report

Mass Spectrum for Sample
RWH-4-71 02.lcd

Operator: Mark Wang

Data Filename: C:\LabSolutions\Data\Schwabacher Alan\RWH-4-71 02.lcd

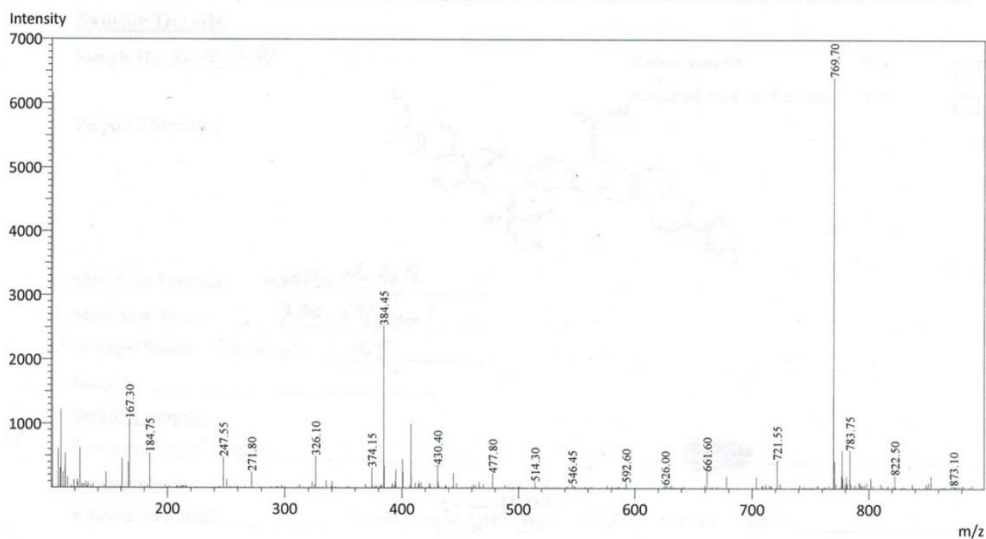
Spectrum Mode: Averaged

Retention Time: ----

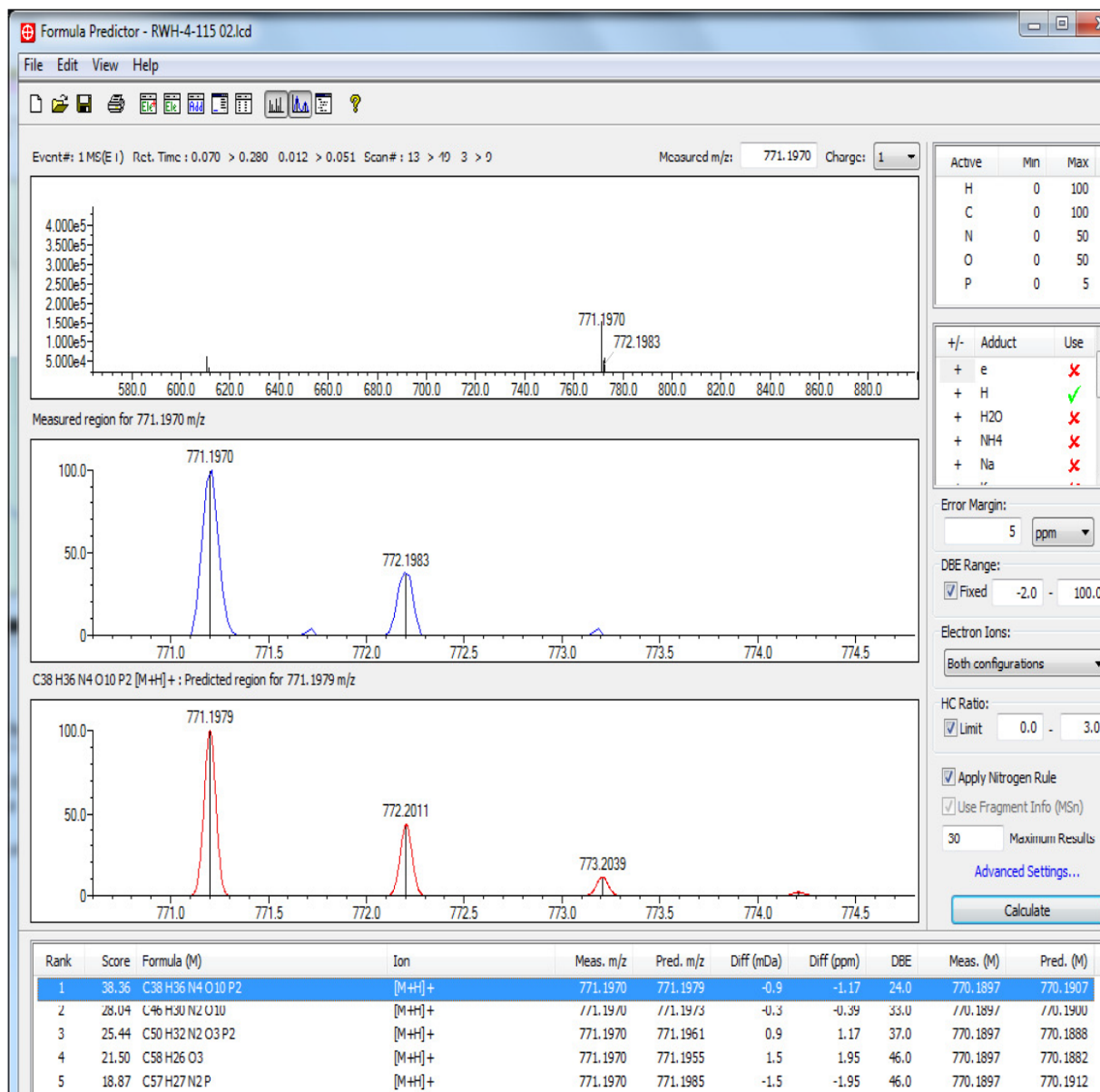
Interface Type (ESI, APCI, DUIS): DUIS

Acquisition Mode (Scan, SIM, Profile): Scan

Polarity: -

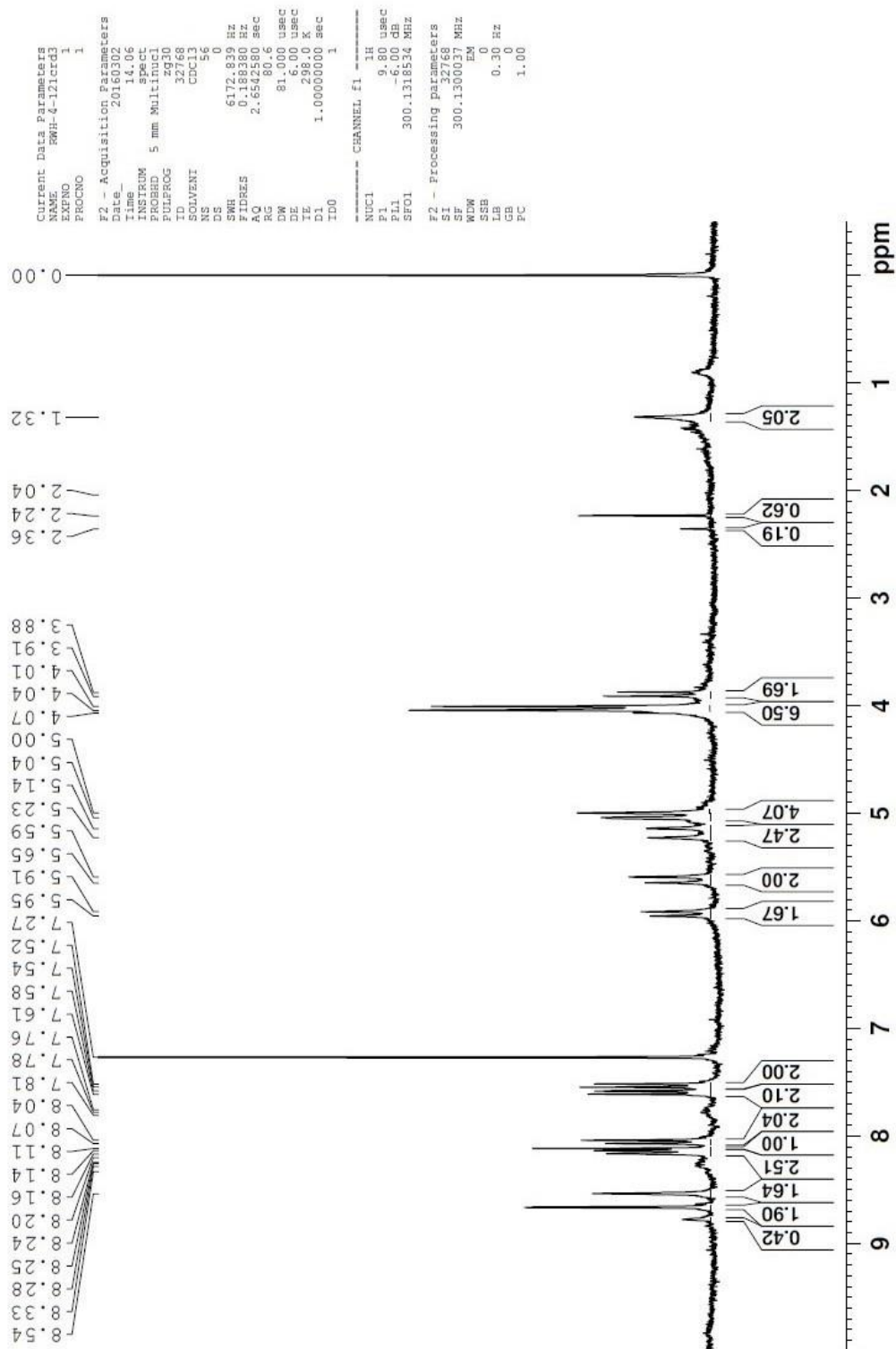


HRMS *meso*- carbethoxy tetra acid isomer (24)



¹H NMR *rac*-methylphosphonate tetra anionic tweezers (25)

¹H NMR (1:1 TFA/CDCl₃) sapon En resub to rxn cond., 2.6mg sample 0.6mL solvent



³¹P NMR rac-methylphosphonate tetra anionic tweezers (25)

31P NMR (TFA, TMS int std) LiOH sapon. rac tweezers 1.9mg sample

```

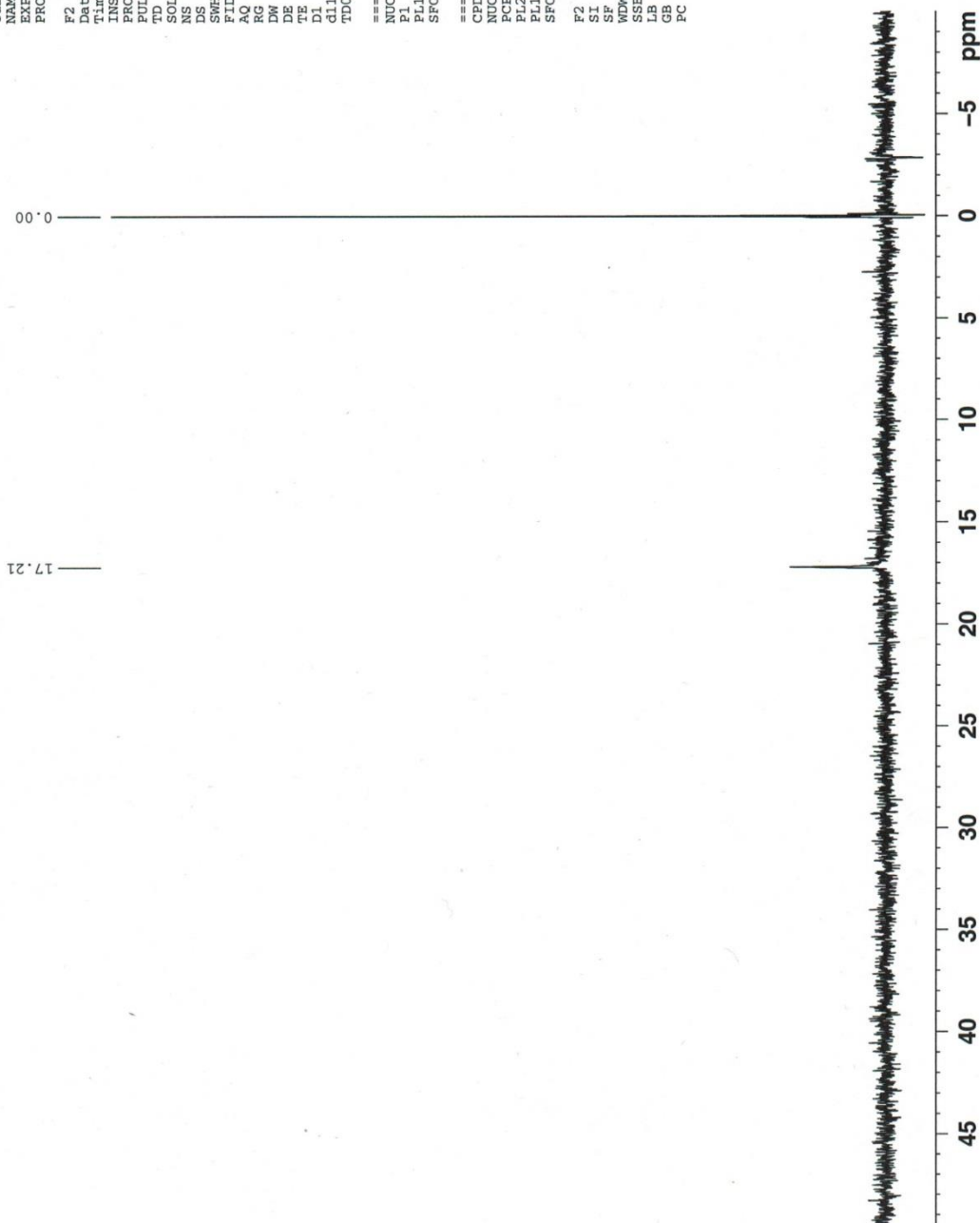
Current Data Parameters:
NAME      RWH-475crd31f
EXPNO     1
PROCNO    1

F2 - Acquisition Parameters
Date_     20140731
Time      18.26
INSTRUM   spect
PROBHD    5 mm Multinucl
PULPROG   zgpg
TD         65536
SOLVENT   Acetone
NS         110
DS         4
SWH        17985.613
FIDRES     0.27443
AQ         1.8219506
RG         9195.2
DW         27.800
DE         6.00
TE         300.2
D1         0.20000000
d11        0.03000000
TDO        0

===== CHANNEL f1 =====
NUC1       31P
P1         8.00
PL1        -6.00
SFO1       121.4972810

===== CHANNEL f2 =====
CPDPRG2    waltz16
NUC2       1H
PCPD2      100.00
PL2        -6.00
PL12       17.80
SFO2       300.1312000

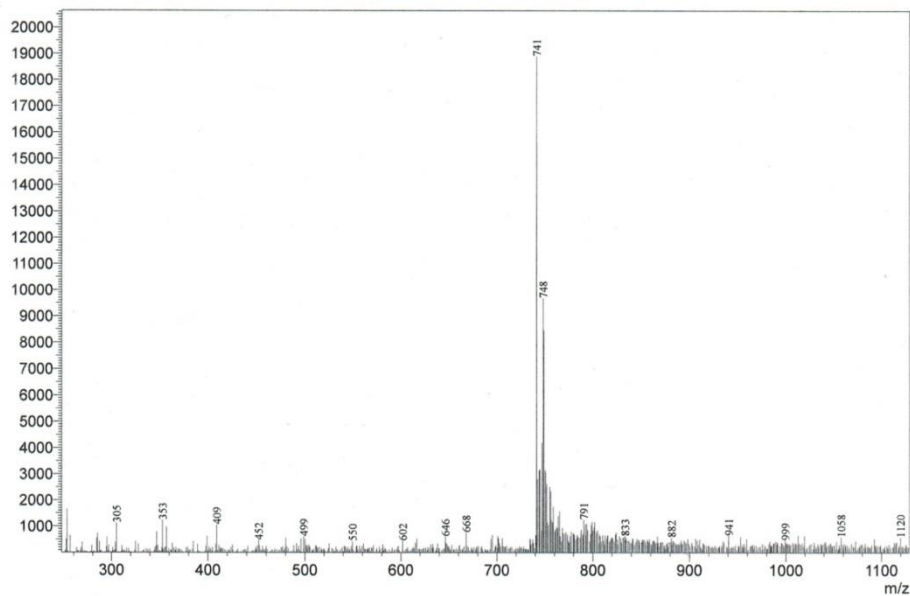
F2 - Processing parameters
SI         32768
SF         121.4947607
WDW        EM
SSB        0
LB         1.00
GB         0
PC         1.40
  
```



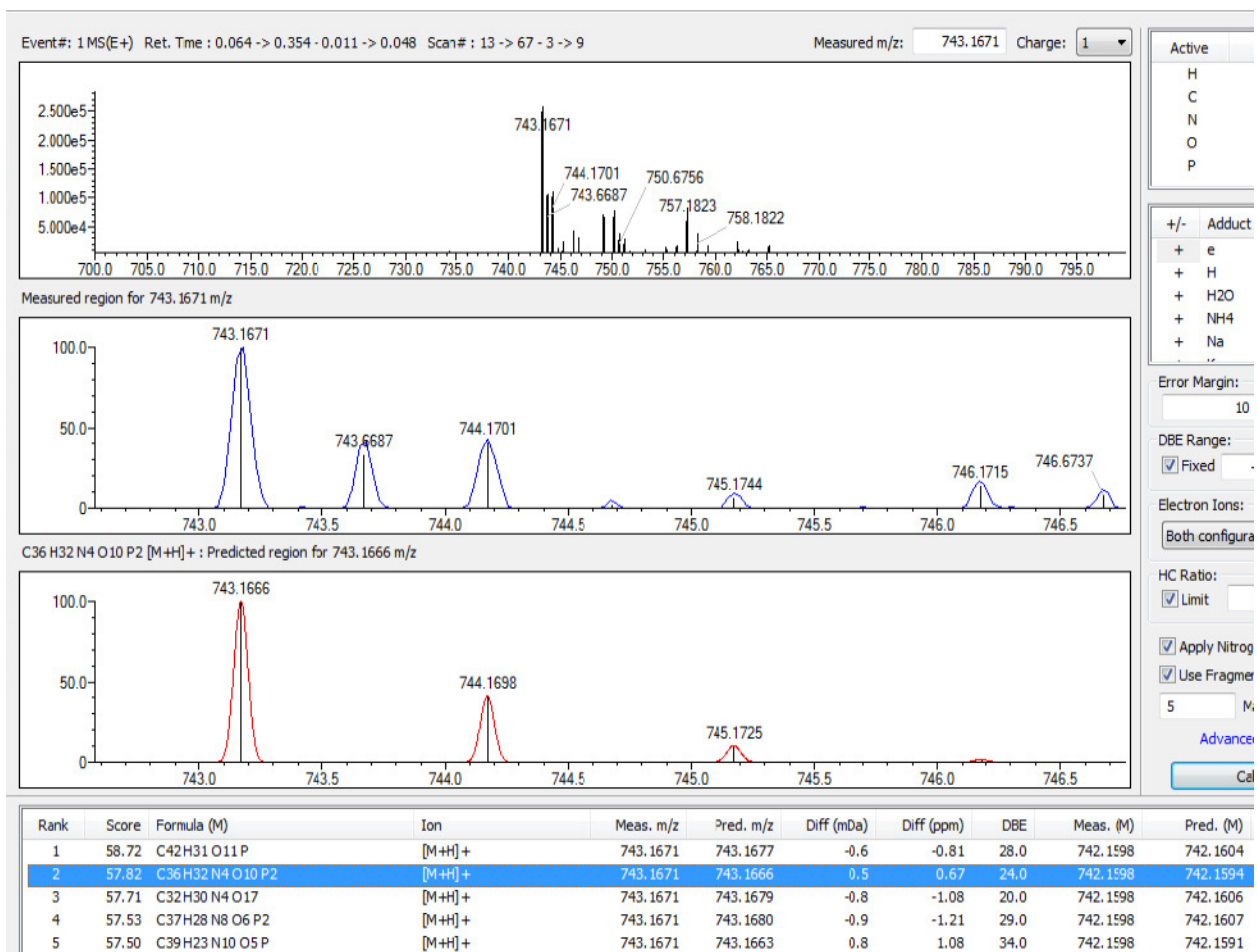
==== Shimadzu LabSolutions Data Report ====

<Spectrum>

Line#:1 R.Time:---(Scan#:---)
MassPeaks:1515
RawMode:Averaged 0.762-1.395(184-336) BasePeak:741(18901)
BG Mode:Averaged 0.012-0.303(4-74) Segment 1 - Event 2

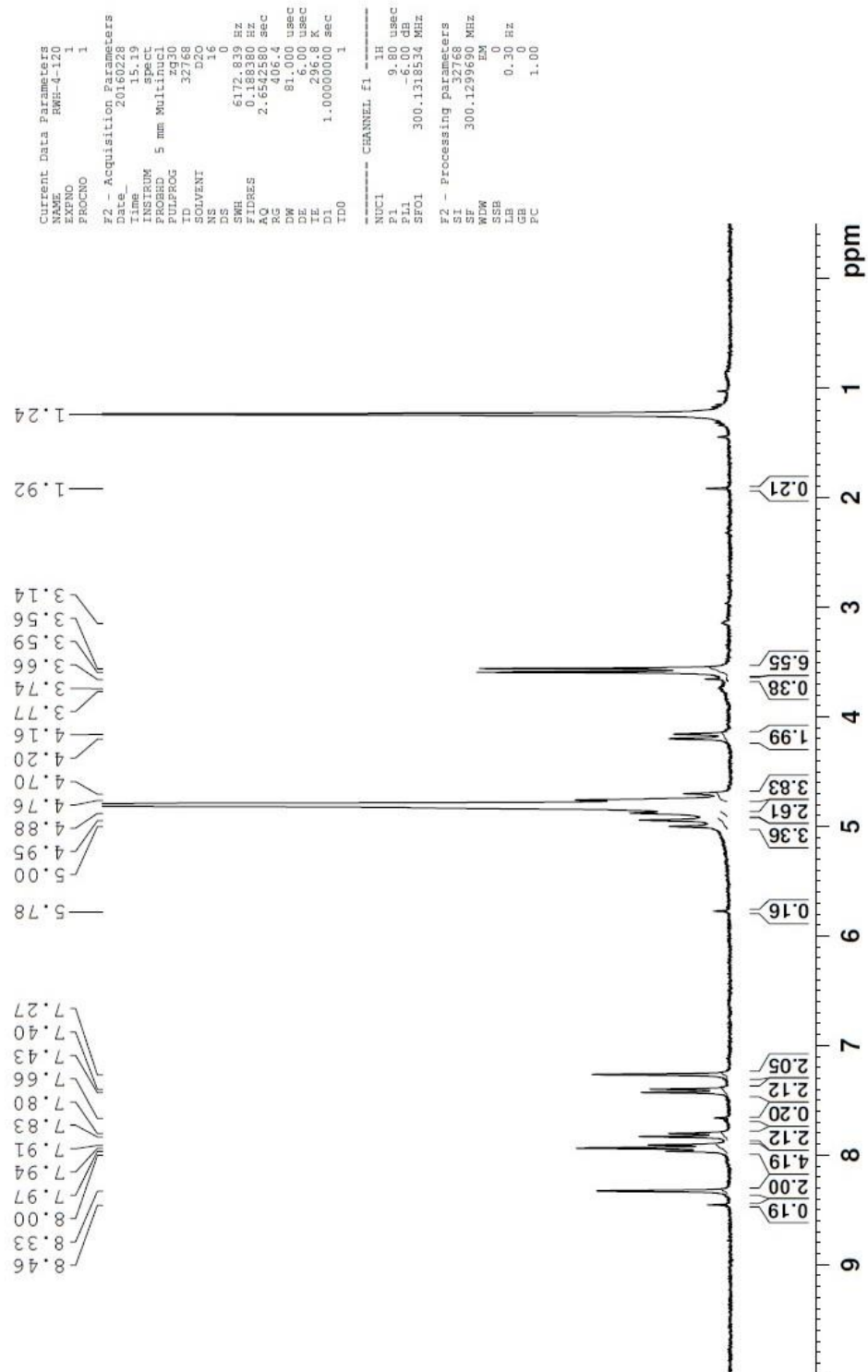


HRMS *rac*-methylphosphonate tetra anionic tweezers (25)



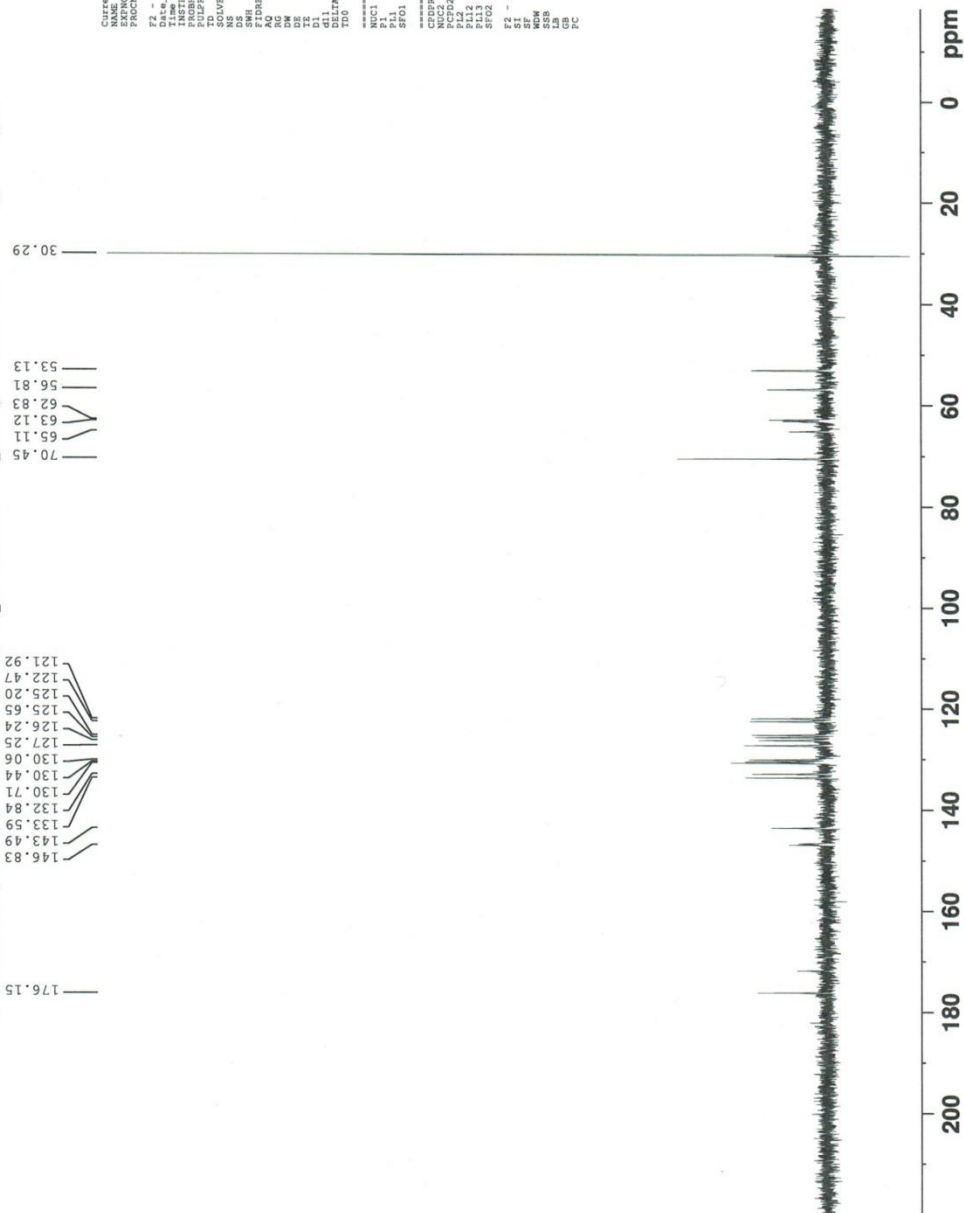
^1H NMR *meso*-methylphosphonate tetra anionic isomer (26)

^1H NMR (D₂O, tBuOH int std) crd prod from sapon of EN, 6.7mg sample



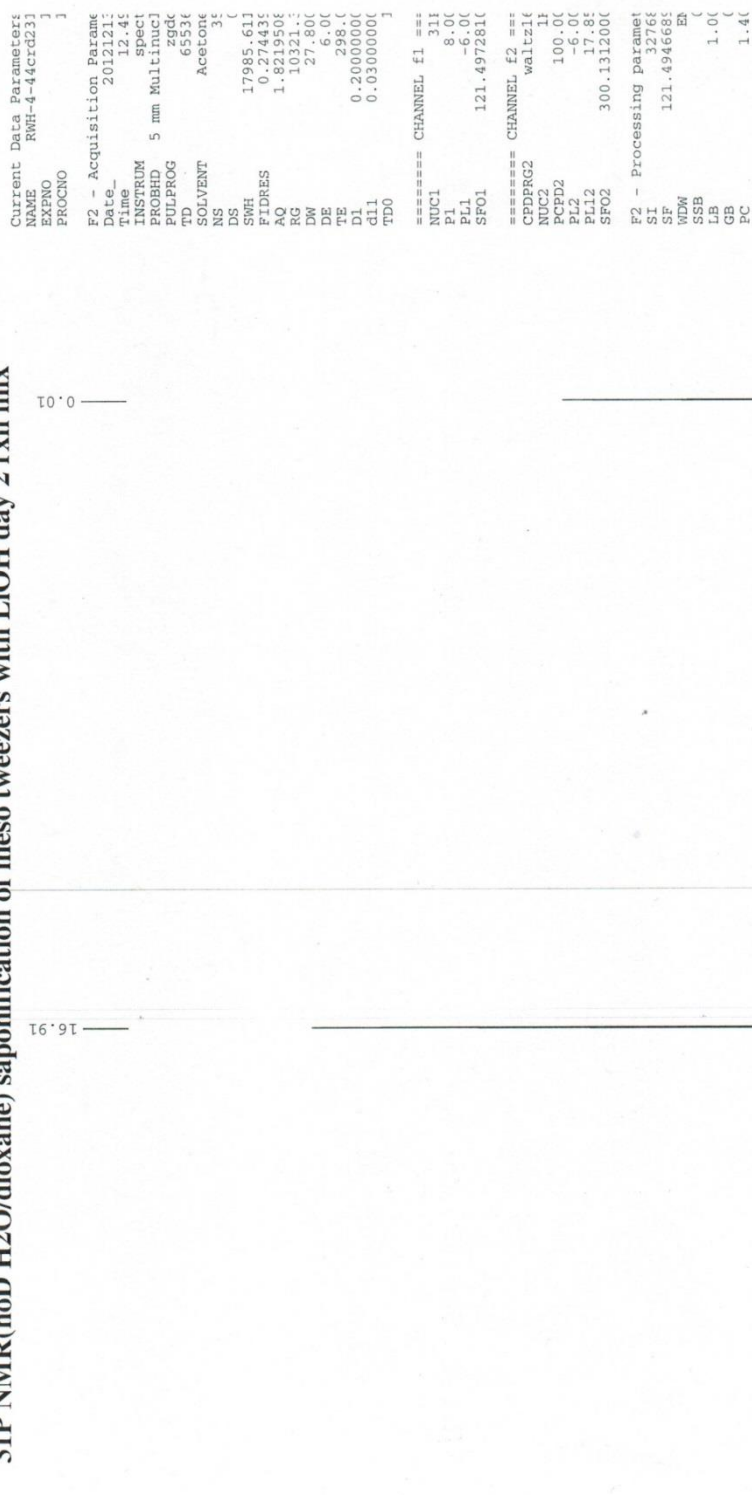
¹³C NMR meso-methylphosphonate tetra anionic isomer (26)

¹³C NMR (D₂O, tBuOH int std) sapon. meso naphthyl tweezers 23.6mg sample



³¹P meso-methylphosphonate tetra anionic isomer (26)

³¹P NMR(noD H₂O/dioxane) saponification of meso tweezers with LiOH day 2 rxn mix

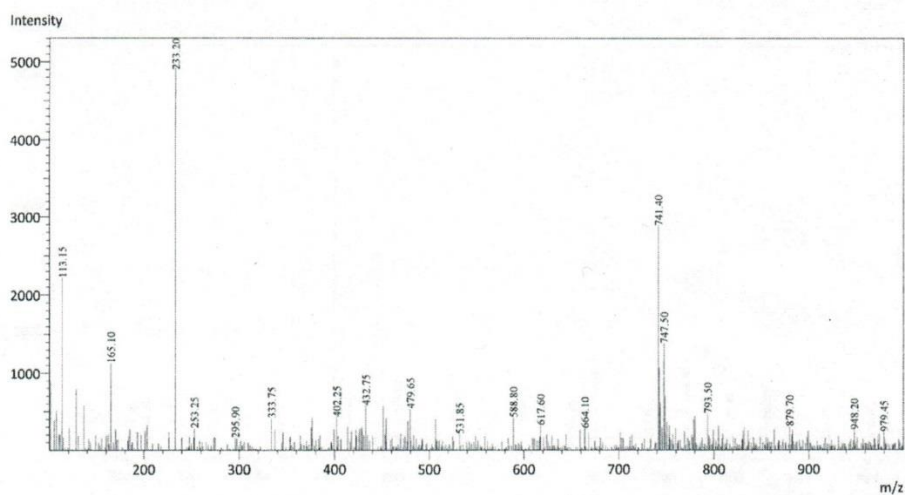


Shimadzu LCMS-2020 Data Report

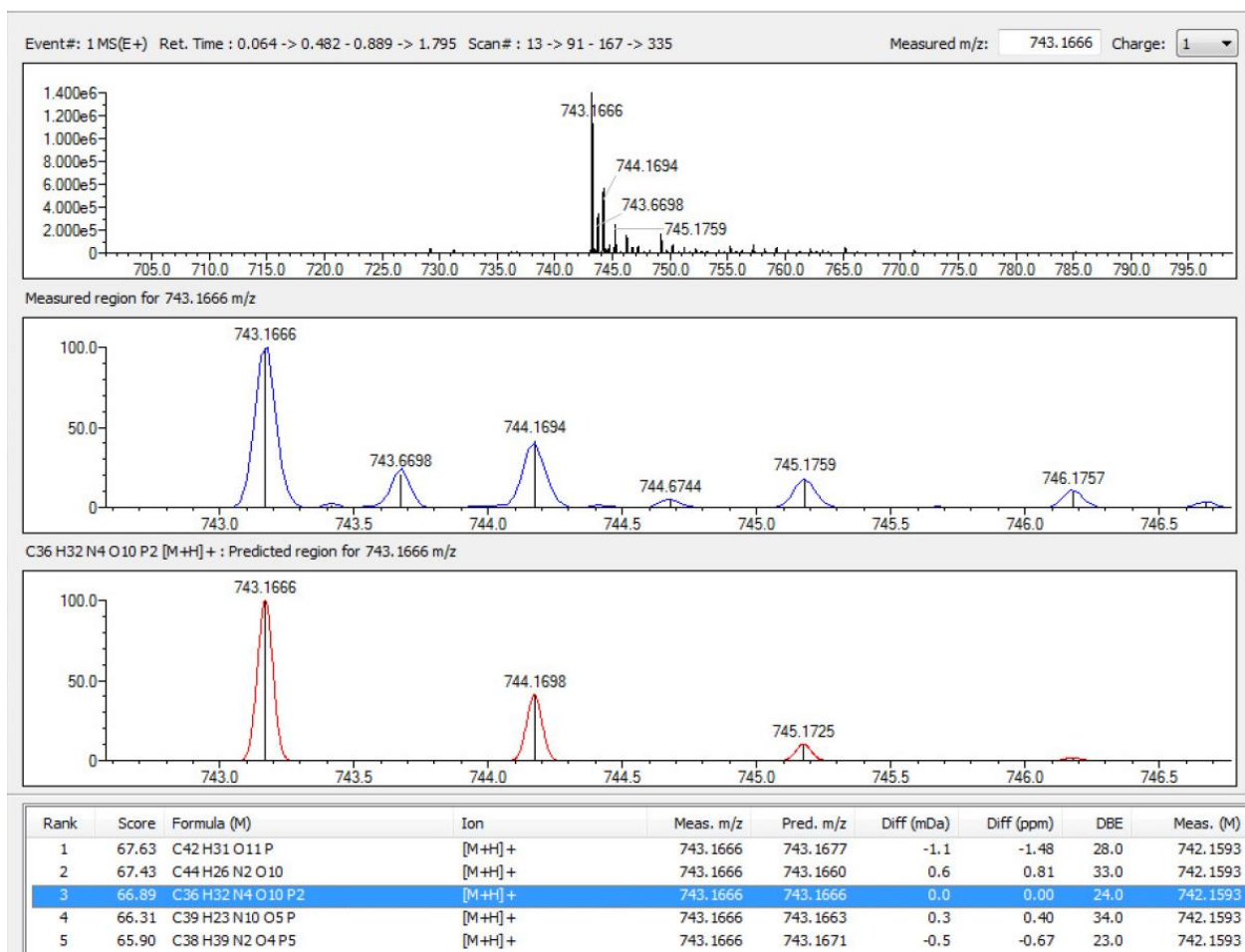
Mass Spectrum for Sample
RWH-4-76 02.lcd

Operator: Mark Wang

Data Filename: C:\LabSolutions\Data\Schwabacher Alan\RWH-4-76 02.lcd
Spectrum Mode: Averaged
Retention Time: ----
Interface Type (ESI, APCI, DUIS): DUIS
Acquisition Mode (Scan, SIM, Profile): Scan
Polarity: -

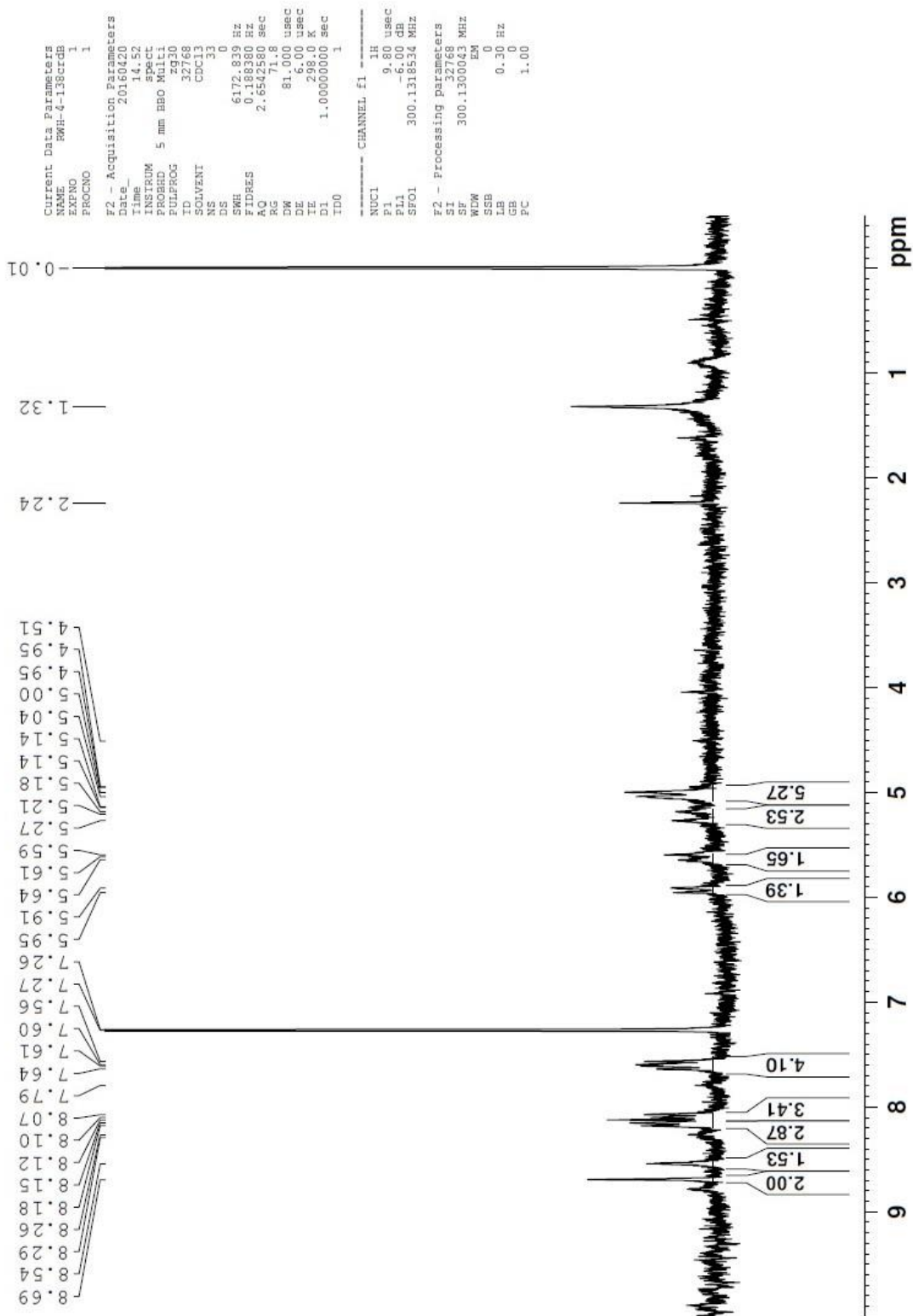


HRMS *meso*-methylphosphonate tetra anionic isomer (**26**)



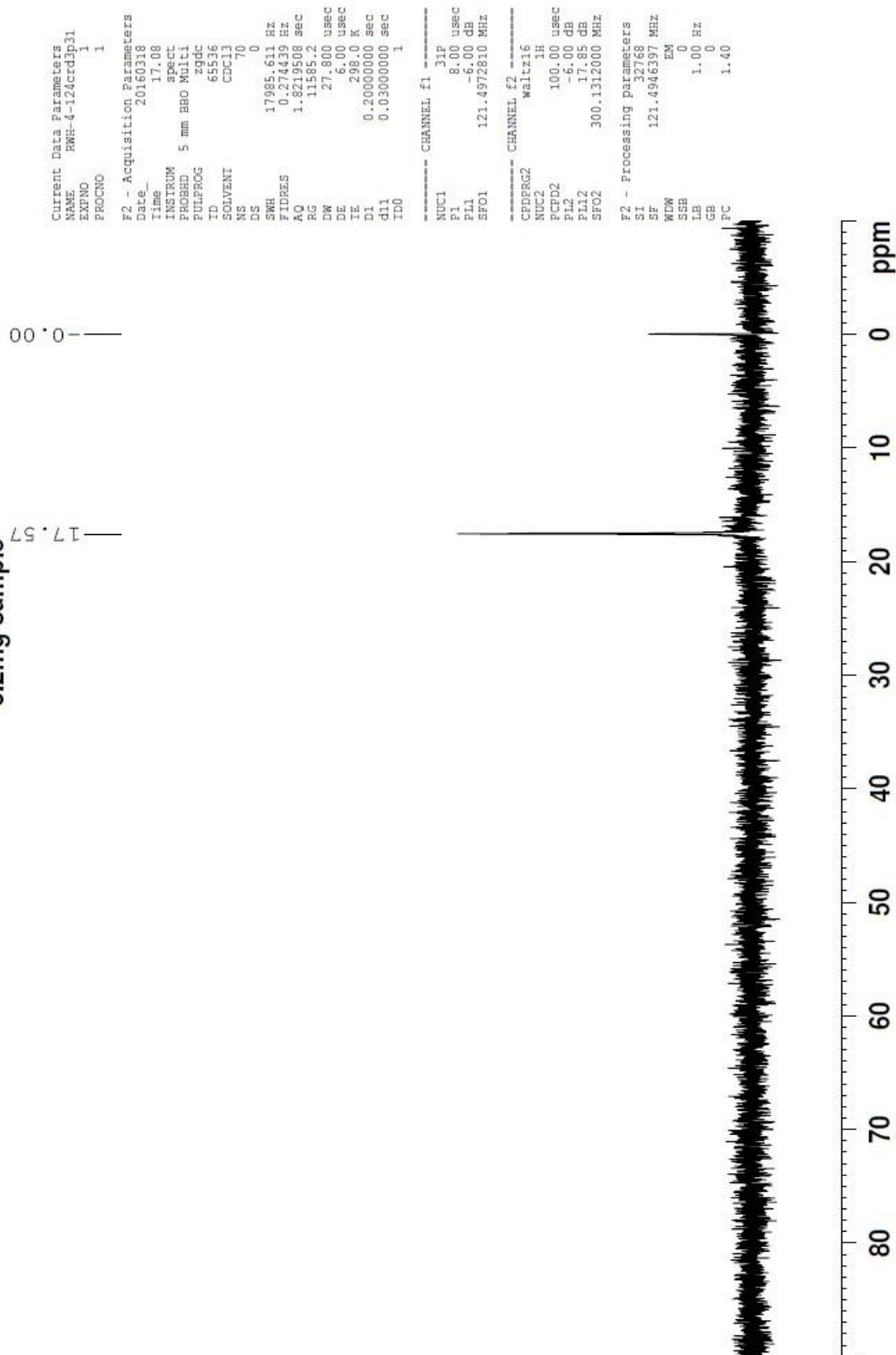
^1H NMR *rac-hexa anionic tweezers* (**27**)

^1H NMR (CDCl_3/TFA) crude prod from *rac-hexa anion synthesis*



³¹P NMR rac-hexa anionic tweezers (27)

³¹P NMR (1:1 TFA/CDCl₃) sapon of rac anphthyl tweezers after 2nd add of LiOH and reflu
3.2mg sample



Shimadzu LCMS-2020 Data Report

Mass Spectrum for Sample
RWH-4-127B01.lcd

Operator: Robert Hoppe

Data Filename: C:\LabSolutions\Data\Schwabacher Alan\RWH-4-127B01.lcd

Spectrum Mode: Averaged

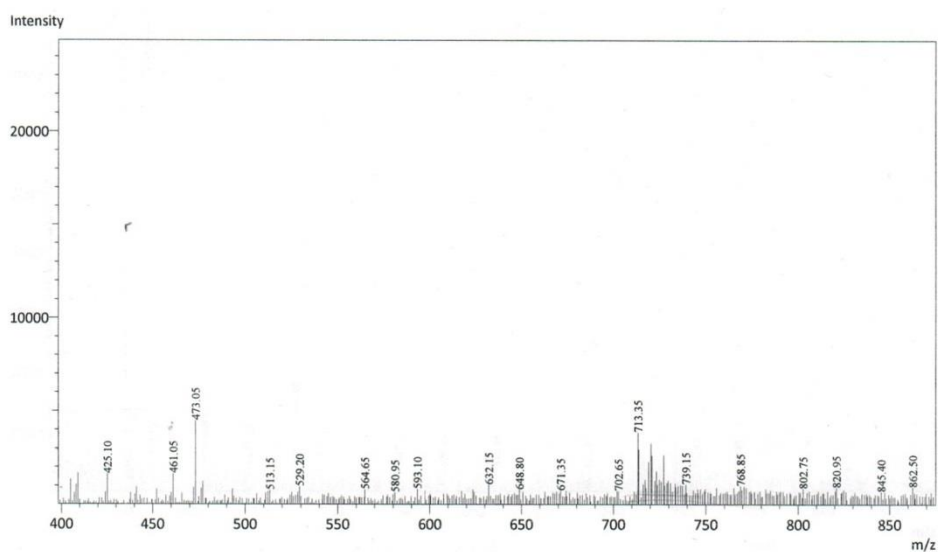
Retention Time: ----

Interface Type (ESI, APCI, DUIS): DUIS

Acquisition Mode (Scan, SIM, Profile): Scan

Polarity: -

H2O/0.1% HCOOH, CH3CN/0.1% HCOOH



HRMS NMR *rac-hexa anionic tweezers* (27)

Formula Predictor Report - RWH-4-127.lcd

Page 1 of 1

Data File: C:\LabSolutions\Data\Training 20160307\RWH-4-127.lcd

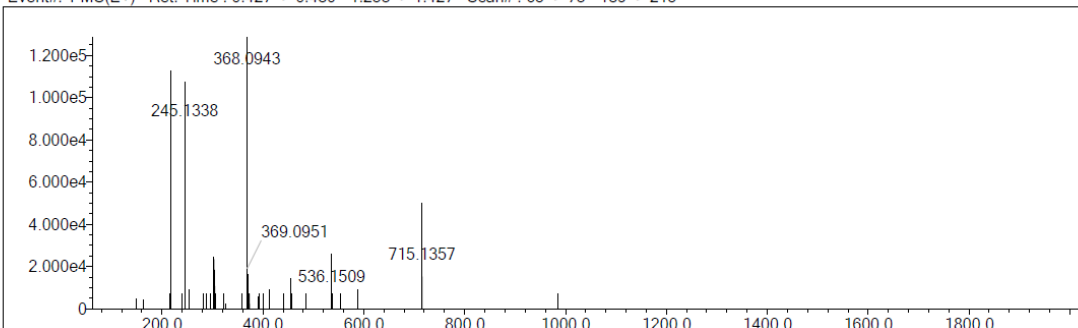
Elmt	Val.	Min	Max	Elmt	Val.	Min	Max	Use Adduct
H	1	0	40	O	2	0	15	H
C	4	0	40	P	3	0	4	
N	3	0	5					

Error Margin (ppm): 5
 HC Ratio: unlimited
 Max Isotopes: all
 MSn Iso RI (%): 75.00

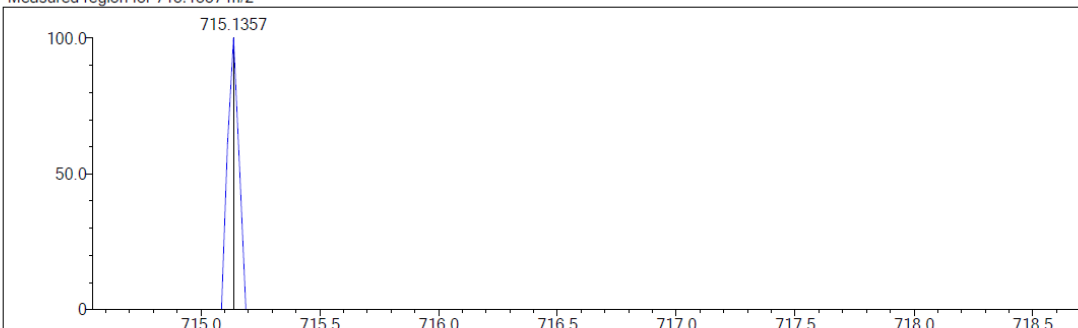
DBE Range: not fixed
 Apply N Rule: yes
 Isotope RI (%): 1.00
 MSn Logic Mode: AND

Electron Ions: both
 Use MSn Info: yes
 Isotope Res: 10000
 Max Results: 50

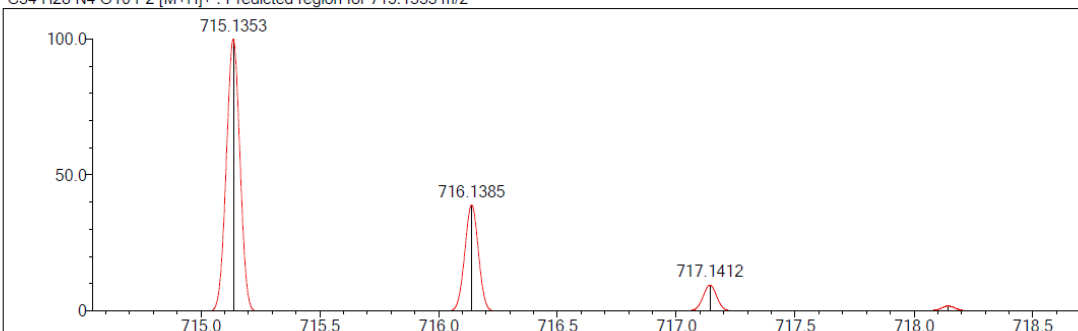
Event#: 1 MS(E+) Ret. Time : 0.427 -> 0.480 - 1.253 -> 1.427 Scan#: 65 -> 73 - 189 -> 215



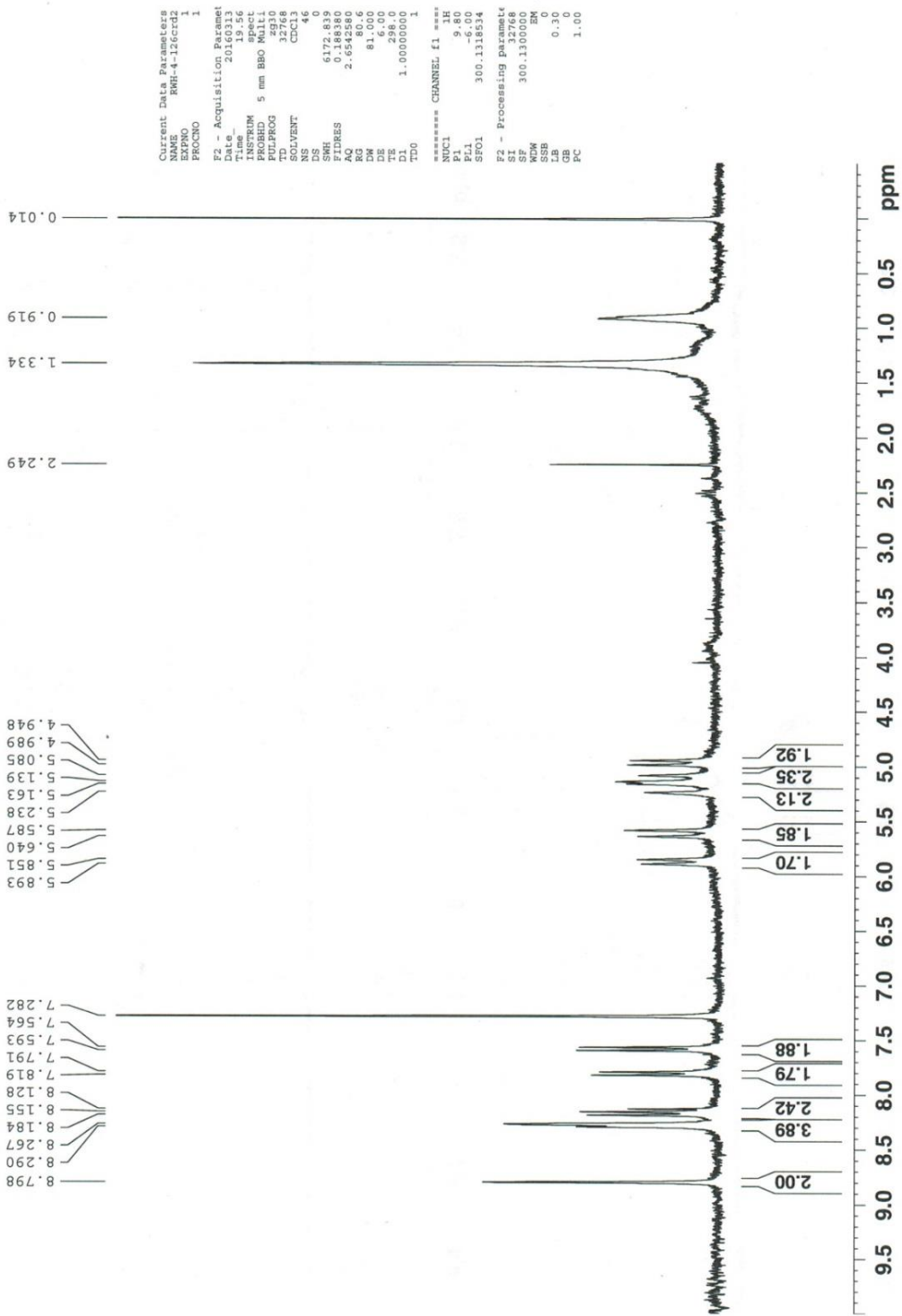
Measured region for 715.1357 m/z



C34 H28 N4 O10 P2 [M+H]⁺ : Predicted region for 715.1353 m/z



Rank	Score	Formula (M)	Ion	Meas. m/z	Pred. m/z	Df. (mDa)	Df. (ppm)	DBE	Meas. (M)	Pred. (M)	Iso
1	0.00	C34 H28 N4 O10 P2	[M+H] ⁺	715.1357	715.1353	0.4	0.56	24.0	714.1284	714.1281	0.00

¹H NMR meso-hexa anionic isomer (**28**)

³¹P NMR *meso*-hexa anionic isomer (28)

³¹P NMR (1:1 TFA/CDCl₃) crude prod of sapon of EN depro, 3.1mg sample, filtered

```

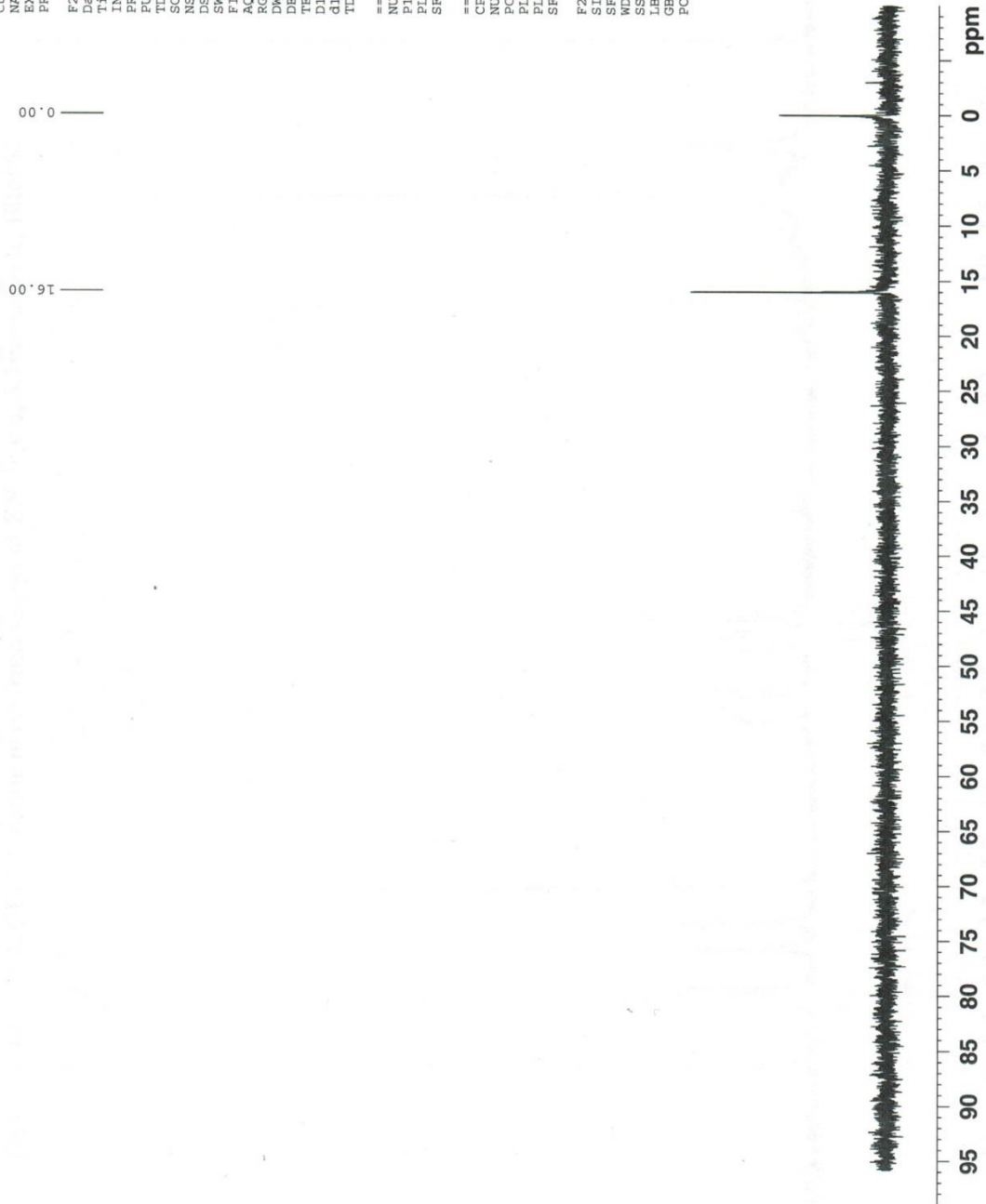
Current Data Parameters
NAME      RWH-4-126crd2f
EXPNO     1
PROCNO    1

F2 - Acquisition Parameters
Date_     20160311
Time      20.52
INSTRUM   spect
PROBHD    5 mm BBO Multi
PULPROG   zgpg30
TD        65536
SOLVENT   CDCl3
NS        74
DS         1
SWH        17985.611
FIDRES     0.274435
AQ         1.8219508
RG         10321.5
DE         27.800
TE         300.2
D1         0.20000000
d11        0.03000000
TD0        1

===== CHANNEL f1 =====
NUC1       31P
P1         8.00
PL1        -6.00
SFO1       121.4972810

===== CHANNEL f2 =====
CPDPRG2    waltz16
NUC2       1H
PCPD2      100.00
PL2        -6.00
PL12       17.85
SFO2       300.1312000

F2 - Processing parameters
SI         32768
SF         121.4946335
WDW         EN
SSB         0
LB          1.00
GB          0
PC          1.40
  
```



Shimadzu LCMS-2020 Data Report

Mass Spectrum for Sample
RWH-4-126.lcd

Operator: Robert Hoppe

Data Filename: C:\LabSolutions\Data\Schwabacher Alan\RWH-4-126.lcd

Spectrum Mode: Averaged

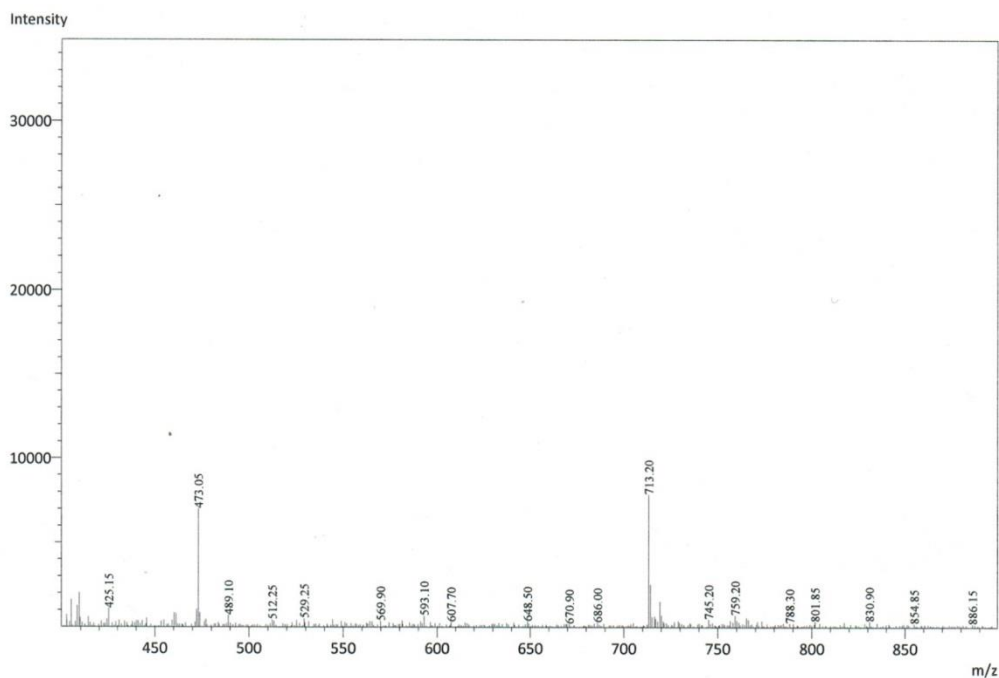
Retention Time: ----

Interface Type (ESI, APCI, DUIS): DUIS

Acquisition Mode (Scan, SIM, Profile): Scan

Polarity: -

H2O/0.1% HCOOH, CH3CN/0.1% HCOOH



HRMS *meso-hexa anionic isomer* (28)

Formula Predictor Report - RWH-4-126.lcd

Page 1 of 1

Data File: C:\LabSolutions\Data\Training 20160307\RWH-4-126.lcd

Elmt	Val.	Min	Max	Elmt	Val.	Min	Max	Use Adduct
H	1	0	50	O	2	0	10	H
C	4	0	50	P	3	0	2	
N	3	0	4					

Error Margin (ppm): 25

HC Ratio: unlimited

Max Isotopes: all

MSn Iso RI (%): 75.00

DBE Range: not fixed

Apply N Rule: yes

Isotope RI (%): 1.00

MSn Logic Mode: AND

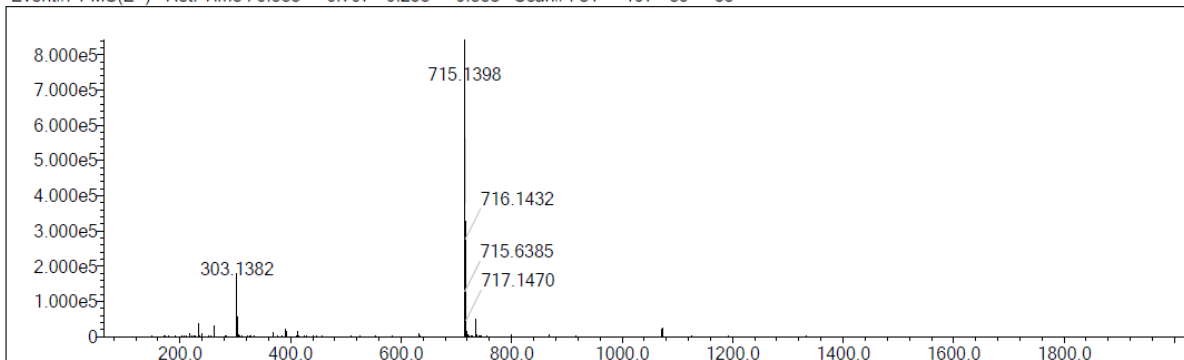
Electron Ions: both

Use MSn Info: yes

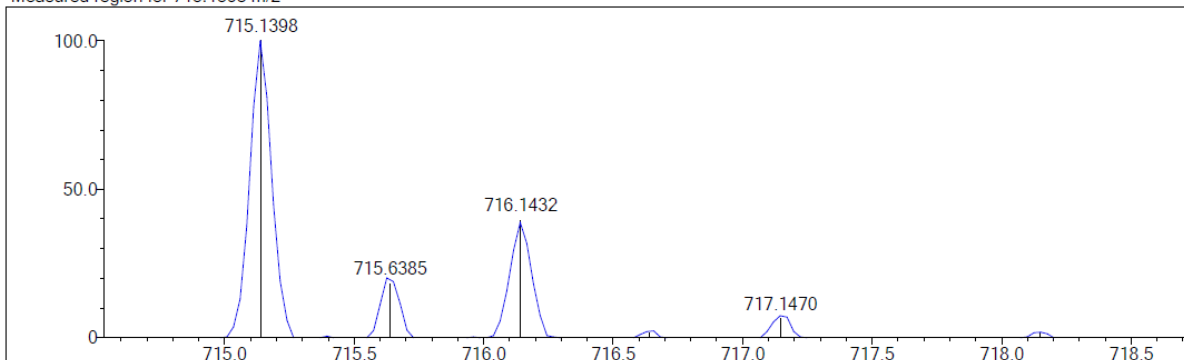
Isotope Res: 10000

Max Results: 50

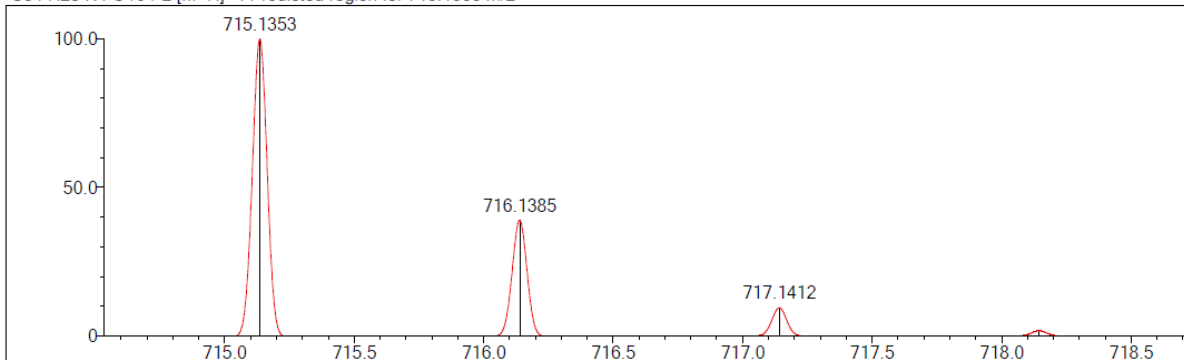
Event#: 1 MS(E+) Ret. Time : 0.533 -> 0.707 - 0.253 -> 0.358 Scan#: 81 -> 107 - 39 -> 55



Measured region for 715.1398 m/z

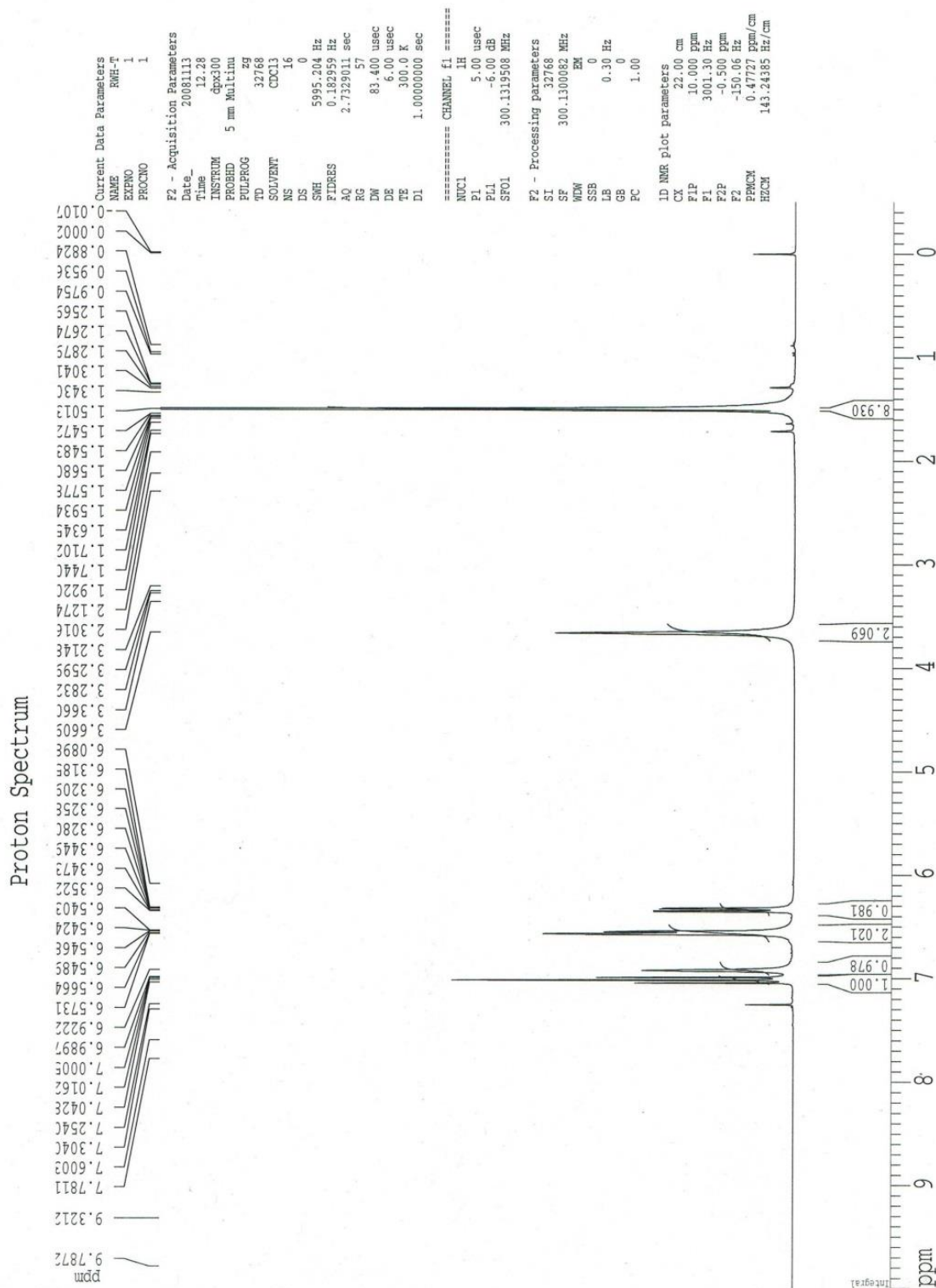


C34 H28 N4 O10 P2 [M+H]⁺ : Predicted region for 715.1353 m/z



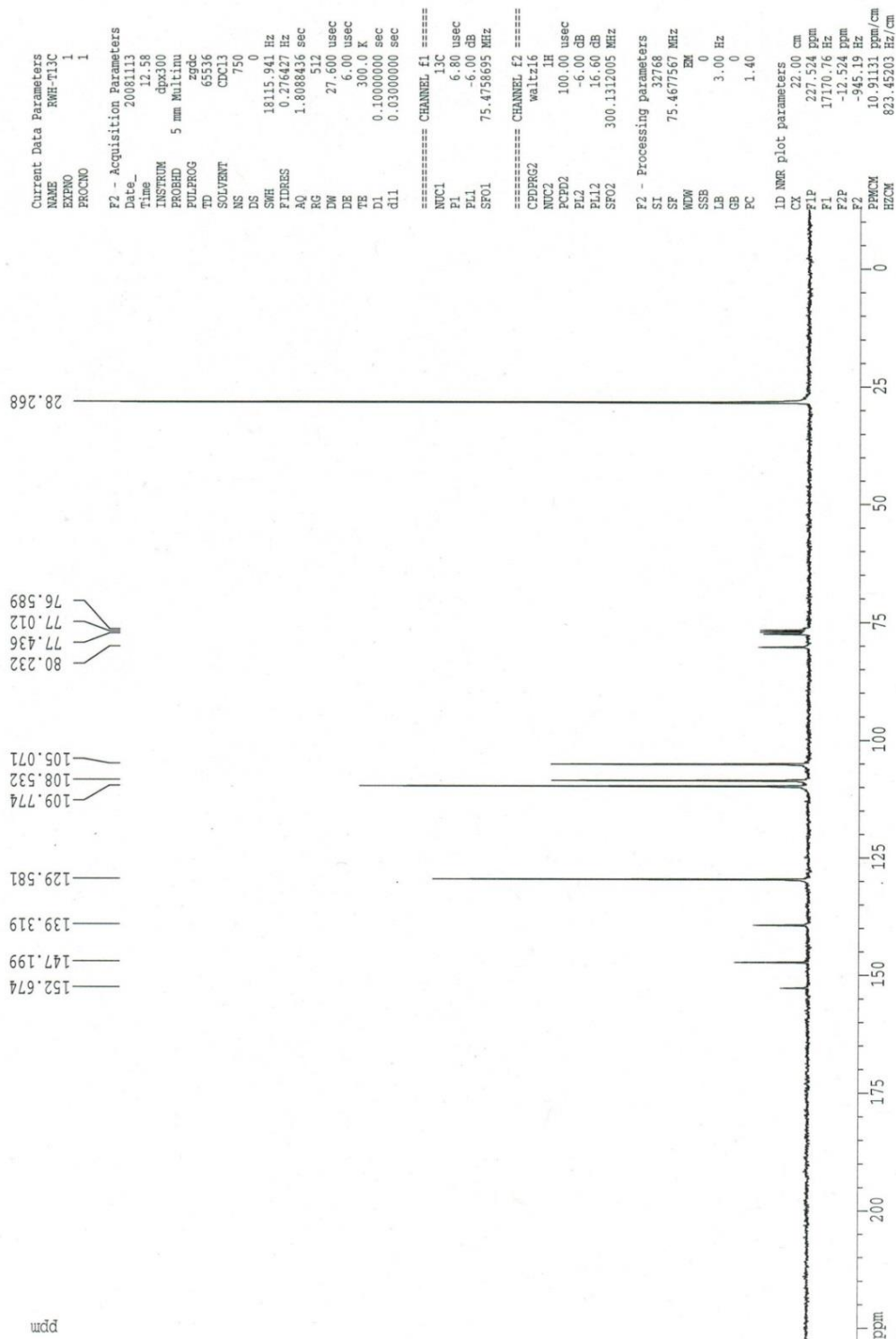
Rank	Score	Formula (M)	Ion	Meas. m/z	Pred. m/z	Df. (mDa)	Df. (ppm)	DBE	Meas. (M)	Pred. (M)	Iso
3	72.38	C34 H28 N4 O10 P2	[M+H] ⁺	715.1398	715.1353	4.5	6.29	24.0	714.1325	714.1281	93.88

¹H NMR *tert*-butyl (3-aminophenyl)carbamate (**29**)



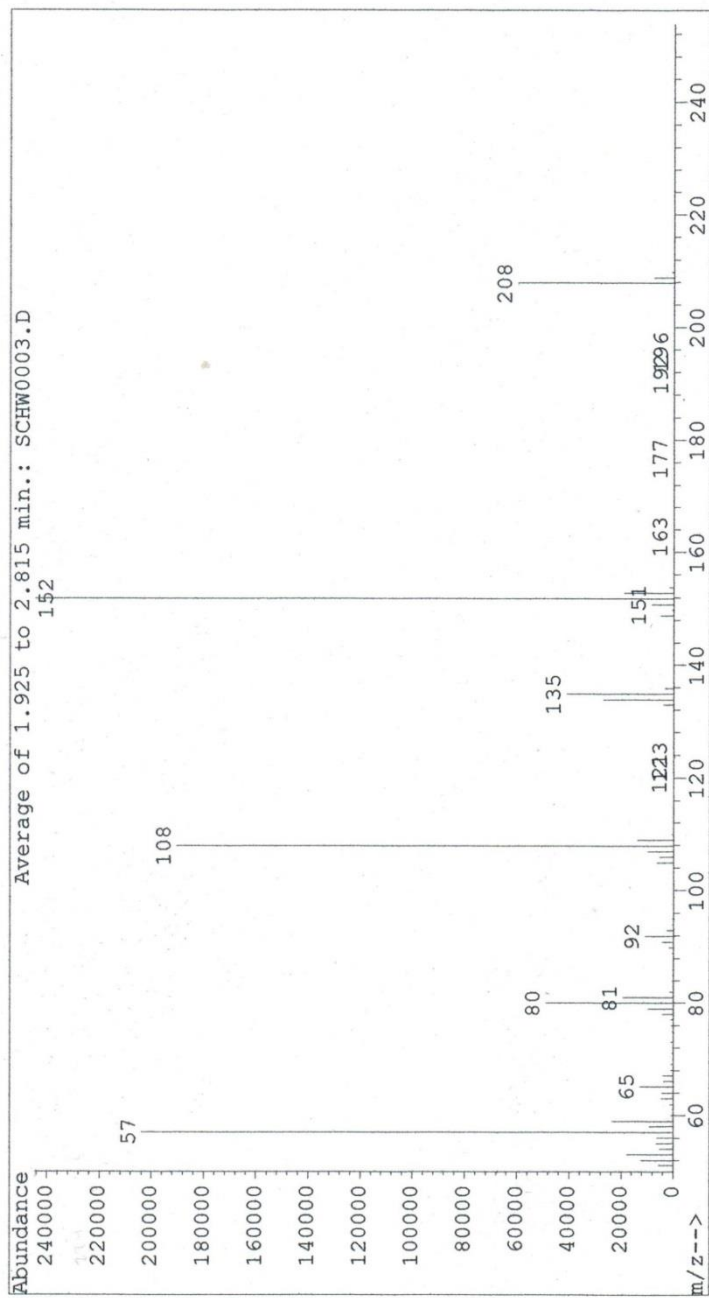
¹³C NMR tert-butyl (3-aminophenyl)carbamate (29)

Carbon Spectrum

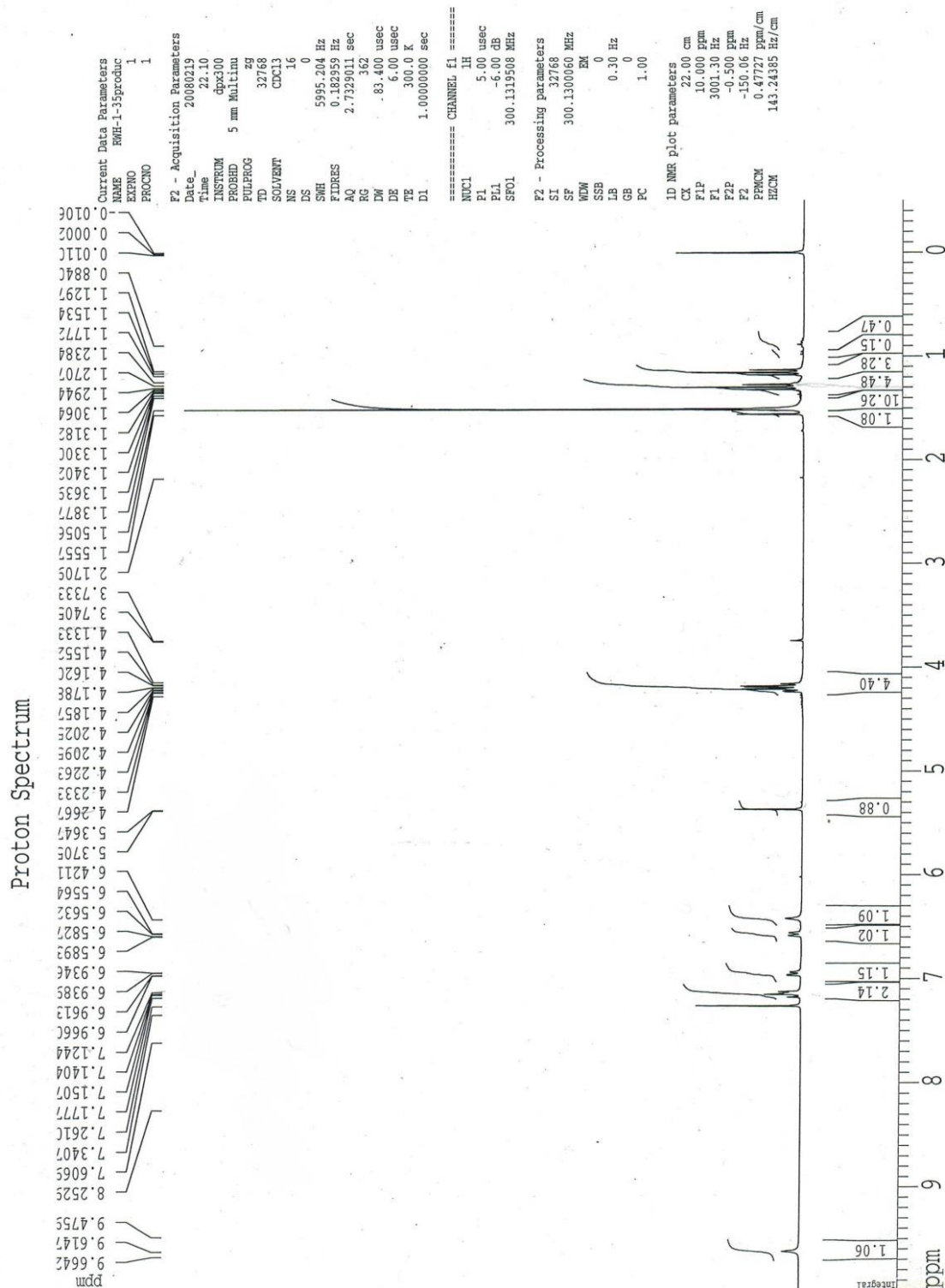


MS (EI, 70eV) tert-butyl (3-aminophenyl)carbamate (29)

File : E:\SCHW0003.D
Operator : LAIB
Acquired : 3 Jul 108 12:38 pm using AcqMethod EI600
Instrument : 5989
Sample Name: RWH-1-34
Misc Info : EI
Vial Number: 1

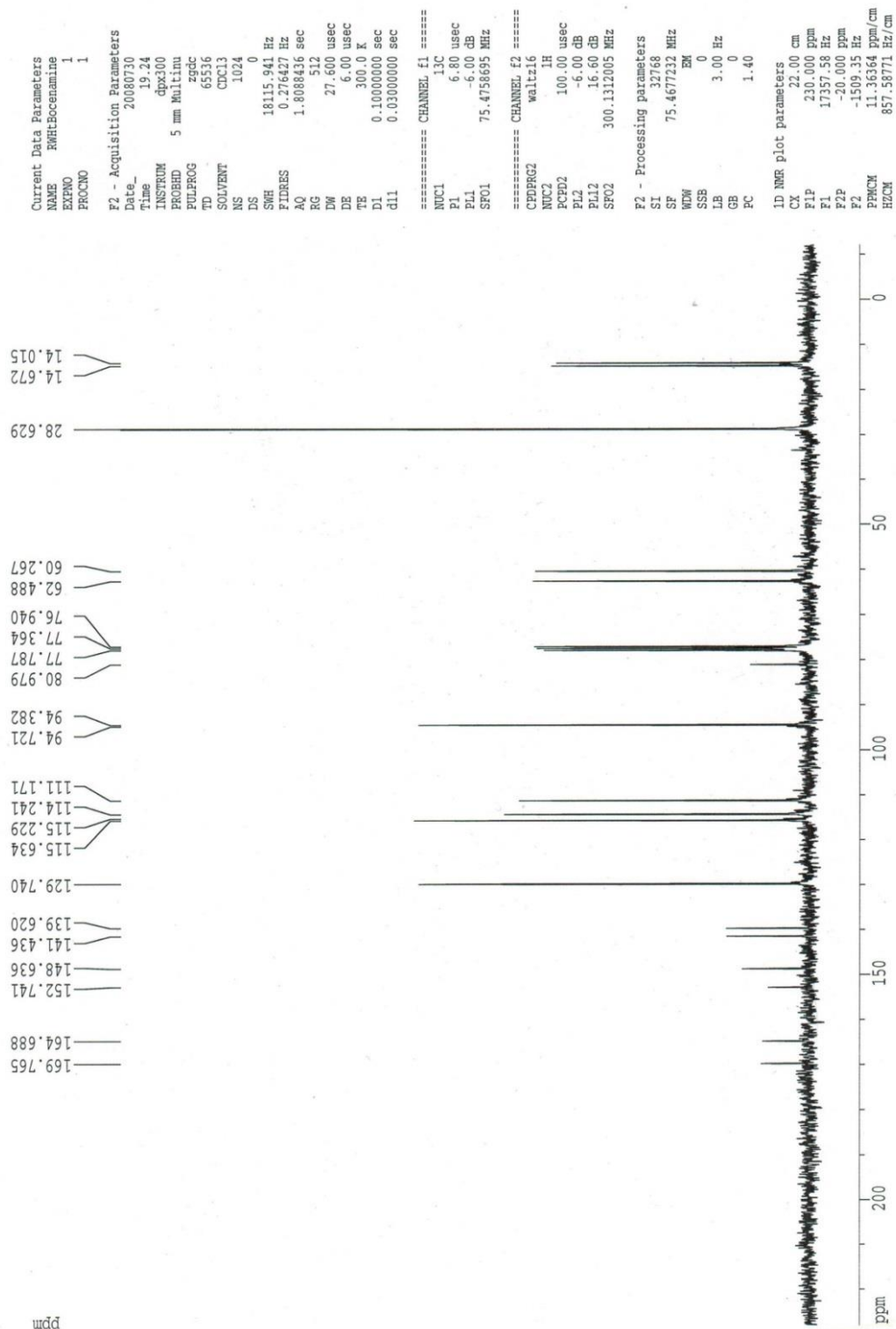


¹H NMR 2-(3-tert-Butoxycarbonylamino-phenylamino)-but-2-enedioic acid diethyl ester (30)



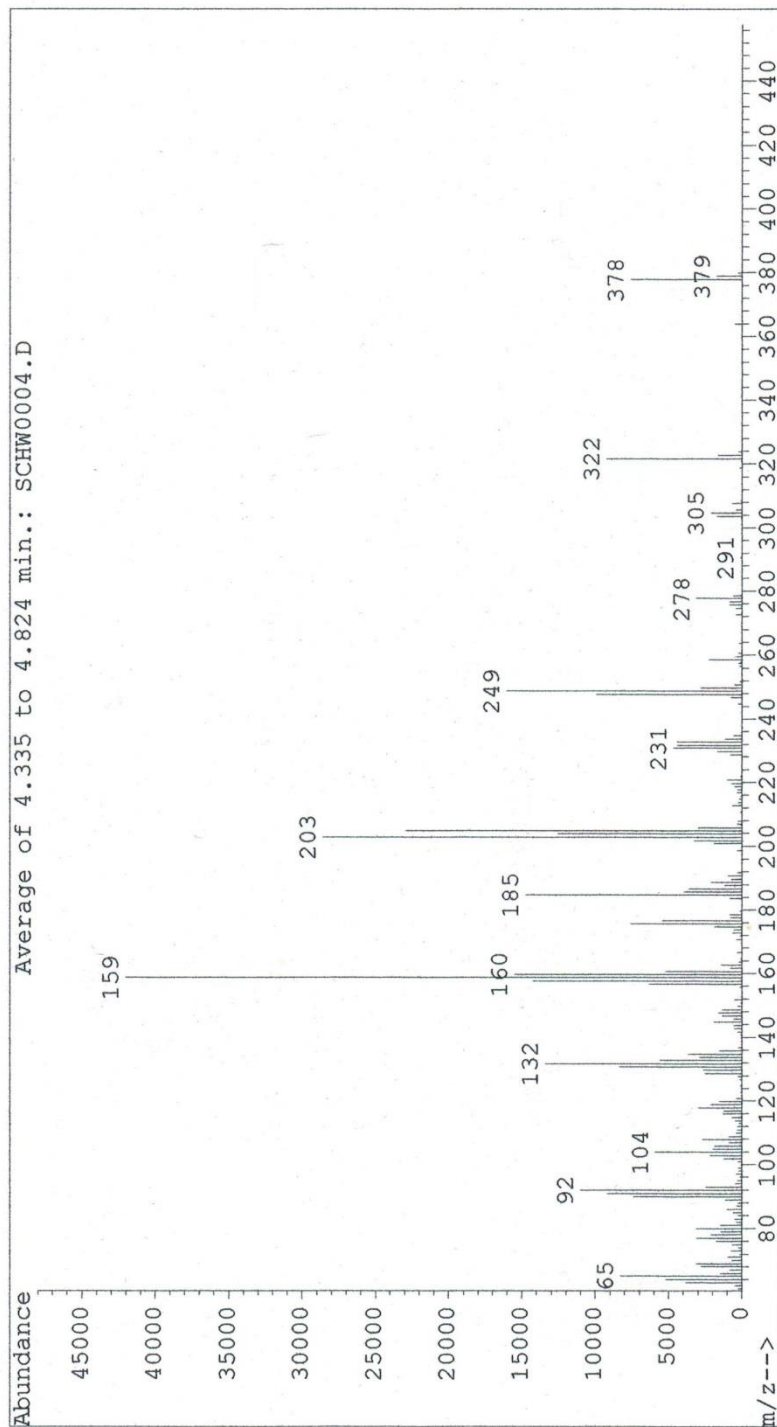
¹³C NMR 2-(3-tert-Butoxycarbonylamino-phenylamino)-but-2-enedioic acid diethyl ester (30)

Carbon Spectrum

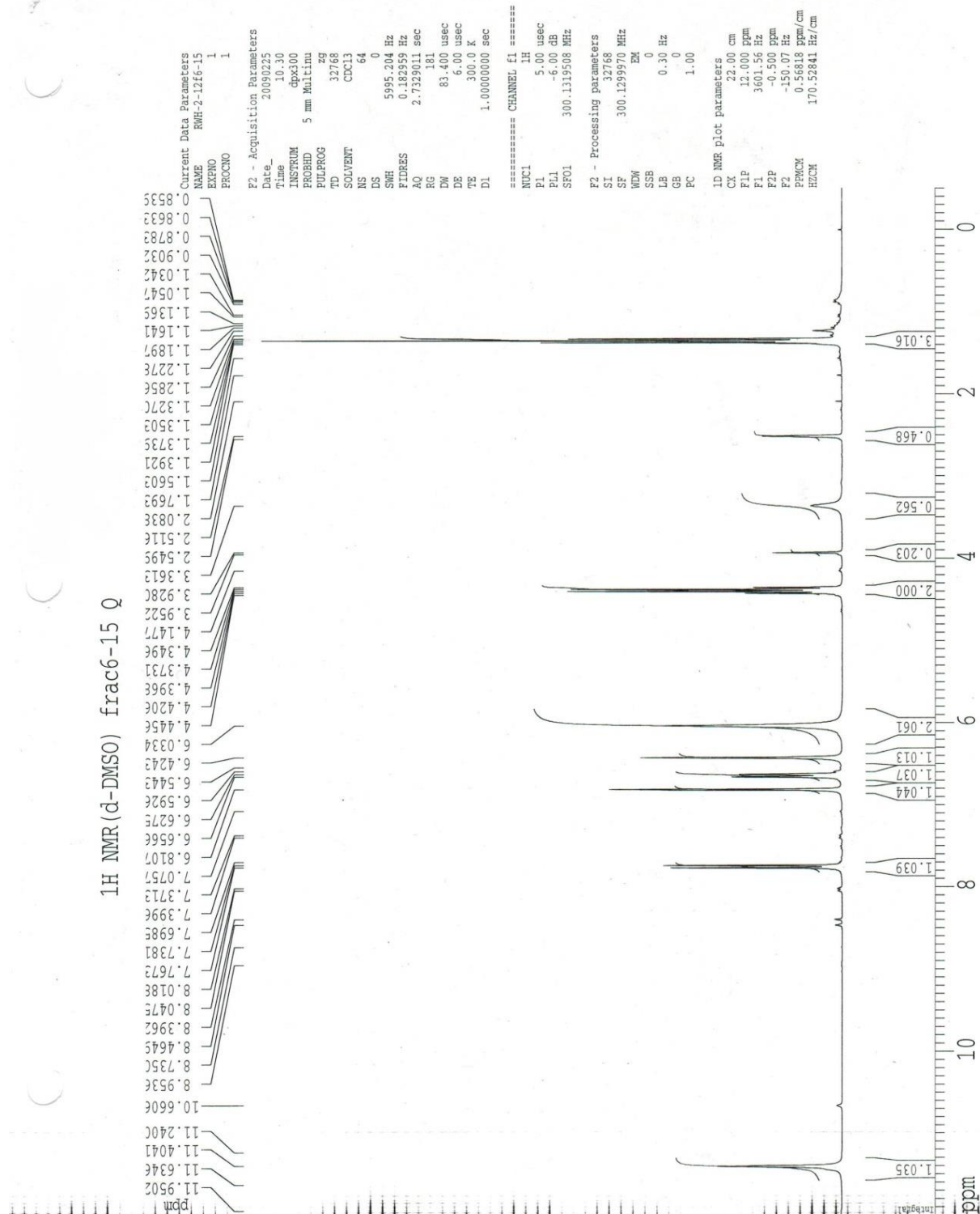


MS (70eV) 2-(3-tert-Butoxycarbonylamino-phenylamino)-but-2-enedioic acid diethyl ester (30)

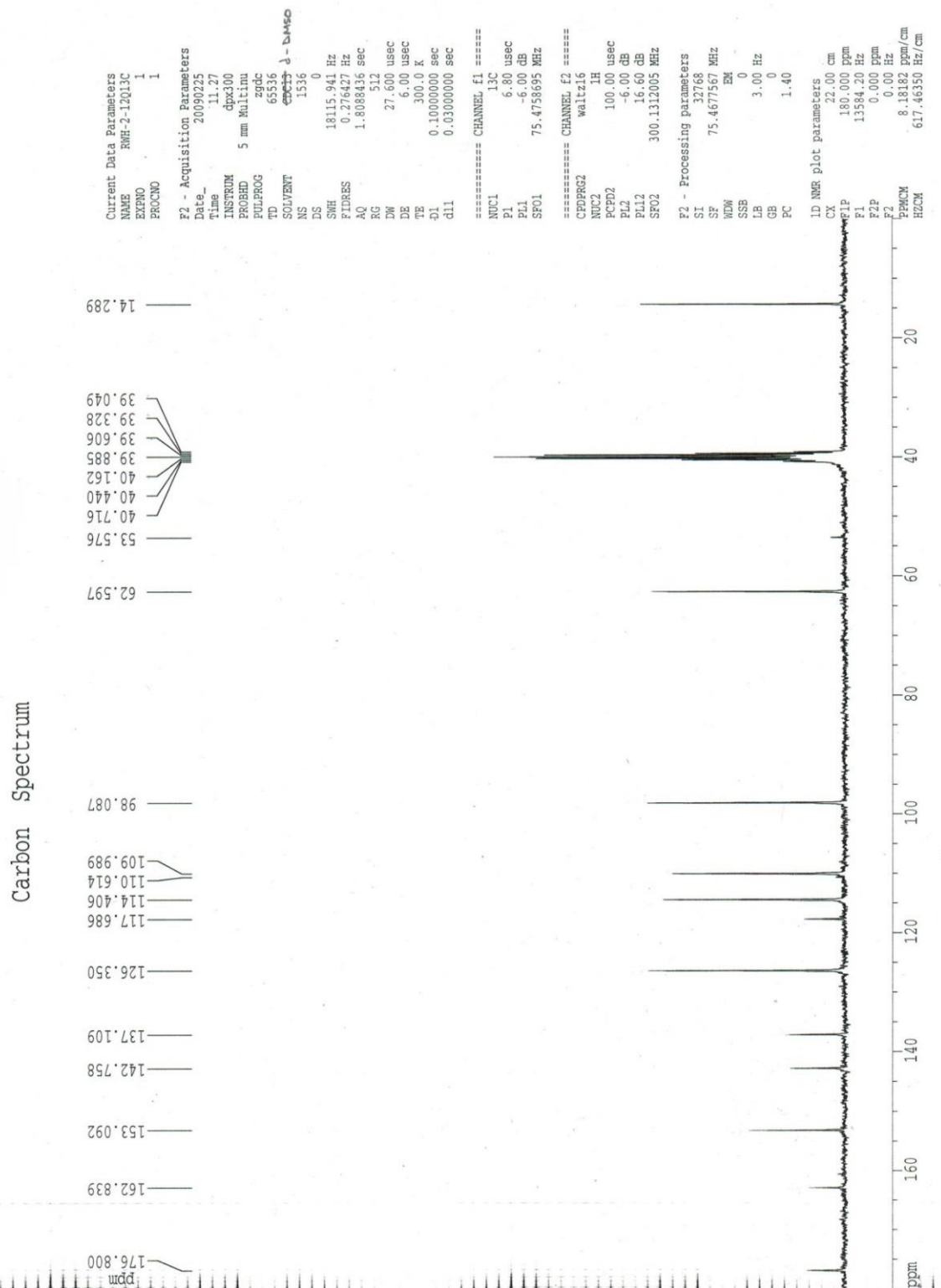
File : E:\SCHW0004.D
Operator : LAIB
Acquired : 3 Jul 108 1:45 pm using AcqMethod EI600
Instrument : 5989
Sample Name: RWH-1-35
Misc Info : EI
Vial Number: 1



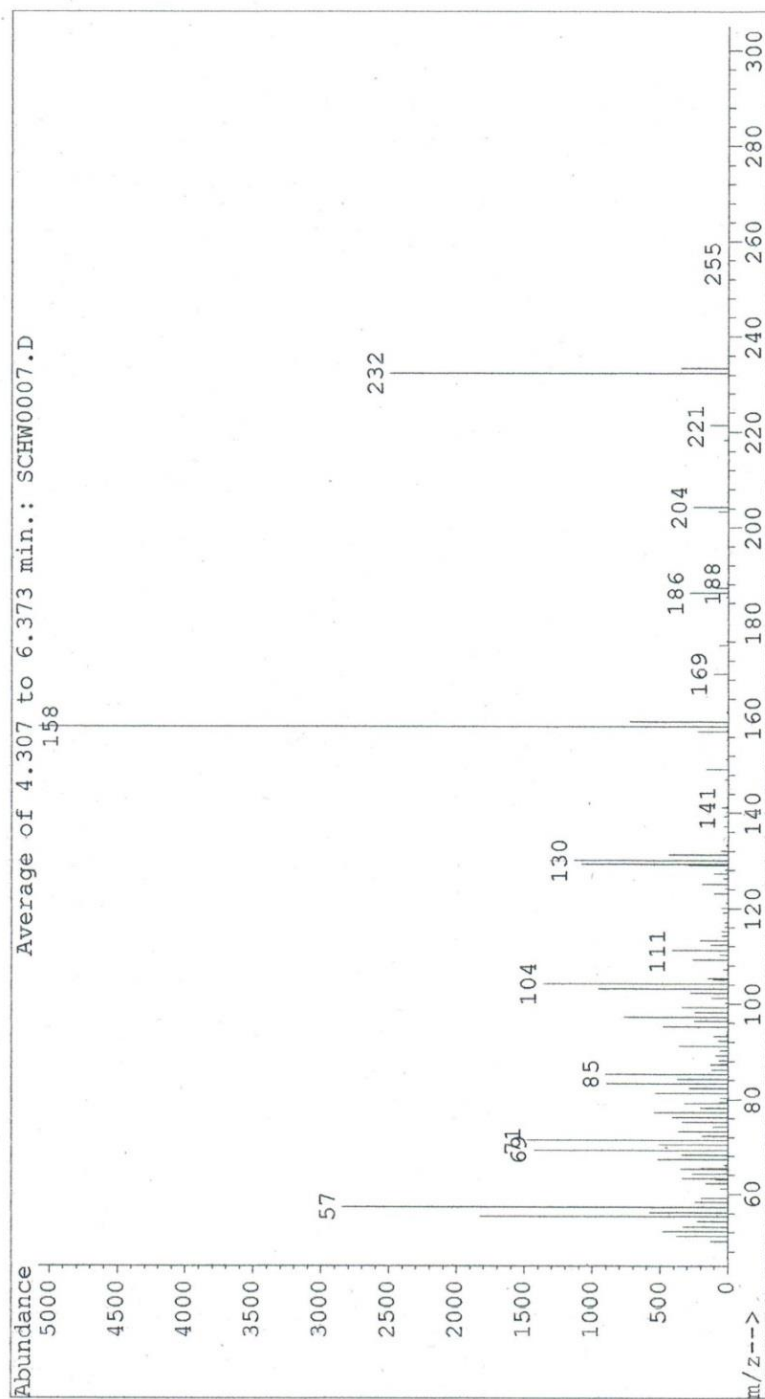
¹H NMR 7-Amino-4-oxo-1,4-dihydro-quinoline-2-carboxylic acid ethyl ester (31)



¹³C NMR 7-Amino-4-oxo-1,4-dihydro-quinoline-2-carboxylic acid ethyl ester (31)



File : E:\SCHW0007.D
Operator : LAIB
Acquired : 26 Aug 108 3:50 pm using AcqMethod EI600
Instrument : 5989
Sample Name: RWH-1-60
Misc Info : EI; (232)
Vial Number: 1

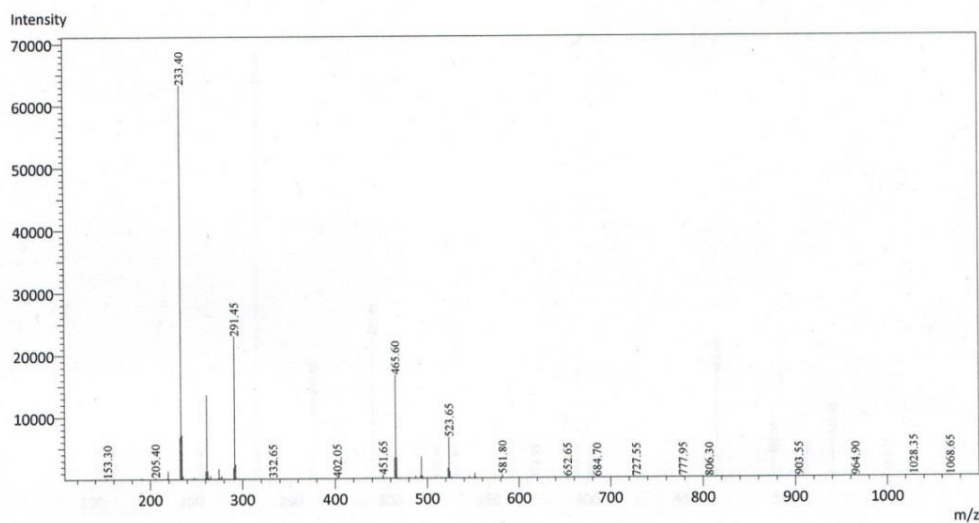


Shimadzu LCMS-2020 Data Report

Mass Spectrum for Sample
RWH-4-83.lcd

Operator: Mark Wang

Data Filename: C:\LabSolutions\Data\Schwabacher Alan\RWH-4-83.lcd
Spectrum Mode: Averaged
Retention Time: ----
Interface Type (ESI, APCI, DUIS): DUIS
Acquisition Mode (Scan, SIM, Profile): Scan
Polarity: +

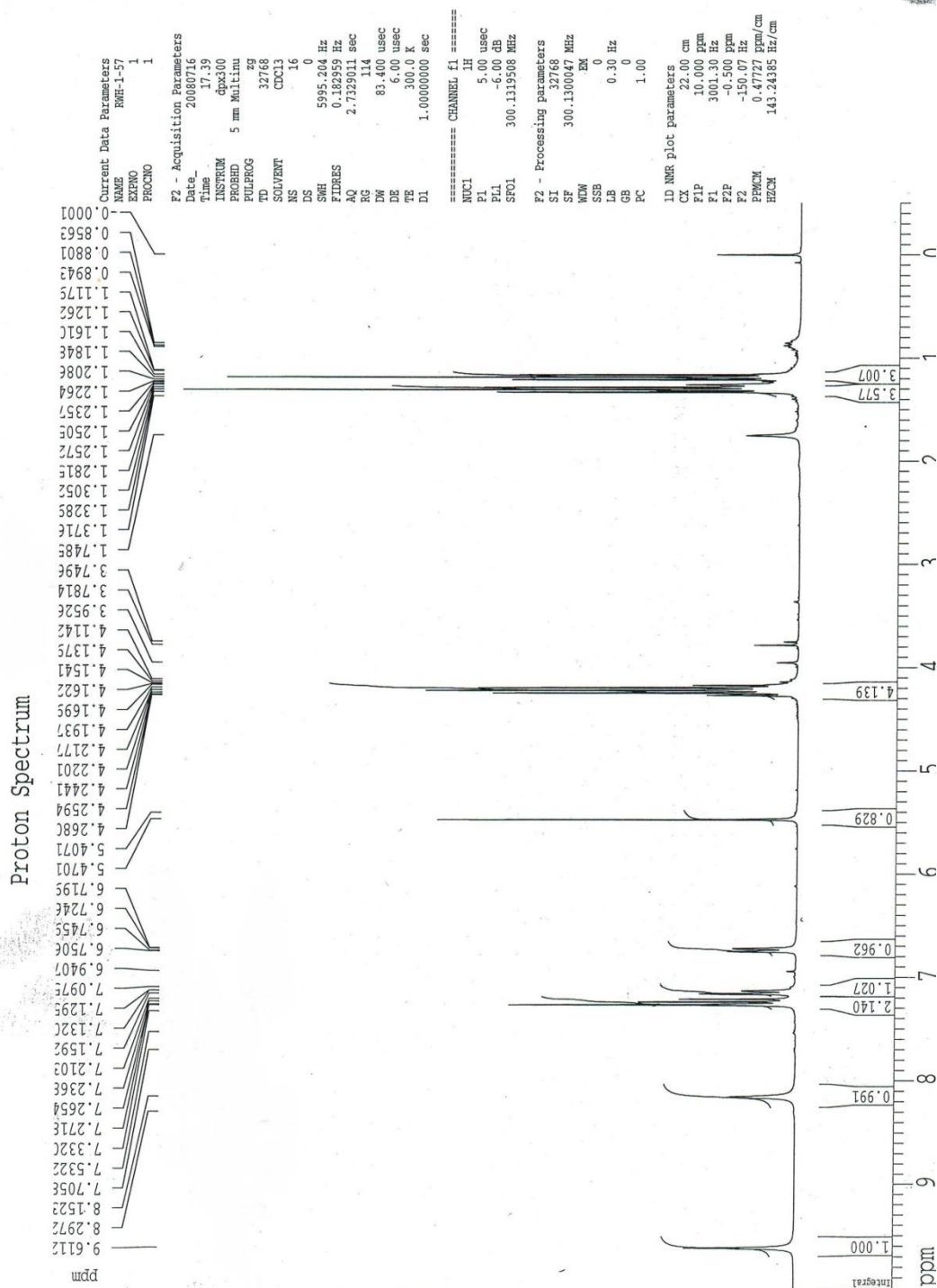


$$233 = M + H^+$$

$$291 = M + 59$$

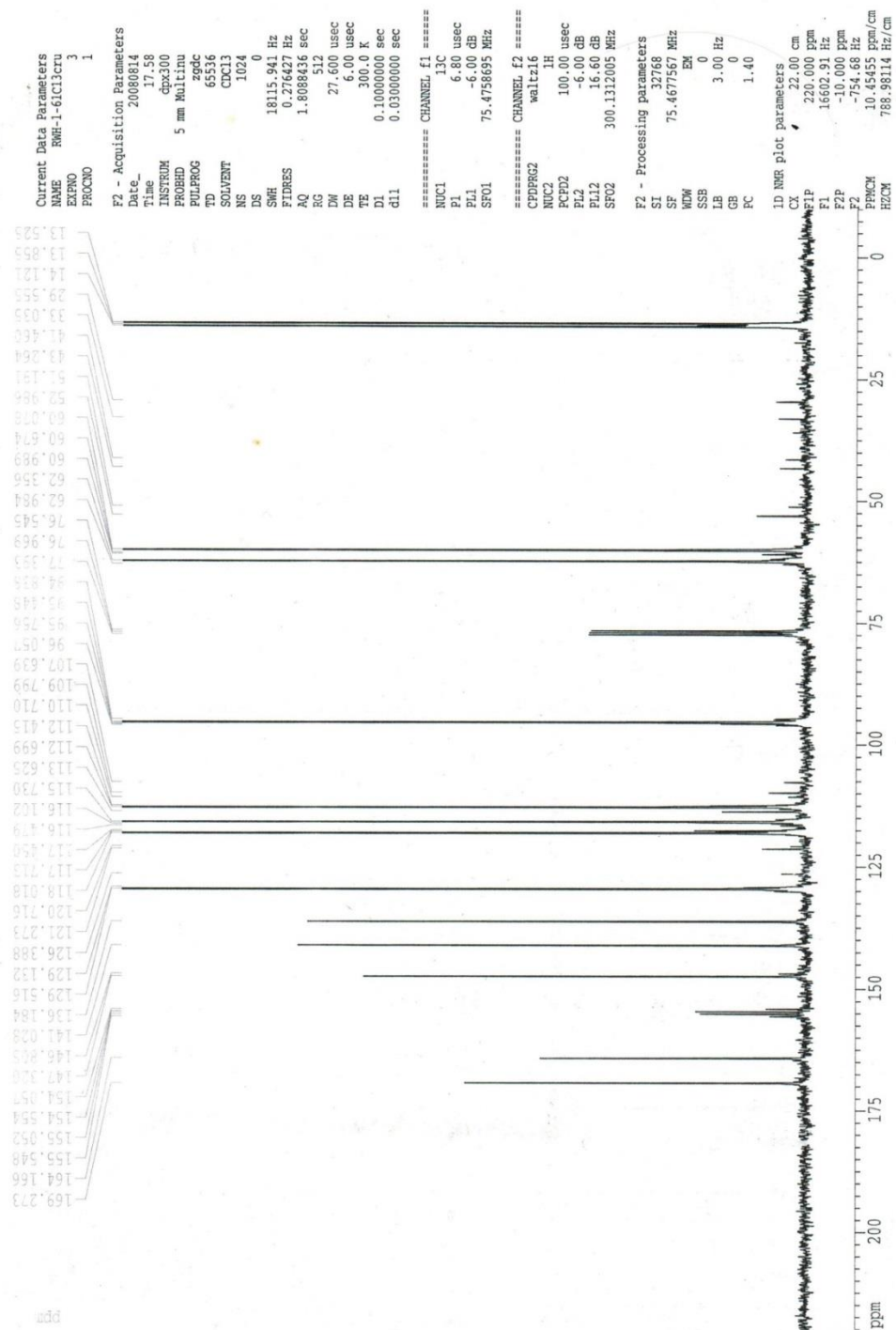
$$465 = 2M + H^+$$

¹H NMR Diethyl 2-((3-(2,2,2-trifluoroacetamido)phenyl)amino)fumarate (34)



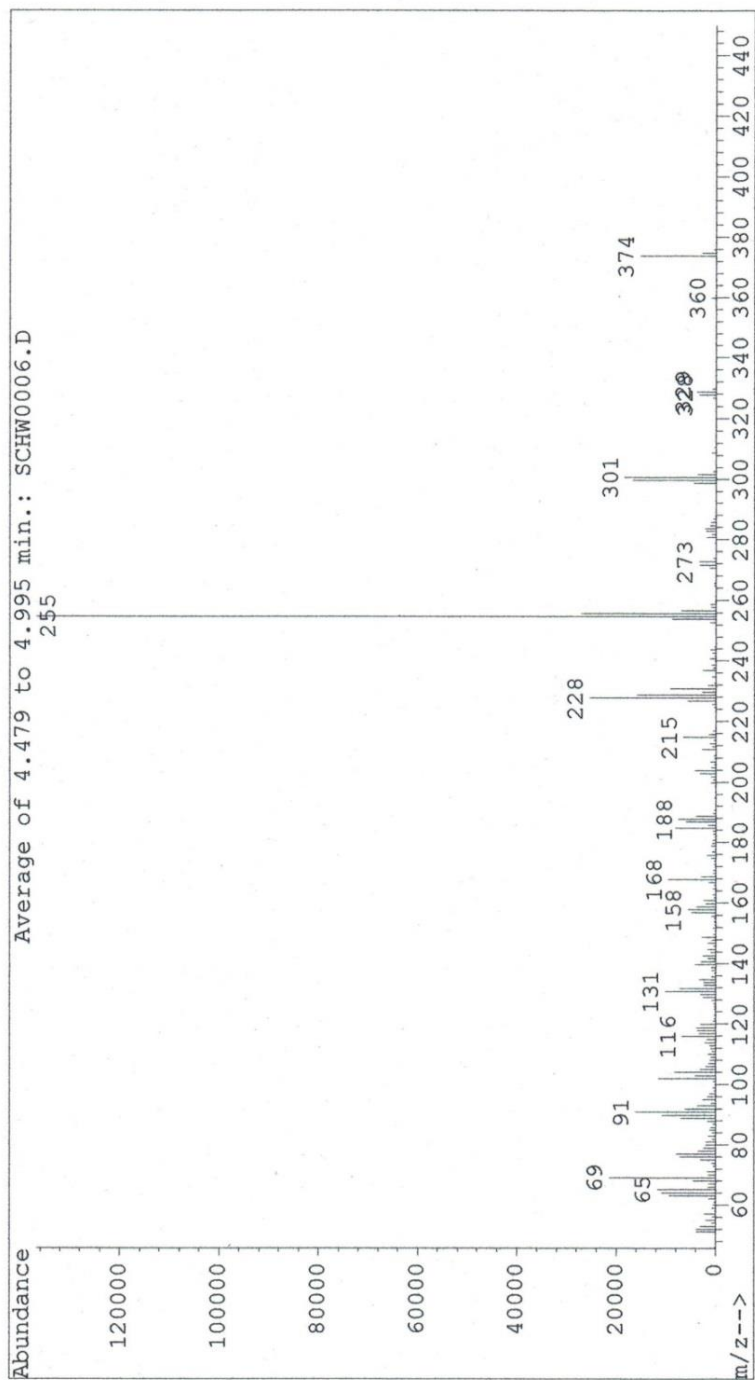
¹³C NMR Diethyl 2-((3-(2,2,2-trifluoroacetamido)phenyl)amino)fumarate (34)

Carbon Spectrum

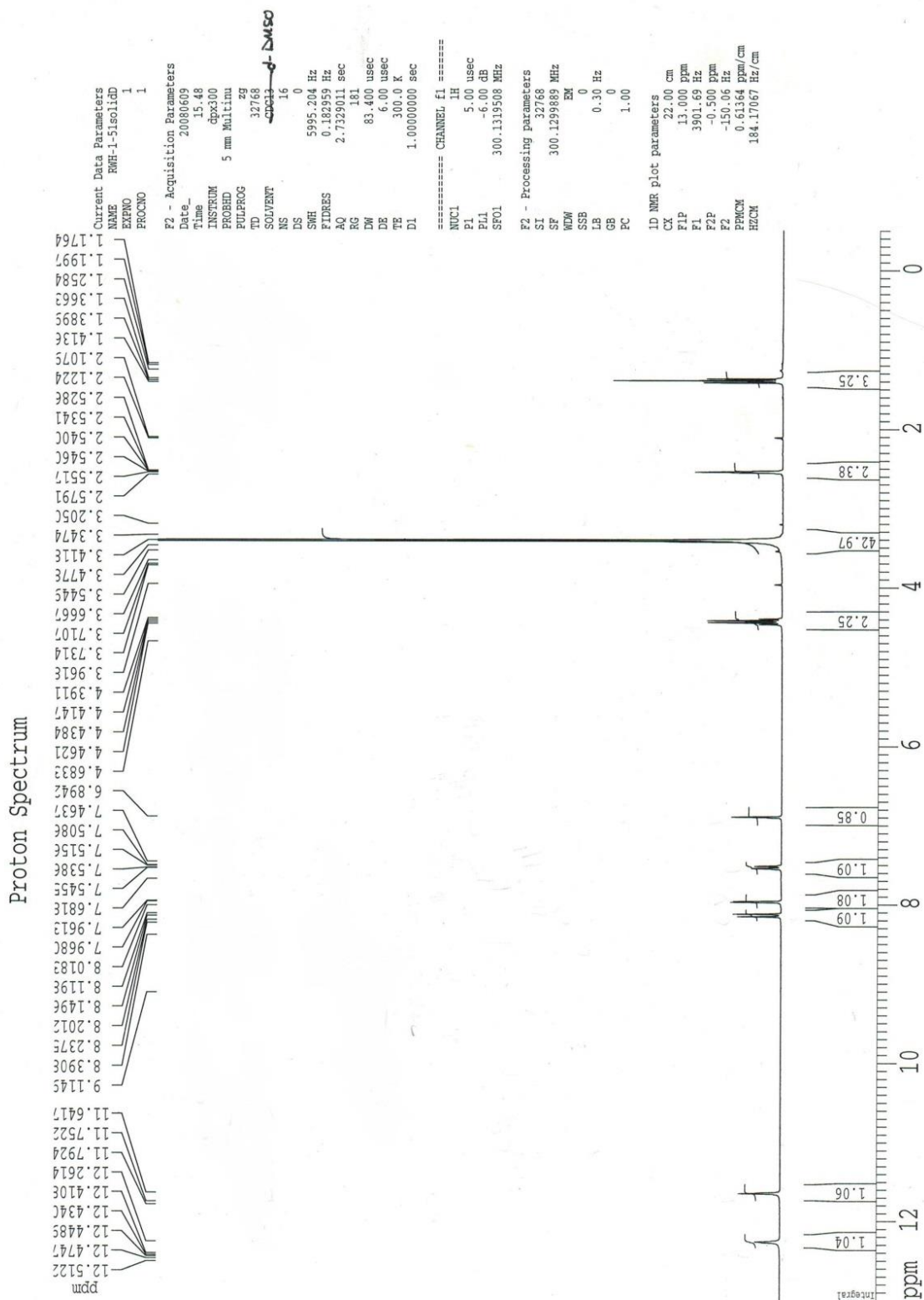


MS (EI, 70eV) Diethyl 2-((3-(2,2,2-trifluoroacetamido)phenyl)amino)fumarate (34)

File : E:\SCHW00006.D
Operator : LAIB
Acquired : 23 Jul 108 1:19 pm using AcqMethod EI600
Instrument : 5989
Sample Name: RWH-1-57
Misc Info : EI
Vial Number: 1

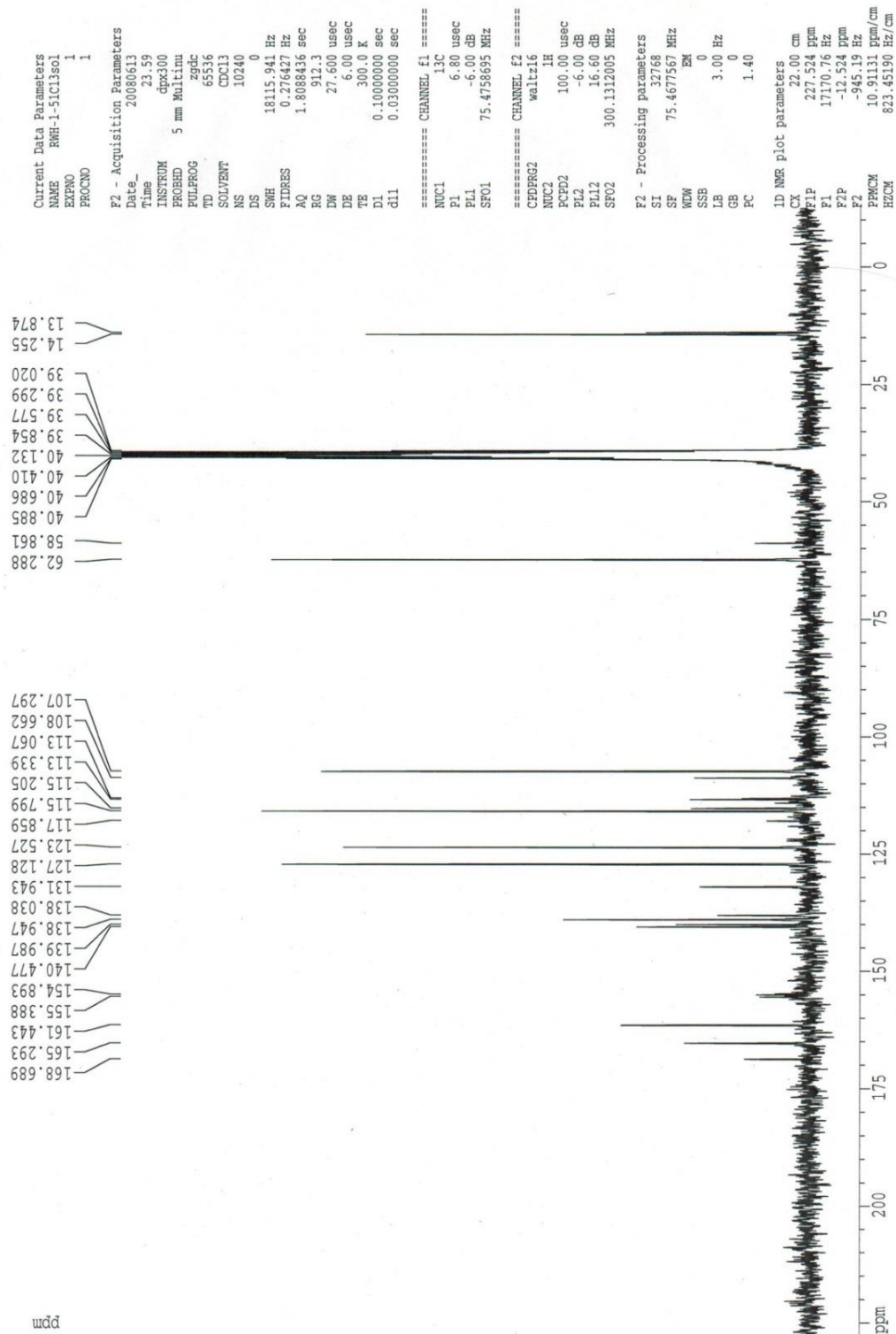


¹H NMR Ethyl 4-oxo-7-(2,2,2-trifluoroacetamido)-1,4-dihydroquinoline-2-carboxylate (35)



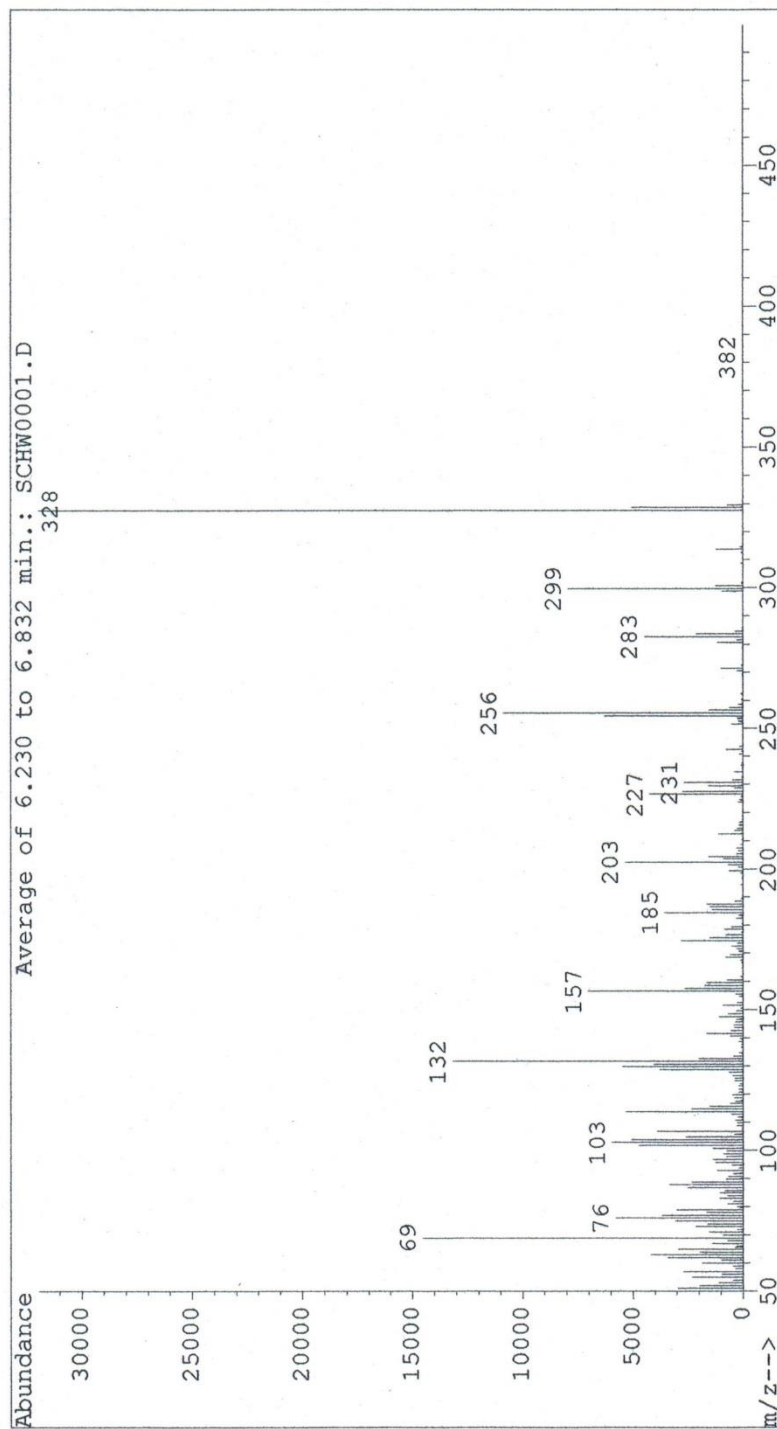
¹³C NMR Ethyl 4-oxo-7-(2,2,2-trifluoroacetamido)-1,4-dihydroquinoline-2-carboxylate (35)

Carbon Spectrum

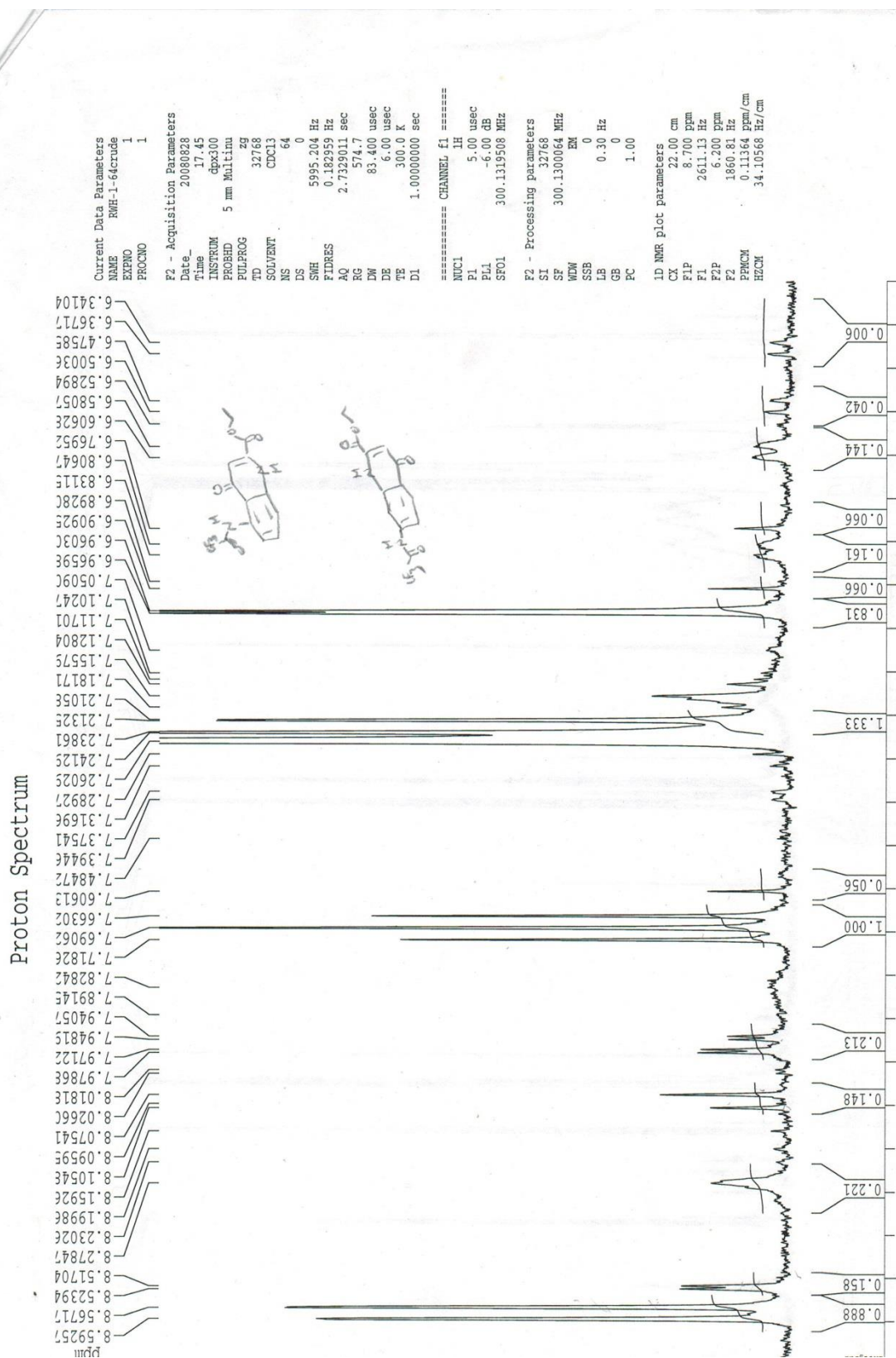


MS (EI, 70eV) Ethyl 4-oxo-7-(2,2,2-trifluoroacetamido)-1,4-dihydroquinoline-2-carboxylate (35)

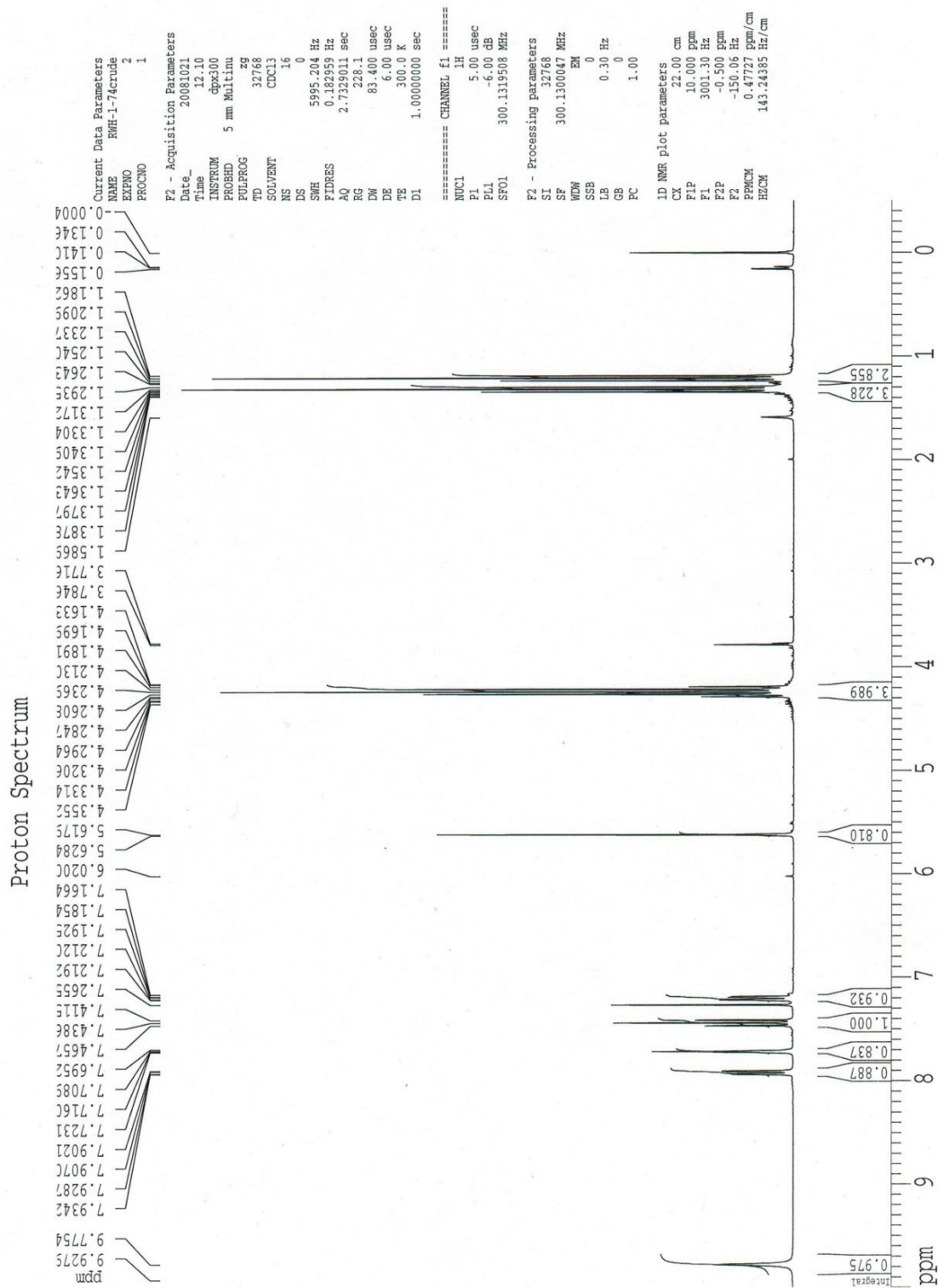
File : E:\SCHW0001.D
Operator : LAIB
Acquired : 26 Jun 108 2:41 pm using AcqMethod EI600
Instrument : 5989
Sample Name: RWH-1-51
Misc Info : EI (328)
Vial Number: 1



¹H NMR Ethyl 4-oxo-5-(2,2,2-trifluoroacetamido)-1,4-dihydroquinoline-2-carboxylate (36)

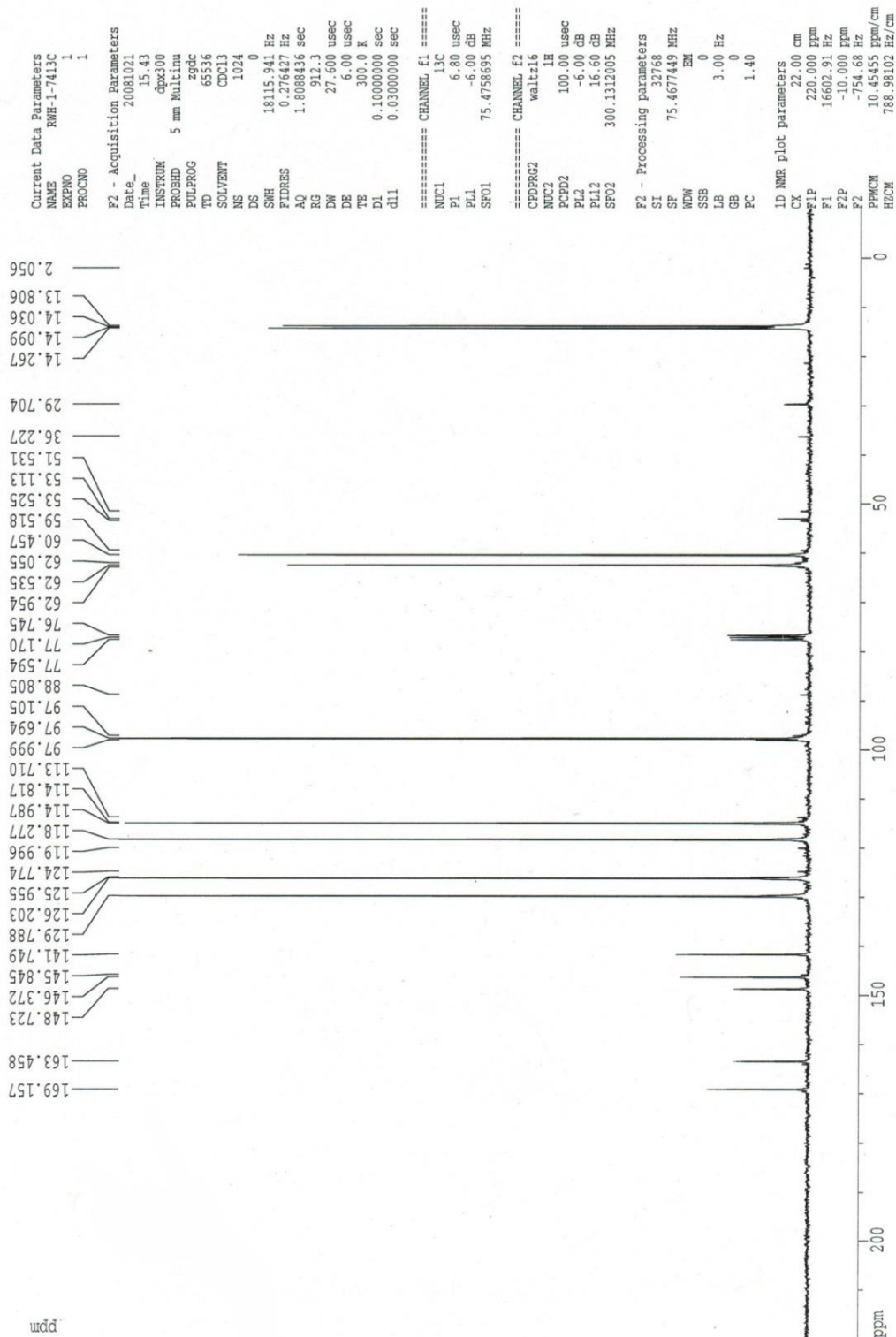


¹H NMR Diethyl 2-((3-nitrophenyl)amino)fumarate (37)



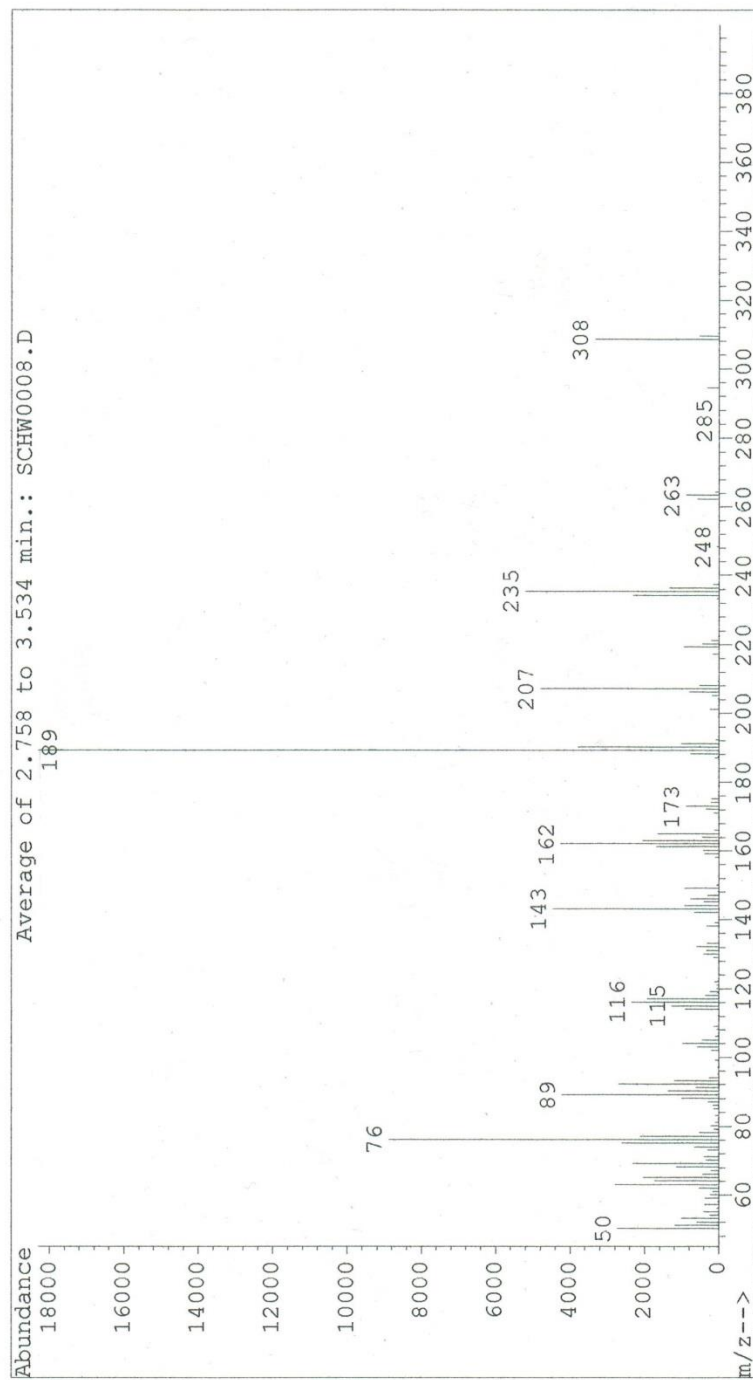
¹³C NMR Diethyl 2-((3-nitrophenyl)amino)fumarate (37)

Carbon Spectrum

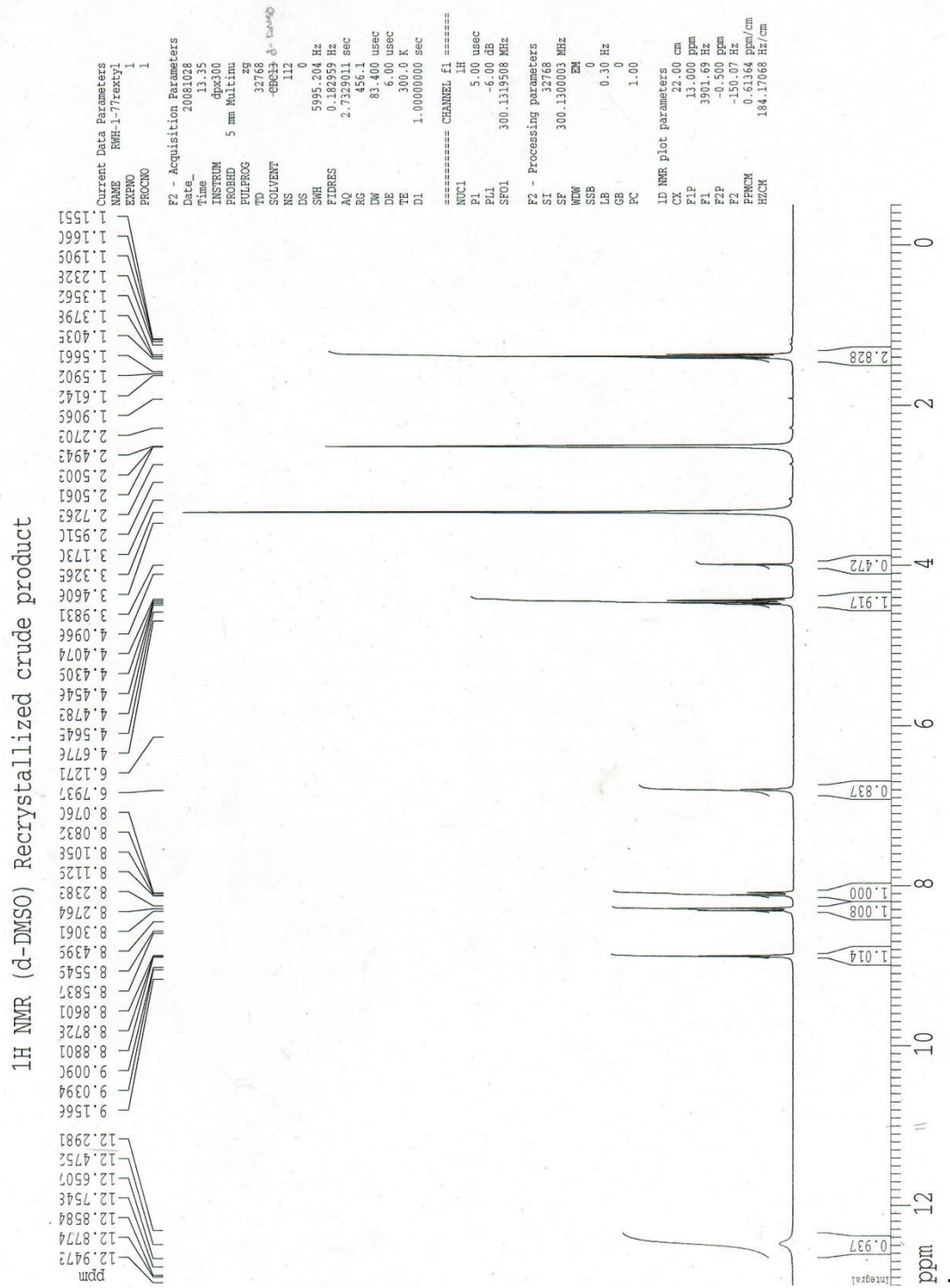


MS (EI, 70eV) Diethyl 2-((3-nitrophenyl)amino)fumarate (37)

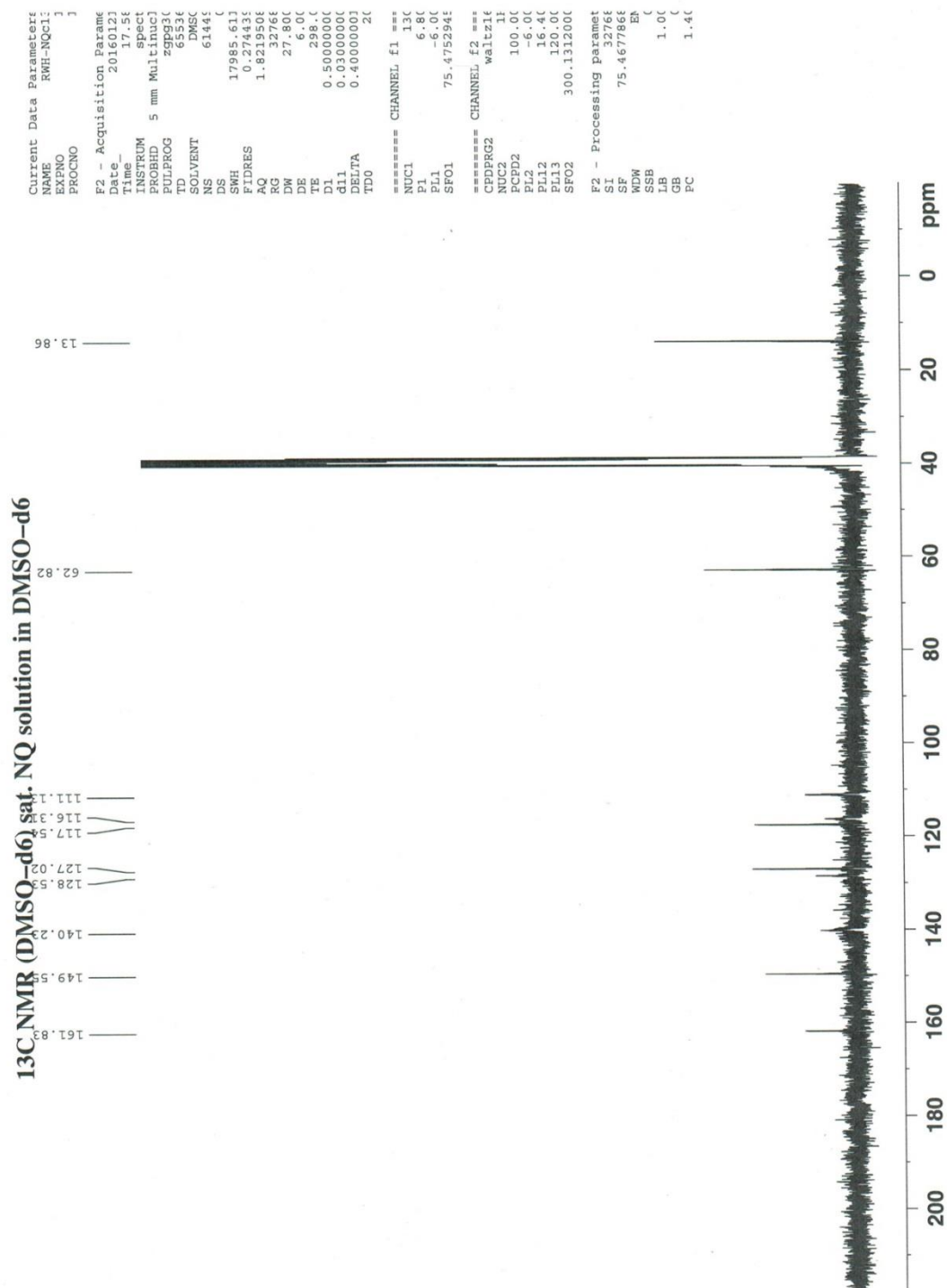
File : E:\SCHW0008.D
Operator : LAIB
Acquired : 23 Oct 108 12:15 pm using AcqMethod EI600
Instrument : 5989
Sample Name: RWH-1-74
Misc Info : EI (308)
Vial Number: 1



¹H NMR Ethyl 7-nitro-4-oxo-1,4-dihydroquinoline-2-carboxylate (38)

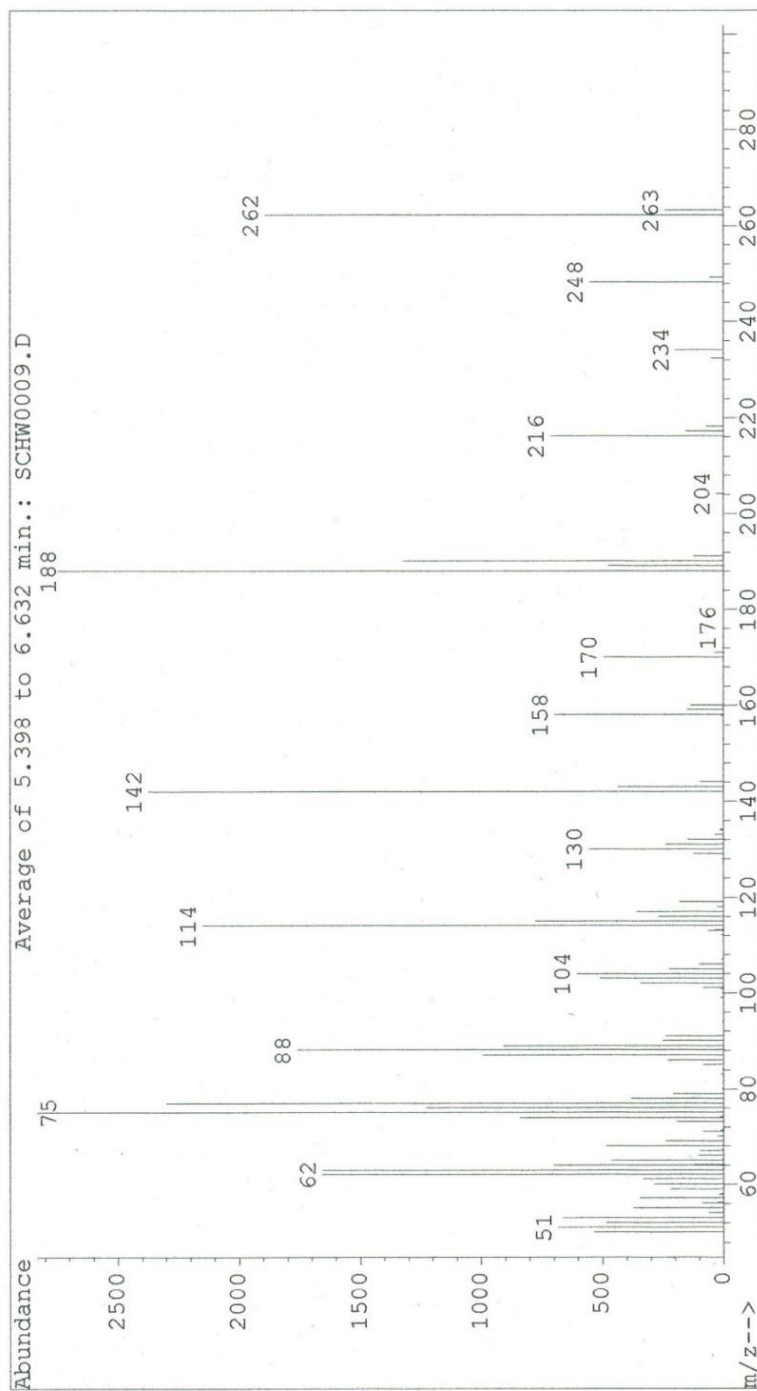


¹³C NMR Ethyl 7-nitro-4-oxo-1,4-dihydroquinoline-2-carboxylate (38)

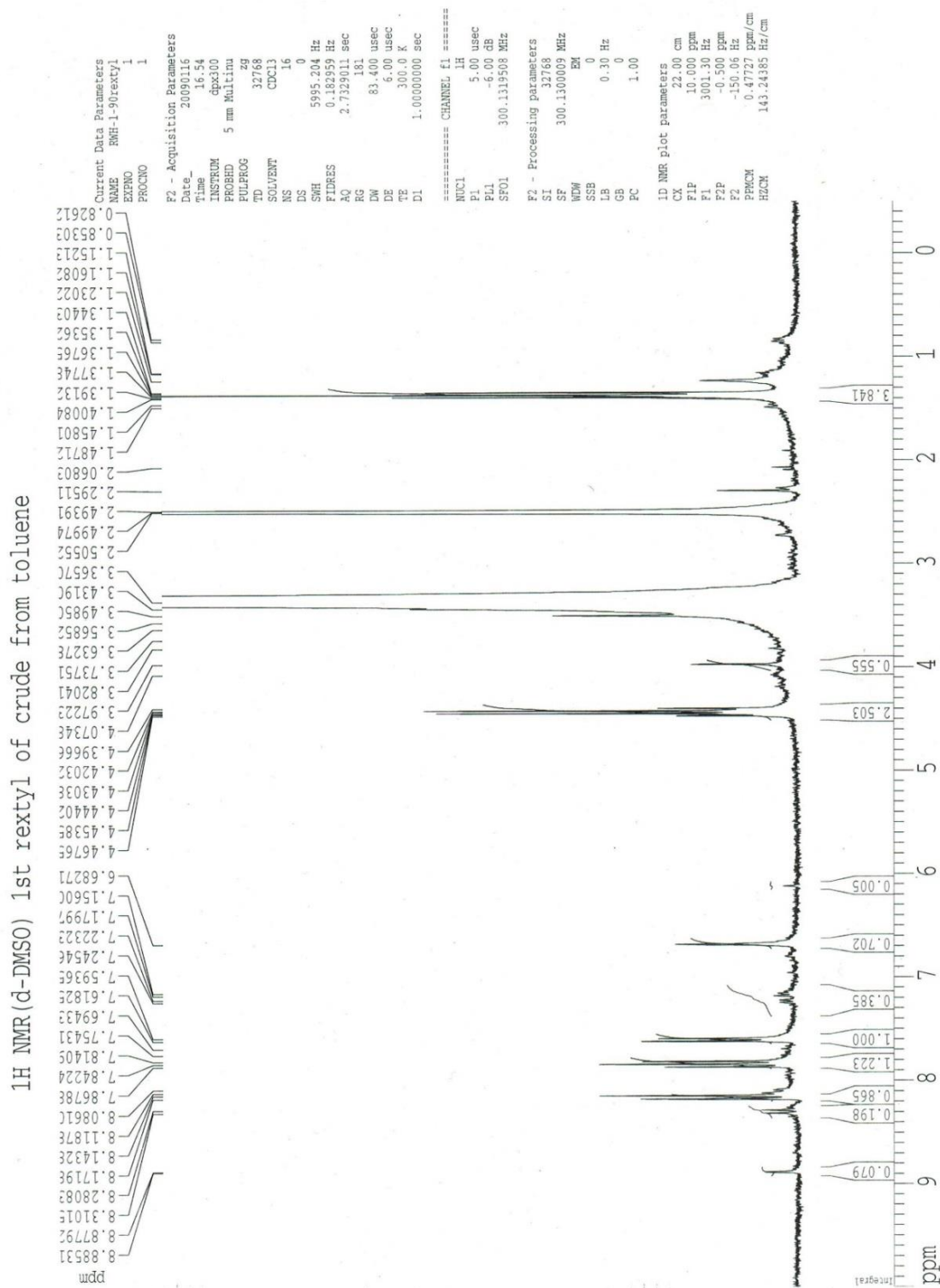


MS (EI, 70eV) Ethyl 7-nitro-4-oxo-1,4-dihydroquinoline-2-carboxylate (38)

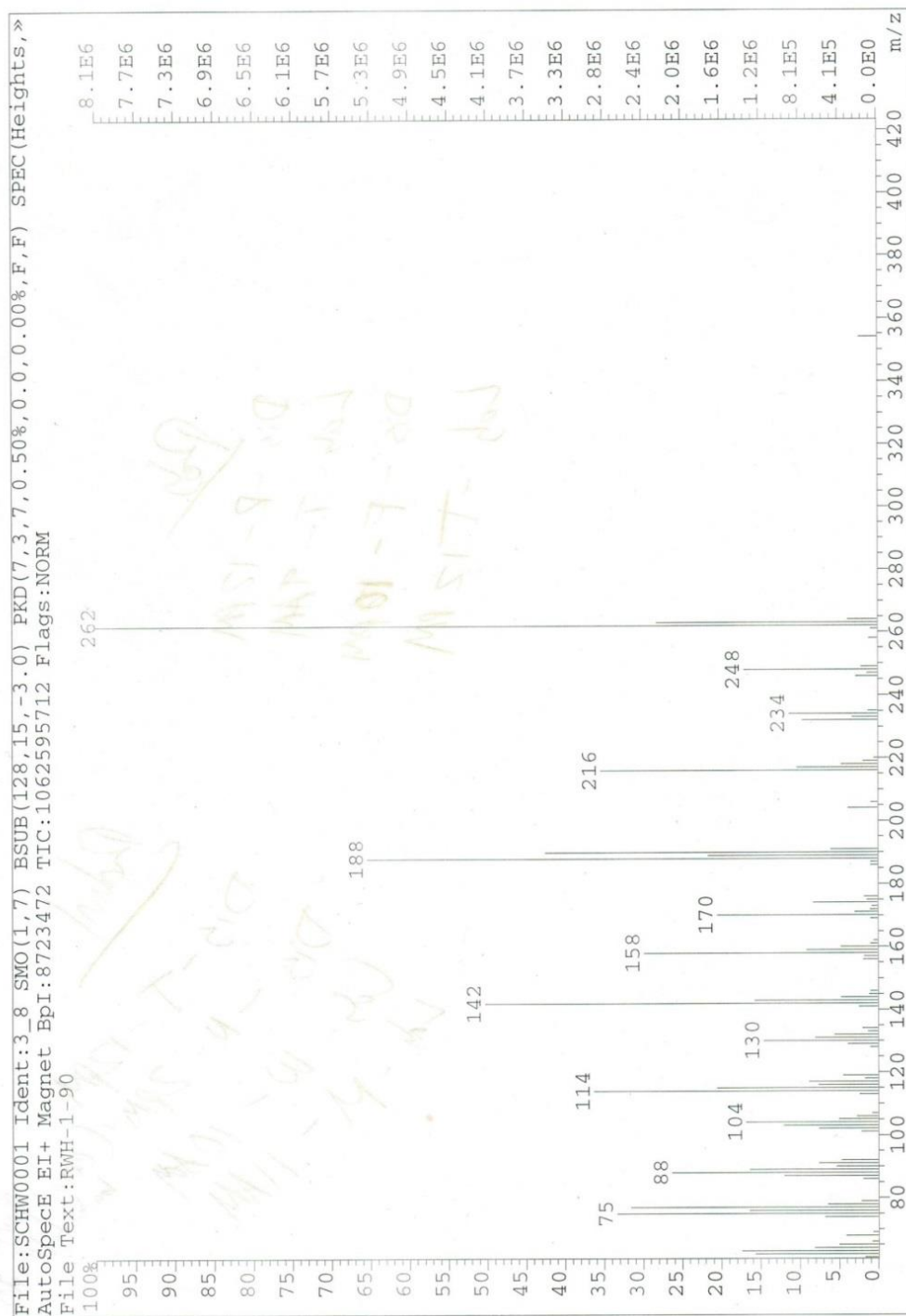
File : E:\SCHW00009.D
Operator : LAIB
Acquired : 13 Nov 108 12:26 pm using AcqMethod EI600
Instrument : 5989
Sample Name: RWH-1-77
Misc Info : EI (262)
Vial Number: 1



¹H NMR *Ethyl 5-nitro-4-oxo-1,4-dihydroquinoline-2-carboxylate* (**39**)

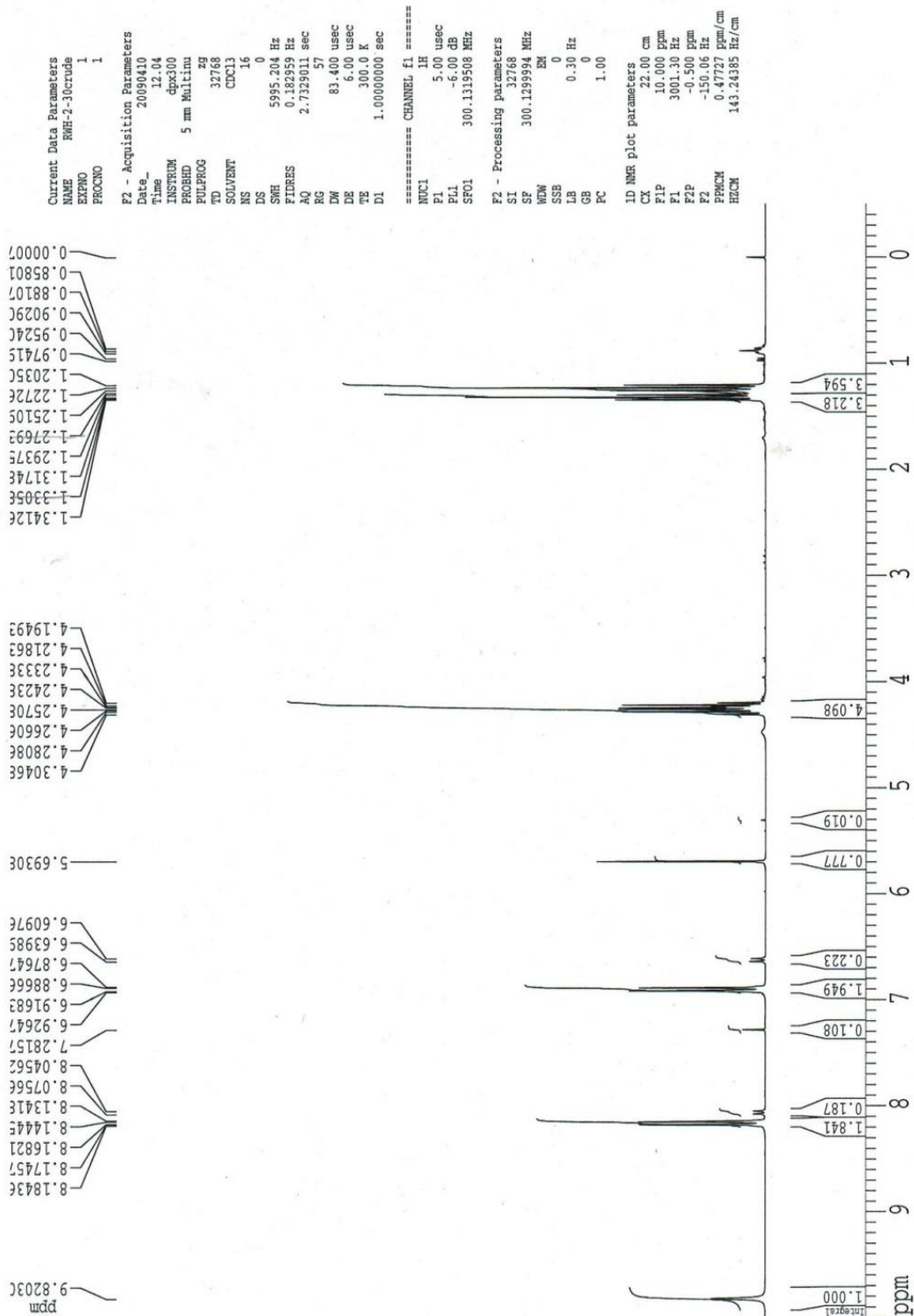


MS (EI, 70eV) Ethyl 5-nitro-4-oxo-1,4-dihydroquinoline-2-carboxylate (39)

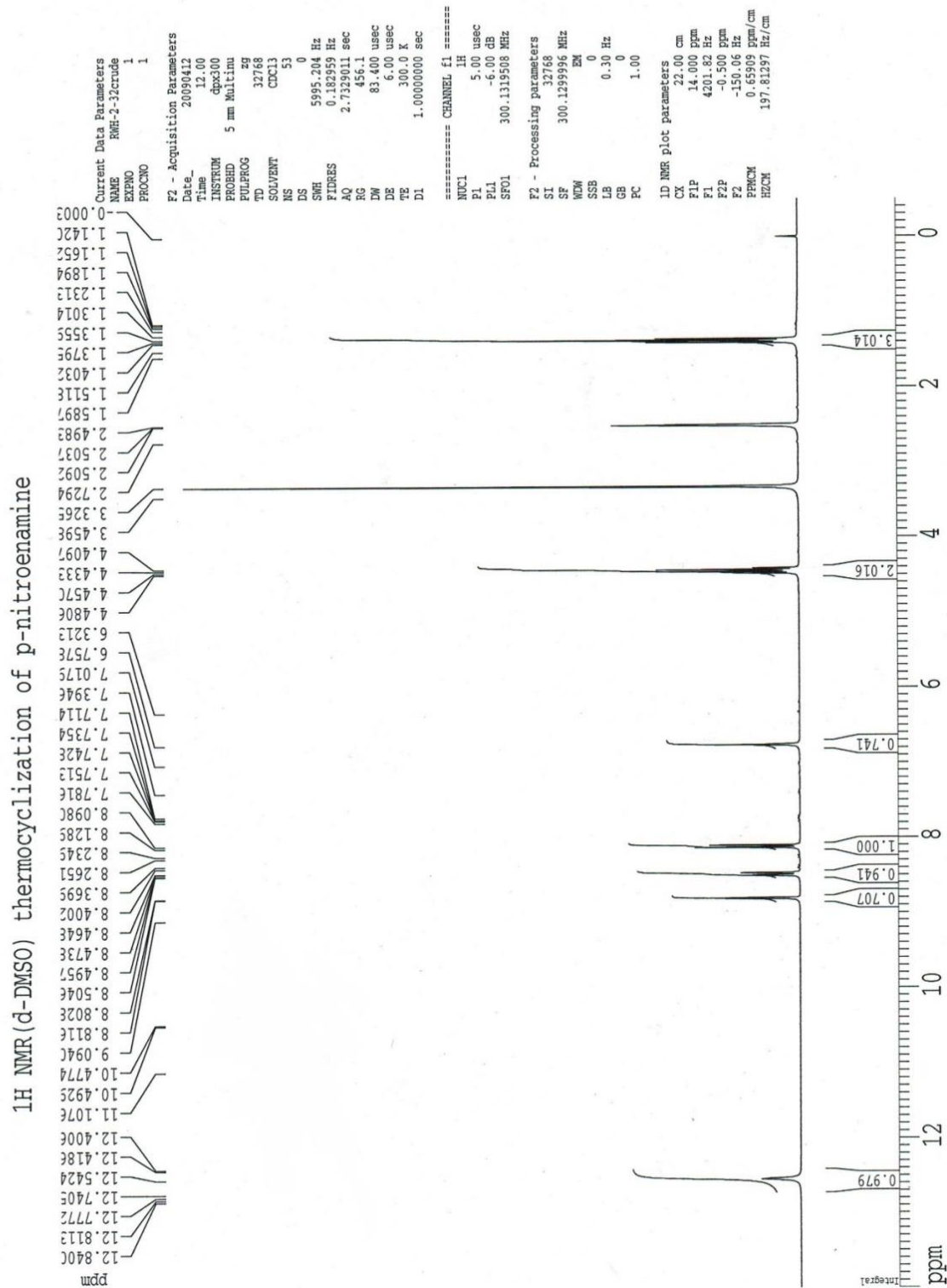


¹H NMR Diethyl 2-((4-nitrophenyl)amino)fumarate (40)

¹H NMR (CDCl₃) crude product of p-nitroenamine

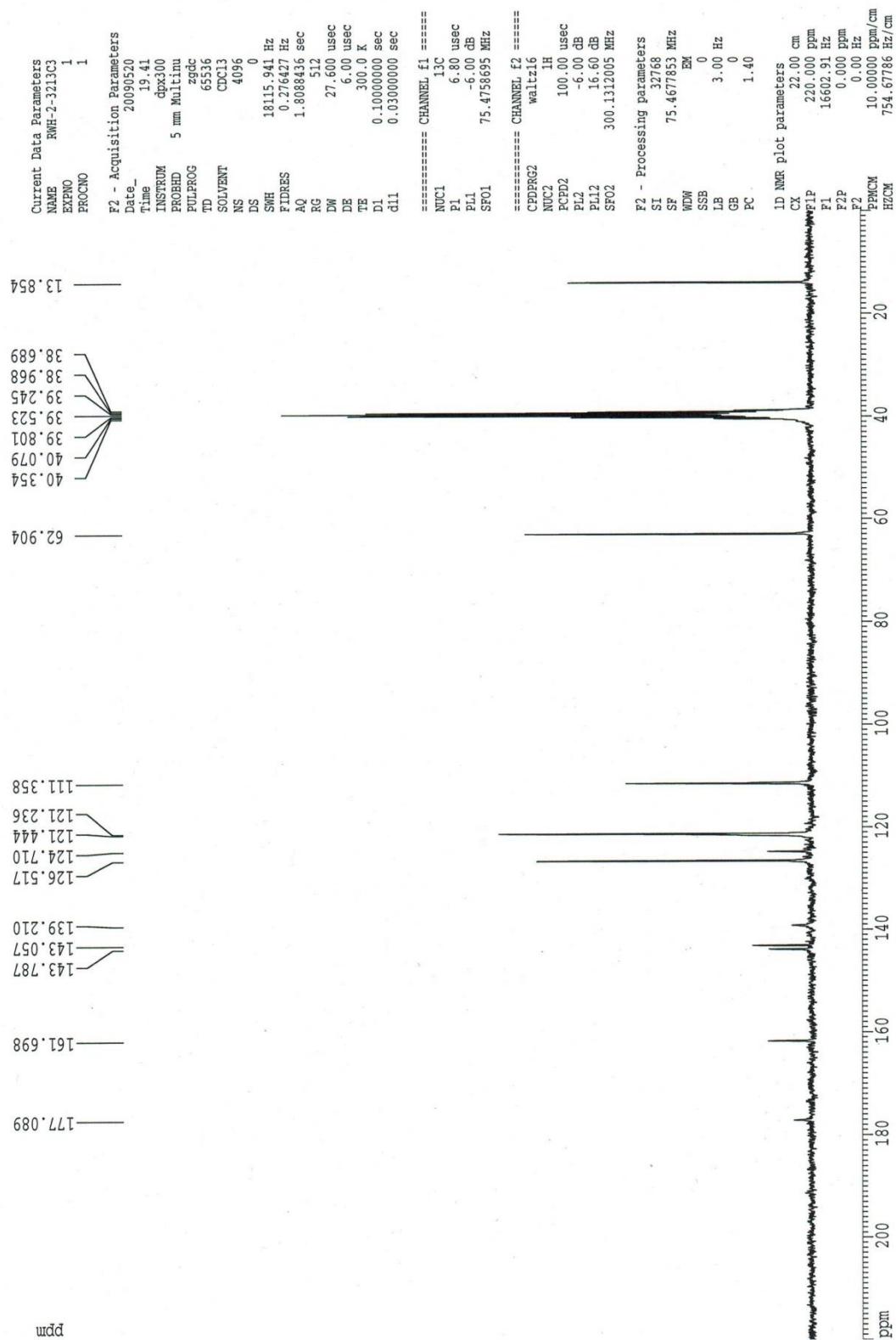


¹H NMR *Ethyl 6-nitro-4-oxo-1,4-dihydroquinoline-2-carboxylate* (**41**)

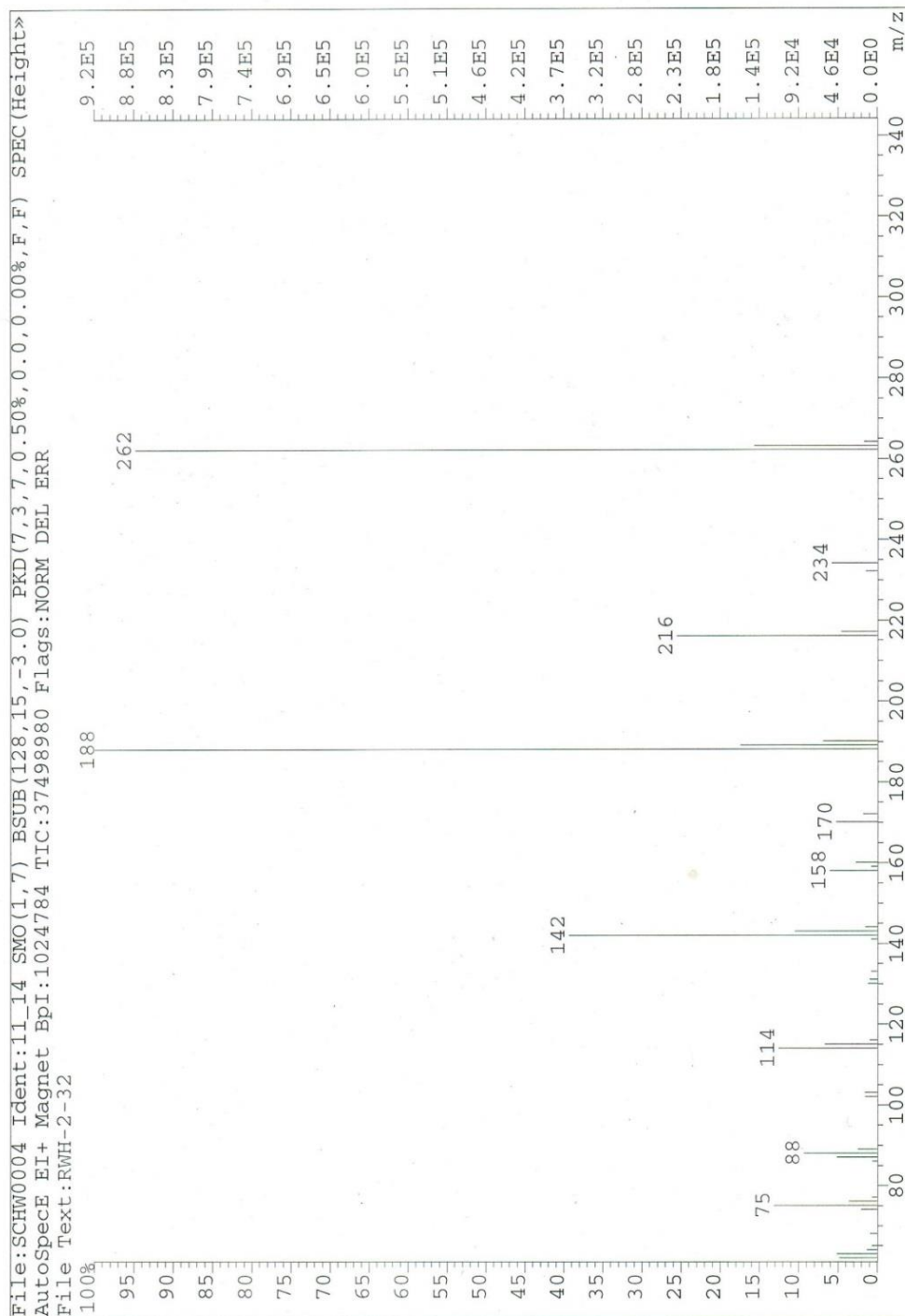


¹³C NMR Ethyl 6-nitro-4-oxo-1,4-dihydroquinoline-2-carboxylate (41)

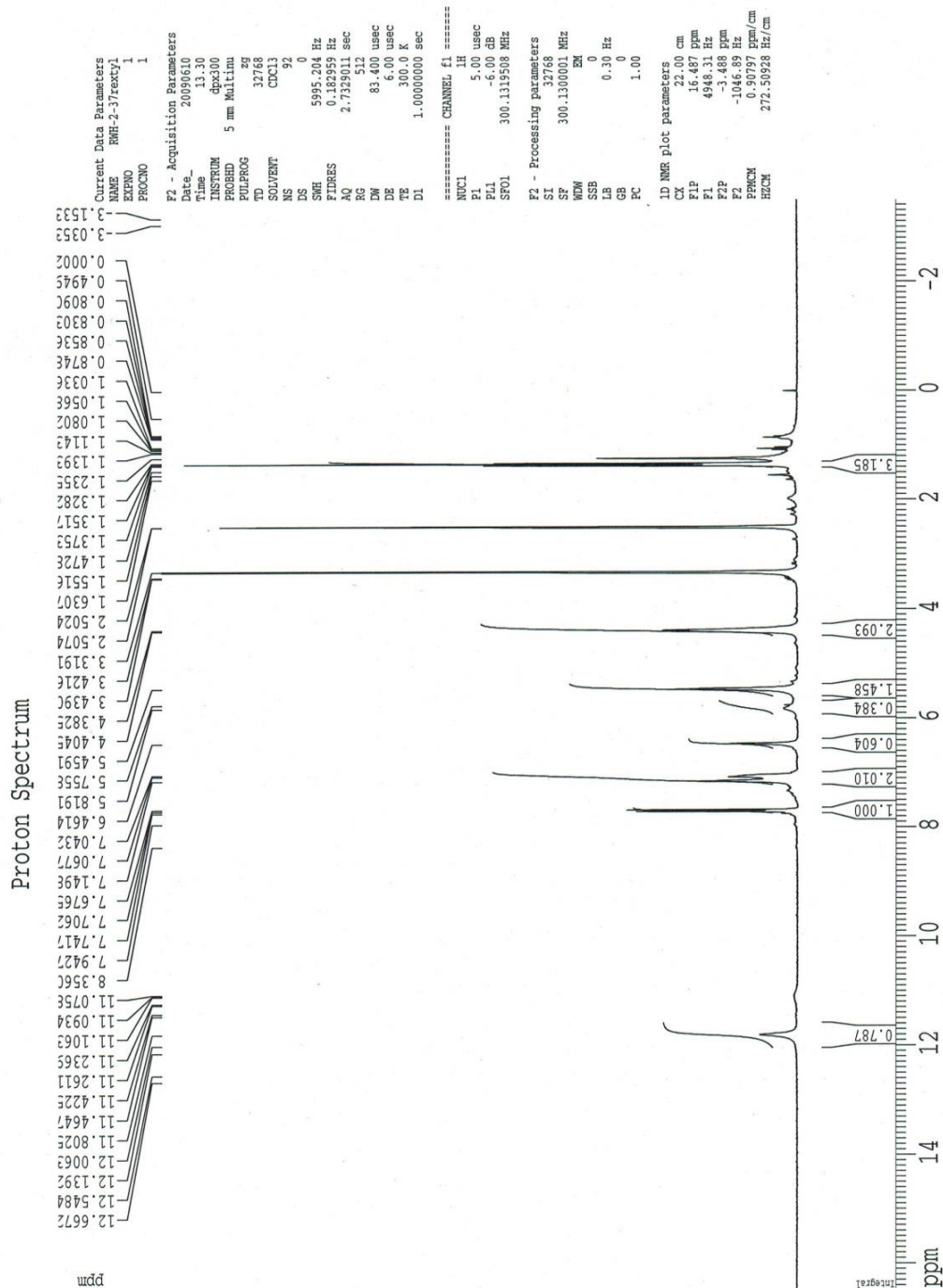
6-nitroquinolone



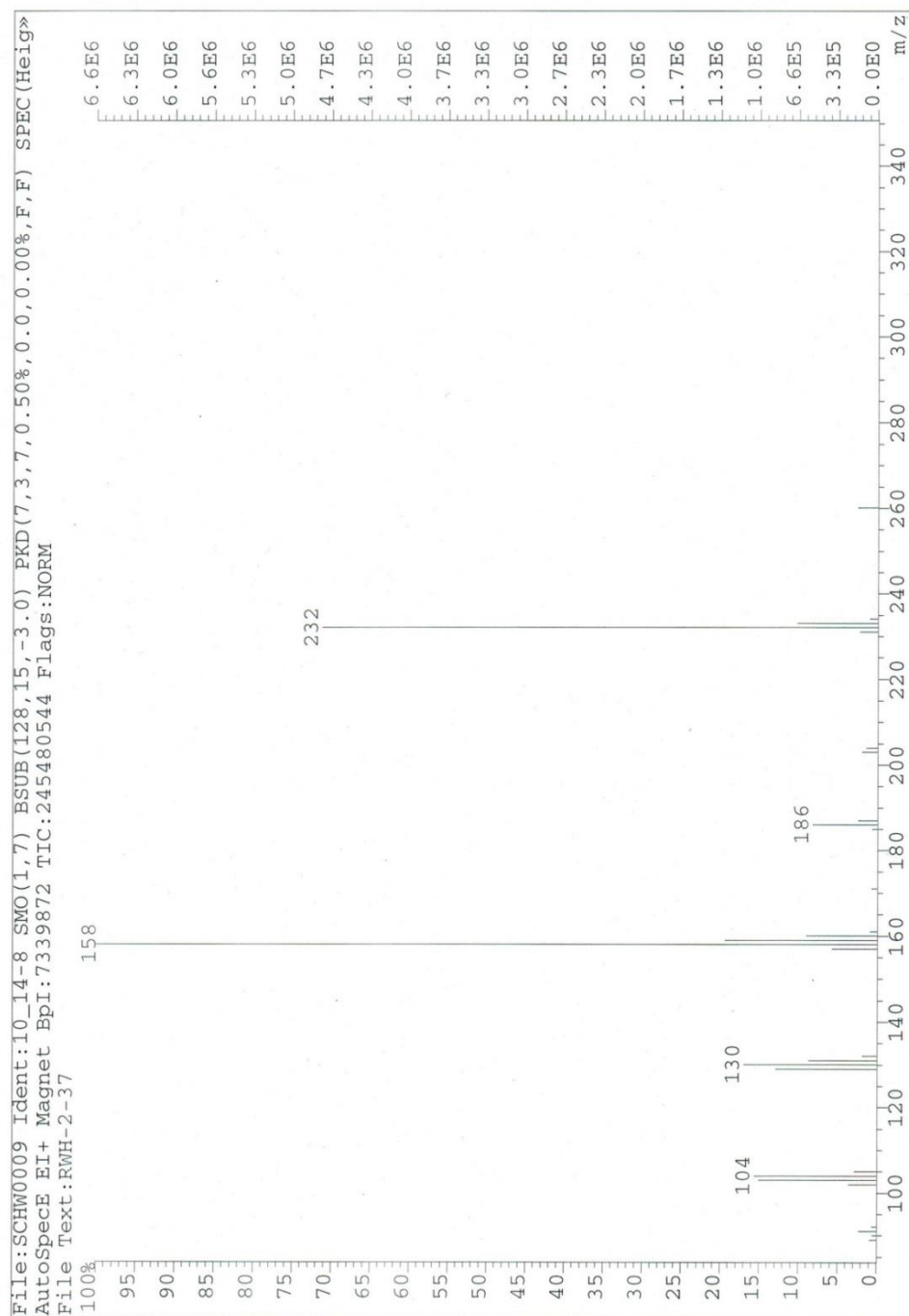
MS (EI, 70eV) Ethyl 6-nitro-4-oxo-1,4-dihydroquinoline-2-carboxylate (41)



¹H NMR Ethyl 6-amino-4-oxo-1,4-dihydroquinoline-2-carboxylate (42)

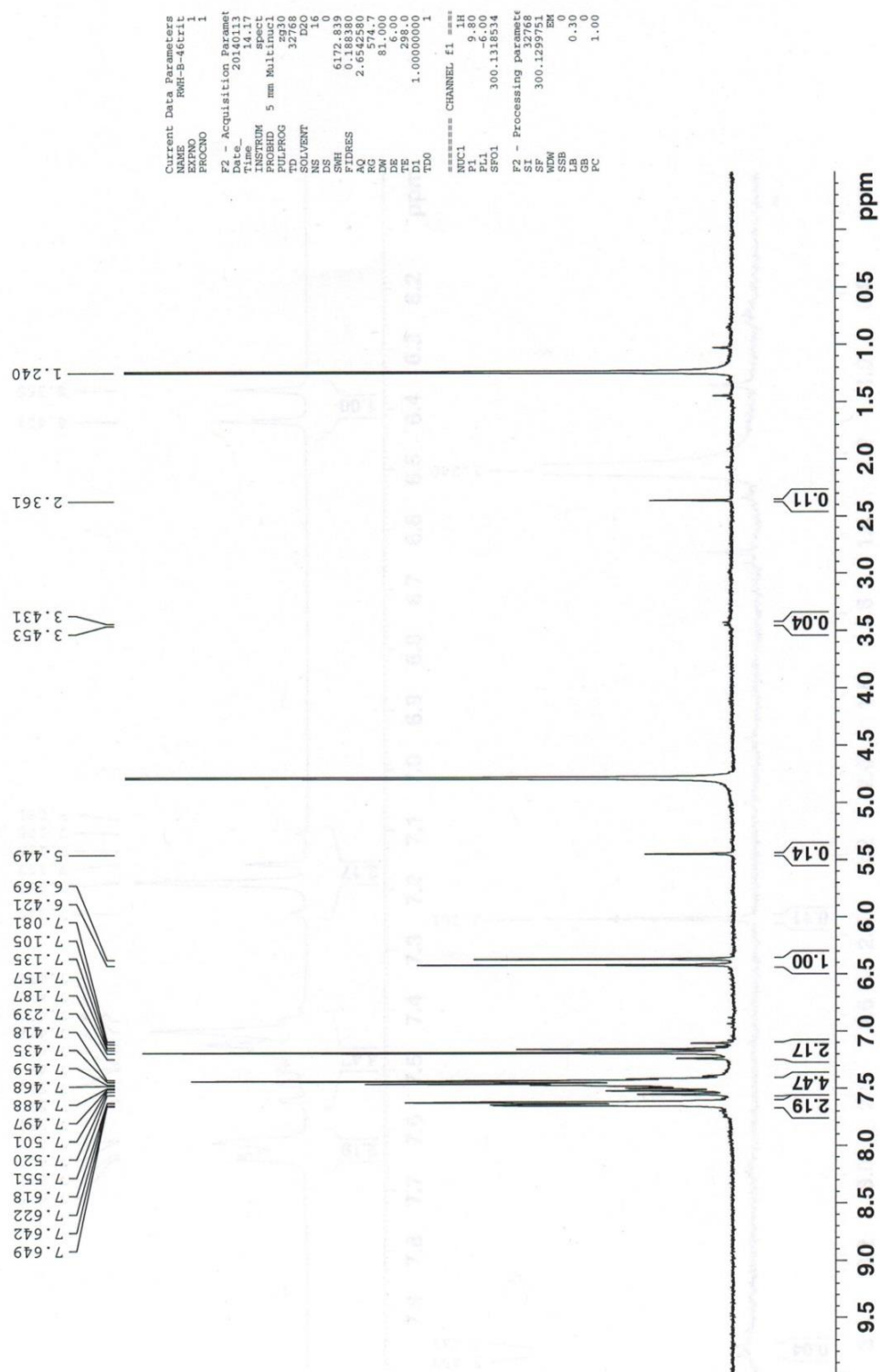


MS (EI, 70eV) Ethyl 6-amino-4-oxo-1,4-dihydroquinoline-2-carboxylate (42)

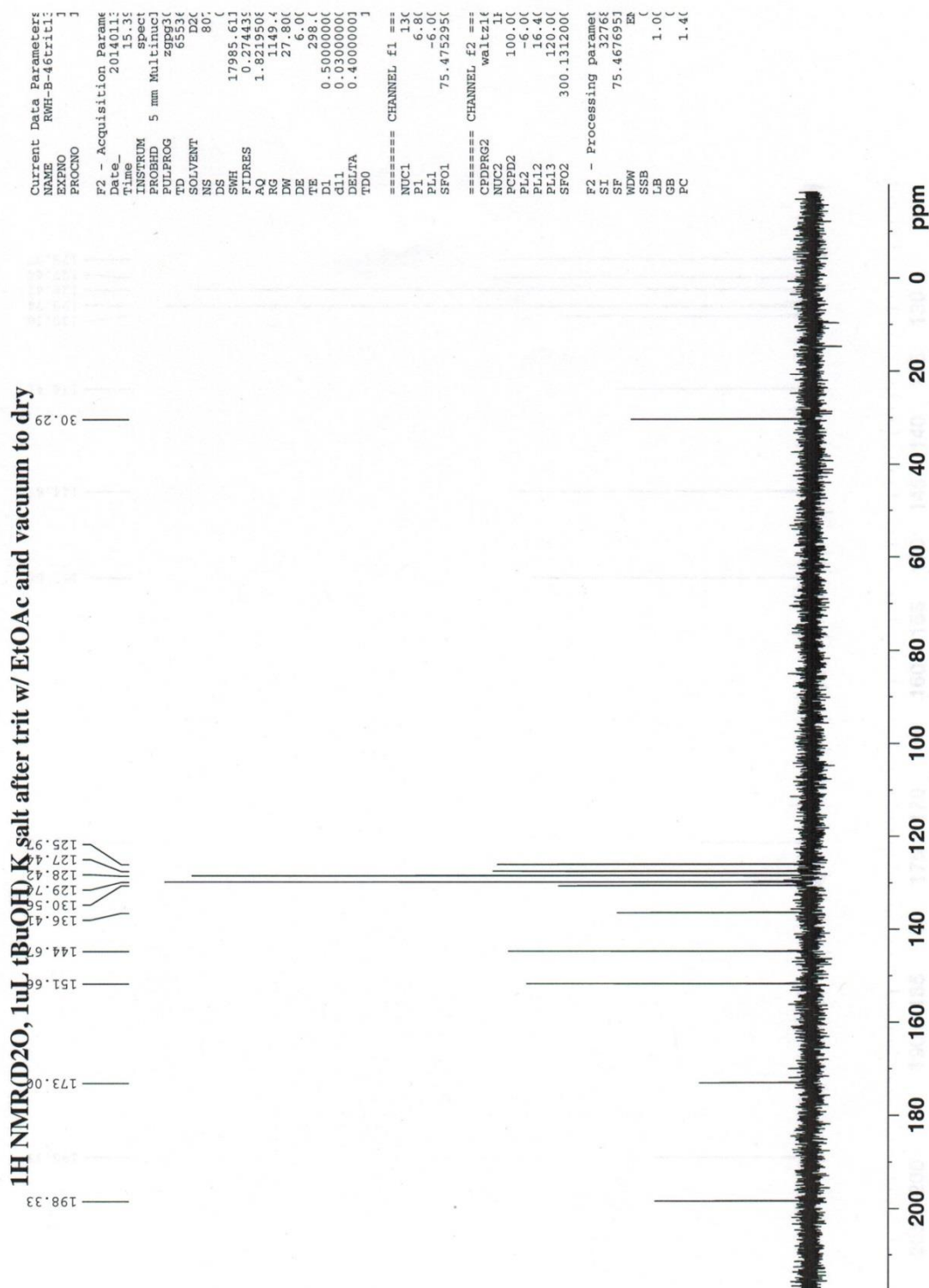


¹H NMR Potassium (3E,5E)-2-oxo-6-phenylhexa-3,5-dienoate (45)

¹H NMR(D₂O, 1uL tBuOH) K salt after trit with EtOAc



¹³C NMR Potassium (3E,5E)-2-oxo-6-phenylhexa-3,5-dienoate (45)

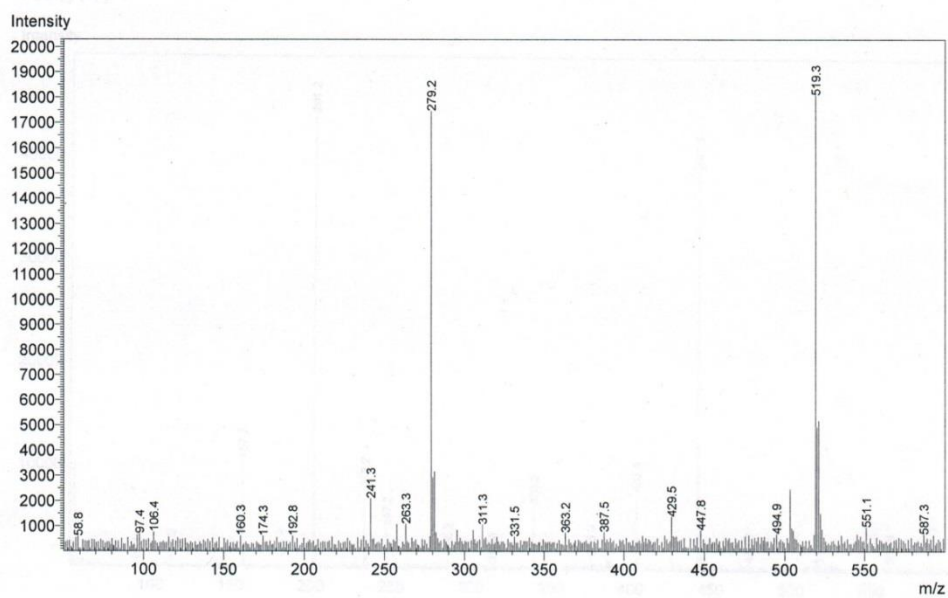


Shimadzu LCMS-2020 Data Report

Mass Spectrum for Sample:
RWH-B-42xtyl

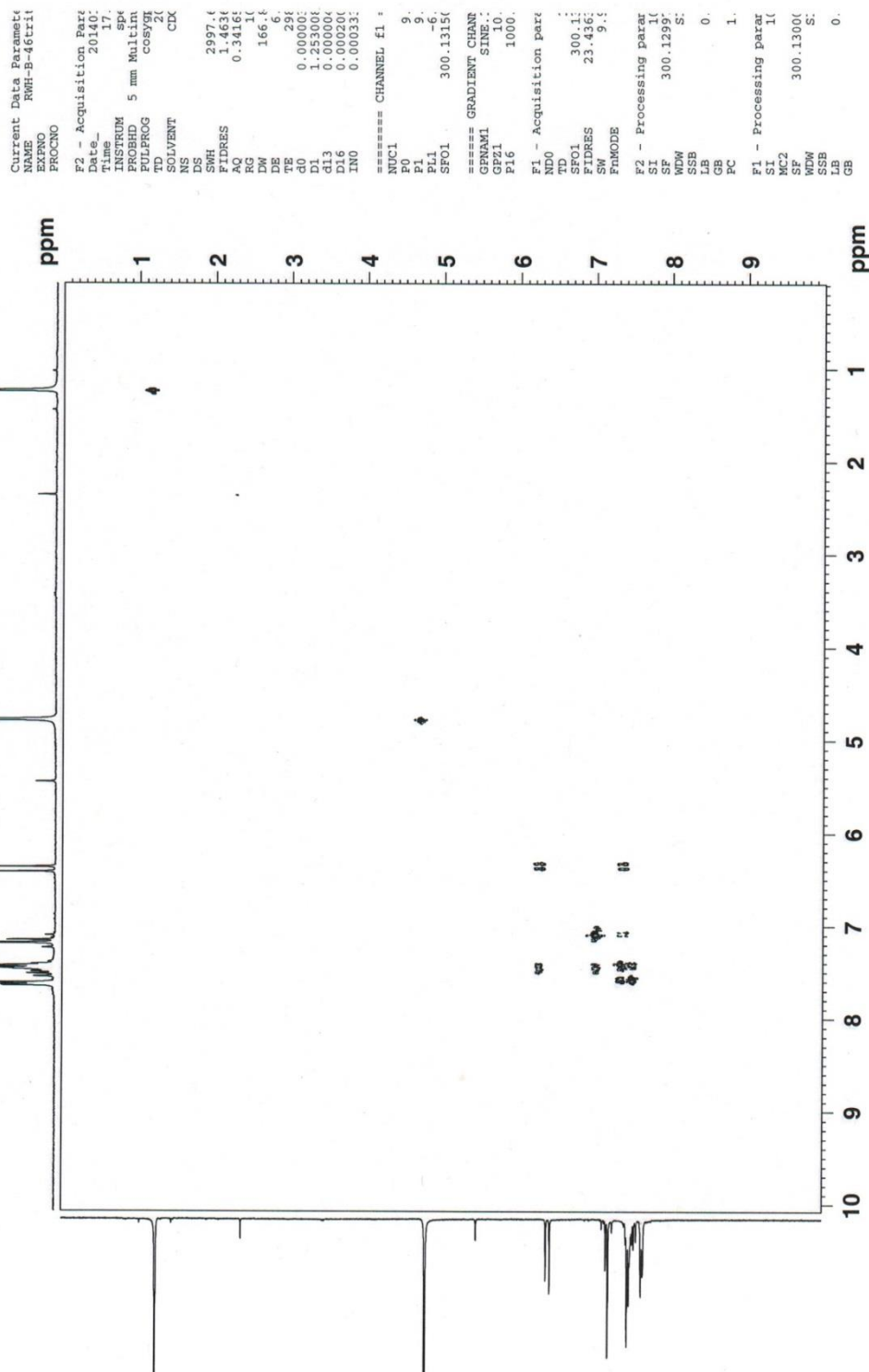
Operator: Mark Wang

Data filename: C:\LabSolutions\Data\Schwabacher Alan\RWH-B-42xtyl.lcd
Spectrum Mode: Single
Retention Time: 0.100 min.
Interface Type (ESI, APCI, DUIS): DUIS
Aquisition Mode (Scan, SIM, Profile): Scan
Polarity (+,-): +



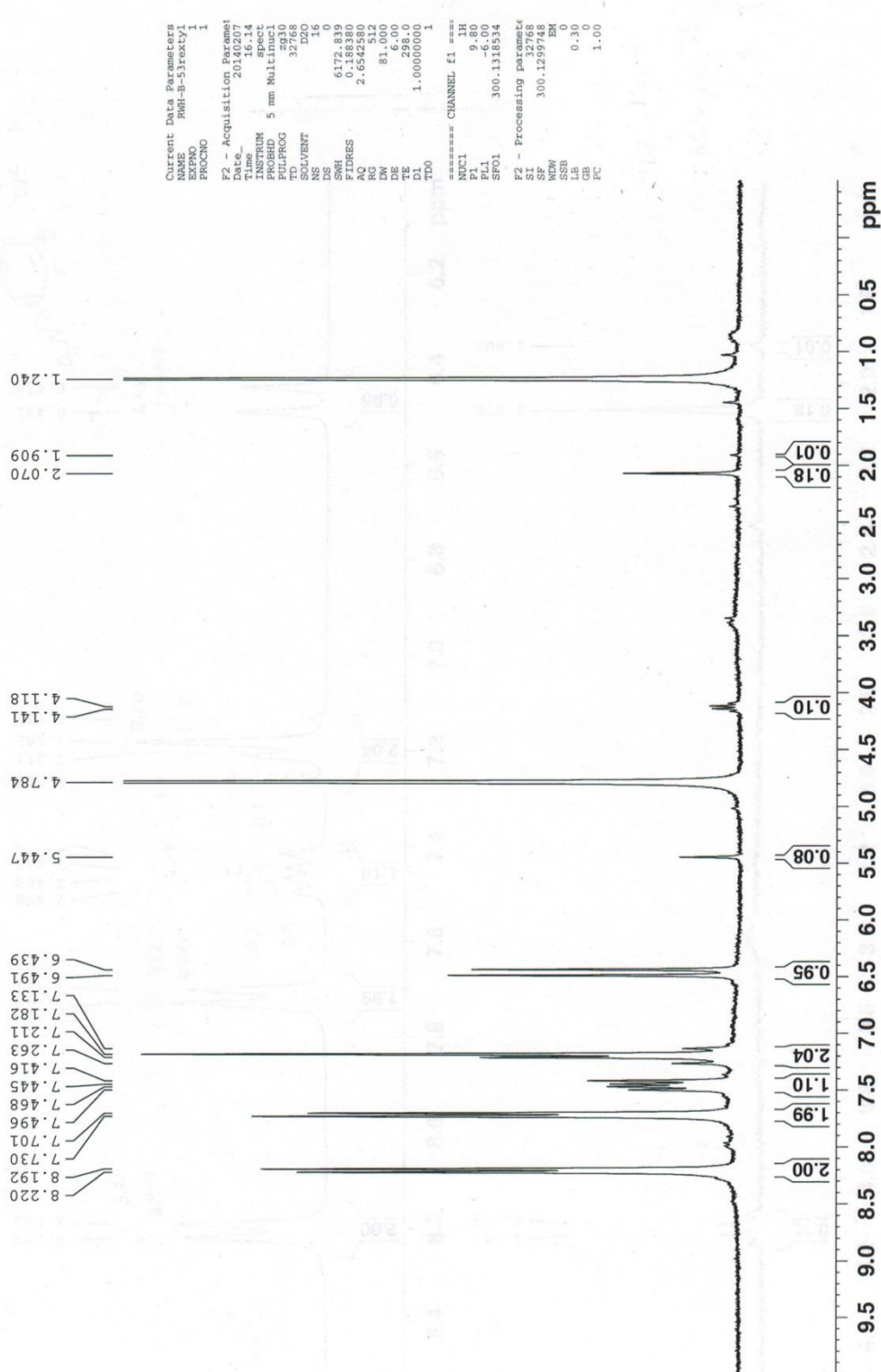
COSY Potassium (3E,5E)-2-oxo-6-phenylhexa-3,5-dienoate (45)

2D COSY S(D2O, 1uL tBuOH int std_ K salt diene of cinn + pyr



¹H NMR *Potassium (3E,5E)-6-(4-nitrophenyl)-2-oxohexa-3,5-dienoate (46)*

¹H NMR (D₂O, 1uL tBuOH int std) rextylled 4-nitrocinnamylidene pyruvate



¹³C NMR Potassium (3E,5E)-6-(4-nitrophenyl)-2-oxohexa-3,5-dienoate (46)

¹³C NMR (D₂O, 1uL, tBuOH int std) rextyl 4-nitrocinnamylidene pyruvate

```

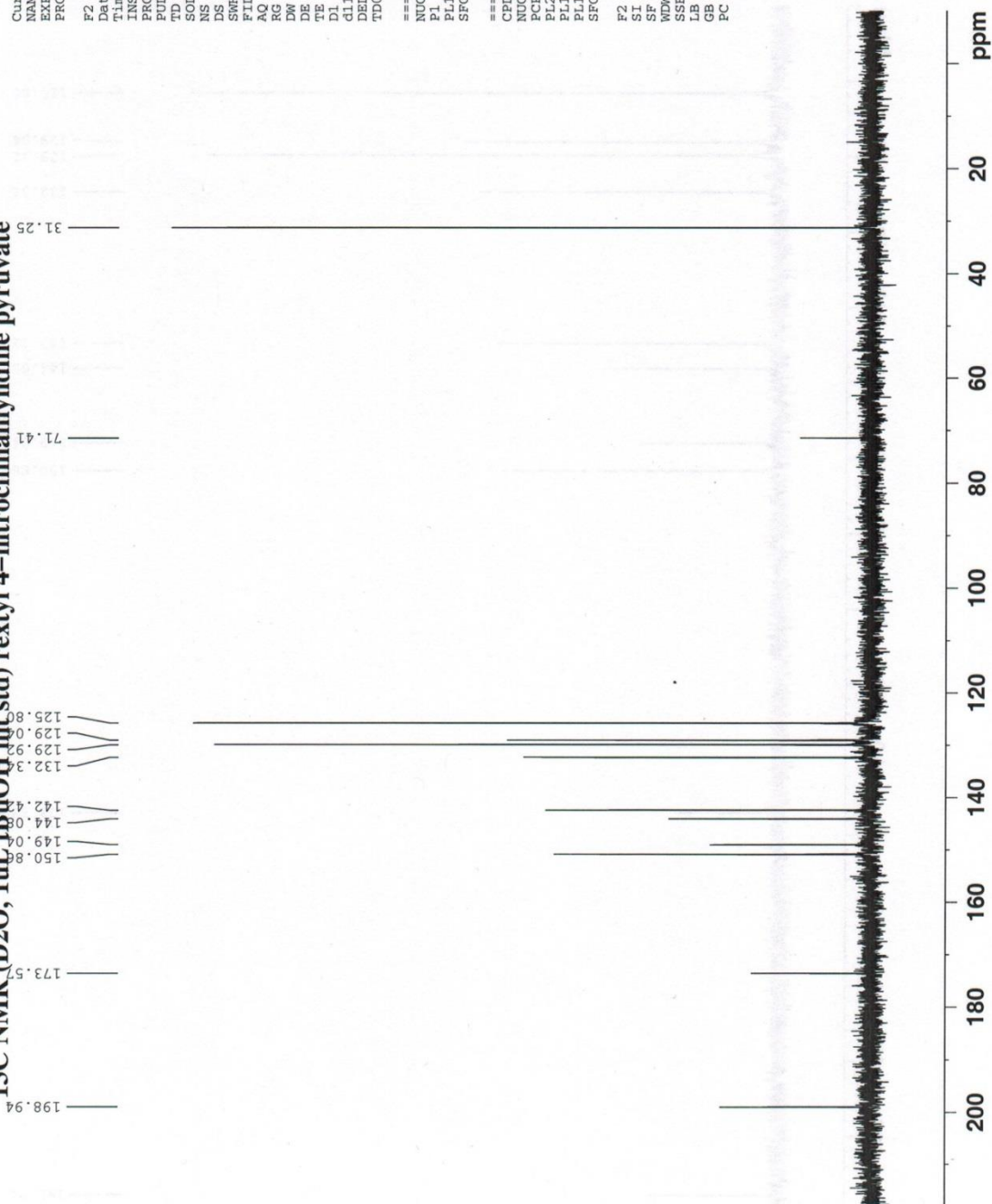
Current Data Parameters:
NAME      RMH-B-53rextyl
EXPNO     1
PROCNO    1

F2 - Acquisition Parameters:
Date_     20140201
Time      17.07
INSTRUM   spect
PROBHD    5 mm Multinucl
PULPROG   zgpg30
TD        65536
SOLVENT   D2O
NS        3375
DS         4
SWH        17985.611
FIDRES     0.27443
AQ         1.821950
RG         456.7
DW         27.80
DE         6.00
TE         298.2
D1         0.500000
d11        0.030000
DELTA     0.400000
TD0        1

===== CHANNEL f1 =====
NUC1       13C
P1         6.80
PL1        -6.00
SFO1       75.475295

===== CHANNEL f2 =====
CPDPRG2    waltz16
NUC2       1H
PCPD2      100.00
PL2        -6.00
PL12       16.40
PL13       120.00
SFO2       300.131200

F2 - Processing parameters:
SI         32768
SF         75.4676214
WDW        EN
SSB        0
LB         1.00
GB         0
PC         1.40
  
```



Shimadzu LCMS-2020 Data Report

Mass Spectrum for Sample:
RWH-B-53xtyl

Operator: Mark Wang

Data filename: C:\LabSolutions\Data\Schwabacher Alan\RWH-B-53xtyl.lcd

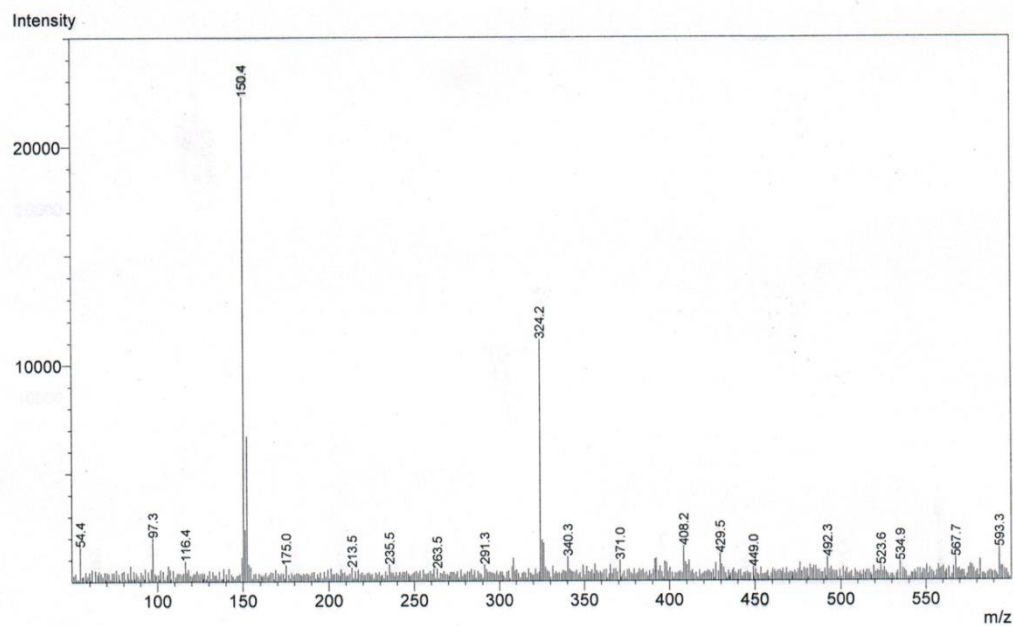
Spectrum Mode: Single

Retention Time: 0.100 min.

Interface Type (ESI, APCI, DUIS): DUIS

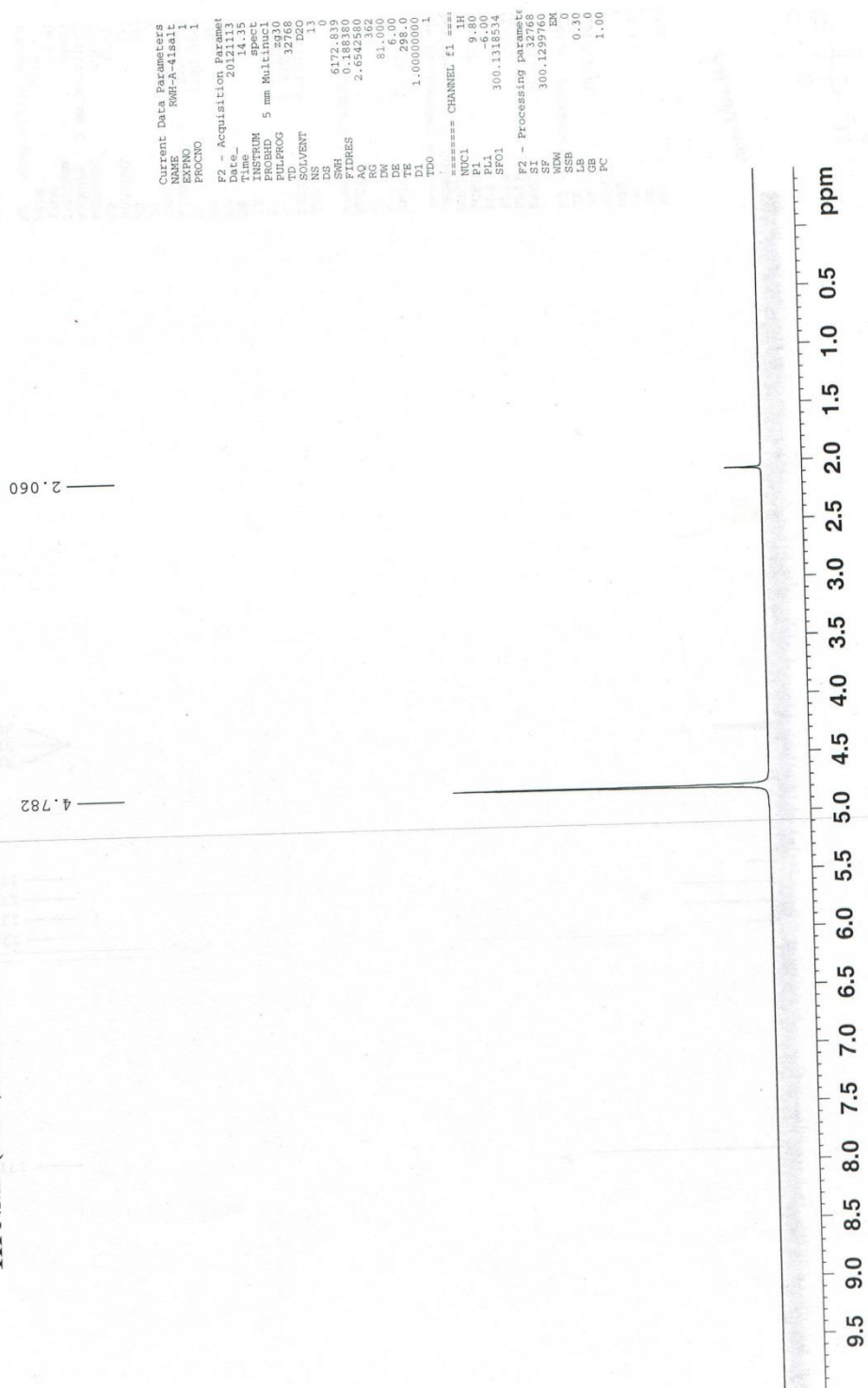
Acquisition Mode (Scan, SIM, Profile): Scan

Polarity (+, -): +



¹H NMR Sodium trifluoropyruvate (47)

¹H NMR(D₂O) sodium trifluoropyruvate 0.03g sample CH₃CN int std



```

Current Data Parameters
NAME      SDF-A-41salt
EXPNO     1
PROCNO    1

F2 - Acquisition Parameters
Date_     20121113
Time      14.35
INSTRUM   spect
PROBHD    5 mm Malt
PULPROG   zg30
TD         32768
SOLVENT   D2O
NS         10
DS         1
SWH        6172.839
FIDRES     0.188380
AQ         2.6542362
RG         81.000
DE         6.00
TE         298.00
D1         1.0000000
D10        1

===== CHANNEL f1 =====
NUC1       1H
P1         9.80
PL1        -6.00
SFO1       300.1318534

F2 - Processing parameters
SI         32768
SF         300.1299760
WDW        EM
SSB        0
LB         0.30
GB         0
PC         1.00
  
```


¹³C NMR Sodium trifluoropyruvate (47)

¹³C NMR(D₂O) sodium trifluoropyruvate 0.03g sample CH₃CN int std

```

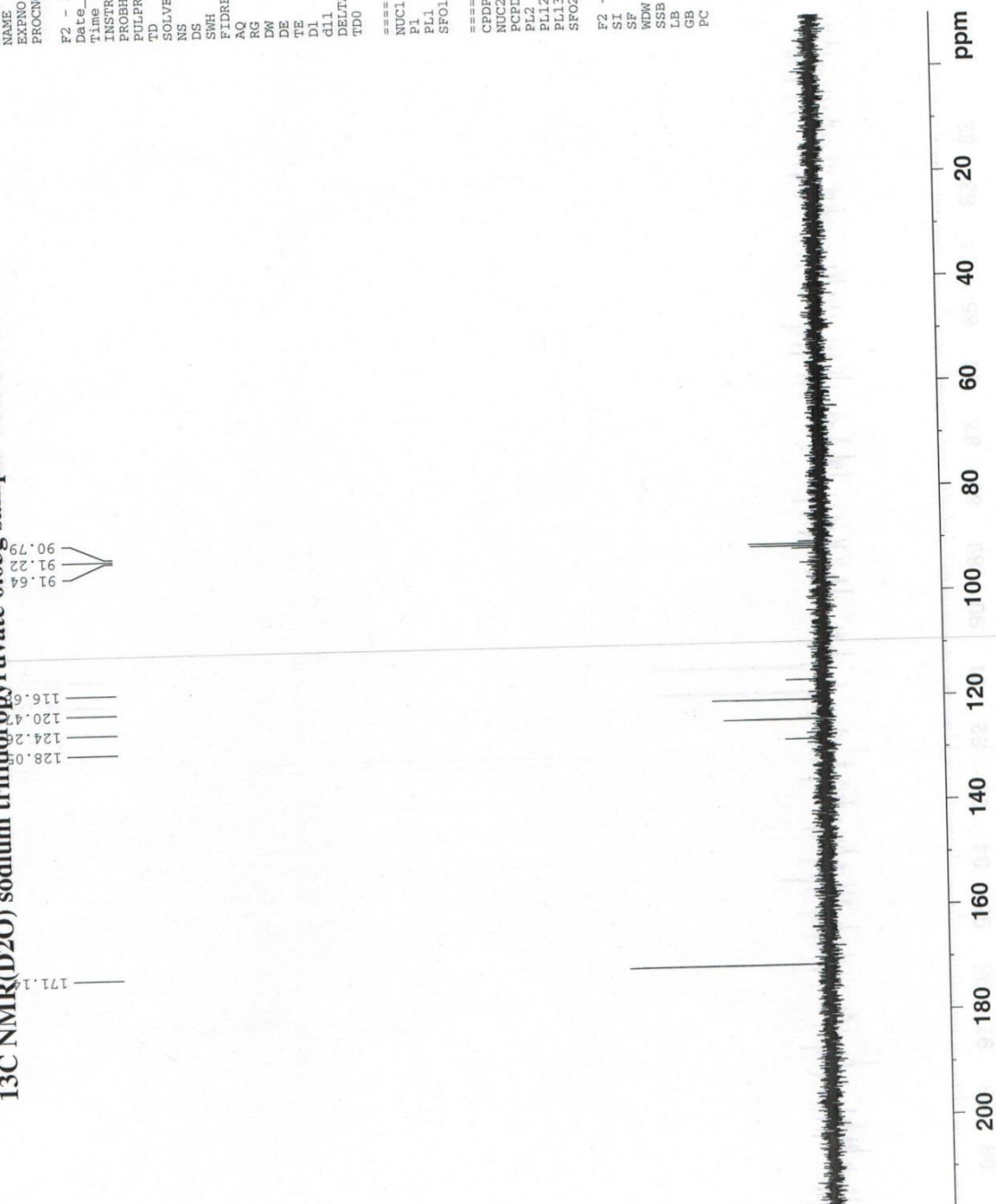
Current Data Parameters:
NAME      RWH-A-41sal11
EXPNO     1
PROCNO    1

F2 - Acquisition Parameters
Date_     20121111
Time      14.40
INSTRUM   spect
PROBHD    5 mm Multinucl
PULPROG   zgpg30
TD        65536
DZ        2
SOLVENT   D2O
NS        512
DS        4
SWH        17985.613
FIDRES     0.274435
AQ         1.8219508
RG         512
DW         27.800
DE         6.00
TE         298.15
D1         0.50000000
d11        0.03000000
DELTA     0.40000001
TD0        1

===== CHANNEL f1 =====
NUC1       13C
P1         6.80
PL1        -6.00
SFO1       75.4752950

===== CHANNEL f2 =====
CPDPRG2    waltz16
NUC2       1F
PCPD2      100.00
PL2        -6.00
PL12       16.40
PL13       120.00
SFO2       300.1312000

F2 - Processing parameters
SI         32768
SF         75.4677490
WDW        EM
SSB        0
LB         1.00
GB         0
PC         1.40
  
```



Shimadzu LCMS-2020 Data Report

Mass Spectrum for Sample
RWH-B-43.lcd

Operator: Mark Wang

Data Filename: C:\LabSolutions\Data\Schwabacher Alan\RWH-B-43.lcd

Spectrum Mode: Averaged

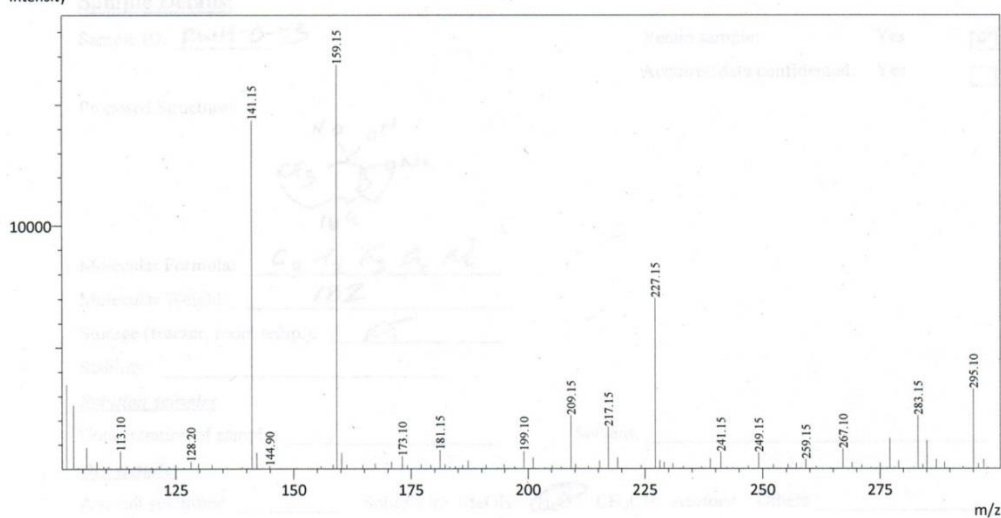
Retention Time: ----

Interface Type (ESI, APCI, DUIS): DUIS

Acquisition Mode (Scan, SIM, Profile): Scan

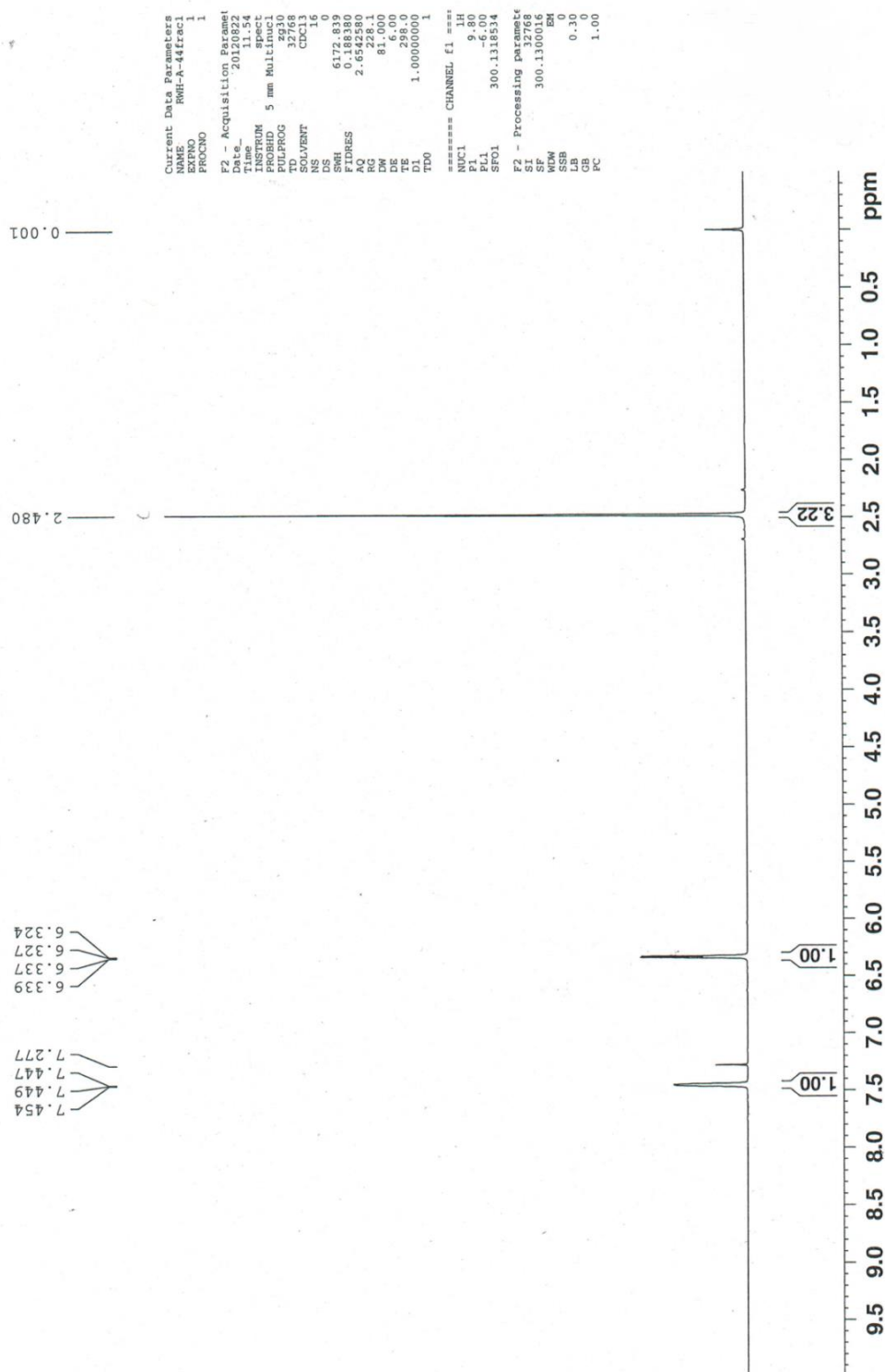
Polarity: -

Intensity



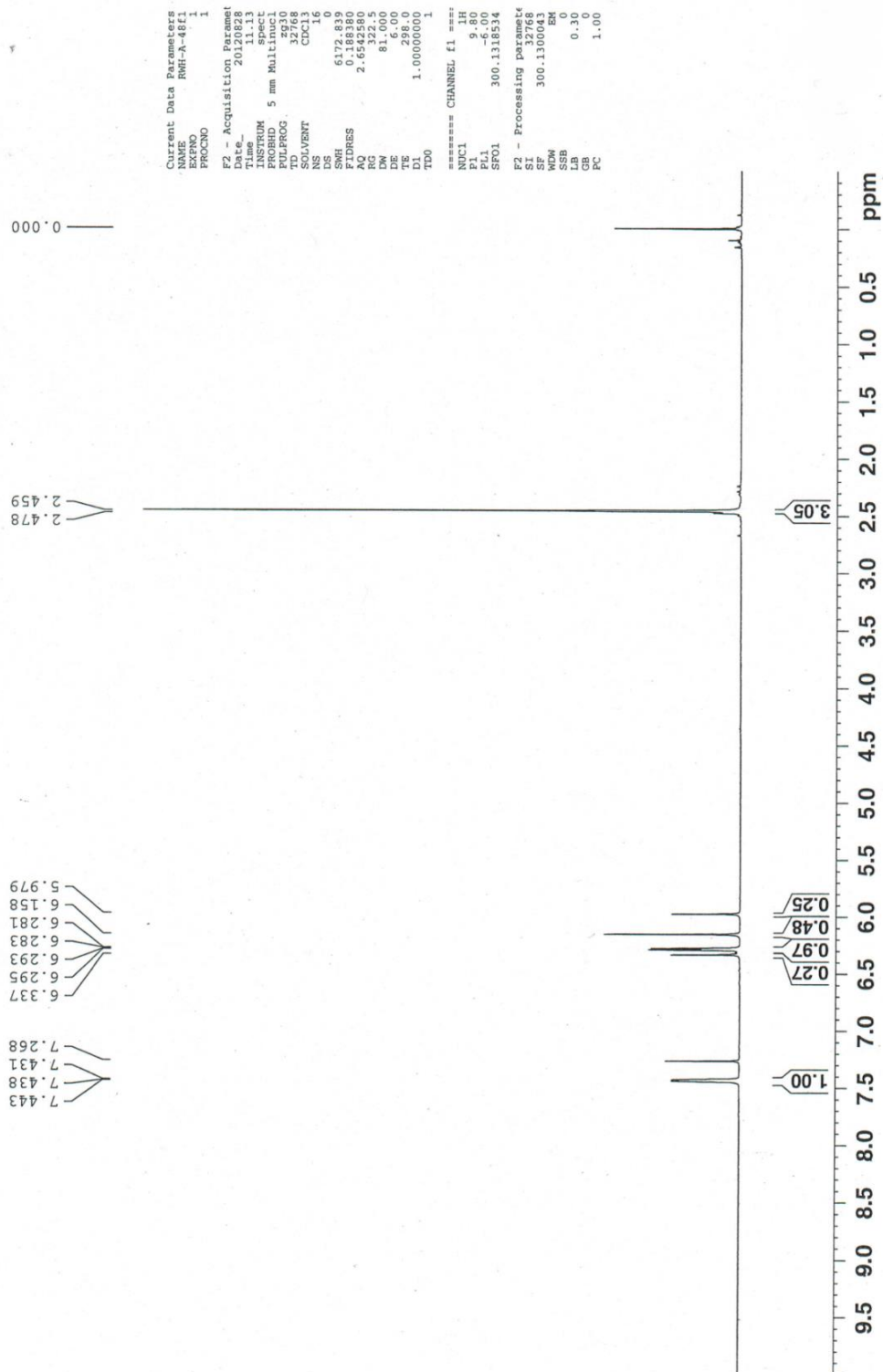
¹H NMR 5-methyl-2-(2,2,2-trifluoroacetyl)furan (50)

¹H NMR(CDCl₃) frac1 from distillation 80C head temp



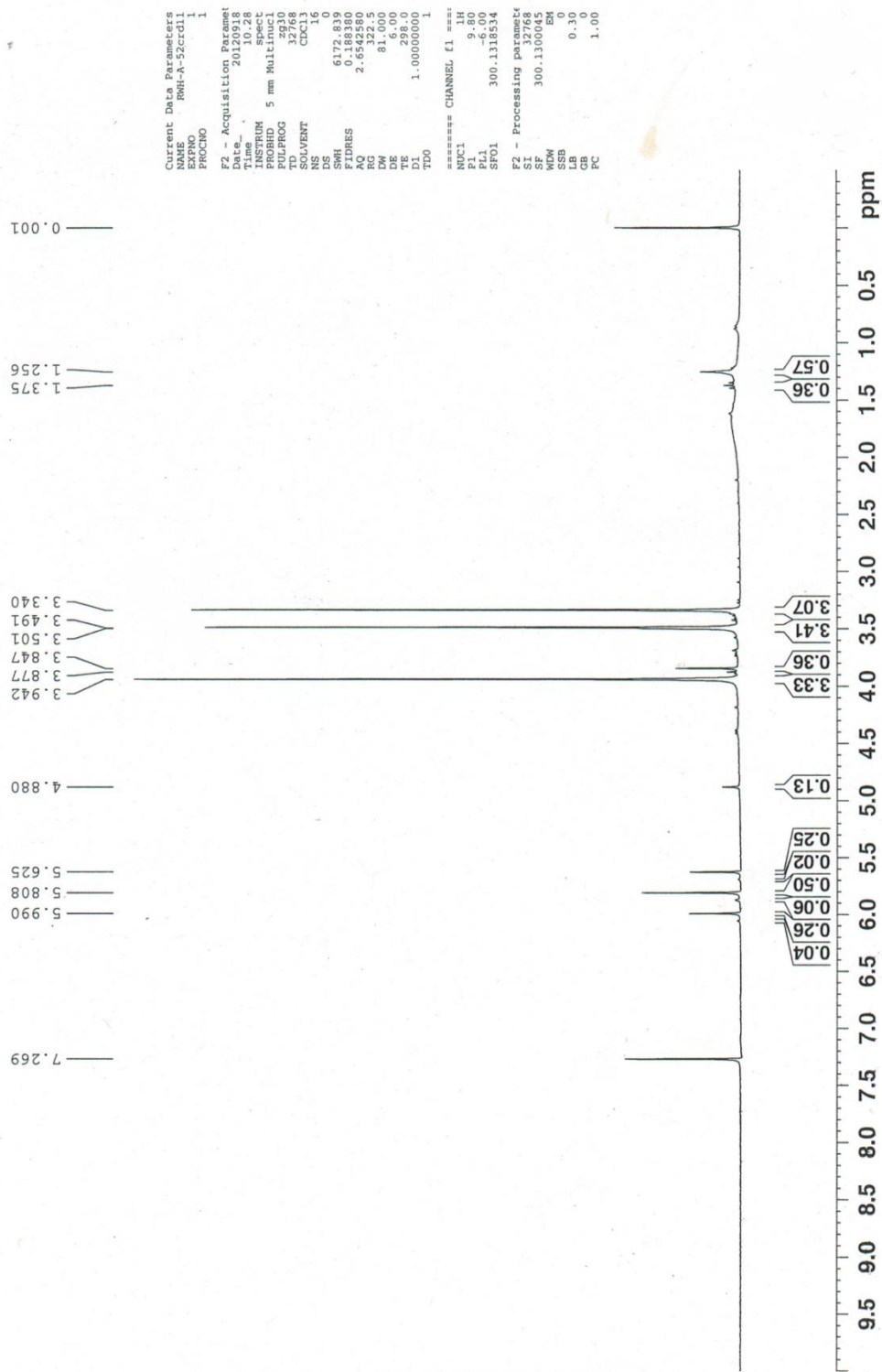
¹H NMR 5-methyl-2-(2,2-difluoroacetyl)furan (51)

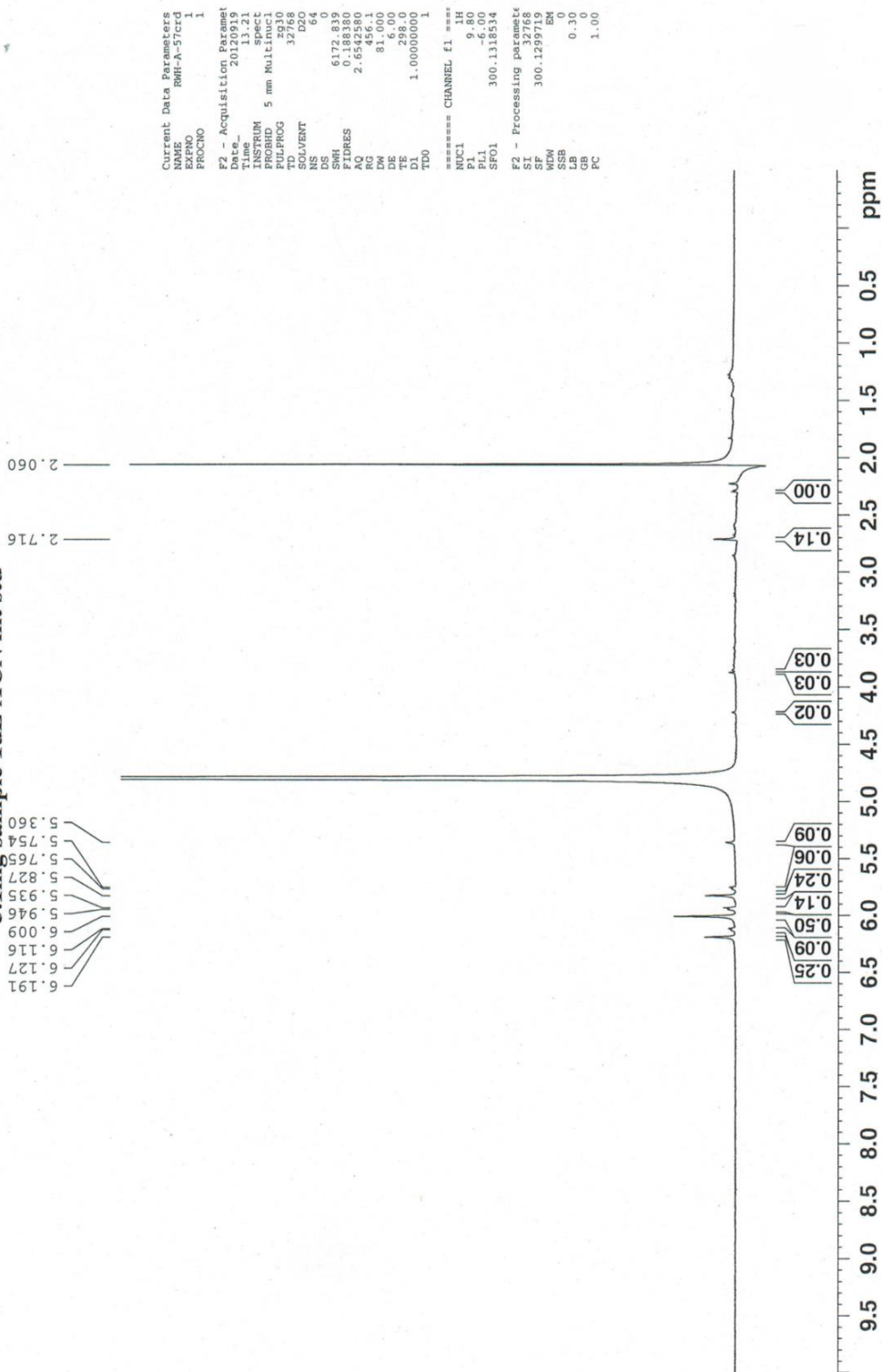
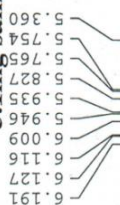
¹H NMR(CDCI₃) frac 1 from vac. distillation of combined 2-difluoroacetyl-5-methylfuran



¹H NMR *Methyl difluoropyruvate methyl hemiacetal (52)*

¹H NMR(CDC13) f9-24 of MeOH effluent 13.9mg sample





MS Sodium difluoropyruvate hydrate (53)

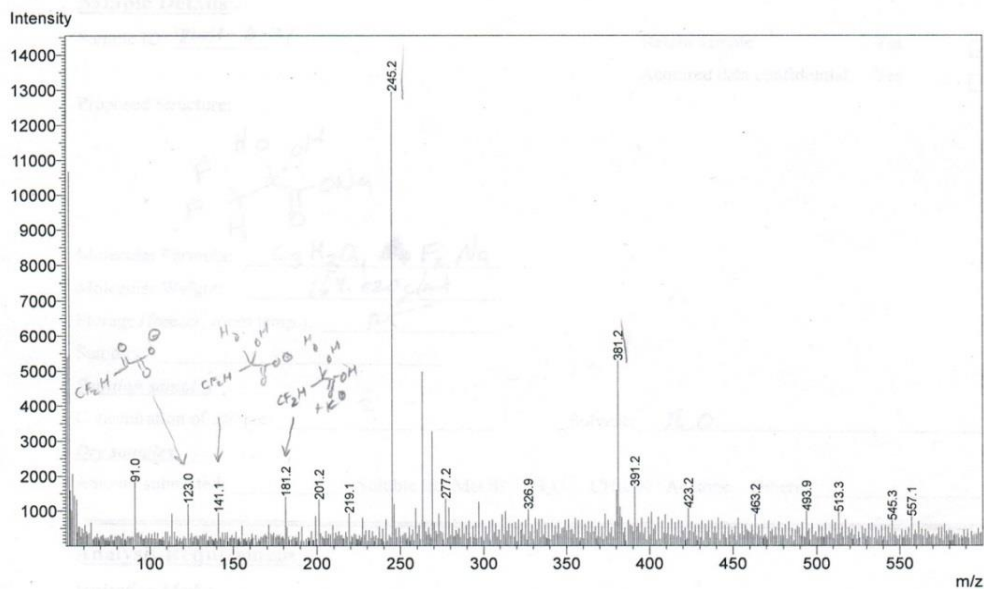
2/19/2014 3:33:23 PM Page 1 / 1

Shimadzu LCMS-2020 Data Report

Mass Spectrum for Sample:
RHW-B-21-1

Operator: Mark Wang

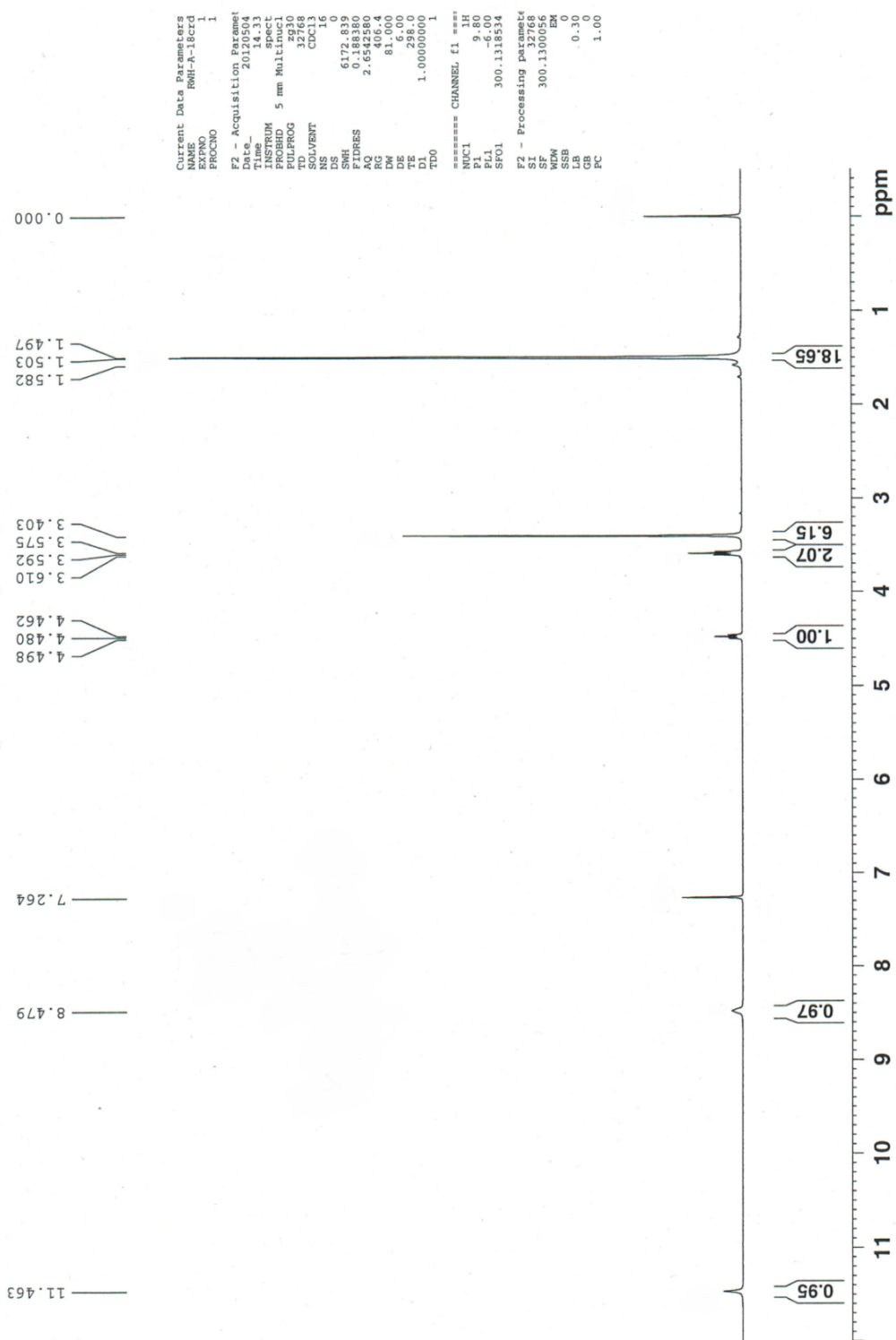
Data filename: C:\LabSolutions\Data\Schwabacher Alan\RHW-B-21-1.lcd
Spectrum Mode: Single
Retention Time: 0.150 min.
Interface Type (ESI, APCI, DUIS): DUIS
Acquisition Mode (Scan, SIM, Profile): Scan
Polarity (+, -): -



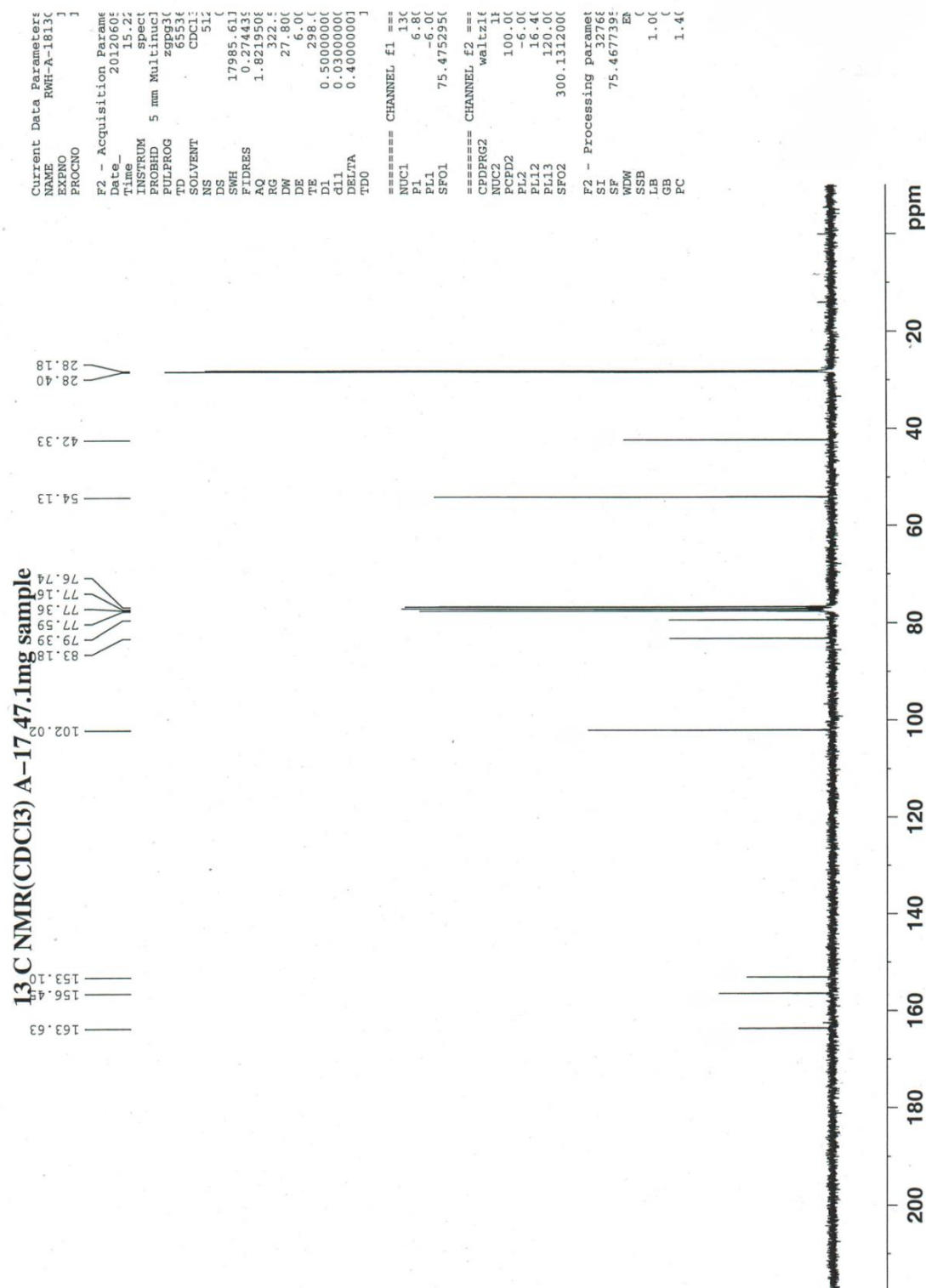
$$M + m^- = 297$$

¹H NMR *N,N'*-Di-Boc-*N''*-(2,2-dimethoxy-ethyl)-guanidine (54)

¹H NMR(CDCI₃) crude reaction product 5.9mg sample



¹³C NMR *N,N'*-Di-Boc-*N''*-(2,2-dimethoxy-ethyl)-guanidine (54)



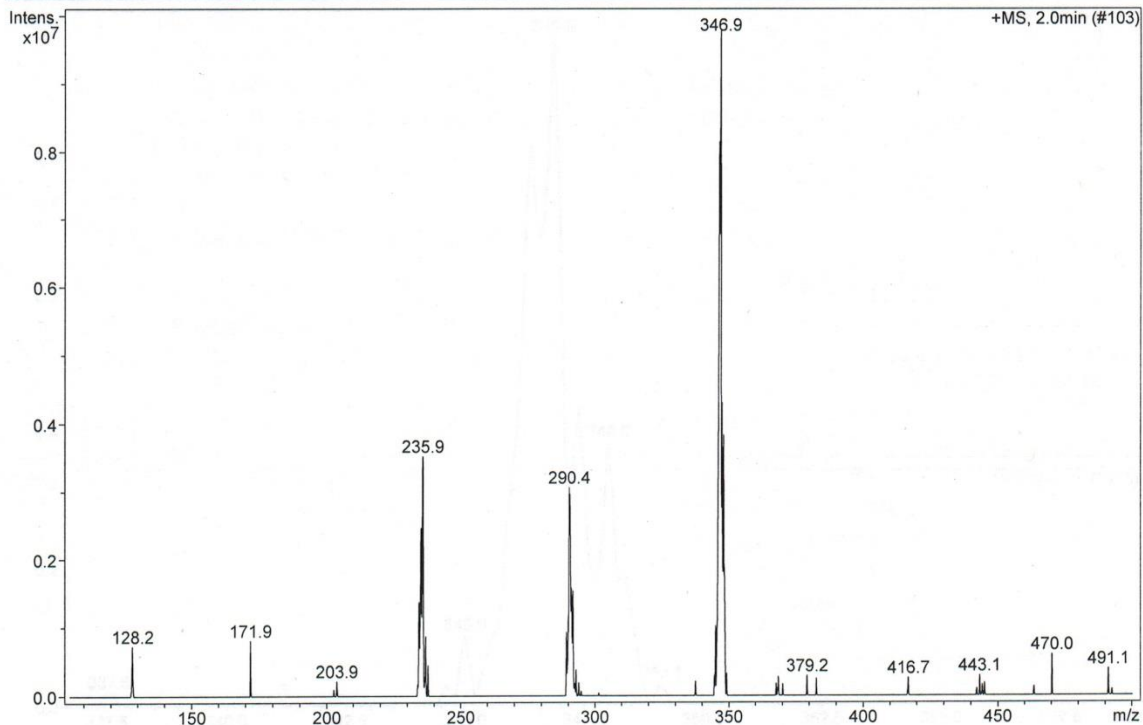
MS *N,N'*-Di-Boc-*N''*-(2,2-dimethoxy-ethyl)-guanidine (54)

Display Report - All Windows Selected Analy

Analysis Name: 06112201.d
Method: Copy of MARK02.M
Sample Na RWH-A-18
Analysis Inf

Instrume LC-MSD-Trap-SL
Operator: Mark Wang

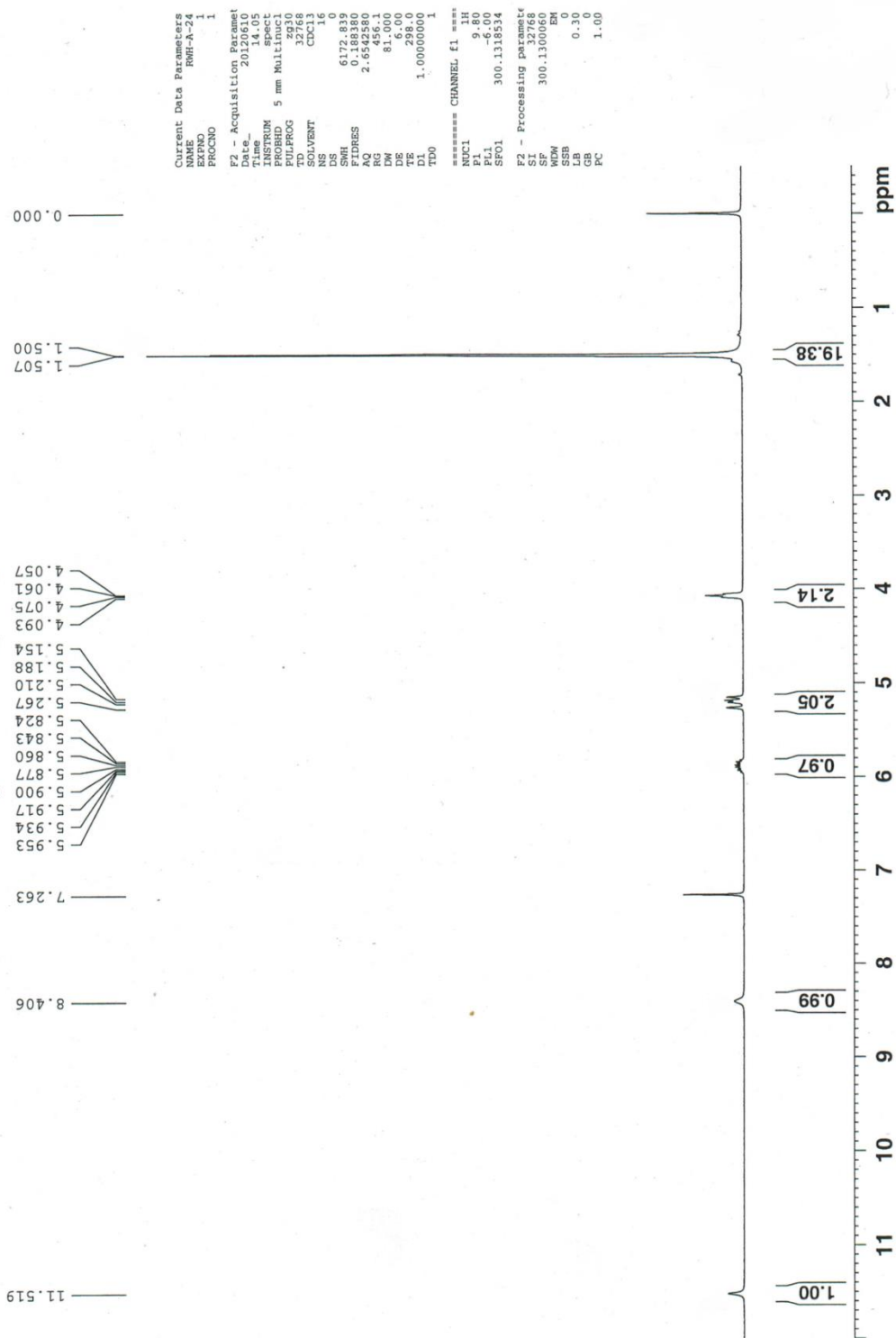
Print Date: 06/12/12 14:21:47
Acq. Date 06/12/12
14:17:35



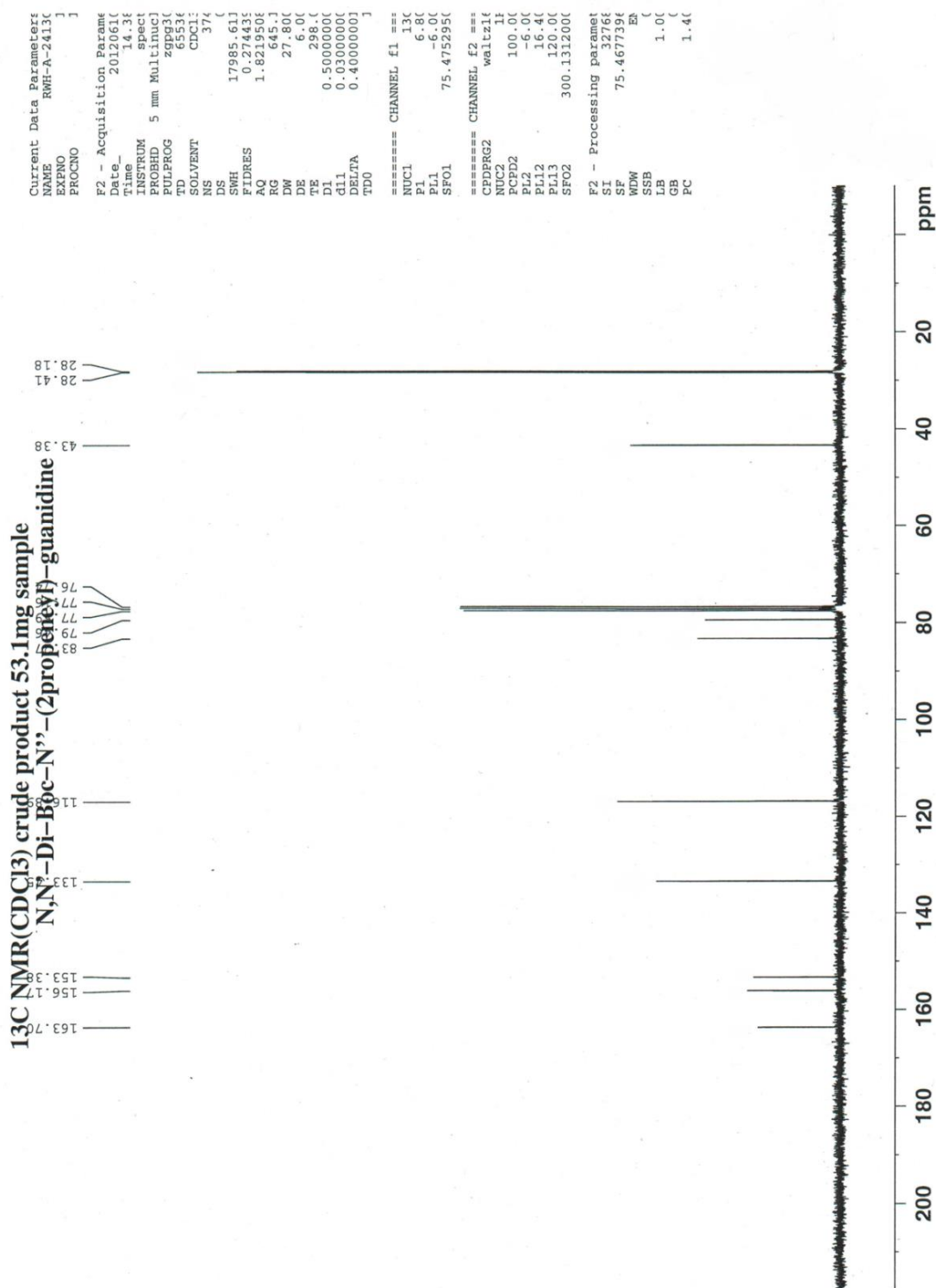
Agilent Technologies

¹H NMR *N*-Allyl-*N'*,*N''*-Di-Boc-quanidine (55)

¹H NMR(CDCl₃) crude product 5.4mg sample



¹³C NMR N-Allyl-N',N''-Di-Boc-quanidine (55)



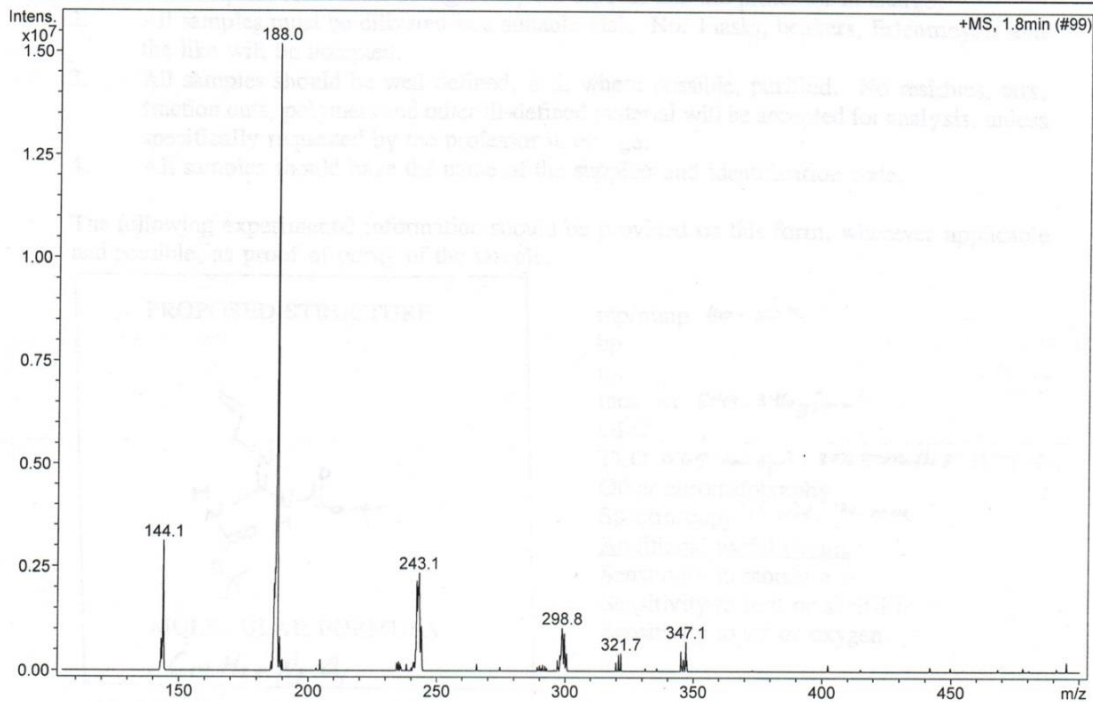
MS N-Allyl-N',N''-Di-Boc-quanidine (55)

Display Report - All Windows Selected Analy

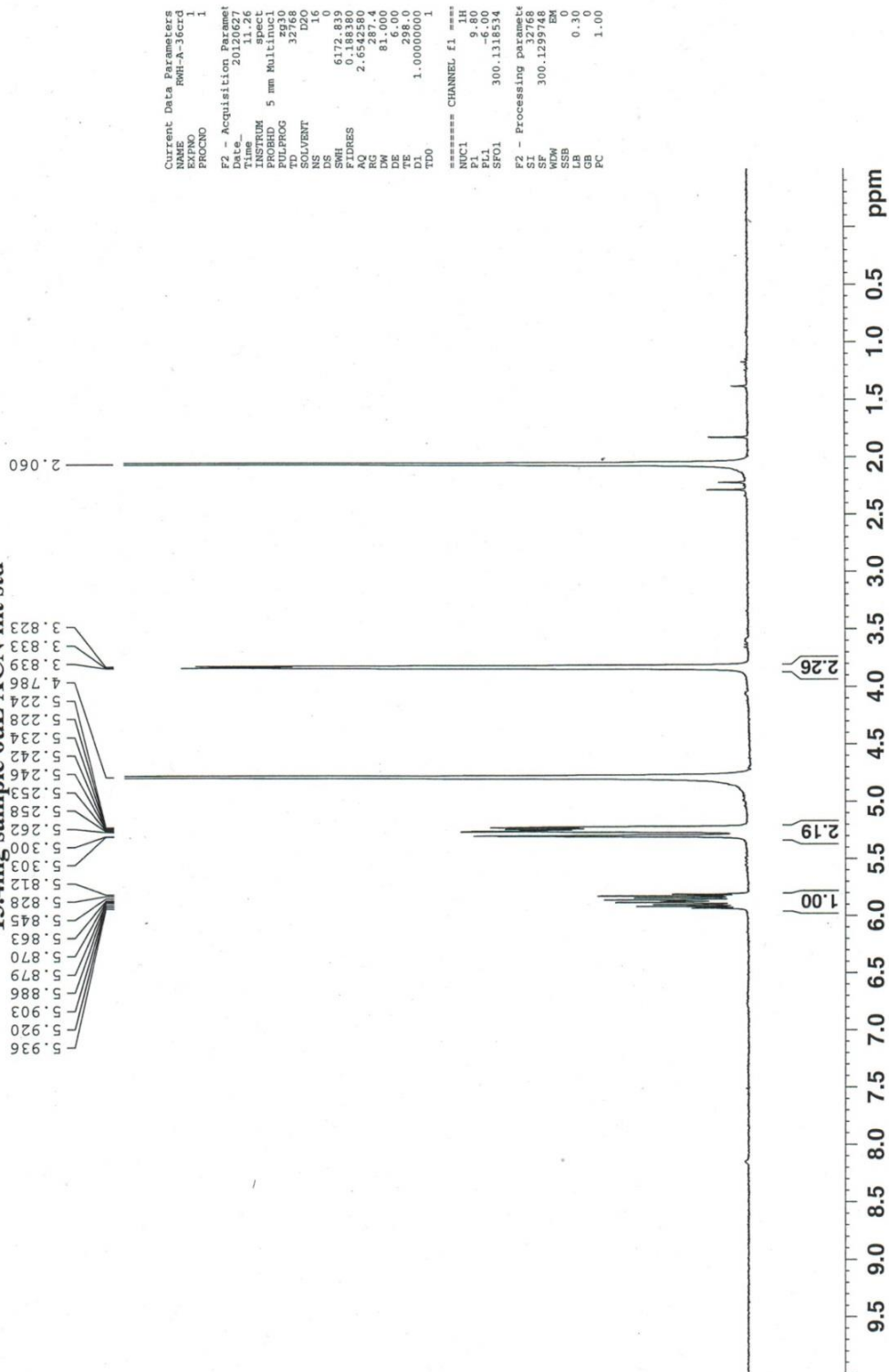
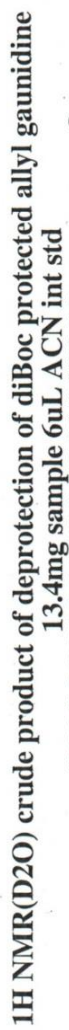
Analysis Name: 06121203.D
Method: Copy of MARK02.M
Sample Na RWH-A-24
Analysis Inf

Instrume LC-MSD-Trap-SL
Operator: Mark Wang

Print Date: 06/12/12 14:38:44
Acq. Date 06/12/12
14:34:41

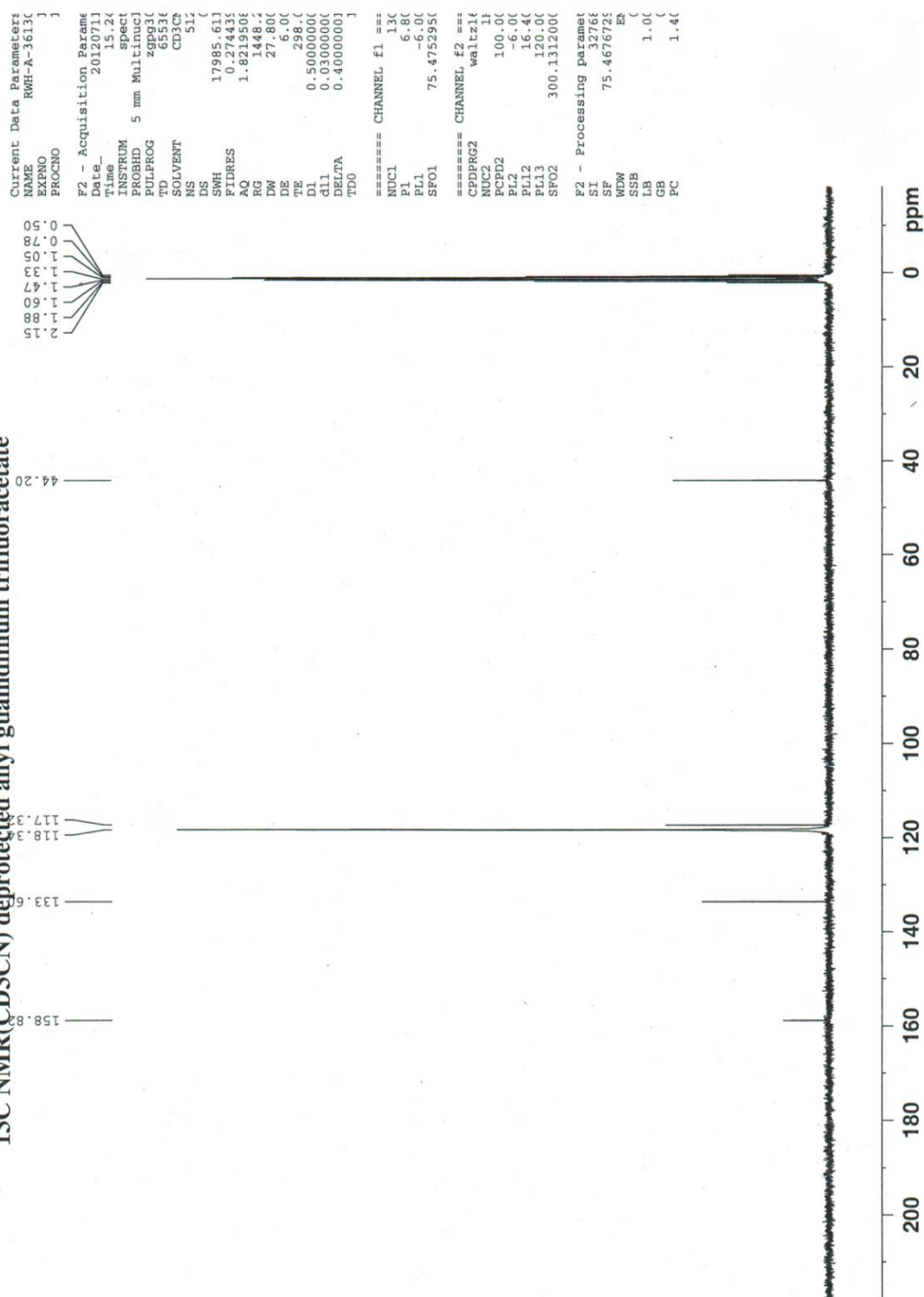


Agilent Technologies

¹H NMR *N*-allyl guanidinium trifluoroacetate (57)

¹³C NMR *N*-allyl guanidinium trifluoroacetate (57)

¹³C NMR(CD₃CN) deprotected allyl guanidinium trifluoroacetate



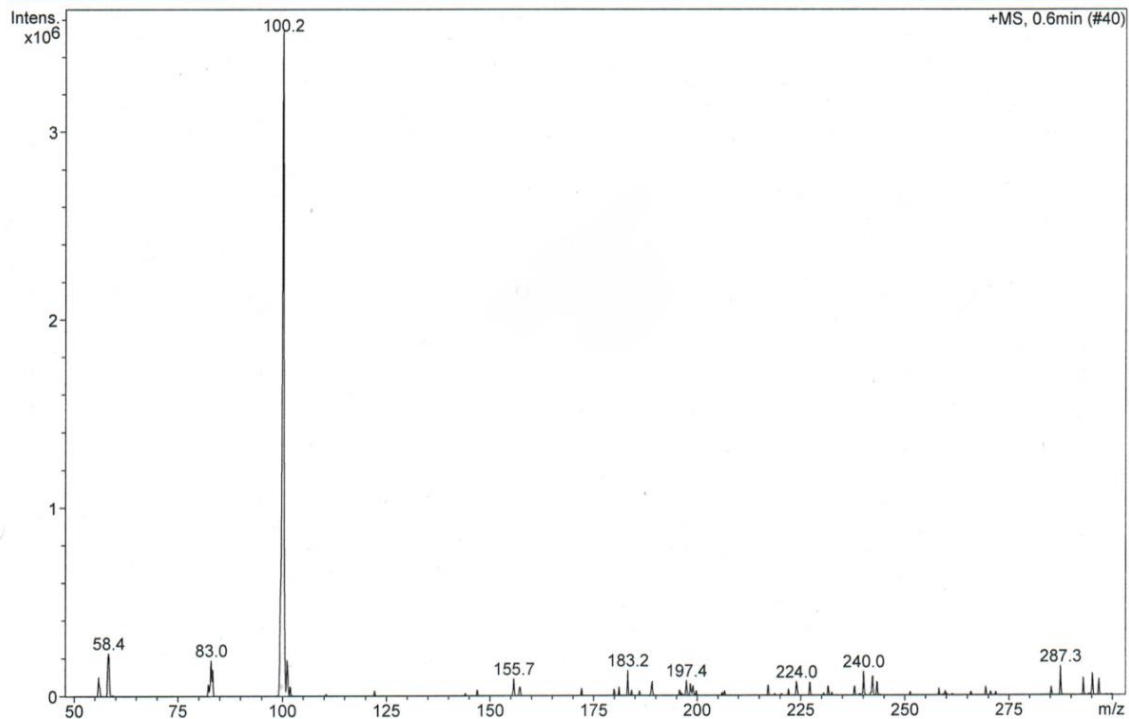
MS N-allyl guanidinium trifluoroacetate (57)

Display Report - All Windows Selected Analy

Analysis Name: 07181201.D
Method: Copy of MARK02.M
Sample Na RWH-A-36
Analysis Inf

Instrume LC-MSD-Trap-SL
Operator: Mark Wang

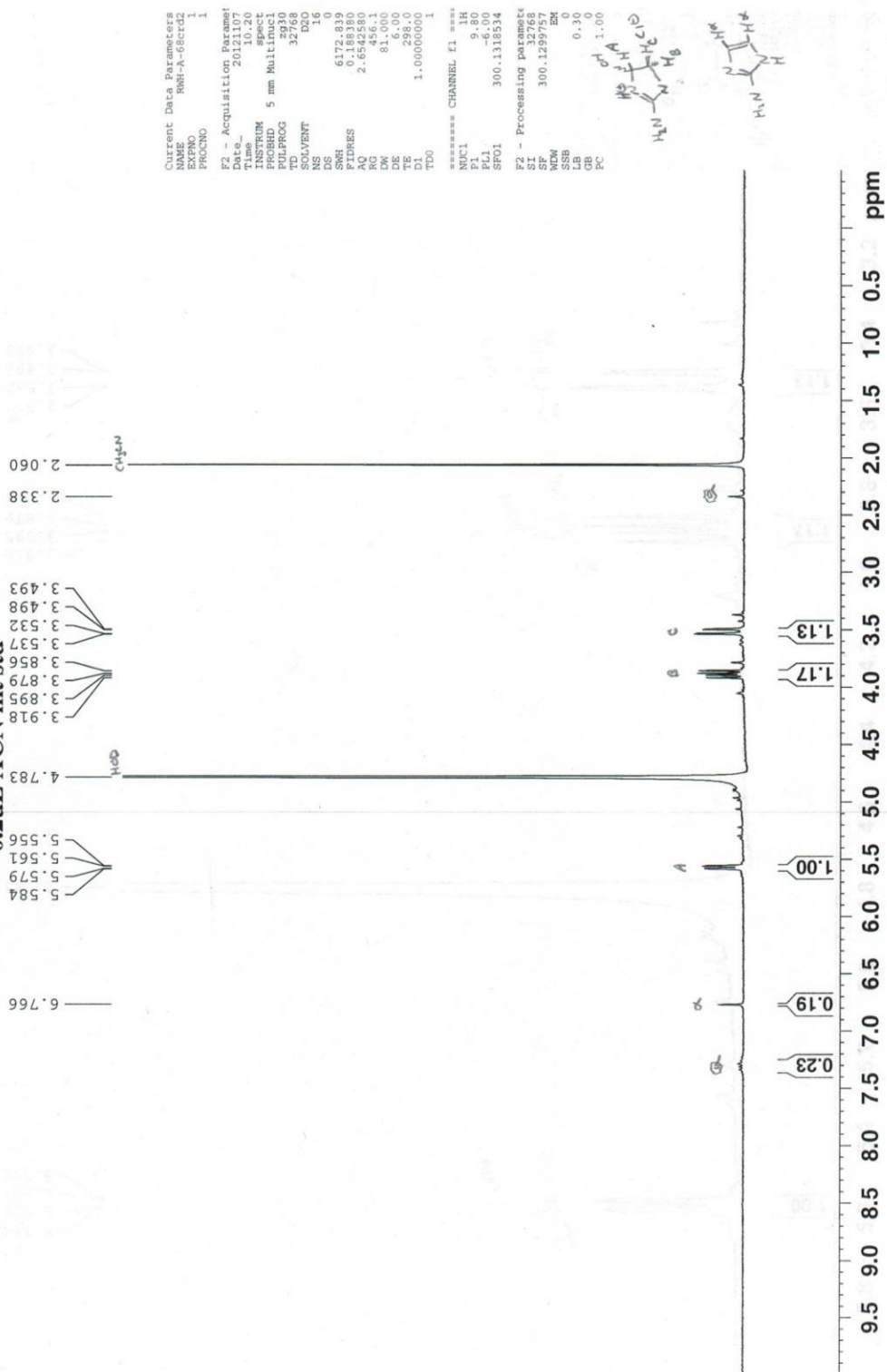
Print Date: 07/18/12 13:17:14
Acq. Date 07/18/12
13:08:45



Agilent Technologies

¹H NMR 2-Amino-5-hydroxy-4,5-dihydro-3H-imidazolium chloride (58)

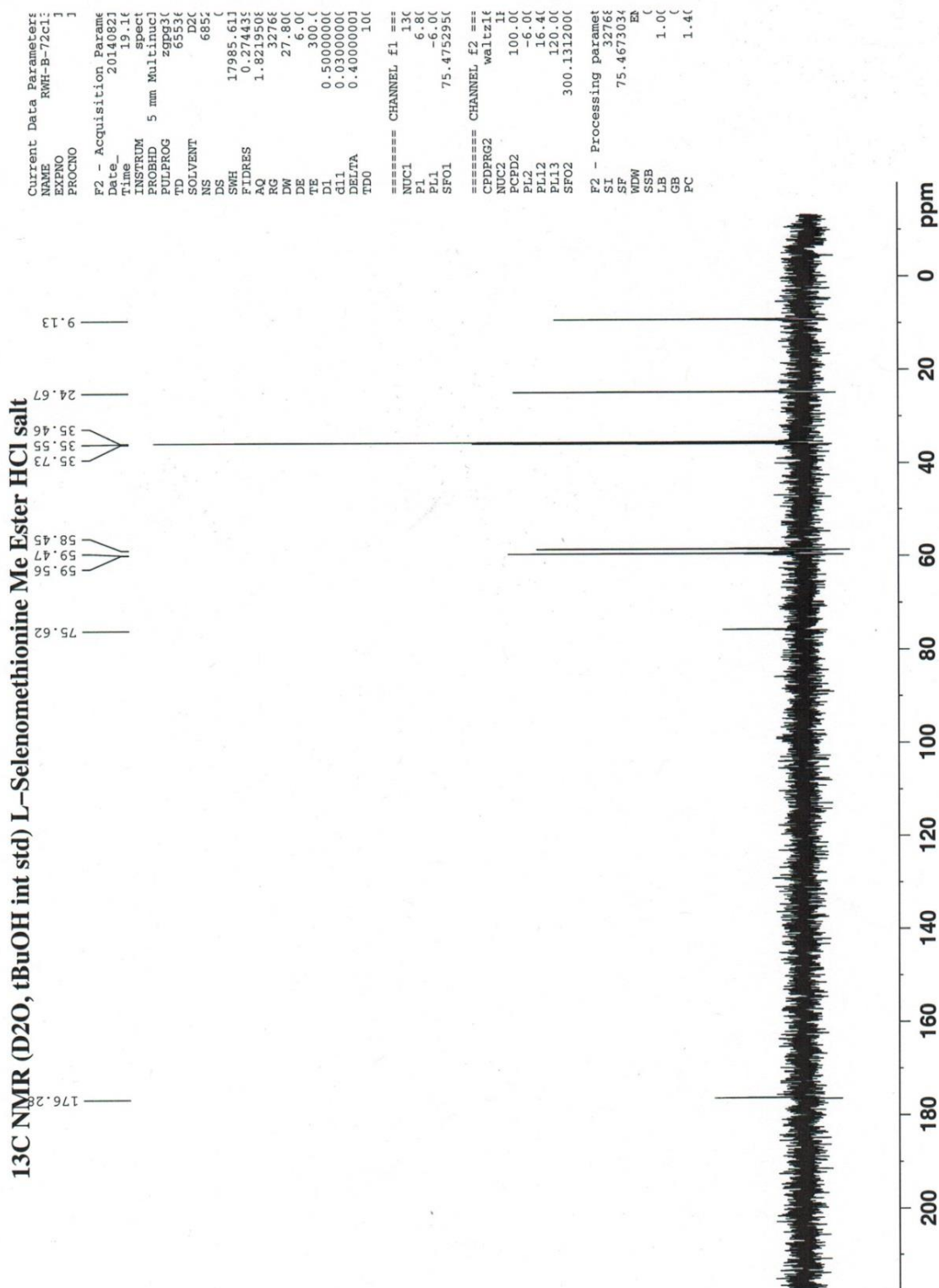
¹H NMR(D2O) deprotected guanidinium cyclized hemiaminal chloride
0.2uL ACN int std



¹H NMR(D₂O) C-methyl ester L-selenomethionine HCl 1uL CH₃CN int std
subtract 0.04 ppm from all δ to correct



¹³C NMR *L*-Selenomethionine methyl ester hydrochloride (62)

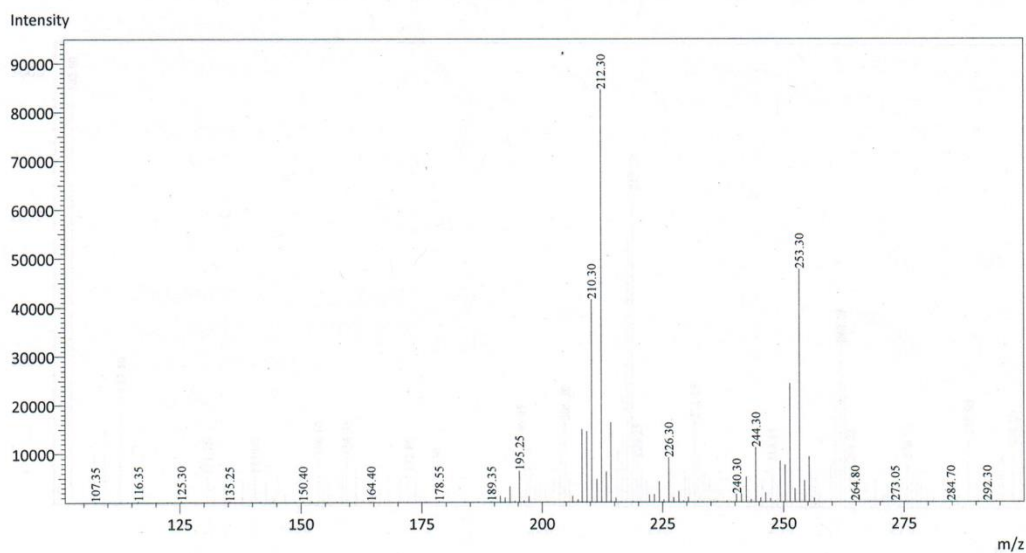


Shimadzu LCMS-2020 Data Report

Mass Spectrum for Sample
RWH-A-72 01.lcd

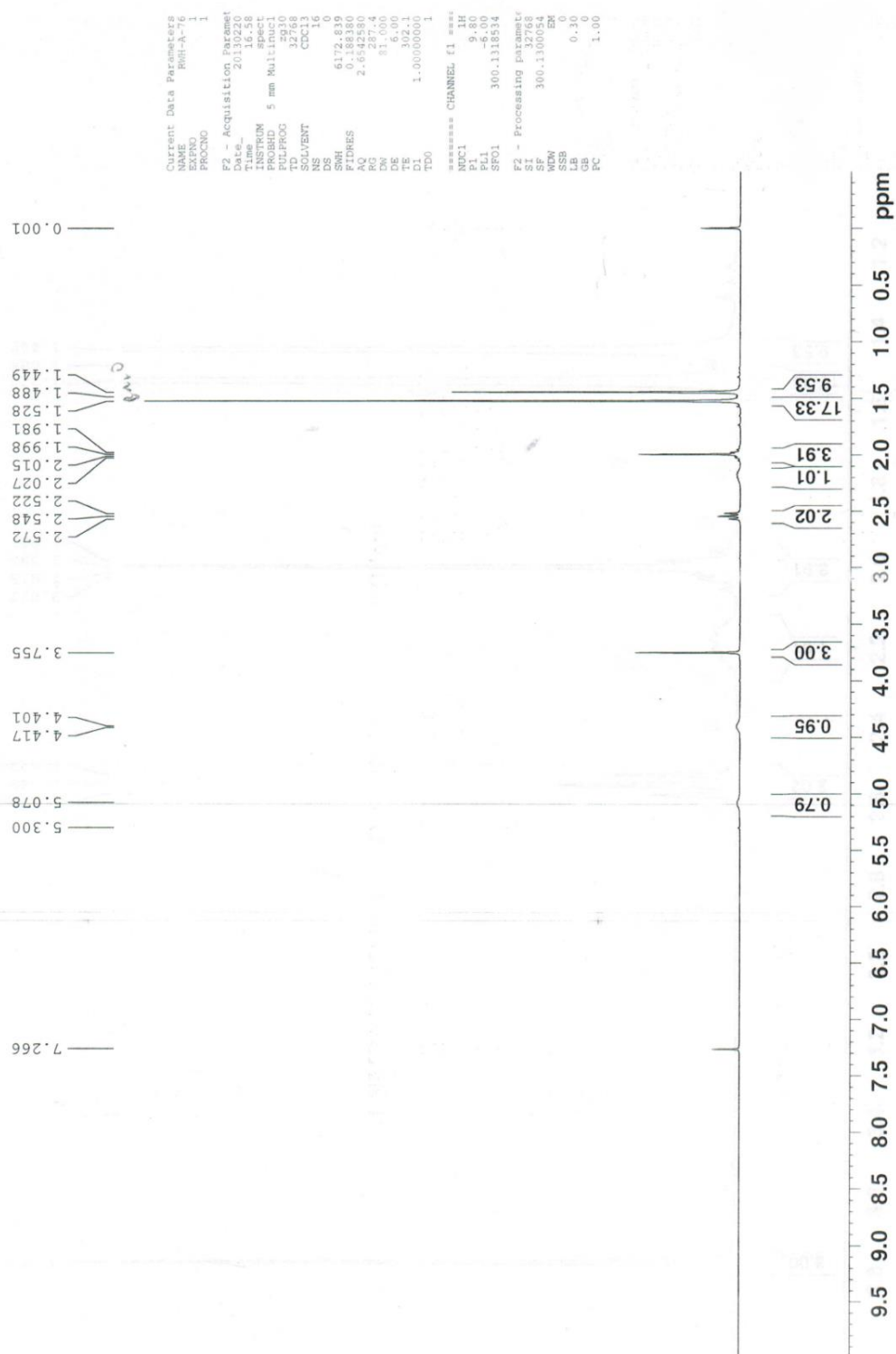
Operator: Mark Wang

Data Filename: C:\LabSolutions\Data\Schwabacher Alan\RWH-A-72 01.lcd
Spectrum Mode: Averaged
Retention Time: ----
Interface Type (ESI, APCI, DUIS): DUIS
Acquisition Mode: (Scan, SIM, Profile): Scan
Polarity: +

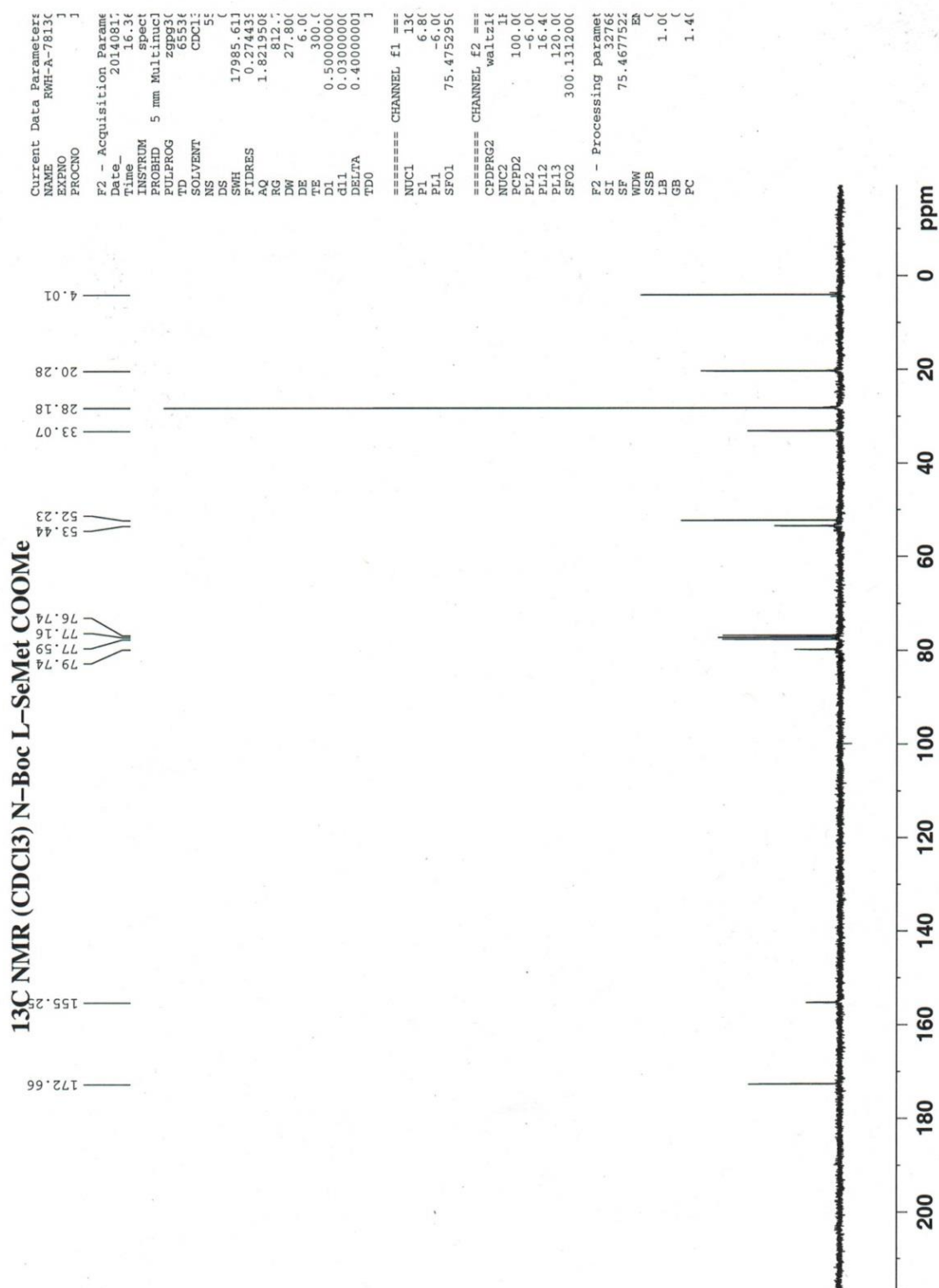


¹H NMR *N*-Boc-*L*-Selenomethionine methyl ester (63)

¹H NMR(CDCl₃) *N*-Boc, C-methyl *L*-selenomethionine



¹³C NMR *N*-Boc-*L*-Selenomethionine methyl ester (**63**)



Shimadzu LCMS-2020 Data Report

Mass Spectrum for Sample
RWH-A-78 02.lcd

Operator: Mark Wang

Data Filename: C:\LabSolutions\Data\Schwabacher Alan\RWH-A-78 02.lcd

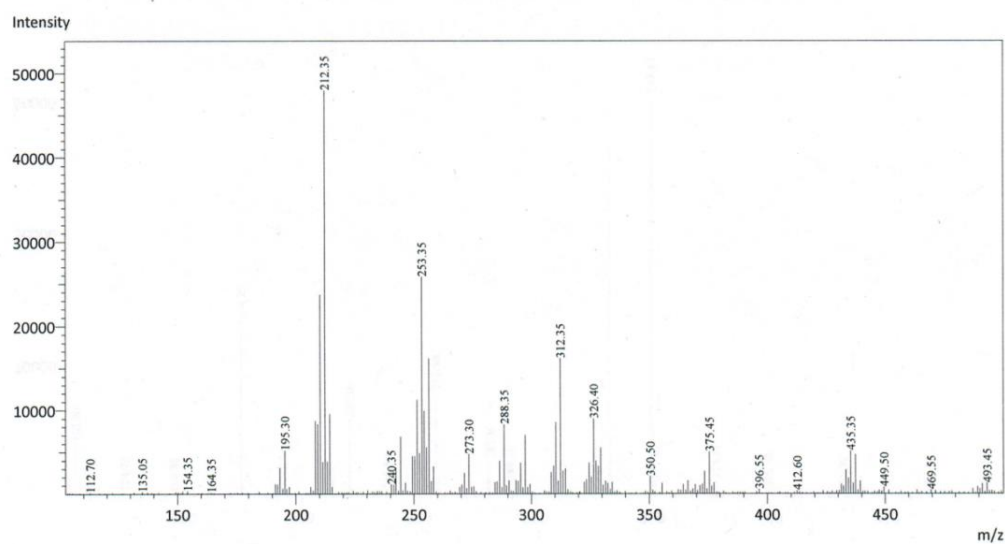
Spectrum Mode: Averaged

Retention Time: ----

Interface Type (ESI, APCI, DUIS): DUIS

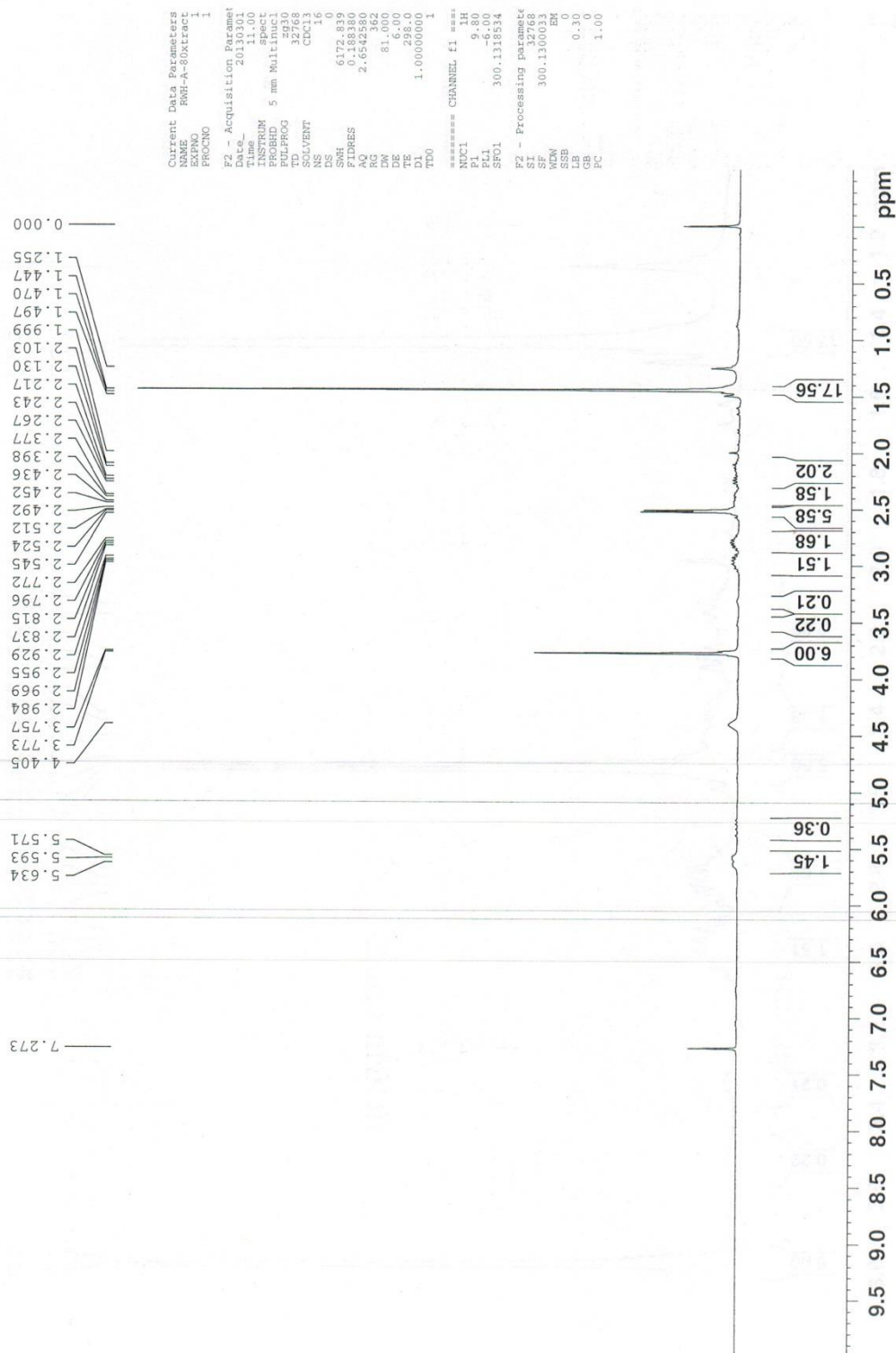
Acquisition Mode: (Scan, SIM, Profile): Scan

Polarity: +



¹H NMR *N*-Boc-L-Selenomethionine oxide methyl ester (64)

¹H NMR(CDCI₃) CH₂Cl₂ extracts from conc. aq. phase



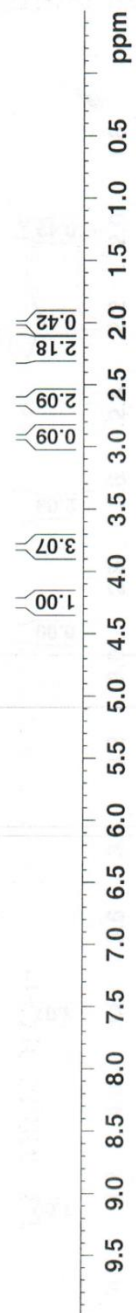
¹H NMR L-Methionine methyl ester hydrochloride (66)

¹H NMR(D₂O) C-methyl ester L-Met HCl 6.0mg sampl1 1uL ACH3CN int. std.

add 0.057 ppm
to all signals

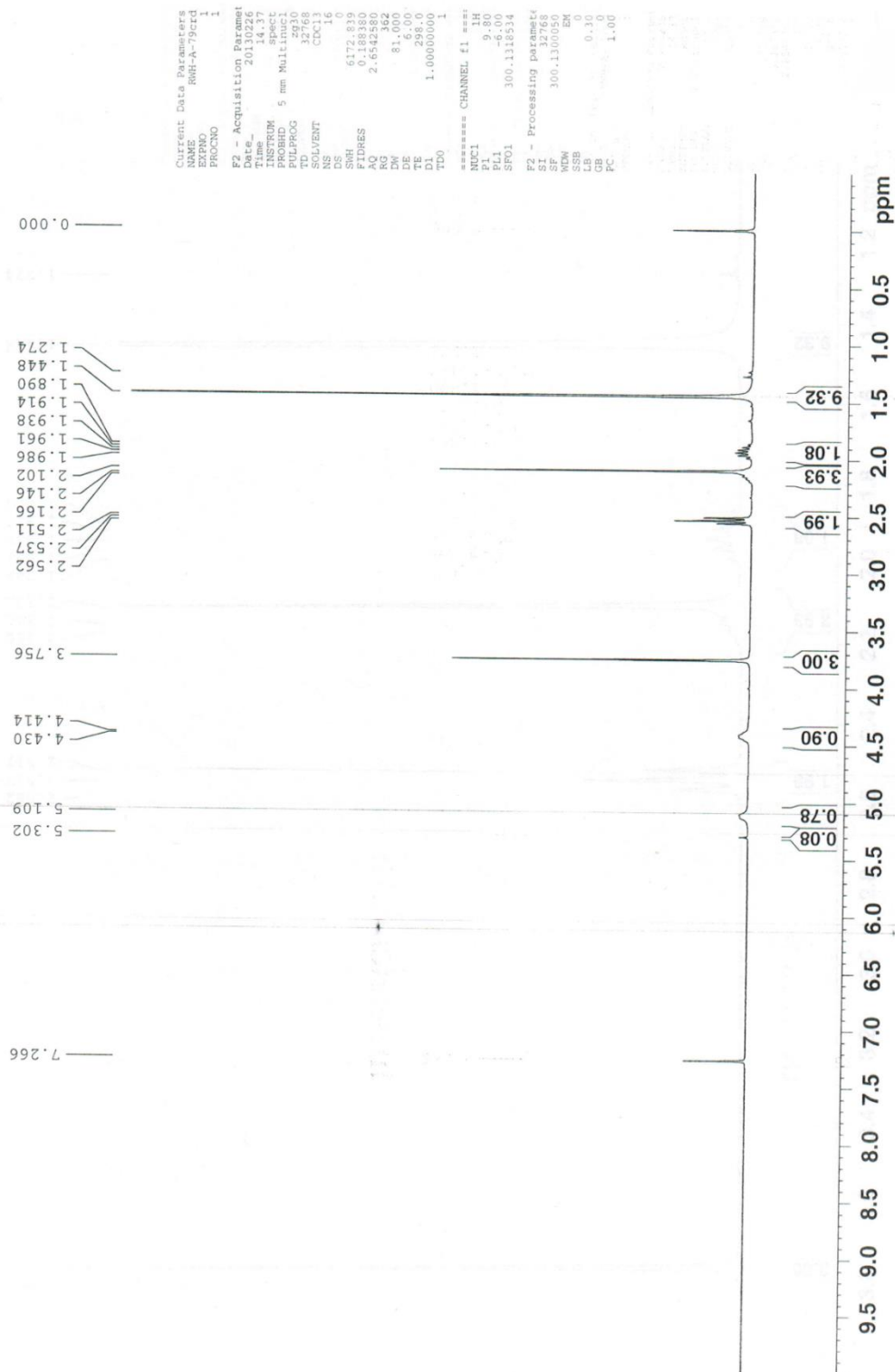
4.270
4.249
4.228
3.801
2.921
2.656
2.632
2.608
2.294
2.269
2.245
2.223
2.212
2.200
2.188
2.164
2.140
2.115
2.061
2.004

Current Data Parameters
NAME RMR-A-73
EXPNO 1
PROCNO 1
F2 - Acquisition Parameters
Date_ 20100611
Time 11.03
INSTRUM spect
PROBHD 5 mm Multinucl
PULPROG zgpg30
TD 65536
SOLVENT D2O
NS 16
DS 0
SWH 6172.830
FIDRES 0.188380
AQ 2.6542580
RG 456.1
WV 81.000
DE 6.000
TE 302.4
D1 1.00000000
TD0 1
***** CHANNEL f1 ****
NUC1 1H
P1 9.80
PL 0.00
SFO1 300.1115534
F2 - Processing parameters
SI 32768
SF 300.130077
WDW EM
SSB 0
LB 0.30
GB 0
PC 1.00



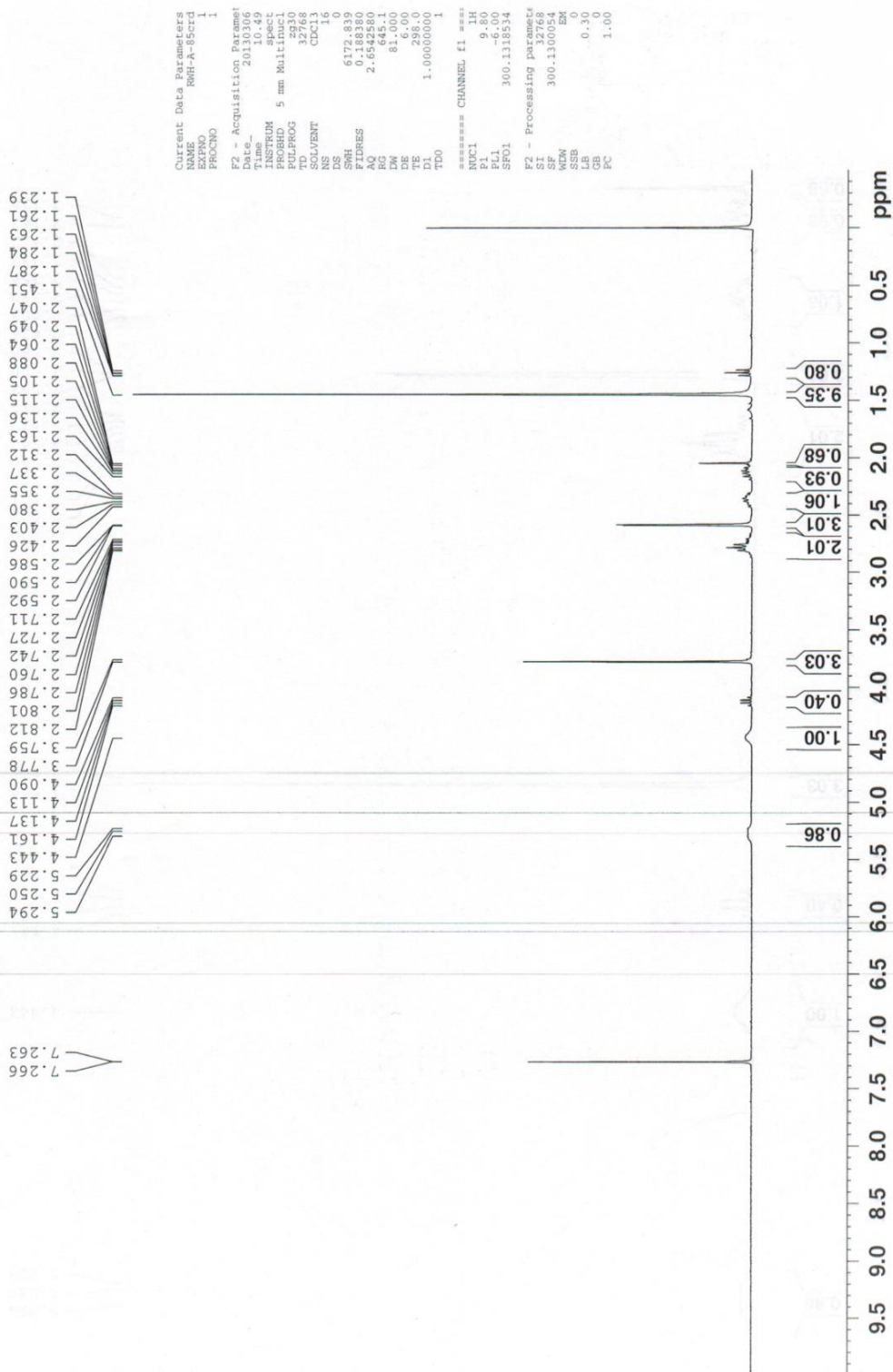
¹H NMR N-Boc-L-Methionine methyl ester (67)

¹H NMR(CDCI₃) N-Boc C-Me ester L-Met



¹H NMR *N*-Boc-L-Methionine sulfoxide methyl ester (68)

¹H NMR(CDCl₃) L-Met SO crude product?



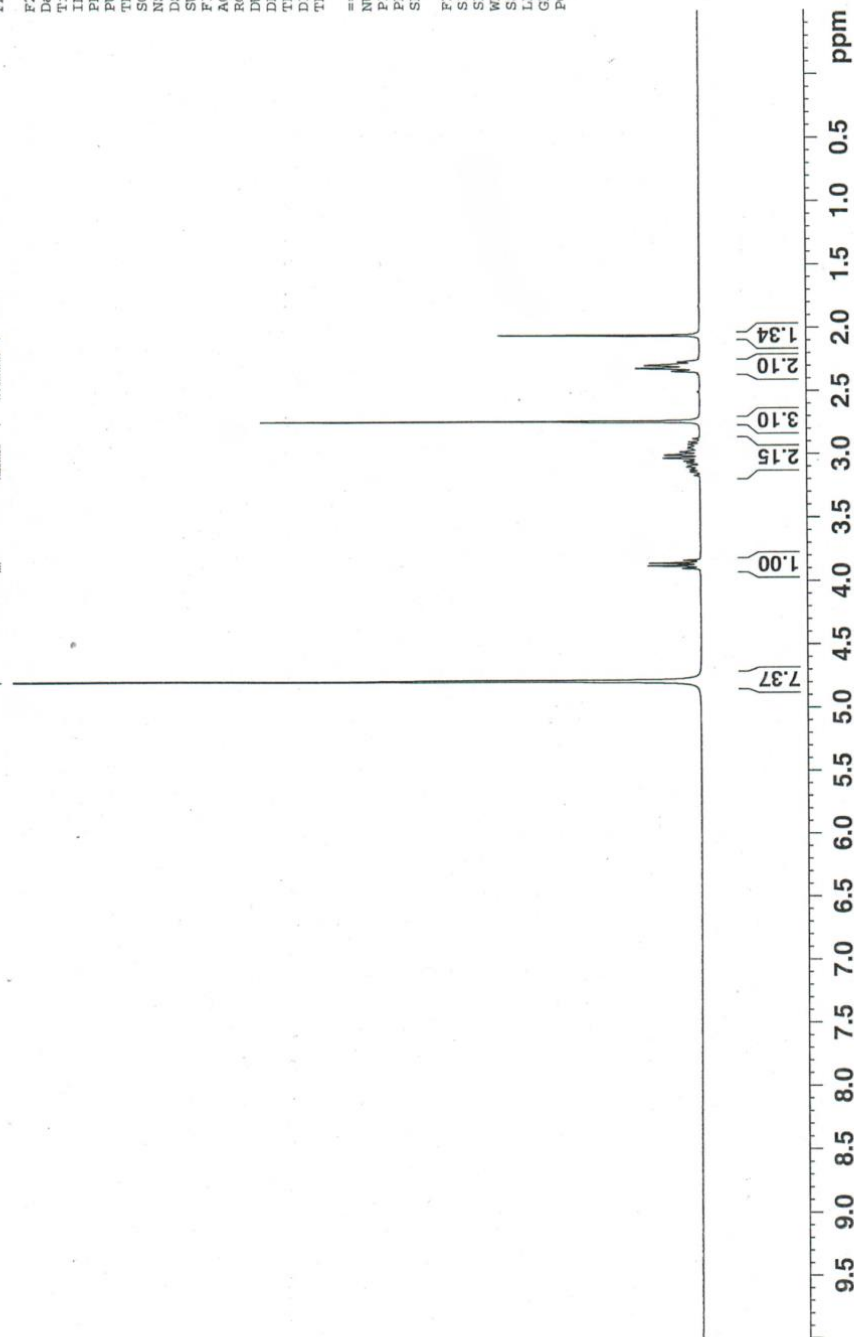
¹H NMR *L*-Methionine sulfoxide (70)

1 ¹H NMR(D₂O) White ppt after treatment of *L*-Met with 30% H₂O₂ and dilution with EtOH 8.6mg s

4uL ACN internal std.

4.786
3.900
3.879
3.858
3.837
3.170
3.143
3.125
3.115
3.102
3.094
3.071
3.057
3.031
3.008
2.984
2.963
2.954
2.946
2.925
2.905
2.742
2.536
2.507
2.464
2.425
2.419
2.408
2.389
2.367
2.343
2.318
2.294
2.270
2.236
2.213
2.183
2.059

Current Data Parameters
NAME RMH-A-2
EXPNO 1
PROCNO 1
F2 - Acquisition Parameters
Date_ 20110520
Time 11.09
INSTRUM spect
PROBHD 5 mm Multinucl
PULPROG zg30
TD 32768
SOLVENT D₂O
NS 32
DS 0
SWH 6172.839
FIDRES 0.188380
AQ 2.6542580
RG 362
DW 81.000
DE 6.00
TE 298.0
D1 1.00000000
TD0 1
===== CHANNEL f1 =====
NUC1 1H
P1 9.80
PL1 -6.00
SFO1 300.1318534
F2 - Processing parameters
SI 32768
SF 300.1299747
WDW EM
SSB 0
LB 0.30
GB 0
FC 1.00



¹³C NMR L-Methionine sulfoxide (70)

¹³C NMR(D₂O) L-Met Sulfoxide 32.8mg sample 6uL ACN int. std.



```

Current Data Parameters:
NAME      RWH-A-2-13
EXPNO     1
PROCNO    1

F2 - Acquisition Parameters:
Date_     20110521
Time      17.21
INSTRUM   spect
PROBHD    5 mm Multinu
PULPROG   zgpg3
TD        65534
SOLVENT   CDC1
NS        64
DS        4
SWH        17985.61
FIDRES     0.27443
AQ         1.821950
RG         406.4
DW         27.80
DE         6.0
TE         303.2
D1         0.5000000
d11        0.0300000
DELTA     0.4000000
TD0        1

===== CHANNEL f1 =====
NUC1       13C
P1         6.80
PL1        -6.00
SF01       75.475295

===== CHANNEL f2 =====
CPDPRG2    waltz16
NUC2       1H
PCPD2      100.00
PL2        -6.00
PL12       16.40
PL13       120.00
SFO2       300.131200

F2 - Processing parameters:
SI         32768
SF         75.467704
WDW         EM
SSB         1.00
GB          1.40
PC          1.40
  
```

200 180 160 140 120 100 80 60 40 20 0 ppm

MS L-Methionine sulfoxide (70)

Display Report - All Windows Selected Analy

Analysis Name: 06141109.d

Instrume LC-MSD-Trap-SL

Print Date: 06/14/11 12:06:12

Method: Copy of Mark01.MS

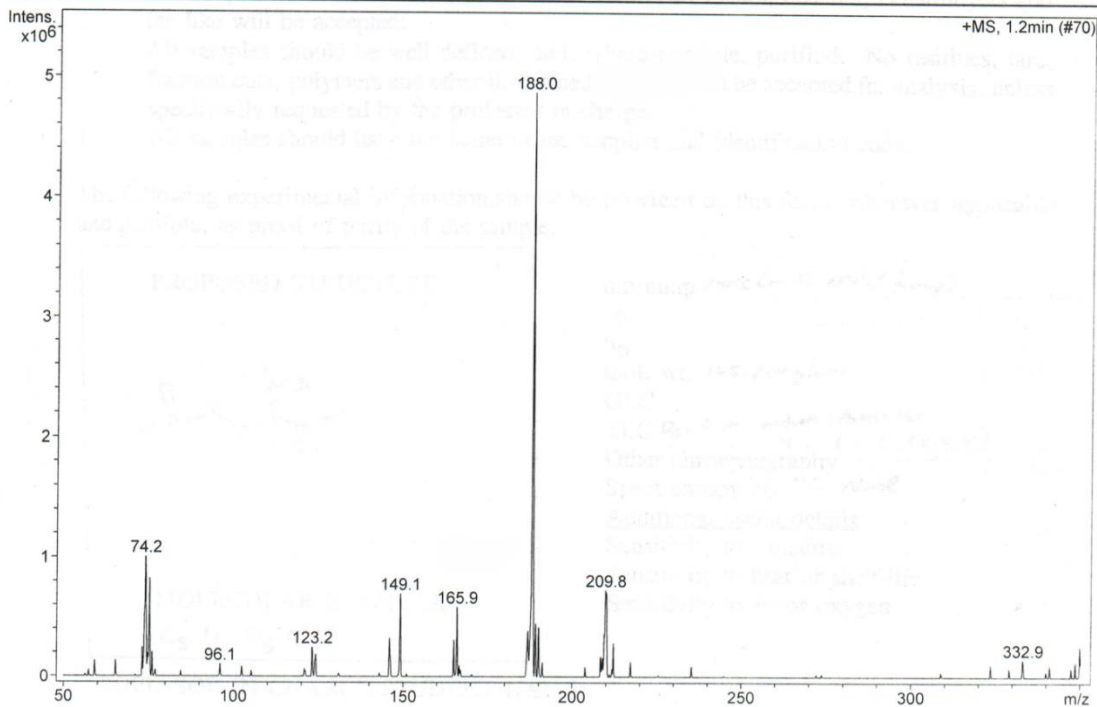
Operator: Mark Wang

Acq. Date 06/14/11

Sample Na RWH-A-2

12:02:54

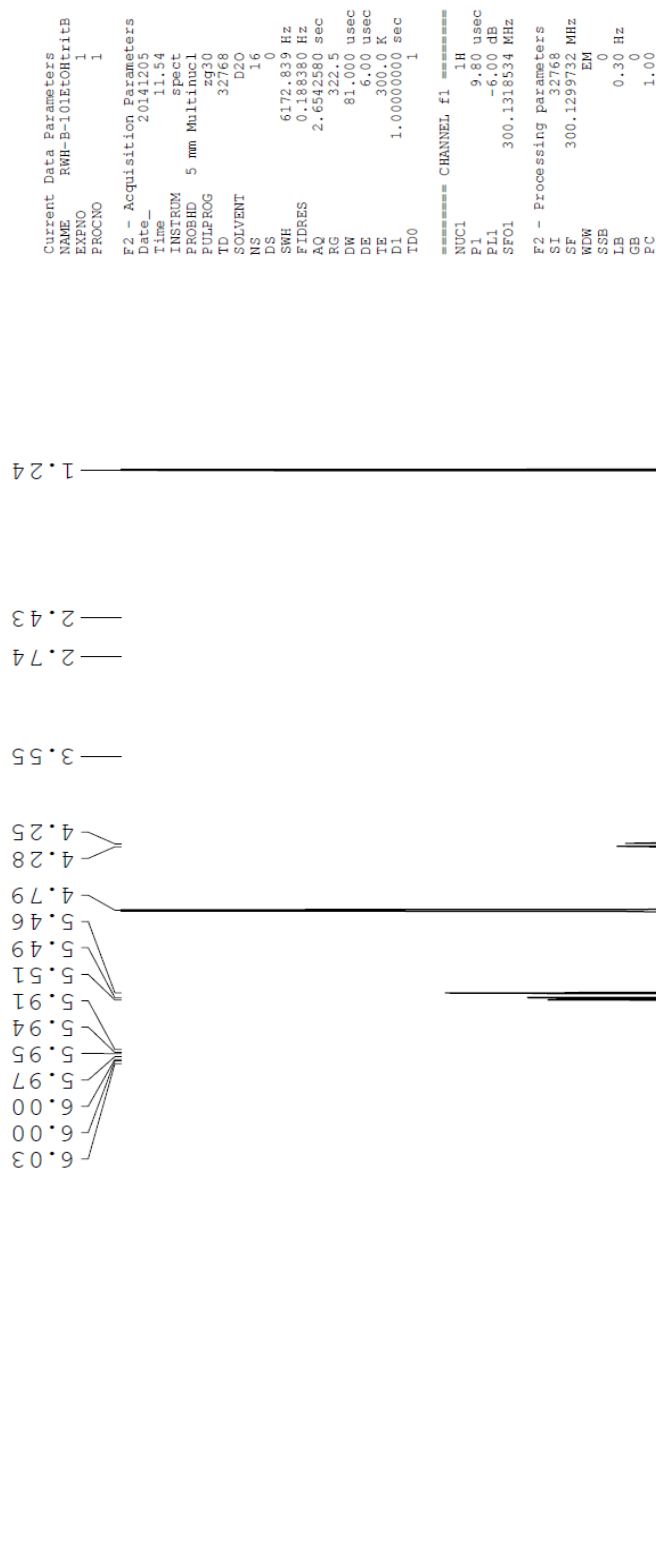
Analysis Inf Sample RWH-A-2 in Water, ESI positive mode



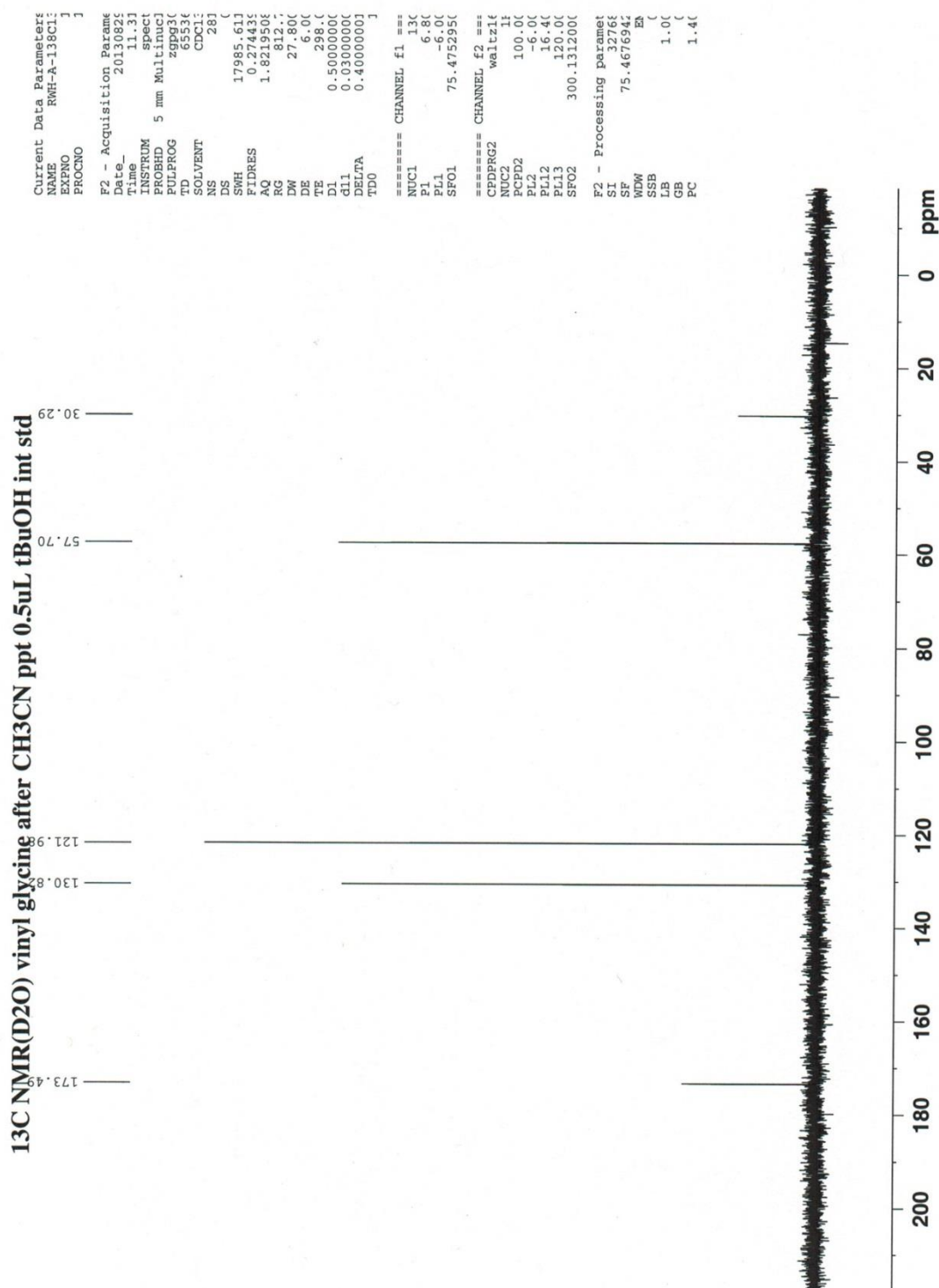
Agilent Technologies

¹H NMR L-Vinylglycine (71)

¹H NMR (D₂O, tBuOH int std) L-Vinylglycine from EtOH trituration, t=3days in D₂O



¹³C NMR L-Vinylglycine (71)



Shimadzu LCMS-2020 Data Report

Mass Spectrum for Sample
RWH-B-83A_03.lcd

Operator: Margaret Guthrie

Data Filename: C:\LabSolutions\Data\Guthrie, Margaret\RWH-B-83A_03.lcd

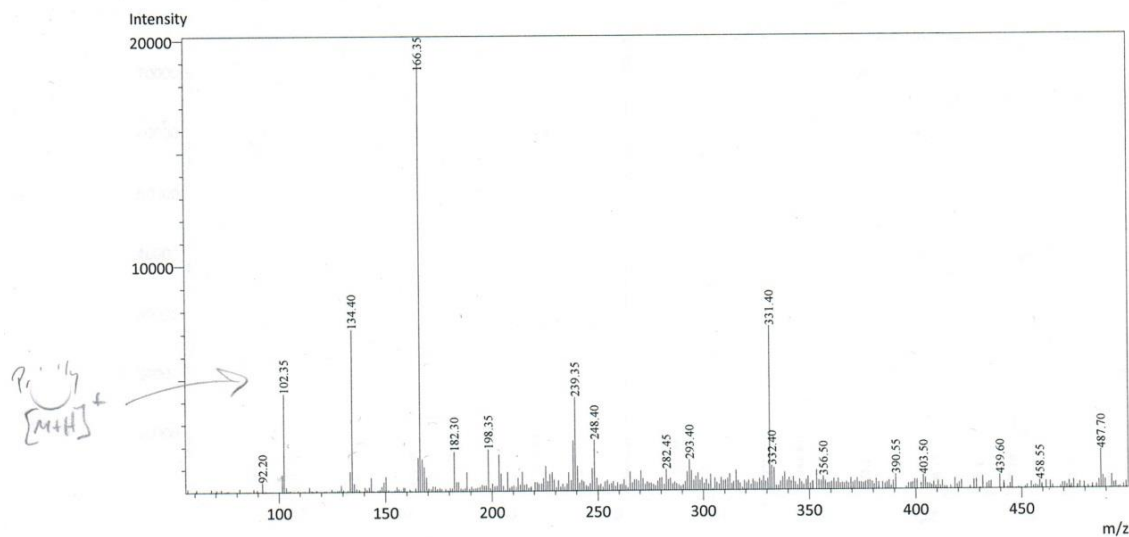
Spectrum Mode: Averaged

Retention Time: ----

Interface Type (ESI, APCI, DUIS): DUIS

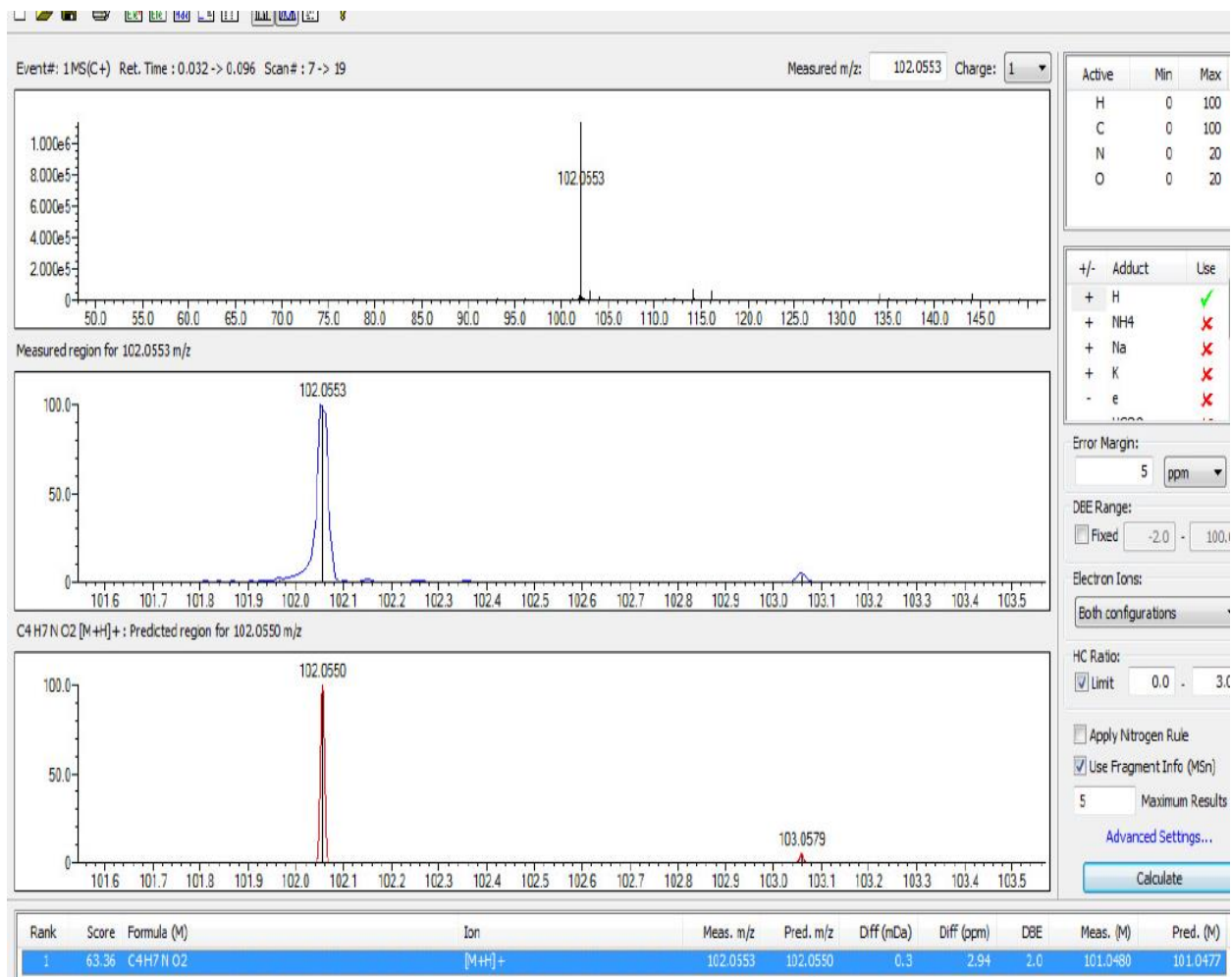
Acquisition Mode: (Scan, SIM, Profile): Scan

Polarity: +



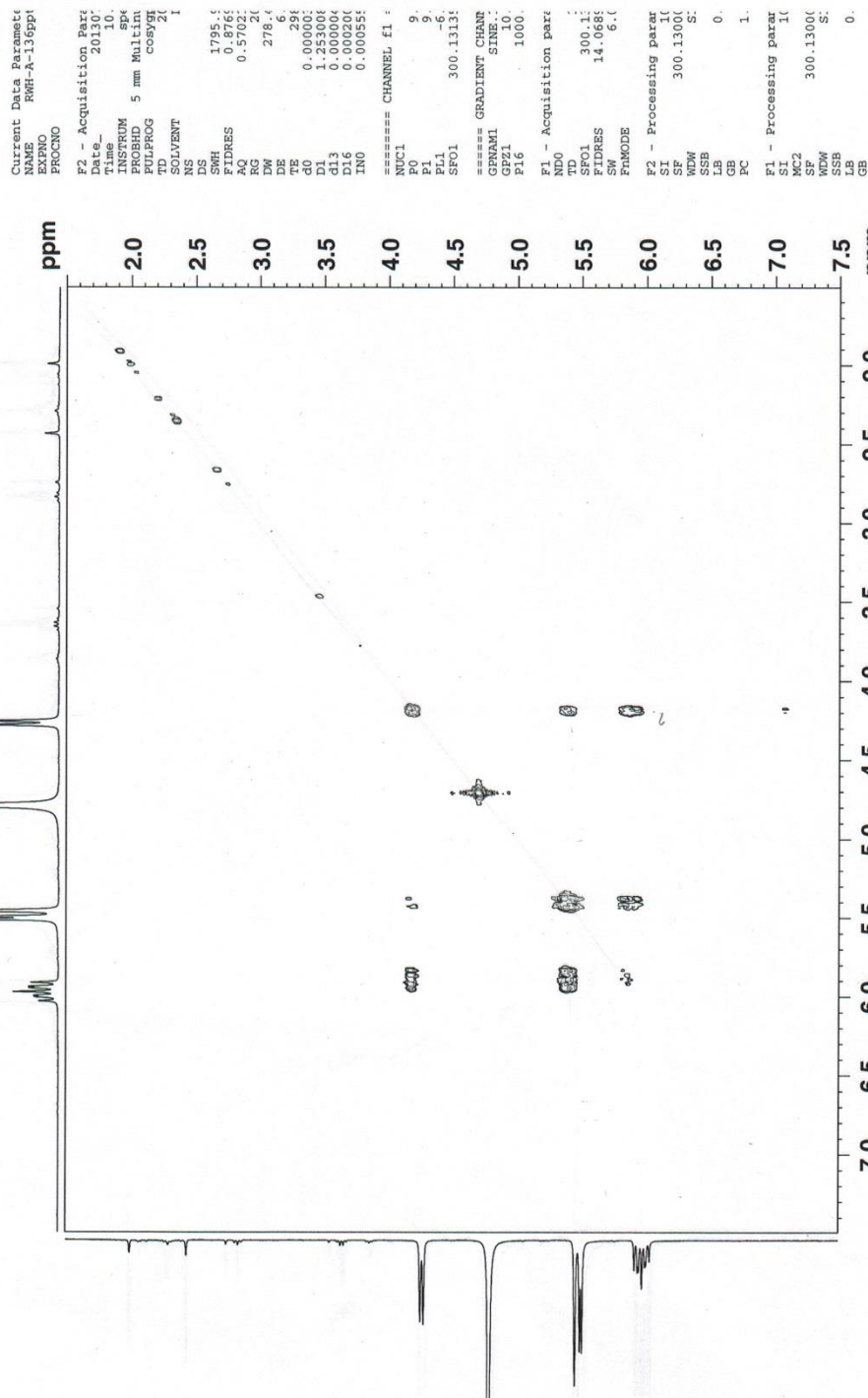
Handwritten:
90% MeOH
10% H₂O
No modifiers

HRMS (IT-TOF) *L*-Vinylglycine (71)



COSY L-Vinylglycine (71)

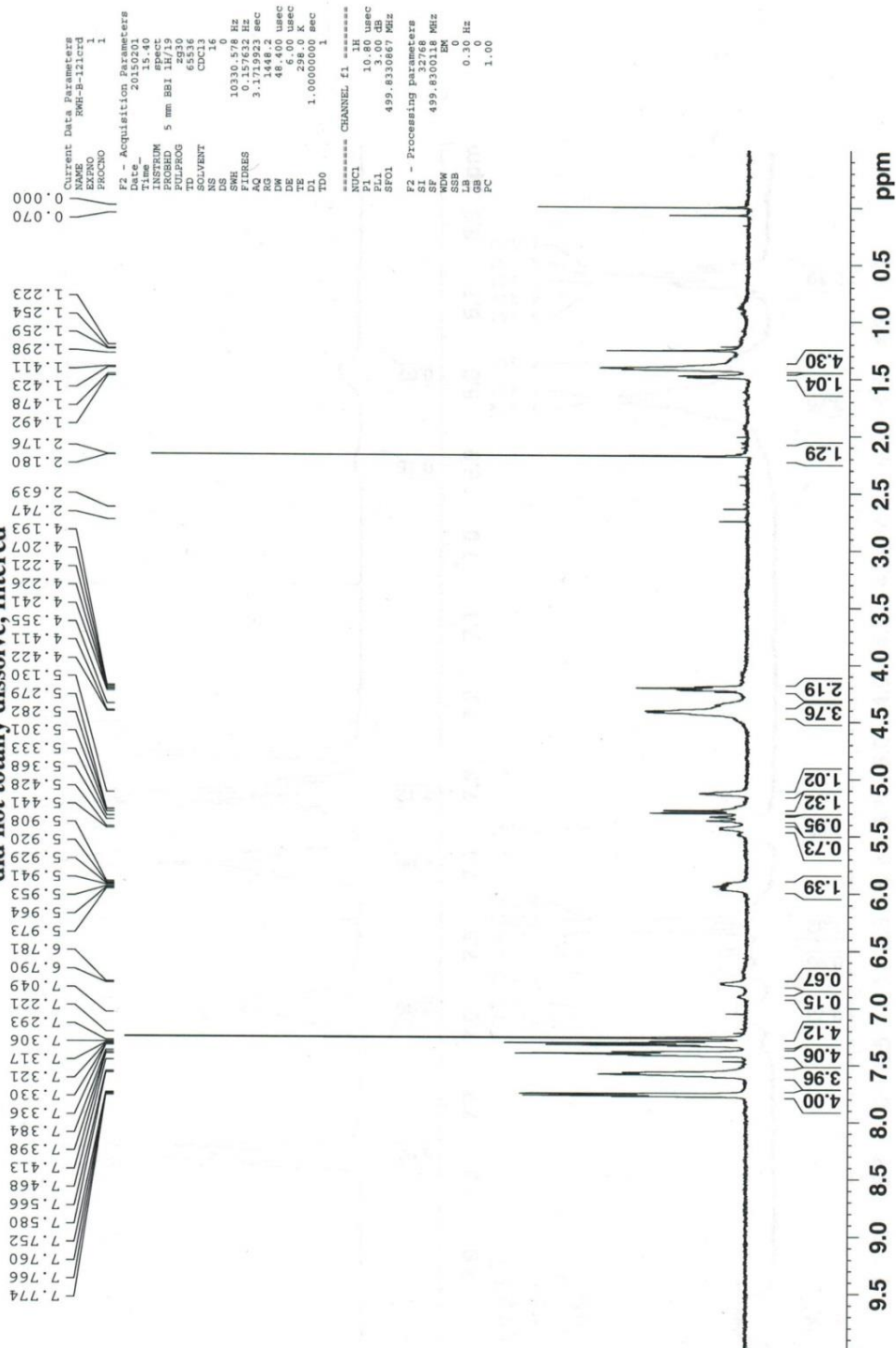
2D COSY NMR (D₂O) Ppt crude of vinyl glycine from ~~EtOH~~ ^{H₂O} w/~~EtOH~~ ^{EtOH}
0.5uL tBuOH int std



¹H NMR

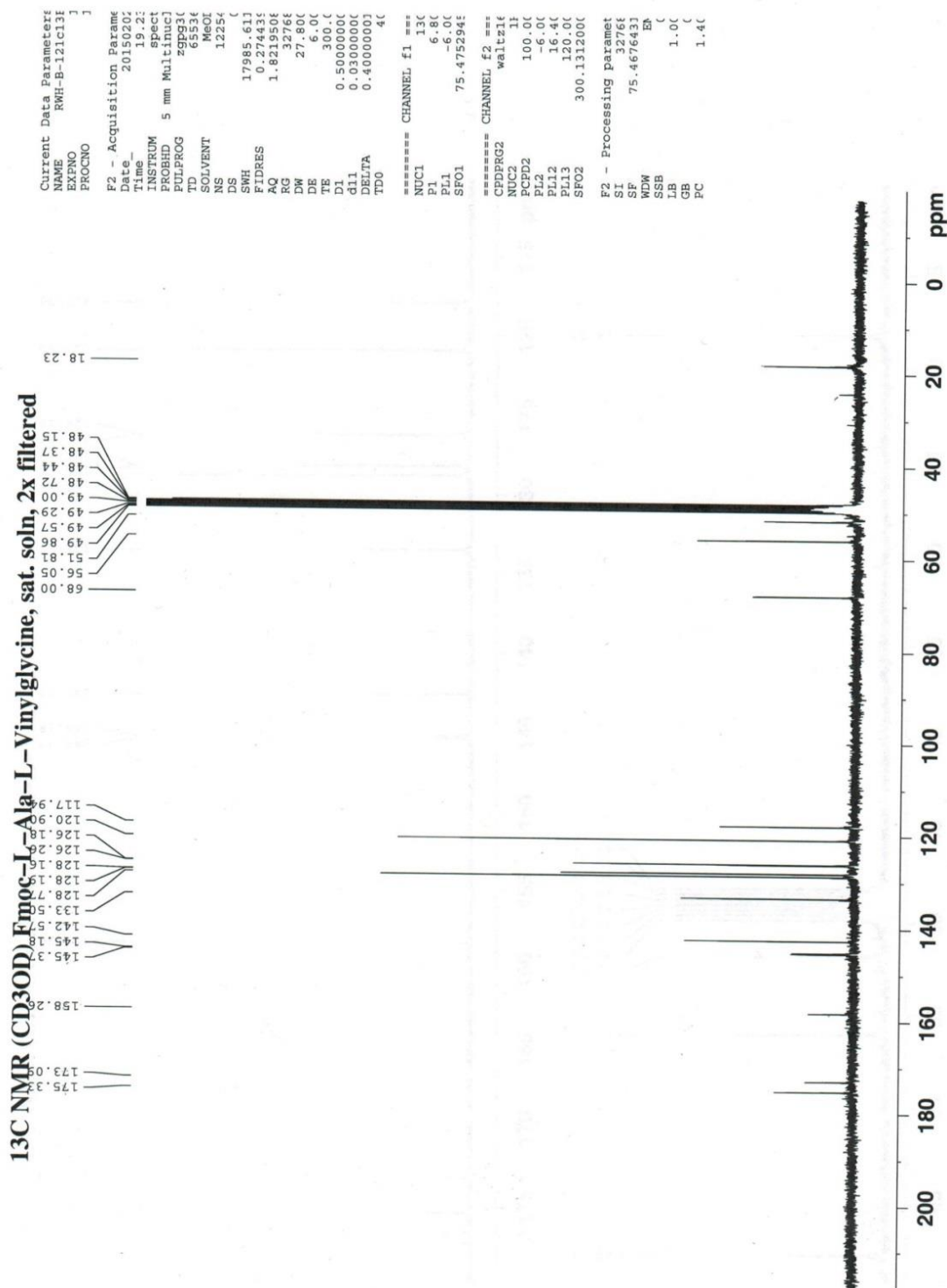
(S)-2-((R)-2-((((9H-fluoren-9-yl)methoxy)carbonyl)amino)propanamido)but-3-enoic acid (72)

**¹H NMR (CDCl₃) Fmoc-L-Ala derivatized vinylglycine, 8.4mg sample
did not totally dissolve, filtered**



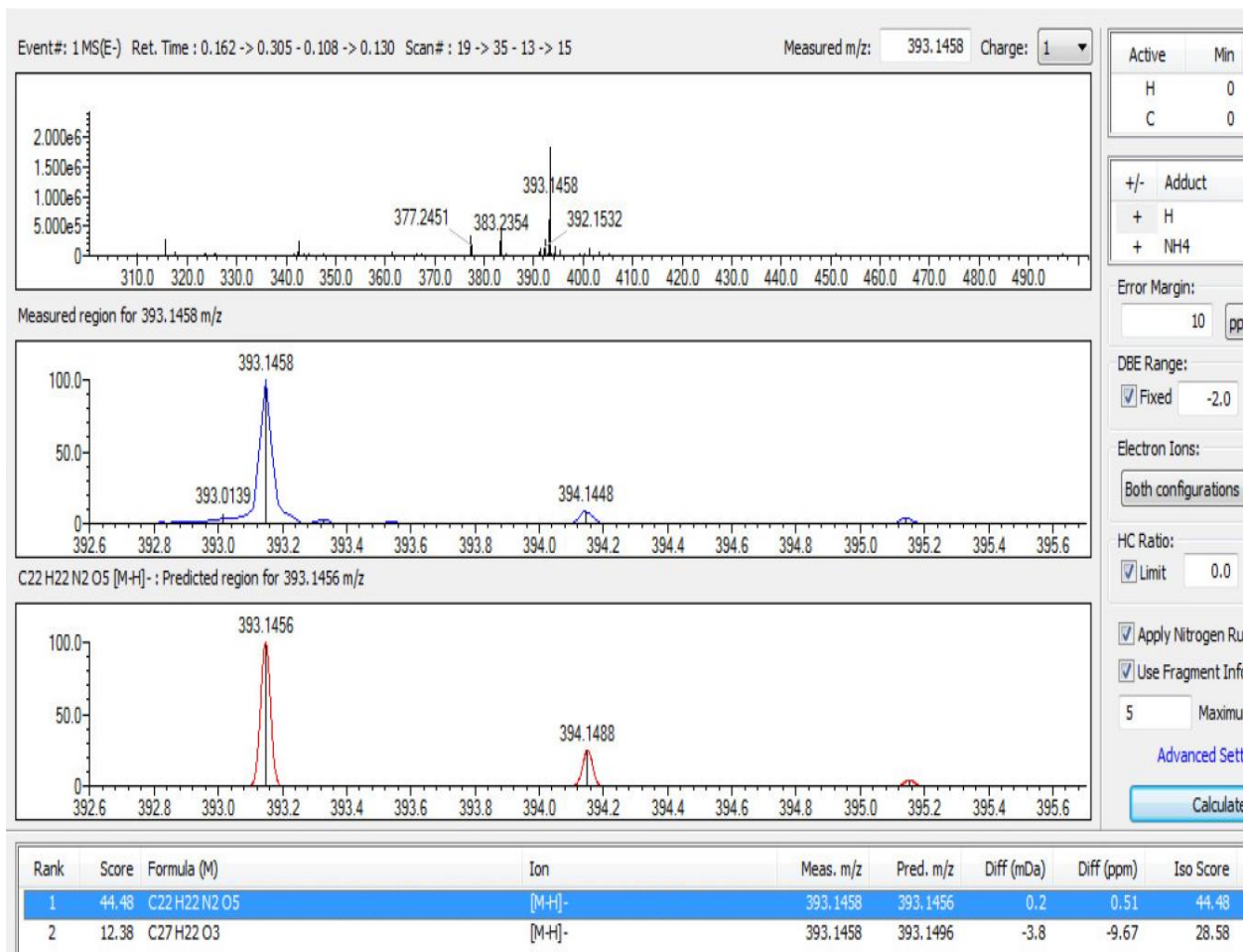
¹³C NMR

(S)-2-((R)-2-((((9H-fluoren-9-yl)methoxy)carbonyl)amino)propanamido)but-3-enoic acid (72)



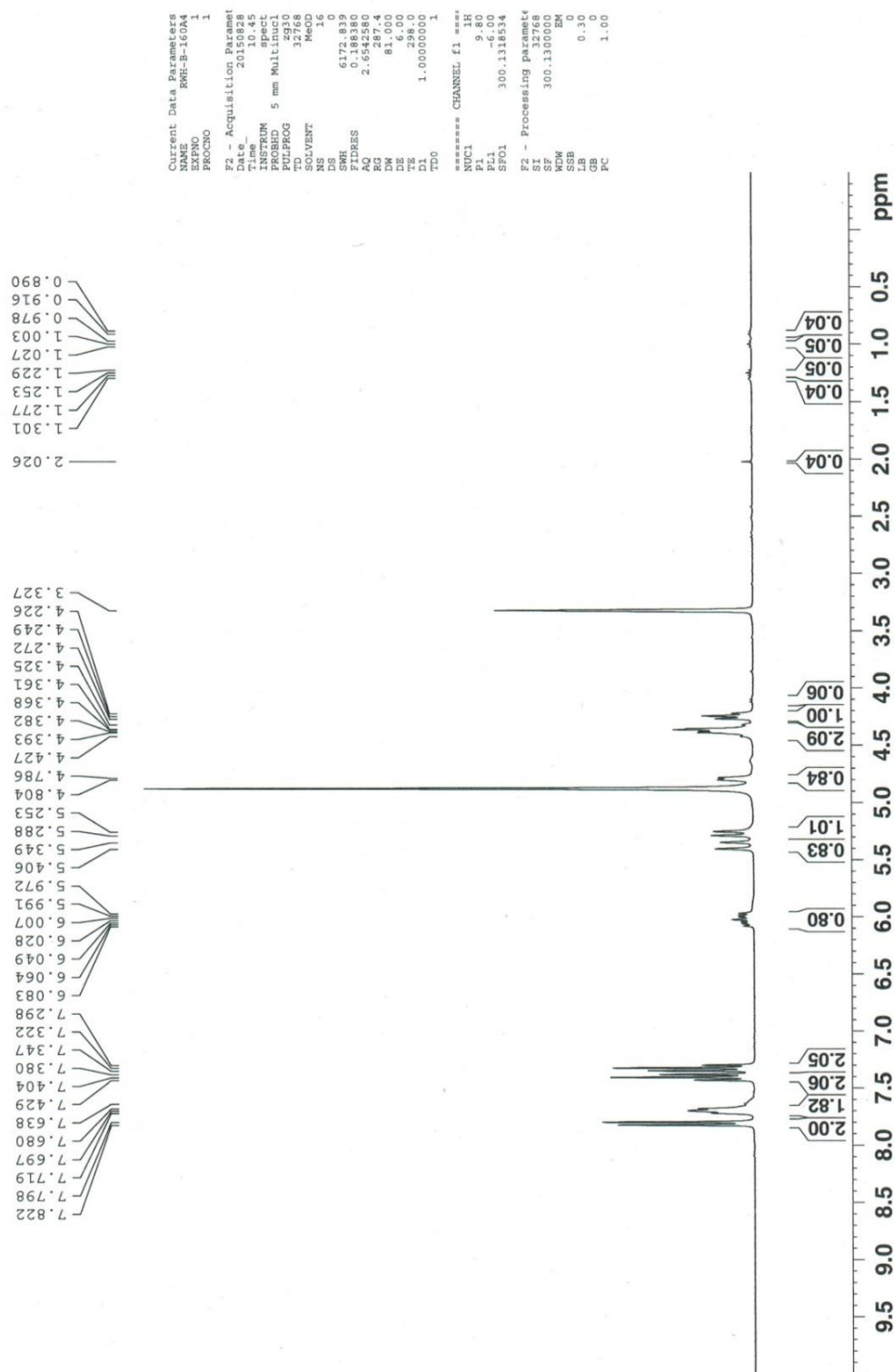
HRMS (IT-TOF)

(S)-2-((R)-2-((((9H-fluoren-9-yl)methoxy)carbonyl)amino)propanamido)but-3-enoic acid (72)

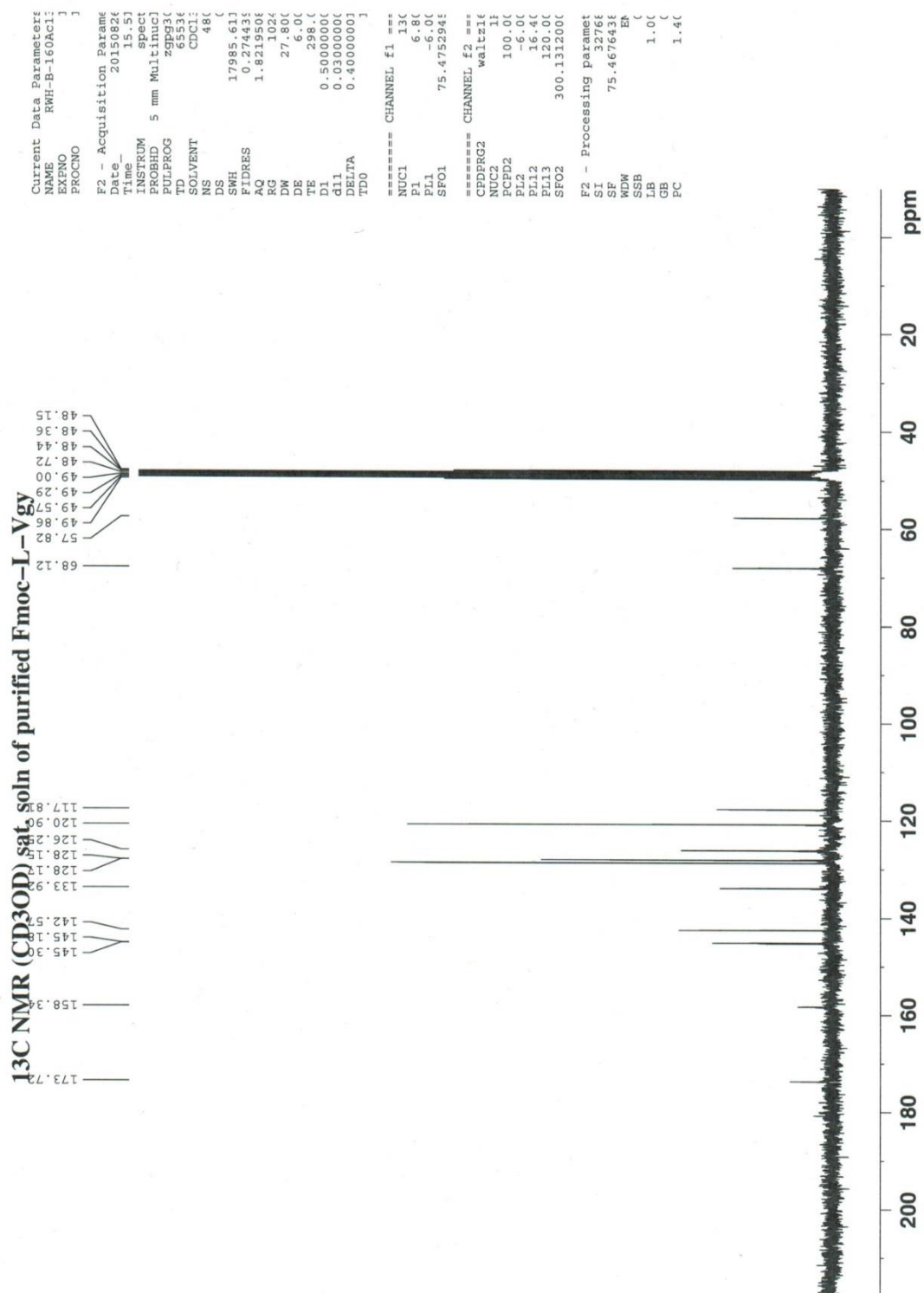


¹H NMR (S)-2-((((9H-fluoren-9-yl)methoxy)carbonyl)amino)but-3-enoic acid (73)

¹H NMR (CD3OD) purified Fmoc-L-Vgy 18.5hr in Abderhalden (hexane/paraffin)



¹³C NMR (S)-2-((((9H-fluoren-9-yl)methoxy)carbonyl)amino)but-3-enoic acid (73)

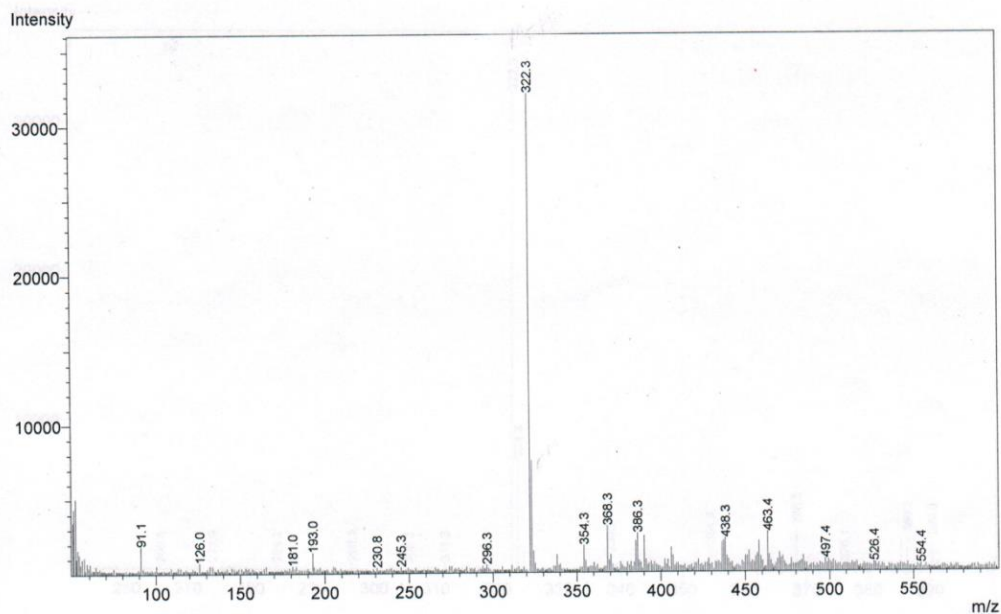


Shimadzu LCMS-2020 Data Report

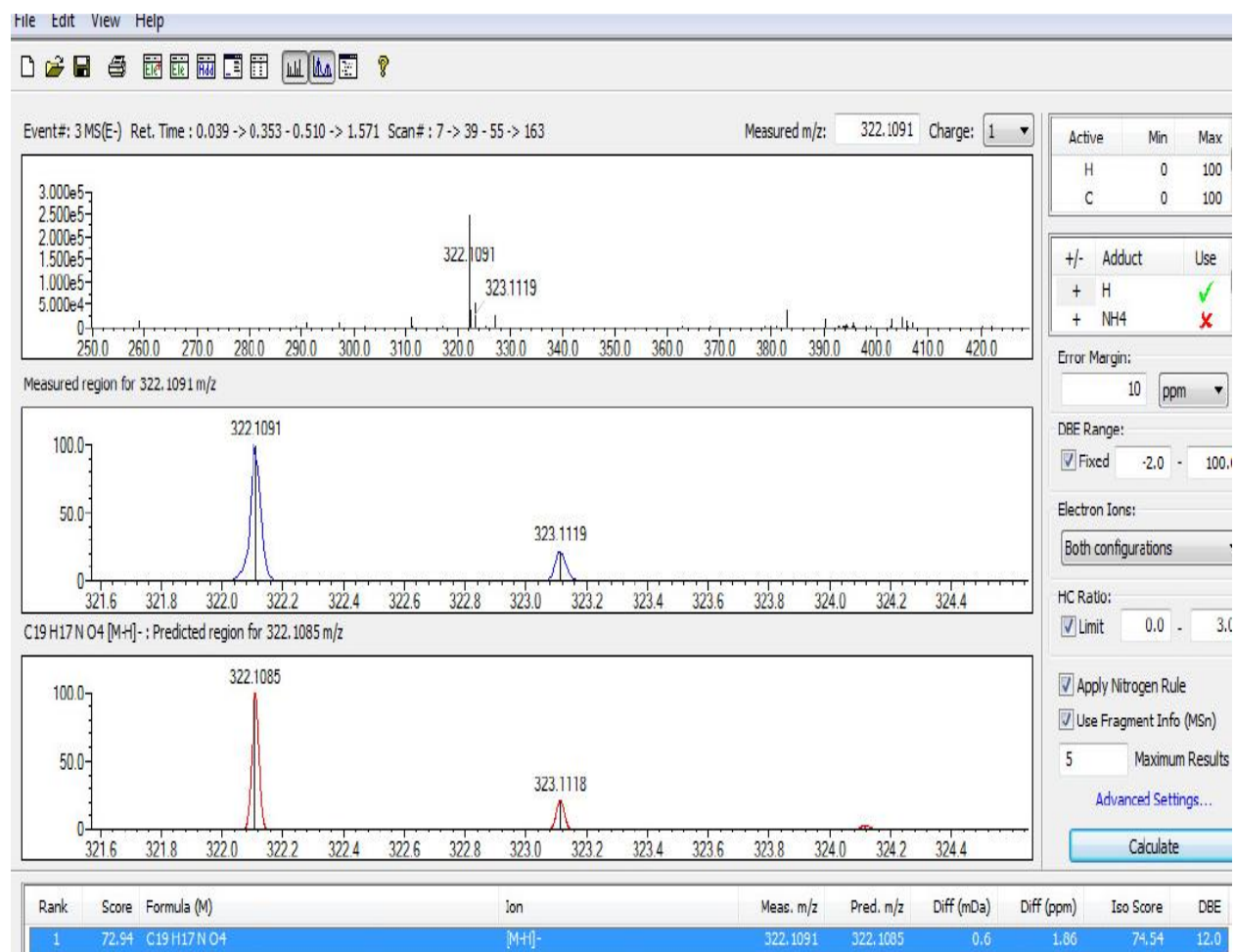
Mass Spectrum for Sample:
RWH-B-33

Operator: Mark Wang

Data filename: C:\LabSolutions\Data\Schwabacher Alan\RWH-B-33.lcd
Spectrum Mode: Single
Retention Time: 0.150 min.
Interface Type (ESI, APCI, DUIS): DUIS
Acquisition Mode (Scan, SIM, Profile): Scan
Polarity (+, -): -

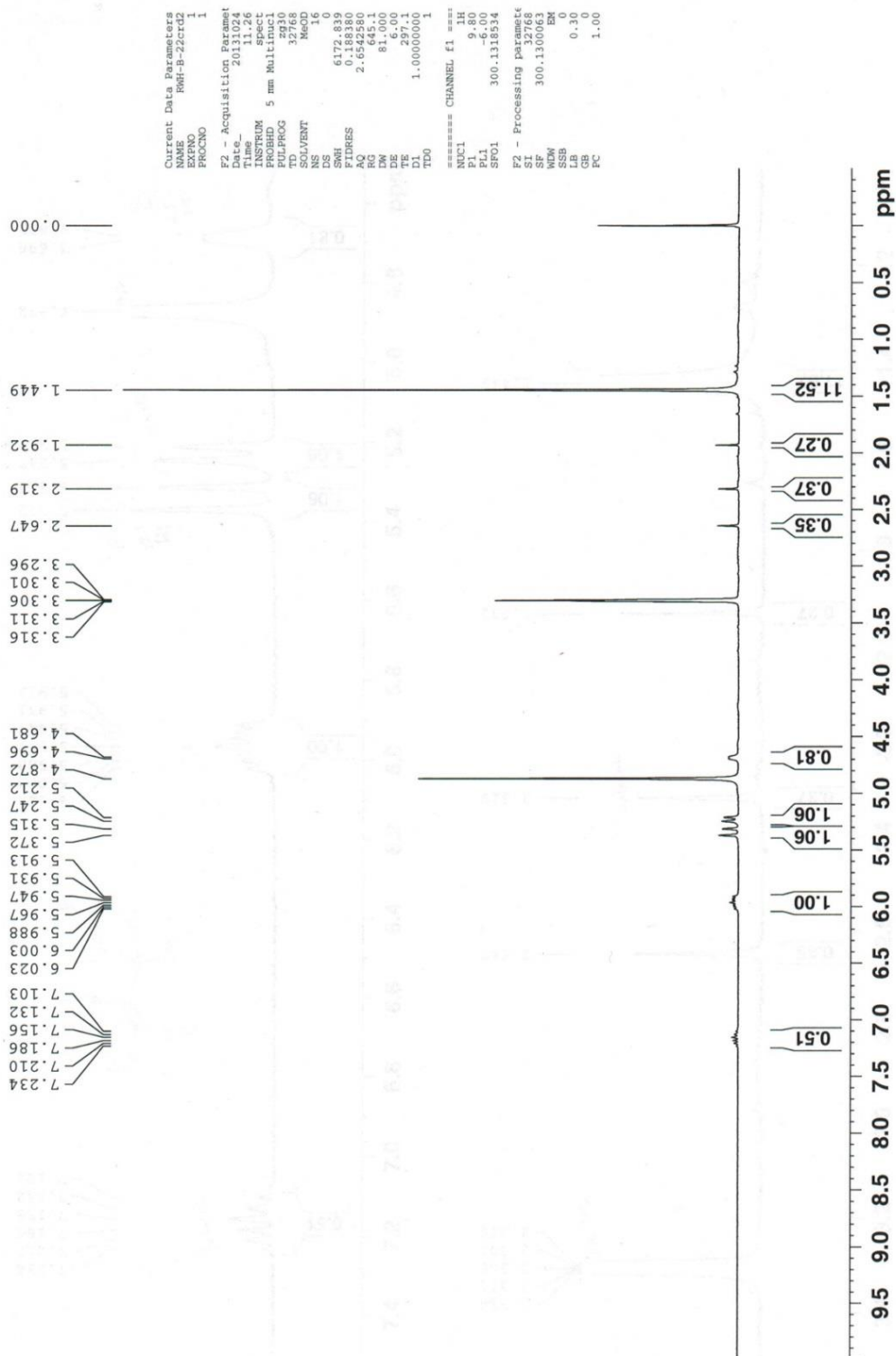


HRMS (IT-TOF) (S)-2-((((9H-fluoren-9-yl)methoxy)carbonyl)amino)but-3-enoic acid (73)

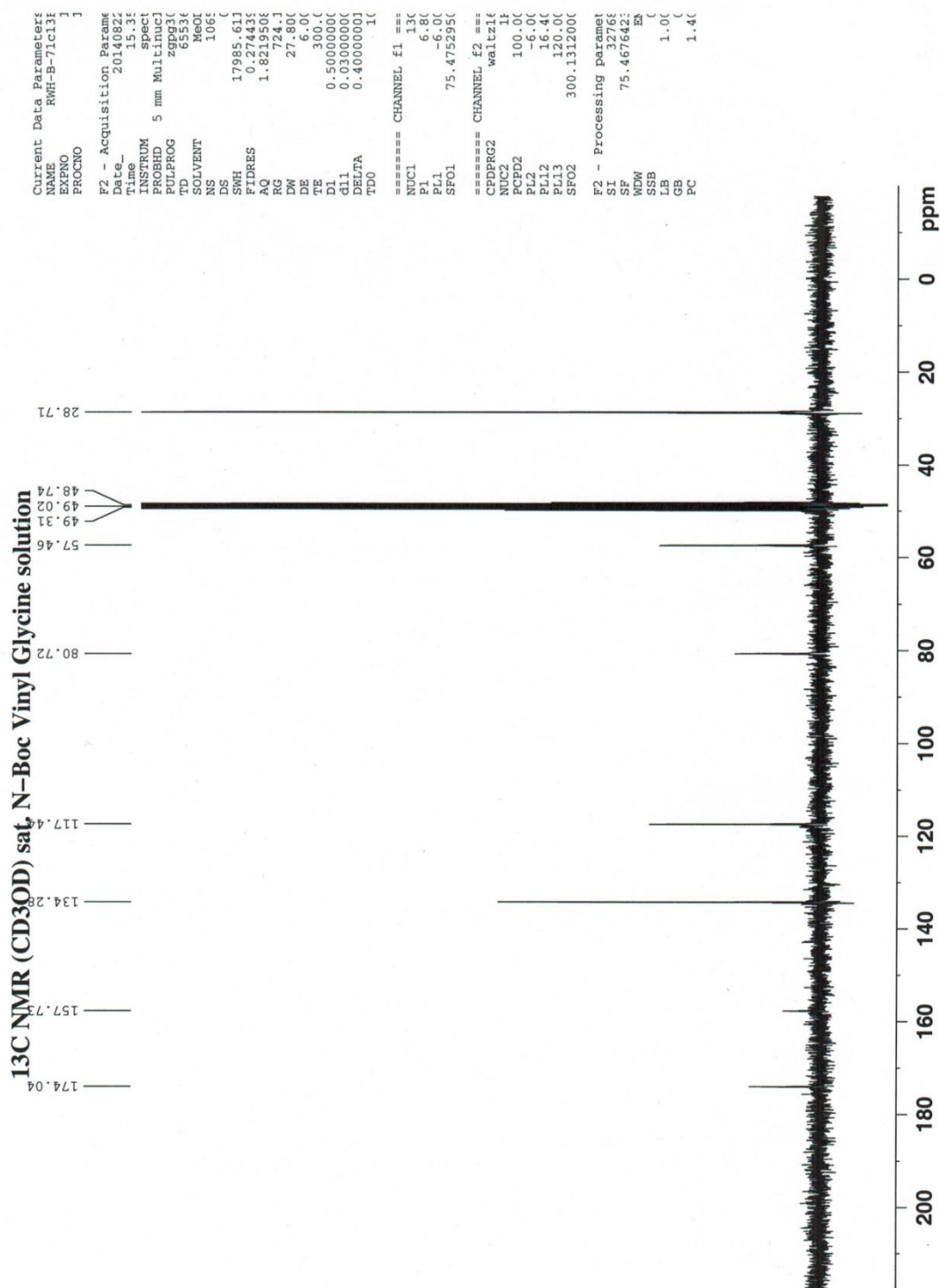


¹H NMR (*S*)-2-((*tert*-butoxycarbonyl)amino)but-3-enoic acid (**74**)

¹H NMR(CD₃OD) crude N-Boc protected vinyl glycine



¹³C NMR (S)-2-((tert-butoxycarbonyl)amino)but-3-enoic acid (74)

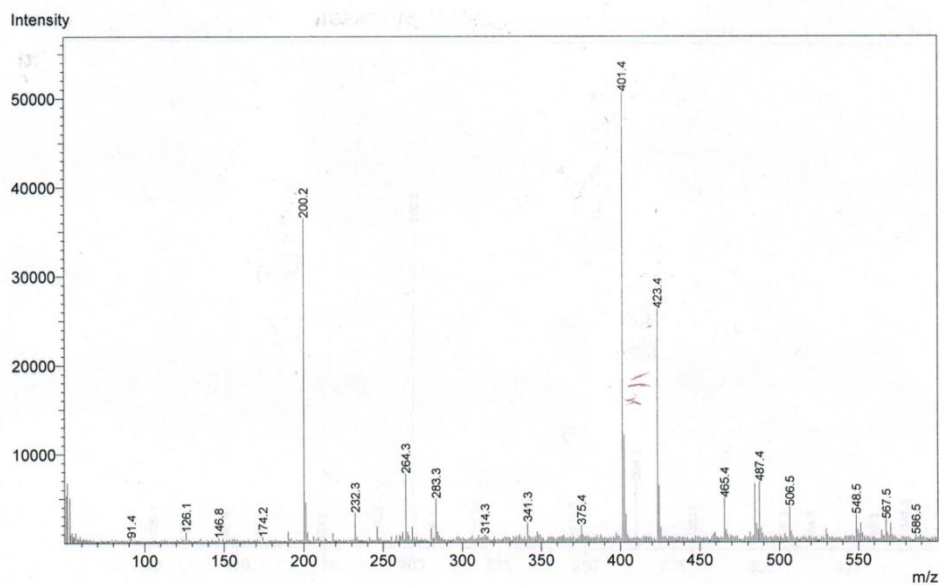


Shimadzu LCMS-2020 Data Report

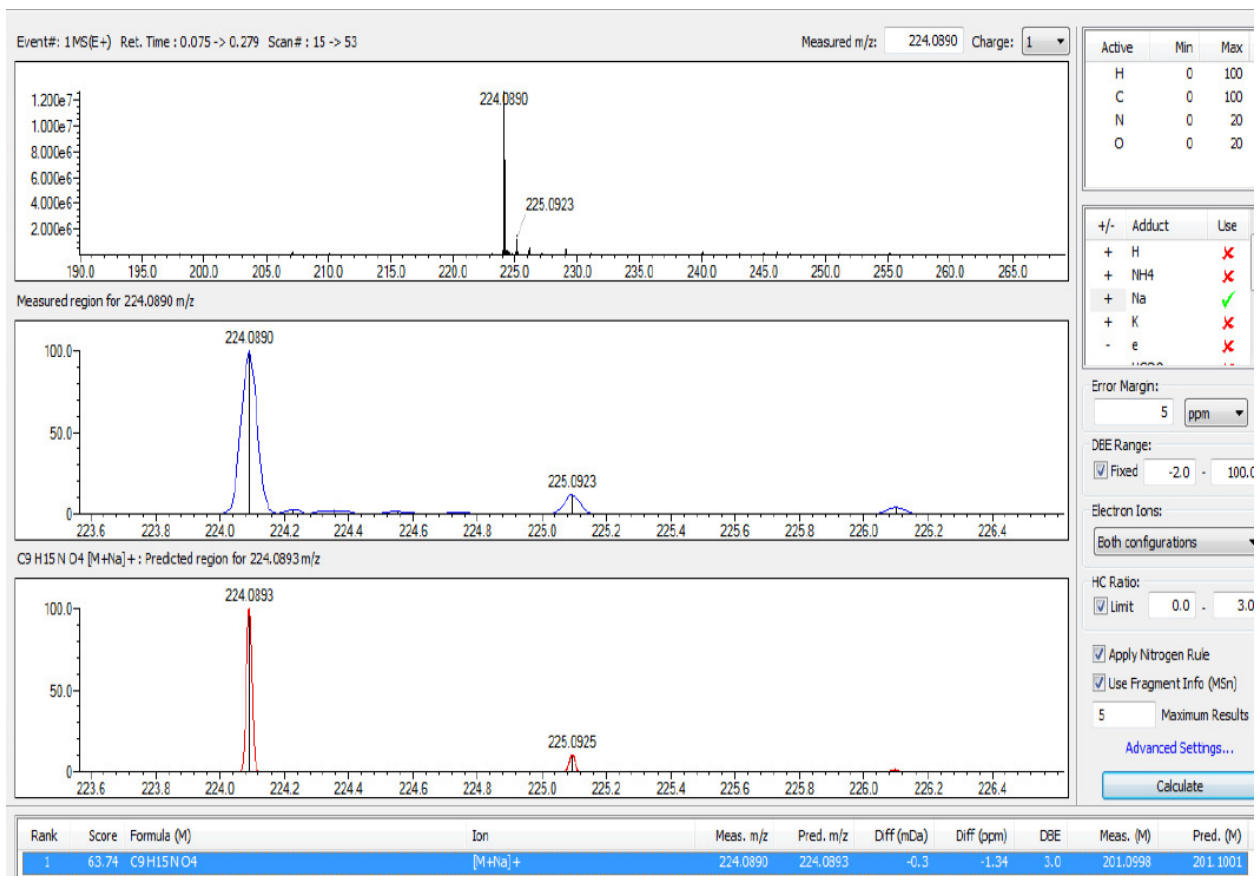
Mass Spectrum for Sample:
RWH-B-22

Operator: Mark Wang

Data filename: C:\LabSolutions\Data\Schwabacher Alan\RWH-B-22.lcd
Spectrum Mode: Single
Retention Time: 0.150 min.
Interface Type (ESI, APCI, DUIS): DUIS
Acquisition Mode (Scan, SIM, Profile): Scan
Polarity (+, -): -

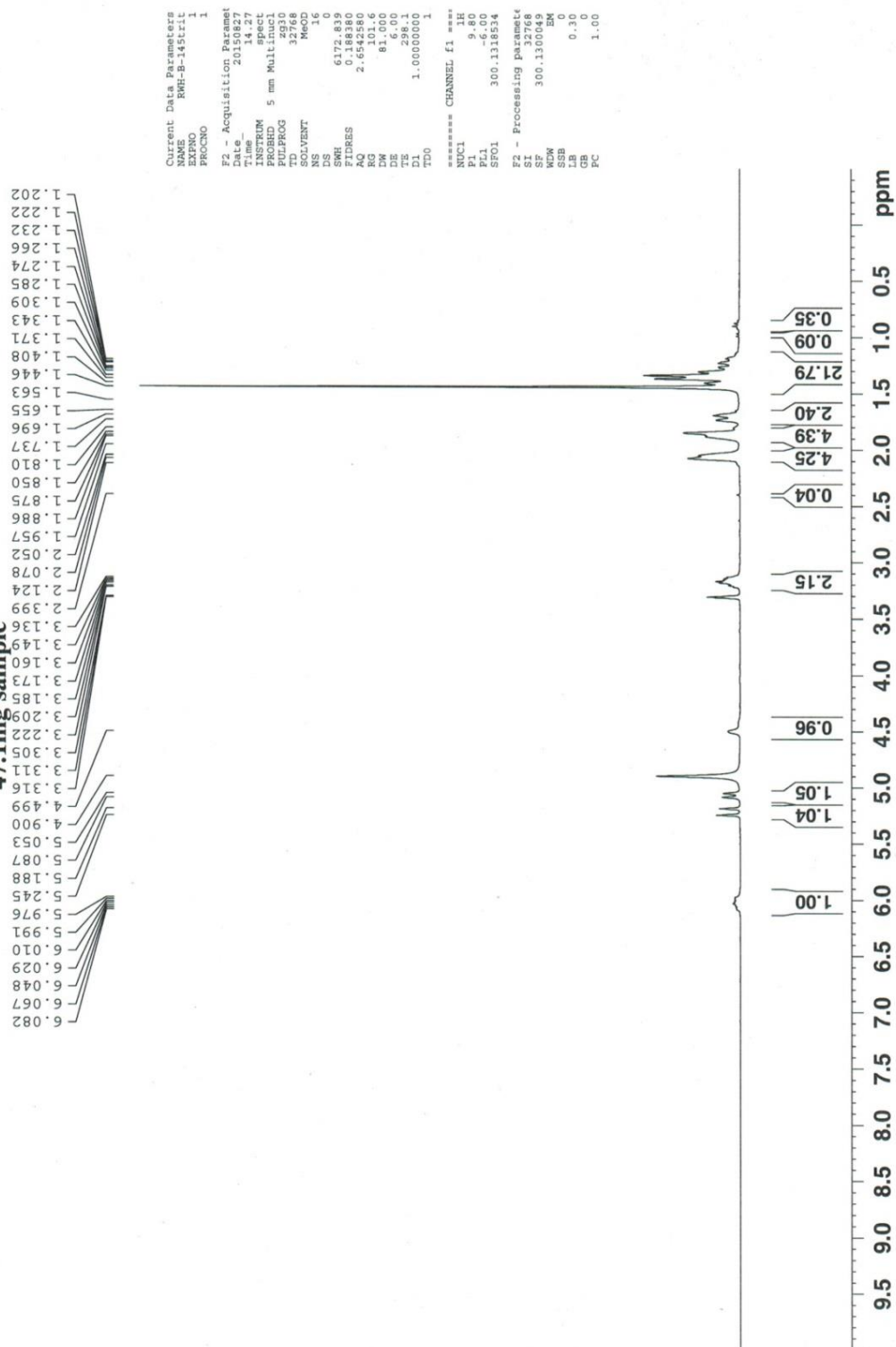


HRMS (IT-TOF) (S)-2-((tert-butoxycarbonyl)amino)but-3-enoic acid (74)

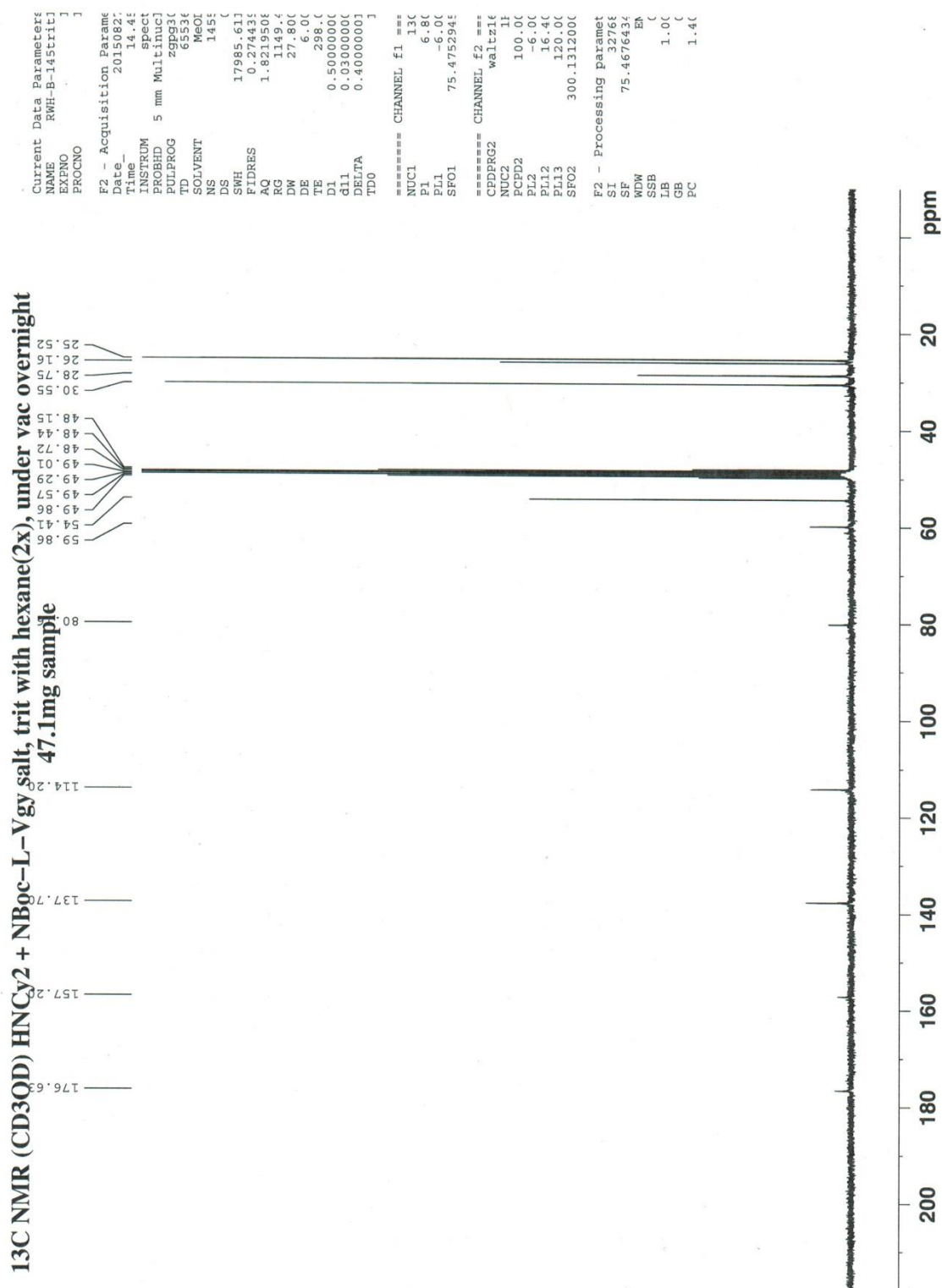


¹H NMR Dicyclohexyl ammonium 2-((tert-butoxycarbonyl)amino)but-3-enoate (75)

¹H NMR (CD₃OD) HNCy₂ salt NBoc-L-Vgy salt, trit with hexane, under vac overnight
47.1mg sample



¹³C NMR Dicyclohexyl ammonium 2-((tert-butoxycarbonyl)amino)but-3-enoate (75)

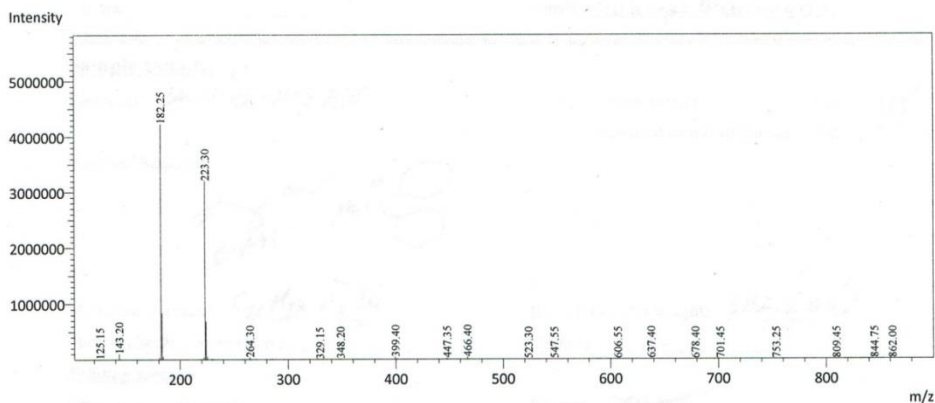


Shimadzu LCMS-2020 Data Report

Mass Spectrum for Sample
RWH-B-145(repeat).lcd

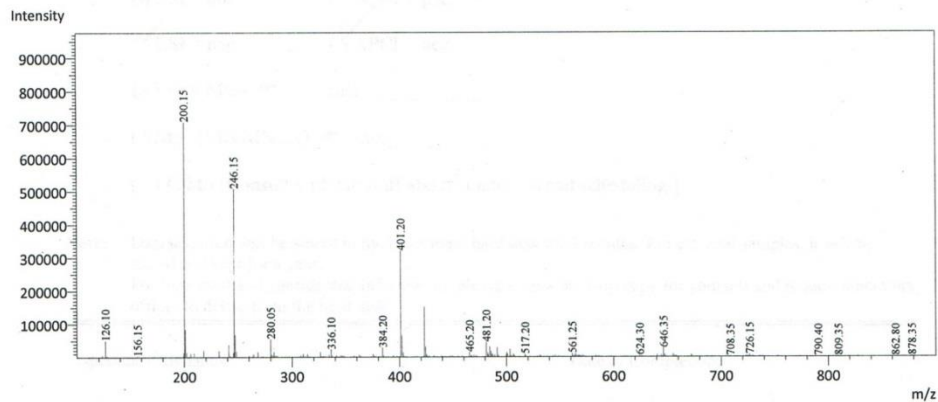
Operator: Tyler Fenske

Data Filename: C:\LabSolutions\Data\Schwabacher Alan\RWH-B-145(repeat).lcd
Spectrum Mode: Averaged
Retention Time: ----
Interface Type (ESI, APCI, DUIS): DUIS
Acquisition Mode: (Scan, SIM, Profile): Scan
Polarity: +
H₂O/0.1% HCOOH, CH₃CN/0.1% HCOOH

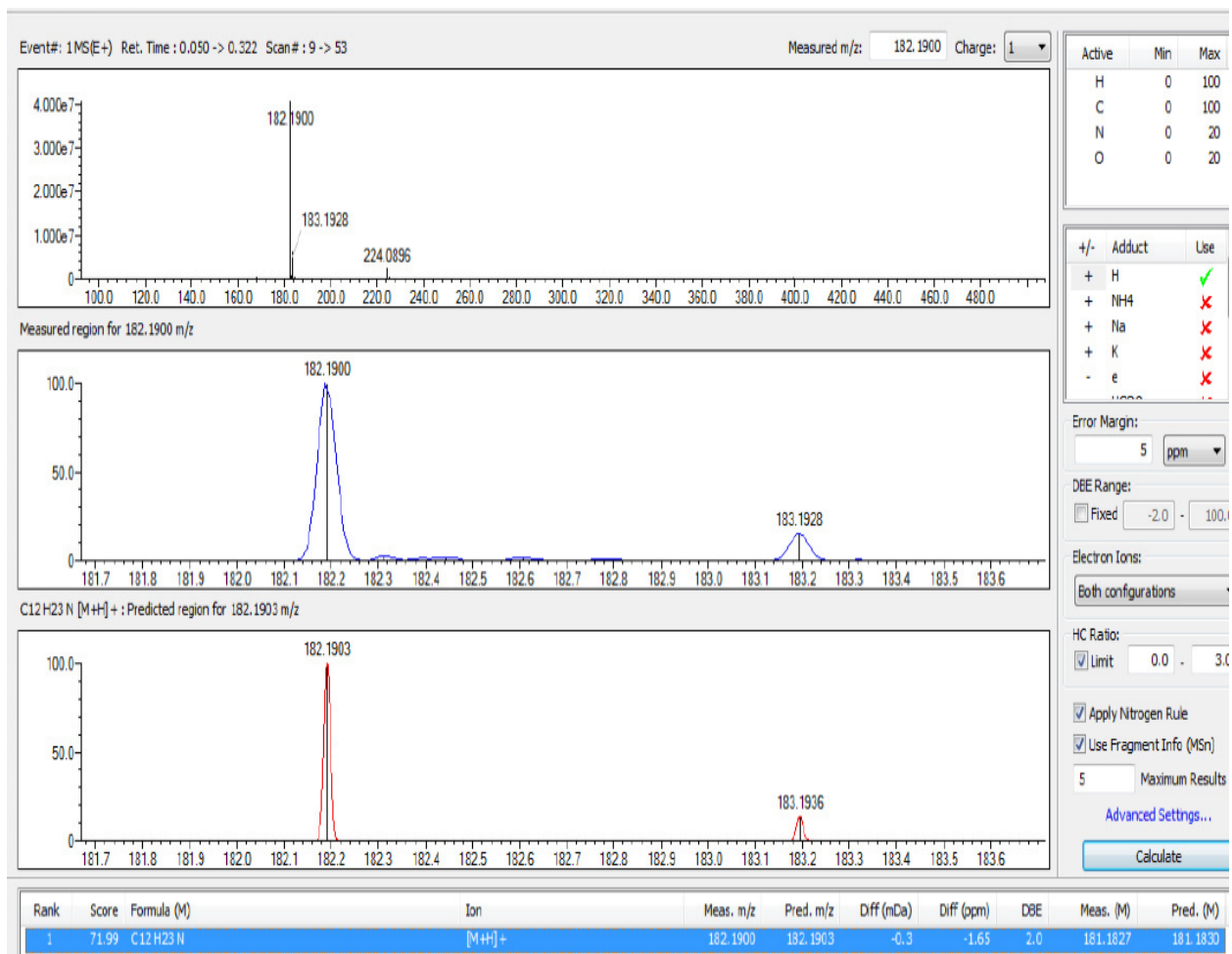


Operator: Tyler Fenske

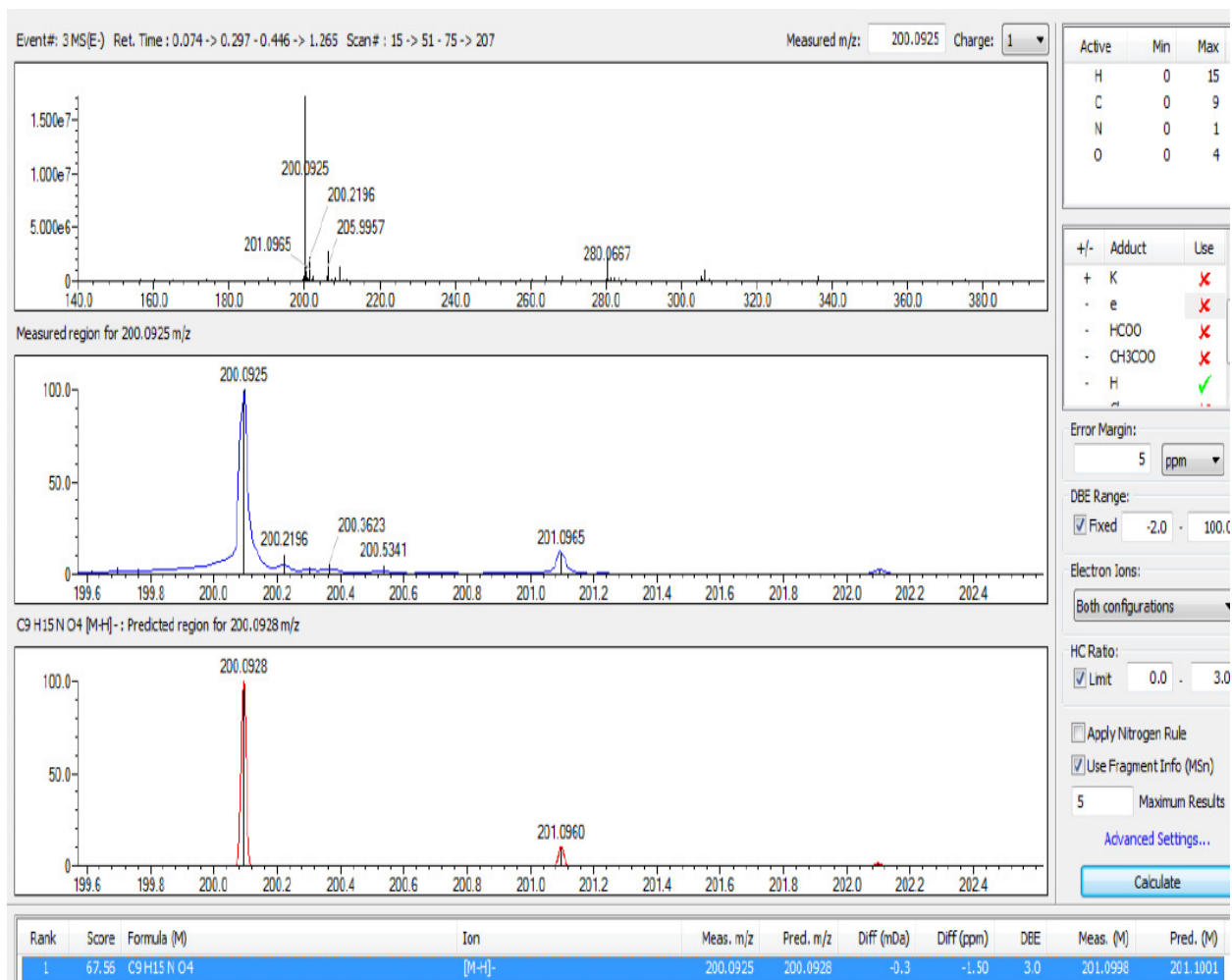
Data Filename: C:\LabSolutions\Data\Schwabacher Alan\RWH-B-145(repeat).lcd
Spectrum Mode: Averaged
Retention Time: ----
Interface Type (ESI, APCI, DUIS): DUIS
Acquisition Mode: (Scan, SIM, Profile): Scan
Polarity: -
H₂O/0.1% HCOOH, CH₃CN/0.1% HCOOH



HRMS (IT-TOF, + ion) Dicyclohexyl ammonium 2-((tert-butoxycarbonyl)amino)but-3-enoate (75)

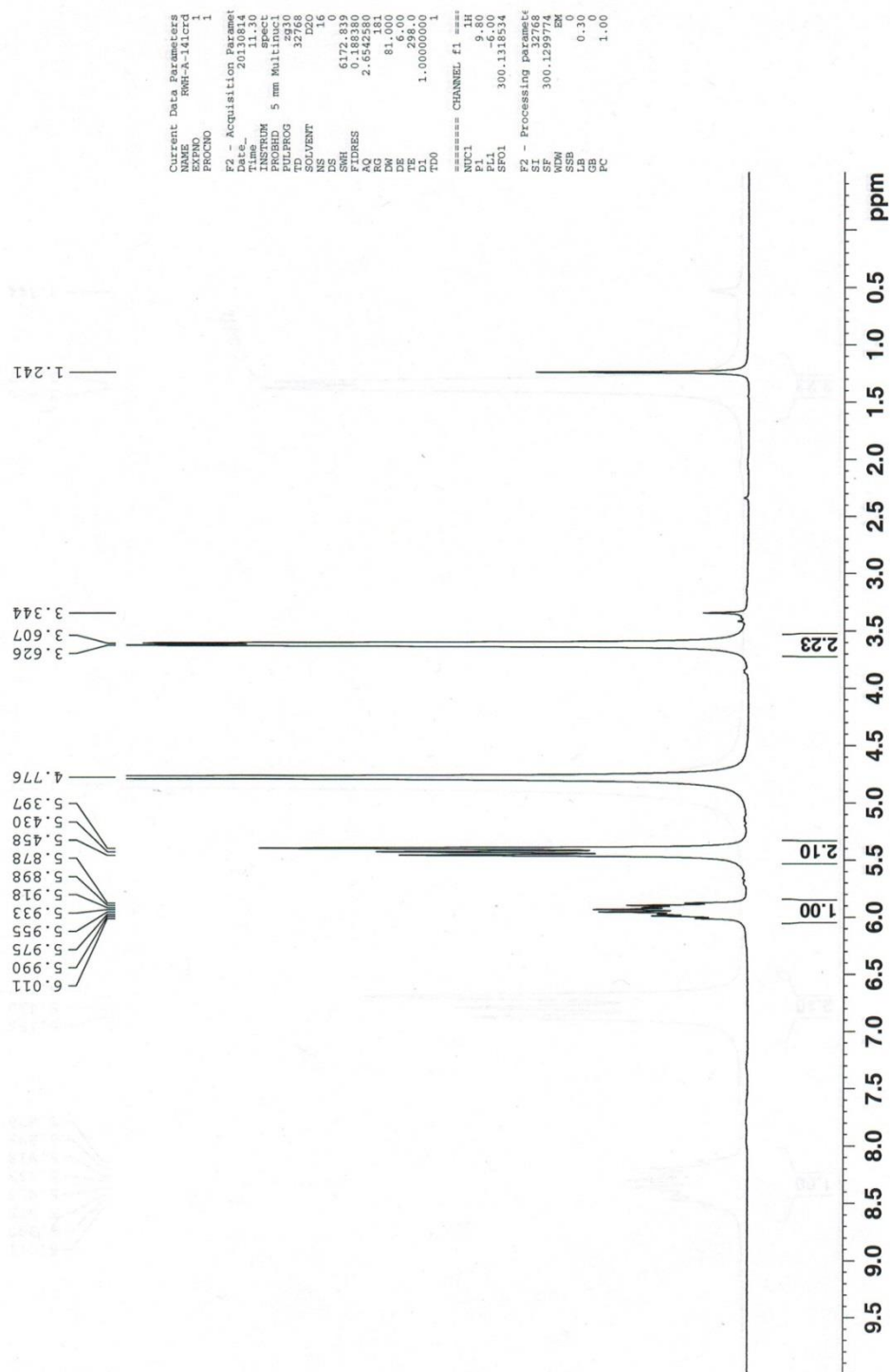


HRMS (IT-TOF, -ion) Dicyclohexyl ammonium 2-((tert-butoxycarbonyl)amino)but-3-enoate (75)



¹H NMR Allylammonium chloride (76)

¹H NMR (D2O) crude allyl amine hydrochloride 0.5uL tBuOH int std



Shimadzu LCMS-2020 Data Report

Mass Spectrum for Sample:
RWH-B-2B

Operator: Mark Wang

Data filename: C:\LabSolutions\Data\Schwabacher Alan\RWH-B-2B.lcd

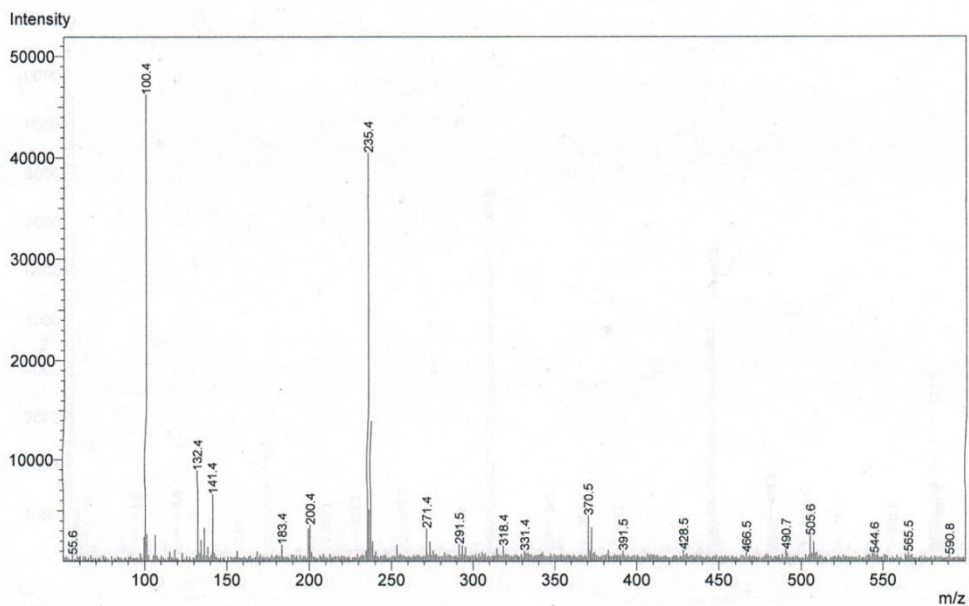
Spectrum Mode: Single

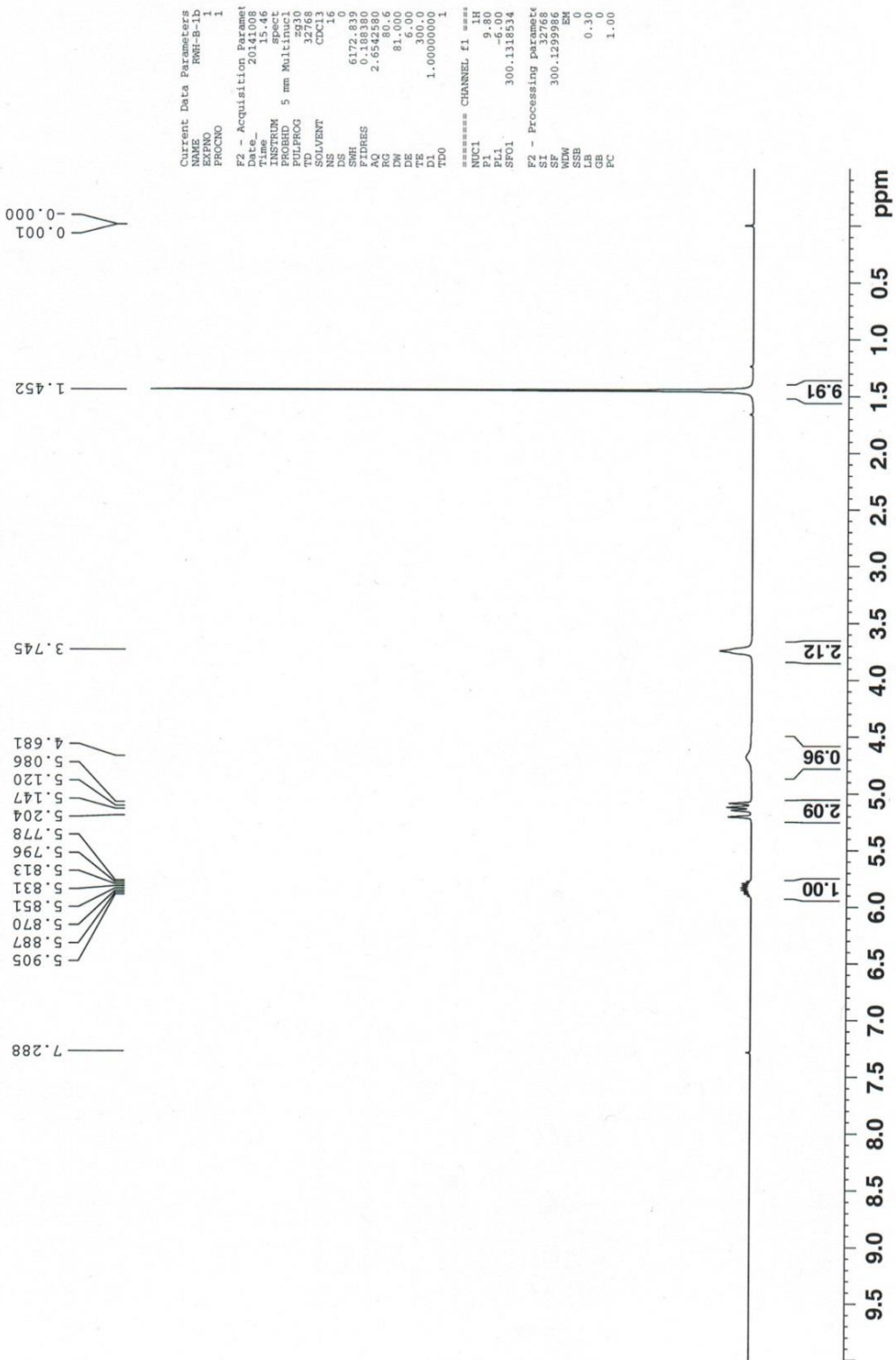
Retention Time: 0.133 min.

Interface Type (ESI, APCI, DUIS): DUIS

Acquisition Mode (Scan, SIM, Profile): Scan

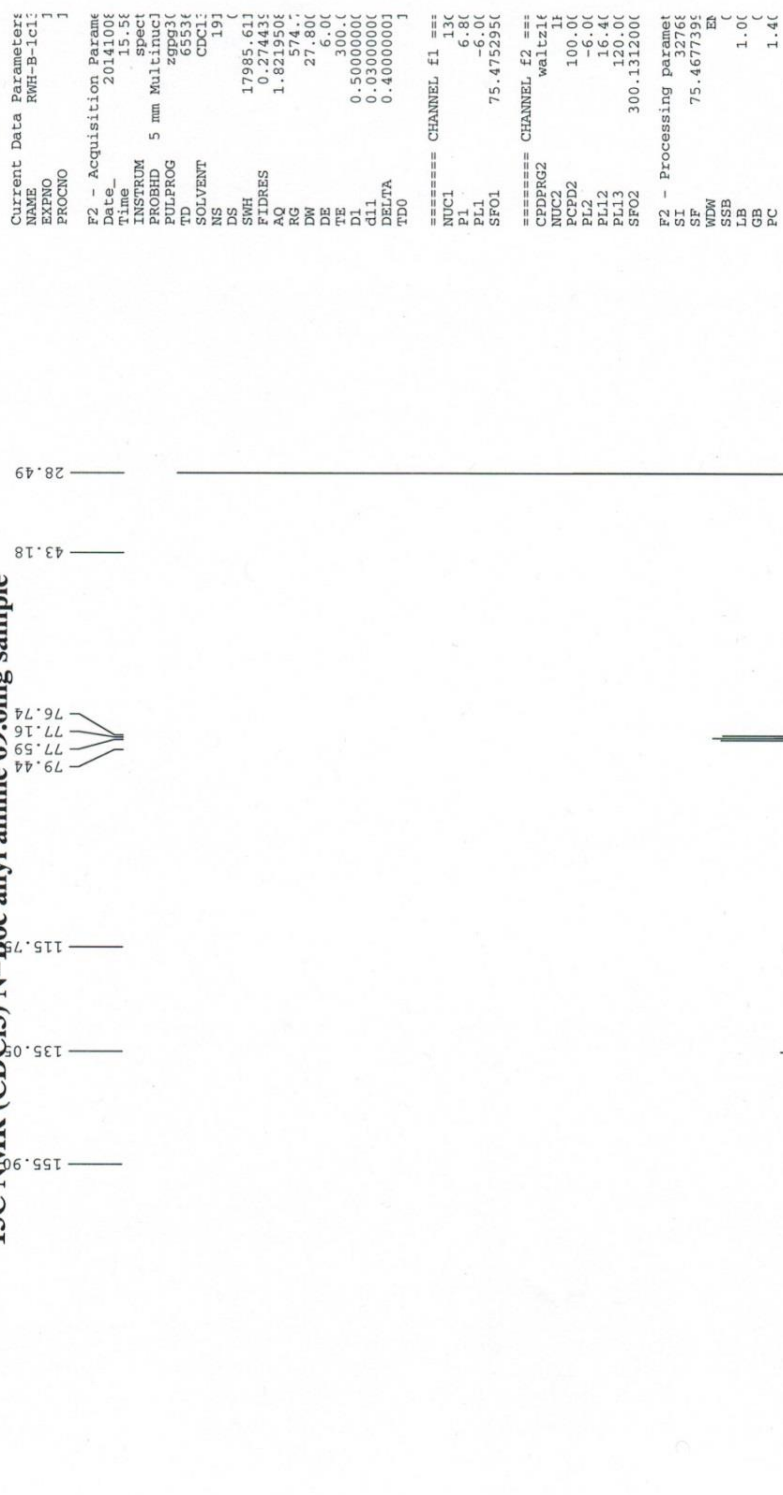
Polarity (+, -): +



¹H NMR *tert*-butyl allylcarbamate (78)

¹³C NMR tert-butyl allylcarbamate (78)

¹³C NMR (CDCl₃) N-Boc allyl amine 69.6mg sample



Shimadzu LCMS-2020 Data Report

Mass Spectrum for Sample:
RWH-B-1

Operator: Mark Wang

Data filename: C:\LabSolutions\Data\Schwabacher Alan\RWH-B-1.lcd

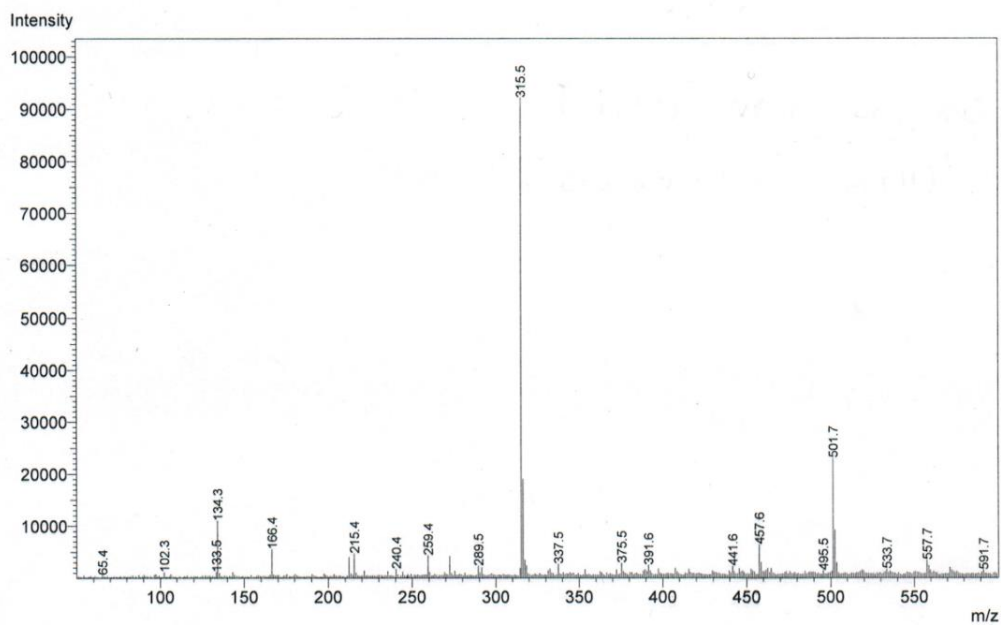
Spectrum Mode: Single

Retention Time: 0.133 min.

Interface Type (ESI, APCI, DUIS): DUIS

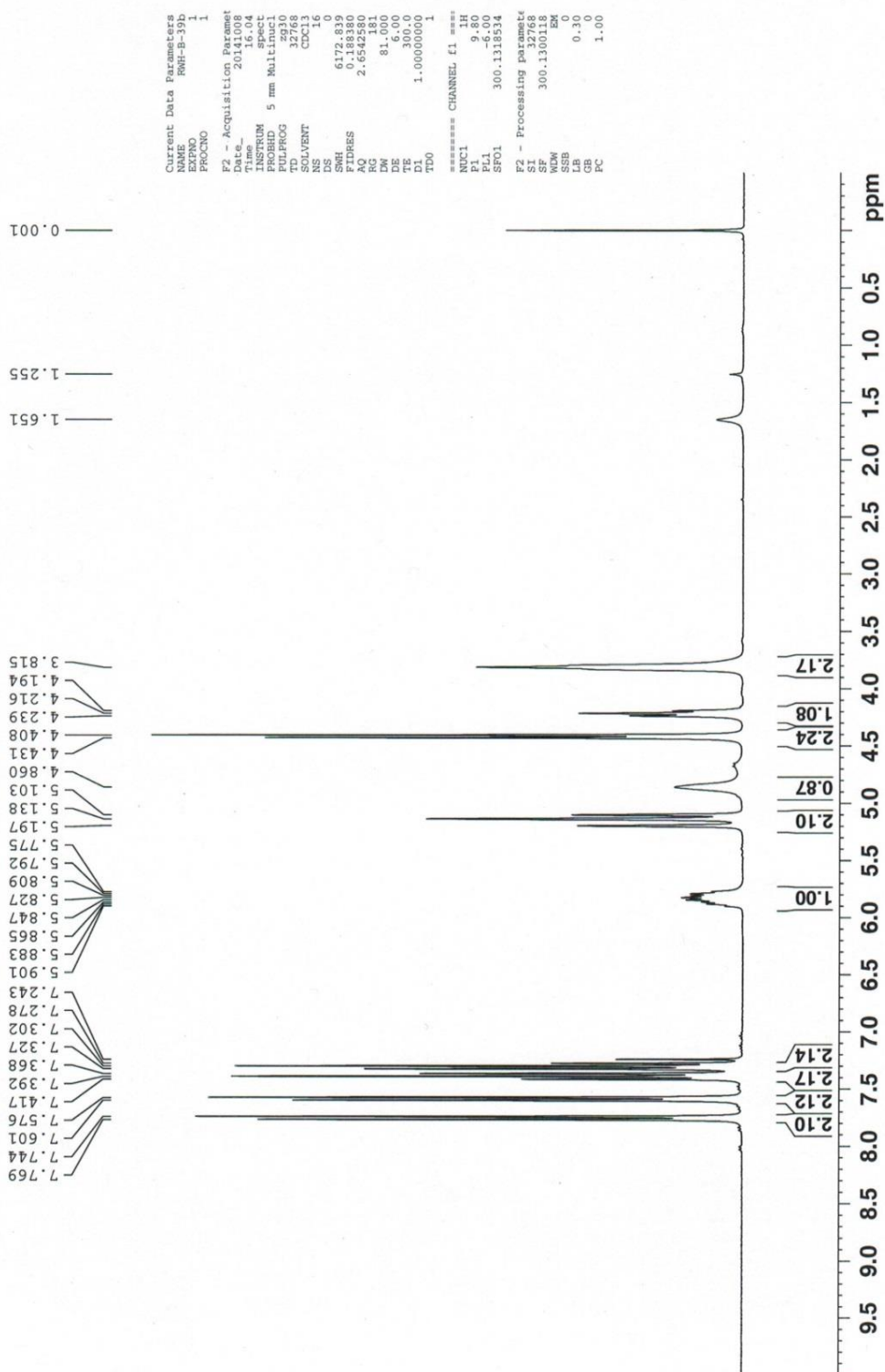
Aquisition Mode (Scan, SIM, Profile): Scan

Polarity (+, -): +

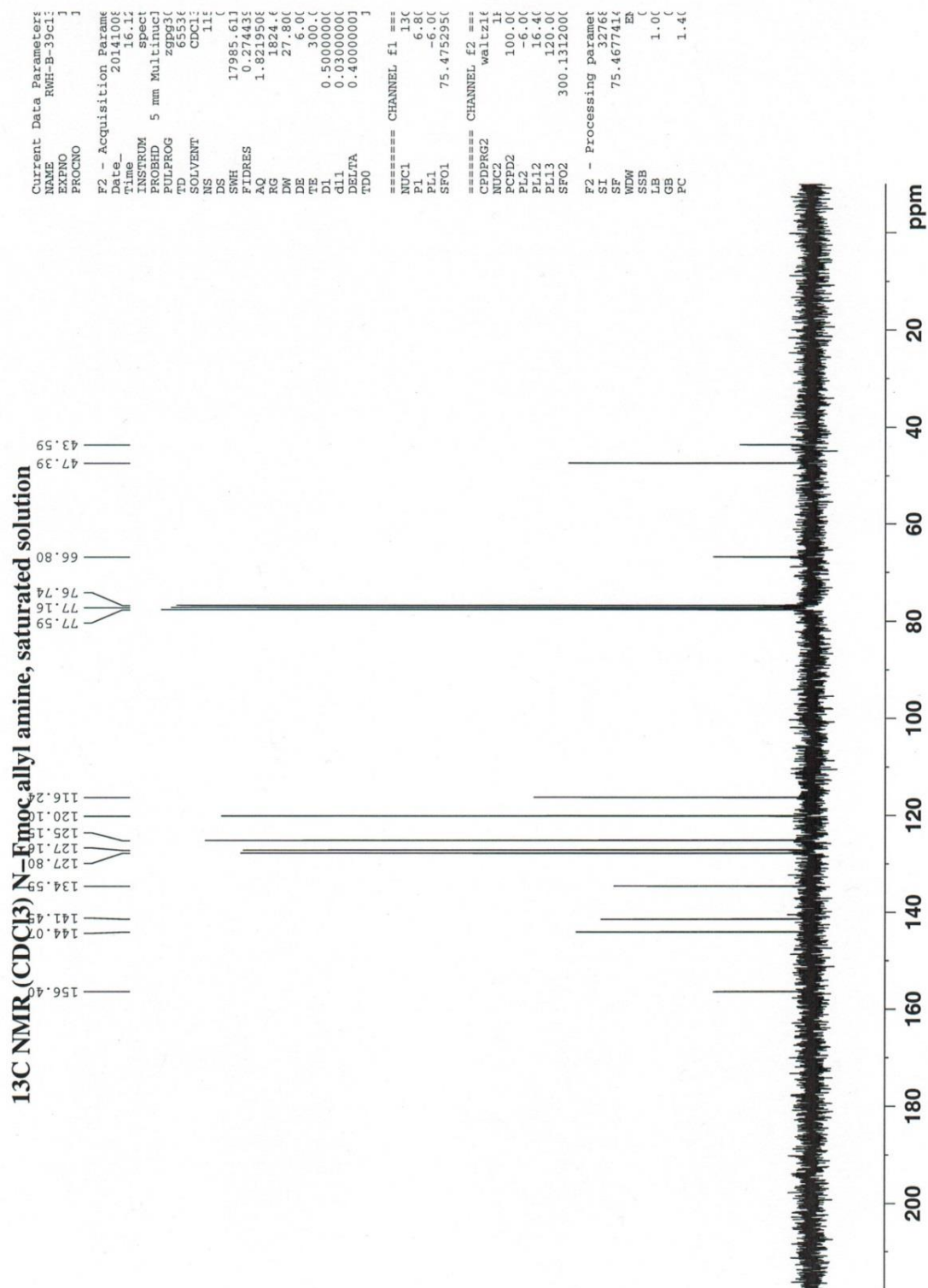


¹H NMR (9H-fluoren-9-yl)methyl allylcarbamate (79)

¹H NMR (CDCl₃) N-Fmoc allyl amine, saturated solution



¹³C NMR (9H-fluoren-9-yl)methyl allylcarbamate (79)



Shimadzu LCMS-2020 Data Report

Mass Spectrum for Sample:
RWH-B-37

Operator: Mark Wang

Data filename: C:\LabSolutions\Data\Schwabacher Alan\RWH-B-37.lcd

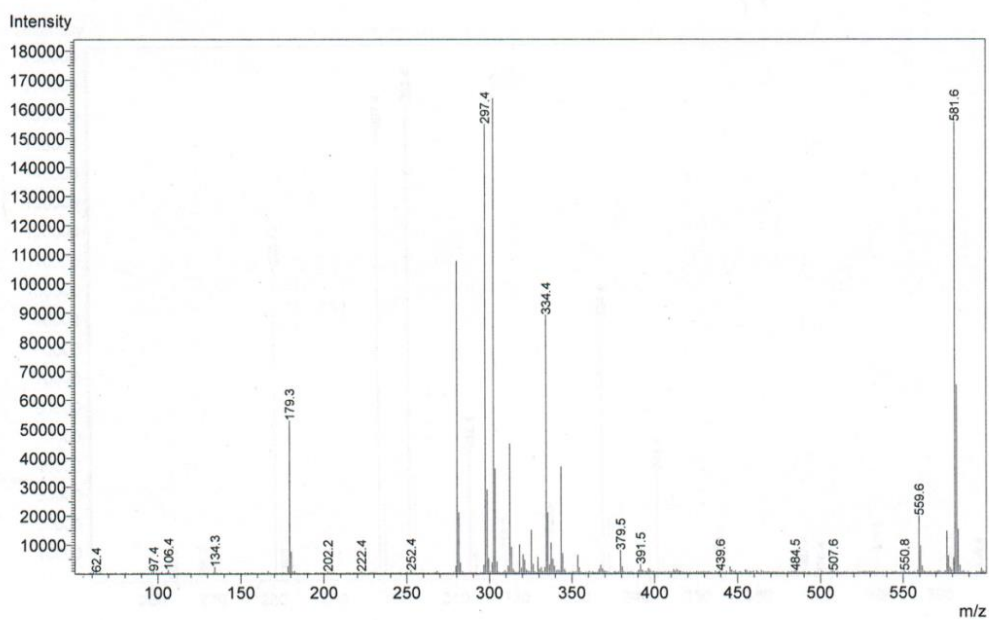
Spectrum Mode: Single

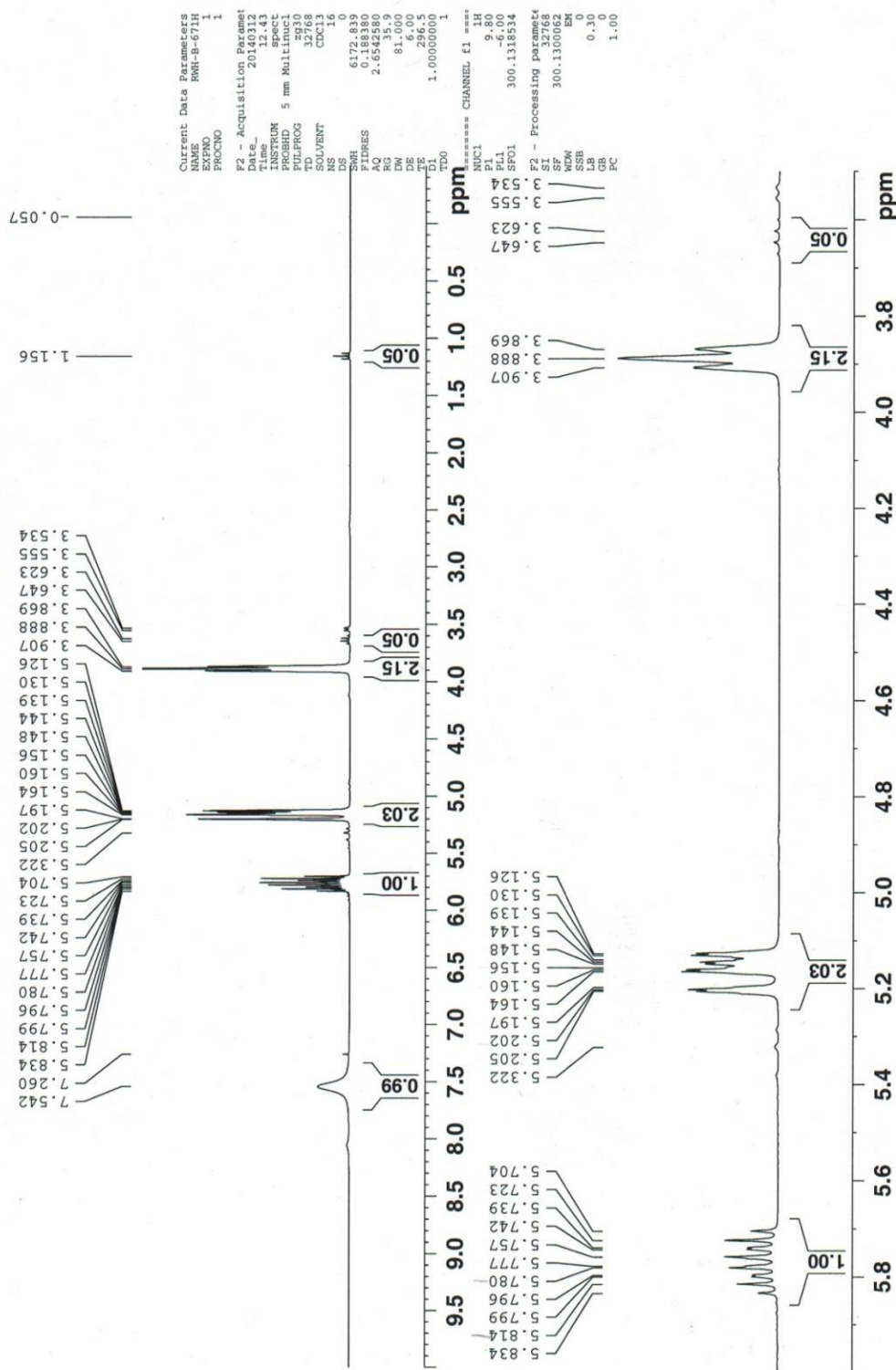
Retention Time: 0.200 min.

Interface Type (ESI, APCI, DUIS): DUIS

Aquisition Mode (Scan, SIM, Profile): Scan

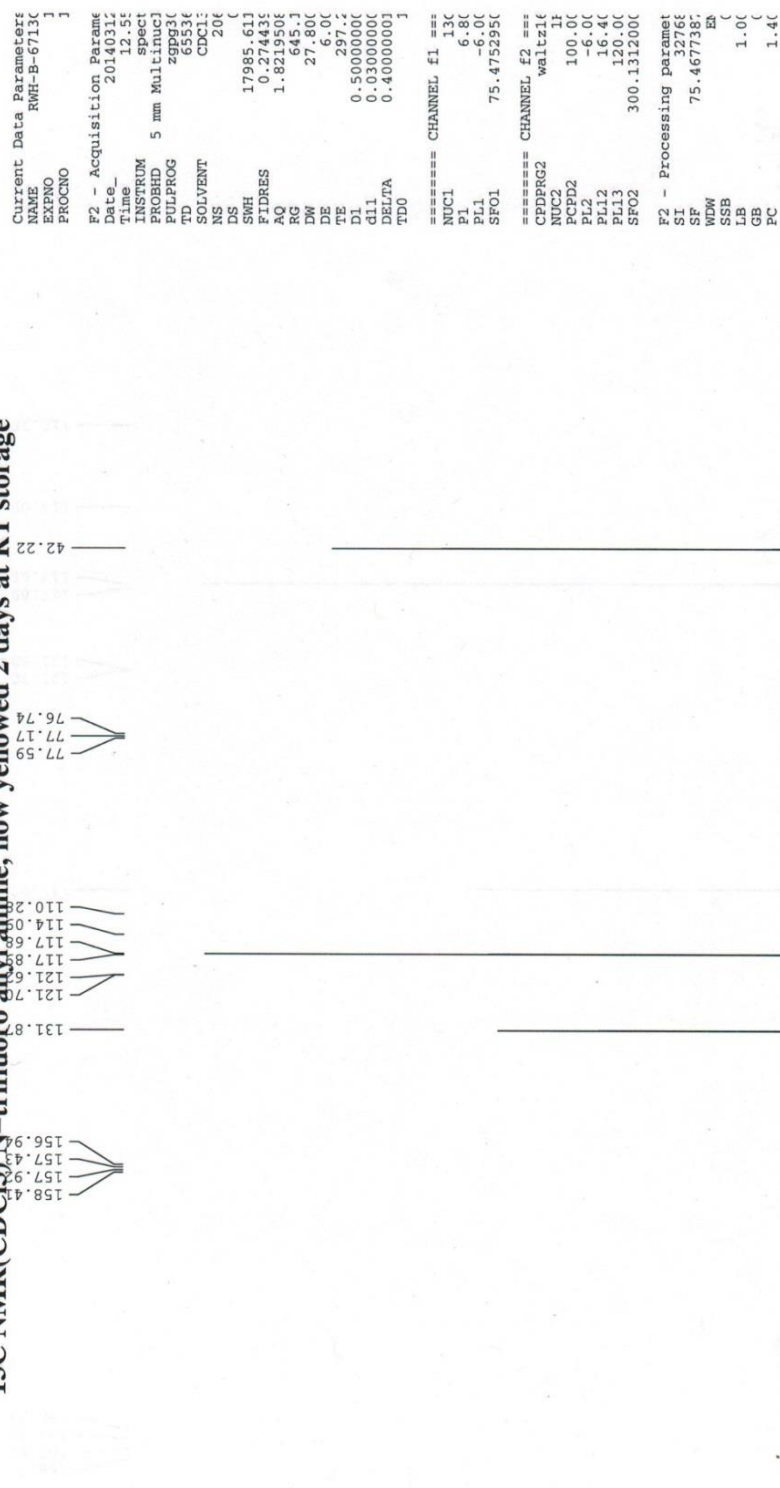
Polarity (+, -): +



¹H NMR *N*-allyl-2,2,2-trifluoroacetamide (80)

¹³C NMR *N*-allyl-2,2,2-trifluoroacetamide (**80**)

¹³C NMR(CDCl₃) *N*-trifluoro allyl amine, now yellowed 2 days at RT storage

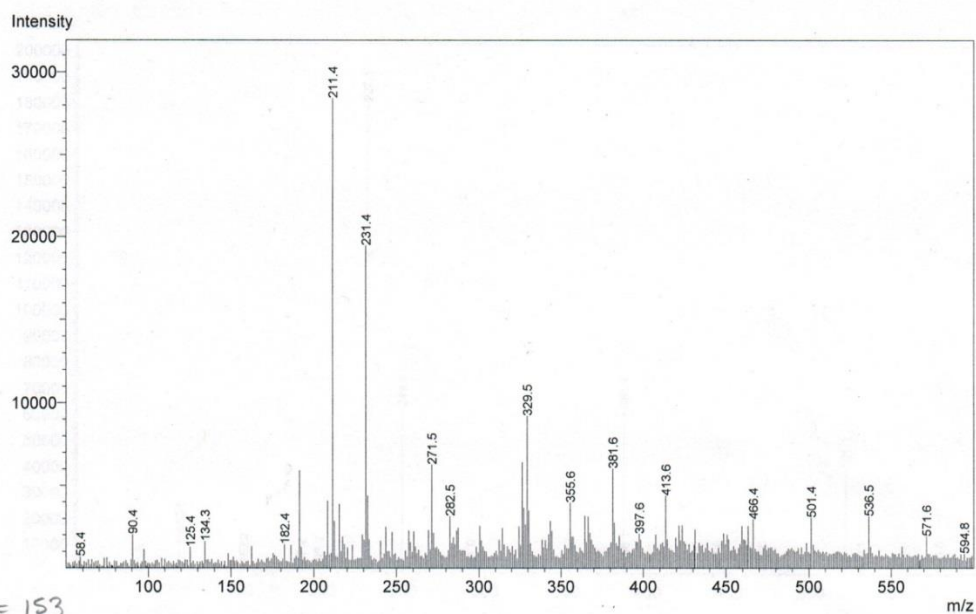


Shimadzu LCMS-2020 Data Report

Mass Spectrum for Sample:
RWH-B-67

Operator: Mark Wang

Data filename: C:\LabSolutions\Data\Schwabacher Alan\RWH-B-67.lcd
Spectrum Mode: Single
Retention Time: 0.100 min.
Interface Type (ESI, APCI, DUIS): DUIS
Acquisition Mode (Scan, SIM, Profile): Scan
Polarity (+, -): +



$$M = 153$$

$$2M = 306$$

$$2M + Na^+ = 306 + 23 = 329$$

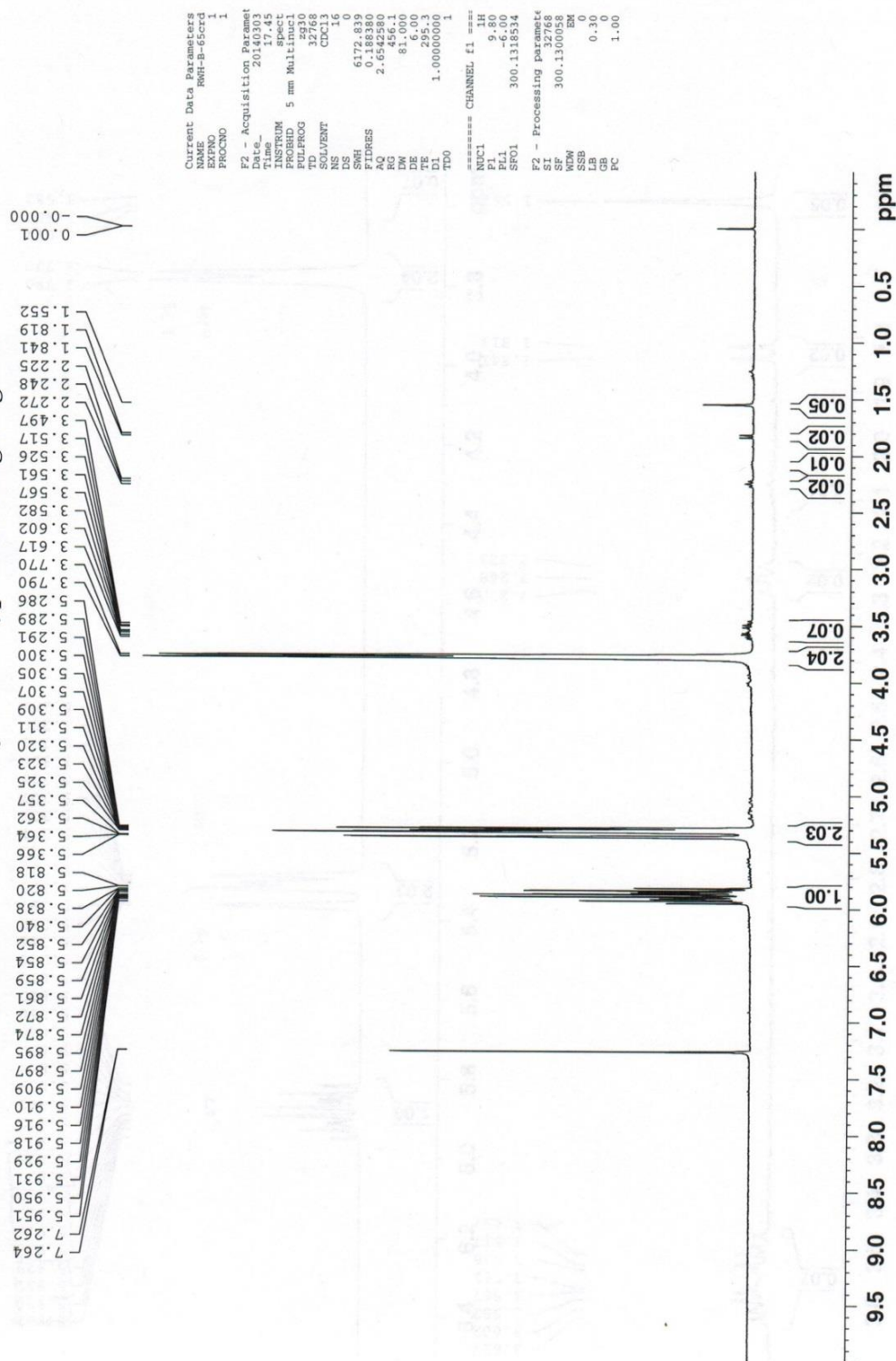
$$\begin{array}{r} 211 \\ -153 \\ \hline 58 \end{array}$$

$$\begin{array}{r} 231 \\ -153 \\ \hline 78 \end{array}$$

$$\begin{array}{r} 271 \\ -153 \\ \hline 118 \end{array}$$

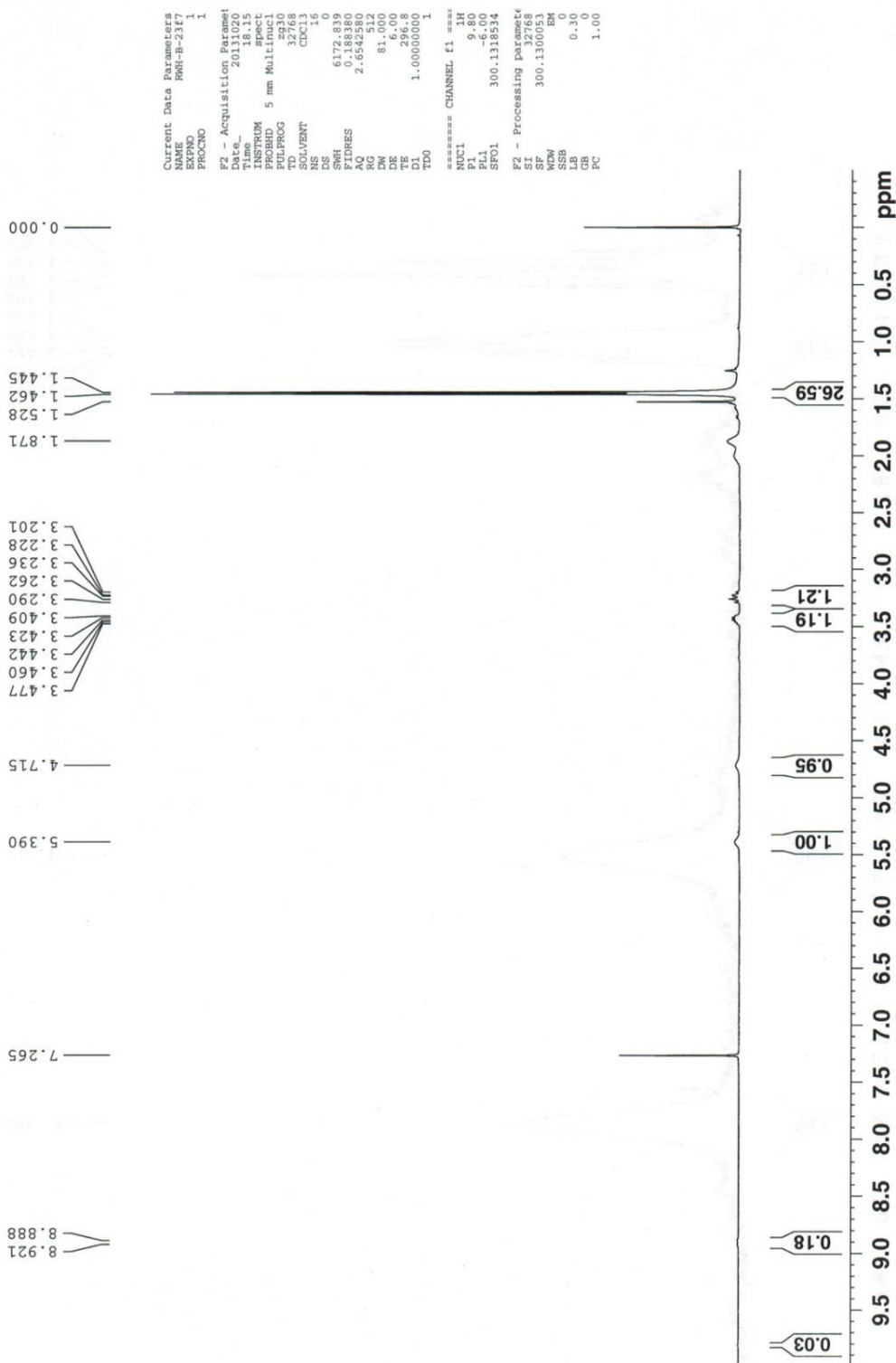
¹H NMR 3-azidoprop-1-ene (**81**)

¹H NMR(CDCI₃) crude product from NaN₃+allyl bromide, passed through MgSO₄



¹H NMR (Z)-di-tert.-butyl but-2-ene-1,4-diyl dicarbamate (82)

¹H NMR(CDCl₃) f7-10 10% CH₃CN/CH₂Cl₂



Shimadzu LCMS-2020 Data Report

Mass Spectrum for Sample:
RWH-B23f7

Operator: Mark Wang

Data filename: C:\LabSolutions\Data\Schwabacher Alan\RWH-B23f7.lcd

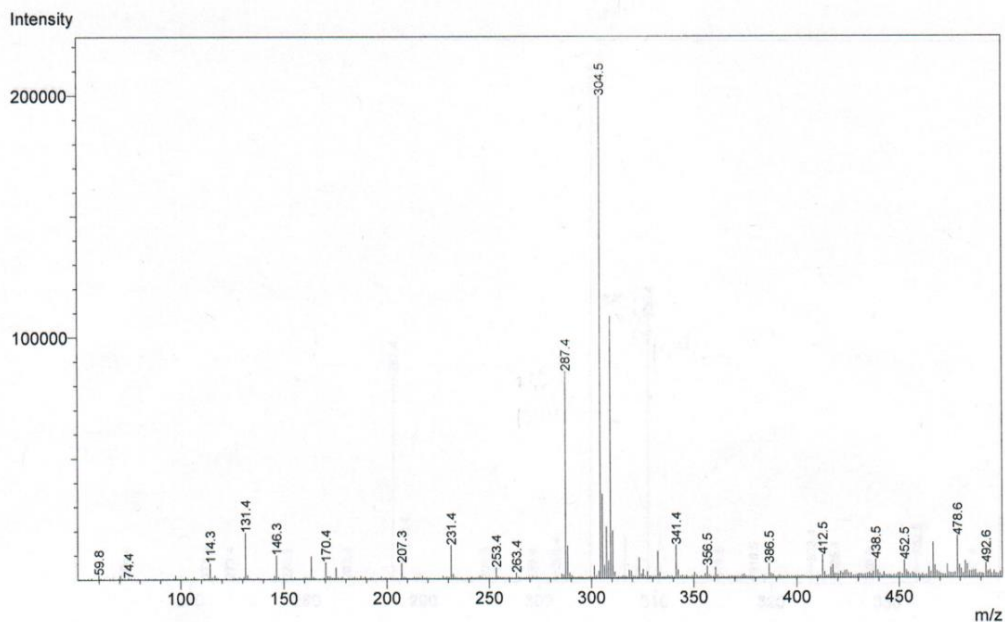
Spectrum Mode: Single

Retention Time: 0.133 min.

Interface Type (ESI, APCI, DUIS): DUIS

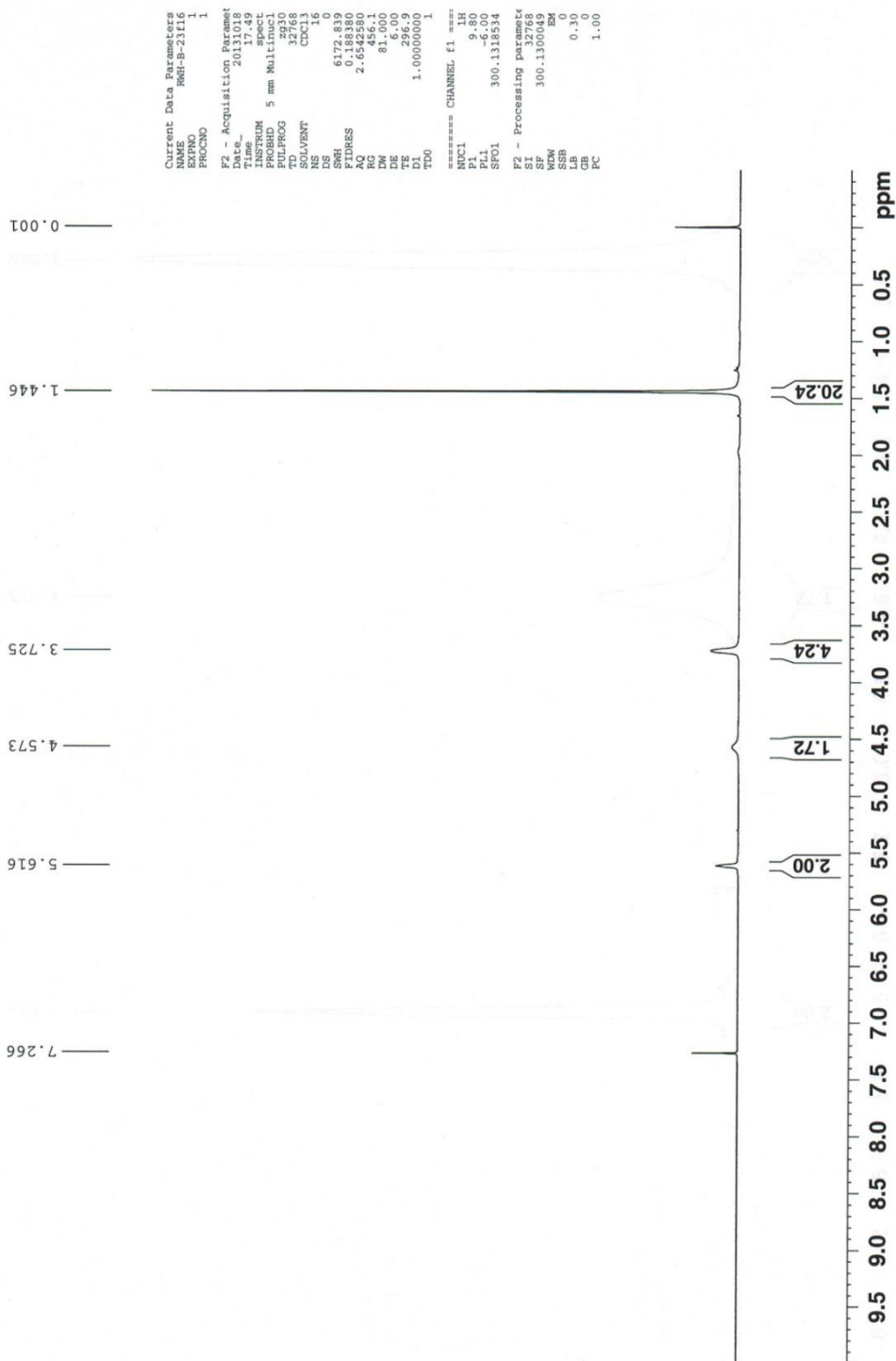
Acquisition Mode (Scan, SIM, Profile): Scan

Polarity (+, -): +



¹H NMR (*E*)-di-*tert*.-butyl but-2-ene-1,4-diyl dicarbamate (**83**)

¹H NMR(CDCl₃) f16-21 10% CH₃CN/CH₂Cl₂



Shimadzu LCMS-2020 Data Report

Mass Spectrum for Sample:
RWH-B23f16-1

Operator: Mark Wang

Data filename: C:\LabSolutions\Data\Schwabacher Alan\RWH-B23f16-1.lcd

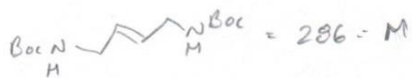
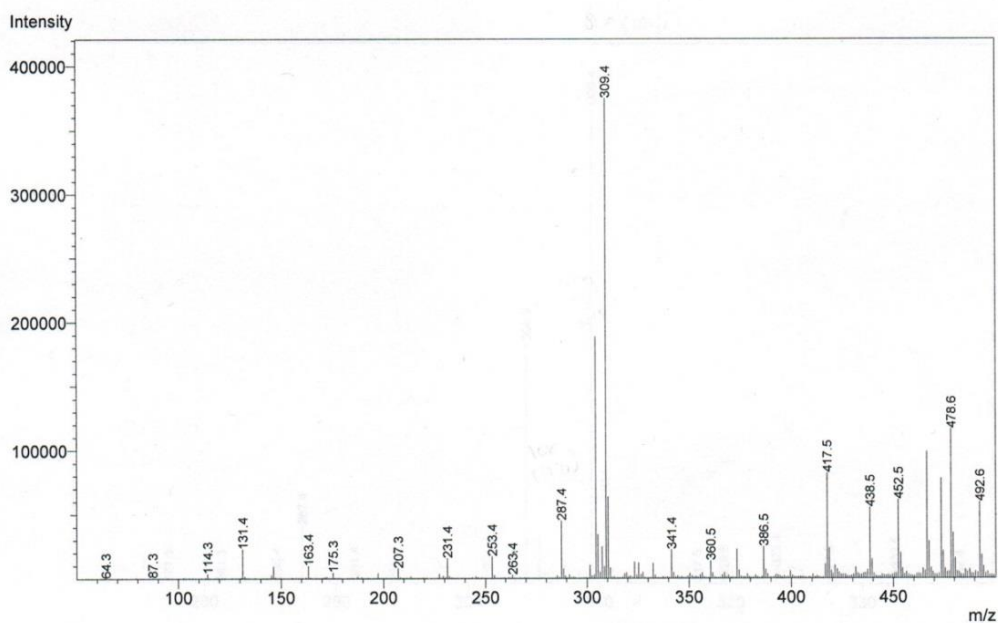
Spectrum Mode: Single

Retention Time: 0.133 min.

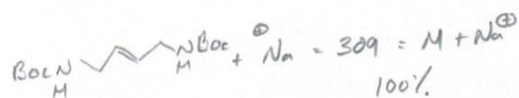
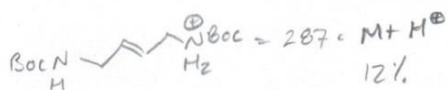
Interface Type (ESI, APCI, DUIS): DUIS

Acquisition Mode (Scan, SIM, Profile): Scan

Polarity (+, -): +

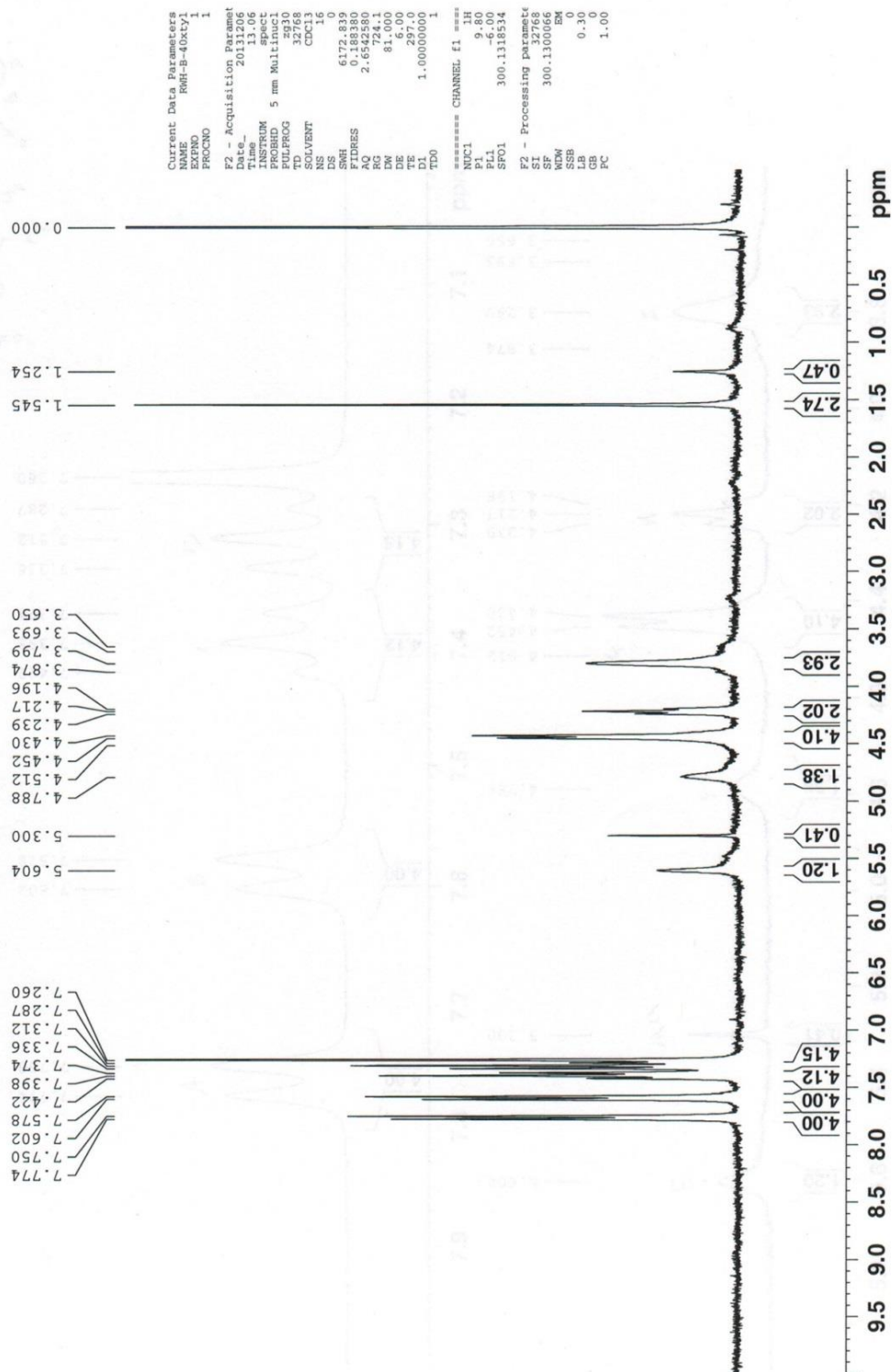


$$304/305 = M+17 / M+18 \\ 50\%$$



¹H NMR (*E*-bis((9H-fluoren-9-yl)methyl) but-2-ene-1,4-diyl)dicarbamate (84)

¹H NMR(CDCl₃) white solid from rxn mixture



Shimadzu LCMS-2020 Data Report

Mass Spectrum for Sample:
RWH-B-40

Operator: Mark Wang

Data filename: C:\LabSolutions\Data\Schwabacher Alan\RWH-B-40-1.lcd

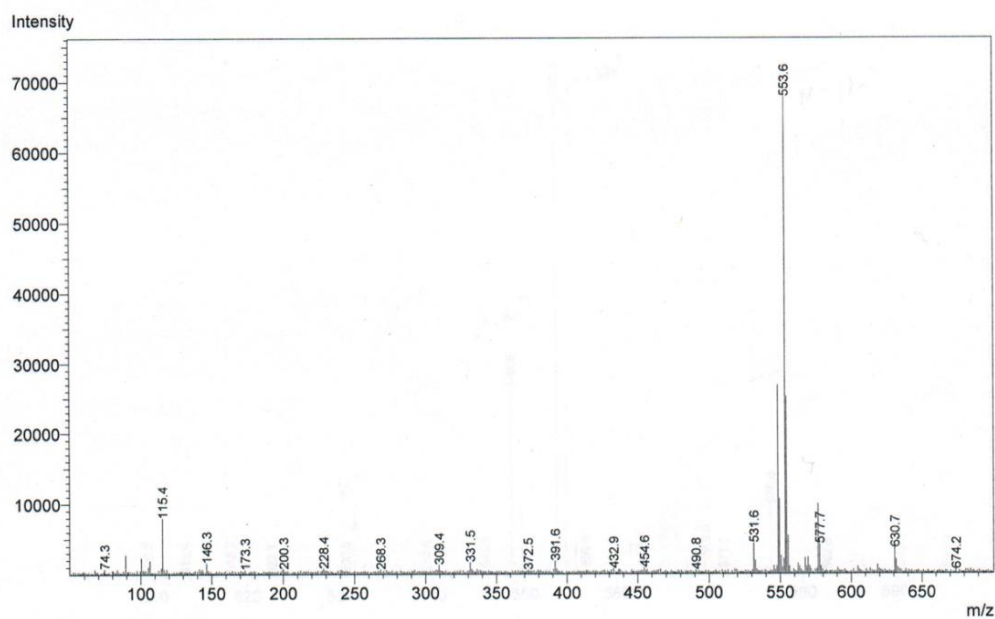
Spectrum Mode: Single

Retention Time: 0.133 min.

Interface Type (ESI, APCI, DUIS): DUIS

Aquisition Mode (Scan, SIM, Profile): Scan

Polarity (+,-): +



ESI-MS (E/Z)-N,N'-(but-2-ene-1,4-diyl)bis(2,2,2-trifluoroacetamide) (85)

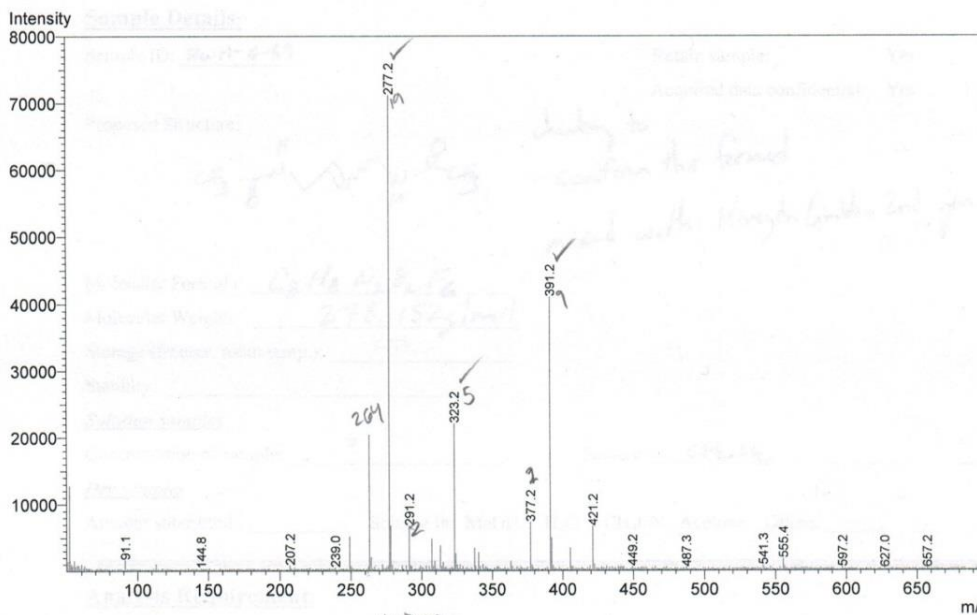
3/14/2014 2:11:21 PM Page 1 / 1

Shimadzu LCMS-2020 Data Report

Mass Spectrum for Sample:
RWH-B-69

Operator: Mark Wang

Data filename: C:\LabSolutions\Data\Hossain, Mahmud\RWH-B-69.lcd
Spectrum Mode: Single
Retention Time: 0.150 min.
Interface Type (ESI, APCI, DUIS): DUIS
Acquisition Mode (Scan, SIM, Profile): Scan
Polarity (+, -): -



$$278 = M$$

$$276 = M - 2H^+ \Rightarrow 188$$

$$277 = M - H^+, 100\%$$

$$323 = M + HCOO^-, 26\%$$

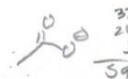
$$391 = M + CF_3COO^-, 47\%$$

monomer = 153

$$\begin{array}{r} 323 \\ - 278 \\ \hline 45 \end{array}$$

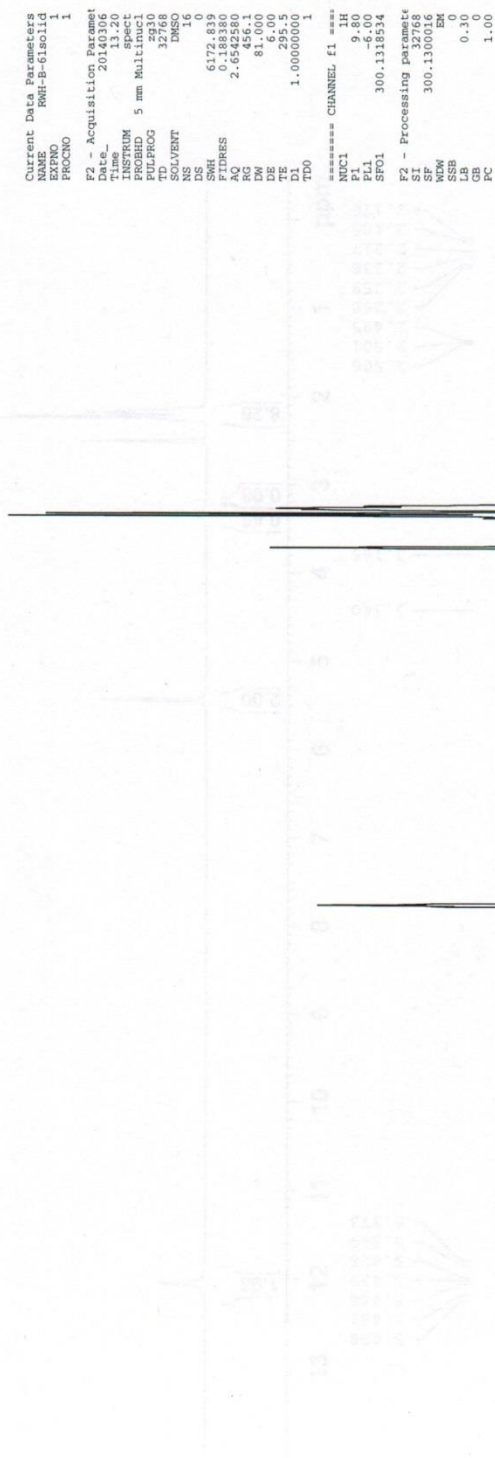
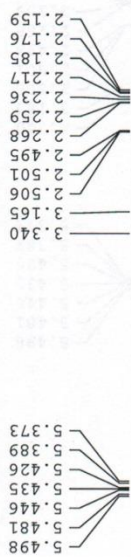
$$\begin{array}{r} 391 \\ - 278 \\ \hline 113 \end{array}$$

$$\begin{array}{r} 421 \\ - 278 \\ \hline 143 \end{array}$$



¹H NMR (*E*)-oct-4-enedioic acid (**86**)

¹H NMR(dMSO) white solid filtered from initial rxn mix

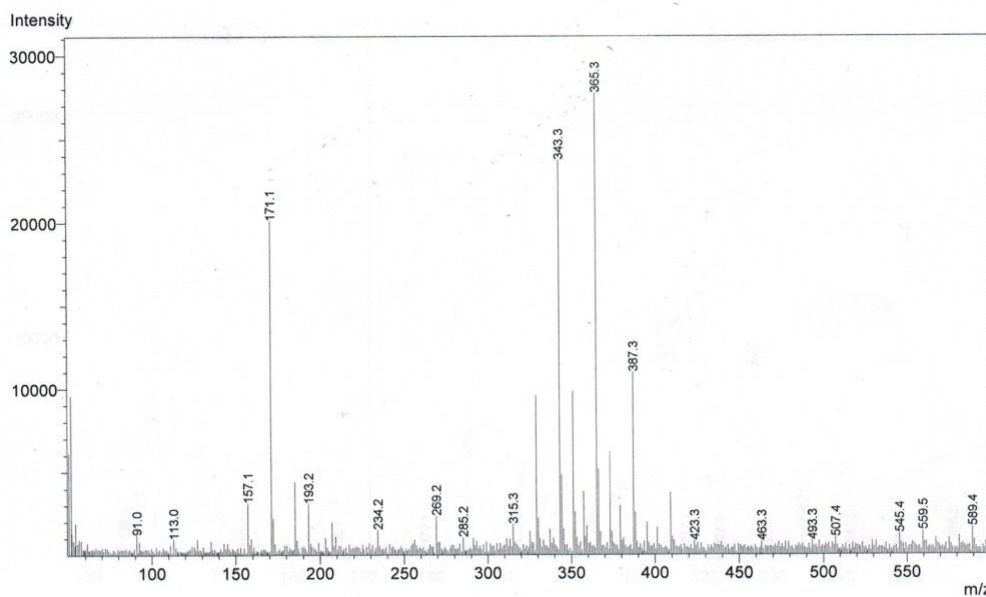


Shimadzu LCMS-2020 Data Report

Mass Spectrum for Sample:
RWH-B-59

Operator: Mark Wang

Data filename: C:\LabSolutions\Data\Schwabacher Alan\RWH-B-59.lcd
Spectrum Mode: Single
Retention Time: 0.150 min.
Interface Type (ESI, APCI, DUIS): DUIS
Acquisition Mode (Scan, SIM, Profile): Scan
Polarity (+, -): -



$$171 = M - H^+$$

72%

$$2M^- = 342$$

$$387 - 2M^- = 45$$

$$CO_2 = 44$$

$$387 - M - M^- = 44$$

$$343 = M + M^-$$

86%

$$365 = 2M^- + Na^+$$

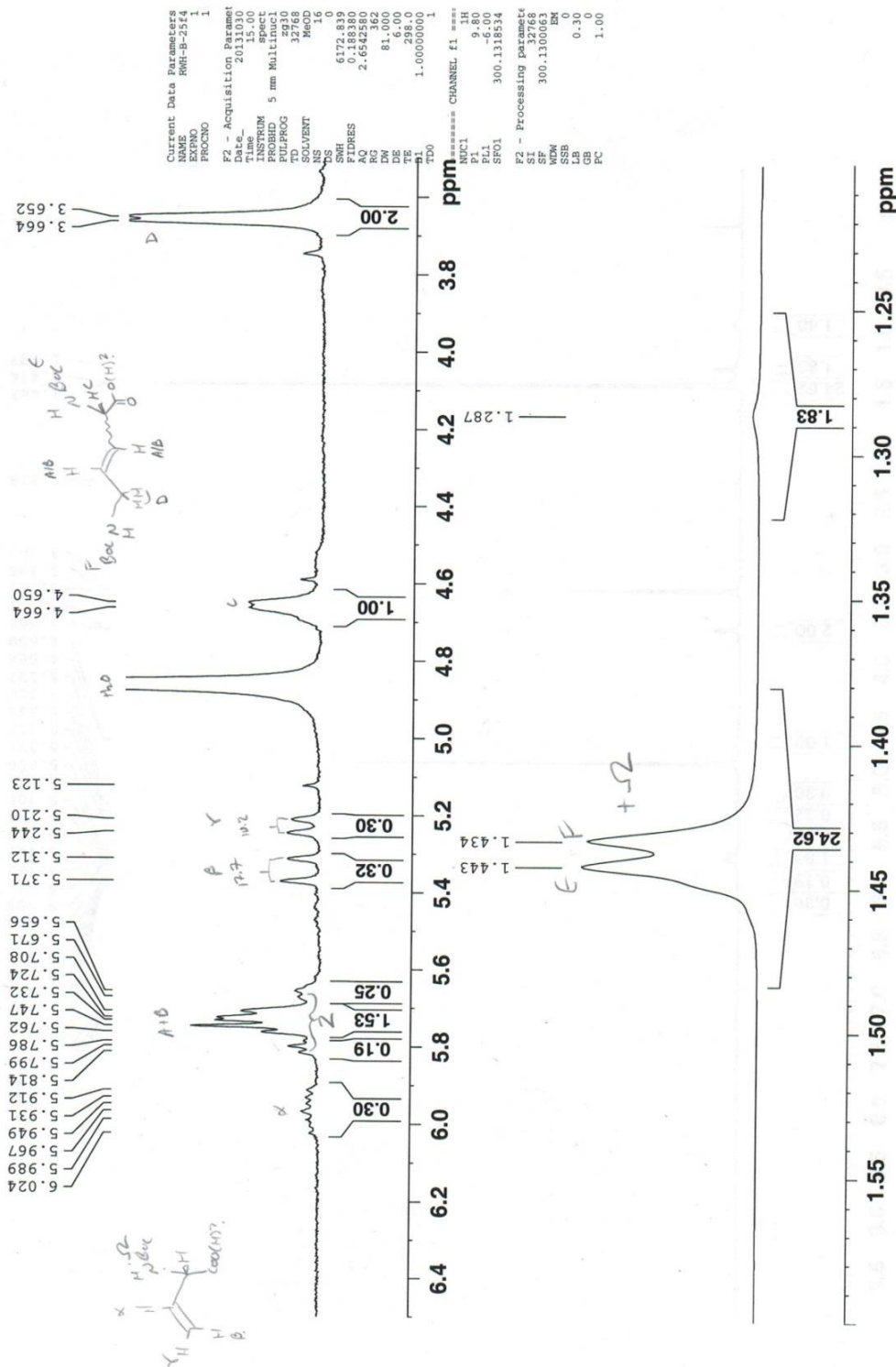
100%

$$C_8H_8 = 44$$

$$44 = 2 \times 22$$

¹H NMR (*S,E*)-2,5-bis((*tert*-butoxycarbonyl)amino)hept-3-enoic acid (**87**)

¹H NMR(CDCl₃) f4 2.5% AcOH/ 7.5% IpOH/ 90% CH₂Cl₂



Shimadzu LCMS-2020 Data Report

Mass Spectrum for Sample:
RWH-B-25

Operator: Mark Wang

Data filename: C:\LabSolutions\Data\Schwabacher Alan\RWH-B-25.lcd

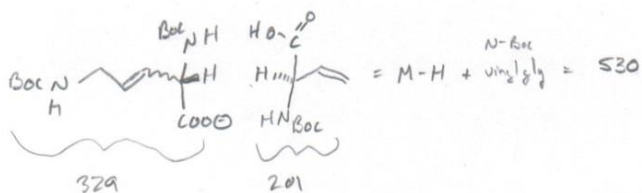
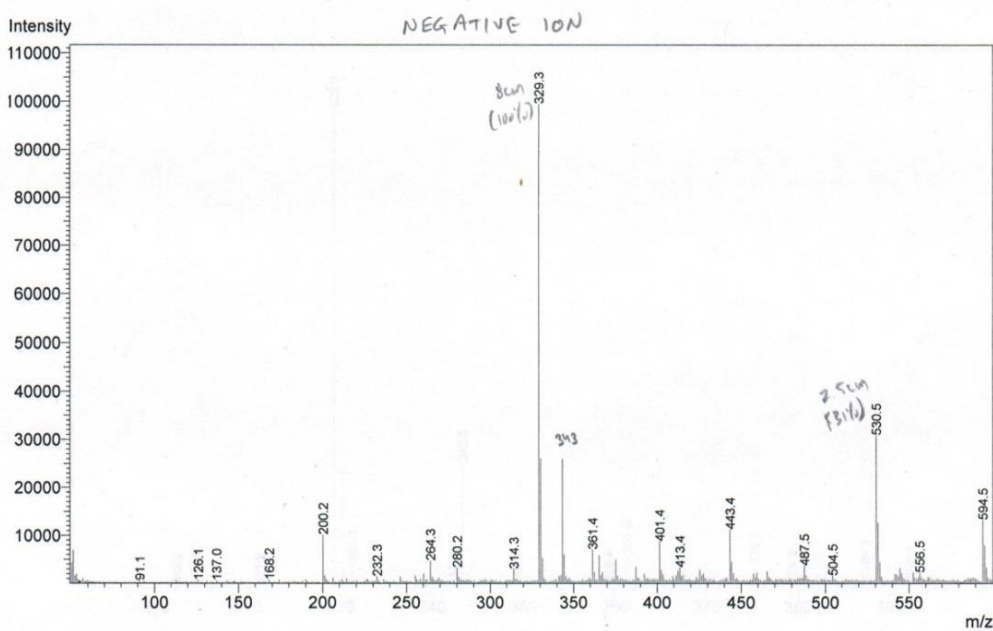
Spectrum Mode: Single

Retention Time: 0.116 min.

Interface Type (ESI, APCI, DUIS): DUIS

Aquisition Mode (Scan, SIM, Profile): Scan

Polarity (+, -): -



ESI-MS

(S,E)-5-((((9H-fluoren-9-yl)methoxy)carbonyl)amino)-2-((tert-butoxycarbonyl)amino)pent-3-enoic acid (88)

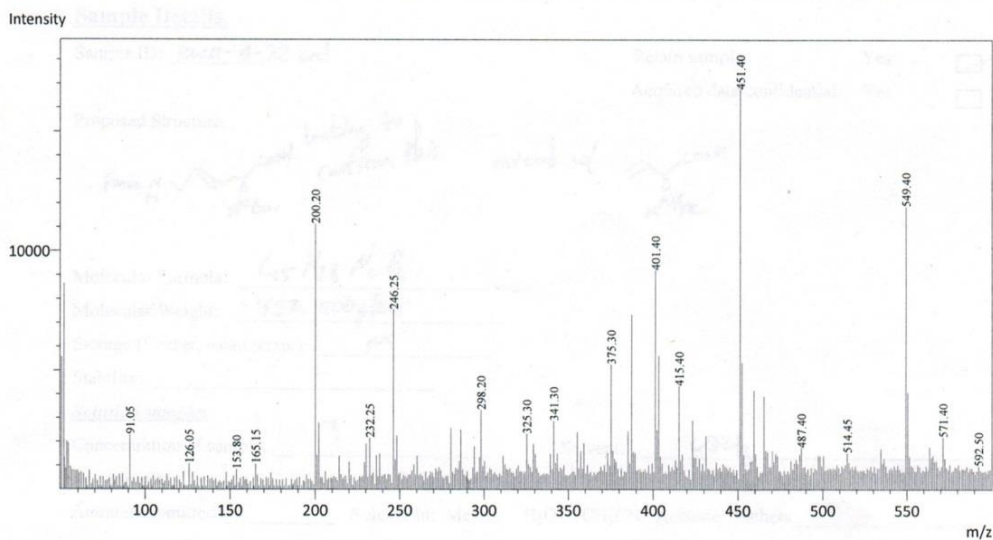
3/24/2014 2:50:28 PM Page 1 /

Shimadzu LCMS-2020 Data Report

Mass Spectrum for Sample
RWH-B-72 cld.lcd

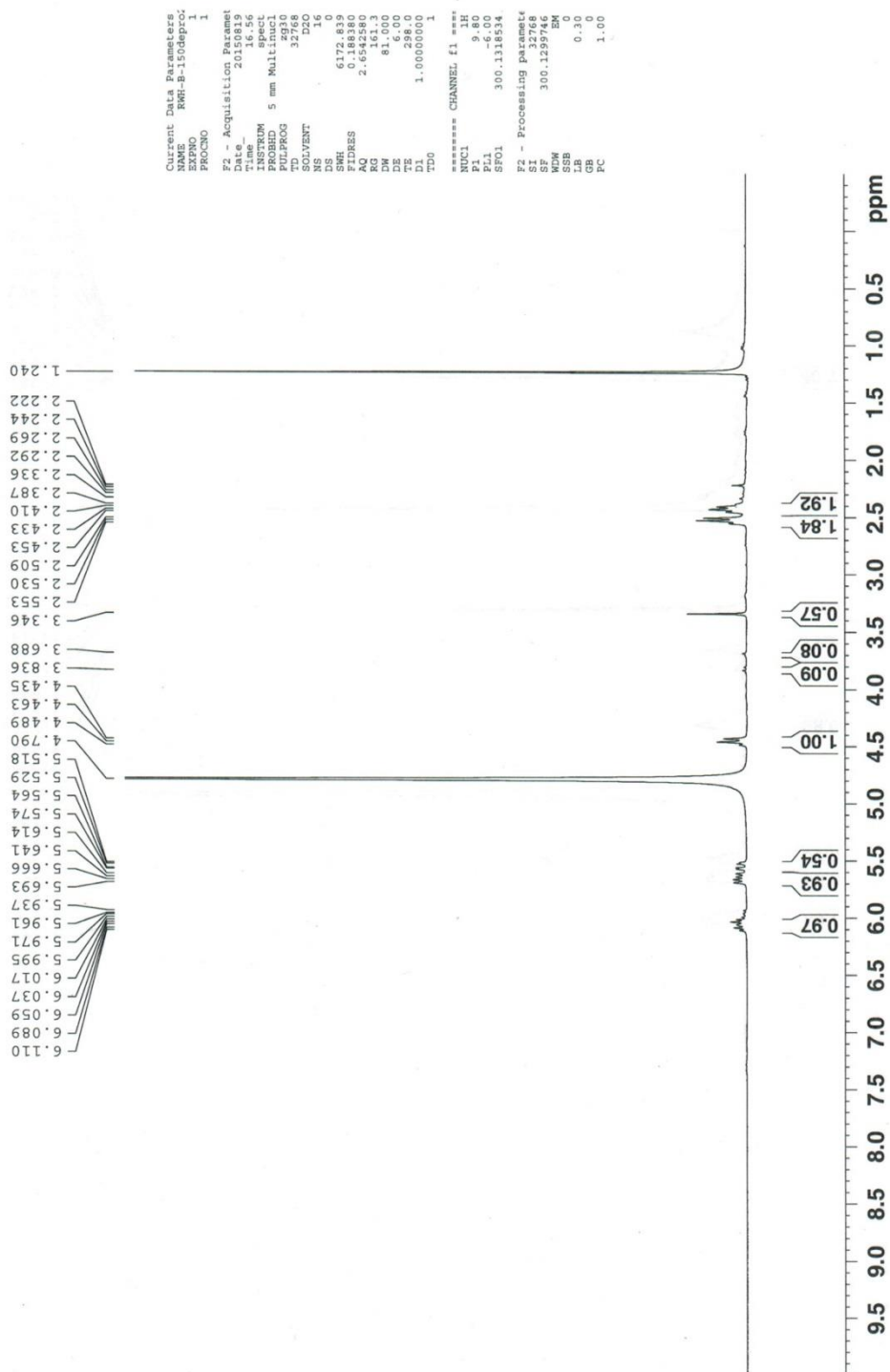
Operator: Mark Wang

Data Filename: C:\LabSolutions\Data\Schwabacher Alan\RWH-B-72 cld.lcd
Spectrum Mode: Single
Retention Time: 0.150
Interface Type (ESI, APCI, DUIS): DUIS
Acquisition Mode (Scan, SIM, Profile): Scan
Polarity: -



¹H NMR (S,E)-2-((tert-butoxycarbonyl)amino)hept-3-enoic acid (89)

¹H NMR (D₂O) deprotected NBoc-L-Vgy + 4PA cross metathesis crude product



Shimadzu LCMS-2020 Data Report

<Spectrum>

Mass Spectrum for Sample
RWH-B-74 depro 01.lcd

Operator: Mark Wang

Data Filename: C:\LabSolutions\Data\Schwabacher Alan\RWH-B-74 depro 01.lcd

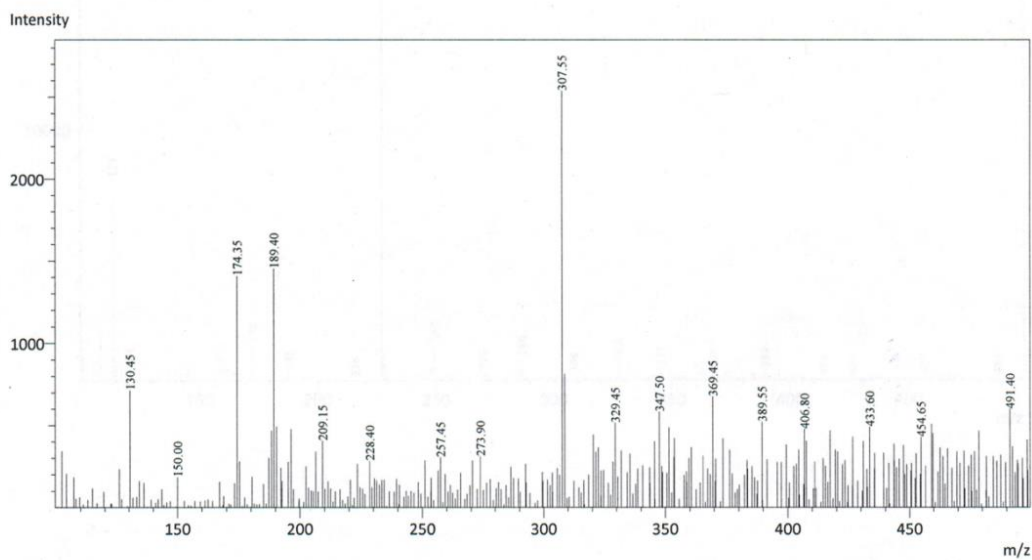
Spectrum Mode: Averaged

Retention Time: ----

Interface Type (ESI, APCI, DUIS): DUIS

Acquisition Mode (Scan, SIM, Profile): Scan

Polarity: +



XI. CURRICULUM VITAE

Robert W. Hoppe

Highlights

- Experience in developing, optimizing and scaling up organic synthetic procedures
- Extensive experience in characterization of molecular structure and behavior using NMR, MS, HPLC, and fluorescence spectroscopy
- Directed research of multiple undergraduates emphasizing fundamental synthetic technique, prudent record keeping, and spectroscopic analysis
- Managing daily laboratory operations including chemical purchasing, organization and storage, and maintenance and repair of equipment

Education

- Dissertation Title: "Molecular Recognition in Water: Rigid Synthetic Receptors and Enzymatic Mechanistic Probes"
Adviser: Professor Alan W. Schwabacher
- BS, Chemistry, University of Wisconsin-Oshkosh, Oshkosh WI, 2006
Adviser: Professor Brant L. Kedrowski

Research Experience

2007-Present Graduate Assistant, University of Wisconsin-Milwaukee

Adviser: Professor Alan W. Schwabacher

- Synthesis and characterization of a water soluble artificial molecular receptor
- Dramatic simplification of thermal reactions: L-Vinylglycine synthesis
- Small molecule synthesis for catalytic and kinetic characterization of enzymes
- Identification of a novel synthesis of diaryl amines in optimization of a large scale synthesis
- Quinolone heterocycles synthesis and correlating factors in regioselectivity in formation

2004-2006 Undergraduate Research Assistant, University of Wisconsin Oshkosh

Adviser: Brant L. Kedrowski

- Studied natural product synthesis

Teaching Experience

General Chemistry (5 terms), Survey of Biochemistry (4 terms), Organic Chemistry (4 terms),
Advanced Organic Laboratory (5 terms)

Affiliations

- American Chemical Society

Publications

- Mueller, L.; Hoppe, R.; Ochsenwald, J.; Berndt, R.; Severin, G.; Schwabacher, A. W.; Silvaggi, N. "Sbi00515, a Protein of Unknown Function from *Streptomyces bingchenggensis*, Highlights the Functional Versatility of the Acetoacetate Decarboxylase Scaffold" *Biochemistry*, 2015, 54 (25), 3978-3988
- Burroughs, A. M.; Hoppe, R.; Goebel, N.; Sayyed, B.; Voegtline, T.; Schwabacher, A. W.; Zabriskie, T. M.; Silvaggi, N. "Structural and Functional Characterization of MppR, an Enduracididine Biosynthetic Enzyme from *Streptomyces hygroscopicus*: Functional Diversity in the Acetoacetate Decarboxylase-like Superfamily" *Biochemistry*, 2013, 52 (26), 4492-4506
- Kedrowski, B.; Hoppe, R. "A Concise Synthesis of (\pm)-Cacalol" *J. Org. Chem.*, 2008, 73 (13), 5177-5179

References

Professor Alan W. Schwabacher, Dept. of Chemistry & Biochemistry, Univ. of Wisconsin-
Milwaukee, Milwaukee WI 414-229-4410 awschwab@uwm.edu

Professor Nicholas Silvaggi, Dept. of Chemistry & Biochemistry, Univ. of Wisconsin-
Milwaukee, Milwaukee WI 414-229-2647 silvaggi@uwm.edu

Professor Anja Blecking, Dept. of Chemistry & Biochemistry, Univ. of Wisconsin- Milwaukee,
Milwaukee WI 414-229-2974 blecking@uwm.edu